AUTISM SIGNALING PATHWAYS

EDITED BY: Yu-Chih Lin and Yi-Ping Hsueh
PUBLISHED IN: Frontiers in Cellular Neuroscience and Frontiers in Genetics

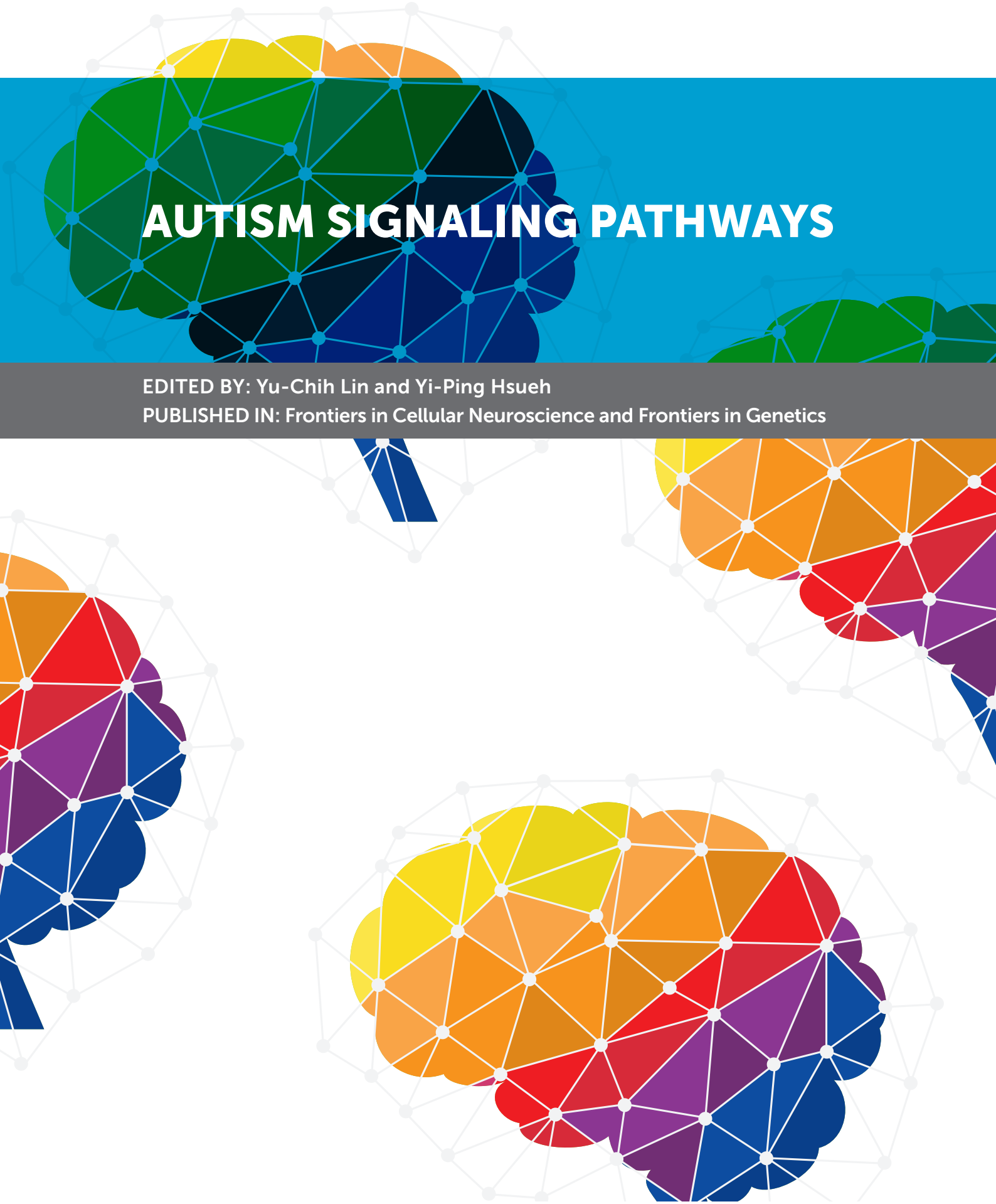

frontiers Research Topics

ISSN 1664-8714
ISBN 978-2-88971-657-9
DOI 10.3389/978-2-88971-657-9

About Frontiers

Frontiers is more than just an open-access publisher of scholarly articles: it is a pioneering approach to the world of academia, radically improving the way scholarly research is managed. The grand vision of Frontiers is a world where all people have an equal opportunity to seek, share and generate knowledge. Frontiers provides immediate and permanent online open access to all its publications, but this alone is not enough to realize our grand goals.

Frontiers Journal Series

The Frontiers Journal Series is a multi-tier and interdisciplinary set of open-access, online journals, promising a paradigm shift from the current review, selection and dissemination processes in academic publishing. All Frontiers journals are driven by researchers for researchers; therefore, they constitute a service to the scholarly community. At the same time, the Frontiers Journal Series operates on a revolutionary invention, the tiered publishing system, initially addressing specific communities of scholars, and gradually climbing up to broader public understanding, thus serving the interests of the lay society, too.

Dedication to Quality

Each Frontiers article is a landmark of the highest quality, thanks to genuinely collaborative interactions between authors and review editors, who include some of the world's best academicians. Research must be certified by peers before entering a stream of knowledge that may eventually reach the public - and shape society; therefore, Frontiers only applies the most rigorous and unbiased reviews.
Frontiers revolutionizes research publishing by freely delivering the most outstanding research, evaluated with no bias from both the academic and social point of view. By applying the most advanced information technologies, Frontiers is catapulting scholarly publishing into a new generation.

What are Frontiers Research Topics?

Frontiers Research Topics are very popular trademarks of the Frontiers Journals Series: they are collections of at least ten articles, all centered on a particular subject. With their unique mix of varied contributions from Original Research to Review Articles, Frontiers Research Topics unify the most influential researchers, the latest key findings and historical advances in a hot research area! Find out more on how to host your own Frontiers Research Topic or contribute to one as an author by contacting the Frontiers Editorial Office: frontiersin.org/about/contact

AUTISM SIGNALING PATHWAYS

Topic Editors:
Yu-Chih Lin, Hussman Institute for Autism, United States
Yi-Ping Hsueh, Academia Sinica, Taiwan

Citation: Lin, Y.-C., Hsueh, Y.-P., eds. (2021). Autism Signaling Pathways. Lausanne: Frontiers Media SA. doi: 10.3389/978-2-88971-657-9

Table of Contents

frontiers in Cellular Neuroscience

EDITORIAL
published: 28 September 2021
doi: 10.3389/fncel.2021.760994

Editorial: Autism Signaling Pathways

Yi-Ping Hsueh[1]* *and Yu-Chih Lin*[2]

[1] Institute of Molecular Biology, Academia Sinica, Taipei City, Taiwan, [2] Program in Neuroscience, Hussman Institute for Autism, Baltimore, MD, United States

Keywords: autism spectrum disorders, cell adhesion, G-protein coupled receptor, IL-17A, parvalbumin, repetitive behaviors, transcriptomic analysis, valproic acid

Editorial on the Research Topic

Autism Signaling Pathways

INTRODUCTION

Autism spectrum disorders (ASD), a group of heterogeneous neurodevelopmental disorders, are characterized by two main behavioral features, termed the ASD dyad (https://www.cdc.gov/ncbddd/autism/hcp-dsm.html). The first is defective social interaction and impaired verbal and non-verbal communication. The second is abnormal sensory responses and stereotypic repetitive behaviors (Grzadzinski et al., 2013). As a neurodevelopmental disorder, genetic variation plays a critical role in ASD (De Rubeis et al., 2014; Gaugler et al., 2014; Iossifov et al., 2014; Krumm et al., 2015; Grove et al., 2019). In the SFARI collection (https://gene.sfari.org/database/gene-scoring/), a total of 549 genes (from syndromic and category 1 and 2 groups) have been evidenced as strongly linked to ASD. In addition to diverse genetic factors, various environmental factors also contribute to ASD (Karimi et al., 2017; Modabbernia et al., 2017), rendering study of ASD even more complex and difficult. When investigating ASD etiology and therapeutics, age-dependent effects and homeostasis of neural activity also need to be considered. In this special Research Topic on "Autism Signaling Pathways," 10 significant publications have been collected to summarize our current understanding of various aspects of ASD and to report on some new findings.

SIGNALING PATHWAYS AND NEURAL CIRCUITS IN ASD

Filice et al. and Janickova and Schwaller have contributed articles related to the roles of parvalbumin and parvalbumin-positive interneurons (PV neurons in short) in ASD. Many autism mouse models display an altered number of PV neurons and/or expression levels of parvalbumin, suggesting involvement of PV neurons in ASD. The physiological significance of PV neurons to ASD is summarized by Filice et al. However, genetic evidence is still lacking to show whether mutation of the paravalbumin gene contributes to ASD. The study by Janickova and Schwaller showed that deletion of the parvalbumin gene results in increased oxidative stress in the brain of mice aged 3 or 6 months but not in younger mice, even though $PV^{-/-}$ mice aged 1 month display autism-like behaviors. Thus, even though PV neurons are critical players in ASD, the disruption of PV neurons in ASD is likely caused by indirect neural circuit alterations as the nervous system tends to adapt to those changes to maintain homeostasis (Fazel Darbandi et al., 2018; Antoine et al., 2019).

As highlighted by Gandhi and Lee, the brain's cerebral cortex, striatum, thalamus, hypothalamus, amygdala, olfactory tubercle, ventral tegmental area (VTA), substantia nigra pars complex (SN), and cerebellum are all involved in ASD, though brain regions respond differentially to diverse genetic variations. Details of the signaling pathways, neural circuits, and anatomical changes related to repetitive behaviors in mice have been explored by Gandhi and Lee. They have also summarized the pharmacological treatments used for repetitive behaviors, representing

OPEN ACCESS

Edited and reviewed by:
Dirk M. Hermann, University of Duisburg-Essen, Germany

***Correspondence:**
Yi-Ping Hsueh
yph@gate.sinica.edu.tw

Specialty section:
This article was submitted to Cellular Neuropathology, a section of the journal Frontiers in Cellular Neuroscience

Received: *19 August 2021*
Accepted: *31 August 2021*
Published: *28 September 2021*

Citation:
Hsueh Y-P and Lin Y-C (2021) Editorial: Autism Signaling Pathways. Front. Cell. Neurosci. 15:760994. doi: 10.3389/fncel.2021.760994

potential therapeutic treatments for ASD. The corticostriatal circuitry was the focus of articles contributed by Mizuno et al., Brandenburg et al., and Caubit et al. Mizuno et al. investigated the transcriptomic profiles of BTBRTF/ArtRbrc mice as an ASD model, reinforcing the notion of complex signaling pathways and interconnectivity among many ASD-associated genes in the brain cortex and striatum. Brandenburg et al. utilized postmortem brains of ASD patients to analyze expression of GABA and serotonin receptors in the basal ganglia and their results indicate that alterations in an indirect pathway of the corticostriatal circuitry are involved in ASD. Finally, Caubit et al. applied the *Camk2a-Cre* transgene to selectively control expression of the zinc finger transcriptional factor TSHZ3, a high-confidence causative gene of ASD, providing a model to further characterize the impact of deleting *Tshz3* from specific cell types in terms of ASD phenotypes.

This special Research Topic also covers other ASD-associated molecules, including cell adhesion molecules (Gandawijaya et al.), G protein-coupled receptors (GPCR, DelaCuesta-Barrutia et al.) and NMDAR GluN2B (Bahry et al.). Gandawijaya et al. report how deletion of human chromosome 3p that results in absence of three closely related genes encoding neuronal immunoglobulin cell adhesion molecules, i.e. *Close Homolog of L1* (*CHL1*), *Contactin-6* (*CNTN6*), and *Contactin-4* (*CNTN4*), is relevant to ASD. DelaCuesta-Barrutia et al. summarize heterooligomer formation of various neurotransmitter receptors, such as the GPCRs of glutamate, dopamine, oxytocin and serotonin, and they discuss current advances in pharmacological approaches targeting GPCR heteromers. The impact of an early termination mutation at amino acid residue 724 of GluN2B on dendritic outgrowth is reported by Bahry et al. As a voltage-gated glutamate receptor, the finding that mutation of *GluN2B* promotes dendritic pruning is intriguing, but the underlying mechanism remains unclear and warrants further investigation.

Finally, Béroule discusses the paradoxical effects of the inflammatory cytokine IL-17A and anticonvulsant valproic acid (VPA) on the brain. Exposure to either IL-17A or VPA during pregnancy increases the likelihood of the offspring developing ASD, yet their effects on adult brains differ. Béroule has hypothesized that as a shared downstream target of IL-17A and VPA, type A monoamine oxidase (MAOA) exerts context-dependent paradoxical effects. He also discusses the roles of neuroinflammation and regulated MAOA expression in ASD.

PERSPECTIVE

Overall, ASD represents a highly complex group of disorders. Emerging studies in this Research Topic dissect their pathologies in neurotransmission (including both ion channels and GPCR), cell adhesion, transcriptional regulation, interconnections among different types of neurons and different brain regions. These studies provide foundations for future investigations. Certainly, other detailed discussions, such as chromatin remodeling and synaptic organization, development and signaling are not covered. Here, we further extend and emphasize three worth considering points for ASD research. First, what is the true cause of ASD? One should be cautious in interpreting results from postmortem brain tissues. Differences in postmortem tissues may be a consequence but not the cause

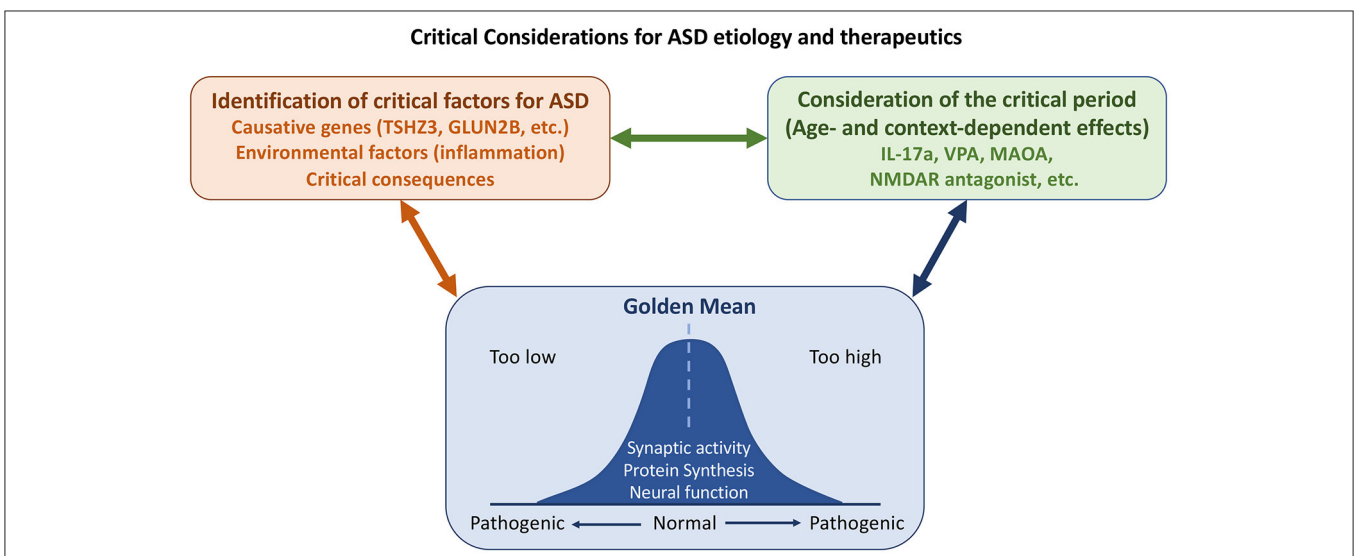

FIGURE 1 | Some considerations on etiology, critical period, and homeostasis (the "golden mean") for ASD study. Both genetic and environmental factors contribute to ASD. Some changes observed in patients and/or mouse models are consequences and not causes of ASD. It is essential to distinguish the causes of ASD from its consequences. Some causative genes and environmental factors that had been discussed in this Research Topic are indicated. As critical factors of ASD may act opposingly at different developmental stages or in different contexts, the critical period needs to be considered for ASD etiology and treatment. Finally, homeostasis of neuronal responses and nervous system activity must be maintained. Defects in either direction give rise to ASD pathological conditions.

of ASD pathology. Similarly, the aforementioned articles on PV neurons imply that altered parvalbumin-mediated regulation of oxidative stress does not cause ASD, even though PV neurons are indeed affected by ASD and are a feature of ASD phenotypes. Second, context- or age-dependent effects of ASD must be considered. Dr. Eunjoon Kim (Korea Advanced Institute of Science and Technology) and colleagues have shown that Shank2-knockout neurons exhibit NMDAR hyperfunction before weaning but NMDAR hypoactivity after weaning (Chung et al., 2019). Consequently, treatment with the NMDAR antagonist memantine exerted the opposite effects on Shank2-knockout mice before and after weaning. The differential effects of IL-17A and VPA on mice of different ages described by Béroule further echo this concept. Thus, to evaluate the effect of pharmacological treatment and signaling pathways of autism, age is one of critical factors for consideration. Finally, although it was not clearly addressed in the articles collected for this Research Topic, it is generally accepted that deviations from homeostasis (the "golden mean," see **Figure 1**) are common in ASD. For instance, both increases and decreases in protein synthesis and signaling have been linked to ASD-associated neuronal defects (Lu and Hsueh, 2021). Synaptic morphology and responses must also be controlled within appropriate thresholds so that neuronal activity or function is neither excessive nor inadequate, since any such defects may lead to ASD pathological conditions.

AUTHOR CONTRIBUTIONS

Y-PH edited manuscripts published in the Research Topic, wrote the current manuscript, prepared the figure, and approved submission to the journal. Y-CL edited manuscripts published in the Research Topic, contributed discussion, and approved submission to the journal. All authors contributed to the article and approved the submitted version.

FUNDING

This work was supported by Academia Sinica (AS-IA-106-L04 and AS-TP-110-L10) and the Ministry of Science and Technology, Taiwan (MOST 108-2311-B-001-008-MY3). Hussman Foundation grant HIAS18004.

ACKNOWLEDGMENTS

We thank Dr. John O'Brien for English editing.

REFERENCES

Antoine, M. W., Langberg, T., Schnepel, P., and Feldman, D. E. (2019). Increased excitation-inhibition ratio stabilizes synapse and circuit excitability in four autism mouse models. *Neuron* 101, 648–661.e644. doi: 10.1016/j.neuron.2018.12.026

Chung, C., Ha, S., Kang, H., Lee, J., Um, S. M., Yan, H., et al. (2019). Early correction of N-Methyl-D-Aspartate Receptor function improves autistic-like social behaviors in adult Shank2(-/-) mice. *Biol. Psychiatry* 85, 534–543. doi: 10.1016/j.biopsych.2018.09.025

De Rubeis, S., He, X., Goldberg, A. P., Poultney, C. S., Samocha, K., Cicek, A. E., et al. (2014). Synaptic, transcriptional and chromatin genes disrupted in autism. *Nature* 515, 209–215. doi: 10.1038/nature13772

Fazel Darbandi, S., Robinson Schwartz, S. E., Qi, Q., Catta-Preta, R., Pai, E. L., Mandell, J. D., et al. (2018). Neonatal Tbr1 dosage controls cortical layer 6 connectivity. *Neuron* 100, 831–845.e837. doi: 10.1016/j.neuron.2018.09.027

Gaugler, T., Klei, L., Sanders, S. J., Bodea, C. A., Goldberg, A. P., Lee, A. B., et al. (2014). Most genetic risk for autism resides with common variation. *Nat. Genet.* 46, 881–885. doi: 10.1038/ng.3039

Grove, J., Ripke, S., Als, T. D., Mattheisen, M., Walters, R. K., Won, H., et al. (2019). Identification of common genetic risk variants for autism spectrum disorder. *Nat. Genet.* 51, 431–444. doi: 10.1038/s41588-019-0344-8

Grzadzinski, R., Huerta, M., and Lord, C. (2013). DSM-5 and autism spectrum disorders (ASDs): an opportunity for identifying ASD subtypes. *Mol. Autism* 4:12. doi: 10.1186/2040-2392-4-12

Iossifov, I., O'Roak, B. J., Sanders, S. J., Ronemus, M., Krumm, N., Levy, D., et al. (2014). The contribution of de novo coding mutations to autism spectrum disorder. *Nature* 515, 216–221. doi: 10.1038/nature13908

Karimi, P., Kamali, E., Mousavi, S. M., and Karahmadi, M. (2017). Environmental factors influencing the risk of autism. *J. Res. Med. Sci.* 22:27. doi: 10.4103/1735-1995.200272

Krumm, N., Turner, T. N., Baker, C., Vives, L., Mohajeri, K., Witherspoon, K., et al. (2015). Excess of rare, inherited truncating mutations in autism. *Nat. Genet.* 47, 582–588. doi: 10.1038/ng.3303

Lu, M. H., and Hsueh, Y. P. (2021). Protein synthesis as a modifiable target for autism-related dendritic spine pathophysiologies. *FEBS J.* doi: 10.1111/febs.15733. [Epub ahead of print].

Modabbernia, A., Velthorst, E., and Reichenberg, A. (2017). Environmental risk factors for autism: an evidence-based review of systematic reviews and meta-analyses. *Mol. Autism* 8:13. doi: 10.1186/s13229-017-0121-4

Conflict of Interest: The authors declare that the research was conducted in the absence of any commercial or financial relationships that could be construed as a potential conflict of interest.

Publisher's Note: All claims expressed in this article are solely those of the authors and do not necessarily represent those of their affiliated organizations, or those of the publisher, the editors and the reviewers. Any product that may be evaluated in this article, or claim that may be made by its manufacturer, is not guaranteed or endorsed by the publisher.

frontiers in Cellular Neuroscience

ORIGINAL RESEARCH
published: 28 September 2020
doi: 10.3389/fncel.2020.571216

Parvalbumin-Deficiency Accelerates the Age-Dependent ROS Production in Pvalb Neurons *in vivo*: Link to Neurodevelopmental Disorders

*Lucia Janickova and Beat Schwaller**

Department of Neurosciences amd Movement Science, Section of Medicine, University of Fribourg, Fribourg, Switzerland

In neurodevelopmental disorders (NDDs) including autism spectrum disorder (ASD) and schizophrenia, impairment/malfunctioning of a subpopulation of interneurons expressing the calcium-binding protein parvalbumin (PV) –here termed Pvalb neurons– has gradually emerged as a possible cause. These neurons may represent a hub or point-of-convergence in the etiology of NDD. Increased oxidative stress associated with mitochondria impairment in Pvalb neurons is discussed as an essential step in schizophrenia etiology. Since PV downregulation is a common finding in ASD and schizophrenia individuals and PV-deficient (PV−/−) mice show a strong ASD-like behavior phenotype, we investigated the putative link between PV expression, alterations in mitochondria and oxidative stress. In a longitudinal study with 1, 3, and 6-months old PV−/− and wild type mice, oxidative stress was investigated in 9 Pvalb neuron subpopulations in the hippocampus, striatum, somatosensory cortex, medial prefrontal cortex, thalamic reticular nucleus (TRN) and cerebellum. In Pvalb neuron somata in the striatum and TRN, we additionally determined mitochondria volume and distribution at these three time points. In all Pvalb neuron subpopulations, we observed an age-dependent increase in oxidative stress and the increase strongly correlated with PV expression levels, but not with mitochondria density in these Pvalb neurons. Moreover, oxidative stress was elevated in Pvalb neurons of PV−/− mice and the magnitude of the effect was again correlated with PV expression levels in the corresponding wild type Pvalb neuron subpopulations. The PV-dependent effect was insignificant at 1 month and relative differences between WT and PV−/− Pvalb neurons were largest at 3 months. Besides the increase in mitochondria volume in PV's absence in TRN and striatal PV−/− Pvalb neurons fully present already at 1 month, we observed a redistribution of mitochondria from the perinuclear region toward the plasma membrane at all time points. We suggest that in absence of PV, slow Ca^{2+} buffering normally exerted by PV is compensated by a (mal)adaptive, mostly sub-plasmalemmal increase in mitochondria resulting in increased oxidative stress observed in 3- and 6-months old mice. Since PV−/− mice display core ASD-like symptoms already at 1 month, oxidative stress in Pvalb neurons is not a likely cause for their ASD-related behavior observed at this age.

Keywords: parvalbumin, autism, schizophrenia, ROS, mitochondria

OPEN ACCESS

Edited by:
Yu-Chih Lin,
Hussman Institute for Autism,
United States

Reviewed by:
Alberto Granato,
Catholic University of the Sacred Heart, Italy
Matteo Caleo,
University of Padua, Italy

***Correspondence:**
Beat Schwaller
beat.schwaller@unifr.ch

Specialty section:
This article was submitted to Cellular Neuropathology, a section of the journal Frontiers in Cellular Neuroscience

Received: *10 June 2020*
Accepted: *12 August 2020*
Published: *28 September 2020*

Citation:
Janickova L and Schwaller B (2020) Parvalbumin-Deficiency Accelerates the Age-Dependent ROS Production in Pvalb Neurons in vivo: Link to Neurodevelopmental Disorders. Front. Cell. Neurosci. 14:571216. doi: 10.3389/fncel.2020.571216

INTRODUCTION

The etiology of neurodevelopmental disorders (NDDs) including autism spectrum disorder (ASD), schizophrenia and attention deficit hyperactivity disorder remains unclear. Although each NDD is characterized by a specific trajectory with respect to onset, symptoms or behavioral alterations, as well as brain regions and cell types implicated in this process, they share genetic etiology (Schork et al., 2019) and also disorder-associated comorbidities. This hints toward impairments of similar and/or convergent pathways in the various NDD. Such a point-of-convergence may exist in the malfunctioning/impairment of GABAergic interneurons (Marin, 2012; Schork et al., 2019) mostly in the ones expressing the calcium-binding protein parvalbumin (PV) (Ferguson and Gao, 2018) hereafter called Pvalb neurons. This interneuron type present, e.g., in cortex, hippocampus, striatum and cerebellum of rodents and humans (for details, see, Celio, 1990; del Rio et al., 1994; Hashemi et al., 2017; Soghomonian et al., 2017) is characterized by fast, non-adaptive firing and rapid AP kinetics. Pvalb neurons target the perikarya or axon initial segments of excitatory (and inhibitory) neurons and form strong autapses (Deleuze et al., 2019), which make them particularly suitable for enabling and controlling synchronization of neuron ensembles (Sohal et al., 2009; Bohannon and Hablitz, 2018) resulting in oscillatory activity. At the morphological level, a majority of Pvalb neurons is surrounded by perineuronal nets (PNN) that allow for their identification irrespective of PV expression levels as shown before (Filice et al., 2016).

In schizophrenia, a decrease in the number of PV-immunoreactive (PV^+) neurons resulting from PV downregulation (initially presumed to result from Pvalb neuron loss) is observed in postmortem brains of affected individuals, as well as in mouse models of schizophrenia (Do et al., 2009; Powell et al., 2012). In most cases, a concomitant decrease in GAD67 (*GAD1*) occurs indicative of a common/similar regulation of the *PVALB* and *GAD1* genes. The decrease of PV and GAD67 is considered as a downstream effect of NMDA receptor (NMDAR) hypofunction in pyramidal cells resulting in decreased activity of Pvalb neurons (Gonzalez-Burgos and Lewis, 2012; Gonzalez-Burgos et al., 2015) proposed to reduce network gamma oscillatory activity (Volman et al., 2011). An extensively studied hypothesis is centered on oxidative stress-mediated Pvalb neuron impairment likely associated with mitochondrial dysfunction (Steullet et al., 2017), as was also proposed for the etiology of ASD (Bader et al., 2011; Tang et al., 2013). In the redox dysregulation model of schizophrenia oxidative stress is viewed as the "integrator" leading to Pvalb neuron impairment (Steullet et al., 2017). Accordingly, genetic and/or environmental factors weaken antioxidant defense systems leading to NMDAR hypofunction and PV downregulation (reviewed in Hardingham and Do, 2016). However, during hippocampal maturation *in vitro*, NMDAR inhibition and oxidative stress differentially alter PV expression and gamma oscillation activity (Hasam-Henderson et al., 2018) indicating that general oxidative stress cannot be the main mechanism underlying the decrease in PV expression and that it cannot mechanistically explain the effects of NMDAR hypofunction (Hasam-Henderson et al., 2018).

In the case of ASD, GABA system dysfunction including impaired Pvalb neuron function is a well-accepted hypothesis (Chattopadhyaya and Cristo, 2012; Coghlan et al., 2012; Marin, 2012). Yet, the putative role of the protein PV lending its name to the Pvalb neuron subpopulation has been investigated to a much lesser extent in ASD (and schizophrenia). Reduced numbers of PV^+ neurons in ASD patients and in animal models of ASD were initially presumed to be the result of a lower number of Pvalb neurons (Gogolla et al., 2009), reviewed in Schwaller (2020). However, in many cases the observed decreased number of PV^+ neurons –at least in mice– is the result of PV downregulation, i.e., in low PV-expressing neurons PV expression levels fall below the detection threshold [e.g., in Shank1−/−, Shank3B−/− (Filice et al., 2016), Cntnap2−/− (Lauber et al., 2018), and VPA mice (Lauber et al., 2016)]. In line, the most strongly downregulated transcript in cerebral cortex of ASD patients is *PVALB* mRNA (Parikshak et al., 2016) and several transcripts of genes related to synaptic transmission and mitochondria (Schwede et al., 2018). Transcriptomic network analysis of three mouse ASD and schizophrenia models identified four modules [M; two cortical (c) and two hippocampal (h)] of co-expressed genes dysregulated in all three animal models (Gordon et al., 2019). The upregulated cM1 module is enriched for genes implicated in 'morphogenesis of branching structures,' while the downregulated cM2 is annotated as mitochondrial related energy balance ('energy-coupled proton transport' and 'respiratory electron transport chain'). Importantly, Expression Weighted Cell-Type Enrichment (EWCE) analysis uncovered a significant increase in cM2 (mitochondrial) genes in fast-firing inhibitory neurons, presumably Pvalb neurons.

We have previously shown that a reduction or complete elimination of PV in PV+/− and PV−/− mice results in a robust ASD-like behavior phenotype showing all ASD core symptoms, as well as ASD-associated comorbidities (Wöhr et al., 2015). Moreover, in all systems investigated so far [fast-twitch muscle, PV-overexpressing epithelial (MDCK), oligodendrocyte-like (CG4) cells (for details, see, Schwaller, 2020)] and Pvalb neurons *in vivo* (Janickova et al., 2020), PV downregulation leads to a compensatory/homeostatic upregulation of mitochondria volume (Schwaller, 2020), while ectopic PV expression in all neurons of Thy-PV transgenic mice decreases the mitochondria volume evidenced in the striatum (Maetzler et al., 2004). In distinct Pvalb neuron populations in adult PV−/− mice, the mitochondrial volume is augmented and the relative increase strongly correlates with the PV concentration prevailing in the various WT Pvalb neuron subpopulations in the different brain regions, i.e., the higher the concentration of PV, the higher the PV loss-induced increase in mitochondria volume (Janickova et al., 2020). Interestingly, both in CG4 cells and more relevant in PV−/− Pvalb neurons, the increase in mitochondria volume and dendritic mitochondria length is associated with increased branching and length of dendrites (Lichvarova et al., 2019; Janickova et al., 2020), in full agreement with the reported increase in genes of module cM1 ('morphogenesis of branching structures') in three ASD and schizophrenia mouse models

(Gordon et al., 2019). Thus, we set out to investigate the timeline of events caused by the absence of PV. More precisely, we analyzed the trajectory (temporal changes) in mitochondria volume and mitochondria distribution in selected Pvalb neurons and the level of oxidative stress in the same Pvalb neuron subpopulations, where we had had previously observed an increase in mitochondria volume in adult (3–5 months) PV−/− mice (Janickova et al., 2020). We chose three time points: 1, 3, and 6 months. The first one, since mice deficient for PV (PV+/−, PV−/−) show ASD core symptoms –reduced communication and social interaction and repetitive/stereotyped behavior– already at PND25-30, as well as changes in the morphology (dendrites) of striatal Pvalb neurons (Wöhr et al., 2015). At 3 months, some ASD-like behavior persists in PV−/− mice (Wöhr et al., 2015) and moreover, clear increases in mitochondria volume occur in 3–5 months-old PV−/− Pvalb neurons (Janickova et al., 2020). This is also the time point, when increased oxidative stress (and PV downregulation) is observed in mouse schizophrenia models (Steullet et al., 2018; Cabungcal et al., 2019). Our results indicate that the ASD-like phenotype in PV−/− mice emerges before the onset of an increase in oxidative stress hinting toward absence/reduction of PV as the main contributor to the behavioral ASD-like phenotype.

RESULTS

Age-Dependent Increase in Oxidative Stress in WT Pvalb Neurons Evidenced by 8-Oxo-dG Staining

The strong activity of Pvalb neurons (fast, high-frequency firing) is coupled to elevated metabolism, high mitochondrial activity and associated ROS production. Subsequently, Pvalb neurons contain substantially more mitochondria in their somata, dendrites and axons than any other interneuron subpopulation or pyramidal cells (reviewed in Kann et al., 2014) and are thus highly susceptible to oxidative stress (Kann, 2016). Resulting from the high mitochondria density, the outline of Pvalb cells can be often recognized on brain sections simply by a general staining for mitochondria, particularly in Pvalb neurons of PV−/− mice (Janickova et al., 2020); examples in TRN are shown in **Supplementary Figure 1**. In this study, we made use of two transgenic mouse lines, where EGFP is selectively expressed in Pvalb neurons (Orduz et al., 2013). In the control (WT) line, mice have two functional *Pvalb* alleles, while the other one is null-mutant (PV−/− or KO) for *Pvalb*. Since the transgene driving EGFP expression is not associated with the endogenous *Pvalb* gene locus, EGFP expression is not coupled to endogenous PV expression. That is, EGFP expression is indistinguishable in WT and KO mice (Janickova et al., 2020). Oxidative stress was determined by immunofluorescence detection of the DNA oxidation product 8-oxo-dG, globally at low magnification on sagittal sections and moreover, in the same Pvalb neuron subpopulations, where we had previously investigated the effect of PV on mitochondria volume and cell morphology, i.e., in the somatosensory and medial prefrontal cortex (SSC, mPFC), striatum, thalamic reticular nucleus (TRN), hippocampal regions DG, CA3 and CA1 and cerebellum [Purkinje cells and molecular layer interneurons (MLI)]. On sagittal sections of 3-months old WT mice scanned by the NanoZoomer at low magnification (**Figure 1A**), several brain regions showed rather strong 8-oxo-dG staining: higher magnification images of the hippocampal DG granule cell layer and the CA3–CA1 pyramidal cell layer, the TRN, the medial vestibular nucleus (MVN) and the cerebellum, in particular the Purkinje cell layer and MLI are shown in **Figure 1B**. In the MVN, staining was mostly confined to fibers, but was also observed in some $EGFP^+$ Pvalb neuron somata present in the parvocellular part of the MVN (**Supplementary Figure 2**) as reported before in rat (Puyal et al., 2002). Essentially all regions showing strong 8-oxo-dG staining also contained higher densities of $EGFP^+$ Pvalb neurons and/or neuropil (fibers) resulting in partial yellow staining in the merged images (**Figures 1A,B**). In Pvalb neuron populations of WT mice analyzed by confocal microscopy, 8-oxo-dG fluorescence signals (in arbitrary units) were first normalized, taking into consideration the different sizes and morphologies of Pvalb neurons as described before (Janickova et al., 2020). We observed a near-linear age-dependent increase in 8-oxo-dG signals in mice of 1, 3, and 6 months (**Figure 1C** and **Table 1**), most evident in the group of high PV-expressing neurons (TRN, MLI, and PC). Linear regression analyses (R^2) revealed high linearity values ≥ 0.97 for medium-to-high PV-expressing Pvalb neurons including TRN, MLI, PC, SSC, and striatum (**Figure 1C** and **Table 1**). Of note, 8-oxo-dG signals in TRN Pvalb neurons at 1 month were already considerably higher than in all other Pvalb neuron subpopulations [ANOVA: $F(8,36) = 64.63$; $p < 0.0001$; Tukey's multiple comparison test: $p < 0.0001$ for all other Pvalb subpopulations], yet the time-dependent increase (slope) was not much higher than for medium PV-expressing Pvalb neurons (striatum, SSC) and clearly smaller than for MLI and PC that showed the strongest time-dependent increase. An exception was the subpopulation of mPFC Pvalb neurons ($R^2 = 0.82$), where 8-oxo-dG signals at 6 months were only marginally higher than at 3 months. In low PV-expressing hippocampal (DG, CA3, CA1) neurons, 8-oxo-dG signal intensities in young (1 month) mice were the lowest of all tested Pvalb neuron subpopulations, and the relative age-dependent increase was marginal. Thus, both parameters (WT fluorescence intensity at 3 months, slope) generally correlated positively with the PV concentration previously estimated in the various Pvalb neuron populations [see Figure 1E in Janickova et al. (2020) and **Supplementary Figure 4B**]. Of note, these changes were not correlated with the relative densities of the mitochondria in the soma cytoplasm of different Pvalb neuron populations, which are rather constant in all Pvalb neurons: 7.8 ± 1.5 vol./vol.% (Janickova et al., 2020).

Increased Oxidative Stress in PV−/− Pvalb Neurons Evident in Mice ≥ 3 Months

A comparison of 8-oxo-dG signals between 1-month old WT and PV−/− mice (5 mice/genotype) revealed no significant

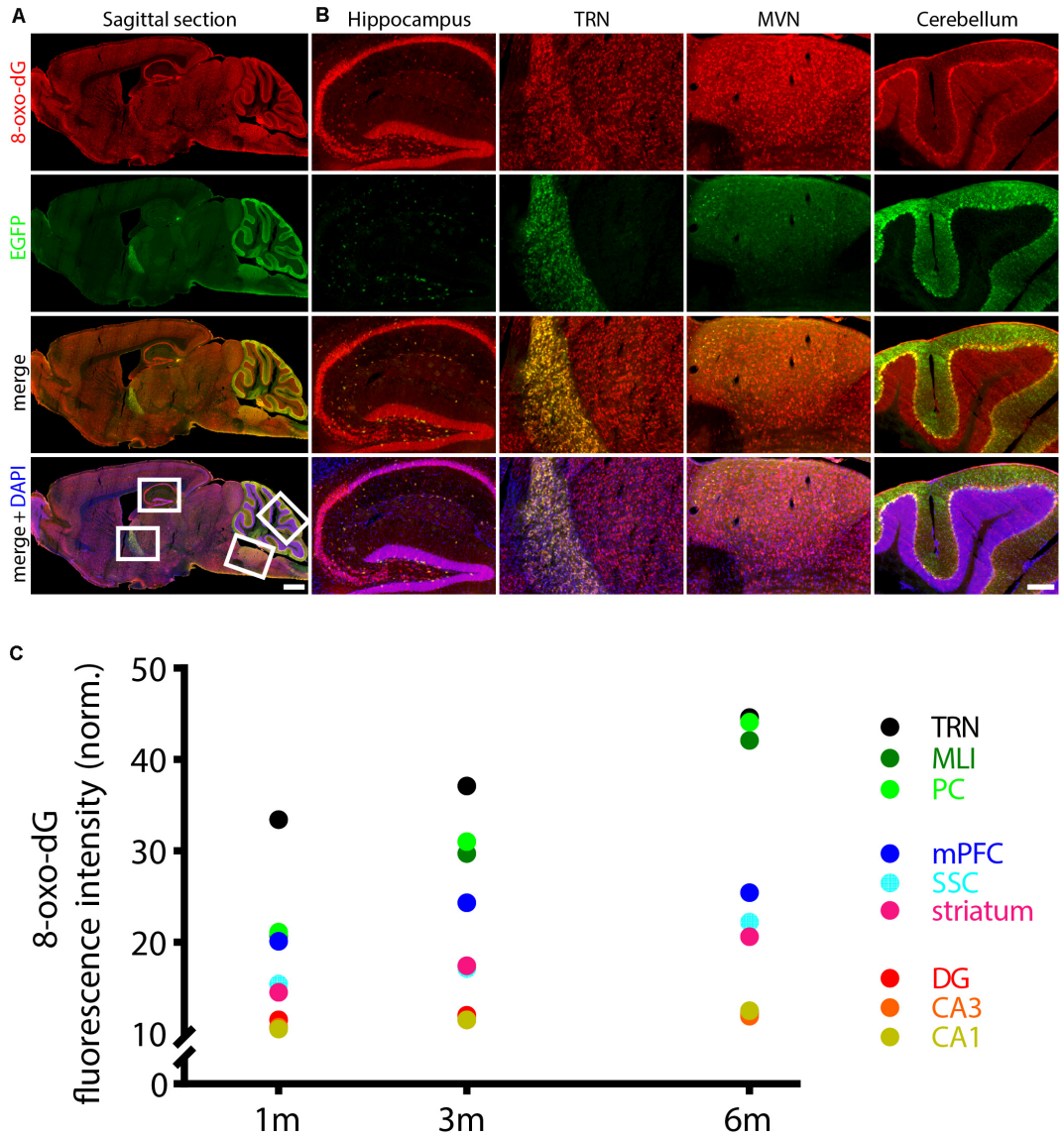

FIGURE 1 | Age-dependent increase in oxidative stress in WT Pvalb neurons evidenced by 8-oxo-dG staining. **(A)** Sagittal brain section from a 3-month old WT mouse stained for 8-oxo-dG (oxidative stress marker, red), EGFP (Pvalb neurons expressing EGFP, green) and DAPI (nuclei, blue). Regions with strong 8-oxo-dG staining (white boxes in low-left image in **A**) –hippocampus, TRN, MVN and cerebellum– are shown at higher magnification in **(B)**. Note the higher densities of $EGFP^+$ Pvalb neurons and/or neuropil (fibers) in these regions resulting in partial yellow staining in the merged images. Scale bar in **(A)** 1 mm, in **(B)** 200 μm. Sagittal brain sections scanned by the NanoZoomer serve for demonstration purposes and were not analyzed in the study. **(C)** Quantitative analyses were performed on confocal microscopy images. Brain sections were scanned in nine regions – 3 hippocampal regions (CA1, CA3, and DG), striatum, SSC, mPFC, 2 cerebellar regions [Purkinje cell layer (PC) and in molecular layer interneurons (MLI)] and TRN. Fluorescence signal quantifications were carried out in 1, 3, and 6-months old mice [normalized values (mean ± SD) are reported in **Table 1**]; for clarity, error bars and regression lines are omitted; R^2 values are from linear regression analyses using the three time points: 1, 3, and 6 months and are listed in **Table 1**.

differences in all nine investigated Pvalb neuron subpopulations as shown for hippocampus (**Figure 2**; DG, CA3, CA1), striatum, SSC and mPFC (**Figure 3**), cerebellum (PC, MLI) and TRN (**Figure 4**). In all cases signals were marginally (average: 5.2 ± 2.1% for all 9 Pvalb neuron populations), but not significantly increased in PV−/− Pvalb neurons. Measurement of acute oxidative stress accumulating during 18.5 h by the DHE method confirmed the results obtained by 8-oxo-dG staining. At 1 month, DHE signals were indistinguishable between WT and PV−/− Pvalb neurons in all investigated Pvalb neuron subpopulations (**Supplementary Figure 3** and **Table 1**).

In 3-month old mice 8-oxo-dG signals were significantly higher in PV−/− mice in all Pvalb neurons with the exception of hippocampal (DG, CA3, CA1) Pvalb neurons, the latter shown in **Figure 2**. Quantitative immunofluorescence results and representative images for the 9 Pvalb neuron subpopulations

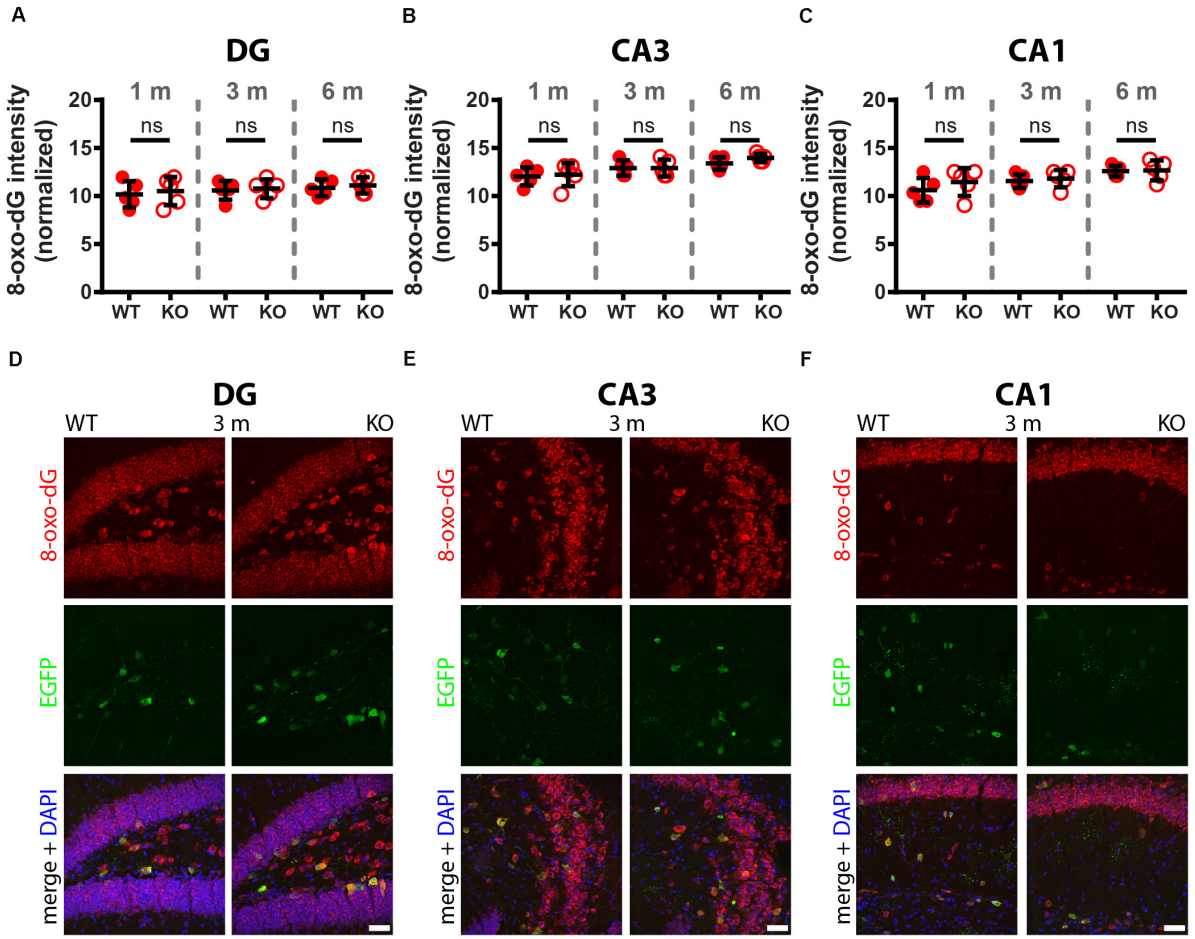

FIGURE 2 | Comparison of 8-oxo-dG signal intensity between WT and KO mice in hippocampal regions of 1, 3, and 6-months old mice. The 8-oxo-dG fluorescence signal intensities (a.u.) analyzed in DG **(A)**, CA3 **(B)**, and CA1 **(C)** were normalized, taking into consideration the different sizes and morphologies of Pvalb neurons. Representative images with immunofluorescence labeling for 8-oxo-dG (red), EGFP (green) and merged images with DAPI (blue) are shown for DG **(D)**, CA3 **(E)** and CA1 **(F)** regions of 3-months old WT (left panels) and KO (right panels) mice. Scale bars: 50 μm. Each dot in the graphs represents the average obtained in 1 animal (5 mice per genotype) and at least 15 cells per animal resulting in > 75 cells per brain region (DG, CA3, CA1) and genotype. No significant differences were observed between WT and KO mice, ns – not significant. Values are reported in **Table 1**.

in the analyzed brain regions are shown in **Figures 2–4** and summarized in **Table 1**. Of note, the magnitude of the increase in 3-month old PV−/− mice was also in a graded manner and ranged from + 20% in striatal to + 36% in TRN Pvalb neurons (**Table 1** and **Supplementary Figure 4C**). The magnitude in increase of oxidative stress strongly correlated with the PV concentration pertaining in the corresponding WT Pvalb neuron populations (compare to Supplementary Figure 3 in Janickova et al., 2020), and moreover with the increase in mitochondria volume in adult (3–5 months-old) PV-/- mice shown previously (Supplementary Figure 3 in Janickova et al., 2020). Thus, the higher the increase in mitochondria volume, the higher the oxidative stress in these PV-deficient Pvalb neurons. In addition to measuring (cumulative) oxidative stress by 8-oxo-dG staining, we used the DHE method to determine acute oxidative stress accumulated during a shorter time period (18.5 h). At 3 months, DHE signals were significantly increased in PV−/− Pvalb neurons in essentially all regions, except SSC (p = 0.0503) and hippocampus. In the latter low PV-expressing neurons, no differences existed between WT and PV−/− in all three subfields (DG, CA3, CA1; for all; $p > 0.97$), thus nearly perfectly replicating the results obtained by staining for 8-oxo-dG (**Supplementary Figure 3** and **Table 1**).

In 6-months old mice, differences in 8-oxo-dG staining intensities persisted between WT and PV−/− Pvalb neurons, however effect sizes were generally smaller. Significant differences between genotypes were observed only in the groups of high PV-expressing Pvalb neurons including mPFC, MLI and TRN (**Figures 3**, **4** and **Table 1**). The smaller differences between genotypes in the other Pvalb neuron subpopulations (striatum, SSC, PC) were mostly resulting from a relatively larger (near-linear) increase in oxidative stress from 3- to 6-month old mice in the WT group, while the increase from 3 to 6 month in PV−/− Pvalb neurons leveled off. Thus, absence of PV leads

TABLE 1 | Quantitative results and statistical analyses of 8-oxo-dG and DHE staining intensities are shown as mean ± standard deviations in all investigated brain regions.

8-oxo-dG	1 month		3 months		6 months						
	WT	KO	WT	KO	WT	KO					WT
	Mean ± SD	Mean ± SD	Mean ± SD	Mean ± SD	Mean ± SD	Mean ± SD	Effect of age →	*p*-value	Effect of genotype →	*p*-value	R^2−value
DG	10.17 ± 1.36	10.51 ± 1.46	10.60 ± 0.97	10.77 ± 0.97	10.85 ± 0.88	11.11 ± 0.85	$F(2,24) = 0.8305$	0.4480	$F(1,24) = 0.3980$	0.5341	0.9306
CA3	12.04 ± 0.93	12.23 ± 1.21	12.91 ± 0.81	12.91 ± 0.88	13.40 ± 0.65	13.98 ± 0.41	$F(2,24) = 8.3030$	0.0018	$F(1,24) = 0.6919$	0.4137	0.9263
CA1	10.60 ± 1.27	11.47 ± 1.44	11.55 ± 0.71	11.81 ± 0.89	12.59 ± 0.56	12.67 ± 1.03	$F(2,24) = 6.0060$	0.0077	$F(1,24) = 1.1330$	0.2977	0.9921
Striatum	14.46 ± 0.97	15.36 ± 1.71	17.41 ± 1.81	20.89 ± 1.71	20.54 ± 1.75	21.88 ± 1.33	$F(2,24) = 41.2000$	<0.0001	$F(1,24) = 10.8800$	0.0030	0.9905
SSC	15.35 ± 2.32	16.41 ± 1.27	17.06 ± 1.53	20.82 ± 2.25	22.20 ± 1.18	23.67 ± 2.08	$F(2,24) = 34.0800$	<0.0001	$F(1,24) = 8.94900$	0.0063	0.9725
mPFC	20.09 ± 1.45	20.87 ± 1.87	24.24 ± 3.09	30.82 ± 3.60	25.37 ± 3.10	32.99 ± 3.54	$F(2,24) = 25.4600$	<0.0001	$F(1,24) = 22.2800$	<0.0001	0.8232
PC	21.05 ± 2.47	22.62 ± 1.61	30.99 ± 4.88	41.22 ± 2.82	44.01 ± 4.53	49.48 ± 2.24	$F(2,24) = 141.600$	<0.0001	$F(1,24) = 22.5200$	<0.0001	0.9986
MLI	20.68 ± 2.97	21.70 ± 1.95	29.66 ± 3.22	39.66 ± 2.35	42.03 ± 2.84	47.46 ± 2.68	$F(2,24) = 191.000$	<0.0001	$F(1,24) = 30.8000$	<0.0001	0.9994
TRN	33.33 ± 3.07	34.79 ± 1.74	37.08 ± 3.09	50.42 ± 3.17	44.58 ± 4.25	53.96 ± 2.37	$F(2,24) = 63.8900$	<0.0001	$F(1,24) = 52.4600$	<0.0001	0.9944

	1 month WT vs. KO *p*-value	3 months WT vs. KO *p*-value	6 months WT vs. KO *p*-value	PV conc. in WT neurons	Mito. volume increase 3 m
DG	0.9962	0.9999	0.9990	20 μM	11.3
CA3	0.9991	>0.9999	0.8843	20 μM	10.6
CA1	0.7731	0.9986	>0.9999	20 μM	13.4
Striatum	0.9446	0.0210*	0.7610	70 μM	109.2
SSC	0.9489	0.0496*	0.8271	90 μM	117.4
mPFC	0.9980	0.0163*	0.0042**	120 μM	130.8
PC	0.9736	0.0007***	0.1356	100 μM	58.2
MLI	0.9904	<0.0001****	0.0421*	570 μM	103.9
TRN	0.9721	<0.0001****	<0.0007***	750 μM	161.1

(Continued)

TABLE 1 | Continued

DHE	1 month		3 months		6 months						
	WT	KO	WT	KO	WT	KO					WT
	Mean ± SD	Mean ± SD	Mean ± SD	Mean ± SD	Mean ± SD	Mean ± SD	Effect of age →	*p*-value	Effect of genotype →	*p*-value	R^2 value
DG	5.73 ± 2.50	6.154 ± 1.82	6.068 ± 2.14	6.75 ± 1.33	6.67 ± 1.87	7.01 ± 1.92	$F(2,24) = 0.5208$	0.6006	$F(1,24) = 0.4548$	0.5065	0.9983
CA3	6.80 ± 1.64	7.670 ± 1.43	8.155 ± 1.15	7.67 ± 2.33	8.93 ± 1.48	8.93 ± 2.44	$F(2,24) = 2.2250$	0.1299	$F(1,24) = 0.0382$	0.8466	0.9283
CA1	5.86 ± 2.08	6.466 ± 1.52	6.552 ± 1.86	6.64 ± 2.18	7.33 ± 1.69	7.41 ± 2.00	$F(2,24) = 1.0280$	0.3729	$F(1,24) = 0.1379$	0.7137	0.9934
Striatum	8.43 ± 1.22	9.29 ± 0.96	9.375 ± 1.51	12.23 ± 0.81	10.18 ± 0.71	12.23 ± 1.50	$F(2,24) = 10.5300$	0.0005	$F(1,24) = 18.6200$	0.0002	0.9745
SSC	9.31 ± 1.45	9.71 ± 1.16	10.29 ± 1.05	12.57 ± 1.05	12.73 ± 1.01	14.04 ± 1.21	$F(2,24) = 27.4600$	<0.0001	$F(1,24) = 9.7400$	0.0046	0.9843
mPFC	11.08 ± 0.89	11.69 ± 1.01	13.33 ± 0.77	15.06 ± 0.83	14.89 ± 0.51	15.93 ± 0.83	$F(2,24) = 61.5200$	<0.0001	$F(1,24) = 13.7000$	0.0011	0.9527
PC	12.62 ± 1.11	12.67 ± 0.88	14.71 ± 0.97	18.14 ± 1.06	16.22 ± 1.03	17.91 ± 1.22	$F(2,24) = 51.1200$	<0.0001	$F(1,24) = 20.0000$	0.0002	0.9575
MLI	18.81 ± 2.89	20.00 ± 1.75	19.49 ± 3.97	27.80 ± 2.57	22.54 ± 1.75	29.83 ± 3.51	$F(2,24) = 14.2600$	<0.0001	$F(1,24) = 28.5300$	<0.0001	0.9450
TRN	17.08 ± 2.50	20.21 ± 2.28	22.08 ± 4.25	32.08 ± 3.63	24.17 ± 3.85	34.38 ± 4.71	$F(2,24) = 23.6200$	<0.0001	$F(1,24) = 34.0400$	<0.0001	0.8839

	1 month WT vs. KO *p*-value	3 months WT vs. KO *p*-value	6 months WT vs. KO *p*-value	PV conc. in WT neurons	Mito. volume increase 3 m
DG	0.9993	0.9993	0.9998	20 μM	11.3
CA3	0.9713	0.9980	>0.9999	20 μM	10.6
CA1	0.9957	>0.9999	>0.9999	20 μM	13.4
Striatum	0.8955	0.0116*	0.1152	70 μM	109.2
SSC	0.9932	0.0503	0.5052	90 μM	117.4
mPFC	0.8550	0.0325*	0.3858	120 μM	130.8
PC	>0.9999	0.0004***	0.1566	100 μM	58.2
MLI	0.9853	0.0015**	0.0059**	570 μM	103.9
TRN	0.7530	0.0028**	0.0022**	750 μM	161.1

*Two-way ANOVA was performed for each brain region (upper parts) followed by Tukey's multiple comparison (lower parts) for 8-oxo-dG and DHE signals. In addition, values of estimated PV concentrations in 3–5 months-old WT mice and mitochondria volume increase between 3-months old WT and KO mice are shown. The mean 8-oxo-dG and ox-DHE signal intensities were compared among groups using multivariate ANOVA followed by Tukey test for multiple comparisons. P-values > 0.05: not significant; *p < 0.05; **p < 0.01; ***p < 0.001; ****p < 0.0001. From WT 8-oxo-dG and ox-DHE data (1, 3, and 6 months), linear regression analysis was performed and R^2 values are listed.*

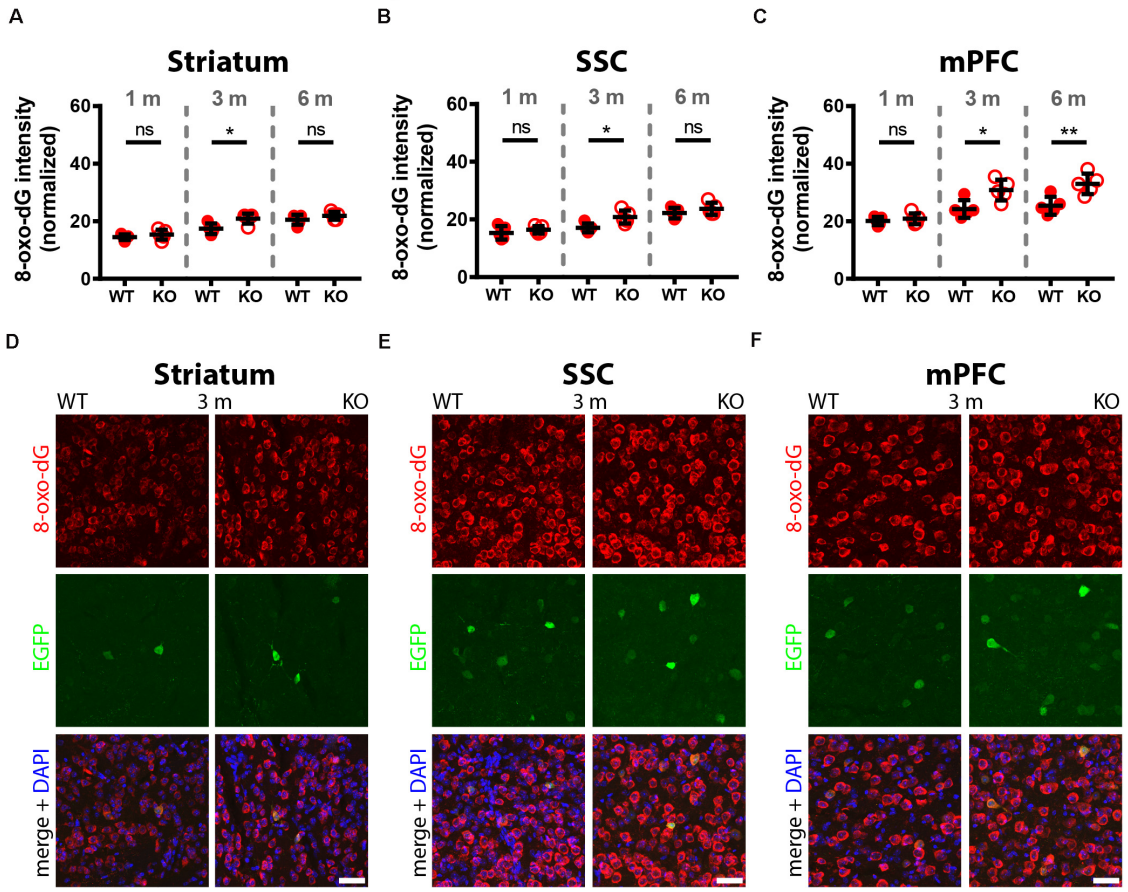

FIGURE 3 | Comparison of 8-oxo-dG signal intensity in striatum, SSC and mPFC of 1, 3, and 6-months old WT and KO mice. Normalized 8-oxo-dG fluorescence signal intensities (a.u.) analyzed in striatum **(A)**, SSC **(B)** and mPFC **(C)** are shown. Representative images with immunofluorescence labeling for 8-oxo-dG (red), EGFP (green) and merged images with DAPI (blue) are shown in striatum **(D)**, SSC **(E),** and mPFC **(F)** of 3-months old WT (left panels) and KO (right panels) mice. Scale bars: 40 μm. Each dot in the graphs represents the average obtained in 1 animal (5 mice per genotype) and 10–15 cells per animal resulting in > 50 cells per brain region (striatum, SSC, mPFC) and genotype. ns not significant; $^{*}p < 0.05$; $^{**}p < 0.01$. Values are reported in **Table 1**.

to a different trajectory of ROS production, i.e., accelerated at 3 months and then approaching the WT condition at 6 months. The same tendency was also observed in mice subjected to DHE treatment. Using this approach, the further increase in DHE signal intensity in PV-deficient mice was significant in two Pvalb subpopulations (MLI and TRN), which are characterized by the highest PV expression levels, namely MLI (stellate and basket cells; [PV]: ∼570 μM (Eggermann and Jonas, 2012)) and TRN Pvalb neurons ([PV]: 600–900 μM, see Supplementary Figure 3 in Janickova et al. (2020).

Trajectory of Increase in Mitochondria Density and Changes in Mitochondria Localization in TRN and Striatal Pvalb Neurons From 1 to 6 Months in WT and PV−/− Mice

While a significant increase in mitochondria density is present in adult (3–5-month old) PV−/− mice that strongly correlates with the PV concentration of various Pvalb neuron subpopulations (Janickova et al., 2020), nothing was previously known to when and to what extent the mitochondria increase occurred in younger mice. Moreover, whether changes took place also between 3 and 6 months was unknown. To close this knowledge gap, mitochondria volumes were determined in selected Pvalb neuron subpopulations at the age of 1, 3, and 6 months. For this analysis, we chose striatal and TRN Pvalb neurons in WT and PV−/− mice. The former, since we intended to correlate presumed mitochondria increases with increased branching observed already at PND18-24 (Wöhr et al., 2015) and persisting to adulthood (Janickova et al., 2020) and the latter, because the increase in mitochondria density and oxidative stress was largest in PV−/− TRN Pvalb neurons (**Figure 4**). In addition to determining soma mitochondria volume, we were interested in the distribution of mitochondria in the soma, since we had previously reported that in Purkinje cells of adult (3–5 months) PV−/− mice, the ∼40% increase in mitochondria volume was essentially restricted to a subplasmalemmal region of 1.5 μm (Chen et al., 2006). A comparison of the soma mitochondria density in TRN neurons revealed a significant increase in the

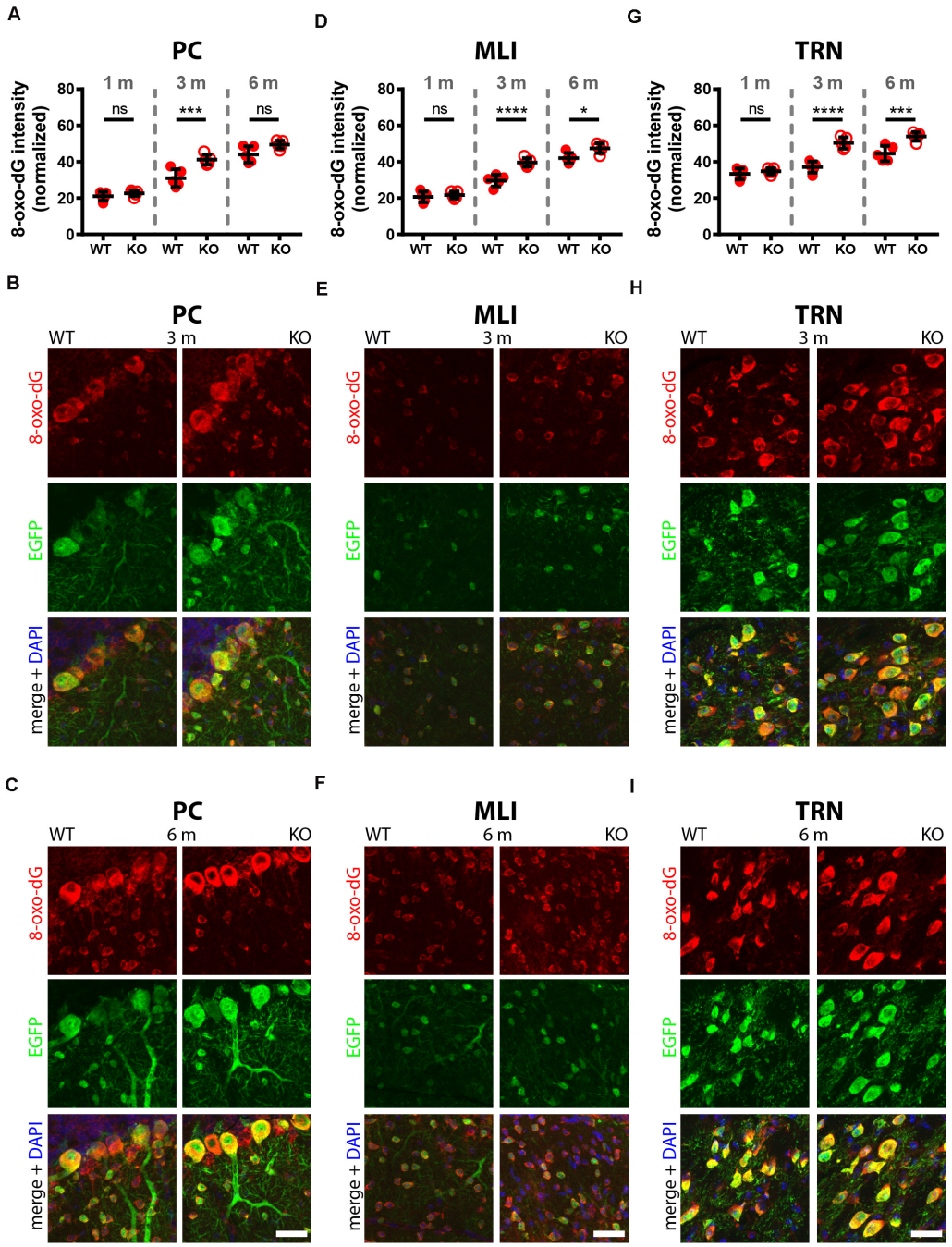

FIGURE 4 | Comparison of 8-oxo-dG signal intensity in cerebellum (PC, MLI) and TRN of 1, 3, and 6-months old WT and KO mice. Normalized 8-oxo-dG fluorescence signal intensities (a.u.) analyzed in PC **(A)**, MLI **(D)**, and TRN Pvalb neurons **(G).** Representative images with immunofluorescence labeling for 8-oxo-dG (red), EGFP (green) and merged + DAPI (blue) in PC from 3 **(B)** and 6-months old **(C)** mice are shown. In **(E,F)** the same is shown for MLI; and in **(H,I)** for TRN Pvalb neurons in WT (left panels) and KO (right panels) mice. Scale bars: 30 μm. Each dot in the graphs represents the average obtained in 1 animal (5 mice per genotype) and at least 20 cells per animal resulting in > 100 cells per brain region (PC, MLI, TRN) and genotype. ns not significant; *$p < 0.05$; **$p < 0.01$; ***$p < 0.001$; ****$p < 0.0001$. Values are reported in **Table 1**.

order of 119% already at 1 month caused by the absence of PV. A similar increase persisted at 3 (+102%) and 6 (+109%) months and was essentially identical to the differences already prevailing at 1 month (**Figure 5B**). As observed previously (Janickova et al., 2020), absence of PV not only resulted in an increase in mitochondria volume, but also in the volume of the cytoplasm (**Figure 5A**) and subsequently of the entire soma (**Figure 5D**). Of note, the small increase in the volume of the nucleus was

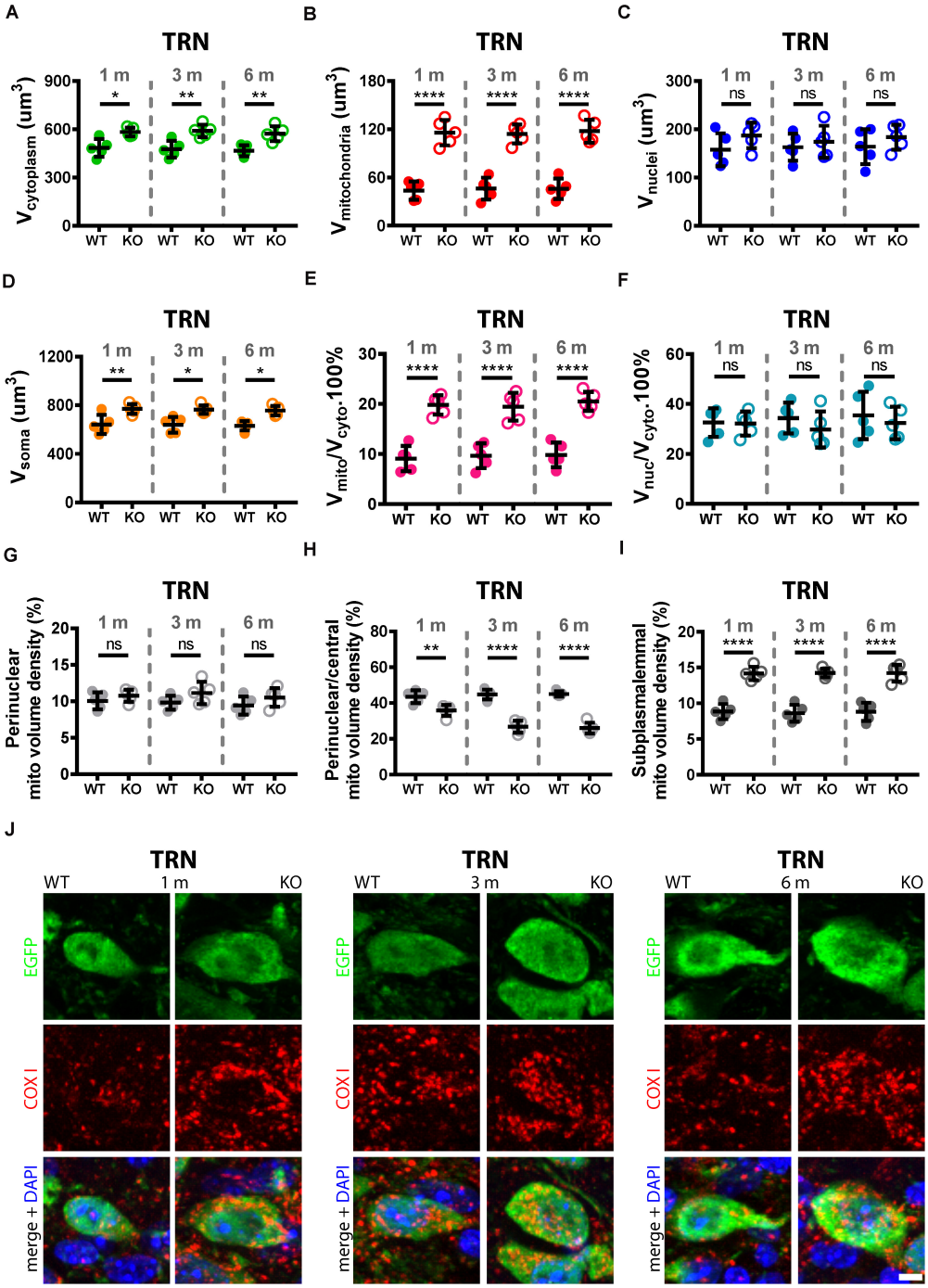

FIGURE 5 | Quantitative morphological analyses of TRN Pvalb neurons. A comparison was carried out in 1, 3, and 6-months old WT and KO mice. Analyzed parameters included volume of cytoplasm **(A)**, volume of mitochondria **(B),** volume of nuclei **(C),** and volume of soma **(D)** in a given Pvalb neuron. Additional parameters were calculated, such as ratio $V_{mitochondria}/V_{cytoplasm}$ **(E)** and $V_{nucleus}/V_{cytoplasm}$ **(F)**. Quantitative analyses of the relative distribution of mitochondria within the cytoplasmic compartment in TRN Pvalb neurons **(G–I)**. Somata and nuclei of selected Pvalb neurons were identified based on EGFP and DAPI staining, respectively and the distribution of mitochondria from the center of the cell (border of nuclei) to the plasma membrane was partitioned into a set of 4 specified zones: 1 being the innermost (perinuclear) and 4 the outermost (subplasmalemmal). Quantitative analyses are shown for zone 1 (perinuclear; **G**), zone 2 (perinuclear/central **H**) and zone 4 (subplasmalemmal; **I**) mitochondrial volume density. Note the mitochondria shift from the perinuclear region to the periphery of the cells in KO mice. Representative confocal images **(J)** show EGFP-stained Pvalb neurons (green; cytoplasm), COX I (red; mitochondria) and DAPI (blue; nuclei) in 1, 3, and 6-months old WT (left panels) and KO (right panels) mice. Scale bar: 5 μm. Each dot in the graphs represents the average obtained in 1 animal (5 mice per genotype) and 20–30 cells per animal resulting in > 100 cells per TRN and genotype. ns: not significant; *$p < 0.05$; **$p < 0.01$; ***$p < 0.001$; ****$p < 0.0001$. Values are reported in **Table 2**.

insignificant (**Figure 5C**). However even when considering the increase in the cytoplasm volume, the mitochondria density ($V_{mitochondria}/V_{cytoplasm}$) was still significantly higher (**Figure 5E**). The ratio $V_{nucleus}/V_{cytoplasm}$ (**Figure 5F**) was also not different indicating that the increase in the volume of the nucleus is approximately paralleled by the increase of the entire soma (**Figure 5D**). Qualitative similar results were observed in striatal Pvalb neurons (**Figure 6**), although effects were somewhat smaller, most probably related to the lower concentration of PV in striatal than in TRN Pvalb neurons (∼70 vs. ∼750 μM, respectively; Janickova et al., 2020). Nonetheless, the increase in mitochondrial density was substantial, in the order of + 60–65% and as in TRN Pvalb neurons already present in 1-month old mice deficient for PV. Thus, constitutive absence of PV during the entire neurodevelopment led to an increase in mitochondria density, which was already maximal at 1 month. Of note, the considerable increase in mitochondria volume (density) present at 1 month had no measurable effect on ROS production in the analyzed Pvalb neuron subpopulations in striatum and TRN. These findings are discussed below in detail with a focus on mechanisms implicated in the development of an ASD-like behavioral phenotype in PV−/− mice.

Importantly, the relative distribution of mitochondria within the cytoplasmic compartment was altered in the absence of PV in TRN (**Figures 5G–I**) and striatal (**Figures 6G–I**) Pvalb neurons. Clearly more mitochondria (+60%) accumulated in the subplasmalemmal region already at 1 month accompanied by relative mitochondria depletion mostly in the central cytoplasmic region that also persisted in mice of 3 and 6 months (values and statistics are listed in **Table 2**). Thus, PV-deficiency led to an overall increase in mitochondria and to an accumulation of subplasmalemmal mitochondria, both effects already maximal at 1 month indicating that absence of PV is rapidly sensed by Pvalb neurons and translated into an increase/redistribution of mitochondria.

MATERIALS AND METHODS

Animals

Two transgenic lines were used in this study: B6.Tg(Pvalb-EGFP)^{1Hmon} mice (WT) expressing normal levels of PV and the enhanced green fluorescent protein (EGFP) selectively in Pvalb neurons (Meyer et al., 2002); the second line B6.Pvalb^{tm11Swal} x B6Tg(Pvalb-EGFP)^{1Hmon} (KO) is additionally devoid of functional *Pvalb* alleles (Orduz et al., 2013). Both lines have been used in previous studies aimed at elucidating the role of PV in Pvalb neurons (Orduz et al., 2013; Janickova et al., 2020). All together 30 female mice were used in this study, sacrificed when they reached 1, 3, and 6 months of age; five mice per age group and genotype. Mice were group-housed in the rodent facility at the University of Fribourg, Switzerland in temperature-controlled rooms (24°C), with 12:12 h light/dark cycle interval. All animals had free access to water and were fed *ad libitum*. Experiments were performed according to institutional guidelines of the present Swiss law and the European Communities Council Directive of 24 November 1986 (86/609/EEC). The authorization number for housing of mice is H-04.2012-Fr and for the experiments 2016_37_FR. All experiments were approved by the Cantonal Veterinary Office (Canton of Fribourg, Switzerland).

In vivo Injections of the Fluorescent Dye Dihydroethidium

To analyze superoxide production in specific brain regions, we used the fluorescent probe dihydroethidium (DHE) (Thermo Fisher Scientific, Switzerland, Cat # D11347). The characterization and validation of DHE for whole animal fluorescence imaging has been successfully carried out before (Hall et al., 2012). When administered systemically, DHE distributes rapidly into the various tissues including the brain (Murakami et al., 1998; Quick and Dugan, 2001). There the uncharged lipophilic compound DHE is converted by superoxide radicals to the positively charged product ox-DHE (Barbacanne et al., 2000; Fink et al., 2004) and, if not oxidized, is cleared from tissues and excreted in the urine (Hall et al., 2012). Importantly, ox-DHE is retained in the brain for a sustained period of time due to its charge (Quick and Dugan, 2001). This then allows for the quantification of the amount of superoxide produced over a defined period of time in a given tissue by measurement of ox-DHE (Hall et al., 2012). Mice at the ages of 1, 3, and 6 months received two serial intraperitoneal injections of freshly prepared DHE solution (27 mg/kg) at 30 min intervals (the first bolus was generally injected at ∼16:00 and the second injection at 16:30). Eighteen hours after the second DHE injection (∼10:30), animals were anesthetized with a lethal dose of Esconarkon® (300 mg/kg body weight; Streuli Pharma AG, Uznach, Switzerland) and perfused as described below.

Tissue Preparation and Immunohistochemistry

Mice were anesthetized with 300 mg/kg body weight Esconarkon® (Streuli Pharma AG, Uznach, Switzerland) and perfused using 0.9% NaCl, followed by perfusion with 4% PFA in 0.9% NaCl. Brains were removed, post-fixed for 24 h in 4% PFA in TBS and cryopreserved in 30% sucrose-TBS (0.1M, pH 7.3) at 4°C, as described before (Lauber et al., 2016). From the entire brains of each mouse coronal sections (40 μm) were cut in the rostro-caudal direction using a freezing microtome (Leica SM2010R, Switzerland) as described before (Filice et al., 2016). For the 9 regions of interest embracing the somatosensory cortex (SSC) and mPFC, striatum, TRN, hippocampal regions DG, CA3, CA1 and cerebellar Purkinje cell layer (Purkinje cells) and molecular layer (interneurons; MLI), three sections per mouse and brain region of interest were selected according to the Allen brain atlas and Paxinos Franklin atlas, following the rules of stereological systematic random sampling principles (for details, see, Filice et al., 2016). Selected brain slices were used immediately for immunohistochemistry, unused brain sections were stored in antifreeze solution at −20°C. Free-floating brain sections containing all the regions of interest were first blocked for 1 h at RT in TBS (0.1M, pH 7.3) containing

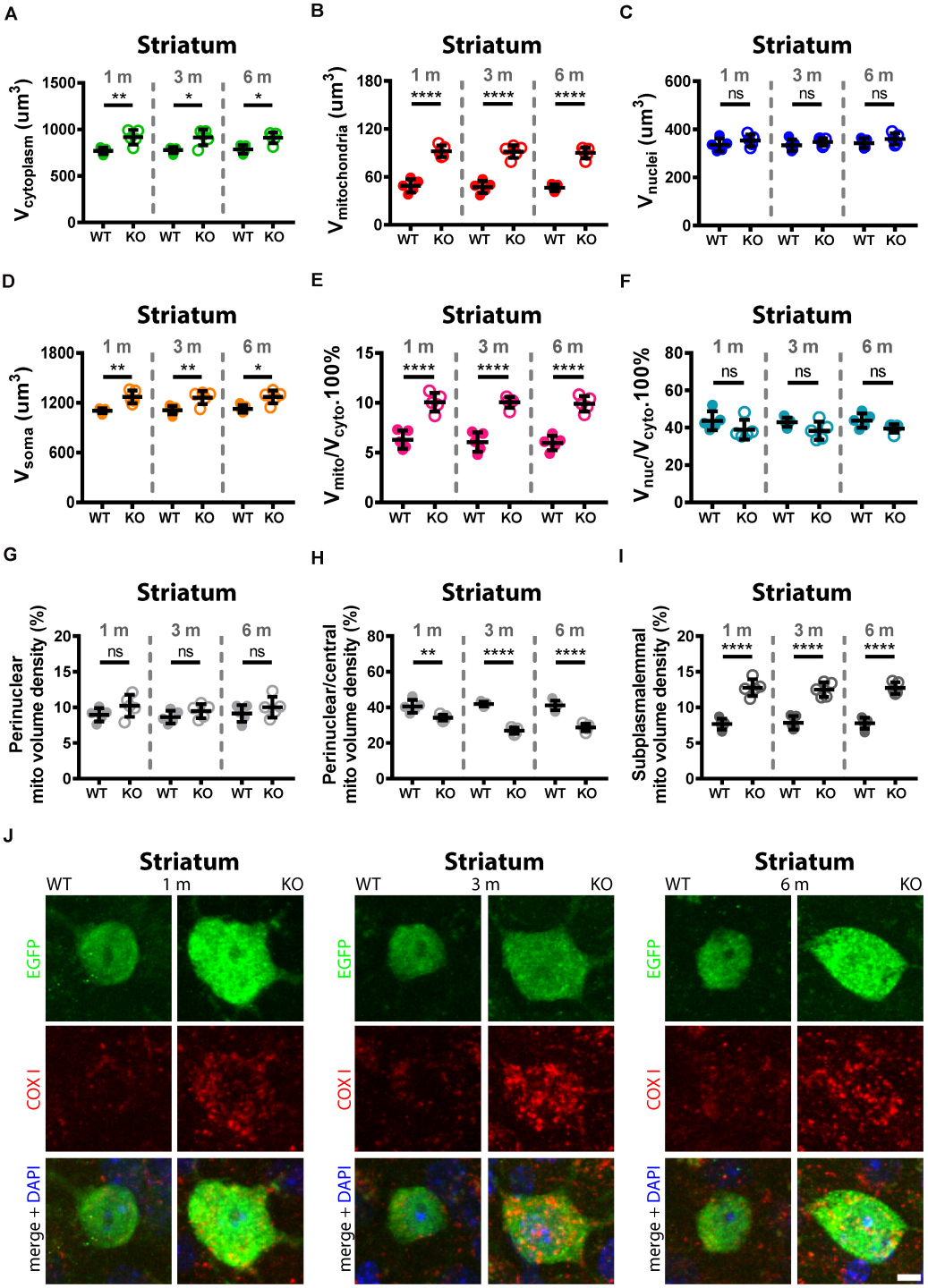

FIGURE 6 | Quantitative morphological analyses of TRN Pvalb neurons. A comparison was carried out in 1, 3, and 6-months old WT and KO mice. Analyzed parameters included volume of cytoplasm **(A)**, volume of mitochondria **(B),** volume of nuclei **(C),** and volume of soma **(D)** in a given Pvalb neuron. Additional parameters were calculated, such as ratio $V_{mitochondria}/V_{cytoplasm}$ **(E)** and $V_{nucleus}/V_{cytoplasm}$ **(F)**. Quantitative analyses of the relative distribution of mitochondria within the cytoplasmic compartment in striatal Pvalb neurons **(G–I)**. Somata and nuclei of selected Pvalb neurons were identified based on EGFP and DAPI staining, respectively and the distribution of mitochondria from the center of the cell (border of nuclei) to the plasma membrane was partitioned into a set of 4 specified zones: 1 being the innermost (perinuclear) and 4 the outermost (subplasmalemmal). Quantitative analyses are shown for zone 1 (perinuclear; **G**), zone 2 (perinuclear/central **H**) and zone 4 (subplasmalemmal; **I**) mitochondrial volume density. Note the mitochondria shift from the perinuclear region to the periphery of the cells in KO mice. Representative confocal images **(J)** of EGFP-stained Pvalb neurons (green; cytoplasm), COX I (red; mitochondria) and DAPI (blue; nuclei) at all observed time points (1, 3, and 6 months) are shown for WT and KO mice. Scale bar: 5 μm. Each dot in the graphs represents the average obtained in 1 animal (5 mice per genotype) and 10–15 cells per animal resulting in > 50 cells per striatal region and genotype. ns: not significant; *$p < 0.05$; **$p < 0.01$; ***$p < 0.001$; ****$p < 0.0001$. Values are reported in **Table 2**.

TABLE 2 | Quantitative results and statistical analyses of volumetric analysis and mitochondria position in four zones are shown as Mean ± SD in striatum and TRN.

TRN

Volumetric analysis

	1 month		3 months		6 months						
	WT	KO	WT	KO	WT	KO					
	Mean ± SD	Mean ± SD	Mean ± SD	Mean ± SD	Mean ± SD	Mean ± SD	Effect of age	→	*p*-value	Effect of genotype	→	*p*-value
V_{cyto}	484.2 ± 55.3	582.8 ± 27.7	476.6 ± 52.4	590.2 ± 39.0	467.0 ± 34.4	572.4 ± 46.6	$F(2,24) = 0.33040$		0.7218	$F(1,24) = 44.07$		<0.0001
V_{mito}	43.6 ± 11.3	115.8 ± 15.8	46.2 ± 13.5	114.2 ± 11.7	46.0 ± 12.8	117.6 ± 14.3	$F(2,24) = 0.06775$		0.9347	$F(1,24) = 210.50$		<0.0001
V_{nuclei}	157.6 ± 34.0	187.2 ± 26.4	162.8 ± 28.2	174.2 ± 33.3	163.8 ± 36.2	183.6 ± 25.9	$F(2,24) = 0.07659$		0.0926	$F(1,24) = 3.22$		0.0853
V_{soma}	641.8 ± 79.6	770.0 ± 39.4	639.4 ± 65.0	764.4 ± 34.6	630.8 ± 38.7	756.0 ± 39.0	$F(2,24) = 0.14990$		0.8616	$F(1,24) = 43.89$		<0.0001
V_{mito}/V_{cyto}	9.1 ± 2.5	19.8 ± 1.9	9.7 ± 2.5	19.4 ± 2.8	9.8 ± 2.5	20.5 ± 1.9	$F(2,24) = 0.26990$		0.7658	$F(1,24) = 144.10$		<0.0001
V_{nuc}/V_{cyto}	32.6 ± 5.7	32.2 ± 4.8	34.4 ± 6.2	29.79 ± 7.2	35.4 ± 9.5	32.4 ± 6.5	$F(2,24) = 0.21200$		0.8105	$F(1,24) = 1.13$		0.2972

	1 month WT vs. KO *p*-value	3 months WT vs. KO *p*-value	6 months WT vs. KO *p*-value
V_{cyto}	0.0171*	0.0047**	0.0096**
V_{mito}	<0.0001****	<0.0001****	<0.0001****
V_{nuclei}	0.6593 ns	0.9913 ns	0.9092 ns
V_{soma}	0.0081**	0.0102*	0.0101*
V_{mito}/V_{cyto}	<0.0001****	<0.0001****	<0.0001****
V_{nuc}/V_{cyto}	>0.9999 ns	0.8934 ns	0.9803 ns

Mito volume density

	1 month		3 months		6 months						
	WT	KO	WT	KO	WT	KO					
	Mean ± SD	Mean ± SD	Mean ± SD	Mean ± SD	Mean ± SD	Mean ± SD	Effect of age	→	*p*-value	Effect of genotype	→	*p*-value
Zone *I*	10.1 ± 1.2	10.8 ± 0.8	9.8 ± 1.0	11.1 ± 1.5	9.4 ± 1.2	10.5 ± 1.3	$F(2,24) = 0.54270$		0.5881	$F(1,24) = 5.76$		0.0245
Zone *II*	43.5 ± 3.5	35.9 ± 3.1	44.8 ± 2.8	26.8 ± 3.3	45.1 ± 1.5	26.0 ± 3.0	$F(2,24) = 6.27000$		0.0064	$F(1,24) = 191.50$		<0.0001
Zone *III*	37.5 ± 3.2	39.2 ± 3.5	36.8 ± 2.6	47.9 ± 3.2	36.7 ± 2.1	49.2 ± 4.0	$F(2,24) = 6.09300$		0.0072	$F(1,24) = 52.09$		<0.0001
Zone *IV*	8.8 ± 1.1	14.2 ± 0.9	8.6 ± 1.2	14.2 ± 0.6	8.8 ± 1.3	14.2 ± 1.2	$F(2,24) = 0.02404$		0.9763	$F(1,24) = 199.50$		<0.0001

	1 month WT vs. KO *p*-value	3 months WT vs. KO *p*-value	6 months WT vs. KO *p*-value
Zone *I*	0.9340 ns	0.5091 ns	0.6882 ns
Zone *II*	0.0048**	<0.0001****	<0.0001****
Zone *III*	0.9639 ns	0.0002***	<0.0001****
Zone *IV*	<0.0001****	<0.0001****	<0.0001****

(Continued)

TABLE 2 | Continued

Striatum

Volumetric analysis

	1 month		3 months		6 months						
	WT	**KO**	**WT**	**KO**	**WT**	**KO**					
	Mean ± SD	**Mean ± SD**	**Mean ± SD**	**Mean ± SD**	**Mean ± SD**	**Mean ± SD**	**Effect of age**	→	***p*-value**	**Effect of genotype** →	***p*-value**
V_{cyto}	769.0 ± 34.9	916.0 ± 78.5	777.6 ± 32.6	914.4 ± 85.4	784.8 ± 44.8	910.2 ± 59.4	$F(2,24) = 0.01856$		0.9816	$F(1,24) = 39.33$	<0.0001
V_{mito}	48.8 ± 8.2	92.0 ± 7.3	47.2 ± 7.6	91.6 ± 7.9	46.4 ± 4.2	90.0 ± 6.9	$F(2,24) = 0.23790$		0.7901	$F(1,24) = 281.3$	<0.0001
V_{nuclei}	335.0 ± 26.2	353.8 ± 24.3	333.8 ± 24.0	347.2 ± 15.1	342.6 ± 19.7	359.8 ± 23.7	$F(2,24) = 0.58060$		0.5672	$F(1,24) = 4.027$	0.0562
V_{soma}	1104 ± 27.6	1270 ± 76.0	1111 ± 50.6	1262 ± 78.9	1127 ± 45.3	1270 ± 76.5	$F(2,24) = 0.12400$		0.8839	$F(1,24) = 45.24$	<0.0001
V_{mito}/V_{cyto}	6.3 ± 0.9	10.1 ± 0.9	6.1 ± 1.0	10.04 ± 0.6	6.0 ± 0.7	9.9 ± 0.8	$F(2,24) = 0.22840$		0.7975	$F(1,24) = 166.1$	<0.0001
V_{nuc}/V_{cyto}	43.7 ± 5.1	38.9 ± 5.2	42.9 ± 2.4	38.3 ± 4.8	43.8 ± 3.9	39.6 ± 2.2	$F(2,24) = 0.16530$		0.8486	$F(1,24) = 8.981$	0.0063

	1 month	3 months	6 months
	WT vs. KO *p*-value	**WT vs. KO *p*-value**	**WT vs. KO *p*-value**
V_{cyto}	0.0078**	0.0148*	0.0297*
V_{mito}	<0.0001****	<0.0001****	<0.0001****
V_{nuclei}	0.7699 ns	0.9311 ns	0.8277 ns
V_{soma}	0.0037**	0.0096**	0.0152*
V_{mito}/V_{cyto}	<0.0001****	<0.0001****	<0.0001****
V_{nuc}/V_{cyto}	0.4699 ns	0.5063 ns	0.6045 ns

Mito volume density

	1 month		3 months		6 months						
	WT	**KO**	**WT**	**KO**	**WT**	**KO**					
	Mean ± SD	**Mean ± SD**	**Mean ± SD**	**Mean ± SD**	**Mean ± SD**	**Mean ± SD**	**Effect of age**	→	***p*-value**	**Effect of genotype** →	***p*-value**
Zone $_{I}$	9.0 ± 0.9	10.2 ± 1.6	8.6 ± 0.9	9.5 ± 1.0	9.1 ± 1.2	10.0 ± 1.5	$F(2,24) = 0.64150$		0.5353	$F(1,24) = 5.166$	0.0323
Zone $_{II}$	40.6 ± 3.6	34.2 ± 1.6	41.9 ± 1.3	26.9 ± 1.8	41.1 ± 2.7	28.7 ± 2.1	$F(2,24) = 4.66200$		0.0195	$F(1,24) = 177.3$	<0.0001
Zone $_{III}$	42.8 ± 4.6	42.8 ± 2.6	41.6 ± 2.2	51.2 ± 2.9	41.9 ± 2.8	48.5 ± 3.3	$F(2,24) = 3.27200$		0.0554	$F(1,24) = 21.73$	<0.0001
Zone $_{IV}$	7.7 ± 0.8	12.8 ± 1.2	7.8 ± 0.9	12.5 ± 1.0	7.8 ± 0.8	12.7 ± 0.8	$F(2,24) = 0.02351$		0.9768	$F(1,24) = 207.6$	<0.0001

	1 month	3 months	6 months
	WT vs. KO *p*-value	**WT vs. KO *p*-value**	**WT vs. KO *p*-value**
Zone $_{I}$	0.5666 ns	0.8726 ns	0.8498 ns
Zone $_{II}$	0.0027**	<0.0001****	<0.0001****
Zone $_{III}$	>0.9999 ns	0.0009***	0.0321*
Zone $_{IV}$	<0.0001****	<0.0001****	<0.0001****

*Two-way ANOVA was performed for each parameter followed by Tukey's multiple comparison. The values were compared among groups using multivariate ANOVA followed by Tukey test for multiple comparisons. ns, not significant; *p < 0.05; **p < 0.01; ***p < 0.001, ****p < 0.0001.*

10% bovine serum albumin (BSA) and 0.4% Triton X-100. Afterward, slices were rinsed three times in TBS. The following primary antibodies were used: rabbit anti-EGFP (Molecular Probes, Thermo Fisher Scientific, Switzerland, Cat # A6455; dilution 1:1000), anti-8-oxo-dG (mouse monoclonal; AMS Biotechnology, Biogio-Lugano, Switzerland, Clone 2E2, Cat # 4354-MC-050, dilution 1:350) as reported before (Cabungcal et al., 2019). 8-oxo-7,8-dihydro-20-deoxyguanine (8-oxo-dG) is a product of DNA oxidation, serving as marker for the evaluation of oxidative stress. Incubation with primary antibodies was performed for 48 h at 4°C (Cabungcal et al., 2019). On parallel sections, COX I antibody (mouse monoclonal anti-cytochrome oxidase 1), clone COX 111 (Molecular Probes, Invitrogen AG, Switzerland, Cat # 35-810; dilution 1:500) and rabbit anti-EGFP antibody (Molecular Probes, Thermo Fisher Scientific, Switzerland, Cat # A6455; dilution 1:1000) were used overnight at 4°C. Sections were rinsed twice with TBS and once with Tris-HCl 0.1M, pH 8.2 for 5 min each and then incubated with anti-rabbit Alexa488-conjugated antibody (Life Technologies, Thermo Fisher Scientific, Switzerland; 1:450 dilution), anti-mouse Cy3-conjugated antibody (Jackson Immunoresearch, Suffolk, United Kingdom) and anti-mouse Alexa647-conjugated antibody (Life Technologies, Thermo Fisher Scientific, Switzerland, 1:450 dilution) used as secondary antibodies for 4 h at 4°C. All sections were washed three times with TBS and nuclei were stained with DAPI (LuBio Science GmbH, Switzerland; 1:1000 dilution), during the last 5 min of the incubation period with secondary antibody in TBS. After final washing, slides were transferred onto MENZEL-GLÄSER SUPERFROST® (Thermo Fisher Scientific, Switzerland) and coverslipped with Hydromount (National Diagnostics, Atlanta, GA, United States).

Whole Slide Scanning

Brain sections were scanned by a fully automated slide scanner NanoZoomer 2.0-HT (Hamamatsu Photonics K.K, Switzerland). Fluorescence images were acquired using the mercury lamp unit L11600-05 and for DAPI, FITC, and Cy3 fluorescence imaging, a filter cube with excitation filters (λ_{Ex}: 387, 485, and 560 nm) and emission filters (λ_{Em} 410, 504, 582 nm) was used. All sections were scanned along the z-axis with a 1.4 μm interval with a 20X objective (numerical aperture 0.75) and using 0.46 μm/pixel as scale factor. Images were exported using NDP.view2 Image viewing software (NanoZoomer, Hamamatsu Photonics K.K, U12388-01) and adjusted in Fiji software (RRID:SCR_002285), an open-source platform for image analysis of biological samples.

Confocal Microscopy and Image Post-processing

Mounted brain sections were examined by laser scanning confocal microscopy using a Leica TCS-SP5 instrument (Leica Microsystems, Inc., Buffalo Grove, IL, United States) equipped with a 40X oil-immersion APO plan objective (numerical aperture 1.3). Fluorescence of oxidized DHE was obtained by excitation at λ_{Ex} 516 nm and recording the emission at λ_{Em} 570–600 nm. For EGFP-stained neurons, confocal settings were λ_{Ex} 477 nm, λ_{Em} 485–510. Specific brain regions were scanned along the z-axis with a 1.4 μm interval as described before (Behrens et al., 2008) with constant acquisition parameters; 1240 × 1240 pixels, 200 Hz scan speed and 1AU pinhole diameter. Fluorescence of 8-oxo-dG was acquired by excitation at λ_{Ex} 561 nm and recording the emission at λ_{Em} 565–660 nm. For volumetric analyses confocal settings were as follows: λ_{Ex} 405 nm, λ_{Em} 410–480 (DAPI), EGFP λ_{Ex} 488 nm, λ_{Em} 495–600 nm (EGFP) and λ_{Ex} 633 nm, λ_{Em} 640–800 (COX I). Sections were scanned along the z-axis at 0.42-μm step intervals, as described previously (Janickova et al., 2020), with constant acquisition parameters; 1240 × 1240 pixels, 200 Hz scan speed and 1AU pinhole diameter. After acquisition, all images were deconvoluted using the Huygens deconvolution software (Scientific Volume Imaging, Netherlands) to eliminate blurring and noise and filtered with a Gaussian filter to remove unwanted background noise and to sharpen cell profile contours.

Image Analysis

Coronal brain sections from 30 mice, 15 WT and 15 KO (n = 5 animals per genotype and age) were used. From each brain, nine specific regions (DG, CA3, CA1, striatum, mPFC, SSC, PC, MLI, and TRN) were selected. From sections containing the above brain regions, three parallel sections were collected following stereological systematic random sampling principles (West et al., 1991). Each section (40 μm) was scanned by laser scanning confocal microscope and z-stacks were acquired. From each defined brain region, a single field was randomly selected and only neuron somata completely positioned within the xyz-stack volume were analyzed, i.e., 3–10 neurons per section. The number of analyzed neurons per section fulfilling the criteria varied based on the density of Pvalb neurons in each brain region; e.g., a relatively low density of Pvalb neurons is characteristic for striatum and a high density of Pvalb neurons is typical for cerebellum and TRN (for more details, see Supplementary Figure 1 in Janickova et al., 2020). The minimum number of neurons that were analyzed from the three sections of each brain region is listed in the figure legends of **Figures 2–4**. To quantify the overall 8-oxo-dG or DHE fluorescence signal intensity within the ROI, we first used Imaris 9.5.1 software (Bitplane, AG, Switzerland, RRID:SCR_007370) to confirm that the soma of an $EGFP^+$ neuron is completely within the boundaries of the xyz volume. Next the proportion of all 8-oxo-dG or DHE immunolabeled voxels contained in the center 8 images of the z-stacks and the mean fluorescence intensity was calculated as previously reported (Cabungcal et al., 2019) using the LAS AF software (Leica Application Suite X, RRID:SCR_013673). We used maximum intensity projections to obtain the values for ROIs, a ROI was drawn using the "free hand tool" based on the $EGFP^+$ neuron morphology. For background subtraction, a similar-sized ROI within the tissue characterized by weak and diffuse staining not overlapping with EGFP or clearly discernible 8-oxo-dG or DHE fluorescence signals was randomly selected from each microscopy field. The values obtained after background subtraction from all analyzed neurons from each section were averaged resulting in a single

value per animal and brain region. Since fluorescence intensity values were obtained from maximal density projections (z-stacks) and the morphology of the different Pvalb neuron subpopulations is quite variable, a correction factor based on Pvalb neuron morphology was calculated (Janickova et al., 2020). Briefly, assuming that neuron somata and nuclei can be approximated by spheres, from the volume of the entire soma and the nucleus, the radii of these two spheres (r2: soma; r1: nucleus) were calculated (see Supplementary Table S1 in Janickova et al., 2020). The difference in the radii is then the thickness (d) of the shell comprising the cytoplasmic volume. Hence, fluorescence values listed in **Table 1** are the ones after applying the d-factor correction. To determine the volume of soma, nucleus and mitochondria of $EGFP^+$ neurons entirely localized within z-stack images, the 'Cell' and 'Surface' module of the Imaris software was used as described before (Janickova et al., 2020). The volume of the cytoplasm, nuclei and mitochondria were calculated for each neuron using the same parameter and algorithm settings. Statistical analyses were performed using the 'Imaris Measurement Pro' module as described previously (Lichvarova et al., 2019).

Mitochondria Distribution in Pvalb Neuron Somata

To analyze mitochondria distribution in the somata of Pvalb neurons, the CellProfiler^{TM} (Cell Image Analysis software, Broad Institute Imaging Platform, RRID:SCR_007358) with the 'Measure Object Intensity Distribution' module was used. This module allows to measure the spatial distribution of intensities within each identified object. First, morphologically fully intact Pvalb neuron somata contained in the z-stack were selected and somata and nuclei of selected neurons were identified based on EGFP and DAPI staining, respectively. Next, the distribution from the center of the cell (nucleus) to the edge (i.e., the plasma membrane of a selected neuron soma) was partitioned into a set of four specified zones excluding the nucleus: 1 being the innermost and 4 the outermost for details, see CellProfiler. The software then measured automatically the fraction of total staining intensity in an object at a given radius. Data are shown as perinuclear mitochondrial volume (zone1), perinuclear/central mitochondrial volume (zone 2) and subplasmalemmal mitochondrial volume (zone 4).

Statistical Analysis

GraphPad Prism 7.05 software (RRID:SCR_002798) was used for statistical analysis. Two-way multivariate ANOVA followed by Tukey multiple comparison test was performed in order to compare the ratios between PV-EGFP (WT) and PVKO-EGFP (PV−/− or KO) mice and age in different brain regions. For all experiments a p-value < 0.05 was considered as statistically significant. Values are expressed as mean ± SD. The mean 8-oxo-dG and ox-DHE signal intensities were compared among groups using multivariate ANOVA followed by Tukey test for multiple comparisons. Detailed statistical analysis with mean ± SD, age and genotype as factors, as well as exact p-values are reported in **Tables 1**, **2**.

DISCUSSION

Release of mitochondrial ROS (mROS) is suggested to have evolved as a communication system linking mitochondrial function with physiological cellular processes to maintain homeostasis in the brain and to sustain adaptation to stress (reviewed in Sena and Chandel, 2012). In the brain mROS act as physiological modulators of signaling pathways and transcription factors involved in cell proliferation, differentiation and maturation (e.g., in axon formation); in mature neurons mROS also participate in the regulation of synaptic plasticity [details are provided in Figure 1 and the references cited in the review by Beckhauser et al. (2016)]. Converse to their important physiological functions, elevated ROS levels causing an imbalance between ROS production and antioxidant defenses (principally provided by glutathione), as found in post-mortem brain tissue of children with ASD (Siddiqui et al., 2016), and adult schizophrenia patients (Tosic et al., 2006) might be implicated in ASD and schizophrenia etiology. The link between redox dysregulation and schizophrenia has been investigated in a mouse model, i.e., in Gclm−/− mice deficient for the glutamate cysteine ligase modifier subunit, the rate-limiting enzyme for glutathione biosynthesis (Cabungcal et al., 2019). The early-onset developmental redox dysregulation caused by constitutive absence of Gclm most strongly affects the Pvalb neuron circuitry evidenced by increased 8-oxo-dG staining in VVA^+ Pvalb neurons. The authors provide evidence "that PV neurons located in different cortical and sub-cortical brain regions exhibit selective vulnerability to oxidative stress during different phases of neurodevelopment" (see Figure 6 in Cabungcal et al., 2019). Potential explanations for these region-specific variances include "differences in (1) maturation time course of PV neurons and their PNN, (2) neuronal and metabolic activity, (3) antioxidant capacity of PV neurons and their neighbored cells, (4) levels of catecholamines (dopamine, noradrenaline)" and possibly temporal changes in functional connectivity between brain regions (Cabungcal et al., 2019).

Results from our longitudinal study indicate that the magnitude and moreover, the age-dependent increase in oxidative stress in Pvalb neurons is highly correlated with the PV concentration in those neurons of WT mice (**Supplementary Figure 4**). In absence of PV, the elevated oxidative stress is strongly correlated with the PV deficiency-induced increase in mitochondria volume (density) reported before (Janickova et al., 2020) and shown here for TRN and striatal Pvalb neurons (**Figures 5**, **6**). Compared to WT mice enhanced oxidative stress was detectable in PV−/− mice from 3 months on, although the increase in mitochondrial volume was already maximal at 1 month evidenced in striatal and TRN Pvalb neurons. Yet, at this age oxidative stress was not increased in absence of PV. In summary, the larger the increase in mitochondria volume caused by the absence of PV in Pvalb neurons, the larger the oxidative stress, evident only in older (>3 months) mice.

Inverse (antagonistic) regulation of PV and mitochondria is observed in several *in vitro* and *in vivo* models (reviewed in Schwaller, 2020) including Pvalb neurons of PV−/− mice (Janickova et al., 2020). In this study, a strong correlation between

the PV deficiency-induced increase in mitochondria and the prevailing PV concentration in Pvalb neurons of WT mice was observed. The increase in mitochondria is likely regulated by the master regulator of mitochondria biosynthesis PGC-1α, as previously shown in fast-twitch muscle of PV−/− mice, where mitochondria volume is also upregulated in absence of PV (Ducreux et al., 2012). Of note, PGC-1α overexpression also increases expression of ROS defense systems likely to maintain redox balance (St-Pierre et al., 2006). In line, in MDCK (epithelial) cells mRNA levels of *Ucp2* are higher in PV-negative control cells (a proxy measure for PV-deficient Pvalb cells) compared to PV-overexpressing cells characterized by a decreased mitochondria volume (Henzi and Schwaller, 2015). The same holds true for CG4 cells, where *Ucp2* levels are higher in PV-negative control cells than in PV-expressing CG4 cells (L. Janickova, unpublished). Upregulation of uncoupling proteins decreases the mitochondrial membrane potential $\Delta\Psi$ and concomitantly is expected to reduce mROS production. Thus, possibly elevated ROS defense systems [as found in the MDCK cell model (Henzi and Schwaller, 2015) and CG4 cells] despite a significant increase in mitochondria volume in PV−/− Pvalb neurons of 1-month old mice might prevent elevated ROS production at this age.

Thus, we propose the following timeline for events taking place in Pvalb neurons, if PV expression is constitutively lacking in PV−/− mice. Absence of PV is rapidly detected by Pvalb neurons possibly sensed as changes in the shape of Ca^{2+} transients shown to occur in Purkinje cells (Schmidt et al., 2003), MLI (Collin et al., 2005) and in a large Pvalb neuron presynapse, the calyx of Held (Muller et al., 2007). At the functional level this results in increased paired-pulse facilitation (PPF) as seen at synapses involving cerebellar (Caillard et al., 2000; Collin et al., 2005), striatal (Orduz et al., 2013), and hippocampal (Vreugdenhil et al., 2003) Pvalb neurons. These alterations are then leading to modifications in excitation-transcription coupling inducing several changes including mitochondria biosynthesis resulting in mitochondria that are tuned to optimally contribute to slow Ca^{2+} buffering. This mitochondria-mediated process is energy-expensive and can only be maintained by increased ATP production (Palmieri and Persico, 2010) paralleled by increases in mROS production (for reviews, see, Devine and Kittler, 2018; Giorgi et al., 2018) that are manifest in PV−/− mice only at older (>3 months) age. We assume that although increased mitochondria volume (density) in absence of PV is already maximal at 1 month, the possibly concomitant increase in ROS defense systems including UCP2 might be sufficient to prevent augmentation of oxidative stress at this age.

Of relevance, transcriptional regulation of PV is mediated not by the prototypical CaMKII or IV, but by the "atypical" γCaMKI (Cohen et al., 2016). In line, *CAMK1G* mRNA is among the most strongly downregulated transcripts in cortical samples from ASD individuals initially reported in Parikshak et al. (2016) and further analyzed in Schwede et al. (2018), thus providing the link to decreased levels of *PVALB* mRNA and elevated mitochondrial genes in human ASD including *UCP2*. The elevated mitochondria density previously determined in Pvalb neurons of 3–5 months-old mice is ranging from ∼5% (hippocampus) to ∼108% (TRN) and is approximately proportional to the PV concentration prevailing in WT Pvalb neurons (see Supplementary Figure 3 in Janickova et al., 2020). Of importance, in 1-month old PV−/− mice, when PV expression has reached adult levels (as shown in cerebellar Pvalb neurons; see Figure 2 in Collin et al., 2005), the increase in mitochondria density is already maximal: ∼60–65% in striatal and ∼115% in TRN Pvalb neurons. Of importance, in none of the investigated Pvalb neuron subpopulations, an increase in oxidative stress is evident at this time point. However, at the behavioral level PV−/− mice show ASD-like core symptoms at PND25–30 (Wöhr et al., 2015). This essentially precludes oxidative stress as causative for the ASD-like behavioral phenotype of PV−/− mice. It rather supports the hypothesis that altered Ca^{2+} signals in PV−/− Pvalb neurons subtly modify synaptic plasticity likely translating into changes in neuron ensemble synchrony and oscillations. Notwithstanding additional alterations affecting Pvalb neuron firing caused by the absence of PV might be implicated as well: e.g., striatal PV−/− Pvalb neurons show besides increased paired-pulse facilitation, higher excitability and spontaneous spiking is more regular, likely involving changes in the activation of small conductance (SK) Ca^{2+}-dependent K^+ channels (Orduz et al., 2013).

First signs of oxidative stress evidenced by increased 8-oxo-dG and DHE signal intensity were observed at the age of 3 months in PV−/− mice. Preliminary behavioral experiments (3-chamber assay) carried out in 3 months-old male PV−/− mice indicate that the ASD-like phenotype is rather attenuated (Filice, unpublished) compared to PND25-30 mice (Filice et al., 2018) further supporting that most probably oxidative stress is not causally implicated in the development of the ASD-like phenotype of PV−/− mice. Whether this is also the case in other ASD mouse models with reduced PV levels (Supplementary Table S1 in Wöhr et al., 2015) or restricted to PV−/− mice remains to be shown.

DATA AVAILABILITY STATEMENT

All datasets generated for this study are included in the article/**Supplementary Material**.

ETHICS STATEMENT

The animal study was reviewed and approved by Animal care committee (Canton of Fribourg, Switzerland); the authorization number for housing is H-04.2012-Fr and for experiments 2016_37_FR.

AUTHOR CONTRIBUTIONS

LJ carried out the experiments, performed data analysis, and wrote the manuscript. BS conceived the study, performed data analysis and together with LJ wrote the manuscript. All authors read and approved the final manuscript.

FUNDING

The project was supported by the Swiss National Science Foundation (SNF) grants # 155952 and 184668 to BS.

ACKNOWLEDGMENTS

We would like to thank Simone Eichenberger for her excellent technical assistance in the maintenance of the mouse facility and staff members of the Bioimage Light Microscopy Facility of the University of Fribourg for the excellent technical support. We also thank Dr. Thomas Henzi and Dr. Federica Filice, University of Fribourg for feedback and comments on the manuscript.

SUPPLEMENTARY MATERIAL

The Supplementary Material for this article can be found online at: https://www.frontiersin.org/articles/10.3389/fncel.2020.571216/full#supplementary-material

REFERENCES

Bader, P. L., Faizi, M., Kim, L. H., Owen, S. F., Tadross, M. R., Alfa, R. W., et al. (2011). Mouse model of Timothy syndrome recapitulates triad of autistic traits. *Proc. Natl. Acad. Sci. U.S.A.* 108, 15432–15437. doi: 10.1073/pnas.1112667108

Barbacanne, M. A., Souchard, J. P., Darblade, B., Iliou, J. P., Nepveu, F., Pipy, B., et al. (2000). Detection of superoxide anion released extracellularly by endothelial cells using cytochrome c reduction, ESR, fluorescence and lucigenin-enhanced chemiluminescence techniques. *Free Radic. Biol. Med.* 29, 388–396. doi: 10.1016/s0891-5849(00)00336-1

Beckhauser, T. F., Francis-Oliveira, J., and De Pasquale, R. (2016). Reactive oxygen species: physiological and physiopathological effects on synaptic plasticity. *J. Exp. Neurosci.* 10, 23–48.

Behrens, M. M., Ali, S. S., and Dugan, L. L. (2008). Interleukin-6 mediates the increase in NADPH-oxidase in the ketamine model of schizophrenia. *J. Neurosci.* 28, 13957–13966. doi: 10.1523/jneurosci.4457-08.2008

Bohannon, A. S., and Hablitz, J. J. (2018). Optogenetic dissection of roles of specific cortical interneuron subtypes in GABAergic network synchronization. *J. Physiol.* 596, 901–919. doi: 10.1113/jp275317

Cabungcal, J. H., Steullet, P., Kraftsik, R., Cuenod, M., and Do, K. Q. (2019). A developmental redox dysregulation leads to spatio-temporal deficit of parvalbumin neuron circuitry in a schizophrenia mouse model. *Schizophr. Res.* 213, 96–106. doi: 10.1016/j.schres.2019.02.017

Caillard, O., Moreno, H., Schwaller, B., Llano, I., Celio, M. R., and Marty, A. (2000). Role of the calcium-binding protein parvalbumin in short-term synaptic plasticity. *Proc. Natl. Acad. Sci. U.S.A.* 97, 13372–13377. doi: 10.1073/pnas.230362997

Celio, M. R. (1990). Calbindin D-28k and parvalbumin in the rat nervous system. *Neuroscience* 35, 375–475. doi: 10.1016/0306-4522(90)90091-h

Chattopadhyaya, B., and Cristo, G. D. (2012). GABAergic circuit dysfunctions in neurodevelopmental disorders. *Front. Psychiatry* 3:51. doi: 10.3389/fpsyt.2012.00051

Chen, G., Racay, P., Bichet, S., Celio, M. R., Eggli, P., and Schwaller, B. (2006). Deficiency in parvalbumin, but not in calbindin D-28k upregulates mitochondrial volume and decreases smooth endoplasmic reticulum surface selectively in a peripheral, subplasmalemmal region in the soma of Purkinje cells. *Neuroscience* 142, 97–105. doi: 10.1016/j.neuroscience.2006.06.008

Coghlan, S., Horder, J., Inkster, B., Mendez, M. A., Murphy, D. G., and Nutt, D. J. (2012). GABA system dysfunction in autism and related disorders: from synapse to symptoms. *Neurosci. Biobehav. Rev.* 36, 2044–2055.

Cohen, S. M., Ma, H., Kuchibhotla, K. V., Watson, B. O., Buzsaki, G., Froemke, R. C., et al. (2016). Excitation-transcription coupling in parvalbumin-positive interneurons employs a novel CaM Kinase-dependent pathway distinct from excitatory neurons. *Neuron* 90, 292–307. doi: 10.1016/j.neuron.2016.03.001

Collin, T., Chat, M., Lucas, M. G., Moreno, H., Racay, P., Schwaller, B., et al. (2005). Developmental changes in parvalbumin regulate presynaptic Ca2+ signaling. *J. Neurosci.* 25, 96–107. doi: 10.1523/jneurosci.3748-04.2005

del Rio, J. A., De Lecea, L., Ferrer, I., and Soriano, E. (1994). The development of parvalbumin-immunoreactivity in the neocortex of the mouse. *Brain Res. Dev. Brain Res.* 81, 247–259. doi: 10.1016/0165-3806(94)90311-5

Deleuze, C., Bhumbra, G. S., Pazienti, A., Lourenco, J., Mailhes, C., Aguirre, A., et al. (2019). Strong preference for autaptic self-connectivity of neocortical PV interneurons facilitates their tuning to gamma-oscillations. *PLoS Biol.* 17:e3000419. doi: 10.1371/journal.pbio.3000419

Devine, M. J., and Kittler, J. T. (2018). Mitochondria at the neuronal presynapse in health and disease. *Nat. Rev. Neurosci.* 19, 63–80. doi: 10.1038/nrn.2017.170

Do, K. Q., Cabungcal, J. H., Frank, A., Steullet, P., and Cuenod, M. (2009). Redox dysregulation, neurodevelopment, and schizophrenia. *Curr. Opin. Neurobiol.* 19, 220–230. doi: 10.1016/j.conb.2009.05.001

Ducreux, S., Gregory, P., and Schwaller, B. (2012). Inverse regulation of mitochondrial volume and the cytosolic Ca2+ buffer parvalbumin in muscle cells via SIRT-1/PGC-1α axis. *PLoS One* 7:e44837. doi: 10.1371/journal.pone.0044837

Eggermann, E., and Jonas, P. (2012). How the 'slow' Ca2+ buffer parvalbumin affects transmitter release in nanodomain-coupling regimes. *Nat. Neurosci.* 15, 20–22. doi: 10.1038/nn.3002

Ferguson, B. R., and Gao, W. J. (2018). PV interneurons: critical regulators of e/i balance for prefrontal cortex-dependent behavior and psychiatric disorders. *Front. Neural Circuits* 12:37. doi: 10.3389/fncir.2018.00037

Filice, F., Lauber, E., Vorckel, K. J., Wöhr, M., and Schwaller, B. (2018). 17-beta estradiol increases parvalbumin levels in Pvalb heterozygous mice and attenuates behavioral phenotypes with relevance to autism core symptoms. *Mol. Autism* 9:15.

Filice, F., Vorckel, K. J., Sungur, A. O., Wöhr, M., and Schwaller, B. (2016). Reduction in parvalbumin expression not loss of the parvalbumin-expressing GABA interneuron subpopulation in genetic parvalbumin and shank mouse models of autism. *Mol. Brain* 9:10.

Fink, B., Laude, K., Mccann, L., Doughan, A., Harrison, D. G., and Dikalov, S. (2004). Detection of intracellular superoxide formation in endothelial cells and intact tissues using dihydroethidium and an HPLC-based assay. *Am. J. Physiol. Cell Physiol.* 287, C895–C902.

Giorgi, C., Marchi, S., and Pinton, P. (2018). The machineries, regulation and cellular functions of mitochondrial calcium. *Nat. Rev. Mol. Cell Biol.* 19, 713–730. doi: 10.1038/s41580-018-0052-8

Gogolla, N., Leblanc, J. J., Quast, K. B., Sudhof, T. C., Fagiolini, M., and Hensch, T. K. (2009). Common circuit defect of excitatory-inhibitory balance in mouse models of autism. *J. Neurodev. Disord.* 1, 172–181. doi: 10.1007/s11689-009-9023-x

Gonzalez-Burgos, G., Cho, R. Y., and Lewis, D. A. (2015). Alterations in cortical network oscillations and parvalbumin neurons in schizophrenia. *Biol. Psychiatry* 77, 1031–1040. doi: 10.1016/j.biopsych.2015.03.010

Gonzalez-Burgos, G., and Lewis, D. A. (2012). NMDA receptor hypofunction, parvalbumin-positive neurons, and cortical gamma oscillations in schizophrenia. *Schizophr. Bull.* 38, 950–957. doi: 10.1093/schbul/sbs010

Gordon, A., Forsingdal, A., Klewe, I. V., Nielsen, J., Didriksen, M., Werge, T., et al. (2019). Transcriptomic networks implicate neuronal energetic abnormalities in three mouse models harboring autism and schizophrenia-associated mutations. *Mol. Psychiatry*. doi: 10.1038/s41380-019-0576-0 [Epub ahead of print].

Hall, D. J., Han, S. H., Chepetan, A., Inui, E. G., Rogers, M., and Dugan, L. L. (2012). Dynamic optical imaging of metabolic and NADPH oxidase-derived superoxide in live mouse brain using fluorescence lifetime unmixing. *J. Cereb. Blood Flow Metab.* 32, 23–32. doi: 10.1038/jcbfm.2011.119

Hardingham, G. E., and Do, K. Q. (2016). Linking early-life NMDAR hypofunction and oxidative stress in schizophrenia pathogenesis. *Nat. Rev. Neurosci.* 17, 125–134. doi: 10.1038/nrn.2015.19

Hasam-Henderson, L. A., Gotti, G. C., Mishto, M., Klisch, C., Gerevich, Z., Geiger, J. R. P., et al. (2018). NMDA-receptor inhibition and oxidative stress during hippocampal maturation differentially alter parvalbumin expression and gamma-band activity. *Sci. Rep.* 8:9545.

Hashemi, E., Ariza, J., Rogers, H., Noctor, S. C., and Martinez-Cerdeno, V. (2017). The number of parvalbumin-expressing interneurons is decreased in the prefrontal cortex in autism. *Cereb. Cortex* 27, 1931–1943.

Henzi, T., and Schwaller, B. (2015). Antagonistic regulation of parvalbumin expression and mitochondrial calcium handling capacity in renal epithelial cells. *PLoS One* 10:e0142005. doi: 10.1371/journal.pone.0142005

Janickova, L., Rechberger, K. F., Wey, L., and Schwaller, B. (2020). Absence of parvalbumin increases mitochondria volume and branching of dendrites in Pvalb neurons in vivo: a point of convergence of autism spectrum disorder (ASD) risk gene phenotypes. *Mol. Autism* 11:47.

Kann, O. (2016). The interneuron energy hypothesis: implications for brain disease. *Neurobiol. Dis.* 90, 75–85. doi: 10.1016/j.nbd.2015.08.005

Kann, O., Papageorgiou, I. E., and Draguhn, A. (2014). Highly energized inhibitory interneurons are a central element for information processing in cortical networks. *J. Cereb. Blood Flow Metab.* 34, 1270–1282. doi: 10.1038/jcbfm.2014.104

Lauber, E., Filice, F., and Schwaller, B. (2016). Prenatal valproate exposure differentially affects parvalbumin-expressing neurons and related circuits in the cortex and striatum of mice. *Front. Mol. Neurosci.* 9:150. doi: 10.3389/fnmol.2016.00150

Lauber, E., Filice, F., and Schwaller, B. (2018). Dysregulation of parvalbumin expression in the Cntnap2-/- Mouse model of autism spectrum disorder. *Front. Mol. Neurosci.* 11:262. doi: 10.3389/fnmol.2018.00262

Lichvarova, L., Blum, W., Schwaller, B., and Szabolcsi, V. (2019). Parvalbumin expression in oligodendrocyte-like CG4 cells causes a reduction in mitochondrial volume, attenuation in reactive oxygen species production and a decrease in cell processes' length and branching. *Sci. Rep.* 9:10603.

Maetzler, W., Nitsch, C., Bendfeldt, K., Racay, P., Vollenweider, F., and Schwaller, B. (2004). Ectopic parvalbumin expression in mouse forebrain neurons increases excitotoxic injury provoked by ibotenic acid injection into the striatum. *Exp. Neurol.* 186, 78–88. doi: 10.1016/j.expneurol.2003.10.014

Marin, O. (2012). Interneuron dysfunction in psychiatric disorders. *Nat. Rev. Neurosci.* 13, 107–120. doi: 10.1038/nrn3155

Meyer, A. H., Katona, I., Blatow, M., Rozov, A., and Monyer, H. (2002). In vivo labeling of parvalbumin-positive interneurons and analysis of electrical coupling in identified neurons. *J. Neurosci.* 22, 7055–7064. doi: 10.1523/jneurosci.22-16-07055.2002

Muller, M., Felmy, F., Schwaller, B., and Schneggenburger, R. (2007). Parvalbumin is a mobile presynaptic Ca2+ buffer in the calyx of held that accelerates the decay of Ca2+ and short-term facilitation. *J. Neurosci,* 27, 2261–2271. doi: 10.1523/jneurosci.5582-06.2007

Murakami, K., Kondo, T., Kawase, M., Li, Y., Sato, S., Chen, S. F., et al. (1998). Mitochondrial susceptibility to oxidative stress exacerbates cerebral infarction that follows permanent focal cerebral ischemia in mutant mice with manganese superoxide dismutase deficiency. *J. Neurosci.* 18, 205–213. doi: 10.1523/jneurosci.18-01-00205.1998

Orduz, D., Bischop, D. P., Schwaller, B., Schiffmann, S. N., and Gall, D. (2013). Parvalbumin tunes spike-timing and efferent short-term plasticity in striatal fast spiking interneurons. *J. Physiol.* 591, 3215–3232.

Palmieri, L., and Persico, A. M. (2010). Mitochondrial dysfunction in autism spectrum disorders: cause or effect? *Biochim. Biophys. Acta* 1797, 1130–1137.

Parikshak, N. N., Swarup, V., Belgard, T. G., Irimia, M., Ramaswami, G., Gandal, M. J., et al. (2016). Genome-wide changes in lncRNA, splicing, and regional gene expression patterns in autism. *Nature* 540, 423–427.

Powell, S. B., Sejnowski, T. J., and Behrens, M. M. (2012). Behavioral and neurochemical consequences of cortical oxidative stress on parvalbumin-interneuron maturation in rodent models of schizophrenia. *Neuropharmacology* 62, 1322–1331.

Puyal, J., Devau, G., Venteo, S., Sans, N., and Raymond, J. (2002). Calcium-binding proteins map the postnatal development of rat vestibular nuclei and their vestibular and cerebellar projections. *J. Comp. Neurol.* 451, 374–391.

Quick, K. L., and Dugan, L. L. (2001). Superoxide stress identifies neurons at risk in a model of ataxia-telangiectasia. *Ann. Neurol.* 49, 627–635.

Schmidt, H., Stiefel, K. M., Racay, P., Schwaller, B., and Eilers, J. (2003). Mutational analysis of dendritic Ca2+ kinetics in rodent Purkinje cells: role of parvalbumin and calbindin D28k. *J. Physiol.* 551, 13–32.

Schork, A. J., Won, H., Appadurai, V., Nudel, R., Gandal, M., Delaneau, O., et al. (2019). A genome-wide association study of shared risk across psychiatric disorders implicates gene regulation during fetal neurodevelopment. *Nat. Neurosci.* 22, 353–361.

Schwaller, B. (2020). Cytosolic Ca2+ Buffers Are Inherently Ca2+ Signal Modulators. *Cold Spring Harb. Perspect. Biol.* 12:a035543.

Schwede, M., Nagpal, S., Gandal, M. J., Parikshak, N. N., Mirnics, K., Geschwind, D. H., et al. (2018). Strong correlation of downregulated genes related to synaptic transmission and mitochondria in post-mortem autism cerebral cortex. *J. Neurodev. Disord.* 10:18.

Sena, L. A., and Chandel, N. S. (2012). Physiological roles of mitochondrial reactive oxygen species. *Mol. Cell* 48, 158–167.

Siddiqui, M. F., Elwell, C., and Johnson, M. H. (2016). Mitochondrial dysfunction in autism spectrum disorders. *Autism Open Access.* 6, 2389–2396.

Soghomonian, J. J., Zhang, K., Reprakash, S., and Blatt, G. J. (2017). Decreased parvalbumin mRNA levels in cerebellar Purkinje cells in autism. *Autism Res.* 10, 1787–1796.

Sohal, V. S., Zhang, F., Yizhar, O., and Deisseroth, K. (2009). Parvalbumin neurons and gamma rhythms enhance cortical circuit performance. *Nature* 459, 698–702.

Steullet, P., Cabungcal, J. H., Bukhari, S. A., Ardelt, M. I., Pantazopoulos, H., Hamati, F., et al. (2018). The thalamic reticular nucleus in schizophrenia and bipolar disorder: role of parvalbumin-expressing neuron networks and oxidative stress. *Mol. Psychiatry* 23, 2057–2065.

Steullet, P., Cabungcal, J. H., Coyle, J., Didriksen, M., Gill, K., Grace, A. A., et al. (2017). Oxidative stress-driven parvalbumin interneuron impairment as a common mechanism in models of schizophrenia. *Mol. Psychiatry* 22, 936–943.

St-Pierre, J., Drori, S., Uldry, M., Silvaggi, J. M., Rhee, J., Jager, S., et al. (2006). Suppression of reactive oxygen species and neurodegeneration by the PGC-1 transcriptional coactivators. *Cell* 127, 397–408.

Tang, G., Gutierrez Rios, P., Kuo, S. H., Akman, H. O., Rosoklija, G., Tanji, K., et al. (2013). Mitochondrial abnormalities in temporal lobe of autistic brain. *Neurobiol. Dis.* 54, 349–361.

Tosic, M., Ott, J., Barral, S., Bovet, P., Deppen, P., Gheorghita, F., et al. (2006). Schizophrenia and oxidative stress: glutamate cysteine ligase modifier as a susceptibility gene. *Am. J. Hum. Genet.* 79, 586–592.

Volman, V., Behrens, M. M., and Sejnowski, T. J. (2011). Downregulation of parvalbumin at cortical GABA synapses reduces network gamma oscillatory activity. *J. Neurosci.* 31, 18137–18148.

Vreugdenhil, M., Jefferys, J. G., Celio, M. R., and Schwaller, B. (2003). Parvalbumin-deficiency facilitates repetitive IPSCs and gamma oscillations in the hippocampus. *J. Neurophysiol.* 89, 1414–1422.

West, M. J., Slomianka, L., and Gundersen, H. J. (1991). Unbiased stereological estimation of the total number of neurons in thesubdivisions of the rat hippocampus using the optical fractionator. *Anat. Rec.* 231, 482–497.

Wöhr, M., Orduz, D., Gregory, P., Moreno, H., Khan, U., Vorckel, K. J., et al. (2015). Lack of parvalbumin in mice leads to behavioral deficits relevant to all human autism core symptoms and related neural morphofunctional abnormalities. *Transl. Psychiatry* 5:e525.

Conflict of Interest: The authors declare that the research was conducted in the absence of any commercial or financial relationships that could be construed as a potential conflict of interest.

frontiers in Cellular Neuroscience

MINI REVIEW
published: 30 October 2020
doi: 10.3389/fncel.2020.588662

G Protein-Coupled Receptor Heteromers as Putative Pharmacotherapeutic Targets in Autism

Jon DelaCuesta-Barrutia[1], *Olga Peñagarikano*[1,2†] *and Amaia M. Erdozain*[1,2*†]

[1]*Department of Pharmacology, University of the Basque Country (UPV/EHU), Leioa, Spain,* [2]*Centro de Investigación Biomédica en Red en Salud Mental (CIBERSAM), Leioa, Spain*

A major challenge in the development of pharmacotherapies for autism is the failure to identify pathophysiological mechanisms that could be targetable. The majority of developing strategies mainly aim at restoring the brain excitatory/inhibitory imbalance described in autism, by targeting glutamate or GABA receptors. Other neurotransmitter systems are critical for the fine-tuning of the brain excitation/inhibition balance. Among these, the dopaminergic, oxytocinergic, serotonergic, and cannabinoid systems have also been implicated in autism and thus represent putative therapeutic targets. One of the latest breakthroughs in pharmacology has been the discovery of G protein-coupled receptor (GPCR) oligomerization. GPCR heteromers are macromolecular complexes composed of at least two different receptors, with biochemical properties that differ from those of their individual components, leading to the activation of different cellular signaling pathways. Interestingly, heteromers of the above-mentioned neurotransmitter receptors have been described (e.g., mGlu2–5HT2A, mGlu5–D2–A2A, D2–OXT, CB1–D2, D2–5HT2A, D1–D2, D2–D3, and OXT–5HT2A). We hypothesize that differences in the GPCR interactome may underlie the etiology/pathophysiology of autism and could drive different treatment responses, as has already been suggested for other brain disorders such as schizophrenia. Targeting GPCR complexes instead of monomers represents a new order of biased agonism/antagonism that may potentially enhance the efficacy of future pharmacotherapies. Here, we present an overview of the crosstalk of the different GPCRs involved in autism and discuss current advances in pharmacological approaches targeting them.

Keywords: GPCR receptor heteromers, pharmacotherapy, glutamate, oxytocin, serotonin, dopamine, ASD, cannabinoid

OPEN ACCESS

Edited by:
Yu-Chih Lin,
Hussman Institute for Autism, United States

Reviewed by:
Terence Hébert,
McGill University, Canada
Jia-Da Li,
Central South University, China

***Correspondence:**
Amaia M. Erdozain
amaia_erdozain@ehu.eus
orcid.org/0000-0003-0207-9122

†These authors have contributed equally to this work

Specialty section:
This article was submitted to Cellular Neuropathology, a section of the journal Frontiers in Cellular Neuroscience

Received: *29 July 2020*
Accepted: *25 September 2020*
Published: *30 October 2020*

Citation:
DelaCuesta-Barrutia J, Peñagarikano O and Erdozain AM (2020) G Protein-Coupled Receptor Heteromers as Putative Pharmacotherapeutic Targets in Autism. Front. Cell. Neurosci. 14:588662. doi: 10.3389/fncel.2020.588662

INTRODUCTION

Autism spectrum disorder (ASD) is a severe developmental disorder that involves difficulties in two behavioral domains: social interaction, including speech and nonverbal communication, and restricted/repetitive behaviors [American Psychiatric Association (Ed.), 2013]. These core symptoms are frequently associated with other emotional and behavioral disturbances, such as anxiety, irritability, inattention, hyperactivity, and sleep problems, resulting in a very heterogeneous clinical manifestation. The etiology of ASD is also complex, caused by a combination of

genetic (∼80%) and environmental factors (Bai et al., 2019). The causal neuropathology is largely unknown. As a result, there are currently no medications approved for the management of the core symptoms of ASD; however, most affected individuals follow pharmacological interventions to target associated symptoms, albeit with limited evidence-based efficiency and substantial adverse effects.

Research aimed at developing targeted pharmacotherapies for ASD identifies functional alterations in brain areas and networks involved in emotion and social cognition, such as the prefrontal cortex (PFC) and limbic system (Kennedy and Adolphs, 2012; Ecker et al., 2015; Fernández et al., 2018; Müller and Fishman, 2018). At the molecular level, an alteration in several neurotransmitter systems that modulate the activity of these brain areas and networks has been observed. The imbalance between excitatory glutamatergic and inhibitory GABAergic tones has been the most studied (Uzunova et al., 2016). Hence, one strategy that aimed at restoring this imbalance relies on antagonizing glutamate receptors (e.g., memantine) or using GABA agonists (e.g., arbaclofen), in order to reduce the proposed overstimulated glutamate signaling in ASD (Rojas, 2014; Fernández et al., 2018). However, hypo-glutamate theories have also been proposed, and glutamate receptor agonists such as D-cycloserine are also used in some cases, indicating that the excitatory/inhibitory imbalance might occur in both directions (Fernández et al., 2018). Nonetheless, the oxytocinergic (OXT), serotonergic (5HT), dopaminergic (DA), and cannabinoid (CB) systems are also critical for the fine-tuning of the brain excitation/inhibition balance and thus represent putative therapeutic targets in ASD (Marotta et al., 2020).

Once the role of the OXT system in modulating affiliative and social behavior across vertebrate species was established, efforts in translating these findings to the clinic begun (Insel, 2010; Yamasue and Domes, 2017; Erdozain and Peñagarikano, 2020). Alterations in OXT receptor (OXTR) binding and OXTR gene hypermethylation have been found in different brain structures of individuals with ASD (Purba, 1996; Lee et al., 2007). Several studies have also reported altered plasma OXT levels (Modahl et al., 1998; Andari et al., 2010; Aydın et al., 2018; Strauss et al., 2019), albeit there is still much debate on whether peripheral OXT correlates with the one in brain (Jupiter et al., 1988). An increasing number of clinical trials testing the effect of OXT or OXT agonists in ASD are being carried out. Although based on current results OXT seems to have a potential therapeutic value, there are key questions that remain unanswered as to decide the optimal target groups and treatment course (Erdozain and Peñagarikano, 2020).

Regarding 5HT, hyperserotonemia was the first blood biomarker proposed in ASD, as it is present in more than 25% of affected children (Hanley, 1977; Cook, 1990). Since then, many studies have observed changes in the 5HT system in ASD. One example is the decrease of 5HT receptor 2A (5HT2AR) binding detected by imaging studies (Murphy et al., 2006). In postmortem studies, lower binding of 5HT receptor 1A (5HT1AR), in addition to 5HT2AR, has also been reported (Oblak et al., 2013), suggesting a deficient 5HT signaling in brain, albeit the presence of blood hyperserotonemia. Accordingly, selective serotonin reuptake inhibitors (SSRIs) have long been used to treat symptoms of repetitive behavior and anxiety in autism, although with limited clinical efficacy (King et al., 2009).

There are promising studies about the influence of the CB system in ASD due to CB's pro-social properties and its interaction with the OXT system. Lower serum endocannabinoid levels have been reported in children with ASD (Aran et al., 2019), and there is initial evidence of its effectiveness in improving ASD comorbidities such as self-injury, hyperactivity, and anxiety (Poleg et al., 2019).

Last, dysfunction in the DA system has also been observed in ASD, although with apparently conflicting results, with some studies reporting an overstimulation and others a downregulation of DA transmission. To conceal these results, a DA hypothesis of ASD has been proposed, in which upregulation of the DA nigrostriatal pathway would lead to the stereotypic/repetitive behaviors in ASD, while downregulation of the mesocorticolimbic pathway would lead to social deficits (Paval, 2017). The relevance of the DA system in ASD is evident by the fact that the only Food and Drug Administration (FDA)-approved pharmacotherapy to treat associated symptoms in ASD, such as irritability and aggression, are atypical antipsychotics (i.e., risperidone and aripiprazole) that antagonize D2R, albeit they show significant metabolic adverse effects (De Hert et al., 2011).

The scarceness of effective therapeutic treatments for autism and its comorbidities are startling, and the undesirable effects of the currently prescribed drugs abundant. Therefore, an important effort is being made to identify new putative therapeutic targets (Famitafreshi and Karimian, 2018). Oligomerization of G protein-coupled receptors (GPCRs) is one of the latest breakthroughs in pharmacology and could be one of the keys to overcome this therapeutic barrier. In this review, we first introduce the concept of GPCR heteromers. Second, we present different GPCR heteromers that could be of interest as putative pharmacotherapeutic targets in autism. Last, we present some pharmacological tools that are already available to modulate them (**Figure 1**).

G PROTEIN-COUPLED RECEPTOR HETEROMERS AS PHARMACOLOGICAL TARGETS

Heteromer History

GPCR are seven-transmembrane (TM) domain proteins involved in cell-to-cell signalization and are the target of 30–40% of current pharmaceutical drugs (Albizu et al., 2010). While oligomerization is a common biological process, the concept of GPCR oligomerization was not introduced until the 1980's (Agnati et al., 1980, 1982; Birdsall, 1982; Avissar et al., 1983). A relevant historic episode was the discovery of $GABA_B$ receptor dimerization, an obligate receptor dimer (Jones et al., 1998; Kaupmann et al., 1998; Kuner et al., 1999; White et al., 1998; Margeta-Mitrovic et al., 2000). Since

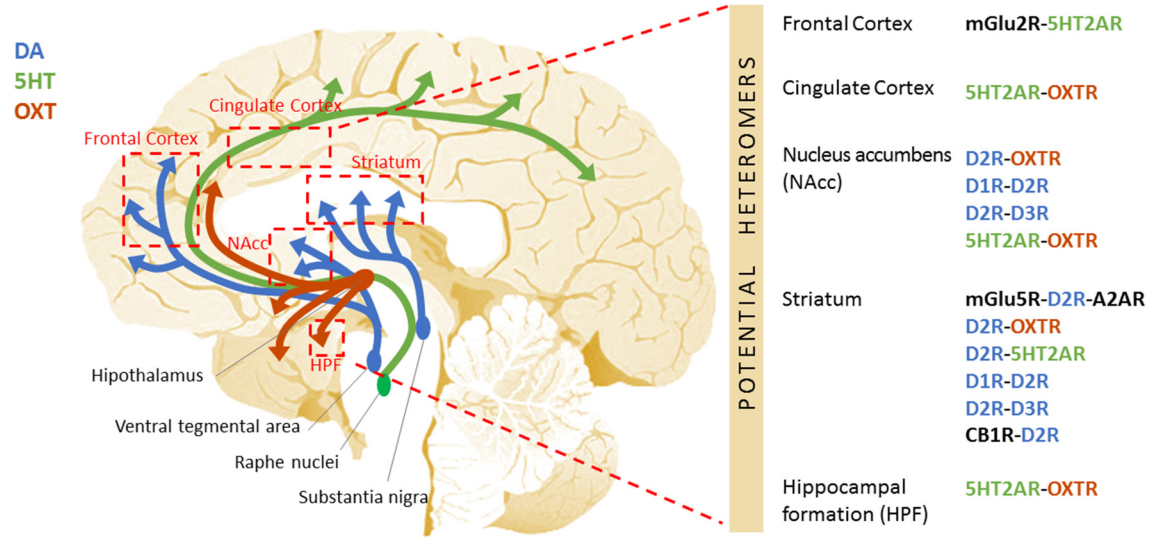

FIGURE 1 | Schematic representation of the potential GPCR heteromers proposed as new therapeutic targets to treat autism. Aside from the widely studied GABAergic and glutamatergic systems, other neurotransmitter systems are critical for the fine-tuning of the excitatory/inhibitory imbalance described in autism. Among these are the dopaminergic, serotonergic, oxytocinergic, and cannabinoid systems. The specific receptors for these neurotransmitters equally represent putative therapeutic targets. Further, these GPCRs heteromers have been shown to display properties that differ from those of their individual components, leading to the activation of distinctive cellular signaling pathways. Differences in the GPCR interactome may underlie the etiology/pathophysiology of autism. This figure shows the DA (blue), 5HT (green), and OXT (red) neural circuits, and the brain regions they connect to (red boxes) where the existence of GPCR heteromers has been described in mammalian brain (mouse, rat, primate, or human). On the right side, the specific GPCR heteromers found in each of these regions are specified.

then, several receptor homomers and heteromers have been discovered in the central nervous system (Moreno et al., 2013). Oligomerization exerts significant impact on receptor function and physiology, offering a platform for the diversification of receptor signaling, pharmacology, regulation, crosstalk, internalization, and trafficking (Farran, 2017). Therefore, heteromers could constitute important therapeutic targets for a wide range of disorders, including ASD.

Heteromer Definition Criteria

Receptor heteromers are oligomeric complexes composed of at least two functional receptor units (i.e., protomers), which interact with each other through the TM domains and show different biochemical properties from those of their individual components (Ferré et al., 2009; Gomes et al., 2016). The International Union of Basic and Clinical Pharmacology proposed five recommendations for the recognition and acceptance of receptor heteromers in the scientific community, and at least two of these criteria should be met for this designation: (1) evidence for physical association in native or primary cells; (2) colocalization of the protomers within the same subcellular compartment in the same cell; (3) proof of the physical interaction between the two receptor protomers in native tissue using coimmunoprecipitation experiments, energy transfer technologies, or transgenic animals expressing physiological levels of recombinant fluorescent proteins; (4) identification of a unique pharmacological property specific of the heteromer; and (5) demonstration of *in vivo* heteromerization using knockout animals or RNAi technology.

PUTATIVE G PROTEIN-COUPLED RECEPTOR HETEROMERS IMPLICATED IN AUTISM

Several GPCR heteromers containing receptors involved in the etiology/pathophysiology of autism, including glutamatergic, DA, OXT, and 5HT receptors, have been described. Dysfunction in the formation and/or function of such heteromers could potentially contribute to the disorder, as has already been suggested for other brain disorders such as schizophrenia. These GPCR heteromers might, thus, represent new pharmacotherapeutic targets for autism (**Figure 2**).

mGlu2R–5HT2AR

mGlu2R and 5HT2AR have been shown to colocalize and interact with each other in mouse and human frontal cortex (Delille et al., 2013; Moreno et al., 2016). Although mGlu2R is coupled to Gi/o proteins and 5HT2AR to Gq/11, it has been shown that acting through the mGlu2R–5HT2AR heterocomplex, both 5HT and glutamatergic ligands modulate Gq/11- and Gi/o-dependent signaling (Fribourg et al., 2011). The pathophysiological role of the heterocomplex has been mainly studied in relation to psychosis and schizophrenia, where altered signaling through this heteromer has been observed (González-Maeso et al., 2008; Moreno et al., 2016; Shah and González-Maeso, 2019). Further, observations in mice and cultured cells suggest that the mGluR2–5HT2AR complex, and not 5HT2AR alone, is the molecular target responsible for the actions of hallucinogenic drugs such as lysergic acid diethylamide (LSD) and that activation of mGlu2R abolishes hallucinogen-specific

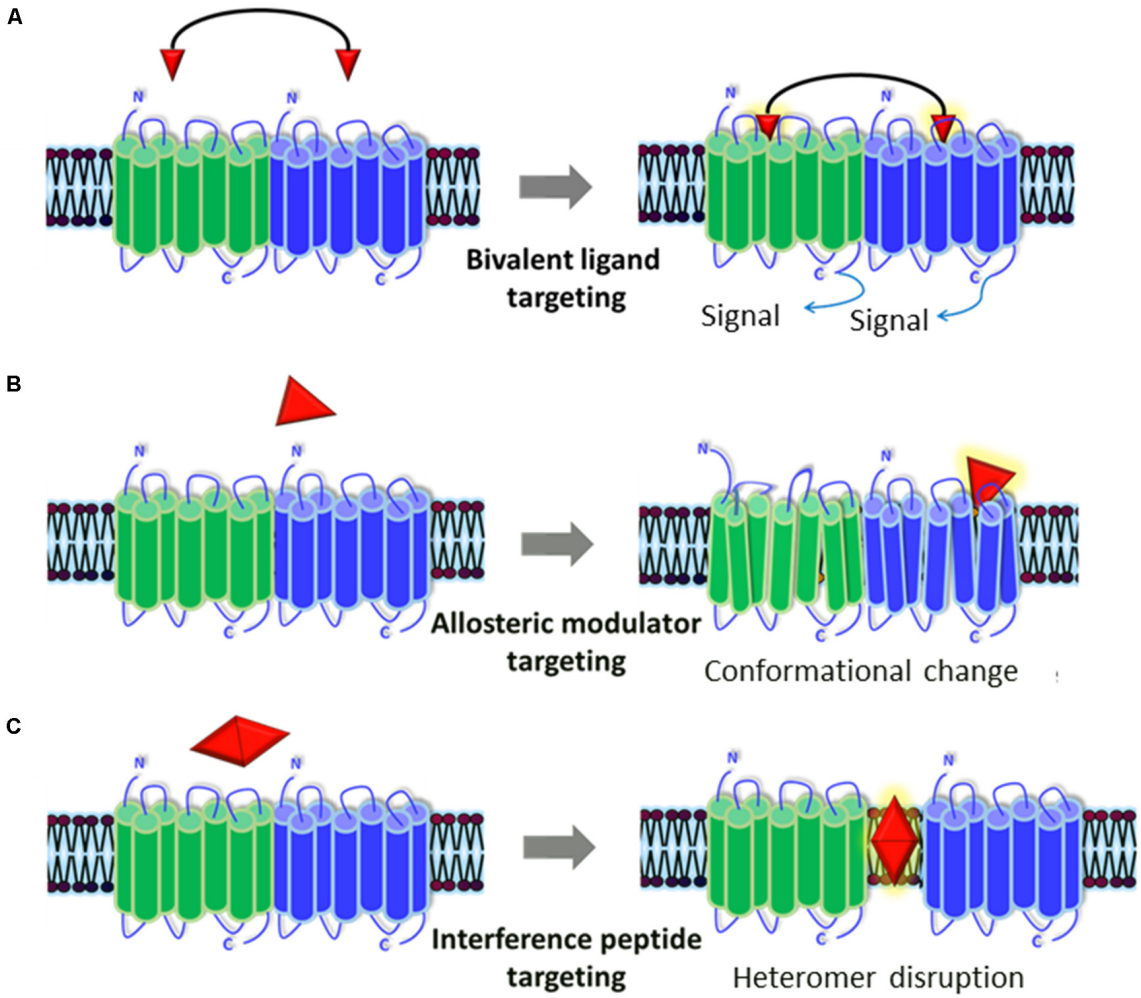

FIGURE 2 | Representation of the pharmacological tools to modulate GPCR heteromers. Currently available pharmacological tools to modulate the generation and/or signaling of receptor heteromers could represent new therapeutic strategies for ASD. **(A)** Bivalent ligands are composed of two functional pharmacophores, linked by a spacer, that interact with each of the protomers of the heteromers and activate/block its cellular signaling cascade(s). **(B)** Allosteric modulators bind to distinct binding sites from the endogenous ligands in one of the protomers and can alter its structure (producing a conformational change), dynamics, and function, which will in turn alter the whole heteromer's functionality. **(C)** Interference peptides are synthetic peptides harboring the same amino acid sequence as the interacting transmembrane (TM) domains between the two receptors that compose the heteromer: they get inserted into TM domains and disrupt the receptor heteromer by preventing binding between the two receptor protomers.

signaling and behavioral responses (González-Maeso et al., 2008; Moreno et al., 2011; Halberstadt et al., 2019). Although so far no study has assessed the role of mGlu2R–5HT2AR heteromer in ASD, its association with schizophrenia, a disorder that shares some risk factors and displays overlapping traits with ASD, including neuroimaging evidence and mutual comorbidity (Chisholm et al., 2015), indicates that its evaluation would be worthwhile. Thus, the evaluation of mGlu2R–5HT2AR complex in ASD animal models and/or postmortem human brain could bring new approaches to understand the disorder and find new pharmacological targets.

mGlu5R–D2R–A2AR

The existence of mGlu5R–D2R–A2AR oligomers has been reported in native rat striatum and GABAergic striatopallidal neurons, where they are mainly formed (Simola et al., 2008; Cabello et al., 2009; Lewis et al., 2019). This heteromer might be of relevance in ASD due to its putative role in repetitive behavior and reward. A recent study has evaluated the potential effect of different drug combinations on the repetitive behaviors characteristic of deer mice: no single drug or double-drug combinations were effective, albeit the combination of a D2R antagonist, an A2AR agonist, and an mGlu5R positive allosteric modulator reduced repetitive behaviors. In contrast, the combination of a D2R agonist, an A2AR antagonist, and an mGlu5R negative allosteric modulator caused a significant increase in repetitive behavior (Lewis et al., 2019). Regarding the reward system, the antidepressant basimglurant, an mGlu5R negative allosteric modulator, has been proposed to reduce the anti-reward effect exerted by

GABA neurons of the ventral striatopallidal pathway, because it inhibits D2R signaling in A2A–D2–mGlu5 receptor heteromers (Fuxe and Borroto-Escuela, 2015). This D2R signal reduction in striatopallidal GABA neurons has also been reported with a combination of an mGlu5R antagonist and an A2AR antagonist (Beggiato et al., 2016). Thus, selectively modulating the functionality of this oligomer through any of its protomers could constitute a novel approach to treat repetitive behaviors in ASD and to improve social interaction through the reward system.

D2R–OXTR

D2R–OXTR heteromers' existence has been revealed in the nucleus accumbens (NAcc) and dorsal striatum of female prairie voles, a species widely used to investigate social behavior (Fuxe et al., 2014). In terms of physiology, radio-ligand experiments in voles with NAcc membrane preparations demonstrated that OXT very significantly modified the affinity of D2R antagonists and agonists, an effect that was blocked by an OXTR antagonist (Fuxe et al., 2014). The co-activation of D2R and OXTR in NAcc has been reported to be necessary for pair bond formation in female voles (Baskerville and Douglas, 2010). Moreover, OXT administration increases NAcc DA release and improves social behavior in rats (Kohli et al., 2019). Hence, difficulties in developing social bonds in ASD could be possibly improved by the activation of D2R–OXTR heteromer in NAcc. In addition, OXT infusion into the central amygdala elicited anxiolytic effects in rats, which was prevented with a simultaneous infusion of a D2/D3 antagonist, suggesting the involvement of the D2R–OXTR heteromer in this brain region. In consequence, OXT's potential benefit for reducing anxiety in ASD may rely on targeting the D2R–OXTR heteromer, possibly in the amygdala.

CB1R–D2R

The presence of the CB1R–D2R heteromer has been recently reported in the globus pallidus in mice (Bagher et al., 2020). The heteromer activation is characterized by an antagonistic interaction between the protomers, with CB1R agonists reducing the affinity and hyper-locomotor activity exerted by D2R agonists (Marcellino et al., 2008). For this reason, targeting CB1R–D2R with CB1R agonists in striatum may be a pharmacological alternative to treat irritability or hyperactivity in ASD. In addition, immunoelectron microscopy suggests that, in mice, CB1R and D2Rs colocalize in GABAergic terminals of the PFC, in which activation of either receptor could suppress GABA release onto layer 5 pyramidal cells (Chiu et al., 2010). Thus, targeting CB1R–D2R might also represent a novel strategy to improve the excitatory/inhibitory imbalance in ASD.

D2R–5HT2AR

Existence of 5HT2AR–D2R heteromers has been demonstrated in rat striatum (Borroto-Escuela et al., 2014). The heteromer displays bidirectional receptor–receptor interaction, D2R agonists increasing hallucinogenic agonists' affinity for 5HT2AR (Albizu et al., 2011), and *vice versa*, hallucinogenic 5HT2AR agonists increasing D2R density (Borroto-Escuela et al., 2014). Thus, the simultaneous antagonization of both protomers has been proposed as an antipsychotic strategy, with fewer side effects and lower doses required (Borroto-Escuela et al., 2014; Zhang et al., 2020). In fact, the advantageous extrapyramidal side-effect profile of the atypical antipsychotic risperidone, which behaves as a D2R and 5HT2A antagonist and is one of the most widely used drugs to treat associated symptoms in ASD, would rely on targeting the dimer and/or inducing its oligomerization (Borroto-Escuela et al., 2014; Kolasa et al., 2018). In agreement with this, a recent computational model of 3D structure–activity relationship of D2R and 5HT2AR antagonists reported that targeting the heteromer simultaneously significantly reduced extrapyramidal side effects of antipsychotic treatment (Zhang et al., 2020).

D1R–D2R

D1R–D2R heteromer was demonstrated in rat and nonhuman primate NAcc (Perreault et al., 2016; Rico et al., 2017) and in human striatum (Pei et al., 2010). The pathophysiological role of this heteromer has been largely studied in depression and anxiety, which are two of the most common comorbidities in ASD (Simonoff et al., 2008). D1R–D2R heteromer formation was found to be increased in human postmortem striatum of subjects with major depression (Pei et al., 2010), and disrupting the dimer in rats produced antidepressant (Hasbi et al., 2014) and anxiolytic effects (Shen et al., 2015). A recent study reported overexpressed D1R–D2R heteromers in female nonhuman primate and rat brain, along with higher depressive-like and anxiety-like behaviors, which are improved by disruption of the dimer (Hasbi et al., 2020). In consequence, D1R–D2R heteromer disruption might be an alternative treatment for individuals with depressive or anxiety symptoms in ASD and potentially more effective in female subjects. Further, the D1R–D2R heteromer might also modulate social behavior through the reward pathway, as disrupting this heteromer in the NAcc has been shown to increase the rewarding effects of drugs of abuse in rats (Perreault et al., 2016).

D2R–D3R

Colocalization of D2R and D3R was detected in the globus pallidus and NAcc of rats (Surmeier et al., 1997), and their interaction was determined by co-immunoprecipitation studies in cultured cells (Scarselli et al., 2001). A putative role for the D2R–D3R heteromer as a target for antipsychotics has been suggested, since antipsychotics with partial D2R agonist properties act as D2R antagonists in the presence of the dimer (Maggio and Millan, 2010). This has strong implications for ASD as aripiprazole, one of the most widely used antipsychotics to treat irritability in autism (Goel et al., 2018), is a partial D2R agonist that would act as antagonist in brain areas where the heterodimer is expressed, gaining brain region-specific effects (Maggio and Millan, 2010). This property of aripiprazole has been proposed to account for the fewer extrapyramidal effects elicited by this drug (Maggio et al., 2015).

5HT2AR–OXTR

Despite the abundant evidence across species of the interaction between the OXT and 5HT systems in the regulation of

socio-cognitive behaviors (Lefevre et al., 2017; Nagano et al., 2018; Tan et al., 2020), anxiety (Yoshida et al., 2009), and reward (Aubert et al., 2013; Dölen et al., 2013), only one recent report has provided evidence of the existence of a 5HT2AR–OXTR heterodimer, which was detected in in rat hippocampus, cingulate cortex, and NAcc, key regions associated with cognition and the above-described behaviors (Chruścicka et al., 2019). The authors, using functional cellular-based assays, proved that the 5HT2AR–OXTR heterocomplex formation leads to bidirectional antagonistic receptor−receptor interactions, reducing Gαq signaling (Chruścicka et al., 2019). The implication of this recently identified heteromer in a pathological state has not been evaluated yet, but it might potentially be an interesting target to improve social behavior and anxiety in ASD.

PHARMACOLOGICAL TOOLS TO MODULATE RECEPTOR HETEROMERS

Currently, there are several pharmacological tools that allow the modulation of receptor heteromers. These include bivalent ligands, allosteric modulators, and interference peptides.

Bivalent Ligands

Bivalent ligands are composed of two functional pharmacophores, linked by a spacer, each with potential of interacting with a protomer of the dimeric receptor (Berque-Bestel et al., 2008). Bivalent ligands of the μ opioid receptor (μOR) were the first to be developed, demonstrating that stimulation of the heteroreceptors δOR-μOR, μOR-CB1R, or μOR-mGlu5R reduced nociception to a bigger extent than morphine and without some of its adverse effects such as tolerance, dependence, and respiratory depression (Gomes et al., 2016; Machelska and Celik, 2018). Hence, using bivalent ligands to target the heteromers potentially affected in ASD, as discussed above, could be more efficient than targeting the receptors separately. For instance, antagonist bivalent ligands targeting D2R–5HT2AR or D2R–D3R heteromers could be an alternative to current antipsychotics to improve irritability, and agonist bivalent ligands targeting D2R–OXTR could be beneficial for social behavior.

Allosteric Modulators

Allosteric sites of GPCR are distinct from binding sites for endogenous ligands and can alter the receptor structure, dynamics, and function in order to achieve a potential therapeutic advantage (Hauser et al., 2017). Positive allosteric modulators increase the effect of agonists, in contrast to negative allosteric modulators that inhibit their effect. Selective modulators of receptor heteromers could expand the range of therapeutic options to treat autism. For instance, mGlu5R positive allosteric modulator targeting mGlu5R–D2R–A2AR heteromer in combination with other drugs, such as a D2R antagonist and an A2AR agonist, as described above (Lewis et al., 2019), may improve repetitive behavior symptoms in ASD.

Interference Peptides

Interference peptides are synthetic peptides harboring the same amino acid sequence as the interacting TM domains between the two receptors that compose the heteromer (Botta et al., 2019). These peptides harbor a small signal peptide that facilitates penetration in the cell. They get inserted into TM domains, disrupting the receptor heteromer by preventing binding between the two receptor protomers. Interference peptides have contributed to validate and understand the functional consequences of receptor oligomerization and could become an alternative to treat ASD. As above mentioned, disrupting D1R–D2R receptor heteromer could be beneficial for individuals with autism due to its anxiolytic and antidepressant effect (Hasbi et al., 2014; Shen et al., 2015). Nevertheless, more efficient interference peptides need to be developed, since their *in vivo* efficacy is often compromised by the loss of secondary structure, deficient cellular penetration, and susceptibility to proteolysis in the digestive system (Botta et al., 2019).

CONCLUSION AND FUTURE DIRECTIONS

There is no doubt that alterations in the GABAergic, glutamatergic, OXT, 5HT, DA, and CB systems are associated with ASD. In an attempt to search for novel targeted therapeutic approaches to treat ASD and overcome the scarceness of effective pharmacological treatments, we propose a potential role for heterocomplexes formed by different receptors of these neurotransmitters. Oligomerization of GPCRs is one of the latest breakthroughs in pharmacology and could be one of the keys to overcome this therapeutic barrier. There is increasing evidence for the role of GPCR heteromers in the pathophysiology of other neuropsychiatric disorders, such as depression or schizophrenia, albeit no study has yet addressed this issue in autism. Postmortem brain samples provide a unique opportunity to advance molecular research in this regard (McCullumsmith et al., 2014). For example, coupling between dopamine D1 and D2 receptors was markedly increased in postmortem brain of subjects suffering from major depression, as detected by co-immunoprecipitation experiments (Pei et al., 2010). Blue native polyacrylamide gel electrophoresis is also a useful technique for this aim, as has already been used to observe alterations in receptor complexes in human brain for other diseases (Falsafi et al., 2016). Further, functional scintillation proximity assays for [35S]GTPγS binding have revealed dysregulated signaling *via* the mGlu2R–5HT2AR heteromer in postmortem human brain samples of schizophrenia subjects (Moreno et al., 2016). Once a potential molecular alteration is identified, existing pharmacological strategies to selectively modulate these GPCR heteromers could be tested to ascertain their potential to become new therapeutic treatments to improve some symptoms of ASD. Animal models provide a useful tool for mechanistic and behavioral outcome measures to address this issue. There are several well-validated animal models of ASD available (Möhrle et al., 2020), in which the expression of the above-mentioned GPCR heteromers could be quantified. In case that any of the complexes are found to be altered compared with those in control mice, a modulation of the heteromer function

could be attempted using the modifiers described above, in order to assess whether it drives a behavioral improvement. In conclusion, the integrative use of ASD animal models and clinical subjects to understand the potential role of GPCR heteromers as mechanistic cause and putative pharmacological targets could open a new direction in understanding and treating ASD.

AUTHOR CONTRIBUTIONS

JD-B drafted the article. AE and OP contributed equally in the conception, design and supervision of the work. All authors contributed adding critical information in the different sections and helped shape the manuscript and design the figures. All authors contributed to the article and approved the submitted version.

FUNDING

This work was funded by the Spanish Ministry of Science, Technology and Research, the Spanish State Research Agency and European Regional Development Fund (MCIU/AEI/FEDER, UE) grants RTI2018-101427-B-I00 to OP and RTI2018-094414-A-I00 to AE, and the UPV/EHU collaborative project (COLAB19/09) to OP and AE.

REFERENCES

Agnati, L. F., Fuxe, K., Zini, I., Lenzi, P., and Hökfelt, T. (1980). Aspects on receptor regulation and isoreceptor identification. *Med. Biol.* 58, 182–187.

Agnati, L. F., Fuxe, K., Zoli, M., Rondanini, C., and Ogren, S. O. (1982). New vistas on synaptic plasticity: the receptor mosaic hypothesis of the engram. *Med. Biol.* 60, 183–190.

Albizu, L., Holloway, T., González-Maeso, J., and Sealfon, S. C. (2011). Functional crosstalk and heteromerization of serotonin 5-HT2A and dopamine D2 receptors. *Neuropharmacology* 61, 770–777. doi: 10.1016/j.neuropharm.2011.05.023

Albizu, L., L. Moreno, J., Gonzalez-Maeso, J., and C. Sealfon, S. (2010). Heteromerization of G protein-coupled receptors: relevance to neurological disorders and neurotherapeutics. *CNS Neurol. Disord. Drug Targets* 9, 636–650. doi: 10.2174/187152710793361586

American Psychiatric Association (Ed.). (2013). *Diagnostic and Statistical Manual of Mental Disorders: DSM-5.* 5th edition. Arlington: American Psychiatric Association.

Andari, E., Duhamel, J.-R., Zalla, T., Herbrecht, E., Leboyer, M., and Sirigu, A. (2010). Promoting social behavior with oxytocin in high-functioning autism spectrum disorders. *Proc. Natl. Acad. Sci. U S A* 107, 4389–4394. doi: 10.1073/pnas.0910249107

Aran, A., Eylon, M., Harel, M., Polianski, L., Nemirovski, A., Tepper, S., et al. (2019). Lower circulating endocannabinoid levels in children with autism spectrum disorder. *Mol. Autism* 10:2. doi: 10.1186/s13229-019-0256-6

Aubert, Y., Allers, K. A., Sommer, B., de Kloet, E. R., Abbott, D. H., and Datson, N. A. (2013). Brain region-specific transcriptomic markers of serotonin-1a receptor agonist action mediating sexual rejection and aggression in female marmoset monkeys. *J. Sex. Med.* 10, 1461–1475. doi: 10.1111/jsm.12131

Avissar, S., Amitai, G., and Sokolovsky, M. (1983). Oligomeric structure of muscarinic receptors is shown by photoaffinity labeling: subunit assembly may explain high- and low-affinity agonist states. *Proc. Natl. Acad. Sci. U S A* 80, 156–159. doi: 10.1073/pnas.80.1.156

Aydın, O., Lysaker, P. H., Balıkçı, K., Ünal-Aydın, P., and Esen-Danacı, A. (2018). Associations of oxytocin and vasopressin plasma levels with neurocognitive, social cognitive and meta cognitive function in schizophrenia. *Psychiatry Res.* 270, 1010–1016. doi: 10.1016/j.psychres.2018.03.048

Bagher, A. M., Young, A. P., Laprairie, R. B., Toguri, J. T., Kelly, M. E. M., and Denovan-Wright, E. M. (2020). Heteromer formation between cannabinoid type 1 and dopamine type 2 receptors is altered by combination cannabinoid and antipsychotic treatments. *J. Neurosci. Res.* 98, 2109–2369. doi: 10.1002/jnr.24716

Bai, D., Yip, B. H. K., Windham, G. C., Sourander, A., Francis, R., Yoffe, R., et al. (2019). Association of genetic and environmental factors with autism in a 5-country cohort. *JAMA Psychiatry* 76, 1035–1043. doi: 10.1001/jamapsychiatry.2019.1411

Baskerville, T. A., and Douglas, A. J. (2010). Dopamine and oxytocin interactions underlying behaviors: potential contributions to behavioral disorders: dopamine and oxytocin interactions underlying behaviors. *CNS Neurosci. Ther.* 16, e92–e123. doi: 10.1111/j.1755-5949.2010.00154.x

Beggiato, S., Tomasini, M. C., Borelli, A. C., Borroto-Escuela, D. O., Fuxe, K., Antonelli, T., et al. (2016). Functional role of striatal A2A, D2 and mGlu5 receptor interactions in regulating striatopallidal GABA neuronal transmission. *J. Neurochem.* 138, 254–264. doi: 10.1111/jnc.13652

Berque-Bestel, I., Lezoualc'h, F., and Jockers, R. (2008). Bivalent ligands as specific pharmacological tools for G protein-coupled receptor dimers. *Curr. Drug Discov. Technol.* 5, 312–318. doi: 10.2174/157016308786733591

Birdsall, N. J. M. (1982). Can different receptors interact directly with each other? *Trends Neurosci.* 5, 137–138. doi: 10.1016/0166-2236(82)90081-9

Borroto-Escuela, D. O., Romero-Fernandez, W., Narvaez, M., Oflijan, J., Agnati, L. F., and Fuxe, K. (2014). Hallucinogenic 5-HT2AR agonists LSD and DOI enhance dopamine D2R protomer recognition and signaling of D2-5-HT2A heteroreceptor complexes. *Biochem. Biophys. Res. Commun.* 443, 278–284. doi: 10.1016/j.bbrc.2013.11.104

Botta, J., Bibic, L., Killoran, P., McCormick, P. J., and Howell, L. A. (2019). Design and development of stapled transmembrane peptides that disrupt the activity of G-protein-coupled receptor oligomers. *J. Biol. Chem.* 294, 16587–16603. doi: 10.1074/jbc.RA119.009160

Cabello, N., Gandía, J., Bertarelli, D. C. G., Watanabe, M., Lluís, C., Franco, R., et al. (2009). Metabotropic glutamate type 5, dopamine D_2 and adenosine A_{2a} receptors form higher-order oligomers in living cells. *J. Neurochem.* 109, 1497–1507. doi: 10.1111/j.1471-4159.2009.06078.x

Chisholm, K., Lin, A., Abu-Akel, A., and Wood, S. J. (2015). The association between autism and schizophrenia spectrum disorders: a review of eight alternate models of co-occurrence. *Neurosci. Biobehav. Rev.* 55, 173–183. doi: 10.1016/j.neubiorev.2015.04.012

Chiu, C. Q., Puente, N., Grandes, P., and Castillo, P. E. (2010). Dopaminergic modulation of endocannabinoid-mediated plasticity at GABAergic synapses in the prefrontal cortex. *J. Neurosci.* 30, 7236–7248. doi: 10.1523/JNEUROSCI.0736-10.2010

Chruścicka, B., Wallace Fitzsimons, S. E., Borroto-Escuela, D. O., Druelle, C., Stamou, P., Nally, K., et al. (2019). Attenuation of oxytocin and serotonin 2A receptor signaling through novel heteroreceptor formation. *ACS Chem. Neurosci.* 10, 3225–3240. doi: 10.1021/acschemneuro.8b00665

Cook, E. H. (1990). Autism: review of neurochemical investigation. *Synapse* 6, 292–308. doi: 10.1002/syn.890060309

De Hert, M., Dobbelaere, M., Sheridan, E. M., Cohen, D., and Correll, C. U. (2011). Metabolic and endocrine adverse effects of second-generation antipsychotics in children and adolescents: a systematic review of randomized, placebo controlled trials and guidelines for clinical practice. *Eur. Psychiatry* 26, 144–158. doi: 10.1016/j.eurpsy.2010.09.011

Delille, H. K., Mezler, M., and Marek, G. J. (2013). The two faces of the pharmacological interaction of mGlu2 and 5-HT2A—relevance of receptor heterocomplexes and interaction through functional brain pathways. *Neuropharmacology* 70, 296–305. doi: 10.1016/ j.neuropharm.2013.02.005

Dölen, G., Darvishzadeh, A., Huang, K. W., and Malenka, R. C. (2013). Social reward requires coordinated activity of nucleus accumbens oxytocin and serotonin. *Nature* 501, 179–184. doi: 10.1038/nature12518

Ecker, C., Bookheimer, S. Y., and Murphy, D. G. M. (2015). Neuroimaging in autism spectrum disorder: brain structure and function across the lifespan. *Lancet Neurol.* 14, 1121–1134. doi: 10.1016/S1474-4422(15)00050-2

Erdozain, A. M., and Peñagarikano, O. (2020). Oxytocin as treatment for social cognition, not there yet. *Front. Psychiatry* 10:930. doi: 10.3389/fpsyt.2019.00930

Falsafi, S. K., Dierssen, M., Ghafari, M., Pollak, A., and Lubec, G. (2016). Reduced cortical neurotransmitter receptor complex levels in fetal Down syndrome brain. *Amino Acids* 48, 103–116. doi: 10.1007/s00726-015-2062-6

Famitafreshi, H., and Karimian, M. (2018). Overview of the recent advances in pathophysiology and treatment for autism. *CNS Neurol. Disord. Drug Targets* 17, 590–594. doi: 10.2174/1871527317666180706141654

Farran, B. (2017). An update on the physiological and therapeutic relevance of GPCR oligomers. *Pharmacol. Res.* 117, 303–327. doi: 10.1016/j.phrs.2017.01.008

Fernández, M., Mollinedo-Gajate, I., and Peñagarikano, O. (2018). Neural circuits for social cognition: implications for autism. *Neuroscience* 370, 148–162. doi: 10.1016/j.neuroscience.2017.07.013

Ferré, S., Baler, R., Bouvier, M., Caron, M. G., Devi, L. A., Durroux, T., et al. (2009). Building a new conceptual framework for receptor heteromers. *Nat. Chem. Biol.* 5, 131–134. doi: 10.1038/nchembio0309-131

Fribourg, M., Moreno, J. L., Holloway, T., Provasi, D., Baki, L., Mahajan, R., et al. (2011). Decoding the signaling of a GPCR heteromeric complex reveals a unifying mechanism of action of antipsychotic drugs. *Cell* 147, 1011–1023. doi: 10.1016/j.cell.2011.09.055

Fuxe, K., and Borroto-Escuela, D. O. (2015). Basimglurant for treatment of major depressive disorder: a novel negative allosteric modulator of metabotropic glutamate receptor 5. *Expert Opin. Investig. Drugs* 24, 1247–1260. doi: 10.1517/13543784.2015.1074175

Fuxe, K., Borroto-Escuela, D. O., Tarakanov, A. O., Romero-Fernandez, W., Ferraro, L., Tanganelli, S., et al. (2014). "Dopamine D2 heteroreceptor complexes and their receptor-receptor interactions in ventral striatum," in *Progress in Brain Research*, eds M. Diana, G. Di Chiara and P. Spano (Amsterdam: Elsevier), 113–139.

Goel, R., Hong, J. S., Findling, R. L., and Ji, N. Y. (2018). An update on pharmacotherapy of autism spectrum disorder in children and adolescents. *Int. Rev. Psychiatry* 30, 78–95. doi: 10.1080/09540261.2018.1458706

Gomes, I., Ayoub, M. A., Fujita, W., Jaeger, W. C., Pfleger, K. D. G., and Devi, L. A. (2016). G protein-coupled receptor heteromers. *Annu. Rev. Pharmacol. Toxicol.* 56, 403–425. doi: 10.1146/annurev-pharmtox-011613-135952

González-Maeso, J., Ang, R. L., Yuen, T., Chan, P., Weisstaub, N. V., López-Giménez, J. F., et al. (2008). Identification of a serotonin/glutamate receptor complex implicated in psychosis. *Nature* 452, 93–97. doi: 10.1038/nature06612

Halberstadt, A. L., van der Zee, J. V. F., Chatha, M., Geyer, M. A., and Powell, S. B. (2019). Chronic treatment with a metabotropic mGlu2/3 receptor agonist diminishes behavioral response to a phenethylamine hallucinogen. *Psychopharmacology* 236, 821–830. doi: 10.1007/s00213-018-5118-y

Hanley, H. G. (1977). Hyperserotonemia and amine metabolites in autistic and retarded children. *Arch. Gen. Psychiatry* 34, 521–531. doi: 10.1001/archpsyc.1977.01770170031002

Hasbi, A., Perreault, M. L., Shen, M. Y. F., Zhang, L., To, R., Fan, T., et al. (2014). A peptide targeting an interaction interface disrupts the dopamine D1-D2 receptor heteromer to block signaling and function *in vitro* and *in vivo*: effective selective antagonism. *FASEB J.* 28, 4806–4820. doi: 10.1096/fj.14-254037

Hasbi, A., Nguyen, T., Rahal, H., Manduca, J. D., Miksys, S., Tyndale, R. F., et al. (2020). Sex difference in dopamine D1–D2 receptor complex expression and signaling affects depression- and anxiety-like behaviors. *Biol. Sex Differ.* 11:8. doi: 10.1186/s13293-020-00285-9

Hauser, A. S., Attwood, M. M., Rask-Andersen, M., Schiöth, H. B., and Gloriam, D. E. (2017). Trends in GPCR drug discovery: new agents, targets and indications. *Nat. Rev. Drug Discov.* 16, 829–842. doi: 10.1038/nrd.2017.178

Insel, T. R. (2010). The challenge of translation in social neuroscience: a review of oxytocin, vasopressin and affiliative behavior. *Neuron* 65, 768–779. doi: 10.1016/j.neuron.2010.03.005

Jones, K. A., Borowsky, B., Tamm, J. A., Craig, D. A., Durkin, M. M., Dai, M., et al. (1998). GABA(B) receptors function as a heteromeric assembly of the subunits GABA(B)R1 and GABA(B)R2. *Nature* 396, 674–679. doi: 10.1038/25348

Jupiter, J. B., First, K., Gallico, G. G. III, and May, J. W. (1988). The role of external fixation in the treatment of posttraumatic osteomyelitis. *J. Orthop. Trauma* 2, 79–93. doi: 10.1097/00005131-198802010-00001

Kaupmann, K., Malitschek, B., Schuler, V., Heid, J., Froestl, W., Beck, P., et al. (1998). GABA(B)-receptor subtypes assemble into functional heteromeric complexes. *Nature* 396, 683–687. doi: 10.1038/25360

Kennedy, D. P., and Adolphs, R. (2012). The social brain in psychiatric and neurological disorders. *Trends Cogn. Sci.* 16, 559–572. doi: 10.1016/j.tics.2012.09.006

King, B. H., Hollander, E., Sikich, L., McCracken, J. T., Scahill, L., Bregman, J. D., et al. (2009). Lack of efficacy of citalopram in children with autism spectrum disorders and high levels of repetitive behavior: citalopram ineffective in children with autism. *Arch. Gen. Psychiatry* 66, 583–590. doi: 10.1001/archgenpsychiatry.2009.30

Kohli, S., King, M. V., Williams, S., Edwards, A., Ballard, T. M., Steward, L. J., et al. (2019). Oxytocin attenuates phencyclidine hyperactivity and increases social interaction and nucleus accumben dopamine release in rats. *Neuropsychopharmacology* 44, 295–305. doi: 10.1038/s41386-018-0171-0

Kolasa, M., Solich, J., Faron-Górecka, A., Żurawek, D., Pabian, P., Łukasiewicz, S., et al. (2018). Paroxetine and low-dose risperidone induce serotonin 5-HT1A and dopamine D2 receptor heteromerization in the mouse prefrontal cortex. *Neuroscience* 377, 184–196. doi: 10.1016/j.neuroscience.2018.03.004

Kuner, R., Köhr, G., Grünewald, S., Eisenhardt, G., Bach, A., and Kornau, H. C. (1999). Role of heteromer formation in GABAB receptor function. *Science* 283, 74–77. doi: 10.1126/science.283.5398.74

Lee, P. R., Brady, D. L., Shapiro, R. A., Dorsa, D. M., and Koenig, J. I. (2007). Prenatal stress generates deficits in rat social behavior: reversal by oxytocin. *Brain Res.* 1156, 152–167. doi: 10.1016/j.brainres.2007.04.042

Lefevre, A., Richard, N., Jazayeri, M., Beuriat, P.-A., Fieux, S., Zimmer, L., et al. (2017). Oxytocin and serotonin brain mechanisms in the nonhuman primate. *J. Neurosci.* 37, 6741–6750. doi: 10.1523/JNEUROSCI.0659-17.2017

Lewis, M. H., Primiani, C. T., and Muehlmann, A. M. (2019). Targeting dopamine D_2, adenosine A_{2A} and glutamate $mGlu_5$ receptors to reduce repetitive behaviors in deer mice. *J. Pharmacol. Exp. Ther.* 370:218. doi: 10.1124/jpet.118.256081err2

Machelska, H., and Celik, M. Ö. (2018). Advances in achieving opioid analgesia without side effects. *Front. Pharmacol.* 9:1388. doi: 10.3389/fphar.2018.01388

Maggio, R., and Millan, M. J. (2010). Dopamine D2-D3 receptor heteromers: pharmacological properties and therapeutic significance. *Curr. Opin. Pharmacol.* 10, 100–107. doi: 10.1016/j.coph.2009.10.001

Maggio, R., Scarselli, M., Capannolo, M., and Millan, M. J. (2015). Novel dimensions of D3 receptor function: Focus on heterodimerisation, transactivation and allosteric modulation. *Eur. Neuropsychopharmacol.* 25, 1470–1479. doi: 10.1016/j.euroneuro.2014.09.016

Marcellino, D., Carriba, P., Filip, M., Borgkvist, A., Frankowska, M., Bellido, I., et al. (2008). Antagonistic cannabinoid CB1/dopamine D2 receptor interactions in striatal CB1/D2 heteromers. A combined neurochemical and behavioral analysis. *Neuropharmacology* 54, 815–823. doi: 10.1016/j.neuropharm.2007.12.011

Margeta-Mitrovic, M., Jan, Y. N., and Jan, L. Y. (2000). A trafficking checkpoint controls GABA(B) receptor heterodimerization. *Neuron* 27, 97–106. doi: 10.1016/s0896-6273(00)00012-x

Marotta, R., Risoleo, M. C., Messina, G., Parisi, L., Carotenuto, M., Vetri, L., et al. (2020). The Neurochemistry of Autism. *Brain Sci.* 10:163. doi: 10.3390/brainsci10030163

McCullumsmith, R. E., Hammond, J. H., Shan, D., and Meador-Woodruff, J. H. (2014). Postmortem brain: an underutilized substrate for studying severe mental illness. *Neuropsychopharmacology* 39, 65–87. doi: 10.1038/npp.2013.239

Modahl, C., Green, L. A., Fein, D., Morris, M., Waterhouse, L., Feinstein, C., et al. (1998). Plasma oxytocin levels in autistic children. *Biol. Psychiatry* 43, 270–277. doi: 10.1016/S0006-3223(97)00439-3

Möhrle, D., Fernández, M., Peñagarikano, O., Frick, A., Allman, B., and Schmid, S. (2020). What we can learn from a genetic rodent model about autism. *Neurosci. Biobehav. Rev.* 109, 29–53. doi: 10.1016/j.neubiorev.2019.12.015

Moreno, J. L., Holloway, T., and González-Maeso, J. (2013). "G protein-coupled receptor heterocomplexes in neuropsychiatric disorders," in *Progress*

in Molecular Biology and Translational Science, eds J. Giraldo and F. Ciruela (Cambridge: Academic Press), 187–205.

Moreno, J. L., Holloway, T., Albizu, L., Sealfon, S. C., and González-Maeso, J. (2011). Metabotropic glutamate mGlu2 receptor is necessary for the pharmacological and behavioral effects induced by hallucinogenic 5-HT2A receptor agonists. *Neurosci. Lett.* 493, 76–79. doi: 10.1016/j.neulet.2011.01.046

Moreno, J. L., Miranda-Azpiazu, P., García-Bea, A., Younkin, J., Cui, M., Kozlenkov, A., et al. (2016). Allosteric signaling through an mGlu2 and 5-HT_{2A} heteromeric receptor complex and its potential contribution to schizophrenia. *Sci. Signal.* 9:ra5. doi: 10.1126/scisignal.aab0467

Müller, R.-A., and Fishman, I. (2018). Brain connectivity and neuroimaging of social networks in autism. *Trends Cogn. Sci.* 22, 1103–1116. doi: 10.1016/j.tics.2018.09.008

Murphy, D. G. M., Daly, E., Schmitz, N., Toal, F., Murphy, K., Curran, S., et al. (2006). Cortical serotonin 5-HT_{2A} receptor binding and social communication in adults with asperger's syndrome: an *in vivo* SPECT study. *Am. J. Psychiatry* 163, 934–936. doi: 10.1176/ajp.2006.163.5.934

Nagano, M., Takumi, T., and Suzuki, H. (2018). Critical roles of serotonin-oxytocin interaction during the neonatal period in social behavior in 15q dup mice with autistic traits. *Sci. Rep.* 8:13675. doi: 10.1038/s41598-018-32042-9

Oblak, A., Gibbs, T. T., and Blatt, G. J. (2013). Reduced serotonin receptor subtypes in a limbic and a neocortical region in autism: reduced serotonin receptors in autism. *Autism Res.* 6, 571–583. doi: 10.1002/aur.1317

Paval, D. (2017). A dopamine hypothesis of autism spectrum disorder. *Dev. Neurosci.* 39, 355–360. doi: 10.1159/000478725

Pei, L., Li, S., Wang, M., Diwan, M., Anisman, H., Fletcher, P. J., et al. (2010). Uncoupling the dopamine D1–D2 receptor complex exerts antidepressant-like effects. *Nat. Med.* 16, 1393–1395. doi: 10.1038/nm.2263

Perreault, M. L., Hasbi, A., Shen, M. Y. F., Fan, T., Navarro, G., Fletcher, P. J., et al. (2016). Disruption of a dopamine receptor complex amplifies the actions of cocaine. *Eur. Neuropsychopharmacol.* 26, 1366–1377. doi: 10.1016/j.euroneuro.2016.07.008

Poleg, S., Golubchik, P., Offen, D., and Weizman, A. (2019). Cannabidiol as a suggested candidate for treatment of autism spectrum disorder. *Prog. Neuropsychopharmacol. Biol. Psychiatry* 89, 90–96. doi: 10.1016/j.pnpbp.2018.08.030

Purba, J. S. (1996). Increased number of vasopressin- and oxytocin-expressing neurons in the paraventricular nucleus of the hypothalamus in depression. *Arch. Gen. Psychiatry* 53, 137–143. doi: 10.1001/archpsyc.1996.01830020055007

Rico, A. J., Dopeso-Reyes, I. G., Martínez-Pinilla, E., Sucunza, D., Pignataro, D., Roda, E., et al. (2017). Neurochemical evidence supporting dopamine D1–D2 receptor heteromers in the striatum of the long-tailed macaque: changes following dopaminergic manipulation. *Brain Struct. Funct.* 222, 1767–1784. doi: 10.1007/s00429-016-1306-x

Rojas, D. C. (2014). The role of glutamate and its receptors in autism and the use of glutamate receptor antagonists in treatment. *J. Neural Transm.* 121, 891–905. doi: 10.1007/s00702-014-1216-0

Scarselli, M., Novi, F., Schallmach, E., Lin, R., Baragli, A., Colzi, A., et al. (2001). D_2/D_3 dopamine receptor heterodimers exhibit unique functional properties. *J. Biol. Chem.* 276, 30308–30314. doi: 10.1074/jbc.M102297200

Shah, U. H., and González-Maeso, J. (2019). Serotonin and glutamate interactions in preclinical schizophrenia models. *ACS Chem. Neurosci.* 10, 3068–3077. doi: 10.1021/acschemneuro.9b00044

Shen, M. Y. F., Perreault, M. L., Bambico, F. R., Jones-Tabah, J., Cheung, M., Fan, T., et al. (2015). Rapid anti-depressant and anxiolytic actions following dopamine D1–D2 receptor heteromer inactivation. *Eur. Neuropsychopharmacol.* 25, 2437–2448. doi: 10.1016/j.euroneuro.2015.09.004

Simola, N., Morelli, M., and Pinna, A. (2008). Adenosine A2A receptor antagonists and parkinsons disease: state of the art and future directions. *Curr. Pharma. Des.* 14, 1475–1489. doi: 10.2174/138161208784480072

Simonoff, E., Pickles, A., Charman, T., Chandler, S., Loucas, T., and Baird, G. (2008). Psychiatric disorders in children with autism spectrum disorders: prevalence, comorbidity and associated factors in a population-derived sample. *J. Am. Acad. Child Adolesc. Psychiatry* 47, 921–929. doi: 10.1097/CHI.0b013e318179964f

Strauss, G. P., Chapman, H. C., Keller, W. R., Koenig, J. I., Gold, J. M., Carpenter, W. T., et al. (2019). Endogenous oxytocin levels are associated with impaired social cognition and neurocognition in schizophrenia. *J. Psychiatr. Res.* 112, 38–43. doi: 10.1016/j.jpsychires.2019.02.017

Surmeier, D. J., Yan, Z., and Song, W.-J. (1997). "Coordinated expression of dopamine receptors in neostriatal medium spiny neurons," in *Advances in Pharmacology*, eds D. S. Goldstein, G. Eisenhofer and R. McCarty (Cambridge: Academic Press), 1020–1023.

Tan, O., Martin, L. J., and Bowen, M. T. (2020). Divergent pathways mediate 5-HT_{1A} receptor agonist effects on close social interaction, grooming and aggressive behaviour in mice: Exploring the involvement of the oxytocin and vasopressin systems. *J. Psychopharmacol.* 34, 795–805. doi: 10.1177/0269881120913150

Uzunova, G., Pallanti, S., and Hollander, E. (2016). Excitatory/inhibitory imbalance in autism spectrum disorders: implications for interventions and therapeutics. *World J. Biol. Psychiatry* 17, 174–186. doi: 10.3109/15622975.2015.1085597

White, J. H., Wise, A., Main, M. J., Green, A., Fraser, N. J., Disney, G. H., et al. (1998). Heterodimerization is required for the formation of a functional GABA(B) receptor. *Nature* 396, 679–682. doi: 10.1038/25354

Yamasue, H., and Domes, G. (2017). "Oxytocin and autism spectrum disorders," in *Behavioral Pharmacology of Neuropeptides: Oxytocin*, eds R. Hurlemann and V. Grinevich (Cham: Springer International Publishing), 449–465.

Yoshida, M., Takayanagi, Y., Inoue, K., Kimura, T., Young, L. J., Onaka, T., et al. (2009). Evidence that oxytocin exerts anxiolytic effects *via* oxytocin receptor expressed in serotonergic neurons in mice. *J. Neurosci.* 29, 2259–2271. doi: 10.1523/JNEUROSCI.5593-08.2009

Zhang, C., Li, Q., Meng, L., and Ren, Y. (2020). Design of novel dopamine D_2 and serotonin 5-HT_{2A} receptors dual antagonists toward schizophrenia: an integrated study with QSAR, molecular docking, virtual screening and molecular dynamics simulations. *J. Biomol. Struct. Dyn.* 38, 860–885. doi: 10.1080/07391102.2019.1590244

Conflict of Interest: The authors declare that the research was conducted in the absence of any commercial or financial relationships that could be construed as a potential conflict of interest.

frontiers in Cellular Neuroscience

ORIGINAL RESEARCH
published: 09 November 2020
doi: 10.3389/fncel.2020.577858

Increased Dopamine Type 2 Gene Expression in the Dorsal Striatum in Individuals With Autism Spectrum Disorder Suggests Alterations in Indirect Pathway Signaling and Circuitry

Cheryl Brandenburg[1,2], Jean-Jacques Soghomonian[3], Kunzhong Zhang[3], Ina Sulkaj[3], Brianna Randolph[3], Marissa Kachadoorian[3] and Gene J. Blatt[1]**

[1]*Autism Neurocircuitry Laboratory, Hussman Institute for Autism, Baltimore, MD, United States,* [2]*Program in Neuroscience, University of Maryland Baltimore School of Medicine, Baltimore, MD, United States,* [3]*Department of Anatomy and Neurobiology, Boston University School of Medicine, Boston, MA, United States*

OPEN ACCESS

Edited by:
Yi-Ping Hsueh, Academia Sinica, Taiwan

Reviewed by:
Wenlin Liao, National Chengchi University, Taiwan
Daniela Neuhofer, Medical University of South Carolina, United States

***Correspondence:**
Cheryl Brandenburg
cbrandenburg@hussmanautism.org
Gene J. Blatt
gblatt@hussmanautism.org

Specialty section:
This article was submitted to Cellular Neuropathology, a section of the journal Frontiers in Cellular Neuroscience

Received: *30 June 2020*
Accepted: *09 October 2020*
Published: *09 November 2020*

Citation:
Brandenburg C, Soghomonian J-J, Zhang K, Sulkaj I, Randolph B, Kachadoorian M and Blatt GJ (2020) Increased Dopamine Type 2 Gene Expression in the Dorsal Striatum in Individuals With Autism Spectrum Disorder Suggests Alterations in Indirect Pathway Signaling and Circuitry. Front. Cell. Neurosci. 14:577858. doi: 10.3389/fncel.2020.577858

Autism spectrum disorder (ASD) is behaviorally defined and diagnosed by delayed and/or impeded language, stereotyped repetitive behaviors, and difficulties with social interactions. Additionally, there are disruptions in motor processing, which includes the intent to execute movements, interrupted/inhibited action chain sequences, impaired execution of speech, and repetitive motor behaviors. Cortical loops through basal ganglia (BG) structures are known to play critical roles in the typical functioning of these actions. Specifically, corticostriate projections to the dorsal striatum (caudate and putamen) convey abundant input from motor, cognitive and limbic cortices and subsequently project to other BG structures. Excitatory dopamine (DA) type 1 receptors are predominantly expressed on GABAergic medium spiny neurons (MSNs) in the dorsal striatum as part of the "direct pathway" to GPi and SNpr whereas inhibitory DA type 2 receptors are predominantly expressed on MSNs that primarily project to GPe. This study aimed to better understand how this circuitry may be altered in ASD, especially concerning the neurochemical modulation of GABAergic MSNs within the two major BG pathways. We utilized two classical methods to analyze the postmortem BG in ASD in comparison to neurotypical cases: ligand binding autoradiography to quantify densities of GABA-A, GABA-B, 5-HT_2, and DA type 1 and 2 receptors and *in situ* hybridization histochemistry (ISHH) to quantify mRNA for D1, D2 receptors and three key GABAergic subunits (α1, β2, and γ2), as well as the GABA synthesizing enzymes (GAD65/67). Results demonstrated significant increases in D2 mRNA within MSNs in both the caudate and putamen, which was further verified by proenkephalin mRNA that is co-expressed with the D2 receptor in the indirect pathway MSNs. In

Abbreviations: 5-HT, serotonin; ADI, Autism Diagnostic Interview; ASD, autism spectrum disorder; BG, basal ganglia; DA, dopamine; D1R, dopamine type 1 receptor; D2R, dopamine type 2 receptor; Drd2, dopamine receptor D2 gene; Drd1, dopamine receptor D1 gene; GPi, globus pallidus internus; GPe, globus pallidus externus; ISHH, *in situ* hybridization histochemistry; MSNs, medium spiny neurons; PPE, preproenkephalin; SNpr, substantia nigra pars reticularis.

contrast, all other GABAergic, serotonergic and dopaminergic markers in the dorsal striatum had comparable labeling densities. These results indicate alterations in the indirect pathway of the BG, with possible implications for the execution of competing motor programs and E/I imbalance in the direct/indirect motor feedback pathways through thalamic and motor cortical areas. Results also provide insights regarding the efficacy of FDA-approved drugs used to treat individuals with ASD acting on specific DA and 5-HT receptor subtypes.

Keywords: autism spectrum disorder, dopamine, GABA, basal ganglia, indirect pathway, risperidone

INTRODUCTION

Characteristic delayed and/or impeded language, stereotyped repetitive behaviors, and difficulties with social interaction/communication are the core features of an autism spectrum disorder (ASD) diagnosis (Geschwind and Levitt, 2007; Fung and Hardan, 2014). Additionally, motor impairment is a cardinal feature of ASD, and language to reflect repetitive motor behaviors has been added to the DSM-5 diagnostic criteria (American Psychiatric Association, 2013). The behaviors associated with disrupted motor processing are widespread and include differences in fundamental motor skills such as eye movement, fine and gross motor skills, gait and balance as well as more complex skills like movement coordination, action chaining, and inhibition control (for a review see: Becker and Stoodley, 2013; Subramanian et al., 2017). Given the clear disruption in sensorimotor processing in individuals with ASD, it is important to examine postmortem brain areas that are responsible for the intention to execute movements.

The basal ganglia (BG) are known to participate in action selection, learned habits, action sequences, and repetitive behaviors (for a review see: Graybiel, 2008; Graybiel and Grafton, 2015) and increasing evidence implicates the BG in the pathogenesis of ASD. Several studies have found volumetric differences in the dorsal striatum (caudate and/or putamen) of ASD subjects compared to neurotypical individuals *via* imaging studies (Sears et al., 1999; Hollander et al., 2005; Rojas et al., 2006; Langen et al., 2007; Sato et al., 2014) and one postmortem study demonstrated similar findings (Wegiel et al., 2014). Thus, neuroanatomical differences in the dorsal striatum in individuals with ASD suggest that critical loops within the BG and their cortical connections may be significantly impacted. Increased caudate volume in ASD (Sears et al., 1999; Hollander et al., 2005; Rojas et al., 2006; Wegiel et al., 2014), for example, has been related to complex mannerisms, compulsions/rituals, stereotypy and/or difficulties in routine scores on the Autism Diagnostic Interview (ADI).

Afferent input from the frontal and cingulate cortices to the dorsal striatum provides motor, limbic, and cognitive information (for a review see: Subramanian et al., 2017) and may participate in ASD-related functions. Glutamatergic inputs provide excitatory drive from the thalamus and cortex and mostly target GABAergic medium spiny neurons (MSNs) and GABAergic interneurons, which, *via* feed-forward synapses, inhibit MSNs, which in turn primarily project to the globus pallidus internus (GPi) or substantia nigra pars reticularis (SNpr; direct pathway; rich in D1 receptors) or the globus pallidus externus (GPe; indirect pathway; rich in D2 receptors). The interplay of these pathways likely affects action performance by facilitation of the selection of action and inhibiting unwanted actions following cortical activation (Lovinger, 2017).

Despite increased recognition that the BG is implicated in ASD, there is a wide gap in our knowledge regarding which aspects of the BG circuitry are impacted in ASD as well as a lack of understanding of defined targets for pharmacotherapeutic treatment. Interestingly, the first drug approved for children with ASD and now the most widely used, Risperidone (Risperdal), has led to significant improvements in behavioral symptoms, such as sensorimotor and repetitive behaviors (McCracken et al., 2002; Shea et al., 2004; McDougle et al., 2005; Pandina et al., 2007; Kent et al., 2013; Goel et al., 2018). Risperidone mainly has high-affinity binding as an antagonist at serotonin (5-HT) 2A receptors and dopamine (DA) type 2 receptors (D2R). Aripiprazole (Abilify), one of the very few other drugs approved by the FDA for ASD (LeClerc and Easley, 2015), acts as a partial agonist to D2R and 5-HT_{1A} receptors and as an antagonist to 5-HT_{2A} receptors (Hirsch and Pringsheim, 2016; Lamy and Erickson, 2018), but targets anxiolytic symptoms (Marcus et al., 2009; Owen et al., 2009; Ichikawa et al., 2017). Although there are clinical reports for use of both of these drugs for ASD patients, there are no postmortem studies from ASD subjects that quantify the density and distribution of DA and 5-HT receptors in key brain structures that are likely involved in repetitive behaviors, such as the BG.

The objective of the current study was to determine if levels of expression of markers of dopaminergic, GABAergic, and serotonergic activity in the striatum are changed in ASD, which could shed light on the mechanisms whereby the BG is impacted. This study utilizes classic methodologies such as *in situ* hybridization histochemistry (ISHH) and ligand binding autoradiography to quantify select GAD/GABA receptor and DA receptor mRNA expression as well as to quantify GABA, DA, and 5-HT receptor densities in the dorsal striatum of postmortem ASD cases as compared to controls. These methodologies were designed to determine whether there are alterations within the circuitry of the dorsal striatum and/or in receptor density, including those which are primary targets for risperidone and aripiprazole, within the corticostriatal and striatopallidal circuits in age, postmortem interval (PMI), and gender-matched cases. Collectively, these data help to improve our understanding of

neurochemical differences within the BG that can inform on likely targets responsible for dysregulation of motor behaviors in ASD. The results indicate a largely normal repertoire of DA, GABA and 5-HT receptors expressed within the dorsal striatum, but reveal an increase of Drd2 mRNA expression within individual MSNs that likely impacts output to the GPe. These insights help to clarify which of the key targets for approved and widely used ASD drugs are altered in the BG of a cohort of postmortem ASD cases.

MATERIALS AND METHODS

Postmortem Tissue

Human postmortem brain tissue was obtained from the University of Maryland Brain and Tissue Bank, a brain and tissue repository of the NIH Neurobiobank. Case demographics are detailed in **Table 1**. Coronal sections (20 μm) from caudate and putamen were cut on a Leica CM1950 cryostat and kept frozen at −80°C (n = 11 control, n = 11 ASD). Note that brain blocks through a portion of the dorsal striatum were matched for level as far as having both caudate and putamen present in the same sections when cut, but the exact level matching of individual sections is a limitation in postmortem studies due to the availability of material through regions of interest. Several blocks did not contain ventral striatum. The number of cases used in individual experiments may vary due to the occasional loss of sections during processing. Total case ages (p = 0.24) and PMI (p = 0.37) were not significantly different between ASD and control cases using a Student's t-test. Three ASD cases had at least one seizure reported and six had reported medications (**Table 1**). All ASD cases had confirmed diagnoses through the Autism Diagnostic Interview-Revised (ADI-R) scores and/or received a clinical diagnosis of autism from a licensed psychiatrist.

As this research did not involve live human subjects, Institutional Review Board approval and informed consent were not necessary. However, the University of Maryland Brain and Tissue Bank (NIH Neurobiobank) is overseen by Institutional Review Board protocol number HM-HP-00042077 and de-identifies all cases before distribution to researchers.

Radioisotopic *In Situ* Hybridization Histochemistry (ISHH)

^{35}S radiolabeled complementary RNA (cRNA) probes were transcribed *in vitro* from cDNAs selective for the human GAD67, GAD65, PPE, dopamine Drd2, and Drd1 receptors and GABAa alpha1, beta2, and gamma 2 receptor subunits. The circular plasmids containing the cDNAs were linearized according to standard protocols (Wood, 1983). Transcription of the radioactive cRNAs was performed for 2 h at 37°C in the presence of 2.5 μM ^{35}S-uracil triphosphate (UTP; specific activity 1,250 Ci/mmol; Perkin Elmer Life Sciences) and 10 μM unlabeled UTP with ATP, cytosine triphosphate (CTP), and guanine triphosphate (GTP) in excess. The cDNA template was then digested with DNAse I. The labeled cRNAs were purified by phenol/chloroform extraction and ethanol precipitation and the probe length was reduced to 100–150 nucleotides by alkaline hydrolysis (Cox et al., 1984).

Two adjacent sections per subject were used. Sections were fixed for 5 min in 3% paraformaldehyde in 0.1 M phosphate buffer saline (pH 7.2). Pre-hybridization washes were in 2× SSC, phosphate buffer saline (0.4 M), 0.25% acetic anhydride with triethanolamine, and Tris-glycine, then followed by dehydration in ethanol. After rinsing with 2× SSC, sections hybridized for 4 h at 52°C with 8 ng of radiolabeled cRNA probe. The probe was diluted in 20 μl of hybridization solution (containing 40% formamide, 10% dextran sulfate, 4× SSC, 10 mM dithiothreitol, 1.0% sheared salmon sperm DNA, 1.0% yeast tRNA, and 1× Denhardt's solution). The sections were subsequently washed in 50% formamide at 52°C for 5 and 20 min, RNAse A (100 μg/ml; Sigma–Aldrich) for 30 min at 37°C, and in 50% formamide for 5 min at 52°C, then dehydrated in ethanol and defatted in xylene. Sections were placed in contact with Kodak BioMax MR film in light-tight cassettes for 10–15 days. The films were then developed. Slides were then processed for emulsion autoradiography. In that case, slides were coated with Kodak NTB3 nuclear emulsion diluted 1:1 with distilled water containing 300 mM ammonium acetate, air-dried for 3 h, and stored at room temperature in light-tight boxes for 14 days. Sections were developed in Kodak D-19 developer for 3.5 min at 14°C and lightly counterstained with eosin and hematoxylin, and mounted with Eukitt.

Quantification of mRNA Labeling

The relative levels of GAD67, GAD65, PPE, Drd2, Drd1, α1, β2, and γ2 mRNA labeling were quantified on X-ray film autoradiographs by computerized densitometry with NIH Image (Macintosh[1]). The autoradiographs were digitized using a CCD Sony video camera and the analog signal was converted to a digital image of 640 × 480 pixels (picture points) with gray values ranging from 0 to 255. Quantification was conducted ensuring most values were in the linear range of the best-fit calibration curve. Relative optical density (OD) measurements were calculated using two adjacent slides from each case. Data were expressed as mean ± S.E.M. Relative differences were compared within groups by Student's t-test.

Following processing with X-ray films, sections were processed for emulsion autoradiography by dipping in Kodak NTB liquid emulsion. Following 2–3 weeks of exposure duration, the emulsion autoradiographs were developed in Kodak D19 developer, processed in fixative and counterstained with eosin-hematoxylin. Following mounting, the autoradiographs were examined on a Nikon microscope and neurons with five or more silver grains were quantified using NIH image as previously described (Nielsen and Soghomonian, 2004; Lanoue et al., 2010). Only probes showing a significant effect on X-ray films were quantified on emulsion autoradiographs. Two sections per case and 50 neurons per section and per region (caudate and putamen) were analyzed. The results were expressed as a number of pixels per neuron. Data from control and ASD cases were plotted for the caudate and the putamen as a frequency distribution of labeling per neuron and comparisons between the

[1] www.zippy.nimh.nih.gov

TABLE 1 | Postmortem brain donor case demographics.

Cases	Diagnosis	Age	PMI	Gender	Ethnicity	Cause of Death
3228	Control	11	20	Male	Caucasian	Internal bleeding
4337	Control	8	16	Male	African american	Neck injury
4599	Control	23	18	Male	African american	Cardiac arrthymia
4787	Control	12	15	Male	African american	Asthma
5163	Control	14	12	Male	Caucasian	Drowning
5170	Control	13	20	Male	African american	Gunshot wound to chest
5334	Control	12	15	Male	Hispanic	Suicide
5387	Control	12	13	Male	Caucasian	Drowning
5391	Control	8	12	Male	Caucasian	Drowning
5408	Control	6	16	Male	African american	Drowning
5813	Control	21	24	Male	African american	Atherosclerotic cardiovascular disease
2004	Autism	10	23	Male	Asian	Accident,
4231[a]	Autism	8	12	Male	African american	Drowning
4434[b*]	Autism	11	27	Male	Hispanic	Acute hemorrhagic tracheobronchitis
4721	Autism	8	16	Male	African american	Drowning
4849	Autism	7	20	Male	African american	Drowning
4899[c]	Autism	14	9	Male	Caucasian	Drowning
5144	Autism	7	3	Male	Caucasian	Cancer
5308	Autism	4	21	Male	Caucasian	Skull fractures
5565[d*]	Autism	12	22	Male	African american	Seizure Disorder
5841[e]	Autism	12	15	Male	Caucasian	Hanging
5864[f*]	Autism	20	42	Male	Caucasian	Seizure Disorder

**At least one documented seizureKnown medications: [a]Zyprexa, Lexapro; [b]Keppra, Lexapro; [c]Keppra; [d]Daytrana; [e]Trileptal, Zoloft, Clonidine, Melatonin; [f]Tegretol, Clonidine, Ativan, Risperdal.*

distributions in controls and ASD cases were analyzed with a Kolmogorov-Smirnov test.

Saturation Ligand Binding Assays

Five tritiated [^{3}H] ligands including spiperone [Perkin Elmer, Boston, MA, USA, NET1187 (2016); Palacios et al., 1981; Filer et al., 2019], SCH 23390 [NET930 (2015); Bourne, 2001], flunitrazepam [NET5627 (2015); Guptill et al., 2007; Oblak et al., 2009], Ketanserin [NET7910 (2015); Leysen et al., 1982] and CGP 54626 [American Radiolabeled Chemicals, St. Louis, MO, USA ART715 (2015); Scheperjans et al., 2005] were processed under conditions specified in **Table 2**. Total binding was quantified from two thawed 20 μm sections while one section from each case was exposed to the ligand and a displacer to determine non-specific binding. Each displacer purchased from Sigma–Aldrich (St. Louis, MO, USA) was used at a concentration of 10 μM for +/− butaclamol hydrochloride [SIG-D033 (2016)] or 100 μM for both Clonazepam [SIG-C1277 (2016)] and CGP-55845 hydrochloride [SIG-SML0594 (2015)]. Imipramine hydrochloride was also used at 100 μM [AAJ6372306 Thermo Fisher Scientific, Waltham, MA, USA (2016)]. Labetalol hydrochloride [SIG L1011 (2016)] and ketanserin +/− tartrate [SIG S006 (2016)] were added to the spiperone buffer to block serotonin receptor 2 and adrenoreceptors.

All tissue went through a pre-incubation in buffer without ligand for 30 min before incubation with a ligand for 1 h. Buffer for ^{3}H spiperone was composed of 50 mM Tris-HCl, 120 mM NaCl, 5 mM KCl, 2 mM $CaCl_2$, 1 mM $MgCl_2$ pH 7.4, ^{3}H SCH 23390 and ^{3}H flunitrazepam was composed of 170 mM Tris-HCl, pH 7.4 and ^{3}H CGP 54626 used 50 mM Tris-HCl and 2.5 mM $CaCl_2$, pH 7.2. After three 5-min rinses in buffer followed by one dip in distilled water, sections were allowed to air-dry overnight. Slides, [^{3}H]-sensitive hyper film [Kodak Biomax MR film Z350389, Sigma–Aldrich, St. Louis, MO, USA (2016)] and a [^{3}H] standard [Tritium standards, American Radiolabeled Chemicals St. Louis, MO, USA ART0123 (2015)] were placed in X-ray cassettes and exposed for 10–14 weeks. Films were processed in the dark for 3 min in developer [Kodak D19 74200, Electron Microscopy Sciences, Hatfield, PA, USA (2015)], fixed [Kodak Rapidfix 74312, Electron Microscopy Sciences, Hatfield, PA, USA (2015)] for 4 min at room temperature, and washed with a stream of water for 1 h and air-dried.

Tissue section autoradiograms from the film were digitized with a QICAM digital camera (QImaging, Surrey, BC, Canada) followed by analysis with MCID Core 7.1 Elite Image analysis system software (InterFocus Imaging Limited, UK). Within the MCID software, one representative standard curve was chosen to normalize all standard curves and images for comparison

TABLE 2 | Ligand binding conditions.

Receptor	Ligand	Specific Activity (Ci/mmol)	Concentration (nM)	Displacer	Exposure (weeks)
D_2	[^{3}H] Spiperone	78.8	2	+/-butaclamol	14
D_1	[^{3}H] SCH 23390	81.9	3	+/-butaclamol	10
$GABA_A$	[^{3}H] Flunitrazepam	79.8	5	Clonazepam	12
$GABA_B$	[^{3}H] CGP 54626	60	3	CGP-5585	14
5-HT_2	[^{3}H] Ketanserin	47.3	3	Imipramine	23

across films. The ribbon tool was employed to sample binding along the length of the observable region of interest that included the caudate and putamen of the BG (as shown by the Nissl in **Figure 1A**). OD values of the sampled areas were converted to nanocuries (nCi) per milligram (mg) through the use of [^{3}H] standards then femtomoles (fmol) per mg of protein-based on the specific activity for each ligand. As non-specific binding was less than 5% of total binding, total binding was taken as representative of the specific binding for each ligand. Student *t*-tests were conducted to compare the binding affinity of each ligand between control and ASD groups.

RESULTS

Dopamine D1 and D2 Receptor Analysis

Radioisotopic ISHH allowed for visualization of mRNA encoding for dopamine receptors (Drd2, Drd1) within the caudate and putamen (**Figure 1A**). Regional quantification on film autoradiographs indicated that Drd2 mRNA expression was significantly elevated in both the caudate (mean: control 0.014 ± 0.002, ASD 0.023 ± 0.002) and putamen (mean: control 0.020 ± 0.002, ASD 0.026 ± 0.002) of the ASD cases (**Figure 1B**), with a more pronounced difference shown in the caudate. The expression of the Drd1 mRNA was not different between controls and ASD for neither the caudate (mean: control 0.106 ± 0.005, ASD 0.109 ± 0.007) or putamen (mean: control 0.102 ± 0.007, ASD 0.105 ± 0.006; **Figure 1B**).

To further examine the increase in Drd2 expression, mRNA levels were quantified at the single-cell level on emulsion autoradiographs (**Figure 2**). The analysis yielded results that confirmed the effects seen on film autoradiographs and further indicated that higher Drd2 mRNA levels in ASD seen on X-ray films are due to an increased expression per neuron rather than an increase in the number of neurons expressing the mRNA.

To determine whether increased Drd2 mRNA levels were paralleled by increased receptor expression at the protein level, ligand binding assays were conducted. D2R binding levels within the caudate (mean: control 210.014 ± 15.946, ASD 234.108 ± 18.529) and putamen (mean: control 249.161 ± 14.201, ASD 244.190 ± 11.614) were similar between ASD and control cases (**Figure 3**), indicating that overall D2R tissue expression within the caudate and putamen is unchanged. The D2Rs are primarily distributed on indirect striatal pathway neurons, on cholinergic and GABAergic interneurons as well as on corticostriatal axonal projections, whereas the Drd2 mRNA is detected in intrinsic striatal neurons only. Also, the population of cholinergic interneurons is much lower than the population of indirect pathway neurons. One explanation for the contradictory results between ISHH and ligand binding experiments could be that the ISHH results primarily reflect a change in mRNA levels in indirect pathway neurons. On the other hand, potential changes in ligand binding in indirect pathway neurons may be obscured by the detection of receptors on other populations of neurons, including corticostriatal axons.

To further assess the possibility that the expression of other mRNAs is altered in the indirect pathway neurons, we also measured pre proenkephalin (PPE; **Figure 4A**), which is selectively expressed in indirect pathway striatal neurons. Although the putamen levels of PPE in ASD cases were not different (mean: control 0.254 ± 0.045, ASD 0.278 ± 0.036; **Figure 4B**), the caudate of ASD had significantly higher levels of PPE compared to controls (mean: control 0.162 ± 0.020, ASD 0.253 ± 0.036).

GABAergic and 5-HT Markers

The mRNA levels of GAD65 caudate (mean: control 0.054 ± 0.005, ASD 0.052 ± 0.006) and putamen (mean: control 0.055 ± 0.007, ASD 0.060 ± 0.005) and GAD67 (**Figure 5**) in the caudate (mean: control 0.063 ± 0.010, ASD 0.069 ± 0.008) and putamen (mean: control 0.074 ± 0.009, ASD 0.079 ± 0.009) as well as the three GABA-A receptor subunits [α1 caudate (mean: control 0.039 ± 0.001, ASD 0.040 ± 0.002), putamen (mean: control 0.041 ± 0.003, ASD 0.040 ± 0.002); β2 caudate (mean: control 0.141 ± 0.009, ASD 0.147 ± 0.012), putamen (mean: control 0.156 ± 0.016, ASD 0.150 ± 0.014); and γ2 caudate (mean: control 0.073 ± 0.005, ASD 0.066 ± 0.002), putamen (mean: control 0.071 ± 0.004, ASD 0.074 ± 0.004); **Figure 6**] were not significantly different between control and ASD cases. Protein levels were not different between ASD and control groups for $GABA_A$ [caudate (mean: control 49.688 ± 11.639, ASD 54.462 ± 8.060), putamen (mean: control 53.421 ± 10.626, ASD 56.352 ± 9.418)] and $GABA_B$ receptors [caudate (mean: control 1.723 ± 0.184, ASD 2.229 ± 0.198), putamen (mean: control 1.540 ± 0.128, ASD 2.141 ± 0.159); **Figure 7**] or 5-HT_2 receptors [caudate (mean: control 234.358 ± 23.548, ASD 223.460 ± 16.143), putamen (mean: control 251.705 ± 17.497, ASD 214.465 ± 19.519); **Figure 8**].

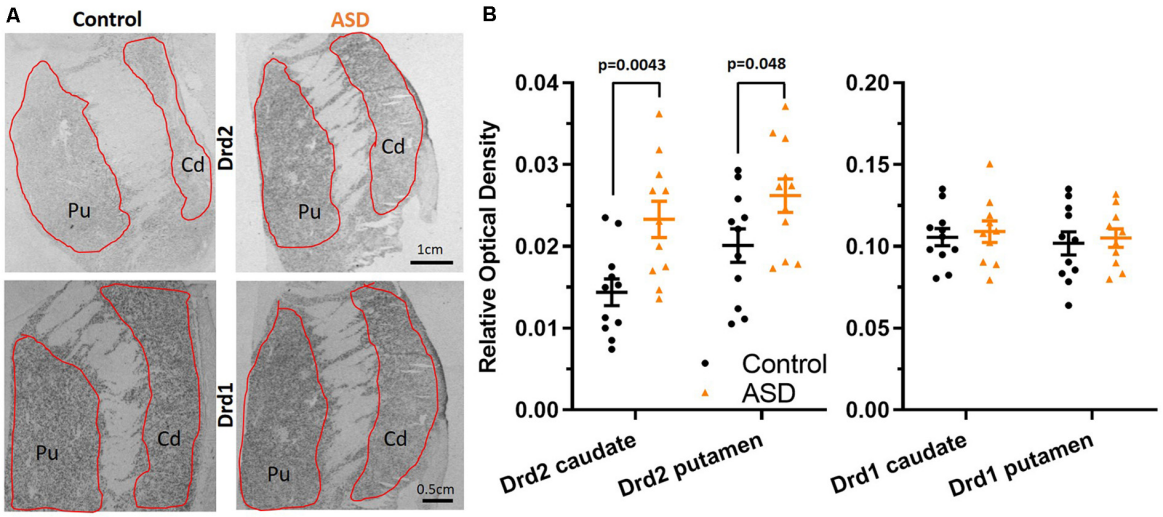

FIGURE 1 | (A) Radioisotopic *in situ* hybridization histochemistry showing labeled mRNA of Drd2 and Drd1. **(B)** Quantification of the relative density of Drd2 measured on film autoradiographs reveals higher expression in autism spectrum disorder (ASD) cases (orange) in both the caudate and putamen. Drd1 expression levels are unchanged in the caudate and putamen in ASD. Drd2 *n* = 11 control, 11 ASD; Drd1 *n* = 11 control, 10 ASD.

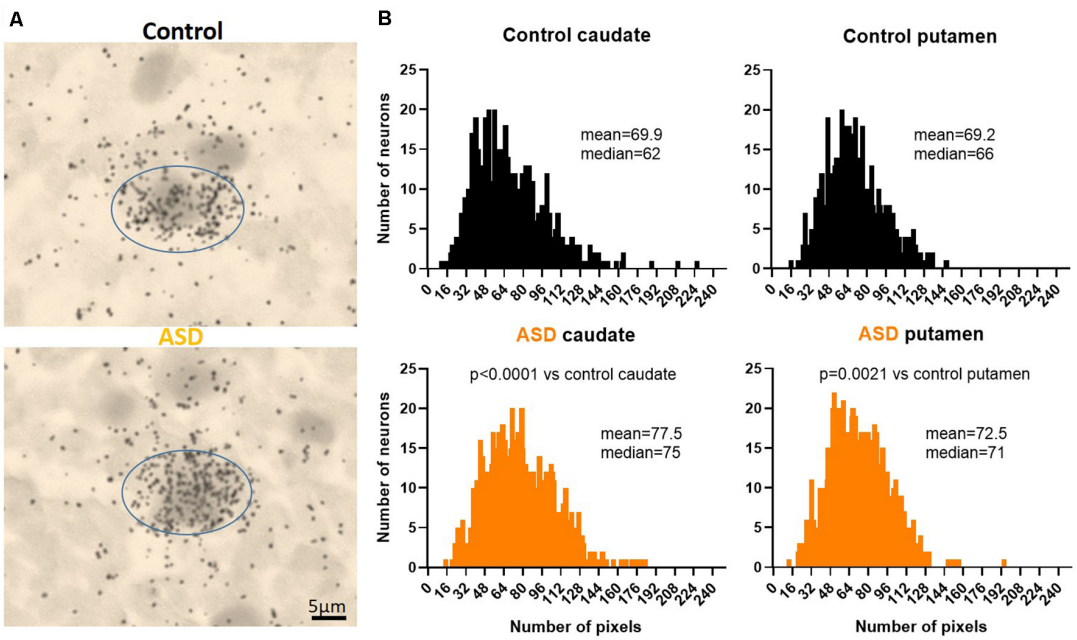

FIGURE 2 | (A) Representative images of control and ASD caudate. Drd2 emulsion autoradiographs. **(B)** Histograms of Drd2 mRNA labeling within individuals cells quantifies the distribution from emulsion autoradiographs in controls (upper panels) and ASD (lower panels). Differences between control and ASD distributions were analyzed with a Kolmogorov–Smirnov test. *n* = 10 control, 11 ASD cases; *n* = 884 control caudate, 1,004 autism caudate, 766 control putamen, 1,000 autism putamen cells.

DISCUSSION

Dopaminergic Expression Differences Are Evident in the Dorsal Striatum in ASD

The objective of the present study was to document possible changes in the expression of key markers of dopaminergic and GABAergic neurons in ASD. Our study presents original evidence for neurochemical imbalance in the dopaminergic system in the caudate and putamen in ASD cases. The functional relevance of differences in the BG of individuals with ASD is unclear but the effect seen on Drd2 receptors suggests that modulation of striatal neurons

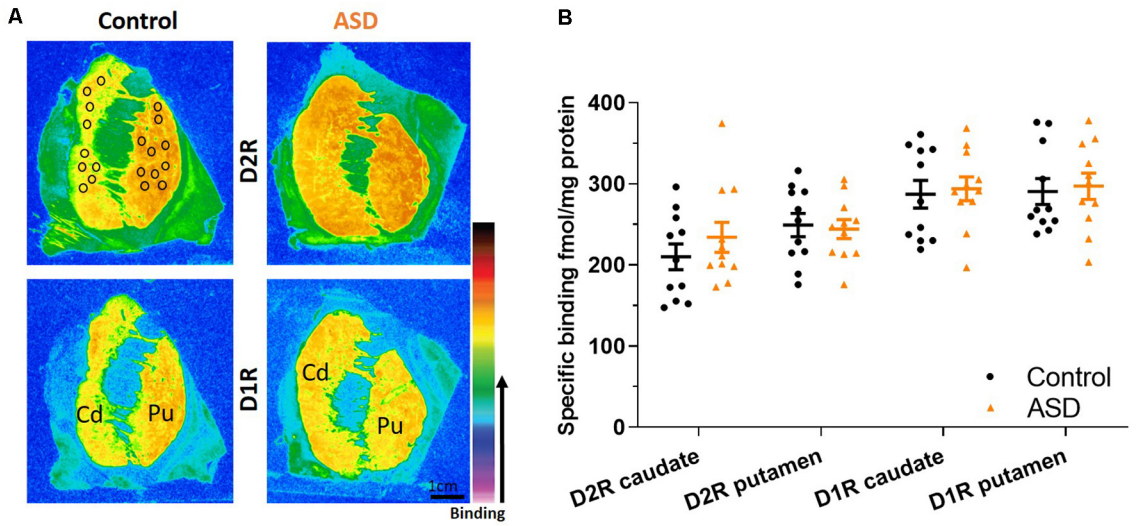

FIGURE 3 | (A) Representative images of control and ASD cases for ligand binding with warmer colors indicating higher binding. Black circles over the control case represent typical sampling areas, where we chose only representative areas with appropriate binding levels for quantification and can be applied to all binding images. **(B)** D2 and D1 receptor expression labeled with tritiated isotopes are similar between ASD (orange) and controls (black) in the caudate/putamen. *n* = 11 control, 11 ASD.

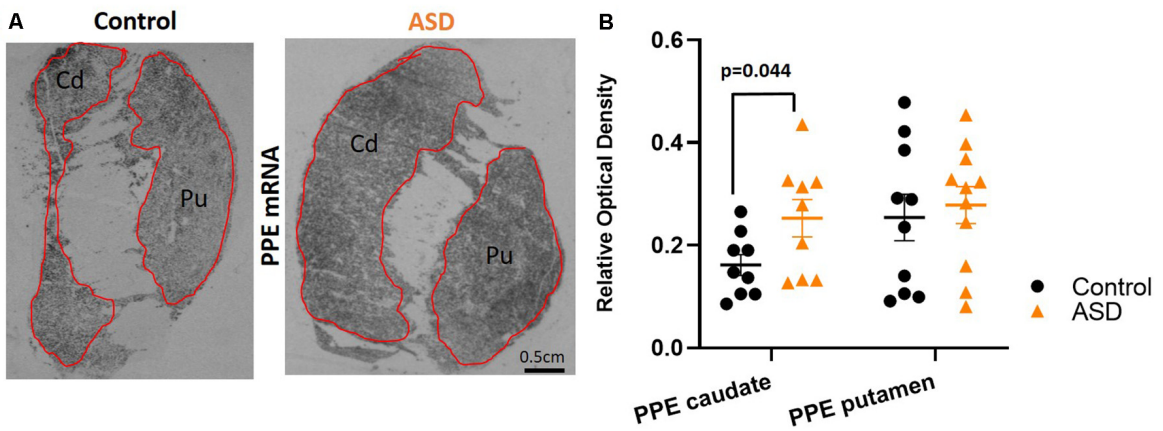

FIGURE 4 | (A) Preproenkephalin mRNA labeling with radioisotopic *in situ* hybridization histochemistry. **(B)** Preproenkephalin is increased in the caudate, but not in the putamen of ASD cases. *n* = 10 control putamen, nine control caudate; 11 ASD putamen, nine ASD caudate.

by dopamine is altered in ASD. Dopamine is a major modulator of striatal neurons and dopamine receptors are expressed in striatal interneurons and striatal projection neurons. Projection neurons in particular constitute a large proportion of the striatal neuronal population representing about 85% of all neurons. Other cells are cholinergic or GABAergic interneurons (Assous and Tepper, 2019). In our ISHH studies, analyses did not distinguish between GABAergic projection neurons and interneurons. Because the population of interneurons is very low compared to projection neurons, the changes in Drd2 mRNA documented here likely occurred in GABAergic projection neurons. Also, we did not include large cell bodies in our analyses, which correspond to cholinergic interneurons. It was somewhat surprising to find that the changes in Drd2 mRNA levels were not accompanied by changes in dopamine D2 receptors in our binding experiments. There are several plausible explanations for this apparent mismatch. First, ligand binding detects receptors present not only on projection neurons and interneurons but also on axon terminals of corticostriatal and thalamostriatal inputs. Second, dopamine receptors expressed in striatal projection neurons can be transported to their targets in the globus pallidus and/or substantia nigra, and changes in mRNA levels may not necessarily translate into changes in receptor levels on cell bodies. D2Rs expressed in striatal projection neurons

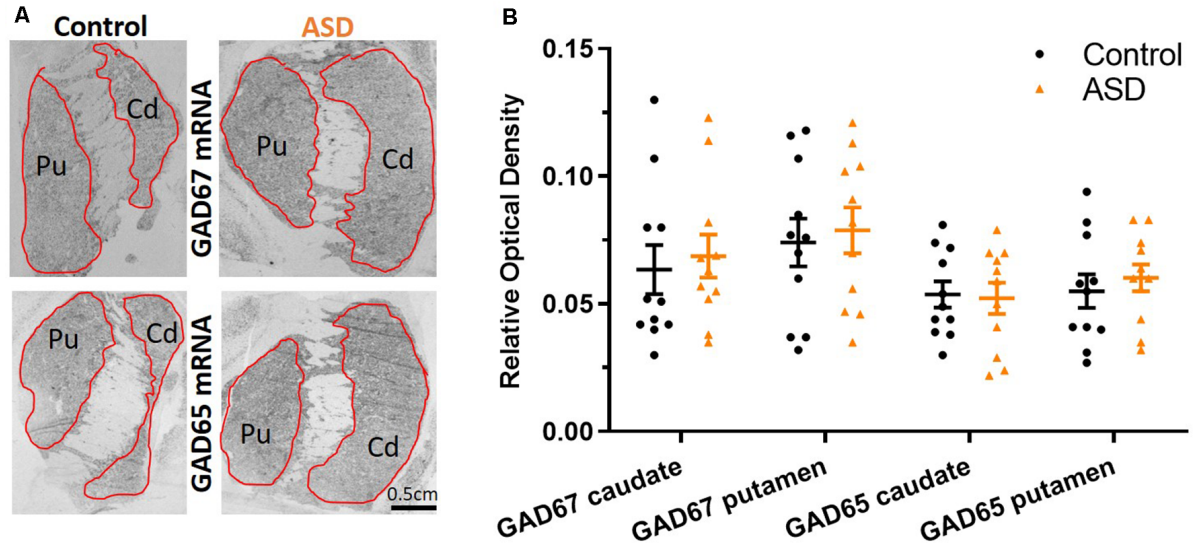

FIGURE 5 | (A) GAD67 and GAD65 mRNA labeling with radioisotopic *in situ* hybridization histochemistry. **(B)** Both GAD65 and GAD67 are similarly expressed between ASD and control cases in the caudate and putamen. *n* = 11 control, 11 ASD.

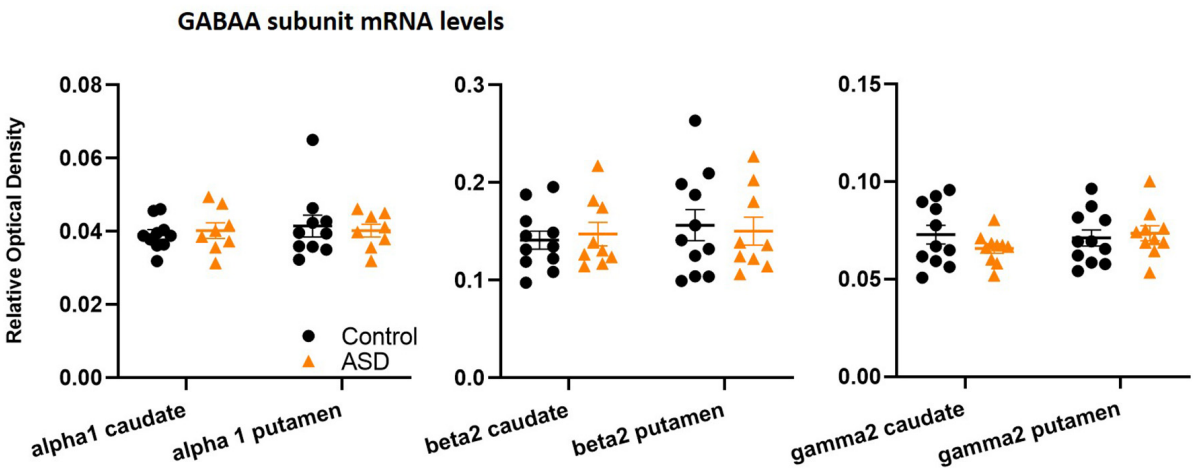

FIGURE 6 | $GABA_A$ subunit mRNA levels are unchanged between control and ASD cases, including α1 (*n* = 10 control, 8 ASD), β2 (*n* = 11 control, 9 ASD), and γ2 (*n* = 11 control, 10 ASD) in both caudate and putamen.

are primarily expressed in indirect pathway neurons that project to the Gpe. This subpopulation of striatal projection neurons co-expressed PPE mRNA (for a review see: Soghomonian, 2016). We found that PPE mRNA levels were also elevated in the caudate, which further supports the interpretation that indirect pathway neurons are impacted in ASD. Drd1 mRNA levels, which are primarily expressed in the direct pathway neurons that project to Gpi were not changed.

Dopamine receptors exert widespread effects on the activity of intrinsic neurons in the caudate and putamen. In particular, Drd2 receptors inhibit striatal indirect pathway neurons. The changes in Drd2 mRNA levels suggest that control of GABAergic indirect pathway projection neurons is affected in ASD, however, a functional change in the striatum is undetermined and there may instead be an impact on D2R in the globus pallidus. A recent study has shown that a DAT mutation identified in an individual with ASD alters dopaminergic transmission in the striatum of a mouse model, an effect paralleled by hyperactive and repetitive behaviors as well as social deficits (DiCarlo et al., 2019). In this context, it would also be important to determine if changes in dopaminergic activity are a developmental feature of ASD. In that regard, it is noteworthy that gene mutations seen in ASD alter corticostriatal activity in mouse models (for a review see: Subramanian et al., 2017). In particular, in Fmr1 mice, a hypoconnectivity of corticostriatal synapses has

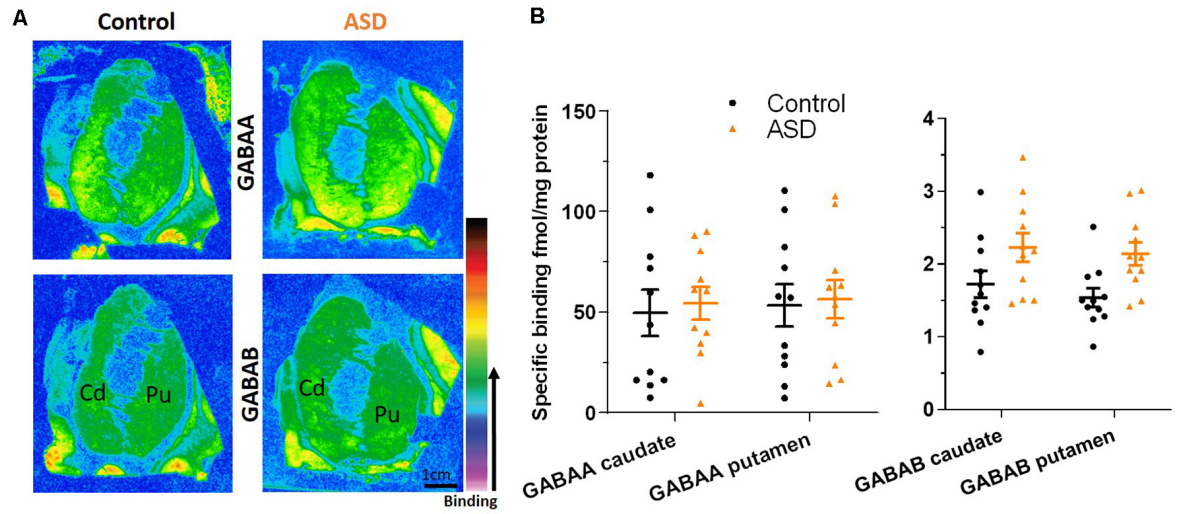

FIGURE 7 | (A) Representative image of ligand binding with warmer colors indicating higher binding. **(B)** $GABA_A$ and $GABA_B$ receptor expression labeled with tritiated isotopes is similar between ASD (orange) and controls (black). *n* = 11 control, 11 ASD.

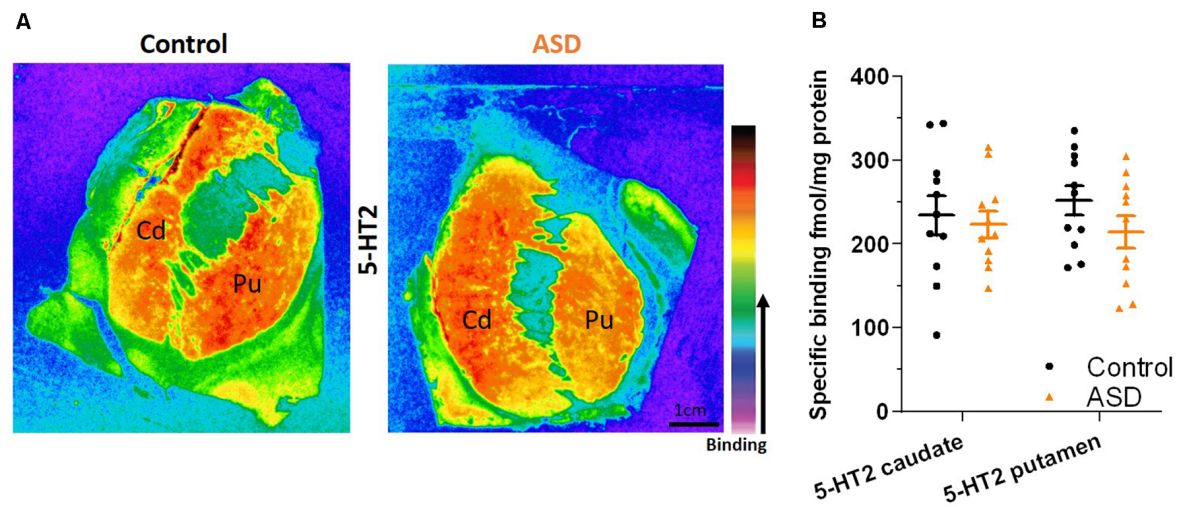

FIGURE 8 | (A) Representative image of ligand binding with warmer colors indicating higher binding. **(B)** 5-HT_2 receptor expression labeled with a tritiated isotope is similar between ASD (orange) and controls (black). *n* = 11 control, 11 ASD.

been documented (Centonze et al., 2008; Jung et al., 2012; Zerbi et al., 2018). Whether or not dopamine plays a role in this hypoconnectivity would be important to determine. The reason why we did not see a parallel effect on GAD or $GABA_A$ receptor expression is unclear. The most likely possibility is that GAD and $GABA_A$ receptors are expressed in direct and indirect pathway neurons as well as in striatal interneurons. Therefore, a specific effect in indirect pathway neurons would be diluted. Future double-labeling anatomical studies at the single-cell level or single-cell transcriptomics could be used to determine if transcriptional changes are selective to indirect pathway neurons and if they involve other markers of activity.

Corticostriatal Inputs to MSNs of the Direct and Indirect Pathways Are Modulated by Dopamine

The caudate and putamen receive widely distributed inputs from the cortex. These corticostriatal projections originate from cortical layers 5A, 5B, and 6 (for a review see: Kuo and Liu, 2019). Averbeck et al. (2014) used anterograde or bidirectional tract tracers in male macaque monkeys to map corticostriatal inputs, which are topographically organized but largely overlapping, especially from frontal cortical areas (for a review see: Haber, 2016). As an example, ventromedial prefrontal cortex (vmPFC), orbitofrontal cortex (OFC), the dorsal part of

the anterior cingulate limbic cortex (dACC) along with parts of dorsal prefrontal cortex (dPFC) project to "hubs" in the medial rostral caudate nucleus, possibly to integrate computations from multiple systems (Buckner et al., 2009; Averbeck et al., 2014) that are involved in decision processes or assigning value associated with actions or stimuli (Seo et al., 2012; Averbeck et al., 2014). These "loops" appear critical for motor functions including motor control, action selection, sequence learning, and formation of habits, but also cognitive/limbic functions that include learning, memory processing, decision making, and planning (Pennartz et al., 2009; Shepherd, 2013; Saunders et al., 2015). The corticostriatal input terminates on GABAergic interneurons and MSNs. GABAergic interneurons exert *via* feed-forward inhibition on MSN and thereby exert a strong impact on MSNs, which receive both motor and non-motor inputs. This distributed input from cortical areas opens several avenues where alterations in cortical systems could lead to disrupted processing in the striatum in ASD. As one example, the dorsal anterior cingulate cortex is an area that heavily innervates the striatum (for a review see: Haber, 2016) and a recent postmortem study from our laboratory revealed differences in serotonin receptor subtype densities that were age-dependent and not evident in the other cortical brain areas examined (Brandenburg and Blatt, 2019). D1R modulates GABA release in the direct pathway whereas D2R modulates GABA release mainly to the GABAergic GPe (i.e., on striatopallidal neurons) in the indirect pathway (for a review see: Gerfen and Bolam, 2010). Recently, it was determined in the macaque that different regions of the dorsal striatum receive unique sets of cortical inputs (i.e., striatal hubs) and their striatopallidal projections are largely topographic with predictive terminal fields from individual injection sites (Heilbronner et al., 2018). Striatal zones receiving unique combinations of cortical afferents (Averbeck et al., 2014; Choi et al., 2017) parcellate into specific functional topography. An example is the convergence of projections from the inferior parietal lobule and prefrontal cortex onto the rostral dorsal caudate, which subsequently projects to the GPe and is critical for the formation of visual bias toward salient environmental stimuli (Steinmetz and Constantinidis, 1995; Corbetta and Shulman, 2002; Corbetta et al., 2008). Thus, disruption of neurochemical modulation *via* dopamine within GABAergic MSNs in the dorsal striatum has the potential to affect neuronal firing to output structures (Mamad et al., 2015), which can influence the control of specific motor and/or non-motor activity and function *via* the reciprocal output projections to cortical areas. As our results demonstrate increased expression of Drd2 and PPE mRNA, we expect that the indirect pathway striatopallidal circuity and its control by corticostriatal inputs are impacted in ASD.

To this end, there are examples of genetic autism-related animal model studies that have demonstrated changes in D2Rs with implications for BG behavioral changes that include repetitive grooming, stereotypic motor routines as well as deficits in decision making and social interactions (Fuccillo, 2016). In the mouse model of the 16p11.2 human copy number variant (CNV), there was an increase in overall numbers of D2R positive MSN phenotypes in the dorsal and ventral striatum and a strong increase in net excitatory strength on D2Rs on MSNs (Portmann et al., 2014). In another genetic animal model, Cntnap4 KOs were administered a D2R antagonist, haloperidol resulting in decreased perseverative grooming by increasing dopaminergic tone (Karayannis et al., 2014). Despite numerous examples of D2R changes in animal models, there is a paucity of studies demonstrating Drd2 mRNA changes in MSNs in animal models and in human studies. Thus, follow-up studies in postmortem autism cases are warranted to further delineate neurochemical differences within human BG circuits.

Implications of Dysfunction of the Indirect Pathway

Disruptions in the indirect striatofugal pathway in ASD could have widespread ramifications. It may contribute to the altered encoding of information relevant to locomotion (Barbera et al., 2016). The indirect pathway projects to the GPe and dopamine controls this pathway *via* receptors expressed on striatal projection neurons or *via* presynaptic D2 receptors transported from the striatum to the Gpe (Rommelfanger and Wichmann, 2010; Mamad et al., 2015). Restricted repetitive behaviors, prevalent in ASD and other neurodevelopmental conditions, include stereotypy, rituals, and compulsions and have been reported to develop, in part, due to decreased indirect pathway activity in a mouse model (Tanimura et al., 2011). Recently, a large study of 2,084 children with ASD $\leq$6 years old measuring motor domain criteria from Vineland tests reported that 35% had significant motor difficulties with another 44% classified as moderately low skilled and included motor stereotypies (hand flapping, spinning, body rocking), and non-verbal behaviors such as use of body postures and gestures (Licari et al., 2020).

While many components in the brain contribute to a variety of these motor functions, MSNs in the dorsal striatum are considered to play a prominent role. The opposing actions of the direct pathway, which facilitates motor activity, vs. the indirect pathway that inhibits competing motor activity, result in smooth motor actions when relayed up to the motor cortex. If either pathway is disturbed, aberrant signals through BG efferent projections may be affected. Dopaminergic transmission dynamically regulates these actions and is critical to maintaining E/I balance within the circuitry. Since D1R excite MSNs of the direct pathway and D2 inhibits MSNs of the indirect pathway, the indirect pathway through the BG can act to terminate or inhibit competing movements selected by the direct pathway (Chu et al., 2015), i.e., if not functioning correctly, dysregulation of the specific part(s) of BG circuitry could lead to stereotypy and repetitive behaviors as seen in ASD.

Pharmacotherapeutic Implications

Pharmacotherapies have been extensively utilized in individuals with ASD, but there are only a few FDA-approved drugs aimed at helping to ameliorate or lessen behavioral symptoms. These include Risperidone (Risperdal), a second-generation antipsychotic, which is the only drug approved by the FDA for children with ASD over 5 years of age with irritability and aggression as well as Aripiprazole (Abilify), a psychotropic drug for irritability and depression (Hirsch and Pringsheim,

2016; Li et al., 2017: Eissa et al., 2018; Lamy and Erickson, 2018). Both drugs target a combination of dopamine and serotonin receptors and both treatments have had paradoxical effects, helping some individuals with ASD but having adverse side effects in others. Each of these drugs targets BG, D2R, and 5-HT_2. However, the present study, which is limited in cases, demonstrated similar binding densities for these key receptor types in the dorsal striatum negating any definitive conclusions regarding the efficacy of the drugs on D2R or 5-HT_2 receptors. Future studies that address dopaminergic innervation to the GPe and possible effects on D2Rs and/or other BG structures will be important, Another consideration that cannot be ruled out is that changes in Drd2 mRNA levels are secondary to pharmacotherapy as our sample size was not suitable to assess the possible impact of treatment on mRNA levels. Earlier experimental studies in rodents and primates have provided inconsistent results on the effects of neuroleptics on mRNA levels for dopamine receptors in the BG (Fox et al., 1994). Therefore, a possible contribution of pharmacotherapy on Drd2 mRNA levels is unclear and should be further investigated.

CONCLUSIONS

The results suggest that the indirect pathway of the BG is implicated in ASD as evidenced by a significant elevation in Drd2 mRNA within MSNs of the caudate and putamen and a similar increase in caudate MSN PPE mRNA, an indirect pathway marker. Since the indirect pathway is thought to contribute to inhibiting competing motor actions so that a chosen action by the direct pathway can proceed, it is therefore likely that a disturbance in a key regulator of action selection may be relevant for motor dysfunction, stereotypy, and/or other repetitive behaviors in individuals with ASD. In addition to these functions, the BG has been implicated in the cognitive control of language processing, and functional interactions between Broca's area and the striatum are well documented (Bohsali and Crosson, 2016). Changes in neurochemical or cellular processes in the BG may thus also have significance to language disorders in ASD.

DATA AVAILABILITY STATEMENT

The raw data supporting the conclusions of this article will be made available by the authors, without undue reservation.

ETHICS STATEMENT

Ethical review and approval was not required for the study on human participants in accordance with the local legislation and institutional requirements. Written informed consent for participation was not required for this study in accordance with the national legislation and the institutional requirements.

AUTHOR CONTRIBUTIONS

GB, J-JS and CB: conceptualization. CB, KZ, IS, BR, and MK: methodology. CB, J-JS, KZ, IS, BR, and MK: analysis. CB, GB, and J-JS: original draft. CB, GB, J-JS, KZ, IS, BR, and MK: review and editing. GB and J-JS: supervision. All authors contributed to the article and approved the submitted version.

FUNDING

This work was supported by Hussman Foundation grants HIAS #15001 and HIAS #17001 (GB, Principal Investigator).

ACKNOWLEDGMENTS

We acknowledge helpful assistance with references from Ms. Abimbola Oladele. We thank Dr. John P. Hussman for his critical review of the manuscript. We also thank the NIH Neurobiobank at the University of Maryland, Baltimore for supplying the postmortem cases for this study. Finally, the authors are indebted to the families who donated the brain tissue from their loved ones, both autism cases as well as neurotypical controls which made this and other research studies possible.

REFERENCES

American Psychiatric Association. (2013). *Diagnostic and Statistical Manual of Mental Disorders.* 5th Edn. Arlington, VA: American Psychiatric Publishing.

Assous, M., and Tepper, J. M. (2019). Excitatory extrinsic afferents to striatal interneurons and interactions with striatal microcircuitry. *Eur. J. Neurosci.* 49, 593–603. doi: 10.1111/ejn.13881

Averbeck, B. B., Lehman, J., Jacobson, M., and Haber, S. N. (2014). Estimates of projection overlap and zones of convergence within frontal-striatal circuits. *J. Neurosci.* 34, 9497–9505. doi: 10.1523/JNEUROSCI.5806-12.2014

Barbera, G., Liang, B., Zhang, L., Gerfen, C. R., Culurciello, E., Chen, R., et al. (2016). Spatially compact neural clusters in the dorsal striatum encode locomotion relevant information. *Neuron* 92, 202–213. doi: 10.1016/j.neuron.2016.08.037

Becker, E. B., and Stoodley, C. J. (2013). Autism spectrum disorder and the cerebellum. *Int. Rev. Neurobiol.* 113, 1–34. doi: 10.1016/B978-0-12-418700-9.00001-0

Bohsali, A., and Crosson, B. (2016). "The basal ganglia and language: a tale of two loops," in *The Basal Ganglia: Novel Perspectives on Motor and Cognitive Functions*, ed. J.-J. Soghomonian (New York, NY: Springer International Publishing), 217–242.

Bourne, J. A. (2001). SCH 23390: the first selective dopamine D1-like receptor antagonist. *CNS Drug Rev.* 7, 399–414. doi: 10.1111/j.1527-3458.2001.tb00207.x

Brandenburg, C., and Blatt, G. J. (2019). Differential serotonin transporter (5-HTT) and 5-HT_2 receptor density in limbic and neocortical areas of adults and children with autism spectrum disorders: implications for selective serotonin reuptake inhibitor efficacy. *J. Neurochem.* 151, 642–655. doi: 10.1111/jnc.14832

Buckner, R. L., Sepulcre, J., Talukdar, T., Krienen, F. M., Liu, H., Hedden, T., et al. (2009). Cortical hubs revealed by intrinsic functional connectivity: mapping, assessment of stability and relation to Alzheimer's disease. *J. Neurosci.* 29, 1860–1873. doi: 10.1523/JNEUROSCI.5062-08.2009

Centonze, D., Rossi, S., Mercaldo, V., Napoli, I., Teresa Ciotti, M., De Chiara, V., et al. (2008). Abnormal striatal GABA transmission in the mouse model for the

fragile X syndrome. *Biol. Psychiatry* 63, 963–973. doi: 10.1016/j.biopsych.2007.09.008

Choi, E. Y., Ding, S.-L., and Haber, S. N. (2017). Combinatorial inputs to the ventral striatum from the temporal cortex, frontal cortex, and amygdala: implications for segmenting the striatum. *eNeuro* 4:ENEURO.0392–17.2017. doi: 10.1523/ENEURO.0392-17.2017

Chu, H.-Y., Atherton, J. F., Wokosin, D., Surmeier, D. J., and Bevan, M. D. (2015). Heterosynaptic regulation of external globus pallidus inputs to the subthalamic nucleus by the motor cortex. *Neuron* 85, 364–376. doi: 10.1016/j.neuron.2014.12.022

Corbetta, M., Patel, G., and Shulman, G. L. (2008). The reorienting system of the human brain: from environment to theory of mind. *Neuron* 58, 306–324. doi: 10.1016/j.neuron.2008.04.017

Corbetta, M., and Shulman, G. L. (2002). Control of goal-directed and stimulus-driven attention in the brain. *Nat. Rev. Neurosci.* 3, 201–215. doi: 10.1038/nrn755

Cox, K. H., DeLeon, D. V., Angerer, L. M., and Angerer, R. C. (1984). Detection of mRNAs in sea urchin embryos by *in situ* hybridization using asymmetric RNA probes. *Dev. Biol.* 101, 485–502. doi: 10.1016/0012-1606(84)90162-3

DiCarlo, G. E., Aguilar, J. I., Matthies, H. J., Harrison, F. E., Bundschuh, K. E., West, A., et al. (2019). Autism-linked dopamine transporter mutation alters striatal dopamine neurotransmission and dopamine-dependent behaviors. *J. Clin. Invest.* 129, 3407–3419. doi: 10.1172/JCI127411

Eissa, N., Al-Houqani, M., Sadeq, A., Ojha, S. K., Sasse, A., and Sadek, B. (2018). Current enlightenment about etiology and pharmacological treatment of autism spectrum disorder. *Front. Neurosci.* 12:304. doi: 10.3389/fnins.2018.00304

Filer, C. N., Laseter, A. G., and Shelton, E. J. (2019). Spiperone: tritium labelling at high specific activity. *Appl. Radiat. Isot.* 147, 211–214. doi: 10.1016/j.apradiso.2019.02.008

Fox, C. A., Mansour, A., and Watson, S. J. Jr. (1994). The effects of haloperidol on dopamine receptor gene expression. *Exp. Neurol.* 130, 288–303. doi: 10.1006/exnr.1994.1207

Fuccillo, M. V. (2016). Striatal circuits as a common node for autism pathophysiology. *Front. Neurosci.* 10:27. doi: 10.3389/fnins.2016.00027

Fung, L. K., and Hardan, A. Y. (2014). Autism in DSM-5 under the microscope: implications to patients, families, clinicians, and researchers. *Asian J. Psychiatr.* 11, 93–97. doi: 10.1016/j.ajp.2014.08.010

Gerfen, C. R., and Bolam, J. P. (2010). "The neuroanatomical organization of the basal ganglia," in *Handbook of Basal Ganglia Structure and Function. Volume 20 of Handbook of Behavioral Neuroscience*, eds H. Steiner and K. Y. Tseng (Amsterdam: Elsevier), 3–28.

Geschwind, D. H., and Levitt, P. (2007). Autism spectrum disorders: developmental disconnection syndromes. *Curr. Opin. Neurobiol.* 17, 103–111. doi: 10.1016/j.conb.2007.01.009

Goel, R., Hong, J. S., Findling, R. L., and Ji, N. Y. (2018). An update on pharmacotherapy of autism spectrum disorder in children and adolescents. *Int. Rev. Psychiatry* 30, 78–95. doi: 10.1080/09540261.2018.1458706

Graybiel, A. M. (2008). Habits, rituals, and the evaluative brain. *Annu. Rev. Neurosci.* 31, 359–387. doi: 10.1146/annurev.neuro.29.051605.112851

Graybiel, A. M., and Grafton, S. T. (2015). The striatum: where skills and habits meet. *Cold Spring Harb. Perspect. Biol.* 7:a021691. doi: 10.1101/cshperspect.a021691

Guptill, J. T., Booker, A. B., Gibbs, T. T., Kemper, T. L., Bauman, M. L., and Blatt, G. J. (2007). [^{3}H]-flunitrazepam-labeled benzodiazepine binding sites in the hippocampal formation in autism: a multiple concentration autoradiographic study. *J. Autism Dev. Disord.* 37, 911–920. doi: 10.1007/s10803-006-0226-7

Haber, S. N. (2016). Corticostriatal circuitry. *Dialogues Clin. Neurosci.* 18, 7–21. doi: 10.31887/DCNS.2016.18.1/shaber

Heilbronner, S. R., Meyer, M. A. A., Choi, E. Y., and Haber, S. N. (2018). How do cortico-striatal projections impact on downstream pallidal circuitry? *Brain Struct. Funct.* 223, 2809–2821. doi: 10.1007/s00429-018-1662-9

Hirsch, L. E., and Pringsheim, T. (2016). Aripiprazole for autism spectrum disorders (ASD). *Cochrane Database Syst. Rev.* 2016:CD009043. doi: 10.1002/14651858.CD009043.pub3

Hollander, E., Anagnostou, E., Chaplin, W., Esposito, K., Haznedar, M. M., Licalzi, E., et al. (2005). Striatal volume on magnetic resonance imaging and repetitive behaviors in autism. *Biol. Psychiatry* 58, 226–232. doi: 10.1016/j.biopsych.2005.03.040

Ichikawa, H., Mikami, K., Okada, T., Yamashita, Y., Ishizaki, Y., Tomoda, A., et al. (2017). Aripiprazole in the treatment of irritability in children and adolescents with autism spectrum disorder in Japan: a randomized, double-blind, placebo-controlled study. *Child Psychiatry Hum. Dev.* 48, 796–806. doi: 10.1007/s10578-016-0704-x

Jung, K.-M., Sepers, M., Henstridge, C. M., Lassalle, O., Neuhofer, D., Martin, H., et al. (2012). Uncoupling of the endocannabinoid signalling complex in a mouse model of fragile X syndrome. *Nat. Commun.* 3:1080. doi: 10.1038/ncomms2045

Karayannis, T., Au, E., Patel, J. C., Kruglikov, I., Markx, S., Delorme, R., et al. (2014). Cntnap4 differentially contributes to GABAergic and dopaminergic synaptic transmission. *Nature* 511, 236–240. doi: 10.1038/nature13248

Kent, J. M., Kushner, S., Ning, X., Karcher, K., Ness, S., Aman, M., et al. (2013). Risperidone dosing in children and adolescents with autistic disorder: a double-blind, placebo-controlled study. *J. Autism Dev. Disord.* 43, 1773–1783. doi: 10.1007/s10803-012-1723-5

Kuo, H.-Y., and Liu, F.-C. (2019). Synaptic wiring of corticostriatal circuits in basal ganglia: insights into the pathogenesis of neuropsychiatric disorders. *eNeuro* 6:ENEURO.0076–19.2019. doi: 10.1523/ENEURO.0076-19.2019

Lamy, M., and Erickson, C. A. (2018). Pharmacological management of behavioral disturbances in children and adolescents with autism spectrum disorders. *Curr. Probl. Pediatr. Adolesc. Health Care* 48, 250–264. doi: 10.1016/j.cppeds.2018.08.015

Langen, M., Durston, S., Staal, W. G., Palmen, S. J., and van Engeland, H. (2007). Caudate nucleus is enlarged in high-functioning medication-naive subjects with autism. *Biol. Psychiatry* 62, 262–266. doi: 10.1016/j.biopsych.2006.09.040

Lanoue, A. C., Dumitriu, A., Myers, R. H., and Soghomonian, J. J. (2010). Decreased glutamic acid decarboxylase mRNA expression in prefrontal cortex in Parkinson's disease. *Exp. Neurol.* 226, 207–217. doi: 10.1016/j.expneurol.2010.09.001

LeClerc, S., and Easley, D. (2015). Pharmacological therapies for autism spectrum disorder: a review. *P T* 40, 389–397.

Leysen, J. E., Niemegeers, C. J., Van Nueten, J. M., and Laduron, P. M. (1982). [^{3}H]Ketanserin (R 41 468), a selective ^{3}H-ligand for serotonin2 receptor binding sites. Binding properties, brain distribution, and functional role. *Mol. Pharmacol.* 21, 301–314.

Li, A., MacNeill, B., Curiel, H., and Poling, A. (2017). Risperidone in combination with other drugs: experimental research in individuals with autism spectrum disorder. *Exp. Clin. Psychopharmacol.* 25, 434–439. doi: 10.1037/pha0000144

Licari, M. K., Alvares, G. A., Varcin, K., Evans, K. L., Cleary, D., Reid, S. L., et al. (2020). Prevalence of motor difficulties in Autism Spectrum Disorder: analysis of the population-based cohort. *Autism Res.* 13, 298–306. doi: 10.1002/aur.2230

Lovinger, D. M. (2017). An indirect route to repetitive actions. *J. Clin. Invest.* 127, 1618–1621. doi: 10.1172/JCI93918

Mamad, O., Delaville, C., Benjelloun, W., and Benazzouz, A. (2015). Dopaminergic control of the globus pallidus through activation of D2 receptors and its impact on the electrical activity of subthalamic nucleus and substantia nigra reticulata neurons. *PLoS One* 10:e0119152. doi: 10.1371/journal.pone.0119152

Marcus, R. N., Owen, R., Kamen, L., Manos, G., McQuade, R. D., Carson, W. H., et al. (2009). A placebo-controlled, fixed-dose study of aripiprazole in children and adolescents with irritability associated with autistic disorder. *J. Am. Acad. Child Adolesc. Psychiatry* 48, 1110–1119. doi: 10.1097/CHI.0b013e3181b76658

McCracken, J. T., McGough, J., Shah, B., Cronin, P., Hong, D., Aman, M. G., et al. (2002). Risperidone in children with autism and serious behavioral problems. *N. Engl. J. Med.* 347, 314–321. doi: 10.1056/NEJMoa013171

McDougle, C. J., Scahill, L., Aman, M. G., McCracken, J. T., Tierney, E., Davies, M., et al. (2005). Risperidone for the core symptom domains of autism: results from the study by the autism network of the research units on pediatric psychopharmacology. *Am. J. Psychiatry* 162, 1142–1148. doi: 10.1176/appi.ajp.162.6.1142

Nielsen, K. M., and Soghomonian, J.-J. (2004). Normalization of glutamate decarboxylase gene expression in the entopeduncular nucleus of rats with a unilateral 6-hydroxydopamine lesion correlates with increased GABAergic

input following intermittent but not continuous levodopa. *Neuroscience* 123, 31–42. doi: 10.1016/j.neuroscience.2003.08.010

Oblak, A., Gibbs, T. T., and Blatt, G. J. (2009). Decreased $GABA_A$ receptors and benzodiazepine binding sites in the anterior cingulate cortex in autism [published correction appears in Autism]. *Autism Res.* 2, 205–219. doi: 10.1002/aur.88

Owen, R., Sikich, L., Marcus, R. N., Corey-Lisle, P., Manos, G., McQuade, R. D., et al. (2009). Aripiprazole in the treatment of irritability in children and adolescents with autistic disorder. *Pediatrics* 124, 1533–1540. doi: 10.1542/peds.2008-3782

Palacios, J. M., Niehoff, D. L., and Kuhar, M. J. (1981). [^{3}H]Spiperone binding sites in brain: autoradiographic localization of multiple receptors. *Brain Res.* 213, 277–289. doi: 10.1016/0006-8993(81)90234-1

Pandina, G. J., Bossie, C. A., Youssef, E., Zhu, Y., and Dunbar, F. (2007). Risperidone improves behavioral symptoms in children with autism in a randomized, double-blind, placebo-controlled trial. *J. Autism Dev. Disord.* 37, 367–373. doi: 10.1007/s10803-006-0234-7

Pennartz, C. M. A., Berke, J. D., Graybiel, A. M., Ito, R., Lansink, C. S., van der Meer, M., et al. (2009). Corticostriatal interactions during learning, memory processing, and decision making. *J. Neurosci.* 29, 12831–12838. doi: 10.1523/JNEUROSCI.3177-09.2009

Portmann, T., Yang, M., Mao, R., Panagiotakos, G., Ellegood, J., Dolen, G., et al. (2014). Behavioral abnormalities and circuit defects in the basal ganglia of a mouse model of 16p11.2 deletion syndrome. *Cell Rep.* 7, 1077–1092. doi: 10.1016/j.celrep.2014.03.036

Rojas, D. C., Peterson, E., Winterrowd, E., Reite, M. L., Rogers, S. J., and Tregellas, J. R. (2006). Regional gray matter volumetric changes in autism associated with social and repetitive behavior symptoms. *BMC Psychiatry* 6:56. doi: 10.1186/1471-244X-6-56

Rommelfanger, K. S., and Wichmann, T. (2010). Extrastriatal dopaminergic circuits of the Basal Ganglia. *Front. Neuroanat.* 4:139. doi: 10.3389/fnana.2010.00139

Sato, W., Kubota, Y., Kochiyama, T., Uono, S., Yoshimura, S., Sawada, R., et al. (2014). Increased putamen volume in adults with autism spectrum disorder. *Front. Hum. Neurosci.* 8:957. doi: 10.3389/fnhum.2014.00957

Saunders, A., Oldenburg, I. A., Berezovskii, V. K., Johnson, C. A., Kingery, N. D., Elliott, H. L., et al. (2015). A direct GABAergic output from the basal ganglia to frontal cortex. *Nature* 521, 85–89. doi: 10.1038/nature14179

Scheperjans, F., Palomero-Gallagher, N., Grefkes, C., Schleicher, A., and Zilles, K. (2005). Transmitter receptors reveal segregation of cortical areas in the human superior parietal cortex: relations to visual and somatosensory regions. *NeuroImage* 28, 362–379. doi: 10.1016/j.neuroimage.2005.06.028

Sears, L. L., Vest, C., Mohamed, S., Bailey, J., Ranson, B. J., and Piven, J. (1999). An MRI study of the basal ganglia in autism. *Prog. Neuropsychopharmacol. Biol. Psychiatry* 23, 613–624. doi: 10.1016/s0278-5846(99)00020-2

Seo, M., Lee, E., and Averbeck, B. B. (2012). Action selection and action value in frontal-striatal circuits. *Neuron* 74, 947–960. doi: 10.1016/j.neuron.2012.03.037

Shea, S., Turgay, A., Carroll, A., Schulz, M., Orlik, H., Smith, I., et al. (2004). Risperidone in the treatment of disruptive behavioral symptoms in children with autistic and other pervasive developmental disorders. *Pediatrics* 114, e634–e641. doi: 10.1542/peds.2003-0264-F

Shepherd, G. M. G. (2013). Corticostriatal connectivity and its role in disease. *Nat. Rev. Neurosci.* 14, 278–291. doi: 10.1038/nrn3469

Soghomonian, J. J. (2016). "Anatomy and function of the direct and indirect striatal pathways," in *The Basal Ganglia: Novel Perspectives on Motor and Cognitive Functions*, ed. J.-J. Soghomonian (New York, NY: Springer), 47–67.

Steinmetz, M. A., and Constantinidis, C. (1995). Neurophysiological evidence for a role of posterior parietal cortex in redirecting visual attention. *Cereb. Cortex* 5, 448–456. doi: 10.1093/cercor/5.5.448

Subramanian, K., Brandenburg, C., Orsati, F., Soghomonian, J. J., Hussman, J. P., and Blatt, G. J. (2017). Basal ganglia and autism—a translational perspective. *Autism Res.* 10, 1751–1775. doi: 10.1002/aur.1837

Tanimura, Y., King, M. A., Williams, D. K., and Lewis, M. H. (2011). Development of repetitive behavior in a mouse model: roles of indirect and striosomal basal ganglia pathways. *Int. J. Dev. Neurosci.* 29, 461–467. doi: 10.1016/j.ijdevneu.2011.02.004

Wegiel, J., Flory, M., Kuchna, I., Nowicki, K., Ma, S. Y., Imaki, H., et al. (2014). Stereological study of the neuronal number and volume of 38 brain subdivisions of subjects diagnosed with autism reveals significant alterations restricted to the striatum, amygdala and cerebellum. *Acta Neuropathol. Commun.* 2:141. doi: 10.1186/s40478-014-0141-7

Wood, E. (1983). Molecular cloning. A laboratory manual. *Biochem. Edu.* 11:82. doi: 10.1016/0307-4412(83)90068-7

Zerbi, V., Ielacqua, G. D., Markicevic, M., Haberl, M. G., Ellisman, M. H., A-Bhaskaran, A., et al. (2018). Dysfunctional autism risk genes cause circuit-specific connectivity deficits with distinct developmental trajectories. *Cereb. Cortex* 28, 2495–2506. doi: 10.1093/cercor/bhy046

Conflict of Interest: The authors declare that the research was conducted in the absence of any commercial or financial relationships that could be construed as a potential conflict of interest.

frontiers in Cellular Neuroscience

HYPOTHESIS AND THEORY
published: 11 November 2020
doi: 10.3389/fncel.2020.585395

Paradoxical Effects of a Cytokine and an Anticonvulsant Strengthen the Epigenetic/Enzymatic Avenue for Autism Research

D. G. Béroule [1,2]*

[1]CNRS, Bat.508, Faculté des Sciences d'Orsay, BP 133, Orsay, France, [2]CRIIGEN, Paris, France

Maternal exposure to the *valproate* short-chain fatty acid (SCFA) during pregnancy is known to possibly induce autism spectrum disorders (ASDs) in the offspring. By contrast, case studies have evidenced positive outcomes of this anticonvulsant drug in children with severe autism. Interestingly, the same paradoxical pattern applies to the *IL-17a inflammatory cytokine* involved in the immune system regulation. Such joint apparent contradictions can be overcome by pointing out that, among their respective signaling pathways, valproate and IL-17a share an enhancement of the "*type A monoamine oxidase*" (MAOA) enzyme carried by the X chromosome. In the *Guided Propagation* (GP) model of autism, such enzymatic rise triggers a prenatal epigenetic downregulation, which, without possible *X-inactivation*, and when coinciding with genetic expression variants of other brain enzymes, results in the delayed onset of autistic symptoms. The underlying imbalance of synaptic monoamines, *serotonin* in the first place, would reflect a mismatch between the environment to which the brain metabolism was prepared during gestation and the postnatal actual surroundings. Following a prenatal exposure to molecules that significantly elicit the MAOA gene expression, a daily treatment with the same metabolic impact would tend to recreate the fetal environment and contribute to rebalance monoamines, thus allowing proper neural circuits to gradually develop, provided behavioral re-education. Given the multifaceted other players than MAOA that are involved in the regulation of serotonin levels, potential compensatory effects are surveyed, which may underlie the autism heterogeneity. This explanatory framework opens up prospects regarding autism prevention and treatment, strikingly in line with current advances along the gut microbiome–brain axis.

Keywords: autism spectrum disorders, brain enzymes, epigenetics, cytokines, short-chain fatty acids, gut microbiome, MAOA, guided propagation networks

OPEN ACCESS

Edited by:
Yu-Chih Lin,
Hussman Institute for Autism, United States

Reviewed by:
Chan Young Shin,
Konkuk University, South Korea
Charles Albert Hoeffer,
University of Colorado Boulder, United States

***Correspondence:**
D. G. Béroule
dominique.beroule@limsi.fr

Specialty section:
This article was submitted to Cellular Neuropathology, a section of the journal Frontiers in Cellular Neuroscience

Received: *20 July 2020*
Accepted: *28 September 2020*
Published: *11 November 2020*

Citation:
Béroule DG (2020) Paradoxical Effects of a Cytokine and an Anticonvulsant Strengthen the Epigenetic/Enzymatic Avenue for Autism Research. Front. Cell. Neurosci. 14:585395. doi: 10.3389/fncel.2020.585395

Abbreviations: ASD, autism spectrum disorder; BBB, blood–brain barrier; BS, Brunner syndrome; BA, butyric acid; COMT, catechol-*O*-methyl transferase; DA, dopamine; ENS, enteric nervous system; EPU, elementary processing unit; FDA, Food and Drug Administration; GP, Guided Propagation; SCFA, short-chain fatty acid; VPA, valproic acid; MAOA, type A monoamine oxidase; MAOB, type B monoamine oxidase; NE, norepinephrine; PPA, propionic acid; SERT, serotonin transporter; TPH2, type 2 tryptophan; 5-HT, serotonin; $5HT_{2B}R$, type 2B serotonin receptor; WT, wild type.

INTRODUCTION

Living organisms do not passively undergo inputs from their biological environment. Whether air particle, radiation, food, or drug, any ambient stimulus generates different net effects depending on both its strength and context of intrusion into the human body. Contradictory global effects can even be initiated by the same input and can raise a paradox deserving examination for possibly gaining insights into the biological mechanisms at work. Although not considered as fully "environmental" (Modabbernia et al., 2017), *autism spectrum disorder* (ASD) cases have followed an asymptotic increase in number over the last 50 years (Demeneix, 2014), too rapidly to argue a clear genetic cause like in *hemophilia* (Evatt, 2010; **Figure 1**). Rather than being attributable to a significant genetic mutation, such as *Fragile X*, *Brunner* (Piton et al., 2014), and *Rett* syndromes among close conditions, ASD is usually described by several symptoms of variable severities. Communication deficits are likely to result from a lack of emotional guiding and control of perception, worsened in most severe cases by irrelevant repetitions of a few acts (*stereotypy*). A high comorbidity evokes a condition of the systemic type, including poor sleep, digestive problems, and epileptic signs.

The survey reported here has been motivated by the identification of an intriguing phenomenon relating recent trials of molecules with potential impact on autism. As a matter of fact, paradoxical data were issued by distinct scientific experiments whose respective molecular targets [i.e., *IL-17a cytokine* and *valproate* (VPA) anticonvulsant] were found to alleviate autistic symptoms (Yim et al., 2017; Aliyev and Aliyev, 2018), albeit previously seen as "at risk" if absorbed by the embryonic brain (Schneider and Przewocki, 2005; Christensen et al., 2013; Wong and Hoeffer, 2018). In other words, separate studies suggest that some molecules can be implicated in the etiology of ASD when interfering with gestation, while providing potential remedies against overt autism. This issue requires clarification, notably in order to avoid promising treatments being shadowed by the knowledge of their adverse effects on pregnancy. More fundamentally, resolving this paradox may shed new light on the genesis of autism, as well as on its prevention and potential treatments.

CONTEXT-DEPENDENT EFFECTS OF DRUGS

Life is communication. Indeed, living beings are driven by complex networks of signal transmission and control, within and between their constituent cells. More precisely, biological interactions between the cell and its microenvironment are performed through "cell signaling", thanks to small proteins named *cytokines*, functionally close to hormones. At the macro-environmental level, drugs contain chemicals aimed at favorably interfering with the signaling cascades that interweave within the human body. Not surprisingly then, any single drug is likely to activate many such pathways, including the subnetworks responsible for protecting the host organism against pathogens: the *immune system*. Moreover, the expression of genes—orchestrated by *epigenetics*—can be disrupted by pharmaceutical formulations (Csoka and Szyf, 2009). In any case, the impact of a given drug depends on possible coincident stimuli (e.g., *polypharmacy*), plus the ongoing business of the host organism, as well as its background (epi)genetic traits. For example, the efficacy of a subclass of anti-hypertension agents (*beta-blockers*) undergoes variations throughout the day, coincidently with systems that control the blood pressure (Morgan and Anderson, 2003). Of note here, pregnancy constitutes a unique period during which most drugs must be either avoided or prescribed with caution, because critical periods of fetal development especially enhance drug side effects involving epigenetic and immune systems. With respect to ASD, exposure to the following molecules, either "during" or "after" pregnancy, may either "induce" or "reduce" symptoms.

1. *Cytokine IL-17a* is a small protein that contributes to cell signaling; it belongs to the *interleukin* family on which the immune system relies for regulating the maturation and responsiveness of cellular populations. IL-17a triggers signals aimed at recruiting white blood cells involved in immunity, while promoting the expression of anti-microbial *peptides*. It is important to add here that IL-17a is known to enhance the action of *IL-13*, an anti-inflammatory interleukin (Hall et al., 2017).
2. VPA is a synthetic short-chain fatty acid (SCFA), chemically similar to a molecule found in valerian. Among several medical uses, VPA is primarily an antiepileptic drug, which, in the early century, turned out to be deleterious for the offspring when prescribed across pregnancy.

TWO MOLECULES IN QUESTION

Temporary improvements have been reported in autistic individuals who experienced fever (Yim et al., 2017; Grzadzinski et al., 2018) or followed an antiepileptic treatment based on VPA (Hollander et al., 2001; Aliyev and Aliyev, 2018; Béroule, 2019). As introduced above, such reduction of symptoms is surprising because both medical conditions can also produce adverse effects during pregnancy (Patterson, 2011; Meador et al., 2013). At first sight, the same initial event (e.g., infection or drug) may therefore result in opposite final effects depending on the context, either embryonic or "postnatal with ASD."

Interleukin-17a

A large-scale study of children born in Denmark between 1980 and 2005 found that severe viral infections occurring within the first trimester of gestation increased by a factor of three the risk for autism in the offspring (Atladóttir et al., 2010). A molecular basis was given to account for this epidemiological study, namely, the elevation of cytokines associated with maternal immune response (Patterson, 2011). Among the set of pro-inflammatory actors that play their part in fighting infection, a significant contribution comes from interleukin-17a signaling. In pregnancy with maternal inflammatory condition, the activation of IL-17a pathways in the placenta may indeed

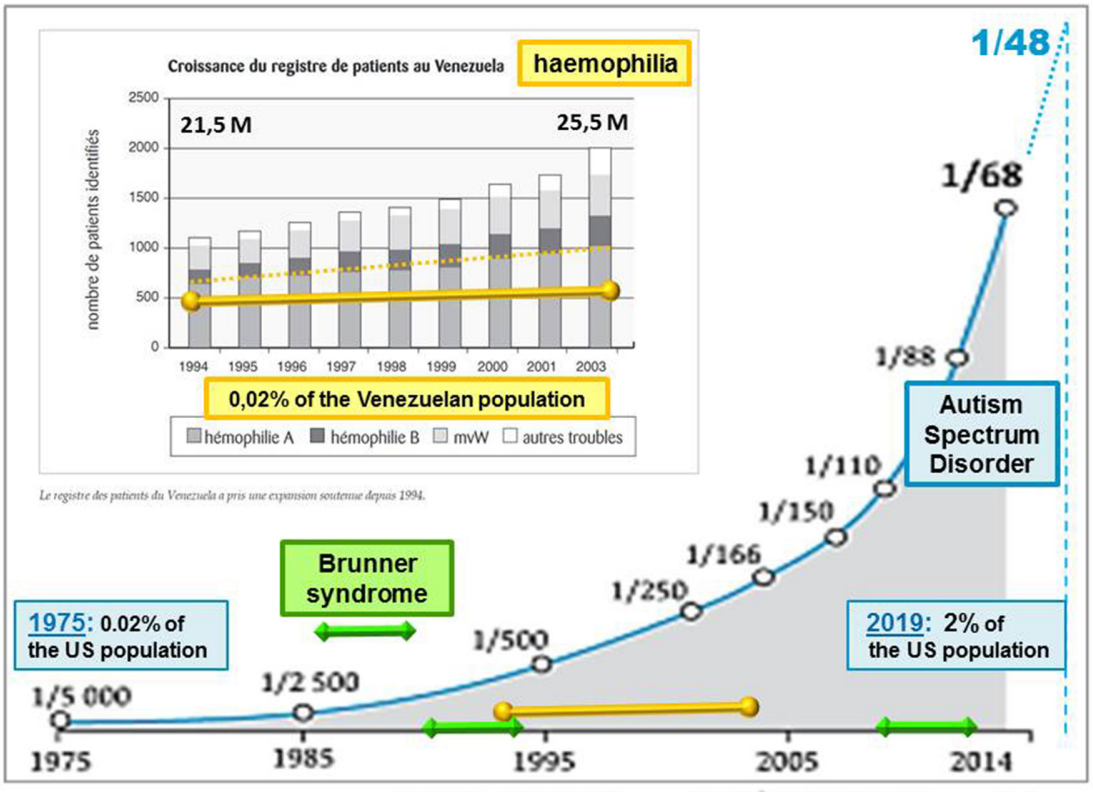

FIGURE 1 | Evolution of the autism rate (blue asymptotic curve, from Demeneix, 2014) compared with genetic diseases: hemophilia (yellow line superimposed on a graph (excerpt from Evatt, 2010) and Brunner syndrome (BS; displayed by green line segments). Intellectual disabilities associated with BS, as observed in only two families around 1993 and 2013 (Piton et al., 2014), prevent transgenerational transmission, contrary to hemophilia, which can be passed on by healthy carriers from one generation to the next. By contrast with BS, the rate of hemophilia follows at least a slight progression, as reflected by a Venezuelan survey of affected patients over a decade (Evatt, 2010). The asymptotic increase of autism spectrum disorder (ASD) cases is proposed here to result from environmental factors inducing the silent inheritance of an epigenetic mark. The latter would remain hidden until genetic features are met across human generations. Accordingly, the ASD rates currently released would only account for cases of "overt autism", irrespective of "healthy carriers" of the epigenetic mark at issue.

predispose to the postnatal onset of ASD-like deficits (Choi et al., 2016; Wong and Hoeffer, 2018). Specifically, in pregnant mice, intestinal *Th17* cells, which produce IL-17a and are released by the human bacteria, are more likely to cause inflammation-associated abnormalities in the offspring (Kim et al., 2017). Other investigations evidenced that cytokine IL-17 participates in several neurological diseases, notably through the disruption of the *blood–brain barrier* (BBB) as well as a direct effect on brain cells (Cipollini et al., 2019). Unexpectedly, then, episodes of fever have been shown to temporarily alleviate aberrant behaviors in some autistic children (Curran et al., 2007). A molecular–behavioral link is now proposed between the release of IL-17a and the temporary reduction of impairments in animal models of autism (Reed et al., 2020). According to the authors of the relevant study, maternal exposure to this cytokine would impact a brain region (*S1DZ*) located in the somatosensory cortex, by getting bound to receptors and thus reducing neural activity in this cortical area (Yim et al., 2017). Autistic symptoms would result from the disturbed development of S1DZ during gestation. Near inhibition of the same region through IL-17a release would then restrict its defective functioning. However, it remains unclear how reducing the activity in this specialized brain area could either generate long-term wide-spectrum deficits or temporarily inhibit them, afterwards.

Valproate

In 2006, building on previous work concerning the effectiveness of VPA against mood lability and irritability (Hollander et al., 2001), a 2-month, double-blind, placebo-controlled trial tested its benefits on stereotypy in ASD (Hollander et al., 2010). Based upon these preliminary results and the link found between isolated epileptiform discharges and deficits in attention, language, and behavior (Spence and Schneider, 2009), a clinical trial was planned in 2014 for investigating several medical outcomes of VPA. Because not enough subjects could satisfy the enrolment criteria, including the presence of epileptiform discharges, this study was withdrawn. No clinical trial was carried out until the end of the decade, preventing VPA from being assessed as a potential treatment against autistic symptoms. Incidentally, the US Food and Drug Administration (FDA) had advised health professionals mid-2013 that anti-seizure drugs

based on VPA were contraindicated for pregnant women. This alert was supported at that time by a study showing that children exposed to VPA while their mothers were pregnant had significantly lower IQs at age 6 than children exposed to other antiepileptic drugs (Patterson, 2011). Consequently, the pregnancy status of VPA had then been shifted from a "possible use despite potential risks" to the "X" category warning that the risk of use clearly outweighs any possible benefit. In France, a 2015 administrative report stated that existing medical alerts had not accurately informed about known risks for pregnant women (Chastel et al., 2015). As a matter of fact, up to 40% of women exposed to VPA during pregnancy had given birth to children with intellectual disabilities and autism. Meanwhile, on the research front, a computational model of autism (Béroule, 2018) predicted that besides its classical anticonvulsant properties, VPA could serve as an autism-modifying drug for its capacity to promote the *type A monoamine oxidase* (MAOA) genetic expression (Gupta et al., 2015). In 2015–2016, a preliminary case study concerned the daily intake of a VPA-based anticonvulsant, monitored over 12 months in an 11-year-old child with severe autism and epileptic signs. Gradual improvements arose across a broad autism spectrum, some of them showing up only 9 months after the trial beginning, and sometimes disturbed by bursts of overactivity. In order to remedy the latter, *methylphenidate* could complete VPA at the pharmacological level, without mutual interference (Béroule, 2019). This favorable outcome has been corroborated by a double-blind placebo-controlled trial of the same VPA-based drug, involving 100 children and using a global rating scale of ASD; 80% of the treated subjects showed significant global improvement, compared with 12% in subjects having received a placebo (Aliyev and Aliyev, 2018). The researchers who conducted this clinical study eventually gave neurobiological interpretations that are often put forward to explain autism, relating the amplitude of sodium-dependent action potentials, as well as the inhibitory GABA neurotransmitters. However, neither heterogeneity of ASD nor paradoxical effects of specific molecules like VPA can currently be enlightened by the only global excitatory/inhibitory imbalance of brain neural circuits (Uzunova et al., 2015).

PERSISTENT ADAPTATION TO THE FETAL ENVIRONMENT

At this stage, the paradox raised by inconsistent effects of two molecules can be addressed through the following couple of questions.

1. What kinds of physiological events, caused by the same input, could either (during gestation) underlie the development of an ASD case or (in the autistic child) facilitate the onset of proper behavior?
2. Are there common signaling pathways at the intersection of those activated by the molecules under focus here? Accordingly, if all autism inducers shared a chemical cascade leading to ASD onset, any of them could form the basis of a potential remedy, regardless of the condition actual initiators.

In attempting to answer the above questions, the human broad adaptability can first be reminded and associated with the trend to keep track of environmental stimuli in the long run. Even early molecular memory acquired in the fetal life may thus modulate the impact of postnatal inputs. By contrast, the seemingly sudden onset of autistic signs in the infancy is still believed to readily result from early medications, especially vaccination, despite epidemiological studies based on large populations evidencing no such causal relationship (Hviid et al., 2019). The occurrence of symptoms before the age of 3 can less directly be linked to prenatal adverse events memorized in some way and silently integrated into the developmental script of the infant until a revealing situation. As a matter of fact, not so many biological systems (e.g., neural and immune) are capable of reliably implementing both "print" and "reading" memory functions in the long run. Of noticeable exception is that the DNA gene pool sustainably crosses generations, although experiencing rare mutations. Additionally, the embryonic genetic programming of stem cells—through epigenetics—propagates unaltered identities along cell lines (e.g., *X chromosome inactivation*; Pinheiro and Heard, 2017) and, under certain conditions, over human generations without genetic mutations: among pathologies of epigenetic origin, defects are still reported in the third generation after the grandmother was treated with *diethylstilbestrol* during a pregnancy carried in the third quarter of the 20th century (Gore et al., 2015). Beyond this transgenerational pathology, it seems that critical periods of embryonic brain development (Kim et al., 2011) exhibit enhanced susceptibility to the environment. Quite possibly, an early "snapshot" of this environment may be taken as reference for the baseline expression of "regulating genes" being fixed once and for all (e.g., MAOA enzyme). In particular, the synaptic concentration of neurotransmitters is likely adapted to the maternal health and feeding resources conveyed by the composition of the mother's blood. With the latter being passed through both placenta and BBB to the fetus neural system, the neurotransmitters' metabolism could be tuned so as to account for environmental signals. But this partial information may not actually reflect the chemical surroundings that the newborn will find after the end of gestation, when breastfeeding is over. In case of significant gap between (maternal) signals received in the womb and (autonomously) after birth, weaning may resemble a sort of withdrawal (a well-known example is the newborn of a smoking mother, whose brain does not receive any more psychotropic molecules). This environmental mismatch would be harmless if the early genetic programming could be refined according to the postnatal context, encompassing the erasure of obsolete epigenetic marks. Otherwise, a closer fit of prenatal and postnatal situations may however be reached by bringing the child chemical environment closer to influential events experienced in the mother's womb. Although unusual, this view is consistent with the paradoxical situations addressed here. Environmental feature(s) to the metabolic effects of which the fetal brain got permanently adapted during a critical stage of gestation would thus favorably be brought into play. But

apart from a few identified factors such as maternal infection, VPA-based treatment, or polluted surroundings (von Ehrenstein et al., 2019), the origin of a given case of autism remains often uncertain. Furthermore, not every environmental item, such as a pesticide, can form the basis of a safe treatment. These difficulties bring us back to the second question concerning the possibility that, although respectively generating various physiological outcomes, all potential initiators of an autistic case could share a subset of signaling pathways. Interestingly, this would allow molecules that are medically safe to partly reinstate the "lost environment" for which neuronal stem cells had been programmed into the womb.

SHARED BRAIN ENZYMATIC PATHWAYS

Among neurotransmitters, *monoamines* are modulating agents involved in the control of behavior and learning. The ongoing synaptic concentration of monoaminergic neurotransmitters is therefore central in the brain function, relying on a subtle balance to be preserved between their production/*synthesis*, *recycling*, and degradation/*catabolism*. Reabsorbed through *reuptake* into the afferent synapse, monoamines can either be used again (recycled) or be degraded in the presynaptic neuron by MAOA, while another enzyme, named *catechol-O-methyl transferase* (COMT), works in the postsynaptic neuron. The potential for regulated trafficking between relevant systems relies on early epigenetic setup, as well as feedback loops to properly adjust metabolic parameters. Provided an optimal range of synaptic levels for a given neurotransmitter, the inner promotion of its catabolism may for instance be set "down" and its synthesis be boosted in case of a too-low concentration. Such out-of-range output may be due to an accidental input involving for instance MAOA. The A type of MAO, carried by the X chromosome and known as a vital regulator of embryonic brain development (Wang et al., 2011), is capable of degrading at least three key monoamines, namely, *dopamine* (DA), *serotonin* (5-HT), and *norepinephrine* (NE), whereas type B monoamine oxidase (MAOB) and COMT cannot catabolize 5-HT. On first analysis, this discrepancy is likely to elicit unbalanced synaptic concentrations between 5-HT and other monoamines. However, as long as MAOA remains the main player to carry on the degradation of all monoamines, their levels consequently decrease at the same rate. In the *Guided Propagation* (GP) model of autism, monoaminergic equilibrium tends to continue if COMT is poorly expressed, if X-inactivation occurs (in women), and until MAOB is fully operational (around 2 years after birth). At the computational level, the higher the local parameter *Da* that codes for DA, the more controlled the response of *elementary processing units* (EPUs) despite possible imbalance of other monoamine-like parameters; this occurs when the "*Da* concentration" is decreased, which in the real world accompanies an increase of MAOB activity. A theoretical scenario therefore begins with an accidental stimulation of MAOA during gestation, eliciting a long-term epigenetic regulation of the same enzyme in the embryonic neurons. This epigenetic mark would become deleterious when meeting high-functioning COMT promoter, and without protection by X-inactivation (because all X chromosomes carry the downregulated MAOA). The relatively poor degradation of 5-HT assumed here would only initiate visible effects in the early childhood, when the third metabolizer (MAOB) is mature enough to supply the baseline catabolism of DA. This enzymatic reading provides an explanation for the regressive feature of ASD, while the X-inactivation and COMT polymorphism (low to high expressions) can together account for the male prevalence (Béroule, 2018, 2019). Consequent structural deficits are represented by a GP network in which the local *5ht* parameters decrease slower than *Ne* across offline encoding, inducing either aberrant or lacking memory pathways (Béroule, 2016). The higher the *5ht*/*Ne* ratio, the wider the misconnections, namely, the chaining of meaningless sensorimotor patterns, magnified convergence of inner stimuli towards EPUs inducing their overactivity, and missing links between channels that normally cooperate in sensorimotor tasks. For the sake of simplicity, the way the above events are represented in the GP model can be displayed by an assembly of puzzle pieces (**Figure 2**).

Given that the downregulation of MAOA is being proposed as key crossover point between prenatal signaling and a spectrum of postnatal symptoms, the second question to be addressed is about the generic nature of this central feature. Ultimately, is IL-17a able to affect MAOA just as VPA?

As stated above, VPA is already known to stimulate the MAOA gene promotion, through select signal pathways (Gupta et al., 2015). Of note, several "medium-chain" fatty acids and SCFAs share chemical and structural properties with VPA, making them potential MAOA inducers; they are named *pelargonic/nonanoic*, *decenoic*, *propionic*, *butyric*, and *valeric* from which VPA is made. Now, with regard to the IL-17 cytokine, no direct action was reported towards MAOA. But other molecules activated by IL-17 could promote MAOA and therefore be responsible for ASD cases through a mathematical *transitive relation*. Indeed, MAOA is one of the most strongly upregulated gene within cells activated by the IL-13 anti-inflammatory interleukin (Dhabal et al., 2018), which gives the following: (1) IL-13 → MAOA+. Not surprisingly then, elevated gestational IL-13 associated with maternal inflammatory immune response and maternal–fetal cytokine signaling increases the risk for the offspring to develop abnormalities, namely, ASD, hyperactivity, and inattention (Thürmann et al., 2019). Importantly here, the genetic expression of IL-13 is enhanced by the pro-inflammatory IL-17, i.e., (2) IL-17 → IL-13, provided that their signaling pathways are present in the same cell (Hall et al., 2017). Indeed, IL-13 can be produced inside the brain, where its receptors have been evidenced (Mori et al., 2016); for its part, the IL-17 generated outside the brain is conveyed by the blood, can get across the fetal BBB, and then reach receptors (IL-17R) found in neural cells (Luo et al., 2019), together with IL-13 receptors. Taken together, (1) and (2) lead to IL-17 → MAOA+.

To sum up, the paradoxes that motivated this study only appear from a distant point of view. A close-range focus shows an immediate common effect of molecules at issue, regardless of

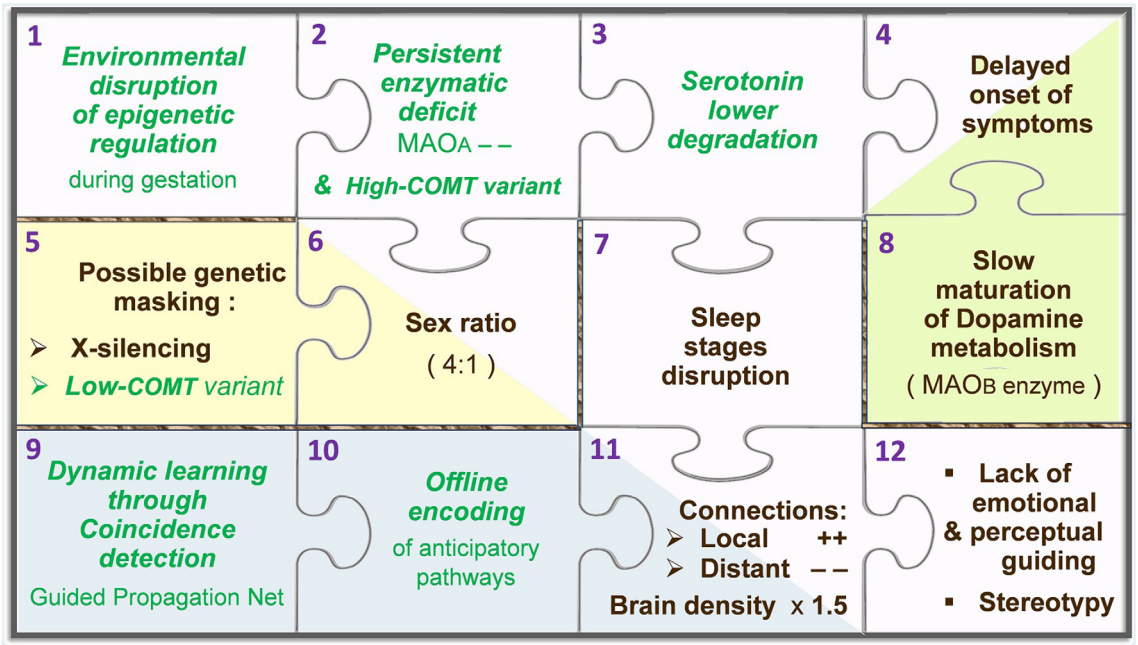

FIGURE 2 | Puzzle of autism, according to the Guided Propagation (GP) model. Pieces containing a green label in italics represent hypotheses, while labels in black indicate actual facts. The main stream of pieces goes from the epigenetic regulation hypothesis (top-left piece, no. 1) towards core symptoms (bottom-right piece, no. 12). Two-tone pieces (nos. 4, 6, and 11) stand for facts that appear downstream of two pieces coding for a hypothesis and another fact: in this theoretical framework, the disrupted architecture of sleep (no. 7) is caused by a poor degradation of serotonin (no. 3), which leads to aberrant neural paths (no. 11) that are built "offline" in the anticipation mode normally only relevant "online" (no. 10). For further details, see Béroule (2018).

context, namely, an increased promotion of the MAOA enzyme. In the GP model, second-order effects differ according to the context of exposure:

1. Blank situation, critical period of neurulation: The monoamine metabolism is durably adapted to the current fetal environment through MAOA downregulation (MAOA–in **Figure 2**). When the transport of causal molecule(s) by maternal blood/milk is discontinued, no later than the end of gestation/breastfeeding, the MAOA setting remains.
2. Then, the occurrence of MAOA inducers is expected by the epigenetic memory to comply with its prenatal regulation. A metabolic imbalance may otherwise result from the high-expression variant of COMT and be enhanced by matured MAOB.
3. In case of epigenetic masking (i.e., X-inactivation in women) or genetic variant (low/medium COMT), the MAOA downregulation is silently transferred to the next offspring where it may occur in a different genetic context leading to overt autism (case 2 above).

According to this possible etiology of ASD (**Figure 3**), only the erasure of specific epigenetic traits supporting the MAOA downregulation could permanently reverse the brain enzymatic imbalance at issue. Disease-modifying treatments based on MAOA stimulation nevertheless represent an alternative thanks to neurogenesis and targeted neural migration. Favored by an educational program, the gradual growth of proper neural structures is assumed to support the enrichment of social conduct, at the price of a sustained supply of drugs aimed at approaching the embryonic microenvironment. The sooner the treatment initiation, the better its expected outcomes. However, while shown to be effective against both epileptic signs and some ASD symptoms, VPA-based drugs can be toxic to detoxification organs, most commonly below 6 years of age (Star et al., 2014), encompassing the earlier time at which behavioral deficits start arising. Alternative treatments remain to be established with the aim of being safe at an early age. Accordingly, one should care about recent strides in the understanding of the *gut microbiome* function.

THE MICROBIOME RESOURCES

The *enteric nervous system* (ENS), also referred to as the "second brain," notably allows some autonomy in the management of digestion, however mediated by the same chemical mediators as those at work in the "first" brain. It logically follows that a systemic metabolic imbalance of monoamines is likely to affect the neural cells of both nervous systems. In the close neighborhood of trillions of microbes, some of which induce inflammation and produce SCFAs, the ENS appears to be better equipped than the brain to deal with a metabolic dysregulation. Molecules elicited by the gut microbiota mostly serve local functions before being degraded in the liver, but those which can reach the blood circulation (*via* the *distal colon* bypass) and get through the BBB are eventually able to spread their

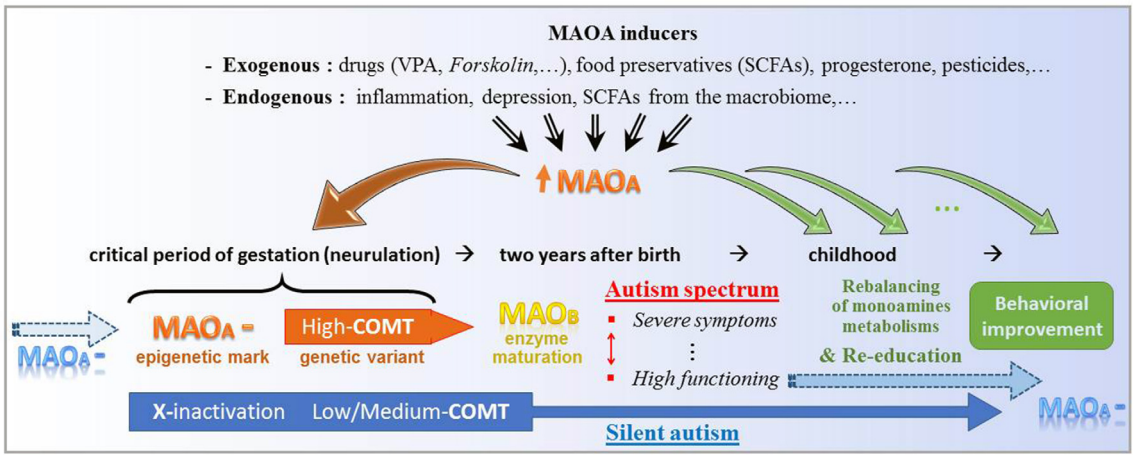

FIGURE 3 | Theoretical key functions of the molecular stimulation of type A monoamine oxidase (MAOA) in either initiation or alleviation of autism. At the top, several non-genetic factors share the property to significantly promote the expression of the MAOA gene. In the early gestation, an epigenetic downregulation of MAOA (MAOA—), which notably combines here with genetic variants of the catechol-*O*-methyl transferase (COMT) enzyme, may be inherited (blue arrow at the left-hand side) and/or favored/caused by MAOA enhancers (brown down arrow to the left). At the right-hand side, the series of smaller green arrows stand for a daily intake of MAOA inducer, which may bridge the gap between gestational and postnatal respective environments by reducing the metabolic imbalance of monoamines and consequently support behavioral re-education. At the bottom, a genetic variant (low-to-medium expression of COMT) and the classical epigenetic X-inactivation may hide the "MAOA—" mark, which is however silently carried towards the next human generation.

metabolic influence across the brain. In particular, regulatory outcomes primarily aimed at the second brain may benefit the first one. Besides a common lowered diversity of the autistic children microbiome, a trend seems to emerge from existing data, reminiscent of the alternative ASD inducer/remedy represented here by cytokines and SCFAs. In absence of medical intervention involving antibiotics, the microbiota would develop along the inflammatory arm and its associated digestive troubles: any shift towards a gut pro-inflammatory state can in turn trigger the activation of neuro-inflammatory responses in the brain (Golubeva et al., 2017), with potential improvement of ASD. A relatively low concentration of SCFAs can then be observed in the plasma of autistic children (El-Ansary et al., 2011). When reset by a strong antibiotic, short diet, and replaced by typical germs, following a *microbiota transfer therapy*, the SCFA by-products arm can be privileged in a long-lasting way (Kang et al., 2017). Data obtained *in vitro* by using a neuron-like embryonic cell-line notably demonstrate the regulation exerted by propionic acid (PPA) and butyric acid (BA; i.e., *propionate* and *butyrate*) over the expression of neural genes (Nankova et al., 2014). Among a large set of genes tested for their link with ASD, the MAOA expression is doubled by each of these acids, while COMT is decreased by a factor of 2.7 (which means a total of 7.3 if assuming a multiplicative combination of the two acids). Whereas both genetic modulations alleviate the harmful setting pointed out by the GP model (MAOA–and high COMT), therefore suggesting a corrective action of the microbiome, the latter is rather usually believed to exacerbate ASD symptoms (Goines and Ashwood, 2013; Slattery et al., 2016). Even at odds with the theory presented here, immediate behavioral worsening has been proposed to result from exposure to SCFA. Rats whose brain directly receives PPA show epileptiform activity within the 30 min of infusion, accompanied by a variety of abnormal responses (retropulsion, hyperextension, turning, and dystonia) considered as "bearing some resemblance" to bouts of irrelevant actions found in autism (MacFabe et al., 2007). Bacteria that produce SCFAs and elicit inflammation can thus be viewed as unwelcome guests in the gut of subjects with ASD. This position is now challenged by a study in which significant improvements of 18 children with ASD occurred together with the colonization of the gut by antibiotic-resistant and SCFA-producing bacteria (*Bifidobacterium*, *Prevotella*, and *Desulfovibrio*). Persistency of this favorable effect has been confirmed in the same subjects, 2 years after their initial enrollment. Both *Prevotella* and *Desulfovibrio* were on average more abundant in ASD subjects following treatment than in the donor samples: *Prevotella* was 712 times higher after 6 weeks and maintained an 84-times increase after 2 years (Kang et al., 2019). Although Clostridia and *Bacteroides* are also reported as PPA producers in ASD, they share with *Sutterella* the joint occurrence of gastrointestinal disorders such as inflammatory bowel disease (Bezawada et al., 2020). An added plus in favor of the *Prevotella* prevalence is the production of up to three times more PPA than the *Bacteroides*-dominated microbiota associated with high-fat intake (Chen et al., 2017). If PPA was confirmed as effective against overt autism, evidence of its deleterious effects on gestation would provide further support to the present theory. Unexpectedly, such indication already exists. As a matter of fact, *propionic acidemia* is a genetic disease—obviously affecting early gestation—in which the accumulation of PPA elicits several metabolic disorders, including seizures, gastrointestinal disturbances, intellectual disability, and delayed development (Pena and Burton, 2012).

In addition, a microbiome shift in maternal gut, leading to formation of PPA and BA by-products during the early stages of the fetus' neural development, has been linked to ASD (Abdelli et al., 2019).

Through daily intake, VPA primarily protects against epilepsy. A preliminary trial led to its association with the methylphenidate psychostimulant for balancing the monoaminergic metabolism (Béroule, 2019). By comparison, the possible natural production of propionate and butyrate by the microbiome, following a process for initiating the relevant change (Kang et al., 2017), may be preserved by a high-fiber diet. Furthermore, PPA and BA would properly regulate MAOA and COMT, whereas VPA proved to require a complementary medication. Although this avenue still requires closer analyses and refinements, the gut microbiota are therefore likely to provide an alternative to the pharmacological approach of ASD. Regarding now the protection of gestation, SCFA gut by-products should be restricted, particularly when realizing that they would add to similar substances widely used as anti-mold/preservative ingredients in the food industry (Abdelli et al., 2019). Together with the immune system, the microbiome may consequently require follow-up when planning pregnancy, as part of a strategy aimed at limiting autism development (Paysour et al., 2019).

DISCUSSION: ALLOCATION OF ROLES AMONG NETWORKS OF PLAYERS

Facing the Autism Complexity

In 2020, a wide-angle approach to the wide spectrum of autism can be adopted (e.g., Marotta et al., 2020). Given the myriad of various factors that have been linked to ASD over the past decades, a shared responsibility is assumed today, however possibly modulated by emphasis on a selection of signaling pathways. At the molecular level, interdependent systems control the expression of numerous susceptibility genes constrained by their respective polymorphisms and rare mutations, and moreover submitted to environmental stimuli through epigenetics. A strict focus on any of these participants is thus challenged by the known involvement of many other players. With regard to neurotransmitters (Cetin et al., 2015), their metabolic breakdown by brain enzymes only concludes a series of contributions for them to be synthesized, released in the synaptic space, and either recycled or degraded in the presynaptic neuron thanks to *transporters*, towards several subtypes of receptors. All along repetitive rounds of this "neurotransmitter cycle", any player disruption is likely to alter the functions of its partners. Conversely and more positively, several partners may respond by implementing compensatory mechanisms, hence possibly repairing/masking an original impairment. An irrelevant molecular activity can thus be elicited in signaling cascades by upstream previous alterations as well as feedbacks from downstream events, whereas the impact of a local deficit may be hidden by the genetic background and ongoing homeostatic regulations. This situation confirms that the actual picture is obviously more complicated than the representation displayed in **Figure 3**.

Pivotal Role of Serotonin

Despite the complex crosstalk between numerous candidates likely to underlie the ASD heterogeneity, a leading role can be attributed to one monoamine for its recognized contribution to the brain development. Among neurotransmitters, 5-HT has truly become a main biomarker of autism (Benza and Chugani, 2015; Muller et al., 2016). Half a century ago, elevated whole blood 5-HT (*hyperserotonemia*) was the first molecular phenomenon found in a subset of ASD subjects, today associated with 25–30% of cases. The fact that hyperserotonemia is not detected in every autistic case is consistent with the correlation of this feature with ASD severity (Abdulamir et al., 2018) and also reveals individual variations in the biological inner management of disturbances impacting the 5-HT system. Along this line, it is worth knowing first that the level of 5-HT contained in blood *platelets* does not reflect its synaptic concentration. The opposite relationship rather applies, notably through the SERT transporter, which transfers 5-HT from the "extra-" to "intra-" cellular space of neurons, glial cells, and platelets. The 5-HT 2B receptor (5-HT_{2B}R) signaling has recently been proposed to control this process thanks to a feedback loop that keeps synaptic 5-HT at tonic concentrations necessary for brain functions (Baudry et al., 2019). Consequently, a high synaptic level of 5-HT would promote its low uptake. 5-HT_{2B}R, among other auto-receptors, thus participates in 5-HT tuning, which also relies on opposed contributions, namely, synthesis and degradation. The brain 5-HT precursor, named "type 2 tryptophan" (TPH2), is key in 5-HT synthesis and affects both 5-HT availability and synaptic levels in the opposite way as MAOA. These various agents form a team that allows a player irrelevant action to be alleviated by the overexpression/subexpression of other team members. Studies concerning either knock-out (KO) or overexpressed genes are informative of this partnership, aimed at keeping sufficient 5-HT concentrations in both presynaptic vesicles and synaptic cleft.

Multiple-Source Serotonin Tuning

Targeted genetic modifications of the "5-HT team" members have provided animal models of autism to be compared with wild-type (WT) subjects (Muller et al., 2016). In SERT-KO mice, the aforementioned vesicles lack the "recycled 5-HT" input; 5-HT availability then depends on its upgraded synthesis and/or reduced breakdown. On the opposite side, in high-functioning SERT (*Ala56*) gain-of-function mutants, the related high-rate uptake favors the storage of 5-HT into vesicles at the expense of synaptic 5-HT signaling extent and duration. In both out-of-range situations, whether regulating factors could on the one hand optimize the availability of 5-HT packaged into vesicles and, on the other hand, could maintain tonic concentrations in the synapse represents a known conceptual problem for the mechanism of vesicular release (Blakely and Edwards, 2012). However, 5-HT-enhanced synthesis and reduced degradation can be suspected to: (a) better feed the pool of releasable 5-HT despite inactive reuptake (in SERT-KO mice); and (b)

maintain the 5-HT synaptic level required for receptor activation despite hyperactive reuptake (in Ala56 mice). Consistent with this common solution, the 5-HT synthesis capacity has been found to increase gradually in autistic children, up to 1.5 times the adult normal value (Chugani et al., 1999), while a 30% deficit of MAOA activity has been identified in the cerebellum (for 70% of autistic children) and in the frontal cortex (for 55% of young subjects; Gu et al., 2017). Of note, such a depressed enzymatic activity cannot be witnessed by platelets since they only harbor MAOB. Amazingly enough, despite a significant *in vivo* increase in the rate of synaptic clearance in Ala56 vs. WT mice, no change was observed in brain tissue 5-HT levels (Veenstra-VanderWeele et al., 2012), which underpins the implication of compensatory processes. Moreover, the male full prevalence suggests the mediation of at least one protein whose gene is carried by the X chromosome (i.e., MAOA), besides sex-specific loci present in the SERT gene (Weiss et al., 2005). In addition, the surprising time delay of positive effects following SERT inhibition aimed at alleviating ASD symptoms in Ala56 mice (Robson et al., 2018) can be explained by the time-consuming neural migration necessary for new neural structures to be encoded and consolidated under well-regulated MAOA (Béroule, 2018).

After having pointed to metabolic implications of out-of-range SERT, let us start now from the downregulated MAOA hypothesis. In order to avoid a 5-HT synaptic overload caused by MAOA deficiency, possible counteractions include a stronger SERT gene expression, possibly less controlled by $5HT_{2B}R$. Indeed, the SERT gene promoter variants determine different levels of expression affecting 5-HT levels and social skills (Tanaka et al., 2018); a potent clearance of synapses can then be linked with the peripheral hyperserotonemia found in a subset of children with autism, likely carriers of the long allelic variants of the SERT gene promoter (Quinlan et al., 2020). On the opposite, low expressing short-allele of SERT in autistic children and SERT knock-out in mice are both associated with increased cortical volume (*macrocephaly*), counted as hallmark of severe autism. Either loss-of-function polymorphism or epigenetic downregulation of TPH2, the rate-limiting enzyme that allows *tryptophan* to be transformed into brain 5-HT, could modulate the biosynthesis of the latter (Chen and Miller, 2012). Consequently, a lower 5-HT concentration in the synapse would in turn generate the observed enhanced sensitivity of $5HT_{1A}$ and $5HT_{2A}$ postsynaptic receptors in mice mutants (Veenstra-VanderWeele et al., 2012). It eventually appears that the modulating agents mentioned above (TPH2 enzyme, SERT-based recycling system, and 5-HT receptors) are likely to counteract a chronic metabolic breakdown of synaptic 5-HT, while exerting a specific influence on ASD-nonspecific behaviors, such as the management of stress (Chen and Miller, 2012).

Reviewed Position of Type A Monoamine Oxidase

The acute excess of MAOA, which is assumed to trigger an epigenetic reaction, may stand downstream a signaling cascade initiated by factors that stimulate the synaptic 5-HT at an early stage of the brain development. Among molecules holding this property, exposure of fetuses to *5-HT selective reuptake inhibitors* increases the risk of ASD (Harrington et al., 2014), unless the $5\text{-}HT_3$ receptor is knocked out (Engel et al., 2013). Within the GP framework, this receptor would be required to detect the 5-HT excess leading to an acute boost of MAOA, fostering then its persistent epigenetic downregulation. The scenario shown in **Figure 3** is more fundamentally challenged by the fact that a MAOA deficit has not been evidenced in every case of autism. An imbalance activity between the transporter proteins in charge of monoamines (e.g., Low SERT) could then induce the 5-HT synaptic excess at issue, in which case MAOA would not represent a key factor in ASD etiology.

To conclude this discussion, variations of synaptic 5-HT induced by several interactive players may combine so as to cover the full ASD spectrum. Not systematically tested in connection with blood levels of 5-HT (Weiss et al., 2005) nor in SERT-oriented models of autism (Quinlan et al., 2020), MAOA and its enzymatic partners however deserve interest, in connection with other concerned agents, including SERT, 5-HT receptors, and TPH2 among a large family of neurotransmission regulators.

First, MAOA is the only enzyme to catabolize 5-HT, whose disruption is a prime ASD biomarker.

Second, the co-occurrence of a weak MAOA, high COMT, and mature MAOB can account for two ASD features that remained unexplained beforehand, namely, the onset of symptoms before 3 years of age and the sex ratio that partly results from the localization of MAOA on the X chromosome. Other characteristics of the condition can be simulated in a computational model that incorporates a representation of monoamine functions.

Third, among genetically modified rodents—whose neuromodulating system is comparable with the human one, MAOA-KO mice exhibit high correspondence to ASD core symptoms, which warrants its status of "animal model of autism." In human, the very rare mutation of MAOA responsible for the BS has only been linked to autism 20 years after the former discovery of a family with serious behavioral troubles (Piton et al., 2014). At that time, according to the GP model of autism, ASD symptoms could have been masked by genetic variants such has low-COMT polymorphism, or immature MAOB enzyme, or DA overexpression. MAOA might have raised more awareness among researchers, otherwise.

Fourth but not false, the extinction of both 5-HT and NE across every sleep cycle cannot take full advantage of the online multiple regulations of 5-HT addressed above. If the balanced offset of these two monoamines turned out to hold a critical functional role, the disparate 5-HT levels observed online within the autism spectrum would eventually appear not so critical for the structural foundation of autism. Essentially, the GP theory puts forward a 5-HT "noise" that improperly remains into the synaptic cleft during sleep whatever the (non-null) baseline level of 5-HT at the beginning of every sleep cycle, therefore relatively irrespective of the online regulation exerted by the players introduced above.

CONCLUSION: NATURAL FATTY ACIDS UNDER FOCUS

In our modern environment, possible enzymatic disruptions during gestation are substantiated by the finding of chemical factors that overexpress the MAOA enzyme and strikingly entail similar paradoxical effects. One purpose of the present article was to clarify this point, which included confronting a theory of autism to experimental data. An avenue for research now appears to widen, already suggesting medical approaches. In a few words, the goal would be to reinstate the enzymatic shift that caused a persistent epigenetic reaction through which the identity of neuron cell lines was irreversibly fixed in the early gestation (**Figure 3**). From a clinical point of view, this global prediction can be tested on the occasion of future trials concerning MAOA-inducing molecules. Relevant biomarkers have been proposed (Béroule, 2019), including the periodic control of sleep electroencephalogram (EEG), levels of monoamines, their metabolizers and metabolites, and, if possible, the family phenotyping of selected genes responsible for the management of monoamines.

Although not initially expected to be relevant, data on the gut microbiome turned out to strengthen the resolution presented in this article, while offering a potential medical resource. Feedbacks from the gut microbiota towards nervous systems can in fact be viewed as an attempt to reduce the enzymatic imbalance assumed here to underlie autism. As an aside, the continuous release of microbiota by-products remains challenging, since it may maintain the causal epigenetic traits in a sort of vicious cycle, a point to be raised in future works. Furthermore, studies focused on the microbiome enlarged the list of "at risk" industrial chemicals, the natural origin of which is often put forward by their marketer. Obviously, "natural" does not mean "safe." It would be wise for women with a parenthood plan to avoid several products that contain SCFAs or medium-chain fatty acids close to VPA (e.g., food ingredient; Martinez-Mayorga et al., 2013), among other MAOA inducers such as *progesterone* (Kobayashi, 1980) and *forskolin*. Studied for inhibiting ASD progression in rat (Sidharth et al., 2020), forskolin is likely to enhance the MAOA promoter activity, at least in *Neuro2a* cells akin to neural stem cells, and particularly responsive to environmental factors (Gupta et al., 2015). It is also known as an effective weight-loss agent extracted from the Indian *coleus* plant, but its consumption is already not recommended for pregnant women (Godard et al., 2005). As an illustration of misleading advertisement, the *glyphosate* herbicide molecule has been replaced by the FDA-approved pelargonic acid, declared to occur naturally in many plants and animals. One may however bear in mind that pelargonic and valproic acids are close molecules and that permitted concentrations of the first one are comparable with the initial dosing of the second one for an anticonvulsant treatment, which is now forbidden during gestation (Béroule, 2019). Although potentially harmful during pregnancy, some of the molecules that stimulate the expression of MAOA could paradoxically form the basis of medications aimed at stopping the growth of aberrant neural structures, as soon as possible after the onset of autistic signs, hopefully giving conventional school a chance to be effective.

A shifted conception of autism emerges from the above organized set of data and hypotheses, as a side effect of systemic adaptation to environmental changes that, incidentally, could participate in the human evolution. Against this background, medical problems occur in case of critical mismatch between the after-birth surroundings of the brain and the gestational "snapshot" on which a persistent metabolic regulation of its monoamines is supposedly based. Accordingly, this instance of transgenerational epigenetics might one day reveal appropriate, if our environment became continuously overwhelmed by small/medium fatty acids in food, cosmetics, drugs, and pesticides, not mentioning inflammation associated with widespread viral dissemination.

DATA AVAILABILITY STATEMENT

Publicly available datasets were analyzed in this study. This data can be found here: https://perso.limsi.fr/domi/Movie-S1_DGB_nov16.mov.

AUTHOR CONTRIBUTIONS

The author confirms being the sole contributor of this work and has approved it for publication.

FUNDING

This work was supported by CNRS salary.

ACKNOWLEDGMENTS

This article is dedicated to the young scientific researcher Joseph J. Mariani, who, in 1983, allowed Guided Propagation Networks to be developed at LIMSI (CNRS former laboratory).

REFERENCES

Abdelli, L. S., Samsam, A., and Naser, S. A. (2019). Propionic acid induces gliosis and neuro-inflammation through modulation of PTEN/AKT pathway in autism spectrum disorder. *Sci. Rep.* 9:8824. doi: 10.1038/s41598-019-45348-z

Abdulamir, H. A., Abdul-Rasheed, O. F., and Abdulghani, E. A. (2018). Serotonin and serotonin transporter levels in autistic children. *Saudi Med. J.* 39, 487–494. doi: 10.15537/smj.2018.5.21751

Aliyev, N. A., and Aliyev, Z. N. (2018). A double-blind placebo-controlled trial of acediprol (valproate sodium) for global severity in child autism spectrum disorders. *Online J. Neurol. Brain Disord.* 2, 93–97. doi: 10.32474/ojnbd.2018.02.000127

Atladóttir, H. O., Thorsen, P., Østergaard, L., Schendel, D. E., Lemcke, S., Abdallah, M., et al. (2010). Maternal infection requiring hospitalization during pregnancy and autism spectrum disorders. *J. Autism Dev. Disord.* 40, 1423–1430. doi: 10.1007/s10803-010-1006-y

Baudry, A., Pietri, M., Launay, J. M., Kellermann, O., and Schneider, B. (2019). Multifaceted regulations of the serotonin transporter: impact on antidepressant response. *Front. Neurosci.* 13:91. doi: 10.3389/fnins.2019.00091

Benza, N., and Chugani, D. (2015). "Serotonin in autism spectrum disorder: insights from human studies and animal models," in *The Molecular Basis of Autism. Contemporary Clinical Neuroscience*, ed. S. Fatemi (New York, NY: Springer), 257–274.

Béroule, D. G. (2016). Available online at: https://perso.limsi.fr/domi/Movie-S1_DGB_nov16.mov. Accessed October 2020.

Béroule, D. G. (2018). Offline encoding impaired by epigenetic regulations of monoamines in the guided propagation model of autism. *BMC Neurosci.* 19:80. doi: 10.1186/s12868-018-0477-1

Béroule, D. G. (2019). Autism-modifying therapy based on the promotion of a brain enzyme: an introductory case-report. *AIMS Mol. Sci.* 6, 52–72. doi: 10.3934/molsci.2019.3.52

Bezawada, N., Phang, T. H., Hold, G. L., and Hansen, R. (2020). Autism spectrum disorder and the gut microbiota in children: a systematic review. *Ann. Nutr. Metab.* 76, 16–29. doi: 10.1159/000505363

Blakely, R. D., and Edwards, R. H. (2012). Vesicular and plasma membrane transporters for neurotransmitters. *Cold Spring Harb. Perspect. Biol.* 4:a005595. doi: 10.1101/cshperspect.a005595

Cetin, F. H., Tunca, H., Guney, E., and Iseri, E. (2015). *Neurotransmitter Systems in Autism Spectrum Disorder, Autism Spectrum Disorder—Recent Advances, Michael Fitzgerald, IntechOpen.* Available online at: https://www.intechopen.com/books/autism-spectrum-disorder-recent-advances/neurotransmitter-systems-in-autism-spectrum-disorder. Accessed October 2020.

Chastel, X., Essid, A., and Lesteven, P. (2015). *Enquête Relative aux Spécialités Pharmaceutiques Contenant du Valproate de Sodium, Inspection Générale des Affaires Sociales, 2015–094R.* Available online at: http://www.igas.gouv.fr/IMG/pdf/2015-094R.pdf. Accessed October 2020.

Chen, G.-L., and Miller, G. M. (2012). Advances in tryptophan hydroxylase-2 gene expression regulation: new insights into serotonin-stress interaction and clinical implications. *Am. J. Med. Genet. B Neuropsychiatr. Genet.* 159B, 152–171. doi: 10.1002/ajmg.b.32023

Chen, T., Long, W., Zhang, C., Liu, S., Zhao, L., and Hamaker, B. R. (2017). Fiber-utilizing capacity varies in Prevotella- versus Bacteroides-dominated gut microbiota. *Sci. Rep.* 7:2594. doi: 10.1038/s41598-017-02995-4

Choi, G. B., Yim, Y. S., Wong, H., Kim, S., Kim, H., Kim, S. V., et al. (2016). The maternal interleukin-17a pathway in mice promotes autism-like phenotypes in offspring. *Science* 351, 933–939. doi: 10.1126/science.aad0314

Christensen, J., Grønborg, T. K., Sørensen, M. J., Schendel, D., Parner, E. T., Pedersen, L. H., et al. (2013). Prenatal valproate exposure and risk of autism spectrum disorders and childhood autism. *JAMA* 309, 1696–1703. doi: 10.1001/jama.2013.2270

Chugani, D. C., Muzik, O., Behen, M., Rothermel, R., Janisse, J. J., Lee, J., et al. (1999). Developmental changes in brain serotonin synthesis capacity in autistic and nonautistic children. *Ann. Neurol.* 45, 287–295. doi: 10.1002/1531-8249(199903)45:3<287::aid-ana3>3.0.co;2-9

Cipollini, V., Anrather, J., Orzi, F., and Iadecola, C. (2019). Th17 and cognitive impairment: possible mechanisms of action. *Front. Neuroanat.* 13:95. doi: 10.3389/fnana.2019.00095

Csoka, A. B., and Szyf, M. (2009). Epigenetic side-effects of common pharmaceuticals: a potential new field in medicine and pharmacology. *Med. Hypotheses* 73, 770–780. doi: 10.1016/j.mehy.2008.10.039

Curran, L. K., Newschaffer, C. J., Lee, L. C., Crawford, S. O., Johnston, M. V., and Zimmerman, A. W. (2007). Behaviors associated with fever in children with autism spectrum disorders. *Pediatrics* 120, 1386–1392. doi: 10.1542/peds.2007-0360

Demeneix, B. (2014). *Losing our Minds How Environmental Pollution Impairs Human Intelligence and Mental Health, Oxford Series in Behavioral Neuroendocrinology.* New York, NY: Oxford University Press.

Dhabal, S., Das, P., Biswas, P., Kumari, P., Yakubenko, V. P., Kundu, S., et al. (2018). Regulation of monoamine oxidase A (MAO-A) expression, activity and function in IL-13-stimulated monocytes and A549 lung carcinoma cells. *J. Biol. Chem.* 293, 14040–14064. doi: 10.1074/jbc.RA118.002321

El-Ansary, A. K., Ben Bacha, A. G., and Al-Ayahdi, L. Y. (2011). Plasma fatty acids as diagnostic markers in autistic patients from Saudi Arabia. *Lipids Health Dis.* 10:62. doi: 10.1186/1476-511X-10-62

Engel, M., Smidt, M. P., and van Hooft, J. A. (2013). The serotonin 5-HT_3 receptor: a novel neurodevelopmental target. *Front. Cell. Neurosci.* 7:76. doi: 10.3389/fncel.2013.00076

Evatt, B. (2010). *Guide Pour la Création D'un Registre National des Patients.* Montreal, World Federation of Hemophilia. 33p.

Godard, M. P., Johnson, B. A., and Richmond, S. R. (2005). Body composition and hormonal adaptations associated with forskolin consumption in overweight and obese men. *Obes. Res.* 13, 1335–1343. doi: 10.1038/oby.2005.162

Goines, P. E., and Ashwood, P. (2013). Cytokine dysregulation in autism spectrum disorders (ASD): possible role of the environment. *Neurotoxicol. Teratol.* 36, 67–81. doi: 10.1016/j.ntt.2012.07.006

Golubeva, A. V., Joyce, S. A., Moloney, G., Burokas, A., Sherwin, E., Arboleya, S., et al. (2017). Microbiota-related changes in bile acid and tryptophan metabolism are associated with gastrointestinal dysfunction in a mouse model of autism. *EBioMedicine* 24, 166–178. doi: 10.1016/j.ebiom.2017.09.020

Gore, A. C., Chappell, V. A., Fenton, S. E., Flaws, J. A., Nadal, A., Prins, G. S., et al. (2015). EDC-2: the endocrine society's second scientific statement on endocrine-disrupting chemicals. *Endocr. Rev.* 36, E1–E150. doi: 10.1210/er.2015-1010

Grzadzinski, R., Lord, C., Sanders, S. J., Werling, D., and Bal, V. H. (2018). Children with autism spectrum disorder who improve with fever: insights from the simons simplex collection. *Autism Res.* 11, 175–184. doi: 10.1002/aur.1856

Gu, F., Chauhan, V., and Chauhan, A. (2017). Monoamine oxidase-A and B activities in the cerebellum and frontal cortex of children and young adults with autism. *J. Neurosci. Res.* 95, 1965–1972. doi: 10.1002/jnr.24027

Gupta, V., Khan, A. A., Sasi, B. K., and Mahapatra, N. R. (2015). Molecular Mechanism of Monoamine oxidase A gene regulation under inflammation and ischemia-like conditions: key roles of the transcriptions factors GATA2, Sp1 and TBP. *J. Neurochem.* 134, 21–38. doi: 10.1111/jnc.13099

Hall, S. L., Baker, T., Lajoie, S., Richgels, P. K., Yang, Y., McAlees, J. W., et al. (2017). IL-17A enhances IL-13 activity by enhancing IL-13-induced signal transducer and activator of transcription 6 activation. *J. Allergy Clin. Immunol.* 139, 462.e14–471.e14. doi: 10.1016/j.jaci.2016.04.037

Harrington, R. A., Lee, L.-C., Crum, R. M., Zimmerman, A. W., and Hertz-Picciotto, I. (2014). Prenatal SSRI use and offspring with autism spectrum disorder or developmental delay. *Pediatrics* 133, e1241–e1248. doi: 10.1542/peds.2013-3406

Hollander, E., Chaplin, W., Soorya, L., Wasserman, S., Novotny, S., Rusoff, J., et al. (2010). Divalproex sodium vs. placebo for the treatment of irritability in children and adolescents with autism spectrum disorders. *Neuropsychopharmacology* 35, 990–998. doi: 10.1038/npp.2009.202

Hollander, E., Dolgoff-Kaspar, R., Cartwright, C., Rawitt, R., and Novotny, S. (2001). An open trial of divalproex sodium in autism spectrum disorders. *J. Clin. Psychiatry* 62, 530–534. doi: 10.4088/jcp.v62n07a05

Hviid, A., Hansen, J. V., Frisch, M., and Melbye, M. (2019). Measles, mumps, rubella vaccination and autism: a nationwide cohort study. *Ann. Intern. Med.* 170, 513–520. doi: 10.7326/M18-2101

Kang, D.-W., Adams, J. B., Coleman, D. M., Pollard, E. L., Maldonado, J., McDonough-Means, S., et al. (2019). Long-term benefit of microbiota transfer therapy on autism symptoms and gut microbiota. *Sci. Rep.* 9:5821. doi: 10.1038/s41598-019-42183-0

Kang, D.-W., Adams, J. B., Gregory, A. C., Borody, T., Chittick, L., Fasano, A., et al. (2017). Microbiota transfer therapy alters gut ecosystem and improves gastrointestinal and autism symptoms: an open-label study. *Microbiome* 5:10. doi: 10.1186/s40168-016-0225-7

Kim, K. C., Kim, P., Go, H. S., Choi, C. S., Yang, S. I., Cheong, J. H., et al. (2011). The critical period of valproate exposure to induce autistic symptoms in Sprague–Dawley rats. *Toxicol. Lett.* 201, 137–142. doi: 10.1016/j.toxlet.2010.12.018

Kim, S., Kim, H., Yim, Y. S., Ha, S., Atarashi, K., Tan, T. G., et al. (2017). Maternal gut bacteria promote neurodevelopmental abnormalities in mouse offspring. *Nature* 549, 528–532. doi: 10.1038/nature23910

Kobayashi, R. (1980). Effects of estradiol and progesterone on monoamoine oxidase activity in various regions of rat brain and endometrium. *J. Showa Med. Assol.* 40, 165–172. doi: 10.14930/jsma1939.40.165

Luo, H., Liu, H.-Z., Zhang, W.-W., Matsuda, M., Lv, N., Chen, G., et al. (2019). Interleukin-17 regulates neuron-glial communications synaptic transmission, and neuropathic pain after chemotherapy. *Cell Rep.* 29, 2384–2397doi: 10.1016/j.celrep.2019.10.085

MacFabe, D. F., Cain, D. P., Rodriguez-Capote, K., Franklin, A. E., Hoffman, J. E., Boon, F. (2007). Neurobiological effects of intraventricular propionic acid in rats: possible role of short chain fatty acids on the pathogenesis and characteristics of autism spectrum disorders. *Behav. Brain Res.* 176, 149–169. doi: 10.1016/j.bbr.2006.07.025

Marotta, R., Risoleo, M. C., Messina, G., Parisi, L., Carotenuto, M., Vetri, L., et al. (2020). The neurochemistry of autism. *Brain Sci.* 10:163. doi: 10.3390/brainsci10030163

Martinez-Mayorga, K., Peppard, T. L., López-Vallejo, F., Yongye, A. B., and Medina-Franco, J. L. (2013). Systematic mining of generally recognized as safe (GRAS) flavor chemicals for bioactive compounds. *J. Agric. Food Chem.* 61, 7507–7514. doi: 10.1021/jf401019b

Meador, K. J., Baker, G. A., Browning, N., Cohen, M. J., Bromley, R. L., Clayton-Smith, J., et al. (2013). Fetal antiepileptic drug exposure and cognitive outcomes at age 6 years (NEAD study): a prospective observational study. *Lancet Neurol.* 12, 244–252. doi: 10.1016/S1474-4422(12)70323-X

Modabbernia, A., Velthorst, E., and Reichenberg, A. (2017). Environmental risk factors for autism: an evidence-based review of systematic reviews and meta-analyses. *Mol. Autism* 8:13. doi: 10.1186/s13229-017-0121-4

Morgan, T. O., and Anderson, A. (2003). Different drug classes have variable effects on blood pressure depending on the time of day. *Am. J. Hypertens.* 16, 46–50. doi: 10.1016/s0895-7061(02)03081-9

Mori, S., Maher, P., and Conti, B. (2016). Neuroimmunology of the interleukins 13 and 4. *Brain Sci.* 6:18. doi: 10.3390/brainsci6020018

Muller, C. L., Anacker, A., and Veenstra-VanderWeele, J. (2016). The serotonin system in autism spectrum disorder: from biomarker to animal models. *Neuroscience* 321, 24–41. doi: 10.1016/j.neuroscience.2015.11.010

Nankova, B. B., Agarwal, R., MacFabe, D. F., and La Gamma, E. F. (2014). Enteric bacterial metabolites propionic and butyric acid modulate gene expression, including CREB-dependent catecholaminergic neurotransmission, in PC12 cells—possible relevance to autism spectrum disorders. *PLoS One* 9:e103740. doi: 10.1371/journal.pone.0103740

Patterson, P. H. (2011). Maternal infection and immune involvement in autism. *Trends Mol. Med.* 17, 389–394. doi: 10.1016/j.molmed.2011.03.001

Paysour, M. J., Bolte, A. C., and Lukens, J. R. (2019). Crosstalk between the microbiome and gestational immunity in autism-related disorders. *DNA Cell Biol.* 38, 405–409. doi: 10.1089/dna.2019.4653

Pena, L., and Burton, B. K. (2012). Survey of health status and complications among propionic acidemia patients. *Am. J. Med. Genet. A* 158A, 1641–1646. doi: 10.1002/ajmg.a.35387

Pinheiro, I., and Heard, E. (2017). X chromosome inactivation: new players in the initiation of gene silencing. *F1000Res.* 6:F1000Faculty Rev-344. doi: 10.12688/f1000research.10707.1

Piton, A., Poquet, H., Redin, C., Masurel, A., Lauer, J., Muller, J., et al. (2014). 20 ans après: a second mutation in MAOA identified by targeted high-throughput sequencing in a family with altered behavior and cognition. *Eur. J. Hum. Genet.* 22, 776–783. doi: 10.1038/ejhg.2013.243

Quinlan, M. A., Robson, M. J., Ye, R., Rose, K. L., Schey, K. L., and Blakely, R. D. (2020). *Ex vivo* quantitative proteomic analysis of serotonin transporter interactome: network impact of the SERT Ala56 coding variant. *Front. Mol. Neurosci.* 13:89. doi: 10.3389/fnmol.2020.00089

Reed, M., Yim, Y. S., Wimmer, R., Kim, H., Ryu, C., Welch, G., et al. (2020). IL-17a promotes sociability in mouse models of neurodevelopmental disorders. *Nature* 577, 249–253. doi: 10.1038/s41586-019-1843-6

Robson, M. J., Quinlan, M. A., Margolis, K. G., Gajewski-Kurdziel, P. A., Veenstra-VanderWeele, J., Gershon, M. D., et al. (2018). p38α MAPK signaling drives pharmacologically reversible brain and gastrointestinal phenotypes in the SERT Ala56 mouse. *Proc. Natl. Acad. Sci. USA* 115, E10245–E10254. doi: 10.1073/pnas.1809137115

Schneider, T., and Przewocki, R. (2005). Behavioral alterations in rats prenatally exposed to valproic acid: animal model of autism. *Neuropsychopharmacology* 30, 80–89. doi: 10.1038/sj.npp.1300518

Sidharth, M., Saloni, R., Aarti, T., Kapoor, T., Rajdev, K., Sharma, R., et al. (2020). Adenylate cyclase activator forskolin alleviates intracerebroventricular propionic acid-induced mitochondrial dysfunction of autistic rats. *Neural Regen. Res.* 15, 1140–1149. doi: 10.4103/1673-5374.270316

Slattery, J., MacFabe, D. F., and Frye, R. E. (2016). The significance of the enteric microbiome on the development of childhood disease: a review of prebiotic and probiotic therapies in disorders of childhood. *Clin. Med. Insights Pediatr.* 10, 91–107. doi: 10.4137/CMPed.S38338

Spence, S., and Schneider, M. (2009). the role of epilepsy and epileptiform EEGs in autism spectrum disorders. *Pediatr. Res.* 65, 599–606. doi: 10.1203/PDR.0b013e31819e7168

Star, K., Edwards, I. R., and Choonara, I. (2014). Valproic acid and fatalities in children: a review of individual case safety reports in VigiBase. *PLoS One* 9:e108970. doi: 10.1371/journal.pone.0108970

Tanaka, M., Sato, A., Kasai, S., Hagino, Y., Kotajima-Murakami, H., Kashii, H., et al. (2018). Brain hyperserotonemia causes autism-relevant social deficits in mice. *Mol. Autism* 9:60. doi: 10.1186/s13229-018-0243-3

Thürmann, L., Herberth, G., Rolle-Kampczyk, U., Röder, S., Borte, M., von Bergen, M., et al. (2019). Elevated gestational IL-13 during fetal development is associated with hyperactivity and inattention in 8-year-old children. *Front. Immunol.* 10:1658. doi: 10.3389/fimmu.2019.01658

Uzunova, G., Pallanti, S., and Hollander, E. (2015). Excitatory/inhibitory imbalance in autism spectrum disorders: implications for interventions and therapeutics. *World J. Biol. Psychiatry* 17, 174–186. doi: 10.3109/15622975.2015.1085597

Veenstra-VanderWeele, J., Muller, C. L., Iwamoto, H., Sauer, J. E., Owens, W. A., Shah, C. R., et al. (2012). Autism gene variant causes hyperserotonemia, serotonin receptor hypersensitivity, social impairment and repetitive behavior. *Proc. Natl. Acad. Sci. U S A* 109, 5469–5474. doi: 10.1073/pnas.1112345109

von Ehrenstein, O. S., Ling, C., Cui, X., Cockburn, M., Park, A. S., Yu, F., et al. (2019). Prenatal and infant exposure to ambient pesticides and autism spectrum disorder in children: population based case-control study. *BMJ* 364:l962. doi: 10.1136/bmj.l962

Wang, C. C., Borchert, A., Ugun-Klusek, A., Tang, L. Y., Lui, W. T., and Chu, C. Y. (2011). Monoamine oxidase A expression is vital for embryonic brain development by modulating developmental apoptosis. *J. Biol. Chem.* 286, 28322–28330. doi: 10.1074/jbc.M111.241422

Weiss, L. A., Abney, M., Cook, E. H. Jr., and Ober, C. (2005). Sex-specific genetic architecture of whole blood serotonin levels. *Am. J. Hum. Genet.* 76, 33–41. doi: 10.1086/426697

Wong, H., and Hoeffer, C. (2018). Maternal IL-17A in autism. *Exp. Neurol.* 299, 228–240. doi: 10.1016/j.expneurol.2017.04.010

Yim, Y. S., Park, A., Berrios, J., Lafourcade, M., Pascual, L. M., Soares, N., et al. (2017). Reversing behavioral abnormalities in mice exposed to maternal inflammation. *Nature* 549, 482–487. doi: 10.1038/nature23909

Conflict of Interest: The author declares that the research was conducted in the absence of any commercial or financial relationships that could be construed as a potential conflict of interest.

frontiers in Cellular Neuroscience

ORIGINAL RESEARCH
published: 10 December 2020
doi: 10.3389/fncel.2020.595607

Comprehensive Profiling of Gene Expression in the Cerebral Cortex and Striatum of BTBRTF/ArtRbrc Mice Compared to C57BL/6J Mice

*Shota Mizuno[1], Jun-na Hirota[1], Chiaki Ishii[1], Hirohide Iwasaki[2], Yoshitake Sano[1] and Teiichi Furuichi[1]**

[1] Department of Applied Biological Science, Faculty of Science and Technology, Tokyo University of Science, Noda, Japan,
[2] Department of Anatomy, Gunma University Graduate School of Medicine, Maebashi, Japan

Mouse line BTBR *T+ Iptr3*^{tf}/J (hereafter referred as to BTBR/J) is a mouse strain that shows lower sociability compared to the C57BL/6J mouse strain (B6) and thus is often utilized as a model for autism spectrum disorder (ASD). In this study, we utilized another subline, BTBRTF/ArtRbrc (hereafter referred as to BTBR/R), and analyzed the associated brain transcriptome compared to B6 mice using microarray analysis, quantitative RT-PCR analysis, various bioinformatics analyses, and *in situ* hybridization. We focused on the cerebral cortex and the striatum, both of which are thought to be brain circuits associated with ASD symptoms. The transcriptome profiling identified 1,280 differentially expressed genes (DEGs; 974 downregulated and 306 upregulated genes, including 498 non-coding RNAs [ncRNAs]) in BTBR/R mice compared to B6 mice. Among these DEGs, 53 genes were consistent with ASD-related genes already established. Gene Ontology (GO) enrichment analysis highlighted 78 annotations (GO terms) including DNA/chromatin regulation, transcriptional/translational regulation, intercellular signaling, metabolism, immune signaling, and neurotransmitter/synaptic transmission-related terms. RNA interaction analysis revealed novel RNA–RNA networks, including 227 ASD-related genes. Weighted correlation network analysis highlighted 10 enriched modules including DNA/chromatin regulation, neurotransmitter/synaptic transmission, and transcriptional/translational regulation. Finally, the behavioral analyses showed that, compared to B6 mice, BTBR/R mice have mild but significant deficits in social novelty recognition and repetitive behavior. In addition, the BTBR/R data were comprehensively compared with those reported in the previous studies of human subjects with ASD as well as ASD animal models, including BTBR/J mice. Our results allow us to propose potentially important genes, ncRNAs, and RNA interactions. Analysis of the altered brain transcriptome data of the BTBR/R and BTBR/J sublines can contribute to the understanding of the genetic underpinnings of autism susceptibility.

Keywords: *in situ* hybridization, co-expression network, bioinformatics analysis, transcriptome, BTBR mouse model, autism spectrum disorder, RNA-RNA interaction network

OPEN ACCESS

Edited by:
Yi-Ping Hsueh,
Institute of Molecular Biology, Academia Sinica, Taiwan

Reviewed by:
Brandon L. Pearson,
Columbia University, United States
Francesco Errico,
University of Naples Federico II, Italy

***Correspondence:**
Teiichi Furuichi
tfuruichi@rs.tus.ac.jp

Specialty section:
This article was submitted to Cellular Neuropathology, a section of the journal Frontiers in Cellular Neuroscience

Received: *17 August 2020*
Accepted: *09 November 2020*
Published: *10 December 2020*

Citation:
Mizuno S, Hirota J-n, Ishii C, Iwasaki H, Sano Y and Furuichi T (2020) Comprehensive Profiling of Gene Expression in the Cerebral Cortex and Striatum of BTBRTF/ArtRbrc Mice Compared to C57BL/6J Mice. Front. Cell. Neurosci. 14:595607. doi: 10.3389/fncel.2020.595607

INTRODUCTION

Autism spectrum disorder (ASD) is a complex neurodevelopmental disorder characterized by altered functionality across two symptom domains: (1) social and communication deficits, and (2) stereotyped repetitive behaviors with restricted interests (American Psychiatric Association, 2013). ASD is highly heterogeneous in terms of clinical symptoms and etiology. The current prevalence rate of ASD is ∼1 in 40 children (Xu et al., 2018). As there is no cure for ASD, understanding its pathophysiology is an important health issue. ASD is highly heritable and is also affected by environmental factors. Recent advances in next generation sequencing have revealed more than 1,000 mutations associated with ASD (Devlin and Scherer, 2012). However, many of the genomic alterations identified thus far are rare variants that represent only a small fraction of cases of ASD (Chaste and Leboyer, 2012; Devlin and Scherer, 2012). Recent ASD studies performed at the molecular, cellular, and behavioral levels, including mouse model studies, suggest that ASD is clinically heterogeneous with diverse pathophysiological processes that lead to similar behavioral manifestations (de la Torre-Ubieta et al., 2016). Integrative analysis of large-scale genetic data reveals distinct gene networks affected in ASD, mainly related to synaptic function and formation within the brain. Network-based analysis of large-scale transcriptome data also highlights that co-expression modules related to synaptic development, neuronal activity, and immune function are deregulated in ASD (Voineagu et al., 2011; Gupta et al., 2014; de la Torre-Ubieta et al., 2016). Thus, the pathophysiological processes in ASD seem to converge on specific molecular pathways and networks, with a clear interplay between immune and synaptic functions (Estes and McAllister, 2015).

The black and tan brachyury (BTBR) mouse strain was originally created by Leslie Clarence Dunn (Columbia University) using stock obtained from Nadine Dobrovolskaia-Zavadskaia (Pasteur Institute); they were maintained by Karen Artzt (the University of Texas, Austin; named as "BTBRTF/Art" in Wu et al., 2007) after passing them to some researchers, according to Clee et al. (2005) and the Jackson Laboratory (Bar Harbor, ME). BTBRTF/Art was then distributed to and bred in many other laboratories, including the Jackson Laboratory (BTBR *T+ Iptr3*^{tf}/J, MGI ID: 4452239, hereafter referred to as "BTBR/J") from 1994 and the RIKEN BioResource Research Center (RBRC) (Tsukuba, Japan; BTBRTF/ArtRbrc, RBRC ID: 01206, hereafter referred to as "BTBR/R") from 1987. Both BTBR subline BTBR/J and BTBR/R mice have the spontaneous mutations *T* (brachyury), *Itpr3*^{tf} (inositol 1,4,5-trisphosphate receptor 3, tufted), and *a*^{t} (black and tan). Interestingly, BTBR/J mice have been shown to have reduced social behavior relevant to ASD (Bolivar et al., 2007; Moy et al., 2007, 2008; McFarlane et al., 2008; Pobbe et al., 2010; Defensor et al., 2011; Pearson et al., 2011; Scattoni et al., 2011, 2013; Wöhr et al., 2011; Silverman et al., 2012, 2015). Gene transcriptional profiling in ASD has been performed by utilizing post-mortem brain samples. The restricted availability of brain tissue from humans with ASD represents a significant challenge. From this point of view, BTBR/J is a valuable animal model of ASD to analyze the molecular and pathological mechanism at the gene and protein expression level. For this purpose, BTBR/J mice have been subjected to transcriptome analyses of the hippocampus (Daimon et al., 2015; Provenzano et al., 2016; Gasparini et al., 2020), frontal cortex (Kratsman et al., 2016), dorsal striatum (Oron et al., 2019), and cerebellum (Shpyleva et al., 2014), as well as proteome analyses of cortical (Jasien et al., 2014; Wei et al., 2016) and hippocampal tissues (Jasien et al., 2014; Daimon et al., 2015).

In this study, we analyzed the brain transcriptome of BTBR/R mice that have enhanced turnover of dendritic spines in the anterior frontal cortex, similar to that seen in ASD model mice, namely patDp/+ with paternal duplication of chromosome 7c and *NLGN-3* R451C with a point mutation of human neuroligin-3, during the postnatal developmental stage (Isshiki et al., 2014). We performed a comprehensive brain transcriptome analysis between BTBR/R mice and C57BL/6J (hereinafter referred to as B6) mice with high sociality, using genome-wide microarray analysis, quantitative RT-PCR (qRT-PCR) analysis, various bioinformatics analyses, and *in situ* hybridization (ISH). We paid particular attention to the cerebral cortex and striatum, since altered cortico-striatal connectivity has been suggested to be present in patients with ASD (Abbott et al., 2018) and in an ASD model mouse with complete knockout (KO) of *Shank3* (Wang et al., 2016). Our results revealed the differential transcription profiles in microarray expression levels as well as cellular-regional levels in the cerebral cortex and striatum of BTBR/R mice and B6 mice. Some genes and non-coding RNAs (ncRNAs) that we detected have also been reported or suggested to be ASD-related genes, or as differentially expressed genes (DEGs) in ASD animal models including BTBR/J mice. Moreover, our behavioral analysis data suggested that BTBR/R mice have a slight autistic-like tendency in terms of social novelty recognition and stereotypic behavior. Taken together, the results of our study suggest the genetic aspects of BTBR/R mice brain function, which is informative to the understanding of the genetics of the observed behavioral defects.

MATERIALS AND METHODS

Animals

All experimental protocols were evaluated and approved by the Regulation for Animal Research at Tokyo University of Science. All experiments were conducted in accordance with the Regulations for Animal Research at The University of Tokyo and Tokyo University of Science. The BTBR/R mouse strain (BTBRTF/ArtRbrc, RBRC01206) was provided by the RBRC through the National Bio-Resource Project of the Ministry of Education, Culture, Sports, Science and Technology, Japan (Isshiki et al., 2014) and were housed in the animal facility at The University of Tokyo and Tokyo University of Science on 12-h light and dark cycle from 8 a.m. to 8 p.m. The B6 mouse strain (C57BL/6J) was purchased from the Japan SLC, Inc. (Hamamatsu, Japan) and were housed in the animal facility at Tokyo University of Science on 12-h light and dark cycle from 8 a.m. to 8 p.m.

Microarray Analysis

Male BTBR/R (4–6 months of age) and B6 (4 months of age) mice were deeply anesthetized with Somnopentyl (64.8 mg/ml pentobarbital sodium, 150 mg/kg, i.p.; Kyoritsu Seiyaku Corporation, Tokyo, Japan) and were decapitated. Brain tissue samples (cerebral cortex and striatum) from four mice ($N = 4$) of each strain were dissected out and treated in an RNA-stabilizing agent (RNAlater, Qiagen, Hilden, Germany). Microarray analysis was performed by RIKEN Genesis Co., Ltd. (Tokyo, Japan). Briefly, total RNA was extracted with the RNeasy Plus Universal Mini Kit (Qiagen) and RNA quality was analyzed using a 2100 Bioanalyzer (Agilent, Santa Clara, CA, USA) and NanoDrop (Thermo Fisher Scientific, Waltham, MA, USA). Only RNA with a high (>8) RNA integrity number was selected. Cys3-labeled complementary RNAs (cRNAs) were prepared using the Low Input Quick Amp Labeling Kit, One-Color (Agilent), and were analyzed by using the SurePrint G3 Mouse Gene Expression 8x60K v2 microarray (Agilent) that features complete coverage of established RefSeq coding transcripts (NM sequences) from the latest build and updated long ncRNA (lncRNA) content (27,122 Entrez genes and 4,578 lncRNAs), according to the manufacturer's protocol. Hybridization images were acquired using the DNA Microarray Scanner (Agilent) and were analyzed with Feature Extraction Software version 10.7.3.1 (Agilent). Signal analysis and batch normalization were carried out using GeneSpring GX (Agilent). The gene expression datasets of the BTBR/R and B6 mice have been deposited in the NCBI Gene Expression Omnibus database (accession number GSE156646).

Analysis of DEGs

Gene expression in BTBR/R mice was normalized to that of B6 mice to obtain the fold change (FC) of all probes (the value obtained in B6 was set to 1). The probes were tested for differential expression using unpaired two-tailed Student's *t*-tests, and the false discovery rate (FDR) was calculated using *P*-values (Benjamini and Hochberg, 1995). An FDR cut-off of <0.05 and FC of ≥ absolute 2.0 were applied. The DEGs are listed in **Supplementary Table 1**.

Bioinformatics Analyses

Transcript types (such as splicing variants) of the detected genes were defined using the gene databases GenBank (NCBI; Sayers et al., 2020a), Refseq (NCBI; O'Leary et al., 2016), Ensembl release 100 (EMBI-EBI; Yates et al., 2020) and Agilent microarray's information. Each transcript type was categorized into "Protein coding," "Non-coding RNA," "Pseudogene," and "Other." The category descriptions are listed in **Supplementary Table 2**.

Enrichment Analysis of GO Annotations and KEGG Pathways by DAVID

For gene description and pathway enrichment analyses of the DEGs, we utilized the Gene Ontology (GO) and Kyoto Encyclopedia of Genes and Genomes (KEGG) bioinformatics databases and visualized as well as integrated the DEGs based on these resources using the Database for Annotation, Visualization, and Integrated Discovery (DAVID) Functional Annotation tool (Huang et al., 2009a,b; Leidos Biomedical Research). For all analyses, the background of animal species was set to *Mus musculus*, and the enrichment threshold was a DAVID-corrected $P < 0.05$. The data of enriched GO descriptions and KEGG pathways are listed in **Supplementary Tables 3, 4**.

Weight Correlation Network Analysis (WGCNA)

WGCNA was run with R version 4.0.2 and the WGCNA package version 1.69 (Langfelder and Horvath, 2008), using microarray data of the most informative (top 20%) probes in terms of per-probe variance, in accordance with previous work (Provenzano et al., 2016). We used the similarity between gene expression profiles to construct a similarity matrix based on pairwise Pearson correlation coefficient matrices. The similarity matrix was transformed into an adjacency matrix using a power adjacency function (Zhang and Horvath, 2005). In this study, we chose the power of 14 that this value was calculated by using the integration function (pickSoftThreshold) in the WGCNA software package. We then calculated the topological overlap measure (TOM), which is a robust measure of network interconnectedness, using an adjacency matrix. Finally, we performed an average linkage hierarchical clustering according to the TOM-based dissimilarity measure. The tree-cut algorithm method was adopted to identify the module of gene co-expression with a minModuleSize of 30 and a mergeCutHeight of 0.25. GO enrichment analysis for each module was performed using the integration function (GOenrichmentAnalysis) of the WGCNA software package. The module genes and the enriched GO results are listed in **Supplementary Tables 5, 6**.

ENCORI and Cytoscape Analyses

RNA interaction data were obtained using the RNA target database ENCORI (Li et al., 2014). In this analysis, we used each DEG and their targets as network nodes. The interactions network was analyzed and visualized by the network visualization software Cytoscape version 3.8.0 (https://cytoscape.org/). The RNA interactions are listed in **Supplementary Table 7**.

AutDB Search

Genes associated with ASD referenced the autism database AutDB (MindSpec; Pereanu et al., 2018). "Gene Score" and "Syndromic" annotations were obtained from the autism gene database SFARI (https://gene.sfari.org/). Mouse ASD gene orthologs were detected using the gene databases Homologene (Sayers et al., 2020b), Ensembl release 100 (Yates et al., 2020) and Mouse Genome Database (The Jackson Laboratory; Bult et al., 2019). The list of Mouse ASD gene orthologs and DEGs identical to ASD-related genes registered in the AutDB are shown in **Supplementary Tables 8, 9**.

qRT-PCR

cDNA libraries were prepared from total corticostriatal RNAs using the SuperScript IV VILO Master Mix (Thermo Fisher Scientific) according to the manufacturer's protocol. qRT-PCR was performed using 7300 systems (Thermo Fisher Scientific) with real-time detection of fluorescence, using the Power SYBR Green PCR Master Mix (Thermo Fisher

Scientific). Mouse glyceraldehyde-3-phosphate dehydrogenase was used as a standard for quantification. Primer sequences (Integrated DNA Technologies, Coralville, IA, USA) are listed in **Supplementary Table 10**. Expression analyses were performed using the 7300 system SDS software version 1.4 (Thermo Fisher Scientific). Quantitative values were obtained from the threshold cycle (CT) number. Fold change was calculated using the ΔΔCT method, with B6 sample data as the control. All transcripts were run in duplicates and plotted as the average of two independent reactions obtained from each cDNA.

ISH

ISH was performed as described previously, with small modification (Sano et al., 2014). Male BTBR/R (2–3 months of age) and B6 (2–4 months of age) were used for this experiment. Brains were perfused with 4% paraformaldehyde (PFA), harvested, post-fixed with 4% PFA at 4°C for 1 d, and then equilibrated in 30% (w/v) sucrose in phosphate-buffered saline (PBS). Coronal sections (50 μm thickness) were prepared using a cryostat. All steps were performed at room temperature unless indicated otherwise. Sections were incubated with methanol (MeOH) for 2 h, then washed three times for 10 min in PBS containing 0.1% Tween-20 (PBST), incubated with 3.3 μg/ml proteinase K (Sigma-Aldrich, St. Louis, MO, USA) in ProK buffer (0.1 M Tris HCl, pH 8.0, 50 mM EDTA) for 30 min at 37°C, incubated with 0.25% Acetic anhydride in 0.1 M triethanolamine, pH 7.0 for 10 min, washed twice for 5 min in PBST and, finally, incubated with hybridization buffer (5 × SSC, 50% formamide, 0.1% Tween-20, 5x Denhardt's solution) for 1 h at 60°C. Prior to hybridization, digoxigenin (DIG)-labeled cRNA probes in hybridization buffer were denatured at 80°C for 5 min and then quickly cooled on ice for 10 min. cRNA probes were generated using a DIG RNA labeling kit (Roche, Penzberg, Germany). Hybridization was performed at 60°C overnight. Sections were washed in 2 × SSC containing 50% formamide and 0.1% Tween-20 (SSCT) twice for 20 min, incubated with 20 μg/ml RNase (Nippon Gene, Tokyo, Japan) in RNase buffer (10 mM Tris-HCl, pH 8.0, 1 mM EDTA, 0.5 M NaCl) for 30 min at 37°C, washed in 2 × SSCT twice for 15 min at 37°C, and 0.2 × SSCT twice for 15 min at 37°C. Then, the sections were incubated with 1% blocking reagent (Roche; 10 mM maleic acid, 15 mM NaCl, pH 7.5) for 1 h, and finally incubated with alkaline phosphatase-conjugated anti-DIG antibody (1:2,000, Roche) in blocking reagent at 4°C overnight. The sections were washed three times in TNT (0.1 M Tris-HCl, pH 7.5, 0.15 M NaCl, 0.05% Tween-20) for 15 min. For staining with nitroblue tetrazolium chloride/5-bromo-4-chloro-3-indolyl phosphate 4-toluidine salt (NBT/BCIP), the signal was developed in 2% (v/v) NBT/BCIP stock solution (Roche) diluted in TS9.5 (0.1 M NaCl, 10 mM $MgCl_2$, 0.1 M Tris pH 9.5) at room temperature overnight. Sections were imaged using a NanoZoomer Digital Pathology virtual slide scanner (Hamamatsu Photonics, Hamamatsu, Japan). ISH images were verified by analyzing at least three different brain sections from 1–3 mice for each strain. ISH data with clarity as well as reproducibility in terms of signal intensities and patterns were used in this study, although many other genes were also analyzed. The probe sequences are listed in **Supplementary Table 11**.

Statistical Analysis

All statistical analyses were performed in Excel 2019 (Microsoft, Redmond, WA, USA). Datasets were analyzed for significance using unpaired two-tailed Student's *t*-tests. All data are presented as mean ± SEM. In this study, $P < 0.05$ were considered significant. The additional information on each statistical analysis is described in the corresponding sections of the Materials and Methods section and the figure legends.

RESULTS

Differential Cortical and Striatal Gene Expression Between BTBR/R and B6 Mice

To compare the transcriptome features in the cerebral cortex and striatum between BTBR/R and B6 mice, we performed DNA microarray analysis for a total of 27,122 Entrez genes and 4,578 lncRNAs. Principal component analysis showed that the total RNA expression in BTBR/R and B6 mice were separated into two distinct groups (**Figure 1A**), indicating that each strain has distinct gene expression patterns and there is no outlier of the arrays. The data indicated that BTBR/R mice exhibited the differential expression of 1,280 transcripts (974 downregulated, 306 upregulated) in the cerebral cortex and striatum compared to B6 mice (**Figures 1B,C**, **Supplementary Table 1**).

For verification of the microarray data, we performed qRT-PCR analyses in the cerebral cortex and striatum samples between BTBR/R and B6 mice for 15 DEGs: eight downregulated genes for plastin 3 (*Pls3*), CD276 antigen (*Cd276*), glycine amidinotransferase (*Gatm*), aldehyde dehydrogenase family 1, subfamily A3 (*Aldh1a3*), parkin RBR E3 ubiquitin protein ligase (*Prkn*), ribonuclease P and MRP subunit p25 (*Rpp25*), calcium channel, voltage-dependent, beta 2 subunit (*Cacnb2*), and nitric oxide synthase 1 adaptor protein (*Nos1ap*; **Figure 1D**); and seven upregulated genes for prune homolog 2 (*Prune2*), folate hydrolase 1 (*Folh1*), lipoprotein lipase (*Lpl*), DPY30 domain containing 2 (*Dydc2*), lysine-specific demethylase 5B (*Kdm5b*), occludin/ELL domain containing 1 (*Ocel1*), and serine peptidase inhibitor, clade A, member 3N (*Serpina3n*; **Figure 1E**). Only ASD-related DEGs and DEGs with high fold change were selected. As a result, we confirmed that the increased and decreased expression of tested genes were consistent with the results of the microarray analysis.

Using the NCBI and Ensembl databases, we classified types of the differentially expressed transcripts identified, as shown in **Figure 2**. Downregulated and upregulated transcript groups consisted of 524 and 184 protein-coding transcripts, 387 and 111 non-coding transcripts, 33 and 6 pseudogenes, and 30 and 5 other transcripts, respectively (**Supplementary Table 2**).

ENCORI and Cytoscape RNA–RNA Interaction Networks Analysis

To understand the coordinated expression of RNAs, we focused on RNA–RNA interactions. By using the Cytoscape network analysis tool, we analyzed the relationship between specific RNA

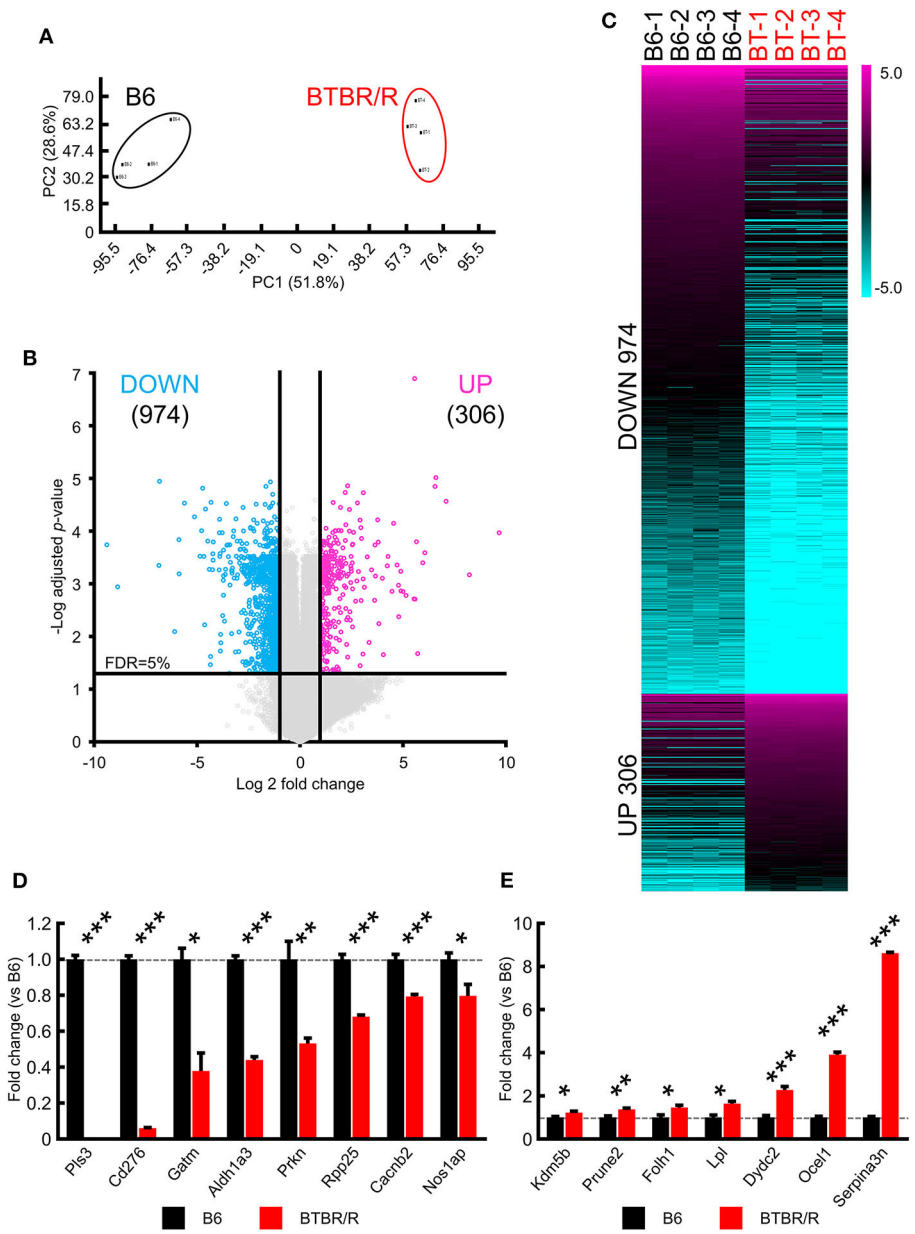

FIGURE 1 | Significant alterations in BTBR/R cortical and striatal gene expression compared to B6. Gene expression changes in the cortical and striatal tissues from BTBR/R mice compared to tissues from B6 mice controls. **(A)** Principal component analysis of gene expression profiles of all samples. **(B)** Volcano plots depicting fold change vs. adjusted *P*-values for gene expression between BTBR/R and B6 mice. **(C)** Heat map of all differentially expressed genes between BTBR/R mice and B6 mice. The threshold was set to fold change ≥2 and *t*-test adjusted *P*-value ≤ 0.05 as illustrated in B. qRT-PCR-mediated validation revealed significantly downregulated **(D)** and upregulated **(E)** transcripts. Histogram black bars represent B6 mice data and red bars represent BTBR/R mice data. Unpaired two-tailed Student's *t*-test; $^{*}P < 0.05$,$^{**}P < 0.01$,$^{***}P < 0.001$.

and its binding target RNAs. For DEGs, both the "DEG and DEG" interactions and the "DEG and non-DEG" interactions were analyzed, while for non-DEGs only the "non-DEG and DEG" interactions were analyzed. We found that DEGs had an RNA interaction network with 3,684 "nodes" (genes) and 5,376 "edges" (interactions; **Figure 3A**, **Supplementary Table 7**). These network nodes included 75 upregulated genes and 253 downregulated genes (**Figure 3D**). Moreover, this network had 227 ASD-related genes connected with 670 edges (**Figures 3D,E**). **Figures 3B,C** list the top 10 "hub" genes that interact highly with DEG and non-DEG nodes, in terms of the number of nodes (**Figures 3B,C**).

In DEGs, predicted gene 37194 (*Gm37194*; downregulated) was the node with the largest RNA–RNA interaction network and acted as a hub RNA interacting with 2,085 target RNAs, including 163 ASD-related genes (**Figure 4A**). In non-DEGs, predicted

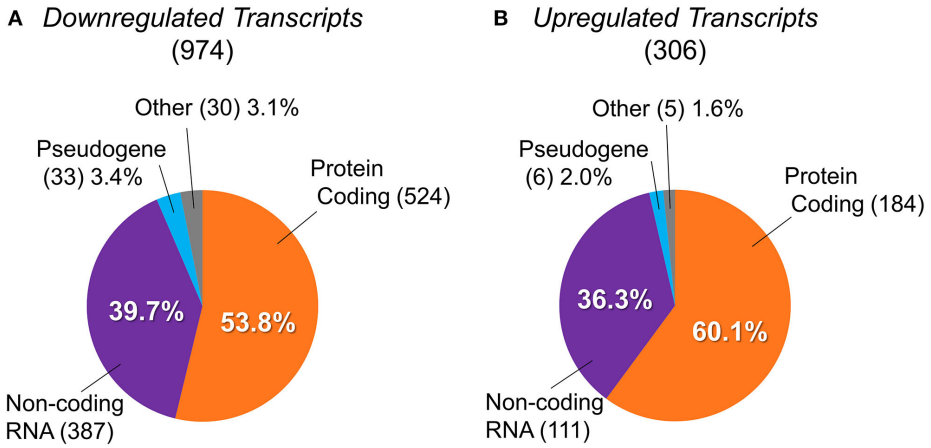

FIGURE 2 | Classification of differentially expressed transcripts into protein-coding genes, non-coding RNAs, pseudogenes, and others. The transcript types of differentially expressed genes between BTBR/R mice and B6 mice. **(A)** 974 downregulated transcripts were classified into 524 protein-coding genes (53.8%), 387 non-coding RNAs (ncRNAs; 39.7%), 33 pseudogenes (3.4%), and 30 others (3.1%). **(B)** 306 upregulated transcripts were classified into 184 protein-coding genes (60.1%), 111 ncRNAs (36.3%), 6 pseudogenes (2.0%), and 5 others (1.6%).

gene 26917 (*Gm26917*; non-DEG) was the node with the largest RNA–RNA interaction network and acted as a hub interacting with 105 nodes including seven ASD-related genes (**Figure 4B**). In ASD-related genes, ankyrin repeat domain 11 (*Ankrd11*; downregulated) and calcium dependent activator protein for secretion 2 (*Cadps2*; non-DEG) were nodes with the largest RNA–RNA interaction networks. *Ankrd11* was a node for 100 RNAs, only two of which were DEGs (both downregulated) and 12 of which were ASD-related genes (**Figure 4C**). *Cadps2* was not a DEG but was a node for 20 RNAs, all of which were DEGs (4 upregulated, 16 downregulated), including three ASD-related genes (*Ccdc88c*, *Cdk13*, and *Cux1*; **Figure 4D**).

Collectively, our comparative whole genome-wide microarray analysis between BTBR/R and B6 found 708 differentially expressed protein-coding genes (524 downregulated and 184 upregulated) that corresponds to ∼3.2% of the total protein-coding genes in mice (22,519 in Ensembl as of April 2020), suggesting complicated alterations in transcriptional regulation of the cerebral cortex and striatum between the two mouse strains, which is also implied by the altered expression of 498 ncRNAs and 39 pseudogenes that may be associated with the differential regulation of transcription and translation between two strains via RNA–RNA interactions.

Bioinformatic Characterization of Differentially Expressed Genes Between BTBR/R and B6 Mice

To functionally characterize the differential gene expression between BTBR/R and B6 mice, identified DEGs were further subjected to various bioinformatics analyses.

Gene Ontology (GO) Functional Classification

To gain an insight into the biological significance in altered gene expression between BTBR/R and B6 mice, we performed the functional gene classification of DEGs by the GO enrichment analysis using the functional annotation and classification tool DAVID (Ashburner et al., 2000; Huang et al., 2009a,b; The Gene Ontology Consortium, 2019). DEGs were enriched in 40 GO terms in *"biological process (BP),"* 16 GO terms in *"cellular component (CC),"* and 22 GO terms in *"molecular function (MF),"* with statistical significance, according to the rule that each gene is annotated with multiple classifications if they match (**Supplementary Table 3**). **Figure 5A** shows the top 10 GO terms of BP, top 5 GO terms of CC, and top 5 GO terms of MF, based on the lowest *P*-value rank (**Figure 5A**). Interestingly, with the BP group, five GO terms ("DNA methylation on cytosine," "DNA replication-dependent nucleosome assembly," "positive regulation of gene expression, epigenetic," "DNA replication-independent nucleosome assembly," and "chromatin silencing at rDNA") were significantly altered in BTBR/R mice compared to B6 mice, since many histone protein variant genes including histone H3 (*Hist1h3f*) and H4 (*Hist1h4d*, *Hist1h4i*, *Hist1h4j*, *Hist1h4k*, *Hist2h4*, and *Hist4h4*) family genes were DEGs of BTBR/R mice (**Supplementary Table 3**); this suggests a difference in DNA and chromatin regulation between the two mouse strains. It is also remarkable that the GO term with the lowest *P*-value in the CC and MF included a large number of annotated DEGs: 137 DEGs of "extracellular exosome" and 161 DEGs of "metal ion binding," respectively (**Figure 5B**). In addition, the enrichment of *"immune signaling"*-related GO terms, 9 in the BP and 2 in the MF, was a characteristic in BTBR/R mice DEGs (**Figure 5B**).

We next focused on *"nervous system"*-related GO terms (**Figure 6**). In the BP group, *"Cell surface receptor signaling pathway"* (80 down- and 15 up-regulated genes) and *"nervous system development"* (59 down- and 18 up-regulated genes) were the first and second ranked groups, respectively, also suggesting possible changes in cellular signaling and development of the cerebral cortex and striatum between the two strains. Sixteen selected GO terms related to brain development included 199

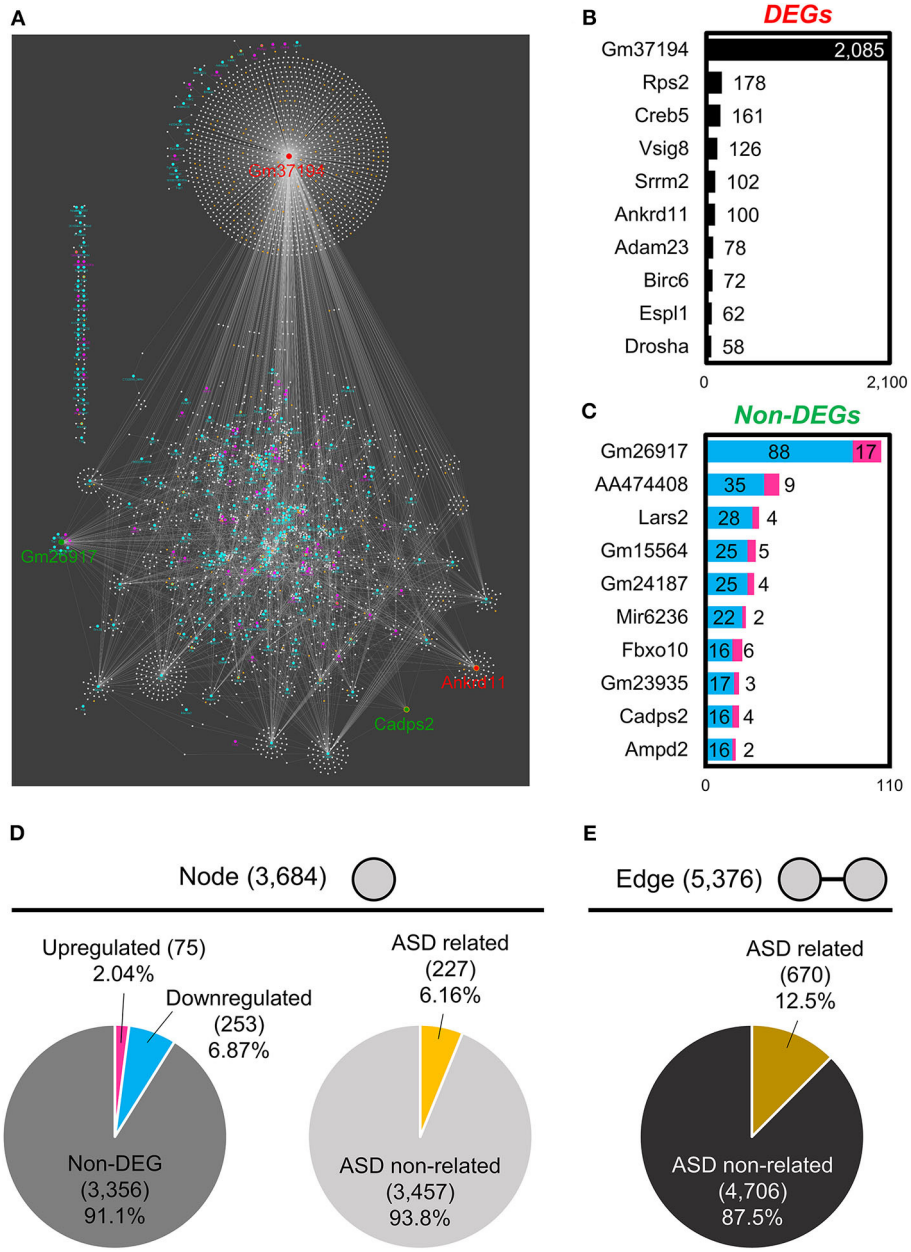

FIGURE 3 | RNA–RNA interaction network analysis of BTBR/R gene expression. **(A)** RNA–RNA interaction networks constructed by 328 differentially expressed genes (DEGs) and 3,356 non-DEGs. The top 10 hub genes of DEGs **(B)** and non-DEGs **(C)** were based on the number of edges. Node's and Edge's attribute. **(D)** Nodes were classified into upregulated genes (2.04%), downregulated genes (6.87%) and non-DEGs (91.1%). Nodes were also classified into autism spectrum disorder (ASD)-related genes (6.16%) and ASD non-related genes (93.8%). **(E)** Edges constructed by ASD-related genes were 12.5%.

down- and 66 up-regulated genes (with redundancy), suggesting that these DEGs may influence developmental differences in the cerebral cortex and striatum between the two strains of mouse (**Supplementary Table 3**).

KEGG Pathway Analysis

We next analyzed the functional connection of DEGs using the KEGG pathway database (Kanehisa et al., 2017). The 12 statistically significant pathways ($P < 0.05$) are summarized in **Supplementary Table 4**. *"Viral carcinogenesis"* (21 DEGs, $P = 0.0002$), *"Alcoholism"* (15 DEGs, $P = 0.013$), and *"Systemic lupus erythematosus"* (12 DEGs, $P = 0.015$) pathways were highly ranked, which may be partly due to the alteration of many histone protein variant genes as described above. Importantly, *"Oxytocin signaling pathway"* (to which 14 DEGs were specified) was included (11 down- and 3 up-regulated, $P = 0.0025$), suggesting the possibility that altered gene expression in this pathway may influence the oxytocin-mediated behavior in BTBR/R mice.

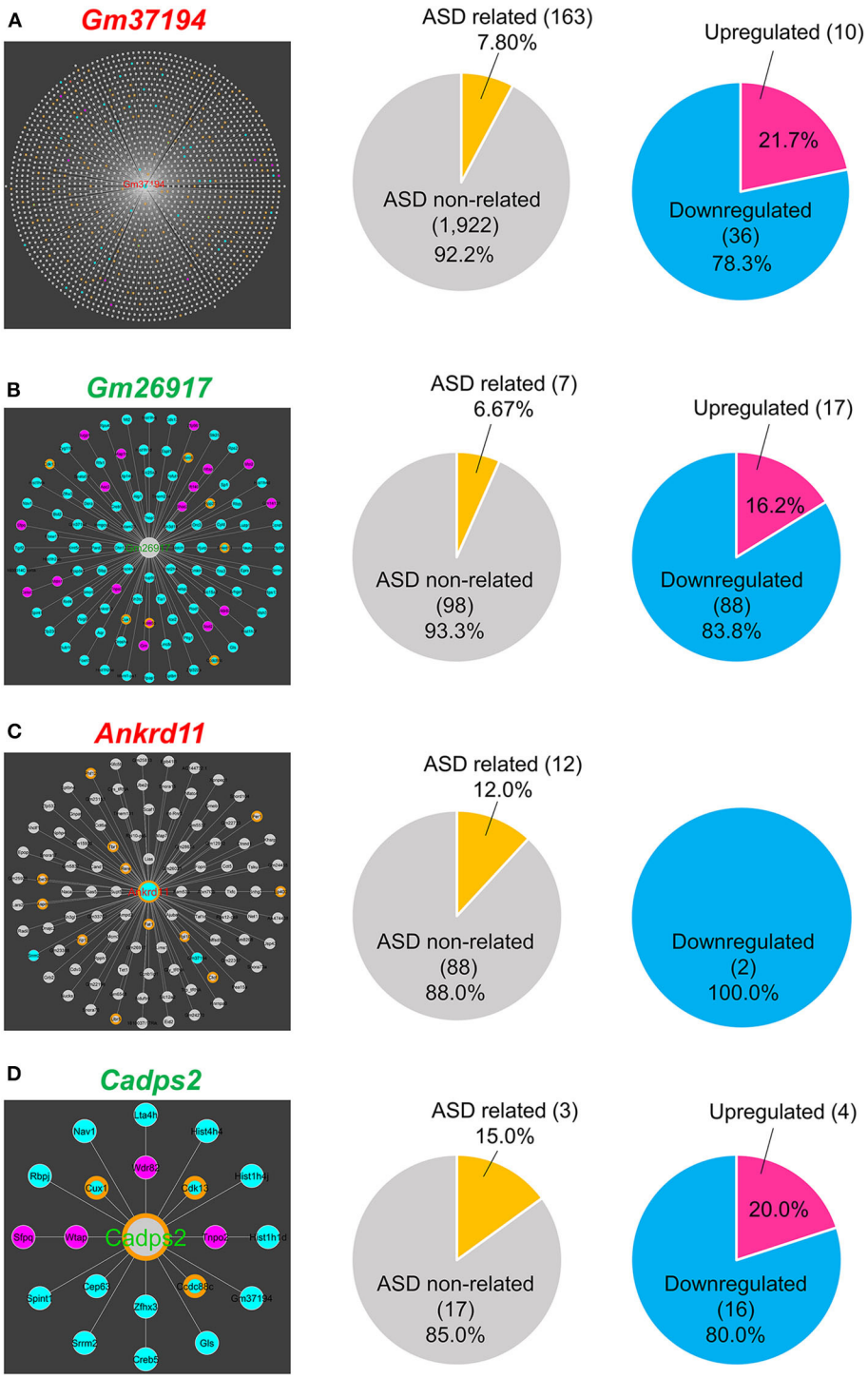

FIGURE 4 | RNA-RNA interaction network hubs. **(A)** *Gm37194* interaction network. *Gm37194*'s nodes had 163 ASD-related genes (7.80%) and 46 DEGs (2.20%). **(B)** *Gm26917* interaction network. *Gm26917*'s nodes had seven ASD-related genes (6.67%), 17 upregulated genes (16.2%), and 88 downregulated genes (83.8%). **(C)** *Ankrd11* interaction network. *Ankrd11*'s nodes had 12 ASD-related genes (12.0%) and 2 DEGs (2.0%). **(D)** *Cadps2* interaction network. *Cadps2*'s nodes had three ASD-related genes (15.0%), four upregulated genes (20.0%), and 16 downregulated genes (80.0%).

To individually assess DEGs mapped to specific pathways regardless of connectivity, we reexamined the KEGG pathway mapping data and picked up 15 pathways (including "*Oxytocin signaling pathway*") in terms of Neuron/Synapse/Receptor, Signaling, and Immune response from all hit pathways including ones with $P \geqq 0.05$ (**Figure 7A** and **Supplementary Table 4**).

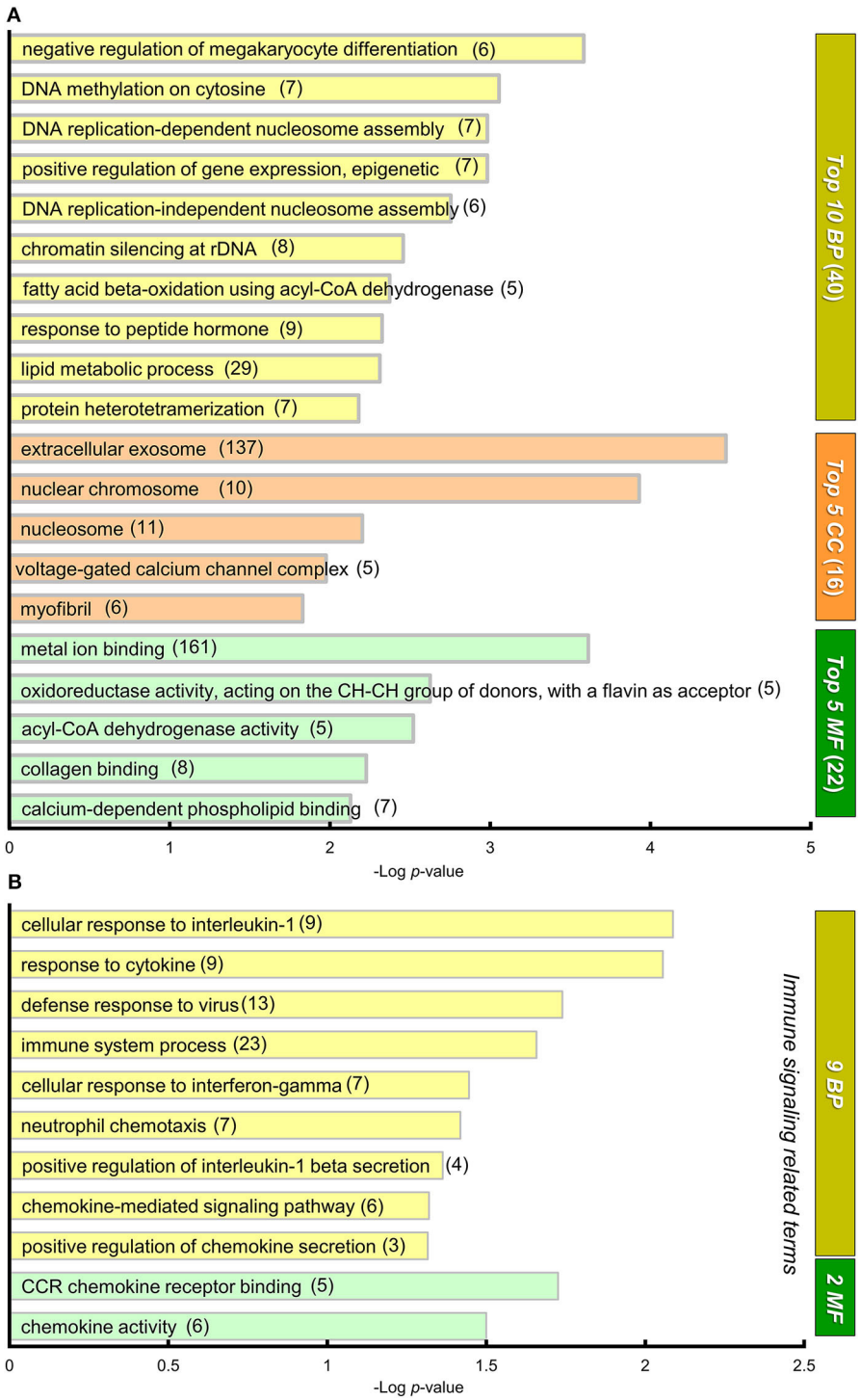

FIGURE 5 | GO annotation and DAVID functional classification of DEGs. **(A)** A graph showing gene ontology (GO) annotations of differentially expressed genes (DEGs) with high statistical significance. DAVID functional classification. DEGs were analyzed for enrichment in GO using DAVID, with an adjusted $P < 0.05$. For each category, adjusted *P*-value is indicated by the length of the horizontal bars (Log *P*-value). DEGs were enriched in 78 GO annotations from three sub-ontologies: 40 biological processes (BP), 16 cellular components (CC), and 22 molecular functions (MF) with statistical significance (**Supplementary Table 3**). Among them, the top 10 BP, top 5 MF, and top 5 CC GO terms are shown in this graph. Numerals in parentheses indicate numbers of DEGs annotated to the terms. **(B)** A graph showing 9 and 2 "immune signaling related" GO terms from BP and MF, respectively. The DEGs were annotated to these 11 "immune signaling" -related GO terms that showed statistical significance.

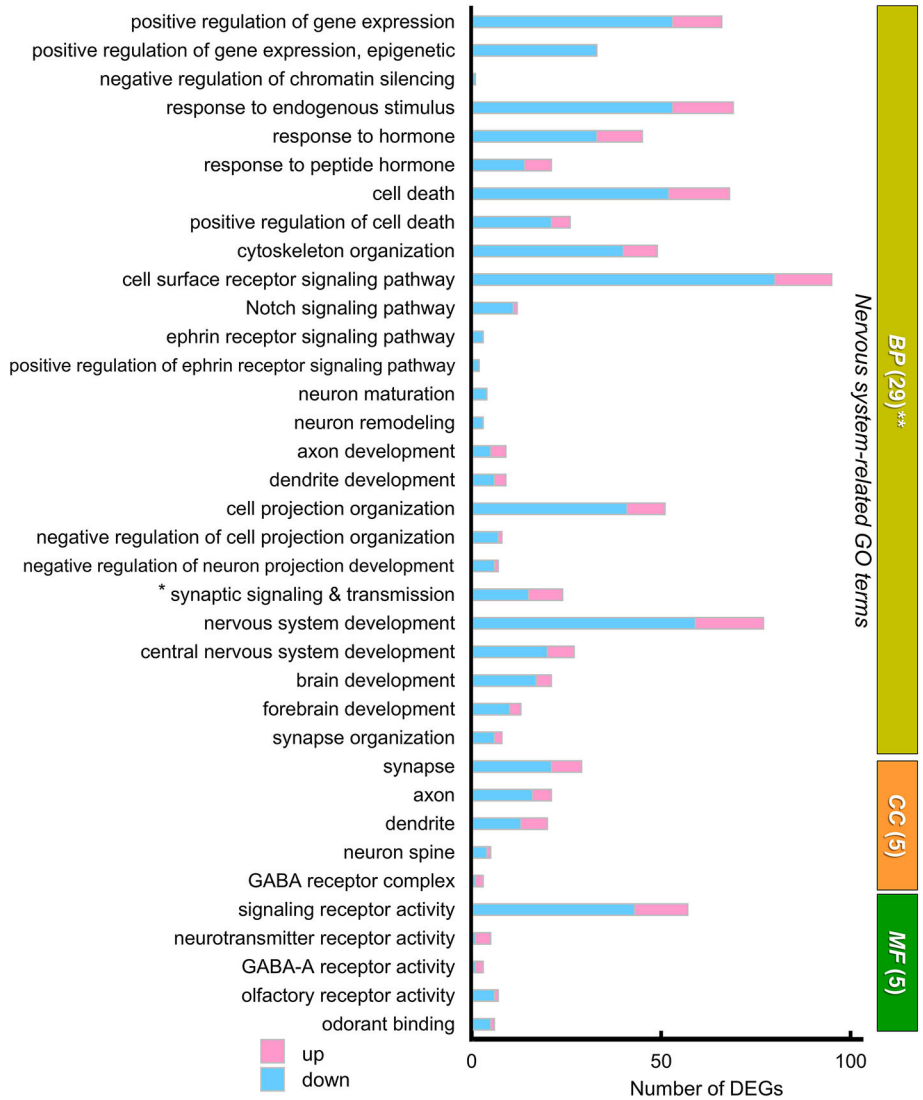

FIGURE 6 | The "nervous system-related" GO terms of DEGs. A graph showing 39 "nervous system-related" GO terms from 29 BP, 5 CC, and 5 MF sub-ontologies. Many DEGs were annotated to a variety of these nervous system related GO terms, although these annotations were not statistically significant. Blue and pink bars represent downregulated and upregulated DEGs, respectively. * "Synaptic signaling and transmission" includes four GO terms: "synaptic signaling," "trans-synaptic signaling," "anterograde trans-synaptic signaling," and "chemical synaptic transmission." **In BP, the GO term "gene expression" (154 downregulated genes, 39 upregulated genes) is not included in this graph. In this GO annotation, each gene is annotated with multiple terms, if they match, so that number of DEGs shown in the graph of GO terms includes redundancy.

The results indicated that there were 11 DEGs mapped to *"Neuroactive ligand-receptor interaction pathway"* of which six genes encoded neurotransmitter receptors for GABA (down: *Gabrg2*; up: *Gabra2*, *Gabrg3*), acetylcholine (up: *Chrm2*, *Chrm3*), and glutamate (down: *Grm7*; **Figure 7B**). The genetic alterations in these receptor genes have been shown to contribute to neuropsychiatric disorders, including GABAergic receptors *Gabrg2* (epilepsy), *Gabra2* (alcohol dependence), and *Gabrg3* (developmental delay, ASD, and Prader-Willi/Angelman syndrome; Braat and Kooy, 2015), muscarinic acetylcholine receptor *Chrm3* (ASD; Petersen et al., 2013), and metabotropic glutamate receptor *Grm7* (ASD; Noroozi et al., 2016). This reexamination also showed the alteration of gene expression for three cell response pathways to cell-cell signaling molecules (Notch, Wnt, and TNF). In addition, the enrichment of 10 DEGs in *"Chemokine signaling pathway"* (7 down and 3 up; **Figure 7B**) was detected, thereby supporting the possibility that the immune signaling is altered between the two mouse strains.

WGCNA

To elucidate gene co-expression networks, we analyzed the microarray sample data by weighted correlation analysis (Zhang and Horvath, 2005; Langfelder and Horvath, 2008). For this analysis, we selected 11,323 probes that were the top 20% most

A

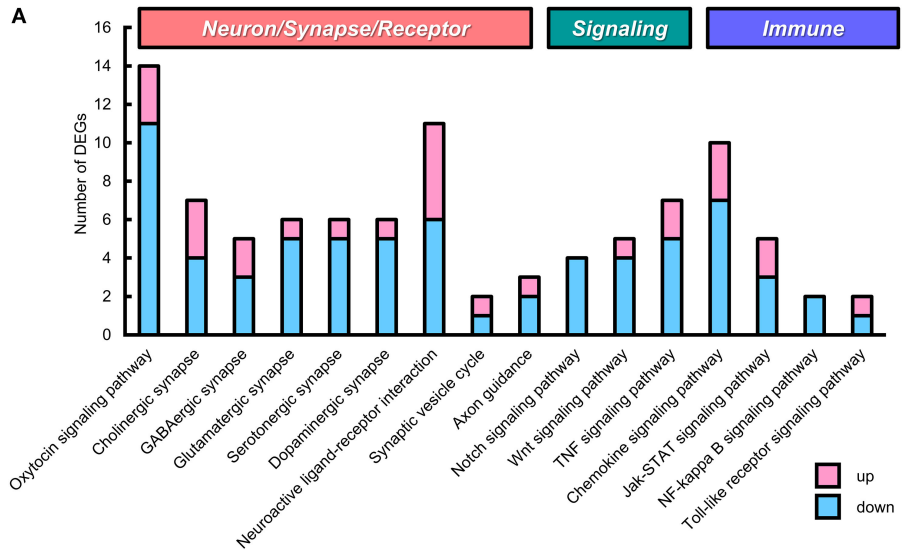

B

KEGG pathway	Downregulated DEGs	Upregulated DEGs
Neuron/Synapse/Receptor		
mmu04921:Oxytocin signaling pathway	*Cacna2d1*, *Cacnb2*, *Cacng1*, *Camk1d*, *Camk2b*, *Ccnd1*, *Cd38*, *Mylk3*, *Pla2g4b*, *Ppp1r12b*, *Prkag3*	*Cacna2d2*, *Fos*, *Pla2g4e*
mmu04725:Cholinergic synapse	*Gng8*, *Creb1*, *Creb5*, *Camk2b*	*Fos*, *Chrm2*, *Chrm3*
mmu04727:GABAergic synapse	*Gng8*, *Gabrg2*, *Gls*	*Gabra2*, *Gabrg3*
mmu04724:Glutamatergic synapse	*Gng8*, *Grik2*, *Grm7*, *Gls*, *Pla2g4b*	*Pla2g4e*
mmu04726:Serotonergic synapse	*Alox12b*, *Alox8*, *Gng8*, *Pla2g4b*, *Slc18a1*	*Pla2g4e*
mmu04728:Dopaminergic synapse	*Camk2b*, *Creb1*, *Creb5*, *Gng8*, *Slc18a1*	*Fos*
mmu04080:Neuroactive ligand-receptor interaction	*Hcrtr1*, *Gabrg2*, *Pard3*, *Ltb4r1*, *Grik2*, *Grm7*	*Gabra2*, *Gabrg3*, *Chrm3*, *Chrm2*, *Sstr1*
mmu04721:Synaptic vesicle cycle	*Slc18a1*	*Atp6v1c2*
mmu:04360:Axon guidance	*Pak6*, *Ablim2*	*Sema3a*
Signaling		
mmu04330:Notch signaling pathway	*Adam17*, *Aph1c*, *Notch1*, *Rbpj*	
mmu04310:Wnt signaling pathway	*Camk2b*, *Ccnd1*, *Fbxw11*, *Wnt8b*	*Daam1*
mmu04668:TNF signaling pathway	*Creb1*, *Creb5*, *Gm5431*, *Il15*, *Tnfrsf1b*	*Fos*, *Junb*
Immune		
mmu04062:Chemokine signaling pathway	*Ccl19*, *Ccl21a*, *Ccl3*, *Gng8*, *Hck*, *Pard3*, *Ppbp*	*Ccl17*, *Ccl24*, *Cx3cr1*
mmu04630:Jak-STAT signaling pathway	*Ccnd1*, *Il15*, *Il22ra1*	*Il12rb1*, *Irf9*
mmu04064:NF-kappa B signaling pathway	*Ccl19*, *Ccl21a*	
mmu04620:Toll-like receptor signaling pathway	*Ccl3*	*Fos*

FIGURE 7 | KEGG pathways that suggest functional alterations in BTBR/R. From Kyoto Encyclopedia of Genes and Genomes (KEGG) pathway analysis data (**Supplementary Table 4**), we selected 15 KEGG pathways which are categorized into the pathways related to "Neuron/Synapse/Receptor" (8 pathways), "Signaling" (3 pathways), and "Immune" (4 pathways). Among these pathways, the "Oxytocin signaling pathway" showed statistical significance ($P < 0.00253$; see **Supplementary Table 4**). **(A)** Number of differentially expressed genes (DEGs) classified into these 15 pathways (with redundancy) are shown. Blue and pink bars represent downregulated and upregulated DEGs, respectively. **(B)** Gene symbols of DEGs classified into each KEGG pathway.

informative probes reliable for the detection of their expression (Provenzano et al., 2016). The WGCNA analysis of BTBR/R data normalized to B6 data showed 10 highly-correlated modules of co-expressed genes (**Figures 8A,B, Supplementary Table 5**). The top 3 large modules "*Turquoise module*" (2,316 genes; 279 GO terms), "*Blue module*" (2,160 genes; 622 GO terms),

and "*Brown module*" (1,589 genes; 428 GO terms) are enriched for genes annotated to the GO terms related to Nucleosome-Chromatin-DNA ("nucleosome," "DNA packaging complex," and "protein-DNA complex"), Neurotransmitter-Synaptic Transmission ("neurotransmitter transport," "chemical synaptic transmission," "regulation of neurotransmitter levels," "neurotransmitter secretion," and "cell-cell signaling"), and Signal Transduction-Translational Regulation ("negative regulation of signal transduction," "negative regulation of signaling," "translational termination," and "regulation of translational termination"), respectively, with the highest statistical significance (**Figure 8C**, **Supplementary Table 6**).

Overall, our comprehensive bioinformatics analyses of gene expression highlighted functional alterations in the cerebral cortex and striatum of BTBR/R mice.

Fifty-Three ASD Candidate Genes Were Included in DEGs Between BTBR/R and B6 Mice

We next explored whether BTBR/R mice DEGs were the known ASD candidate genes by utilizing the autism gene database AutDB (Pereanu et al., 2018). We identified 53 genes (40 downregulated and 13 upregulated) out of 1,280 DEGs to be ASD candidate genes, which corresponds to about 4.7% of total 1,125 genes registered in the AutDB (**Figure 9A**, **Supplementary Table 9**). Considering this result, we entertained the possibility of altered co-expression or combinational expression patterns of these 53 DEGs in BTBR/R mouse brains being partly associated with ASD.

To verify this possibility further, we next analyzed the co-occurrence of differentially-expressed ASD candidate genes between BTBR/R and B6 mice (hereafter referred to as "BTBR/R ASD-DEGs") in the previous studies of three other psychiatric disorder models and human subjects with ASD (**Figures 9B–F**, **Supplementary Tables 12, 13**). Comparing with the genes affected in ASD patients (the largest genome-scale exome-sequencing meta-analysis [n = 35,584 total samples, 11,986 with ASD] by Satterstrom et al., 2020; **Figure 9B**), *Chd8* (chromodomain helicase DNA binding protein 8: ASD-candidate gene) haploinsufficient transgenic mice (with increased connectivity in cortical network and no obvious sociability deficits; P5 mice; one brain hemisphere; Suetterlin et al., 2018; **Figure 9C**), *miR137* haploinsufficient transgenic mice (with synaptic overgrowth, dendritic growth deficits, learning and memory deficits and social behaviors deficits; P14 mice; whole brain; Cheng et al., 2018; **Figure 9D**), the lipopolysaccharide (LPS)-induced maternal immune activation (MIA) rat fetus model (with neural and behavioral abnormalities relevant to ASD; LPS manipulation for the MIA-inducing event on gestational day 15, gene expression measured at 4 h post-LPS injection; Oskvig et al., 2012; Lombardo et al., 2018; **Figure 9E**), and *Fmr1* (Fragile X mental retardation 1: ASD-candidate gene) knockdown *Drosophila* embryos (with neural defects; stage 14 follicles; Greenblatt and Spradling, 2018; **Figure 9F**). The results allowed us to verify *de novo* variations of three ASD-associated BTBR/R DEGs (*Ankrd11*, *Kdm5b*, and *Traf7*) in the large exome sequencing study of patients with ASD (Satterstrom et al., 2020; **Figure 9B** and **Supplementary Table 13**). Similarly, the co-occurrence of BTBR/R ASD DEGs was 3 in the *Chd8* study (**Figure 9C**), 7 in the *miR137* study (**Figure 9D**), 19 in the MIA study (**Figure 9E**), and 4 in the *Fmr1* study (**Figure 9F**). It was

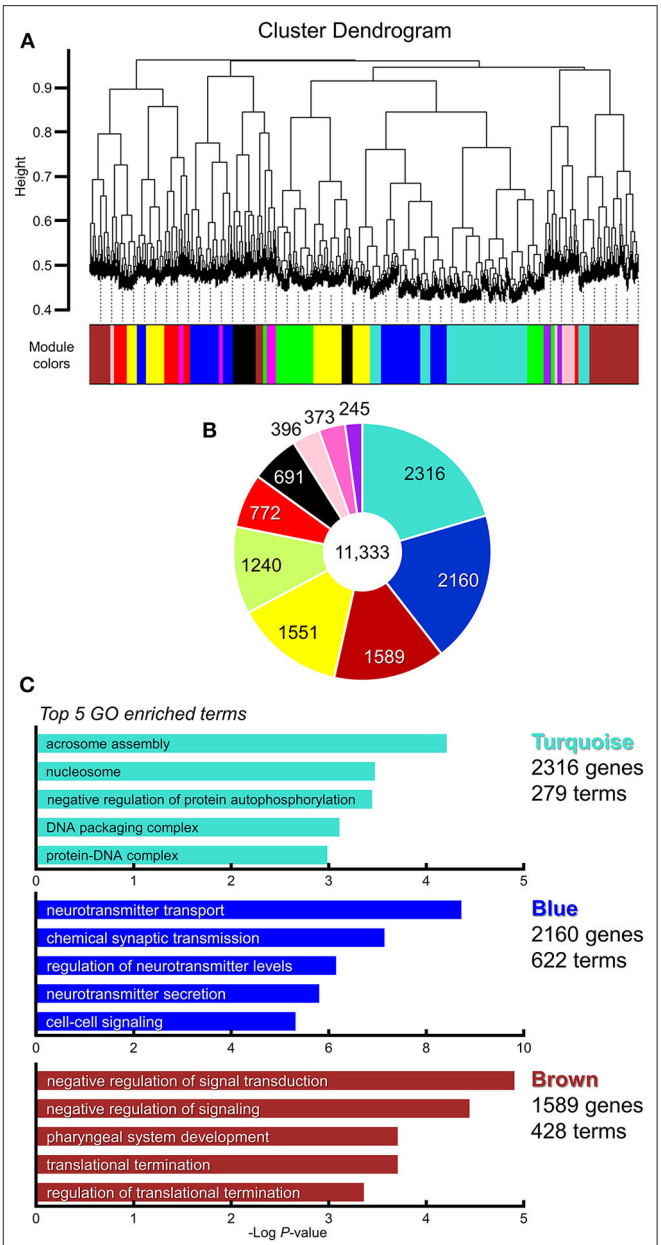

FIGURE 8 | WGCNA identified multiple clusters (modules) of highly correlated genes which were enriched in synapse category. Weighted gene co-expression network analysis (WGCNA). Gene subset containing 11,323 genes is selected for WGCNA analysis (the top 20% of probes; **Supplementary Table 5**). **(A)** Gene dendrogram and clustered 10 modules coded by different colors. **(B)** Pie chart showing gene counts of each module. **(C)** Top 5 enriched gene ontology categories in modules of the highest three ("Turquoise module," "Blue module," and "Brown module"). Horizontal axis indicates the "Log *P*-value" (Enrichment *P*; **Supplementary Table 6**).

remarkable that five BTBR/R ASD genes repeatedly co-occurred in multiple independent studies: *Kdm5b* in all four studies; *Mpp6* in three studies; and *Ankrd11*, *Pde4b*, and *Syn3* in two studies. In addition, 19 out of 53 BTBR/R ASD DEGs co-occurred in the MIA model study. These results suggested that BTBR/R mouse brains have alterations in *Kdm5b*-mediated epigenetic regulation commonly affected in these ASD models together with those in the maternal immune activation model.

We next examined DEGs between two sublines of BTBR mice by comparing our BTBR/R vs. B6 dataset (1,280 DEGs obtained from the cerebral cortex and striatum) with the five independent BTBR/J vs. B6 datasets (1,016 DEGs from the hippocampus by Provenzano et al. (2016); 325 DEGs from the cerebellum by Shpyleva et al. (2014); 448 DEGs in the striatum by Oron et al. (2019); and 328 DEGs from the hippocampus and 328 DEGs from the cerebral cortex by Daimon et al., 2015; **Supplementary Table 14**). The 341 DEGs identified in our BTBR/R study were also reported as DEGs in at least one of the BTBR/J datasets. Five DEGs showed consistent expression patterns in all five datasets: three upregulated DEGs (*Adi1*, *Scg5*, and *Serpina3n*), and two downregulated DEGs (*Nudt19* and *Pop4*). The expression patterns of 136 DEGs (23 upregulated, 113 downregulated) were consistent between the BTBR/R mice cerebral cortex and striatum and the BTBR/J mice striatum (Oron et al., 2019) datasets, while those of 30 DEGs (6 upregulated, 24 downregulated) were consistent between the BTBR/R mice cerebral cortex and striatum and the BTBR/J mice cerebral cortex (Daimon et al., 2015) datasets (**Supplementary Table 14**). In total, 208 DEGs showed consistent expression patterns (45 upregulated, 163 downregulated) between the BTBR/R cerebral cortex and striatum and BTBR/J hippocampus (Provenzano et al., 2016) datasets. The results suggest both differences and similarities in the brain transcriptomes of BTBR/R and BTBR/J mice, although well-controlled direct comparisons between the two sublines of BTBR are required.

Spatial Expression Patterns of DEGs Were Also Different Between B6 and BTBR/R Brain

We comprehensively analyzed the spatial cellular expression of DEGs in the BTBR/R and B6 mice brains in a qualitative manner using the ISH method. We selected 11 DEGs (3 upregulated and 8 downregulated) which are well-annotated in GO. Consistent with microarray analysis, the expression level of *Serpina3n* and *Lpl* in cortical areas and the striatum was higher in BTBR/R mice than B6 mice (**Figure 10**). Higher expression of *Serpina3n* in BTBR/R mice was entirely observed in cortical layers of the primary somatosensory cortex (SSp; **Figure 10A**) and medial prefrontal cortex (mPFC; **Figure 10B**), but the difference between BTBR/R and B6 mice was not prominent in the striatum (**Figure 10C**). Interestingly, the strong expression of *Lpl* in BTBR/R mice was observed in the superficial layer of cortex (**Figures 10A,B**). In the striatum, *Lpl* was highly expressed in BTBR/R compared with B6 mice, especially in the ventral lateral striatum (VL; **Figure 10C**). In contrast, the cortical expression of *Pls3* and *Rpp25* in BTBR/R

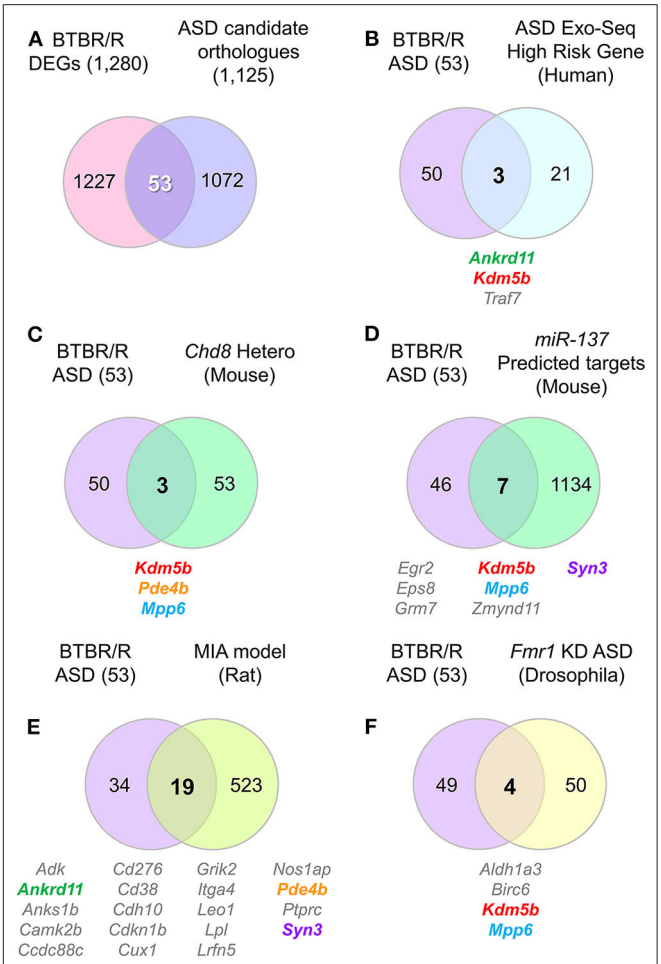

FIGURE 9 | DEG contained several ASD-related orthologs which overlapped with other ASD model and/or human patient altered genes. Venn diagrams show the number of identical genes between BTBR/R differentially expressed genes (DEGs) and autism spectrum disorder (ASD)-related genes registered in the ASD database AutDB **(A)**, and the resultant 53 BTBR/R ASD-related genes and the genes reported in a larger ASD exome sequencing study **(B)** and four ASD model animal studies **(C–F)**. **(A)** 53 genes are identical between 1,280 BTBR/R DEGs and 1,125 ASD-related mouse orthologs to 1,141 human ASD-related genes (AutDB statics, updated Jan 2020). The 53 overlapped genes between BTBR/R DEGs and ASD-related genes are referred to as "BTBR/R ASD genes." **(B)** There were 3 overlapped genes (*Ankrd11*, *Kdm5b*, and *Traf7*) between the large ASD exosome sequencing study (Satterstrom et al., 2020) and this BTBR/R study. **(C)** There were also 3 overlapped genes (*Kdm5b*, *Pde4b*, and *Mpp6*) between the *Chd8* haploinsufficient transgenic mouse study (Suetterlin et al., 2018) and this BTBR/R study. **(D)** There were 7 overlapped genes (*Egr2*, *Eps8*, *Grm7*, *Kdm5b*, *Mpp6*, *Zmynd11*, and *Syn3*) between the *miR137* overexpressing transgenic mouse study (Cheng et al., 2018) and this BTBR/R study. **(E)** There were 19 overlapped genes (*Adk*, *Ankrd11*, *Anks1b*, *Camk2b*, *Ccdc88c*, *Cd276*, *Cd38*, *Cdh10*, *Cdkn1b*, *Cux1*, *Grik2*, *Itga4*, *Leo1*, *Lpl*, *Lrfn5*, *Nos1ap*, *Pde4b*, *Ptprc*, and *Syn3*) between the lipopolysaccharide-induced maternal immune activation rat fetus ASD model study (Oskvig et al., 2012; Lombardo et al., 2018) and this BTBR/R study. **(F)** There were four overlapped genes (*Aldh1a3*, *Birc6*, *Kdm5b*, and *Mpp6*) between the *Fmr1* knockdown *Drosophila* embryo study (Greenblatt and Spradling, 2018) and this BTBR/R study. Five gene symbols that show co-occurrence among multiple independent studies are shown in colored letters; they are: *Ankrd11*, *Kdm5b*, *Pde4b*, *Mpp6*, and *Syn3*.

mice was lower than that of the B6 mice (**Figures 10A,B**). The expression of *Cacnb2* in the nucleus accumbens was decreased in BTBR/R compared with B6 mice (**Figure 10C**). The expression of other DEGs in the cerebral cortex and striatum are shown in the **Supplementary Figures 2–5**. Overall, the expression of 11 DEGs in the cortex and/or striatum from ISH was consistent with the results from the microarray and qRT-PCR analyses (**Figure 10**, **Supplementary Figures 2–5**).

Next, we analyzed the expression of DEGs in other brain areas (**Figure 11**). Similar to the cortical areas, *Serpina3n* expression of BTBR/R mice was higher than that of B6 mice in the hippocampal CA1, CA3, and dentate gyrus (DG) areas (**Figure 11A**). In BTBR/R mice, the expression of *Lpl* was specifically increased in the DG compared with B6 mice (**Figure 11A**). In contrast, the expression of *Cd276* in the CA1 and CA3 areas was lower in BTBR/R than B6 mice (**Figure 11A**). In the piriform cortex (PIR), the expression of *Serpina3n* and *Lpl* was increased, while that of *Pls3* was decreased, in BTBR/R compared to B6 mice (**Figure 11B**). In the amygdala, the expression of *Serpina3n* was higher in BTBR/R than B6 mice, especially in the basolateral amygdala (BLA) (**Figure 11C**). By contrast, the expression of *Pls3* was lower in BTBR/R than B6 mice in the BLA (**Figure 11C**). Consistent with the cortical areas, *Rpp25* expression of BTBR/R mice was decreased in the amygdala compared with that of B6 mice (**Figure 11C**). The expression of other DEGs in the hippocampus, PIR, and amygdala is shown in **Supplementary Figures 6–8**. Finally, we focused on the paraventricular hypothalamic nucleus. The expression of *Serpina3n* and *Pls3* was increased and decreased in BTBR/R mice compared to B6 mice, respectively (**Figure 11D**).

We have summarized the spatial pattern of DEG expression in **Figure 12**. Essentially, messenger RNA (mRNA) expression levels detected by ISH were consistent with the results indicated by the microarray and qRT-PCR analyses. In addition, the comparative ISH analysis provided valuable data on the cellular and regional difference of DEG expression between BTBR/R and B6 mouse brains, which is informative for future studies to consider a relationship between gene expression and brain circuits associated with pathologies.

BTBR/R Behavioral Phenotypes Were Indicative of a Slight Autistic Tendency

Finally, we assessed the basic phenotypes of BTBR/R mice in terms of sociality and associated emotional features. In five-trial social habituation/recognition tasks (**Supplementary Figure 9A**), compared to B6 mice ($n = 12$), BTBR/R mice ($n = 15$) unexpectedly showed no significant differences in four repeated habituation interaction trials with the first social stimulus mouse (**Supplementary Figure 9B**). Interestingly, response to a second novel stimulus mouse at trial five was slightly decreased in BTBR/R compared to B6 mice (**Supplementary Figure 9B**, repeated measurement two-way ANOVA; trial 4–5, $F_{(1, 25)} = 35.80$, $P < 0.001$; mouse strains, $F_{(1, 25)} = 0.15$, $P = 0.70$; trials × strain, $F_{(1, 25)} = 4.31$, $P = 0.048$; *post-hoc* Tukey-Kramer test, BTBR/R vs. B6 at trial 5, $P = 0.026$). Then, we analyzed the social recognition index in which interaction time with a novel mouse at trial five was subtracted from that with a habituated mouse at trial four. The social recognition index was significantly decreased in BTBR/R compared with B6 mice (**Supplementary Figure 9C**, $P = 0.048$). In open field tests (**Supplementary Figures 9D–G**), BTBR/R mice showed a striking increase in repetitive jumping behavior compared with B6 mice ($P < 0.001$), although there were no differences in total distance, time spent in center area, and time spent self-grooming. These findings suggest that, compared to B6 mice, BTBR/R mice have a mild impairment in social recognition as well as increased stereotypic behavior.

DISCUSSION

In this study, we identified a number of transcriptomic changes in the cerebral cortex and striatum of BTBR/R mice (1,280 DEGs with 974 downregulated and 306 upregulated alterations) compared to B6 mice. The GO enrichment analysis showed 78 GO annotations and highlighted the significant alteration of functional gene groups including the DNA-chromatin-related gene group, which may influence DNA replication, transcriptional and epigenetic regulation, and the immune signaling-related gene group, which may result from increased and/or aberrant immune responses. The KEGG pathway analysis showed enrichment of the *"Oxytocin signaling pathway"*-related 14 DEGs with 11 downregulated and three upregulated expression profiles, suggesting the possibility of an overall decline in this important pathway to express the oxytocin-mediated social behavior. The WGCNA co-expression network analysis indicated significant changes in the co-expression modules including a large number of DNA/chromatin-related genes, synaptic transmission-related genes, and signal transduction/translational regulation-related genes. We also showed that 53 ASD-related genes have differential expression patterns between BTBR/R and B6 mice brains. By comparing our DEGs and these ASD-related DEGs to DEGs reported by five independent studies of ASD patients and ASD animal models, we propose some gene candidates critical to similar phenotype(s) among ASD patients and ASD animal models. Moreover, by comparing our DEGs to DEGs reported in four independent BTBR/J studies, we show differences and similarities between the two BTBR sublines, and suggest some critical DEGs that commonly influence brain function and behavior. Finally, we mapped spatial differential expression patterns of 11 DEGs in BTBR/R mice in comparison to those of B6 mice. These transcriptomic features in the cerebral cortex and striatum of BTBR/R mice in contrast to those of highly social B6 mice suggest alterations in expression of brain functions and behavior between these two mouse strains.

RNA Alterations in BTBR/R Mice: ncRNA Expression, Splicing, and RNA–RNA Interactions

In addition to alteration of protein-coding transcripts, abnormalities in splicing patterns as well as ncRNA profiles have been shown in individuals with various psychiatric

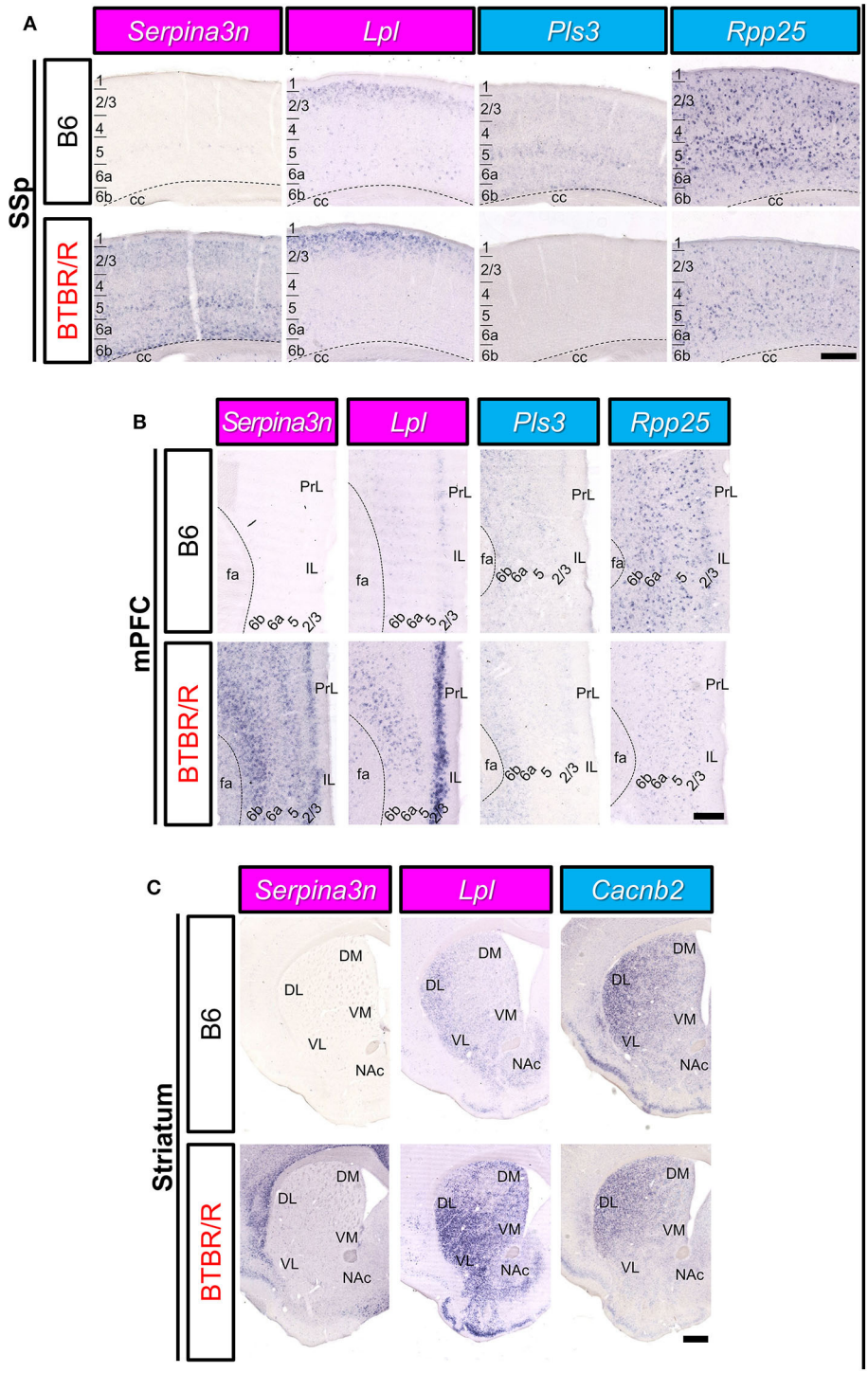

FIGURE 10 | The spatial expression of DEGs in the cerebral cortex and striatum of B6 mice and BTBR/R mice. *In situ* hybridization images for gene expression of *Serpina3n*, *Lpl*, *Pls3*, *Rpp25,* and *Cacnb2* in coronal sections of the primary somatosensory cortex (SSp; **A**), medial prefrontal cortex (mPFC; **B**), and striatum **(C)**. Upper and lower columns show B6 and BTBR/R mouse sections, respectively. Scale bars show 250 μm in cortical images and 500 μm in the striatum images. 1, 2/3, 4, 5, 6a, and 6b, cerebral cortical layer 1, 2/3, 4, 5, 6a, 6b; cc, corpus callosum; fa, corpus callosum, anterior forceps; DL, dorsolateral striatum; DM, dorsomedial striatum; IL, infralimbic cortex, NAc, nucleus accumbens; PrL, prelimbic cortex; VL, ventrolateral striatum; VM, ventromedial striatum. The magenta and light blue indicate upregulated and downregulated genes, respectively.

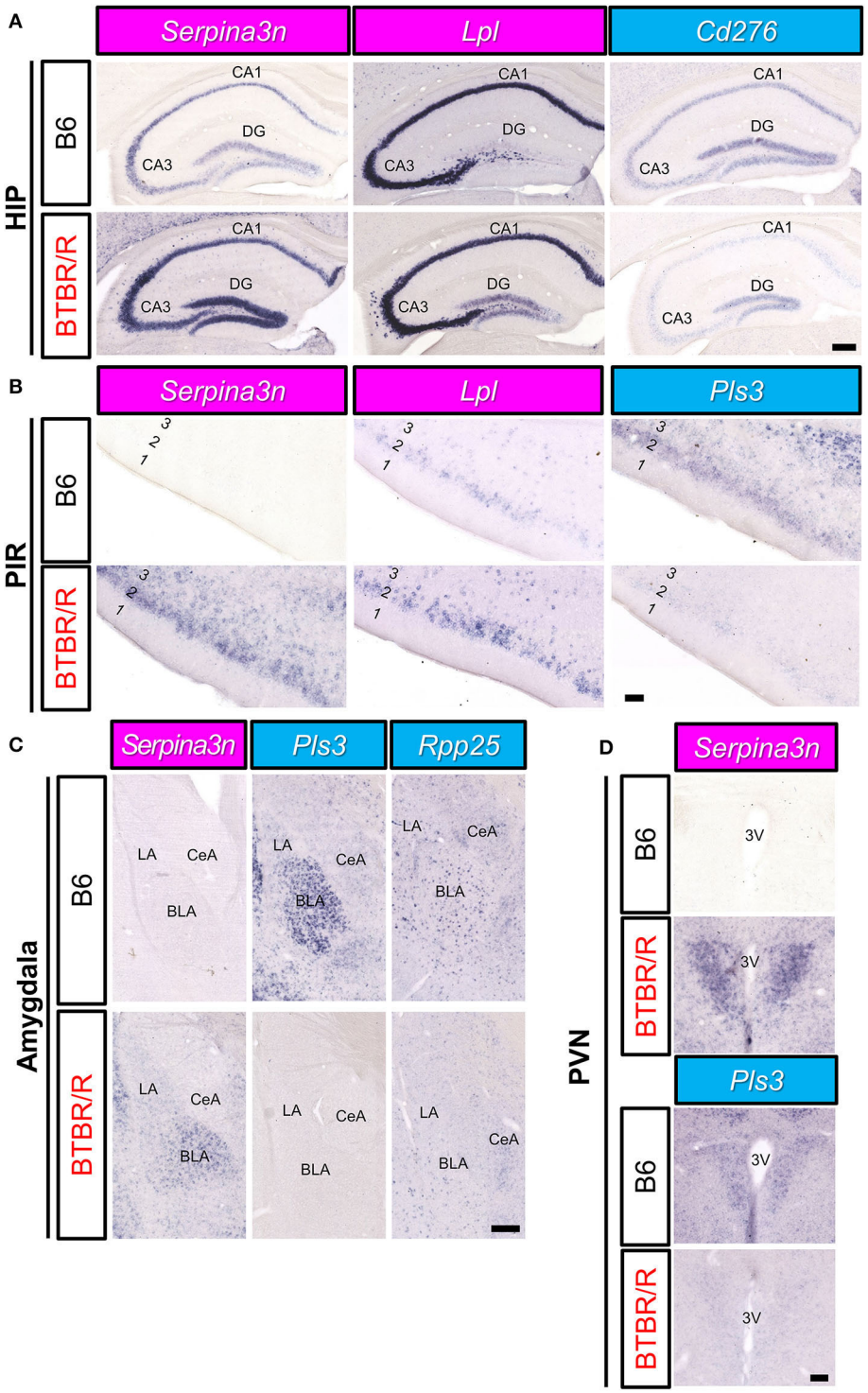

FIGURE 11 | The spatial expression of DEGs in the hippocampus, amygdala, and PIR of B6 mice and BTBR/R mice. *In situ* hybridization images for gene expression of *Serpina3n*, *Lpl*, *Cd276*, *Pls3*, and *Rpp25* in coronal sections of the hippocampus (HIP; **A**), piriform cortex (PIR; **B**), amygdala **(C)**, and paraventricular nucleus (PVN; **D**). Upper and lower columns show B6 and BTBR/R mouse sections, respectively. Scale bars show 250 μm in the HIP and amygdala, 100 μm in the PIR and PVN. In the HIP, CA1, pyramidal layer of the cornu ammonis 1; CA3, pyramidal layer of the cornu ammonis 3; DG, dentate gyrus. In the amygdala, BLA, basolateral amygdala; CeA, central amygdala; LA, lateral amygdala. In the PIR, 1, 2 and 3, cerebral cortical layer 1, 2, and 3. In the PVN, 3V, third ventricle. The magenta and light blue indicate upregulated and downregulated genes, respectively.

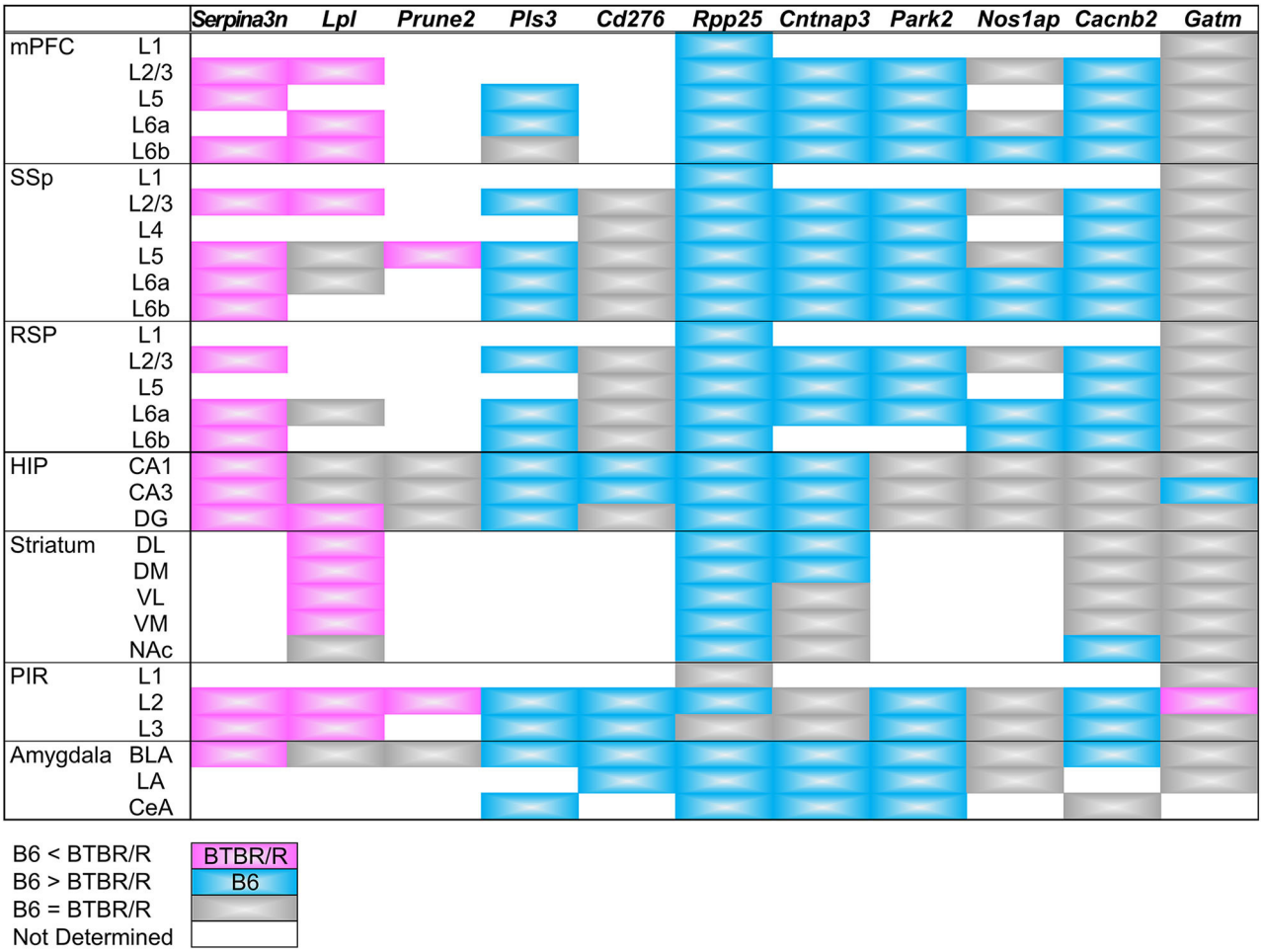

FIGURE 12 | Summary of DEGs expression in the cortical and subcortical areas. Comparative expression levels of differentially expressed genes between BTBR/R mice and B6 mice are shown by color. Magenta and cyan indicate that the *in situ* hybridization signal level is higher in BTBR/R mice and B6 mice than B6 mice and BTBR/R mice, respectively. Gray indicates no detectable difference between two mouse strains. Abbreviations are indicated in the legends of **Figures 10**, **11**.

disorders including ASD (Gandal et al., 2018). Specific ncRNA species such as micro RNAs (miRNAs), small nucleolar RNAs, and lncRNAs are involved in psychiatric disorders by regulating transcriptional and translational systems (Zhang et al., 2019). Abnormal alternative splicing is also associated with neurodevelopmental disorders (Zhang et al., 2016; Gandal et al., 2018); for instance, Rbfox1 is a transcription regulator that controls alternative splicing and its mutation is associated with ASD (Wamsley et al., 2018). In addition, the alternative splicing "Retained intron" is involved in increasing miRNA targets by changing untranslated region's sequence in ASD-related genes (Tan et al., 2007). In this study, we identified 498 ncRNAs (387 downregulated, 111 upregulated) differentially expressed in BTBR/R mice compared to B6 mice. In addition, it was notable that 18.2% of BTBR/R mice DEGs showed alternative splicing (160 downregulated, 47 upregulated; "nonsense mediated decay" and "retained intron"). The altered ncRNA and alternative spliced transcript expression may contribute to a transcriptomic feature in BTBR/R mice brain.

In this study, we identified a huge RNA–RNA interaction network that included DEG- and ASD-related genes. As mentioned above, ncRNA have a regulatory role via ncRNA–RNA interactions. In addition, recent studies have shown that mRNA-mRNA interactions also act as translational regulators in prokaryotes (Ruiz de los Mozos et al., 2013; Masachis and Darfeuille, 2018; Ignatov et al., 2020). In our analysis, we identified *Gm37194* and *Gm26917* as a hub gene that was the most connected node with other node RNAs. Both *Gm37194* and *Gm26917* are predicted genes annotated by an expressed sequence tag (EST; Wilming et al., 2008). *Gm26917* lncRNA expression is regulated by FoxM1 and acts as a competing endogenous RNA source for miRNA-29b, which accelerates apoptosis of muscle satellite cells (Chen et al., 2018). We also identified *Ankrd11* and *Cadps2* as the most connected genes of all the ASD-related genes. ANKRD11 is a potential chromatin regulator implicated in neural development, and its *de novo* mutation was reported in ASD (Iossifov et al., 2014). In mice, ANKRD11 controls cortical precursor proliferation

via histone acetylation, and its knockdown mice showed ASD-like behavior (Gallagher et al., 2015). CADPS2 is a cytosolic protein that regulates the exocytosis of synaptic and dense-core vesicles (Cisternas et al., 2003). In ASD patients, an aberrant increase of a rare alternative splicing variant with exon3-skipping was reported and mice expressing exon3-skipped *Cadps2* variant showed ASD-like behavior (Sadakata et al., 2007, 2012). Among *Ankrd11*-interacting ASD-related genes, six transcriptional repressors (*Phf12*, *Tbr1*, *Rere*, *Ctcf*, *Ep400*, and *Per1*) and three E3 ubiquitin protein ligases (*Ube3b*, *Trip12*, and *Ubr5*) were included. It is of interest that within the *Cadps2*-interacting DEGs, there were three RNA splicing related genes (*Cdk13*, *Srrm2*, and *Sfpq*). Taken together, the RNA–RNA interaction network data demonstrates that *Ankrd11* and *Cadps2* interact with many functionally-related genes, suggesting that these functional mRNA-mRNA interactions may underlie the transcriptional regulation of ASD-related genes.

BTBR/R DEGs Are Commonly Altered in ASD Individuals and Animal Models

We identified 53 ASD candidate genes within BTBR/R mice DEGs (referred to as BTBR/R ASD-DEGs in this study), suggesting that the alteration of this combinatory gene expression pattern may contribute to differences between BTBR/R and B6 mice. Thus, we further analyzed the co-occurrence of BTBR/R mice ASD DEGs in the previously reported five independent studies: in human ASD patients and animal models (mouse, rat, and *Drosophila*) five BTBR/R ASD-DEGs were found that were repeatedly reported in the previous five studies: *Kdm5b* (four times); *Mpp6* (three times); *Ankrd11*, *Pde4b*, and *Syn3* (twice). *Kdm5b* was particularly interesting because of co-occurrence in four independent datasets obtained by analyzing human patients with ASD (Satterstrom et al., 2020) and ASD animal models, including *Chd8*-haploinsufficient transgenic mice (Suetterlin et al., 2018), *miR137*-haploinsufficient transgenic mice (Cheng et al., 2018), and *Fmr1*-knockdown *Drosophila* embryos (Greenblatt and Spradling, 2018). KDM5B (lysine demethylase 5B) is one of the lysine-specific histone demethylase family and demethylates tri/di/mono-methylated lysine-4 of histone H3 (H3K4), which is critical to neural development (Schmitz et al., 2011; Fueyo et al., 2015). *De novo* mutations of *Kdm5b* result in a recognizable syndrome with developmental delay (Faundes et al., 2018). MPP6 (membrane protein, palmitoylated 6) is a member of the peripheral membrane-associated guanylate kinase (MAGUK). MPP6 interacts with 4.1G, Lin7, and CADM4 proteins in Schwann cells and its KO mice showed hypermyelination of sciatic nerves (Saitoh et al., 2019). A *de novo* mutation of *Mpp6* was reported in an individual with ASD (Iossifov et al., 2014). Although MPP2, a member of the MPP family, acts as a scaffold in the postsynaptic density of hippocampal CA1 neurons (Kim et al., 2016), the role of MPP6 in the central nervous system remains to be studied. PDE4B is a member of the cyclic nucleotide phosphodiesterase (PDE) family (PDE4 subfamily). A *de novo* synonymous mutation in *PDE4B* was reported in an individual with ASD (Iossifov et al., 2014; Takata et al., 2016). *PDE4B* has also been identified as one of the subset genes related to a common molecular signature in autism (Diaz-Beltran et al., 2016). SYN3 (Synapsin 3) is a synaptic vesicle associated protein and its KO mice showed impairments in early axon outgrowth and inhibitory neurotransmission in hippocampal neurons (Feng et al., 2002). A *de novo* mutation in *SYN3* was identified in an individual with ASD (Ruzzo et al., 2019). TRAF7 (TNF receptor-associated factor 7), which generally exerts negative control on its targets including NF-κB and p53 by ubiquitination, was identified only in the human ASD dataset (Satterstrom et al., 2020). *TRAF7* mutations were shown to be involved in genesis of human cancer, especially in about 25% of meningiomas (Zotti et al., 2017), and *de novo* missense variants were also identified in ASD probands (Neale et al., 2012; Krumm et al., 2015; Tokita et al., 2018). Together, our results suggest that BTBR/R mice have alterations in the *KDM5B*, *MPP6*, *ANKRD11*, *PDE4B*, *SYN3*, and *TRAF7*-associated pathway(s), some of which are commonly affected in ASD individuals and animal models, that may impact on the development and function of BTBR/R brain.

Maternal infection is a risk for ASD and animal models showed that maternal immune activation is sufficient to impact neuropathology and altered behaviors in offspring (Ehninger et al., 2012; Estes and McAllister, 2015). Recent studies also showed marked neuroinflammation in individuals with ASD, suggesting that can also contribute to ASD risk (Gottfried et al., 2015; Gładysz et al., 2018). Importantly, in addition to changes in gene expression patterns related to the immune signaling and response, which was repeatedly suggested by the GO enrichment and pathway analyses, about 36% of BTBR/R mice ASD DEGs overlapped with DEGs of the LPS-induced MIA rat fetus model (Lombardo et al., 2018). Thus, BTBR/R mice brains may have alterations in the immune-related pathway(s) which impact on brain development and function.

Similarity in DEGs Between Two Sublines of BTBR: BTBR/R and BTBR/J

By comparison of the DEGs between our BTBR/R study and those of previous BTBR/J studies, we identified five DEGs that commonly appeared among these independent studies (upregulated *Adi1*, *Scg5*, and *Serpina3n*; downregulated *Nudt19* and *Pop4*), besides the use of different experimental conditions such as brain regions analyzed (cerebral cortex and striatum in this study; hippocampus in Provenzano et al., 2016; cerebellum in Shpyleva et al., 2014; striatum in Oron et al., 2019; and cortex and hippocampus in Daimon et al., 2015). *Adi1* encodes 1,2-dihydroxy-3-keto-5-methylthiopentene dioxygenase that is involved in methionine salvage: 5′-methylthioadenosine cycle to increase S-adenosylmethionine levels, which altered genome-wide promoter methylation profiles, resulting in altered gene expression in hepatocellular carcinoma (Chu et al., 2019). *Scg5* (secretogranin V, 7B2) encodes a secreted chaperone protein that prevents the aggregation of other secreted proteins inside of secretory vesicles, and its KO mice show a number of endocrine abnormalities (Bartolomucci et al., 2011). *Serpina3n* (Serine protease inhibitor A3N) encodes a secretory serine protease inhibitor that mediates neuroinflammation (Xi et al., 2019) and is upregulated in various neurological diseases (Switonski et al., 2015; Vanni et al., 2017). *Nudt19* (Nucleoside diphosphate linked moiety X [Nudix]-type motif 19) encodes a peroxysomal

nudix hydrolase (Carreras-Puigvert et al., 2017) that exerts a CoA diphosphohydrolase activity in the kidney (Shumar et al., 2018) and its KO mice caused a significant decrease in total CoA levels in the kidney (Shumar et al., 2018). Neuron-specific overexpression of another peroxisomal CoA hydrolase Nudt7 induced reduction in motor coordination (Shumar et al., 2015). *Pop4* (*Rpp29*) encodes ribonuclease P protein subunit P29 that generates mature transfer RNA (tRNA) by cleaving the 5′-leader sequence from the precursor. A recent study showed that Pop4 represses nucleosome deposition of histone H3.3, a regulator of transcription-state change and epigenetic inheritance (Newhart et al., 2016). Although these five DEGs were repeatedly identified in five independent datasets in two BTBR sublines, BTBR/R and BTBR/J, they are not assigned to ASD candidate genes, and their functions may be important for proper development and function of the human brain and thus remain be elucidated.

Altered Spatial Expression Patterns of DEG mRNAs in the BTBR/R Mouse Brain

We mapped mRNA expression of 11 DEGs on BTBR/R mice brains. Three upregulated DEGs (*Serpina3n*, *Lpl*, and *Prune2*) and eight downregulated DEGs (*Pls3*, *Cd276*, *Rpp25*, *Cntnap3*, *Park2*, *Nos1ap*, *Cacnb2*, and *Gatm*) showed similar changing patterns throughout brain regions of BTBR/R and B6 mice. Strikingly, *Serpina3n* was recurrently identified as an upregulated DEG by this BTBR/R study as well as four independent BTBR/J studies, as described above, although it has never been reported as an ASD candidate gene. BTBR/R mice brains showed increased *Serpina3n* mRNA expression: intensely in the cerebral cortex, hippocampus, and amygdala; weakly in the striatum. Together with the transcriptomic data showing the enrichment of the immune signaling pathways in BTBR/R mice DEGs, we suggest that these brain regions in BTBR/R mice may have increased neuroinflammatory responses, as reported in other neurological disorders (Switonski et al., 2015; Vanni et al., 2017; Xi et al., 2019). Upregulated DEG *Lpl* encodes lipoprotein lipase that is the key enzyme in triglyceride metabolism. Highly-increased levels of mRNA expression were remarkable in the cortical layer II/III and striatum of BTBR/R mice compared to B6 mice. LPL activity is critical to regulation of energy balance in the brain (Wang and Eckel, 2012) and is also suggested to play an important role in learning and memory (Xian et al., 2009). Increased expression of *Lpl* in BTBR/R mice brains may cause imbalance of triglyceride-rich plasma lipoproteins, leading to impaired brain function. *Pls3* (*Plastin 3*) encodes an actin binding protein that reduced in a mouse model of spinal muscular atrophy, and its overexpression restored axonal outgrowth of motor neurons in SMA (Alrafiah et al., 2018). *Pls3* mRNA was localized in the cortical layers II/III, V, VIa, VIb, and BLA in B6 mice, but its expression was downregulated in BTBR/R mice, suggesting that BTBR/R mice may have an axonal defect in these regions. *Rpp25* (ribonuclease P and MRP subunit p25) encodes 25 kDa subunit of the ribonuclease P complex and was shown to decrease by about 45% in GABAergic interneurons of the PFC in subjects with ASD (Huang et al., 2010). Importantly, our ISH data also showed a decrease of *Rpp25* mRNA in the mPFC and SSp, probably interneurons, of BTBR/R mice compared to B6 mice, suggesting a possibility that BTBR/R mouse brains may have similar cortical dysfunction to that seen in ASD. Together with *Rpp25*, another key molecule *Pop4* (*Rpp29*) of the ribonuclease P complex is also downregulated in BTBR/R mice as described above, again suggesting a possible defect in tRNA maturation and/or nucleosome formation in these brain regions of BTBR/R mice.

Two BTBR Sublines: BTBR/R vs. BTBR/J

Both sublines BTBR/R and BTBR/J probably originated from the same BTBRTF/Art line and are bred in the RBRC and the Jackson Lab: in this study we conventionally called them BTBR/R and BTBR/J, respectively. We analyzed the brain transcriptome (DEGs, co-expression and interaction RNA networks) of BTBR/R mice and compared them with data reported in the previous studies of human ASD subjects and ASD animal models, including another BTBR subline of BTBR/J mice. There is one previous study showing enhanced turnover of dendritic spines in the anterior frontal cortex of BTBR/R mice similarly to that seen in ASD model mice during the postnatal developmental stage (Isshiki et al., 2014). On the other hand, there has been accumulating information on BTBR/J mice regarding their genetics, neuropathology, and behavior. Many other hallmark symptoms of ASD have been reported in BTBR/J mice, including low sociability (Bolivar et al., 2007; Moy et al., 2007), resistance to change (Moy et al., 2007, 2008), increased repetitive self-grooming behavior (Pobbe et al., 2010), other repetitive behaviors (Pearson et al., 2011), and reduced territorial scent marking (Wöhr et al., 2011). Our behavioral data provide, for the first time, evidence of potential mild but significant deficits in terms of social novelty recognition as well as repetitive behavior in the BTBR/R mouse subline, although further information on detailed behavioral phenotypes of these mice is needed for a comprehensive understanding in this context.

In addition, it is notable that BTBR/J mice have severely reduced hippocampal commissure (HC) and absent corpus callosum (Wahlsten et al., 2003; Dodero et al., 2013; Ellegood et al., 2013; CC). Since in human juveniles and adults with ASD are often reported to have reduced CC volume (Dougherty et al., 2016; Chen et al., 2017; Temur et al., 2019), BTBR/J mice are useful for genetic, anatomical, and behavioral research on the origin and role of the CC and HC. In contrast, the appearances of the CC and HC of BTBR/R mice were normal, although their quantitative examination is required for evaluation of any morphological abnormality. In order to elucidate this striking morphological difference between two BTBR/R and BTBR/J sublines, we researched whether the genes involved in the CC formation (Suárez et al., 2014a) were included within our DEGs. *Wnt8b*, which is one of genes involved in the development of the CC and axonal connections between the left and right sides of the brain (Suárez et al., 2014b), was downregulated in BTBR/R mice brains. FGF signaling is required for the formation of the CC (Smith et al., 2006). Interestingly, *Fgfr1op2*, which encodes the FGFR1 oncogene partner 2 that regulates FGFR1 kinase activity, was commonly downregulated in BTBR/R mice (in the cerebral cortex and striatum, this study) and BTBR/J (in

the cortex and hippocampus, Daimon et al., 2015; and in the cerebellum, Shpyleva et al., 2014). It is yet unclear what genetic alteration(s) generate this drastic morphological change between two sublines and whether the presence and absence of the CC and HC largely impact on their brain function and behavior such as social interaction and repetitive behavior. In other words, BTBR/J mice are a model for ASD subjects completely lacking the CC and HC, while BTBR/R mice may be a model for ASD subjects having intact CC and HC or ones with subtle changes in morphology or neurophysiology. In this study, we found the important similarities and difference between these two BTBR sublines. Further study is needed to clarify these issues.

Our behavioral data indicate potential mild deficits in terms of social novelty recognition and repetitive behavior in BTBR/R mice compared to B6 mice, which is, however, in stark contrast to BTBR/J mice, which are reported to have more severe impairments with regard to autism-related behavior. This also suggests that BTBR/R mice have an autistic-like tendency or susceptibility to autism that may become prominent in BTBR/J mice. Clarifying the differences between the two sublines at the transcriptome level can contribute significantly to understanding the genetics of autism susceptibility.

Transcriptomic Features of Neurotransmitter Systems

Several studies have addressed the involvement of the excitation/inhibition balance in ASD pathologies, especially in the context of dysregulation of glutamatergic and GABAergic neurotransmission systems in ASD patients and models of ASD (Yizhar et al., 2011; Baudouin et al., 2012; Nelson and Valakh, 2015; Horder et al., 2018; Marotta et al., 2020). In previous pharmacological studies, treatment with the mGluR5 antagonist methyl-6-phenylethynyl-pyridine, AMPA receptor positive allosteric modulators, and the GABA-A agonist gaboxadol rescued social deficits or repetitive behavior in BTBR/J mice (Silverman et al., 2012, 2015; Rhine et al., 2019). In our analysis, we highlighted transcriptomic alterations in glutamatergic and GABAergic signaling pathway genes (**Figure 7B**), and the corresponding genes were found to be altered not only in BTBR/R but also BTBR/J mice in several instances (**Supplementary Table 14**). Among the glutamatergic signaling pathway genes, the glutaminase (*Gls*), phospholipase A2 group IVB (*Pla2g4b*), and phospholipase A2 group IVE (*Pla2g4e*) genes were also altered in the hippocampus (Provenzano et al., 2016), dorsal striatum (Oron et al., 2019), and cerebellum (Shpyleva et al., 2014). Of the GABAergic signaling pathway genes, the GABA receptor subunit gamma-2 (*Gabrg2*) and GABA-A receptor subunit alpha2 (*Gabra2*) genes were also altered in the hippocampus (Provenzano et al., 2016), cortex (Daimon et al., 2015), and cerebellum (Shpyleva et al., 2014). In addition, downregulation of *D*-aspartate oxidase (*Ddo*), which is responsible for the degradation of the endogenous NMDA receptor agonist *D*-aspartate, was reported in studies on the hippocampus (Provenzano et al., 2016) and the whole brain (Nuzzo et al., 2020). We also identified some DEGs related to the neurotransmitter signaling pathways for acetylcholine, dopamine, and serotonin, which have also been reported to be involved in ASD (Marotta et al., 2020)—e.g., upregulation of two muscarinic acetylcholine receptors (*Chrm2* and *Chrm3*) and downregulation of the vesicular monoamine transporter 1 (VMAT1, *Slc18a1*), which is predominantly a peripheral VMAT type for neuroendocrine cells. Taken together, there are some difference in the transcriptomic profiles of neurotransmitter signaling pathways, particularly in the glutamatergic and GABAergic signaling pathways that may influence the excitation/inhibition balance, between BTBR/R and B6 mice. The co-expression patterns of these identified DEGs may explain possible differences in corticostriatal neurotransmission systems between BTBR/R and B6 mice, although further studies in this context are warranted.

CONCLUSIONS

In conclusion, we characterized the transcriptomic features of the cerebral cortex and striatum of BTBR/R mice in comparison with B6 mice, using microarray, qRT-PCR, and ISH analyses together with comprehensive bioinformatics approaches. We identified DEGs (upregulated and downregulated) and co-expression as well as interaction RNA networks in BTBR/R mice brains. In addition, the BTBR/R mice data were comprehensively compared to those reported in the previous studies of subjects with ASD as well as ASD animal models, including BTBR/J mice. Our results allow us to propose potentially important genes and ncRNAs that may be associated with brain function and behaviors characteristic to BTBR/R mice that are indicative of an autistic-like phenotype. To contribute further to the understanding of ASD genetics and biology, further studies regarding detailed cellular expression patterns as well as functional aspects of the DEGs in BTBR/R mice brain are required, considering the differences and/or similarities with socially impaired BTBR/J mice and highly social B6 mice.

DATA AVAILABILITY STATEMENT

The datasets generated for this study are available in the NCBI GEO repository under accession numbers GSE156646 and GSM4735682-4735689.

ETHICS STATEMENT

The animal study was reviewed and approved by Animal Experimentation Committee at The University of Tokyo and Tokyo University of Science.

AUTHOR CONTRIBUTIONS

SM designed and performed the experiments, analyzed the data, and wrote the paper. J-nH performed the experiments and wrote the paper. CI performed the experiments and provided funding. HI provided funding. YS and TF conceived the study, provided

funding, and wrote the paper. All authors contributed to the article and approved the submitted version.

FUNDING

This work was supported by a Grant-in-Aid for KAKENHI (19J12771, 17H03563, 17K19638, 26290026, 15K14356, 15K21013, and 18K06499) from Japan Society for the Promotion of Science and the Ministry of Education, Culture, Sports, Science and Technology of Japan, the Novartis Research Grant from the NOVARTIS Foundation (Japan) for the Promotion of Science, and by the Takeda Science Foundation and The Uehara Memorial Foundation.

ACKNOWLEDGMENTS

We thank Dr. Shigeo Okabe for providing BTBRTF/ArtRbrc mice and Mr. Sota Shinozaki, Yosuke Narumi, and Kaiyo Kitakoshi for their technical support of ISH analysis. The BTBRTF/ArtRbrc (RBRC 01206) mice were provided by RBRC through the National Bio-Resource Project of the MEXT, Japan.

SUPPLEMENTARY MATERIAL

The Supplementary Material for this article can be found online at: https://www.frontiersin.org/articles/10.3389/fncel.2020.595607/full#supplementary-material

REFERENCES

Abbott, A. E., Linke, A. C., Nair, A., Jahedi, A., Alba, L. A., Keown, C. L., et al. (2018). Repetitive behaviors in autism are linked to imbalance of corticostriatal connectivity: a functional connectivity MRI study. *Soc. Cogn. Affect. Neurosci.* 13, 32–42. doi: 10.1093/scan/nsx129

Alrafiah, A., Karyka, E., Coldicott, I., Iremonger, K., Lewis, K. E., Ning, K., et al. (2018). Plastin 3 promotes motor neuron axonal growth and extends survival in a mouse model of spinal muscular atrophy. molecular therapy. *Methods Clin. Dev.* 9, 81–89. doi: 10.1016/j.omtm.2018.01.007

American Psychiatric Association (2013). *Diagnostic and Statistical Manual of Mental Disorders, 5th Edn*. Washington, DC: American Psychiatric Association. doi: 10.1176/appi.books.9780890425596

Ashburner, M., Ball, C. A., Blake, J. A., Botstein, D., Butler, H., Cherry, J. M., et al. (2000). Gene ontology: tool for the unification of biology. The gene ontology consortium. *Nat. Genet.* 25, 25–29. doi: 10.1038/75556

Bartolomucci, A., Possenti, R., Mahata, S. K., Fischer-Colbrie, R., Loh, Y. P., and Salton, S. R. (2011). The extended granin family: structure, function, and biomedical implications. *Endocr. Rev.* 32, 755–797. doi: 10.1210/er.2010-0027

Baudouin, S. J., Gaudias, J., Gerharz, S., Hatstatt, L., Zhou, K., Punnakkal, P., et al. (2012). Shared synaptic pathophysiology in syndromic and nonsyndromic rodent models of autism. *Science* 338, 128–132. doi: 10.1126/science.1224159

Benjamini, Y., and Hochberg, Y. (1995). Controlling the false discovery rate: a practical and powerful approach to multiple testing. *J. R Stat. Soc.* 57, 289–300. doi: 10.1111/j.2517-6161.1995.tb02031.x

Bolivar, V. J., Walters, S. R., and Phoenix, J. L. (2007). Assessing autism-like behavior in mice: variations in social interactions among inbred strains. *Behav. Brain Res.* 176, 21–26. doi: 10.1016/j.bbr.2006.09.007

Braat, S., and Kooy, R. F. (2015). The GABAA receptor as a therapeutic target for neurodevelopmental disorders. *Neuron* 86, 1119–1130. doi: 10.1016/j.neuron.2015.03.042

Bult, C. J., Blake, J. A., Smith, C. L., Kadin, J. A., Richardson, J. E., and Mouse Genome Database Group (2019). Mouse genome database (MGD) 2019. *Nucleic Acids Res.* 47, D801–D806. doi: 10.1093/nar/gky1056

Carreras-Puigvert, J., Zitnik, M., Jemth, A. S., Carter, M., Unterlass, J. E., Hallström, B., et al. (2017). A comprehensive structural, biochemical and biological profiling of the human NUDIX hydrolase family. *Nat. Commun.* 8:1541. doi: 10.1038/s41467-017-01642-w

Chaste, P., and Leboyer, M. (2012). Autism risk factors: genes, environment, and gene-environment interactions. *Dialogues Clin. Neurosci.* 14, 281–292. doi: 10.31887/DCNS.2012.14.3/pchaste

Chen, C., Van Horn, J. D., and GENDAAR Research Consortium (2017). Developmental neurogenetics and multimodal neuroimaging of sex differences in autism. *Brain Imaging Behav.* 11, 38–61. doi: 10.1007/s11682-015-9504-3

Chen, Z., Bu, N., Qiao, X., Zuo, Z., Shu, Y., Liu, Z., et al. (2018). Forkhead box M1 transcriptionally regulates the expression of long noncoding RNAs Snhg8 and Gm26917 to promote proliferation and survival of muscle satellite cells. *Stem Cells* 36, 1097–1108. doi: 10.1002/stem.2824

Cheng, Y., Wang, Z. M., Tan, W., Wang, X., Li, Y., Bai, B., et al. (2018). Partial loss of psychiatric risk gene Mir137 in mice causes repetitive behavior and impairs sociability and learning via increased Pde10a. *Nat. Neurosci.* 21, 1689–1703. doi: 10.1038/s41593-018-0261-7

Chu, Y. D., Lai, H. Y., Pai, L. M., Huang, Y. H., Lin, Y. H., Liang, K. H., et al. (2019). The methionine salvage pathway-involving ADI1 inhibits hepatoma growth by epigenetically altering genes expression via elevating S-adenosylmethionine. *Cell Death Dis.* 10:240. doi: 10.1038/s41419-019-1486-4

Cisternas, F. A., Vincent, J. B., Scherer, S. W., and Ray, P. N. (2003). Cloning and characterization of human CADPS and CADPS2, new members of the Ca2+-dependent activator for secretion protein family. *Genomics* 81, 279–291. doi: 10.1016/S0888-7543(02)00040-X

Clee, S. M., Nadler, S. T., and Attie, A. D. (2005). Genetic and genomic studies of the BTBR ob/ob mouse model of type 2 diabetes. *Am. J. Ther.* 12, 491–498. doi: 10.1097/01.mjt.0000178781.89789.25

Daimon, C. M., Jasien, J. M., Wood, W. H., 3rd, Zhang, Y., Becker, K. G., Silverman, J. L., et al. (2015). Hippocampal transcriptomic and proteomic alterations in the BTBR mouse model of autism spectrum disorder. *Front. Physiol.* 6:324. doi: 10.3389/fphys.2015.00324

de la Torre-Ubieta, L., Won, H., Stein, J. L., and Geschwind, D. H. (2016). Advancing the understanding of autism disease mechanisms through genetics. *Nat. Med.* 22, 345–361. doi: 10.1038/nm.4071

Defensor, E. B., Pearson, B. L., Pobbe, R. L., Bolivar, V. J., Blanchard, D. C., and Blanchard, R. J. (2011). A novel social proximity test suggests patterns of social avoidance and gaze aversion-like behavior in BTBR T+ tf/J mice. *Behav. Brain Res.* 217, 302–308. doi: 10.1016/j.bbr.2010.10.033

Devlin, B., and Scherer, S. W. (2012). Genetic architecture in autism spectrum disorder. *Curr. Opin. Genet. Dev.* 22, 229–237. doi: 10.1016/j.gde.2012.03.002

Diaz-Beltran, L., Esteban, F. J., and Wall, D. P. (2016). A common molecular signature in ASD gene expression: following Root 66 to autism. *Transl. Psychiatry* 6:e705. doi: 10.1038/tp.2015.112

Dodero, L., Damiano, M., Galbusera, A., Bifone, A., Tsaftsaris, S. A., Scattoni, M. L., et al. (2013). Neuroimaging evidence of major morpho-anatomical and functional abnormalities in the BTBR T+TF/J mouse model of autism. *PLoS ONE* 8:e76655. doi: 10.1371/journal.pone.0076655

Dougherty, C. C., Evans, D. W., Myers, S. M., Moore, G. J., and Michael, A. M. (2016). A comparison of structural brain imaging findings in autism spectrum disorder and attention-deficit hyperactivity disorder. *Neuropsychol. Rev.* 26, 25–43. doi: 10.1007/s11065-015-9300-2

Ehninger, D., Sano, Y., de Vries, P. J., Dies, K., Franz, D., Geschwind, D. H., et al. (2012). Gestational immune activation and Tsc2 haploinsufficiency cooperate to disrupt fetal survival and may perturb social behavior in adult mice. *Mol. Psychiatry* 17, 62–70. doi: 10.1038/mp.2010.115

Ellegood, J., Babineau, B. A., Henkelman, R. M., Lerch, J. P., and Crawley, J. N. (2013). Neuroanatomical analysis of the BTBR mouse model of autism using magnetic resonance imaging and diffusion tensor imaging. *Neuroimage* 70, 288–300. doi: 10.1016/j.neuroimage.2012.12.029

Estes, M. L., and McAllister, A. K. (2015). Immune mediators in the brain and peripheral tissues in autism spectrum disorder. *Nat. Rev. Neurosci.* 16, 469–486. doi: 10.1038/nrn3978

Faundes, V., Newman, W. G., Bernardini, L., Canham, N., Clayton-Smith, J., Dallapiccola, B., et al. (2018). Histone lysine methylases and demethylases in the landscape of human developmental disorders. *Am. J. Hum. Genet.* 102, 175–187. doi: 10.1016/j.ajhg.2017.11.013

Feng, J., Chi, P., Blanpied, T. A., Xu, Y., Magarinos, A. M., Ferreira, A., et al. (2002). Regulation of neurotransmitter release by synapsin III. *J. Neurosci.* 22, 4372–4380. doi: 10.1523/JNEUROSCI.22-11-04372.2002

Fueyo, R., García, M. A., and Martínez-Balbás, M. A. (2015). Jumonji family histone demethylases in neural development. *Cell Tissue Res.* 359, 87–98. doi: 10.1007/s00441-014-1924-7

Gallagher, D., Voronova, A., Zander, M. A., Cancino, G. I., Bramall, A., Krause, M. P., et al. (2015). Ankrd11 is a chromatin regulator involved in autism that is essential for neural development. *Dev. Cell* 32, 31–42. doi: 10.1016/j.devcel.2014.11.031

Gandal, M. J., Zhang, P., Hadjimichael, E., Walker, R. L., Chen, C., Liu, S., et al. (2018). Transcriptome-wide isoform-level dysregulation in ASD, schizophrenia, and bipolar disorder. *Science* 362:eaat8127. doi: 10.1126/science.aat8127

Gasparini, S., Del Vecchio, G., Gioiosa, S., Flati, T., Castrignano, T., Legnini, I., et al. (2020). Differential expression of hippocampal circular RNAs in the BTBR mouse model for autism spectrum disorder. *Mol. Neurobiol.* 57, 2301–2313. doi: 10.1007/s12035-020-01878-6

Gładysz, D., Krzywdzińska, A., and Hozyasz, K. K. (2018). Immune abnormalities in autism spectrum disorder-could they hold promise for causative treatment? *Mol. Neurobiol.* 55, 6387–6435. doi: 10.1007/s12035-017-0822-x

Gottfried, C., Bambini-Junior, V., Francis, F., Riesgo, R., and Savino, W. (2015). The impact of neuroimmune alterations in autism spectrum disorder. *Front. Psychiatry* 6:121. doi: 10.3389/fpsyt.2015.00121

Greenblatt, E. J., and Spradling, A. C. (2018). Fragile X mental retardation 1 gene enhances the translation of large autism-related proteins. *Science* 361, 709–712. doi: 10.1126/science.aas9963

Gupta, S., Ellis, S. E., Ashar, F. N., Moes, A., Bader, J. S., Zhan, J., et al. (2014). Transcriptome analysis reveals dysregulation of innate immune response genes and neuronal activity-dependent genes in autism. *Nat. Commun.* 5:5748. doi: 10.1038/ncomms6748

Horder, J., Petrinovic, M. M., Mendez, M. A., Bruns, A., Takumi, T., Spooren, W., et al. (2018). Glutamate and GABA in autism spectrum disorder-a translational magnetic resonance spectroscopy study in man and rodent models. *Transl. Psychiatry* 8:106. doi: 10.1038/s41398-018-0155-1

Huang, D. W., Sherman, B. T., and Lempicki, R. A. (2009a). Systematic and integrative analysis of large gene lists using DAVID bioinformatics resources. *Nat. Protoc.* 4, 44–57. doi: 10.1038/nprot.2008.211

Huang, D. W., Sherman, B. T., and Lempicki, R. A. (2009b). Bioinformatics enrichment tools: paths toward the comprehensive functional analysis of large gene lists. *Nucleic Acids Res.* 37, 1–13. doi: 10.1093/nar/gkn923

Huang, H. S., Cheung, I., and Akbarian, S. (2010). RPP25 is developmentally regulated in prefrontal cortex and expressed at decreased levels in autism spectrum disorder. *Autism Res.* 3, 153–161. doi: 10.1002/aur.141

Ignatov, D., Vaitkevicius, K., Durand, S., Cahoon, L., Sandberg, S. S., Liu, X., et al. (2020). An mRNA-mRNA interaction couples expression of a virulence factor and its chaperone in listeria monocytogenes. *Cell Rep.* 30, 4027–4040.e7. doi: 10.1016/j.celrep.2020.03.006

Iossifov, I., O'Roak, B. J., Sanders, S. J., Ronemus, M., Krumm, N., Levy, D., et al. (2014). The contribution of de novo coding mutations to autism spectrum disorder. *Nature* 515, 216–221. doi: 10.1038/nature13908

Isshiki, M., Tanaka, S., Kuriu, T., Tabuchi, K., Takumi, T., and Okabe, S. (2014). Enhanced synapse remodelling as a common phenotype in mouse models of autism. *Nat. Commun.* 5:4742. doi: 10.1038/ncomms5742

Jasien, J. M., Daimon, C. M., Wang, R., Shapiro, B. K., Martin, B., and Maudsley, S. (2014). The effects of aging on the BTBR mouse model of autism spectrum disorder. *Front. Aging Neurosci.* 6:225. doi: 10.3389/fnagi.2014.00225

Kanehisa, M., Furumichi, M., Tanabe, M., Sato, Y., and Morishima, K. (2017). KEGG: new perspectives on genomes, pathways, diseases and drugs. *Nucleic Acids Res.* 45, D353–D361. doi: 10.1093/nar/gkw1092

Kim, K., Heo, D. H., Kim, I., Suh, J. Y., and Kim, M. (2016). Exosome cofactors connect transcription termination to RNA processing by guiding terminated transcripts to the appropriate exonuclease within the nuclear exosome. *J. Biol. Chem.* 291, 13229–13242. doi: 10.1074/jbc.M116.715771

Kratsman, N., Getselter, D., and Elliott, E. (2016). Sodium butyrate attenuates social behavior deficits and modifies the transcription of inhibitory/excitatory genes in the frontal cortex of an autism model. *Neuropharmacology* 102, 136–145. doi: 10.1016/j.neuropharm.2015.11.003

Krumm, N., Turner, T. N., Baker, C., Vives, L., Mohajeri, K., Witherspoon, K., et al. (2015). Excess of rare, inherited truncating mutations in autism. *Nat. Genet.* 47, 582–588. doi: 10.1038/ng.3303

Langfelder, P., and Horvath, S. (2008). WGCNA: an R package for weighted correlation network analysis. *BMC Bioinformatics* 9:559. doi: 10.1186/1471-2105-9-559

Li, J. H., Liu, S., Zhou, H., Qu, L. H., and Yang, J. H. (2014). starBase v2.0: decoding miRNA-ceRNA, miRNA-ncRNA and protein-RNA interaction networks from large-scale CLIP-Seq data. *Nucleic Acids Res.* 42, D92–D97. doi: 10.1093/nar/gkt1248

Lombardo, M. V., Moon, H. M., Su, J., Palmer, T. D., Courchesne, E., and Pramparo, T. (2018). Maternal immune activation dysregulation of the fetal brain transcriptome and relevance to the pathophysiology of autism spectrum disorder. *Mol. Psychiatry* 23, 1001–1013. doi: 10.1038/mp.2017.15

Marotta, R., Risoleo, M. C., Messina, G., Parisi, L., Carotenuto, M., Vetri, L., et al. (2020). The neurochemistry of autism. *Brain Sci.* 10:163. doi: 10.3390/brainsci10030163

Masachis, S., and Darfeuille, F. (2018). Type I toxin-antitoxin systems: regulating toxin expression via shine-dalgarno sequence sequestration and small RNA binding. *Microbiol. Spectr.* 6, 1–18. doi: 10.1128/microbiolspec.RWR-0030-2018

McFarlane, H. G., Kusek, G. K., Yang, M., Phoenix, J. L., Bolivar, V. J., and Crawley, J. N. (2008). Autism-like behavioral phenotypes in BTBR T+tf/J mice. *Genes Brain Behav.* 7, 152–163. doi: 10.1111/j.1601-183X.2007.00330.x

Moy, S. S., Nadler, J. J., Poe, M. D., Nonneman, R. J., Young, N. B., Koller, B. H., et al. (2008). Development of a mouse test for repetitive, restricted behaviors: relevance to autism. *Behav. Brain Res.* 188, 178–194. doi: 10.1016/j.bbr.2007.10.029

Moy, S. S., Nadler, J. J., Young, N. B., Perez, A., Holloway, L. P., Barbaro, R. P., et al. (2007). Mouse behavioral tasks relevant to autism: phenotypes of 10 inbred strains. *Behav. Brain Res.* 176, 4–20. doi: 10.1016/j.bbr.2006.07.030

Neale, B. M., Kou, Y., Liu, L., Ma'ayan, A., Samocha, K. E., Sabo, A., et al. (2012). Patterns and rates of exonic de novo mutations in autism spectrum disorders. *Nature* 485, 242–245. doi: 10.1038/nature11011

Nelson, S. B., and Valakh, V. (2015). Excitatory/inhibitory balance and circuit homeostasis in autism spectrum disorders. *Neuron* 87, 684–698. doi: 10.1016/j.neuron.2015.07.033

Newhart, A., Powers, S. L., Shastrula, P. K., Sierra, I., Joo, L. M., Hayden, J. E., et al. (2016). RNase P protein subunit Rpp29 represses histone H3.3 nucleosome deposition. *Mol. Biol. Cell* 27, 1154–1169. doi: 10.1091/mbc.E15-02-0099

Noroozi, R., Taheri, M., Movafagh, A., Mirfakhraie, R., Solgi, G., Sayad, A., et al. (2016). Glutamate receptor, metabotropic 7 (GRM7) gene variations and susceptibility to autism: a case-control study. *Autism Res.* 9, 1161–1168. doi: 10.1002/aur.1640

Nuzzo, T., Sekine, M., Punzo, D., Miroballo, M., Katane, M., Saitoh, Y., et al. (2020). Dysfunctional d-aspartate metabolism in BTBR mouse model of idiopathic autism. *Biochim. Biophys. Acta Proteins Proteom.* 1868:140531. doi: 10.1016/j.bbapap.2020.140531

O'Leary, N. A., Wright, M. W., Brister, J. R., Ciufo, S., Haddad, D., McVeigh, R., et al. (2016). Reference sequence (RefSeq) database at NCBI: current status, taxonomic expansion, and functional annotation. *Nucleic Acids Res.* 44, D733–D745. doi: 10.1093/nar/gkv1189

Oron, O., Getselter, D., Shohat, S., Reuveni, E., Lukic, I., Shifman, S., et al. (2019). Gene network analysis reveals a role for striatal glutamatergic receptors in dysregulated risk-assessment behavior of autism mouse models. *Transl. Psychiatry* 9:257. doi: 10.1038/s41398-019-0584-5

Oskvig, D. B., Elkahloun, A. G., Johnson, K. R., Phillips, T. M., and Herkenham, M. (2012). Maternal immune activation by LPS selectively alters specific gene expression profiles of interneuron migration and oxidative stress in the fetus

without triggering a fetal immune response. *Brain Behav. Immun.* 26, 623–634. doi: 10.1016/j.bbi.2012.01.015

Pearson, B. L., Pobbe, R. L., Defensor, E. B., Oasay, L., Bolivar, V. J., Blanchard, D. C., et al. (2011). Motor and cognitive stereotypies in the BTBR T+tf/J mouse model of autism. *Genes Brain Behav.* 10, 228–235. doi: 10.1111/j.1601-183X.2010.00659.x

Pereanu, W., Larsen, E. C., Das, I., Estévez, M. A., Sarkar, A. A., et al. (2018). AutDB: a platform to decode the genetic architecture of autism. *Nucleic Acids Res.* 46, D1049–D1054. doi: 10.1093/nar/gkx 1093

Petersen, A. K., Ahmad, A., Shafiq, M., Brown-Kipphut, B., Fong, C. T., and Anwar Iqbal, M. (2013). Deletion 1q43 encompassing only CHRM3 in a patient with autistic disorder. *Eur. J. Med. Genet.* 56, 118–122. doi: 10.1016/j.ejmg.2012.11.003

Pobbe, R. L., Pearson, B. L., Defensor, E. B., Bolivar, V. J., Blanchard, D. C., and Blanchard, R. J. (2010). Expression of social behaviors of C57BL/6J versus BTBR inbred mouse strains in the visible burrow system. *Behav. Brain Res.* 214, 443–449. doi: 10.1016/j.bbr.2010.06.025

Provenzano, G., Corradi, Z., Monsorno, K., Fedrizzi, T., Ricceri, L., Scattoni, M. L., et al. (2016). Comparative gene expression analysis of two mouse models of autism: transcriptome profiling of the BTBR and En2 (-/-) hippocampus. *Front. Neurosci.* 10:396. doi: 10.3389/fnins.2016.00396

Rhine, M. A., Parrott, J. M., Schultz, M. N., Kazdoba, T. M., and Crawley, J. N. (2019). Hypothesis-driven investigations of diverse pharmacological targets in two mouse models of autism. *Autism Res.* 12, 401–421. doi: 10.1002/aur.2066

Ruiz de los Mozos, I., Vergara-Irigaray, M., Segura, V., Villanueva, M., Bitarte, N., Saramago, M., et al. (2013). Base pairing interaction between 5'- and 3'-UTRs controls icaR mRNA translation in Staphylococcus aureus. *PLoS Genet.* 9:e1004001. doi: 10.1371/journal.pgen.1004001

Ruzzo, E. K., Pérez-Cano, L., Jung, J. Y., Wang, L. K., Kashef-Haghighi, D., Hartl, C., et al. (2019). Inherited and *de novo* genetic risk for autism impacts shared networks. *Cell* 178, 850–866.e26. doi: 10.1016/j.cell.2019.07.015

Sadakata, T., Shinoda, Y., Oka, M., Sekine, Y., Sato, Y., Saruta, C., et al. (2012). Reduced axonal localization of a Caps2 splice variant impairs axonal release of BDNF and causes autistic-like behavior in mice. *Proc. Natl. Acad. Sci. U.S.A.* 109, 21104–21109. doi: 10.1073/pnas.1210055109

Sadakata, T., Washida, M., Iwayama, Y., Shoji, S., Sato, Y., Ohkura, T., et al. (2007). Autistic-like phenotypes in Cadps2-knockout mice and aberrant CADPS2 splicing in autistic patients. *J. Clin. Invest.* 117, 931–943. doi: 10.1172/JCI29031

Saitoh, Y., Kamijo, A., Yamauchi, J., Sakamoto, T., and Terada, N. (2019). The membrane palmitoylated protein, MPP6, is involved in myelin formation in the mouse peripheral nervous system. *Histochem. Cell Biol.* 151, 385–394. doi: 10.1007/s00418-018-1745-y

Sano, Y., Shobe, J. L., Zhou, M., Huang, S., Shuman, T., Cai, D. J., et al. (2014). CREB regulates memory allocation in the insular cortex. *Curr. Biol.* 24, 2833–2837. doi: 10.1016/j.cub.2014.10.018

Satterstrom, F. K., Kosmicki, J. A., Wang, J., Breen, M. S., De Rubeis, S., An, J. Y., et al. (2020). Large-scale exome sequencing study implicates both developmental and functional changes in the neurobiology of autism. *Cell* 180, 568–584.e23. doi: 10.1016/j.cell.2019.12.036

Sayers, E. W., Beck, J., Brister, J. R., Bolton, E. E., Canese, K., Comeau, D. C., et al. (2020b). Database resources of the national center for biotechnology information. *Nucleic Acids Res.* 48, D9–D16. doi: 10.1093/nar/gkz899

Sayers, E. W., Cavanaugh, M., Clark, K., Ostell, J., Pruitt, K. D., and Karsch-Mizrachi, I. (2020a). GenBank. *Nucleic Acids Res.* 48, D84–D86. doi: 10.1093/nar/gkz956

Scattoni, M. L., Martire, A., Cartocci, G., Ferrante, A., and Ricceri, L. (2013). Reduced social interaction, behavioural flexibility and BDNF signalling in the BTBR T+ tf/J strain, a mouse model of autism. *Behav. Brain Res.* 251, 35–40. doi: 10.1016/j.bbr.2012.12.028

Scattoni, M. L., Ricceri, L., and Crawley, J. N. (2011). Unusual repertoire of vocalizations in adult BTBR T+tf/J mice during three types of social encounters. *Genes Brain Behav.* 10, 44–56. doi: 10.1111/j.1601-183X.2010.00623.x

Schmitz, S. U., Albert, M., Malatesta, M., Morey, L., Johansen, J. V., Bak, M., et al. (2011). Jarid1b targets genes regulating development and is involved in neural differentiation. *EMBO J.* 30, 4586–4600. doi: 10.1038/emboj.2011.383

Shpyleva, S., Ivanovsky, S., de Conti, A., Melnyk, S., Tryndyak, V., Beland, F. A., et al. (2014). Cerebellar oxidative DNA damage and altered DNA methylation in the BTBR T+tf/J mouse model of autism and similarities with human post mortem cerebellum. *PLoS ONE* 9:e113712. doi: 10.1371/journal.pone.0113712

Shumar, S. A., Fagone, P., Alfonso-Pecchio, A., Gray, J. T., Rehg, J. E., Jackowski, S., et al. (2015). Induction of neuron-specific degradation of coenzyme a models pantothenate kinase-associated neurodegeneration by reducing motor coordination in mice. *PLoS ONE* 10:e0130013. doi: 10.1371/journal.pone.0130013

Shumar, S. A., Kerr, E. W., Geldenhuys, W. J., Montgomery, G. E., Fagone, P., Thirawatananond, P., et al. (2018). Nudt19 is a renal CoA diphosphohydrolase with biochemical and regulatory properties that are distinct from the hepatic Nudt7 isoform. *J. Biol. Chem.* 293, 4134–4148. doi: 10.1074/jbc.RA117.001358

Silverman, J. L., Pride, M. C., Hayes, J. E., Puhger, K. R., Butler-Struben, H. M., Baker, S., et al. (2015). GABAB receptor agonist R-baclofen reverses social deficits and reduces repetitive behavior in two mouse models of autism. *Neuropsychopharmacology* 40, 2228–2239. doi: 10.1038/npp.2015.66

Silverman, J. L., Smith, D. G., Rizzo, S. J., Karras, M. N., Turner, S. M., Tolu, S. S., et al. (2012). Negative allosteric modulation of the mGluR5 receptor reduces repetitive behaviors and rescues social deficits in mouse models of autism. *Sci. Transl. Med.* 4:131ra51. doi: 10.1126/scitranslmed.3003501

Smith, K. M., Ohkubo, Y., Maragnoli, M. E., Rasin, M. R., Schwartz, M. L., Sestan, N., et al. (2006). Midline radial glia translocation and corpus callosum formation require FGF signaling. *Nat. Neurosci.* 9, 787–797. doi: 10.1038/nn1705

Suárez, R., Fenlon, L. R., Marek, R., Avitan, L., Sah, P., Goodhill, G. J., et al. (2014a). Balanced interhemispheric cortical activity is required for correct targeting of the corpus callosum. *Neuron* 82, 1289–1298. doi: 10.1016/j.neuron.2014.04.040

Suárez, R., Gobius, I., and Richards, L. J. (2014b). Evolution and development of interhemispheric connections in the vertebrate forebrain. *Front. Hum. Neurosci.* 8:497. doi: 10.3389/fnhum.2014.00497

Suetterlin, P., Hurley, S., Mohan, C., Riegman, K., Pagani, M., Caruso, A., et al. (2018). Altered neocortical gene expression, brain overgrowth and functional over-connectivity in Chd8 haploinsufficient mice. *Cereb. Cortex* 28, 2192–2206. doi: 10.1093/cercor/bhy058

Switonski, P. M., Szlachcic, W. J., Krzyzosiak, W. J., and Figiel, M. (2015). A new humanized ataxin-3 knock-in mouse model combines the genetic features, pathogenesis of neurons and glia and late disease onset of SCA3/MJD. *Neurobiol. Dis.* 73, 174–188. doi: 10.1016/j.nbd.2014.09.020

Takata, A., Ionita-Laza, I., Gogos, J. A., Xu, B., and Karayiorgou, M. (2016). *De novo* synonymous mutations in regulatory elements contribute to the genetic etiology of autism and schizophrenia. *Neuron* 89, 940–947. doi: 10.1016/j.neuron.2016.02.024

Tan, S., Guo, J., Huang, Q., Chen, X., Li-Ling, J., Li, Q., et al. (2007). Retained introns increase putative microRNA targets within 3' UTRs of human mRNA. *FEBS Lett.* 581, 1081–1086. doi: 10.1016/j.febslet.2007.02.009

Temur, H. O., Yurtsever, I., Yesil, G., Sharifov, R., Yilmaz, F. T., Dundar, T. T., et al. (2019). Correlation between DTI findings and volume of corpus callosum in children with AUTISM. *Curr. Med. Imaging Rev.* 15, 895–899. doi: 10.2174/1573405614666181005114315

The Gene Ontology Consortium (2019). The gene ontology resource: 20 years and still going strong. *Nucleic Acids Res.* 47, D330–D338. doi: 10.1093/nar/gky1055

Tokita, M. J., Chen, C. A., Chitayat, D., Macnamara, E., Rosenfeld, J. A., Hanchard, N., et al. (2018). *De novo* missense variants in TRAF7 cause developmental delay, congenital anomalies, and dysmorphic features. *Am. J. Hum. Genet.* 103, 154–162. doi: 10.1016/j.ajhg.2018.06.005

Vanni, S., Moda, F., Zattoni, M., Bistaffa, E., De Cecco, E., Rossi, M., et al. (2017). Differential overexpression of SERPINA3 in human prion diseases. *Sci. Rep.* 7:15637. doi: 10.1038/s41598-017-15778-8

Voineagu, I., Wang, X., Johnston, P., Lowe, J. K., Tian, Y., Horvath, S., et al. (2011). Transcriptomic analysis of autistic brain reveals convergent molecular pathology. *Nature* 474, 380–384. doi: 10.1038/nature10110

Wahlsten, D., Metten, P., and Crabbe, J. C. (2003). Survey of 21 inbred mouse strains in two laboratories reveals that BTBR T/+ tf/tf has severely reduced hippocampal commissure and absent corpus callosum. *Brain Res.* 971, 47–54. doi: 10.1016/S0006-8993(03)02354-0

Wamsley, B., Jaglin, X. H., Favuzzi, E., Quattrocolo, G., Nigro, M. J., Yusuf, N., et al. (2018). Rbfox1 mediates cell-type-specific splicing in cortical interneurons. *Neuron* 100, 846–859.e7. doi: 10.1016/j.neuron.2018.09.026

Wang, H., and Eckel, R. H. (2012). Lipoprotein lipase in the brain and nervous system. *Annu. Rev. Nutr.* 32, 147–160. doi: 10.1146/annurev-nutr-071811-150703

Wang, X., Bey, A. L., Katz, B. M., Badea, A., Kim, N., David, L. K., et al. (2016). Altered mGluR5-homer scaffolds and corticostriatal connectivity in a Shank3 complete knockout model of autism. *Nat. Commun.* 7:11459. doi: 10.1038/ncomms11459

Wei, H., Ma, Y., Liu, J., Ding, C., Hu, F., and Yu, L. (2016). Proteomic analysis of cortical brain tissue from the BTBR mouse model of autism: evidence for changes in STOP and myelin-related proteins. *Neuroscience* 312, 26–34. doi: 10.1016/j.neuroscience.2015.11.003

Wilming, L. G., Gilbert, J. G., Howe, K., Trevanion, S., Hubbard, T., and Harrow, J. L. (2008). The vertebrate genome annotation (Vega) database. *Nucleic Acids Res.* 36, D753–D760. doi: 10.1093/nar/gkm987

Wöhr, M., Roullet, F. I., and Crawley, J. N. (2011). Reduced scent marking and ultrasonic vocalizations in the BTBR T+tf/J mouse model of autism. *Genes Brain Behav.* 10, 35–43. doi: 10.1111/j.1601-183X.2010.00582.x

Wu, J. I., Centilli, M. A., Vasquez, G., Young, S., Scolnick, J., Durfee, L. A., et al. (2007). Tint maps to mouse chromosome 6 and may interact with a notochordal enhancer of Brachyury. *Genetics* 177, 1151–1161. doi: 10.1534/genetics.107.079715

Xi, Y., Liu, M., Xu, S., Hong, H., Chen, M., Tian, L., et al. (2019). Inhibition of SERPINA3N-dependent neuroinflammation is essential for melatonin to ameliorate trimethyltin chloride-induced neurotoxicity. *J. Pineal Res.* 67:e12596. doi: 10.1111/jpi.12596

Xian, X., Liu, T., Yu, J., Wang, Y., Miao, Y., Zhang, J., et al. (2009). Presynaptic defects underlying impaired learning and memory function in lipoprotein lipase-deficient mice. *J. Neurosci.* 29, 4681–4685. doi: 10.1523/JNEUROSCI.0297-09.2009

Xu, G., Strathearn, L., Liu, B., and Bao, W. (2018). Corrected prevalence of autism spectrum disorder among US children and adolescents. *JAMA* 319:505. doi: 10.1001/jama.2018.0001

Yates, A. D., Achuthan, P., Akanni, W., Allen, J., Allen, J., Alvarez-Jarreta, J., et al. (2020). Ensembl 2020. *Nucleic Acids Res.* 48, D682–D688. doi: 10.1093/nar/gkz966

Yizhar, O., Fenno, L. E., Prigge, M., Schneider, F., Davidson, T. J., O'Shea, D. J., et al. (2011). Neocortical excitation/inhibition balance in information processing and social dysfunction. *Nature* 477, 171–178. doi: 10.1038/nature10360

Zhang, B., and Horvath, S. (2005). A general framework for weighted gene co-expression network analysis. *Stat. Appl. Genet. Mol. Biol.* 4:17. doi: 10.2202/1544-6115.1128

Zhang, S. F., Gao, J., and Liu, C. M. (2019). The role of non-coding RNAs in neurodevelopmental disorders. *Front. Genet.* 10:1033. doi: 10.3389/fgene.2019.01033

Zhang, X., Chen, M. H., Wu, X., Kodani, A., Fan, J., Doan, R., et al. (2016). Cell-type-specific alternative splicing governs cell fate in the developing cerebral cortex. *Cell* 166, 1147–1162.e15. doi: 10.1016/j.cell.2016.07.025

Zotti, T., Scudiero, I., Vito, P., and Stilo, R. (2017). The emerging role of TRAF7 in tumor development. *J. Cell. Physiol.* 232, 1233–1238. doi: 10.1002/jcp.25676

Conflict of Interest: The authors declare that the research was conducted in the absence of any commercial or financial relationships that could be construed as a potential conflict of interest.

frontiers in Cellular Neuroscience

HYPOTHESIS AND THEORY
published: 18 December 2020
doi: 10.3389/fncel.2020.577525

The Parvalbumin Hypothesis of Autism Spectrum Disorder

*Federica Filice, Lucia Janickova, Thomas Henzi, Alessandro Bilella and Beat Schwaller**

Section of Medicine, Anatomy, University of Fribourg, Fribourg, Switzerland

The prevalence of autism spectrum disorder (ASD)—a type of neurodevelopmental disorder—is increasing and is around 2% in North America, Asia, and Europe. Besides the known genetic link, environmental, epigenetic, and metabolic factors have been implicated in ASD etiology. Although highly heterogeneous at the behavioral level, ASD comprises a set of core symptoms including impaired communication and social interaction skills as well as stereotyped and repetitive behaviors. This has led to the suggestion that a large part of the ASD phenotype is caused by changes in a few and common set of signaling pathways, the identification of which is a fundamental aim of autism research. Using advanced bioinformatics tools and the abundantly available genetic data, it is possible to classify the large number of ASD-associated genes according to cellular function and pathways. Cellular processes known to be impaired in ASD include gene regulation, synaptic transmission affecting the excitation/inhibition balance, neuronal Ca^{2+} signaling, development of short-/long-range connectivity (circuits and networks), and mitochondrial function. Such alterations often occur during early postnatal neurodevelopment. Among the neurons most affected in ASD as well as in schizophrenia are those expressing the Ca^{2+}-binding protein parvalbumin (PV). These mainly inhibitory interneurons present in many different brain regions in humans and rodents are characterized by rapid, non-adaptive firing and have a high energy requirement. PV expression is often reduced at both messenger RNA (mRNA) and protein levels in human ASD brain samples and mouse ASD (and schizophrenia) models. Although the human *PVALB* gene is not a high-ranking susceptibility/risk gene for either disorder and is currently only listed in the SFARI Gene Archive, we propose and present supporting evidence for the Parvalbumin Hypothesis, which posits that decreased PV level is causally related to the etiology of ASD (and possibly schizophrenia).

Keywords: parvalbumin, autism (ASD), calcium signal modulator, GABAergic neurons, E/I balance, schizophrenia, ROS, mitochondria

OPEN ACCESS

Edited by:
Yu-Chih Lin,
Hussman Institute for Autism,
United States

Reviewed by:
Nael Nadif Kasri,
Radboud University
Nijmegen, Netherlands
Christopher Pittenger,
Yale University, United States
Rochelle Marie Hines,
University of Nevada, Las Vegas,
United States

***Correspondence:**
Beat Schwaller
beat.schwaller@unifr.ch

Specialty section:
This article was submitted to Cellular Neuropathology, a section of the journal Frontiers in Cellular Neuroscience

Received: *29 June 2020*
Accepted: *10 November 2020*
Published: *18 December 2020*

Citation:
Filice F, Janickova L, Henzi T, Bilella A and Schwaller B (2020) The Parvalbumin Hypothesis of Autism Spectrum Disorder. Front. Cell. Neurosci. 14:577525. doi: 10.3389/fncel.2020.577525

INTRODUCTION

Complex mechanisms underlie neurodevelopmental disorders (NDDs) and neuropsychiatric conditions. From the molecular to the system level, subtle changes at any point during development can lead to impairment of brain functions including cognition, learning, memory, and behavior, which are dynamic and subject to developmental and environmental influences and activity/experience-dependent mechanisms. Genome-wide association studies, investigation of rare genetic disorders, and transcriptome analyses aim to identify genes implicated in the etiology of NDDs, and bioinformatics approaches are used to elucidate dysregulated processes/pathways.

The interplay between altered genes, circuits, and networks giving rise to clinical symptoms in NDDs is illustrated in Figure 1 of Krol et al. (2018).

The motivation for the present article comes from many studies on ASD and schizophrenia focusing on the calcium-binding protein parvalbumin (PV) expressed by a subpopulation of neurons (sometimes referred to as fast-spiking interneurons (FSIs) or PV^+ interneurons; Hu et al., 2014). There is some confusion in the literature regarding the nomenclature. In most morphological studies using immunohistochemical methods, PV^+ neurons are defined as those labeled by anti-PV antibody. A case where the number of PV-immunoreactive neurons is lower than in control animals as a result of experimental treatment or genetic manipulation is either correctly described as a reduction in the number of PV^+ neurons or otherwise as a loss of PV^+ neurons. The latter implies that these neurons either died or did not properly migrate to a specific brain region during development as a result of the manipulation, while a third possibility is that PV was downregulated to a level below the limit of detection by immunohistochemistry (IHC). Thus, distinguishing between PV^+ neuron loss vs. decreased PV expression is critical for accurately interpreting previous studies. For the remainder of this article, we use the term PV^+ neurons only in reference to neurons identified solely by PV IHC; the class of interneurons defined by PV expression as well as additional features (e.g., morphology, electrophysiological properties, and transcriptome profile) is referred to as Pvalb neurons irrespective of PV expression level. As an example, brains of $PV^{-/-}$ mice completely lacking PV expression were found to harbor the same number of Pvalb neurons as wild-type (WT) mice (Filice et al., 2016).

The Parvalbumin Hypothesis of ASD was formulated based on the following lines of evidence: (1) the function of Pvalb neurons is often impaired in NDDs and neuropsychiatric disorders (Marin, 2012; Ferguson and Gao, 2018; Selten et al., 2018); (2) *PVALB* mRNA is the most strongly downregulated transcript in human ASD samples (Schwede et al., 2018); (3) the number of PV^+ neurons is decreased in sections of human ASD brain (Hashemi et al., 2017; Ariza et al., 2018); and (4) transgenic mice with lower ($PV^{+/-}$) or absent ($PV^{-/-}$) expression exhibit the core ASD-like symptoms (Wöhr et al., 2015); the main points of the Parvalbumin Hypothesis are graphically summarized in **Figure 1**.

DATA SUPPORTING THE PARVALBUMIN HYPOTHESIS OF ASD

Decreased Number of PV^+ Neurons in Human ASD Postmortem Brains: Pvalb Neuron Loss vs. PV Downregulation

The cerebral cortex harbors several classes of interneurons including Pvalb neurons. Early classification of these neurons was based on their morphology [most notably of the axon (Kawaguchi and Kubota, 1997; Toledo-Rodriguez et al., 2005)], firing pattern, PV expression, and gene expression profile determined by PCR (Toledo-Rodriguez et al., 2004). More recent classifications based on single-cell or single-nucleus RNA-sequencing (RNA-seq) (Hodge et al., 2019), patch sequencing (Patch-seq) yielding morphoelectric (*met*-type) and transcriptomic (*t*-type) datasets (Gouwens et al., 2020), or machine learning applied to a large patch-seq dataset (Gala et al., 2020) have identified 7 clusters (RNA-seq) as well as 10 *t*-type and 5 *met*-type (patch-seq) Pvalb neurons. Given the different algorithms used to stratify the datasets, it is not surprising that the reported number of Pvalb neuron subtypes varies across studies. Pvalb neurons in the cortex include several types of basket cell, chandelier cell, and translaminar neurons. Basket cells localized in layers 2–6 constitute the majority; chandelier cells are abundant at the boundary between layers 1 and 2 and in layer 6; and the relatively rare translaminar Pvalb neurons are mostly present in layers 5 and 6 (Lim et al., 2018). A similar classification has been applied to hippocampal Pvalb neurons (Somogyi and Klausberger, 2005).

In order to conclude that PV^+ neurons are absent in postmortem ASD brains, it must be demonstrated that neurons with specific morphoelectric, transcriptomic, and biochemical properties are missing/reduced. The typically fixed postmortem human brain tissue samples preclude the assessment of these properties. Besides non-adaptive firing, PV^+ neurons are characterized by PV expression. However, the complete absence of PV cannot be taken as evidence that Pvalb neurons are absent, which must be determined based on the expression of other Pvalb neuron-specific markers including voltage-gated potassium channel $K_V3.1b$ (*KCNC1*), potassium voltage-gated channel modifier subfamily S member 3 $K_V9.3$ (*KCNS3*), or components of perineuronal nets (PNNs), which are a set of extracellular matrix molecules surrounding Pvalb neurons in several brain regions including the cortex (Celio et al., 1998). The presence and/or intensity of PNN immunolabeling must be interpreted with caution because PNN components, like other Pvalb neuron markers besides PV (*PVALB*)—e.g., GAD67 (*GAD1*)—are regulated in an experience/activity-dependent manner (Cohen et al., 2016), and their expression changes over the course of development (Wang and Fawcett, 2012; Ye and Miao, 2013). Earlier studies found no significant changes in the number of PV^+ or calbindin-D28K-positive (CB^+) neurons in the posterior cingulate cortex and fusiform gyrus of postmortem ASD brains (Oblak et al., 2011). However, the mean density of PV^+ neurons was slightly reduced in the superficial and deep layers of both of these areas. In another study, the density of PV^+ cerebellar stellate and basket cells did not differ significantly between ASD ($n = 6$) and control ($n = 4$) samples, although the number of Purkinje cells was reduced in two or three ASD samples (Whitney et al., 2009). Moreover, the mean neuron density of both interneuron subtypes was reduced (basket cells, −15%; stellate cells, −5%), although the difference was not statistically significant. These findings imply that the number of PV^+ neurons is decreased or PV is downregulated in ASD. In a preliminary study (Zikopoulos and Barbas, 2013) comparing the density of CB^+ and PV^+ cortical interneurons in postmortem adult human brain tissue (ASD and control; $n = 2$) from dorsolateral prefrontal area 9, a significant reduction in the number of PV^+ neurons was observed in ASD brains; the ratio of

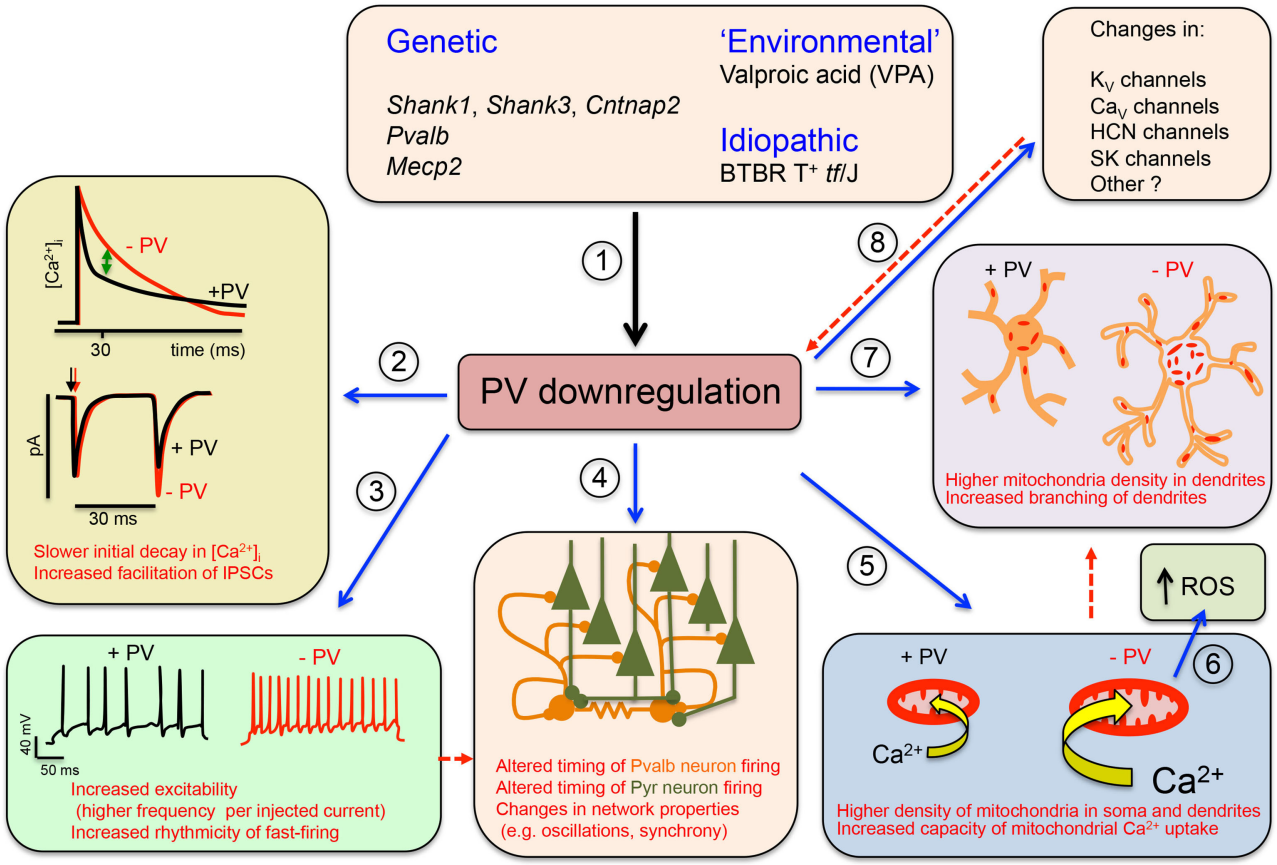

FIGURE 1 | Graphical summary of the Parvalbumin Hypothesis of autism spectrum disorder (ASD) (and putatively, of schizophrenia). (1) Genetic and environmental factors directly or indirectly affecting Pvalb neuron function in mice through impairment of principal neurons, leading to the downregulation of parvalbumin (PV) and reduced neuronal function. (2) (Upper) The initial decline in $[Ca^{2+}]_i$ in Pvalb neurons is accelerated in the presence of PV. Differences in the decay curves (±PV) are largest in the time window of ∼20–50 ms after peak $[Ca^{2+}]_i$, resulting in increased residual Ca^{2+} in the absence of PV (green arrow). (Lower) Larger amounts of residual Ca^{2+} promote γ-aminobutyric acid (GABA) release during further stimulation in this time window, leading to increased facilitation in the paired-pulse protocol. (3) An absence of PV alters other electrophysiological properties: for example, it may increase the excitability of Pvalb neurons, or may result in more regular firing within AP trains (i.e., reducing "jitter") (modified from Orduz et al., 2013). (4) A decrease in PV level affects the electrophysiological properties not only of Pvalb neurons but also of principal (pyramidal) cells and modifies network properties such as oscillation and synchrony. (5) A decrease in PV level alters Ca^{2+}-dependent excitation/transcription coupling by reducing transcript levels of activity-driven genes including *Pvalb* and *Gad1* and prototypical neuronal-activity-associated genes such as *c-Fos*, *Arc*, and *Wnt2*; it also increases messenger RNA (mRNA) levels of genes involved in mitochondrial biogenesis such as *Ppargc1a* encoding the mitochondria master regulator PGC-1α, as well as *Nrf1* and *Tfam*. This results in an increase in mitochondrial volume (density) that is approximately proportional to the PV concentration in corresponding wild-type (WT) Pvalb neurons—i.e., the higher the PV concentration, the greater the increase in mitochondrial density in $PV^{-/-}$ Pvalb neurons. (6) Increased mitochondrial volume associated with a decrease in PV level enhances mitochondrial Ca^{2+}-buffering/sequestration capacity, thereby promoting reactive oxygen species (ROS) production. This slow process may impair mitochondrial function and ultimately impacts Pvalb neuron function, which is thought to produce a schizophrenia phenotype. (7) Absence of PV during (early) postnatal neurodevelopment from ∼PND7 to PND20 increases dendritic branching, yielding Pvalb neurons with a larger dendritic tree and possibly resulting in hyperconnectivity. Increases in mitochondria number and dendritic branching caused by PV downregulation may be subsequent events (red dashed arrow) or could occur via independent mechanisms. (8) Absence of PV perturbs the expression of other putative ASD susceptibility genes that are either directly associated with the electrophysiological properties of Pvalb neurons or are expressed in pyramidal cells that influence Pvalb neuron circuitry; this includes K_V, Ca_V HCN channels, and SK channels. Whether targeted inhibition of these genes also affects PV level is unknown. Solid arrows indicate a causal relationship between events—e.g., altered Ca^{2+} concentration (±PV) and short-term modulation of synaptic plasticity. Dashed lines indicate putative (indirect) mechanism(s) via as yet unknown pathways. Points (1)–(8) are described in detail in the main text (see all subsections in *Data Supporting the Parvalbumin Hypothesis of ASD*).

PV^+/CB^+ interneurons was 0.65 as compared to ∼1 in controls. The lower ratio was assumed to reflect a decreased number of PV^+ interneurons (Zikopoulos and Barbas, 2013). An analysis of cortical interneurons expressing calretinin (CR), CB, and PV in postmortem brains of ASD and age-matched control cases revealed significant differences in three regions of the prefrontal cortex (PFC) (i.e., BA9, BA46, and BA47) that have been implicated in ASD (Hashemi et al., 2017): compared to control cases, the proportion of PV^+ neurons was decreased by 70% in BA46, 45% in BA9, and 38% in BA47 in ASD subjects, while the proportion of neurons expressing CB or CR did not differ between the two groups. Reduced numbers of PV^+ neurons were

equally found in the supra- and infragranular layers. The authors speculated that the decrease in PV^+ neurons was due to the loss of Pvalb neurons or downregulation of PV protein expression. In a follow-up study (Ariza et al., 2018), PV^+ interneuron subtypes (basket and chandelier cells) were separately analyzed in the same samples (Hashemi et al., 2018); double immunolabeling of PV and PNNs with *Vicia villosa agglutinin* (VVA) enabled the differentiation of basket and chandelier cells, as only the former are surrounded by VVA^+ PNNs in human brain. The number of PV^+ chandelier cells was consistently lower in the PFC of ASD specimens ($n = 10$); the number of PV^+/VVA^+ basket cells was also reduced but to a lesser degree. As the authors did not use a second marker to unambiguously identify chandelier cells, they concluded that the reduction in the number of PV^+ cells represents either a true loss of Pvalb neurons (mostly chandelier cells) or a decrease in PV protein level.

PV expression is developmentally regulated in humans and rodents. It has been suggested that gene expression changes in NDDs are related to an immature developmental gene expression program of PV^+ FSIs (Gandal et al., 2012). Cell-type-specific maturation indices calculated from microarray datasets showed that the index for Pvalb neurons was highly correlated with PV expression level in these cells. In all three analyzed diseases (ASD, schizophrenia, and bipolar disorder), the maturation index and PV expression level were significantly reduced, consistent with a delayed/impaired developmental gene expression program. While there are currently no quantitative data on PV expression in human ASD brains, *PVALB* mRNA level has been measured in several studies. Radioisotopic *in situ* hybridization in postmortem brains of ASD and control cases revealed that *PVALB* transcript level was downregulated in cerebellar Purkinje cells of ASD brains, independent of postmortem interval or age at death (Soghomonian et al., 2017). An examination of neocortical architecture in postmortem brain specimens of autistic and normal children aged between 2 and 15 years revealed discrete patches of abnormal and disorganized laminar cytoarchitecture in most samples (Stoner et al., 2014). An analysis of specific molecular markers by RNA *in situ* hybridization showed abnormal gene expression in these neocortical regions: the level of the interneuron marker *PVALB* was decreased, whereas no difference was observed in the total number of neurons by Nissl staining. In accordance with the *in situ* hybridization data, analyses of an RNA-seq dataset (Parikshak et al., 2016) and three microarray datasets (Garbett et al., 2008; Voineagu et al., 2011; Chow et al., 2012) identified *PVALB* mRNA as the most strongly downregulated transcript in the cerebral cortex of ASD patients (Schwede et al., 2018).

The Ca^{2+}/CaM-dependent protein kinase (CaMK) pathway is implicated in Ca^{2+}/activity-dependent gene expression (Ebert and Greenberg, 2013), including in Pvalb neurons (Cohen et al., 2016). Many neurons are regulated by CaMK II and/or IV (reviewed in Bayer and Schulman, 2019). However, Pvalb neurons use the less common isoform γCAMK I (*Camk1g*) to induce cAMP response element-binding protein (CREB) phosphorylation and expression of prototypical activity-driven genes (*c-Fos*, *Arc*, and *Wnt2*) as well as *Gad1* and *Pvalb* (Cohen et al., 2016). The observation that the *CAMK1G* transcript is among the top 40 (out of >250) significantly downregulated mRNAs detected in combined gene array datasets of human ASD samples (Schwede et al., 2018) suggests that impaired activity of Pvalb neurons in ASD results in (likely γCAMK I-dependent) reduced PV expression. Additionally, coordinated dysregulation of genes implicated in synaptic and mitochondrial functions was observed in ASD specimens (Schwede et al., 2018). The possible link between *PVALB* dysregulation and mitochondria is discussed in greater detail in *Effect of PV on Mitochondria, Oxidative Stress, and Pvalb Neuron Morphology: Link to NDDs*.

In summary, *PVALB* transcript level is not only reduced in the brain of ASD cases compared to normal controls but also shows the strongest downregulation among differentially expressed genes. Regarding Pvalb neuron loss, no study to date has provided definitive evidence (using Pvalb neuron markers such as $K_V3.1b$ or $K_V9.3$) of a lower number/density of Pvalb neurons in human ASD brains. Even if this was demonstrated, an outstanding question would be whether this is due to the death of true Pvalb neurons (i.e., Pvalb neuron-selective neurodegeneration), defects in migration or maturation of immature Pvalb neurons during development (e.g., as seen in $Dlx5/6^{-/-}$ mice; Wang et al., 2010), or another mechanism. The downregulation of PV may be linked to loss of Pvalb neuron function, although a partial decrease in function resulting from the abovementioned processes cannot be excluded.

Animal NDD Models of ASD With Reduced PV Expression and/or Decreased Number/Altered Distribution of PV^+ Neurons

Various animal models have been used to investigate NDDs including ASD. ASD risk genes are defined as those that are more frequently mutated in ASD patients than is expected by chance. Large-scale exome sequencing has identified 102 such genes (Satterstrom et al., 2020). An animal (mouse) model harboring the same (or similar) mutations and shows ASD-like behavior has high construct validity. However, in recent years, numerous mouse models (inbred, experimentally induced, and transgenic) have been discovered or established that show varying degrees of typical ASD-like core symptoms. A list of such models (>1,000) is available in the SFARI Gene database (https://gene.sfari.org/), with genes putatively associated with ASD ranked according to several criteria. More models (>3,000) are listed in the AutDB database (http://autism.mindspec.org/autdb/Welcome.do). The number of (mostly mouse) ASD models is constantly increasing, with the models themselves becoming more sophisticated as a result of the possibility of inactivating/deleting genes in a brain region- and neuron type-specific and temporally regulated manner. The last aspect is particularly important for elucidating the etiology of NDDs. Although many mouse models currently used in basic research lack robust construct validity, their strong face validity [anatomic, biochemical, neuropathological, or behavioral phenotype(s) similar to humans] make them highly useful for mechanistic studies on ASD etiology. In this paper, we focus on NDD models affecting Pvalb neurons in terms of neuron number and function and PV expression level,

irrespective whether they are currently classified as models of validated (syndromic) ASD risk genes.

The functional impairment of Pvalb neurons has attracted considerable attention in ASD research (Gogolla et al., 2009; Marin, 2012). The distribution of Pvalb neurons in the rat nervous system has been described before (Celio, 1990). A more detailed and quantitative analysis of Pvalb neuron distribution was carried out using mice in which green fluorescent protein (GFP) fused to histone 2B was selectively expressed in Pvalb neurons (PV-Cre:H2B-GFP) (Kim et al., 2017). In the same study, the distribution of other interneuron classes [somatostatin-positive (SST^+) and vasoactive intestinal polypeptide-positive (VIP^+) interneurons] was analyzed in parallel; the results showed an uneven distribution of the three major interneuron types in the isocortex. The density of the different interneuron subtypes varies in different cortical layers (Kim et al., 2017). Known changes in PV expression (mainly determined by IHC) or in Pvalb neuron function (detected by electrophysiological recordings) are summarized in **Table 1**. In many mouse models, PV IHC has revealed an overall reduction in PV^+ cell numbers in brain regions associated with ASD including the somatosensory cortex (SSC), medial (m)PFC, striatum, hippocampus, thalamic reticular nucleus (TRN), and cerebellum. Importantly, the choice of brain region for investigating PV expression has been somewhat arbitrary and likely dictated by other types of experiments (usually electrophysiology). Thus, if a significant difference in PV expression is observed in a particular brain region, it cannot be assumed that differences also exist in other brain regions. Therefore, systematic analyses are warranted. In some cases, changes in the number/distribution of PV^+ cells in a particular brain region are correlated with altered electrophysiological properties. For example, in $Ambra1^{+/-}$ mice, a likely reduction in PV—observed as a decrease in PV^+ cell number and PV protein level and interpreted as a loss of hippocampal PV interneurons (Nobili et al., 2018)—was correlated with an overall reduction in inhibitory input from Pvalb neurons in CA1 pyramidal cells. Moreover, the perisomatic paired-pulse ratio (PPR) was increased in female $Ambra1^{+/-}$ mice, which was also consistent with PV downregulation. These changes lead to hyperexcitability of CA1 pyramidal neurons and excitatory/inhibitory (E/I) imbalance (**Table 1**). Of note, similar findings were observed in $Ehmt1^{+/-}$ mice—a model for delayed circuit maturation—evidenced by a reduced number of PV^+ neurons at early age (PND14) in several cortical regions and characterized by impaired E/I balance (**Table 1**).

It is unclear whether the previously reported reduction in the number of PV^+ neurons is due to an actual decrease in Pvalb neuron count or PV downregulation because either of these would result in a smaller number of identifiable PV^+ cells. In Pvalb neurons with a low PV expression level (∼10–20 μM in hippocampus; Eggermann and Jonas, 2012)—but also in those with moderate expression (∼100 μM in cortex and striatum)—a reduction in PV level could result in some Pvalb neurons falling below the threshold of detection by PV IHC, and they would thus be considered negative for PV. For example, in $PV^{+/-}$ mice in which PV and *Pvalb* mRNA expression levels are reduced by ∼50% in the forebrain (Filice et al., 2018) and cerebellum (Schwaller et al., 2004), the number of PV^+ neurons quantified by stereological methods was decreased by ∼25–30% in the SSC, mPFC, and striatum (Filice et al., 2016). As a rule of thumb, a decrease in PV protein expression by an average of ∼50% results in 25–30% of Pvalb neurons expressing PV at a level below the threshold of detection by IHC. Importantly, unlike in humans, almost all prototypic Pvalb neurons [expressing γ-aminobutyric acid (GABA)] in the mouse brain are surrounded by PNNs, which can be detected based on the lectin-binding capacity of their glycan components by VVA or *Wisteria floribunda agglutinin* (WFA). In many brain regions, the overlap between PV^+ and PNN^+ neurons is >90% (Härtig et al., 1992). Therefore, the number of VVA^+ cells is a realistic estimate for the number of Pvalb neurons in mice. In $PV^{+/-}$ mice, the number of VVA^+ cells was unaltered in all brain regions known to be associated with ASD—namely, SSC, mPFC, and striatum (Filice et al., 2016). Even in mice completely lacking PV (i.e., the number of PV^+ cells was zero), the number of VVA^+ neurons did not differ from that in WT mice. While there is a global reduction in PV expression in $PV^{+/-}$ mice, in other ASD models, the decrease is brain region specific, yet the number of VAA^+ neurons in these regions is unchanged. Reduced PV level and fewer PV^+ neurons were observed in the SSC of $Shank1^{-/-}$ (−30% PV^+ cells) mice and in the striatum of $Shank3B^{-/-}$ (−30%), $Cntnap2^{-/-}$ (−30%), and *in utero* valproic acid (VPA)-treated (−15%) mice, suggesting that the striatum is a hotspot for the ASD-associated downregulation of PV. Notably, in the abovementioned mouse models, there are other brain regions with unaltered numbers of PV^+ neurons (Schwaller, 2020), and the number of VVA^+ cells is also unchanged. Moreover, in regions with a reduced number of PV^+ neurons, *Pvalb* mRNA and PV protein expression levels were decreased by ∼50% (or by ∼30% in VPA mice). Thus, the $Shank1^{-/-}$, $Shank3B^{-/-}$, $Cntnap2^{-/-}$, VPA, and $PV^{-/-}$ ASD mouse models are characterized by PV downregulation and not the loss of Pvalb neurons. However, such information is unavailable for most of the ASD mouse models listed in **Table 1**, in which a decrease in the number/density of PV^+ neurons has been reported in most cases. Nonetheless, such information can provide mechanistic insights as a decreased number or functional impairment of Pvalb neurons due to a reduction in PV is expected to alter the functioning of the neuronal network in distinct ways.

Irrespective of the cause of the decreased number of PV^+ neurons, the mouse models listed in **Table 1** exhibit changes at the level of electrophysiology and behavior. Notably, many of the genes listed in **Table 1** are associated with ASD and linked to E/I imbalance (Table 1 in Lee et al., 2017). Processes/mechanisms contributing to physiologic E/I balance include the development of excitatory and inhibitory synapses, neurotransmission, and synaptic plasticity comprising homeostatic plasticity, activation of signaling pathways (e.g., excitation–transcription coupling), and modulation of intrinsic excitability (Nelson and Valakh, 2015; Lee et al., 2017). The few models in which such changes in electrophysiological properties are directly attributable to a decrease in PV level are described in detail in *Acute Reduction in PV Expression Induces ASD-Like Behavior in Juvenile Mice, While Promoting PV Expression in* $PV^{+/-}$ *Mice Attenuates*

TABLE 1 | Mouse models with evidence of parvalbumin (PV) alterations and associated changes in electrophysiology and occurrence of autism spectrum disorder (ASD)-like behavior.

Mouse model/*Gene name*/Protein name SFARI classification	Type of PV alteration(s)/age of testing	Electrophysiological alteration(s) relevant to Pvalb neuron function	ASD-like behavioral impairments (core and comorbidity)
(A) GENETIC MODELS LISTED IN THE SFARI GENE DATABASE (https://gene.sfari.org/) (S, SYNDROMIC)			
Cntnap2$^{-/-}$ ***Cntnap2*** Contactin associated protein-like 2 SFARI 2 (S)	**STRIATUM, CORTEX** (Penagarikano et al., 2011;Vogt et al., 2018) Reduction in the number of PV^{+} cells (P14 and P30) **STRIATUM** (Lauber et al., 2018) Reduction in the number of PV^{+} cells and *Pvalb* mRNA, **no change** in the number of VVA^{+} (Pvalb) neurons (P25)	**HIPPOCAMPUS** (Jurgensen and Castillo, 2015) **Altered inhibition onto CA1 pyramidal neurons** • Reduced amplitude of putative perisomatic-evoked IPSCs • Increase in the frequency of spontaneous AP-driven IPSCs **SSC** (Antoine et al., 2019) **Reduced inhibition and (feebly) decreased excitation in L2/L3 pyramidal cells** • Impairment in Pvalb neuron-mediated feedforward eIPSCs • Reduced spontaneous spiking frequency of mEPSCs and mIPSCs	Stereotypic motor movements and communication and social abnormalities. Hyperactivity to thermal sensory stimuli (Penagarikano et al., 2011)
Ehmt1$^{+/-}$ ***Ehmt1*** Euchromatic histone Methyltransferase 1 SFARI Gene Archive 3 (S)	**AUDITORY CORTEX (AC) L2/3 and 4, SSC L2/3 and 4, VISUAL CORTEX (VC) L2/3 and 4** (Negwer et al., 2020) Delay of PV^{+} neuron maturation in early (P14) sensory development, with layer- and region-specific variability later (P28, P56) **AC**: Decrease in PV^{+} neurons in **L2/3 and 4** at P14 only **SSC**: reduced number of PV^{+}/VVA^{+} neurons at all ages in **L4** only **VC**: no differences in **L2/3** at all ages; reduced number of PV^{+} and PV^{+}/VVA^{+} in **L4** at P14	**HIPPOCAMPAL ACUTE SLICES** (Frega et al., 2020) **Impairment in inhibitory transmission** • Strong reduction of mIPSC amplitude and frequency in CA1 pyramidal cells at P21 • Increased inhibitory PPR responses specifically at 50 ms ISI in CA1 pyramidal cells following stimulation in *stratum radiatum* (P21) • Hyperexcitability in CA1 hippocampal excitatory neurons • Results indicate that Ehmt1 plays a role in controlling E/I balance by regulating inhibitory inputs onto CA1 pyramidal cells **AUDITORY CORTEX ACUTE SLICES** (Negwer et al., 2020) • Reduced mIPSC frequency, NOT amplitude in auditory cortex L2/3 pyramidal cells at P14–16. • Increased inhibitory PPR responses at ISI of 50, 100, and 200 ms • Decreased release probability of GABA determined from a 10-Hz stimulus train	Reduced social play in juvenile (P30) male, but not in female mice Prolonged social approach in the social approach assay (3-chamber assay) observed in adult (3 months) male and female Ehmt1$^{+/-}$ mice Delayed (males) or absent (females) preference for social novelty Hypergrooming and reduced exploration in the open field (Balemans et al., 2010)
En2$^{-/-}$ ***En2*** Engrailed 2 SFARI 3	**HIPPOCAMPUS, SSC** (Tripathi et al., 2009) Reduction in the number of PV^{+} cells (3–5 months) **TRN** (Provenzano et al., 2020) Reduction of *Pvalb* mRNA (P30) Reduction in the number of PV^{+} cells (6 weeks) **VISUAL CORTEX (L2/3 and L5/6)** (Pirone et al., 2020) Increase in the number of PV^{+} cells (P30 and adult)	No electrophysiology at cellular level reported	Deficits in reciprocal social interactions as juveniles and adults (Brielmaier et al., 2012)
Fmr1$^{-/-}$ ***Fmr1*** Fragile X-mental retardation protein (FMRP) SFARI 3 (S)	**SSC** (Selby et al., 2007) Reduction in the number of PV^{+} cells (12 months) **DEVELOPING AUDITORY CORTEX** (Wen et al., 2019) Reduction in the number of PV^{+} cells (P14, P21, P30)	**SSC (barrel cortex layer 4)** (Gibson et al., 2008) **Reduced feedback inhibition mediated by FS (Pvalb) neurons** • Decreased EPSC frequency on FS (Pvalb) neurons • Normal feed-forward inhibition > no change in inhibitory drive • Excitatory neurons intrinsically more excitable > increased evoked AP firing rate during 600-ms current injection	ASD-like core symptoms of altered social interaction and repetitive behaviors, hyperactivity (Pietropaolo et al., 2011). Mental retardation, anxiety, increased incidence of epilepsy, auditory hypersensitivity (Chen and Toth, 2001;Frankland et al., 2004)

(Continued)

TABLE 1 | Continued

Mouse model/*Gene name*/Protein name SFARI classification	Type of PV alteration(s)/age of testing	Electrophysiological alteration(s) relevant to Pvalb neuron function	ASD-like behavioral impairments (core and comorbidity)
(A) GENETIC MODELS LISTED IN THE SFARI GENE DATABASE (https://gene.sfari.org/) (S, SYNDROMIC)			
Mecp2$^{-/-}$ ***Mecp2*** Methyl-CpG-binding Protein-2 SFARI 2 (S)	**VISUAL CORTEX (V1)** (Krishnan et al., 2015;Patrizi et al., 2019) Accelerated maturation of PV network (P14 and P30) **HIPPOCAMPUS CA3** (Calfa et al., 2015) Density of PV$^+$ interneurons not altered in CA3 (P40–P60) **VISUAL CORTEX** (Durand et al., 2012) Increased *Pvalb* mRNA levels PV-hyperconnectivity > increased PV immunofluorescence intensity as consequence of increased neurite complexity (from P15 on; persistent also in adulthood)	**HIPPOCAMPUS CA3** (Calfa et al., 2015) **Weaker synaptic inhibition onto CA3 pyramidal neurons resulting in larger E/I ratio in CA3 pyramidal neurons** • Smaller amplitude, but higher mIPSCs frequency in pyramidal neurons; larger amplitude, but lower frequency of mEPSCs • Smaller slope of input/output (I/O) relationship • Lower frequency of spontaneous APs from FS (Pvalb) neurons > smaller and less frequent mEPSCs onto CA3 fast-spiking basket cells **VISUAL CORTEX** (Durand et al., 2012) **Reduction of pyramidal neuron and network activity** • Stronger inhibition of pyramidal neurons caused by a hyperinnervation by PV-expressing interneurons > low spontaneous and evoked neuronal activity and a general silencing of cortical circuitry	Ataxia, stereotyped behaviors, seizures, motor, sensory, memory, and social deficits (Chao et al., 2010;Ito-Ishida et al., 2015)
Nlgn3$^{-/-}$ ***Nlgn3*** Neuroligin 3 SFARI 2	**SSC** (Gogolla et al., 2009) "Patchy" PV$^+$ cells (2–3 months)	**HIPPOCAMPUS CA2** (Modi et al., 2019) **Increased neuronal excitability and reduced inhibition** • Increased frequency of spontaneous EPSCs and decrease in frequency of spontaneous IPSCs in CA2 pyramidal cells • strong reduction of perisomatic inhibition mediated by CCK neurons **HIPPOCAMPUS CA1** (Polepalli et al., 2017) **Decrease in Pvalb interneuron inhibition** • Significant reduction in facilitation of EPSCs and spiking in Pvalb neurons lacking Nlgn3	Impaired social novelty and social memory, hyperactivity, repetitive behaviors (Tabuchi et al., 2007;Rothwell et al., 2014)
Nlgn3 R451C Knock-in substitution of Arg^{451} to Cys ***Nlgn3*** Neuroligin 3 SFARI 2	**SSC** (Speed et al., 2015) PV$^+$ cell number unchanged (P13–17)	**SSC (barrel cortex)** (Tabuchi et al., 2007;Speed et al., 2015) **Increase in inhibitory synaptic transmission** • Increase in spontaneous mIPSC frequency in L2/3 pyramidal neurons • Increased amplitude of evoked IPSCs in L2/3 pyramidal neurons **Pvalb neuron–pyramidal cell synaptic connections NOT altered** • Unitary $IPSC_5/IPSC_1$ ratio unchanged; paired whole-cell recordings between Pvalb neurons and pyramidal neurons **HIPPOCAMPUS CA1** (Etherton et al., 2011) **Increase in AMPA and NMDA receptor-mediated excitatory synaptic transmission** • Increased fEPSP slope and spontaneous mEPSCs frequency **Increased evoked synaptic strength at inhibitory synapses** • Larger eIPSC amplitude in L2/3 pyramidal neurons **mPFC** (*in vivo* recordings) (Cao et al., 2018) **Decreased excitability of FS interneurons and dysfunction of gamma oscillation** • Reduced firing frequency recorded from FS interneurons	Impaired social interaction behaviors and enhanced spatial learning (Tabuchi et al., 2007;Etherton et al., 2011)

(Continued)

TABLE 1 | Continued

Mouse model/*Gene name*/Protein name SFARI classification	Type of PV alteration(s)/age of testing	Electrophysiological alteration(s) relevant to Pvalb neuron function	ASD-like behavioral impairments (core and comorbidity)
(A) GENETIC MODELS LISTED IN THE SFARI GENE DATABASE (https://gene.sfari.org/) (S, SYNDROMIC)			
Shank3$^{-/-}$ ***Shank3*** SH3 and multiple ankyrin repeat domains 3 SFARI 1 (S)	**STRIATUM** (Filice et al., 2016) Reduction in the number of PV^{+} cells and *Pvalb* mRNA, **no change** in the number of VVA^{+} (Pvalb) neurons (P25) **INSULAR CORTEX** (Gogolla et al., 2014) Diminished PV^{+} puncta on pyramidal cells (P70–100)	**CORTICOSTRIATAL ACUTE SLICES** (Peca et al., 2011) **Disruption of striatal glutamatergic signaling** • Decreased corticostriatal population spike amplitude • Reduced frequency and amplitude of AMPA-mediated mEPSC in MSN **SSC** (Chen et al., 2020) **Excitatory neuron hyperactivity and inhibitory neuron hypoactivity** • *in vivo* population calcium imaging (basal recordings and after stimulation: vibrissae motion detection task	Hypergrooming, social deficits, sensory hyperactivity (Peca et al., 2011;Chen et al., 2020)
(B) 'ENVIRONMENTAL' AND IDIOPATHIC MODELS			
VPA Environmental model of ASD (*in utero* exposure to valproic acid	**SSC** (Gogolla et al., 2014) "Patchy" distribution of PV^{+} cells (2–3 months) **SSC, STRIATUM** (Lauber et al., 2016) Reduction in the number of PV^{+} cells and *Pvalb* mRNA, **no change** in VVA^{+} (Pvalb) neurons (P25)	**TEMPORAL CORTEX** (Banerjee et al., 2013) **mIPSC impairment** • Reduced mIPSC frequency, but increased rise time and decay time in L2/3 pyramidal cells • Lower input/output response of evoked IPSCs	Reduced communication, social deficits, repetitive behavior, stimuli hypersensitivity (Schneider and Przewlocki, 2005;Markram et al., 2008;Gandal et al., 2010)
BTBR T^{+} Itpr3^{tf}/J (BTBR T^{+} *tf*/J) strain Idiopathic model of ASD This strain carries the mutations "a^{t}" (non-agouti; black and tan) "*Itpr3^{tf}*" (inositol 1,4,5-triphosphate receptor 3; tufted), and "T" (brachyury)	**INSULAR CORTEX** (Gogolla et al., 2014) Diminished PV^{+} puncta on pyramidal cells (P70–100) **ANTERIOR CINGULATE CORTEX** (Stephenson et al., 2011) Reduction in PV^{+} cells (8–10 weeks)	**INSULAR CORTEX** (Gogolla et al., 2014) **Impaired multisensory integration—weakened inhibitory circuitry** • Decreased mIPSCs frequency recorded in pyramidal cells	Social deficits, impairments in vocal communication, stereotypic, repetitive behaviors, exaggerated auditory responses at low-moderate tones (McFarlane et al., 2008;Scattoni et al., 2011;Gogolla et al., 2014)
(C) GENETIC NDD MODELS WITH A FEEBLER LINK TO PV AND ASD			
Ambra1$^{+/-}$ (female mice) ***Ambra1*** Activating molecule in Beclin1-regulated autophagy SFARI Gene Archive 5	**HIPPOCAMPUS** (Nobili et al., 2018) Reduction in the number of PV^{+} cells and PV protein levels (2–3 months)	**HIPPOCAMPUS** (Nobili et al., 2018) **Reduction of inhibitory drive on CA1 pyramidal neurons** • Reduced amplitude of dendritic eIPSCs • Reduced amplitude of Pvalb neuron-mediated perisomatic eIPSCs	Sociability and communication deficits (Nobili et al., 2018)
Aspm$^{1-7}$ ***Aspm*** Abnormal spindle-like microcephaly associated	**HIPPOCAMPUS, TRN** (Garrett et al., 2020) Reduction in the number of PV^{+} cells (23 weeks)	n/a	Impaired short- and long-term object recognition memory (Garrett et al., 2020)
PV-Lmo4$^{-/-}$ Lmo4 deletion in Pvalb neurons ***Lmo4*** LIM domain only	**ANTERIOR CINGULATE CORTEX** (Zhang et al., 2020a) No detectable loss of PV^{+} neurons (2–4 months)	**ANTERIOR CINGULATE CORTEX (ACC) L2/3** (Zhang et al., 2020a) **Altered properties of Pvalb neurons** • Increased membrane excitability and shortened latency to the first AP • Increased amplitude of spontaneous inhibitory inputs (mostly from Pvalb neurons) to the somata of ACC L2/3 pyramidal cells **Increased Pvalb neuron-mediated perisomatic feedforward inhibition**	Repetitive behaviors and deficits in social interaction (Zhang et al., 2020a)

Social Behavioral Impairment. Permanent changes in the firing properties of Pvalb neurons, their inputs, or their targets in ASD mouse models alter the steady-state equilibrium (i.e., E/I balance). It was initially proposed that an increase in the E/I ratio could be causally related to ASD (Rubenstein and Merzenich, 2003); however, it has since been demonstrated in many models that a homeostatic or maladaptive change in the E/I balance in either direction is a hallmark of ASD. The relative contribution of E/I imbalance to ASD can vary according to ASD risk/susceptibility gene mutation, brain region, specific features of synapses, and developmental time point. Even in mice harboring the same mutation, the E/I balance is differentially affected across neuron subpopulations. For example, mice carrying the neuroligin 3 mutation R451C ($NL3^{R451C}$) show an increase in inhibitory synaptic transmission in SSC pyramidal cells—that is, increases in spontaneous inhibitory postsynaptic current (sIPSC) and evoked (e)IPSC frequency (Tabuchi et al., 2007) leading to a lower E/I ratio. However, in CA1 pyramidal neurons of the same mice, excitatory transmission mediated by N-methyl-D-aspartate (NMDA)- and α-amino-3-hydroxy-5-methyl-4-isoxazolepropionic acid (AMPA)-type glutamate receptors is increased. As the former shows greater involvement, the NMDA/AMPA ratio as well as E/I ratio are increased. The increase in NMDA/AMPA ratio does not occur in layer 2/3 pyramidal neurons of the SSC (Etherton et al., 2011). In the hippocampal CA1 pyramidal cells of $Cntnap2^{-/-}$ mice, putative perisomatic input (likely via the axon initial segment, soma, and proximal dendrites) and eIPSC amplitude are decreased, while miniature excitatory postsynaptic current (mEPSC) frequency and amplitude are unchanged (Jurgensen and Castillo, 2015). However, there is a trend toward a lower NMDA/AMPA ratio in $Cntnap2^{-/-}$ mice. On the contrary, the frequency (but not amplitude) of spontaneous action potential (AP)-driven IPSC is increased in mutant mice, whereas mIPSC is unchanged (both in frequency and amplitude). Strongly reduced layer 4 stimulation-evoked feedforward inhibition (i.e., eIPSC) and a smaller decrease in feedforward excitation (i.e., evoked EPSC) onto layer 2/3 SSC pyramidal cells results in a higher E/I ratio in several ASD mouse models including $Cntnap2^{-/-}$ and $Fmr1^{y/-}$ mice (Antoine et al., 2019). This only weakly affects spontaneous (basal) spiking in layer 2/3 pyramidal cells *in vitro*; however, the whisker-evoked firing rate of FSI (likely Pvalb neurons) is reduced in these two ASD models (Antoine et al., 2019). The above examples provide evidence that dysfunctional GABAergic transmission—often perisomatic inhibition by Pvalb basket cells—is a critical aspect of ASD. How the absence of PV is directly implicated in altered GABAergic transmission is discussed in *PV Affects Pvalb Neuron Targets and Inputs*.

Acute Reduction in PV Expression Induces ASD-Like Behavior in Juvenile Mice, While Promoting PV Expression in $PV^{+/-}$ Mice Attenuates Social Behavioral Impairment

Based on findings from ASD patients and ASD animal models discussed in *Decreased Number of PV^{+} Neurons in Human ASD Postmortem Brains: Pvalb Neuron Loss vs. PV Downregulation* and *Animal NDD Models of ASD With Reduced PV Expression and/or Decreased Number/Altered Distribution of PV^{+} Neurons*, respectively, as well as our own *in vitro* studies (reviewed in Schwaller, 2020), we investigated the role of PV in the development of an ASD-like behavioral phenotype using genetically modified mice. Experimental approaches typically used to demonstrate causality between an experimental manipulation at the molecular or cellular level and higher-order brain function(s) (e.g., network activity or behavioral phenotype) are based on perturbation of the system. For instance, removing a component (e.g., a protein) hypothesized to be directly implicated in a behavior is predicted to lead to its appearance, whereas when the same component has lower abundance (e.g., in haploinsufficiency), upregulation to a normal level is expected to attenuate/alleviate the behavior (rescue experiment). There are several caveats to this concept. During the process of downregulation and/or reappearance of the investigated protein, additional adaptive, compensatory, or homeostatic changes may occur, likely over varying time scales and to different degrees. Nonetheless, the knockdown and rescue approaches have been successful in many instances, including in the field of ASD. Re-expression of Shank3 in a Shank3 conditional knock-in mouse model rescued social interaction deficits and attenuated repetitive grooming behavior in adult mice (Mei et al., 2016); early genetic restoration of WT Shank3 in $Shank3^{E13}$ mutant mice rescued the same deficits as well as those in locomotion and rearing (Jaramillo et al., 2020). In MeCP2-overexpressing mice, reducing MeCP2 level (e.g., by antisense oligonucleotide treatment) reversed behavioral deficits associated with *MECP2* duplication syndrome (Sztainberg et al., 2015). Of note, null mutant *Shank3* and *Mecp2* mice are models for delayed and precocious circuit maturation during development, respectively, and especially for perisomatic Pvalb neuronal circuit function (Gogolla et al., 2014). Both mutants show impaired multisensory integration in the insular cortex, likely due to an E/I circuit imbalance skewed toward excitation ($Shank3^{-/-}$) or inhibition ($Mecp2^{-/-}$), respectively. This suggests that an optimal E/I circuit balance depends on precise Pvalb neuronal circuit function (Figure 7 in Gogolla et al., 2014). Alterations in the time course of network development/maturation—especially during critical periods of plasticity [postnatal days (PND) 5–15 in mice]—are thought to contribute to the appearance of ASD-like behavioral traits (Leblanc and Fagiolini, 2011).

We applied the perturbation (removal/readdition) approach to investigate the role of PV in the occurrence of ASD-like core symptoms in mice. We previously showed that $PV^{-/-}$ mice constitutively lacking PV expression exhibited all of the core ASD symptoms—i.e., reduced reciprocal social interaction, impaired communication (ultrasonic vocalization), and repetitive and stereotyped behaviors (Wöhr et al., 2015); they also showed several ASD-associated comorbidities such as increased susceptibility to epilepsy (Schwaller et al., 2004), reduced pain sensitivity (Wöhr et al., 2015), slight impairment of motor coordination, and mild hyperactivity (measured as characteristic speed) (Farre-Castany et al., 2007). The same but weaker core ASD-like phenotype is seen in $PV^{+/-}$ mice (Wöhr et al., 2015), in which the level of PV is about 50% lower than

in WT mice (Schwaller et al., 2004; Filice et al., 2018). ASD-like behaviors in $PV^{-/-}$ and $PV^{+/-}$ mice have been consistently observed in the juvenile reciprocal social interaction assay and three-chamber assay evaluating direct social interaction and social preference, respectively. In the former, the most robust parameter distinguishing WT mice from those with reduced PV level ($PV^{+/-}$ and $PV^{-/-}$) was behavior following social behavior (Figure 3 legend and Figure 1D in Wöhr et al., 2015) and Figure 2C in Filice et al. (2018). In the three-chamber assay, the most relevant findings were related to sniff time—i.e., the time a mouse spent in close proximity (2 cm) to a caged stranger mouse – and not simply the time spent in the compartment with the stranger mouse; described in detail in the Supplementary Materials of Filice et al. (2018). To define the experimental conditions for the knockdown/rescue experiments, it is important to consider the developmental regulation of PV in Pvalb neurons. PV in mice is expressed starting from PND5 to PND7 (depending on the brain region), with peak expression occurring at approximately PND25–40 (Okaty et al., 2009). The developmental timeline of Pvalb neurons in the SSC (Figure 3 in Butt et al., 2017) and auditory cortex (Takesian et al., 2018) has been reported. An overview of cortical interneuron development can be found in Lim et al. (2018).

Quantitative data on PV expression levels during juvenile development in mice are available only for the cerebellum, which contains Purkinje cells and molecular layer interneurons (MLI) expressing PV (Figure 2B in Collin et al., 2005). These data were used to generate the blue curve for WT mice shown in **Figure 2B**. PV expression increases sharply starting at PND10 and reaches a plateau at PND20. The second postnatal week is also the start of the GABA switch from depolarizing to hyperpolarizing (observed in cultured hippocampal neurons) (Leonzino et al., 2016) that is essentially complete by PND12, as evidenced by the disappearance of giant depolarizing potentials (Ben-Ari et al., 1989; reviewed in Ben-Ari, 2002). Thus, the steep increase in PV expression begins at around the time when GABA action turns hyperpolarizing. The developmental course of PV expression may be different in other Pvalb neurons (in the cortex, hippocampus, and TRN). In $PV^{+/-}$ mice, we assumed the same temporal course as in WT mice; however, PV level reaching only 50% of WT at PND25 (Filice et al., 2018) (red curve in **Figure 2B**). For the rescue experiment, $PV^{+/-}$ mice were treated with 17-β-estradiol (E2) from PND5 to PND15, resulting in a PV expression level that was ∼90% that of WT mice at PND25 (Filice et al., 2018). Hypothetical PV expression levels during the development of E2-treated mice are shown in **Figure 2B** (green curve). E2 has been shown to increase PV expression *in vitro* (Fujimoto et al., 2004) and in $PV^{+/-}$ mice (Filice et al., 2018); in the latter, this effect is mediated by an as-yet unidentified estrogen-responsive element (ERE) in the mouse *Pvalb* promoter. As E2 most likely affects the expression of several genes with identified EREs, what are the evidences that E2-mediated upregulation of PV is a most likely cause for the attenuation of the ASD-like phenotype in E2-treated $PV^{+/-}$ mice? Moreover, one has to take into account that E2 modulates social behavior in rats (Reilly et al., 2015) and more generally affects neural circuits via direct or indirect activation of multiple downstream signaling pathways (Marino et al., 2006). First, in $PV^{-/-}$ mice, E2 had no obvious effect on PV expression or ASD-related behaviors (Filice et al., 2018). Second, although E2 treatment in WT mice does not increase global PV protein level, it is possible that PV protein is upregulated in some Pvalb neurons including those with low PV expression. Unexpectedly, E2 treatment provoked ASD-like behaviors in WT mice (e.g., decreased sociability and an increase in repetitive behavior). Possible reasons for this antisocial effect of E2 treatment in WT mice and additional arguments about the positive effect of E2 treatment selectively in $PV^{+/-}$ mice are discussed in Filice et al. (2018). Stronger PV IHC signals indicative of elevated PV level were also observed in $MeCP2^{-/-}$ ASD model mice (Patrizi et al., 2019), in accordance with the concept of optimal PV circuit function (Figure 7 in Gogolla et al., 2014). For the inverse experiment, we used the $B6PV^{Cre}$-Tg(hPGK-eGFP/RNAi; Pvalb)^{1Swal} mouse line (abbreviated as shPV22 or shPV), which permits temporally controlled PV downregulation upon isopropyl-β-D-thiogalactoside (IPTG) administration (Filice et al., 2019). Induced expression of sh*Pvalb* from PND18 to PND25 decreased PV level to approximately 50–60% of the WT level (Filice et al., 2019), which was also comparable to the PV level in constitutive $PV^{+/-}$ mice. The hypothesized course of PV expression level is shown in **Figure 2B** (orange curve). It should be noted that the only experimentally verified PV levels in the rescue and downregulation experiments are those measured at PND25 (**Figure 2A**)—that is, the time point of behavioral testing; the green and orange curves in **Figure 2B** depicting PV expression levels in the two models are thus estimates that are not yet supported by experimental data.

ASD-like behavior was tested at PND25 for four conditions/genotypes: (1) WT; (2) constitutive $PV^{+/-}$; (3) $PV^{+/-}$ rescue, in which PV expression was enhanced by E2 treatment; and (4) shPV22 (downregulation), in which PV expression declined starting from PND18 to 50–60% at PND25. Results from the first three groups have been published (Wöhr et al., 2015; Filice et al., 2018), while behavioral data from shPV22 mice have not yet been reported. WT mice showed a strong preference (>60%) for engaging in another social behavior after a previous one (Wöhr et al., 2015; Filice et al., 2018) (**Figure 3**); this preference was not observed in $PV^{+/-}$ mice but was induced by increasing PV level through E2 treatment (Filice et al., 2018) and abolished after PV downregulation mediated by shPV22 starting from PND18. Almost identical results were observed in the three-chamber assay evaluating social preference: WT mice showed a stronger interest in the small cage with the stranger mouse than in the empty cage (object), as measured by sniff time (**Figure 4**). $PV^{+/-}$ mice showed no preference for the stranger mouse, but this was restored by E2-mediated PV upregulation. Transient PV reduction induced by IPTG in shPV22 mice attenuated preference for the stranger mouse compared to WT mice [$p = 0.024$ in the first cohort ($n = 6$) and $p = 0.179$ in the second cohort ($n = 4$)]. However, when results from the two cohorts were combined, a preference ($p = 0.0049$) for the stranger mouse is maintained—as to a lesser extent (n.s.)—in constitutive $PV^{+/-}$ mice (red and orange bars in **Figure 4**). In conclusion, induced downregulation of PV produces an

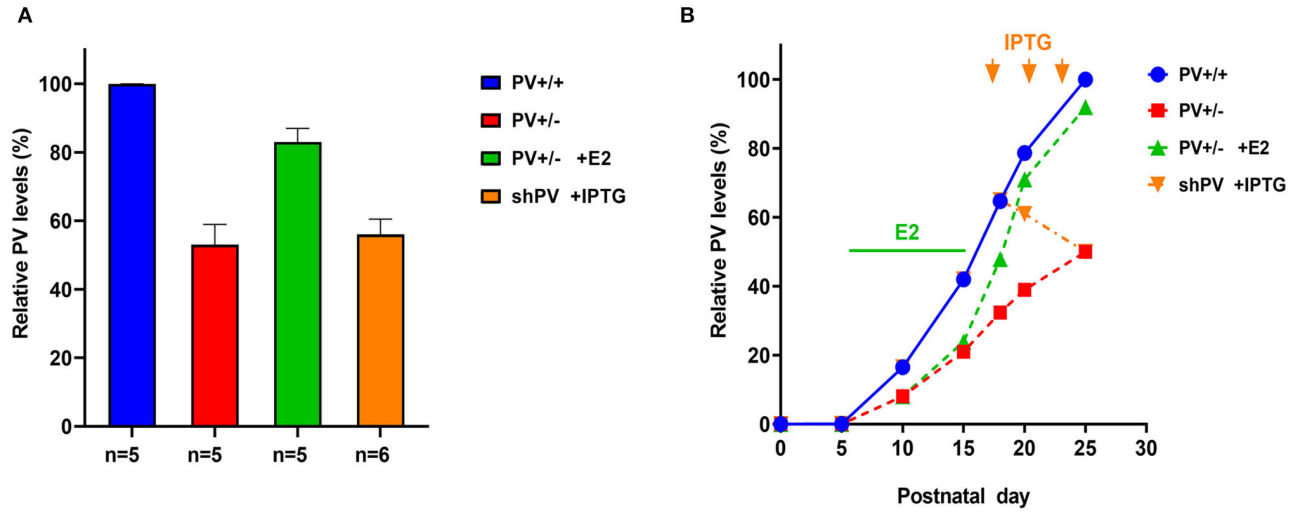

FIGURE 2 | (A) Relative parvalbumin (PV) expression level determined by semi-quantitative western blot analysis in mouse forebrain extracts from PND25. Data for $PV^{+/+}$ (defined as 100%), $PV^{+/-}$, and $PV^{+/-}$ mice treated with E2 are from Filice et al. (2018); data for isopropyl-β-D-thiogalactoside (IPTG)-treated shPV mice are from Filice et al. (2019). The number of mice is indicated; values represent mean ± SD. **(B)** Autism spectrum disorder (ASD)-like behavior shown in **Figures 3**, **4** was tested at PND25 in four conditions/genotypes: (1) wild-type (WT) mice; (2) constitutive $PV^{+/-}$ mice; (3) $PV^{+/-}$ rescue mice, in which PV expression was enhanced by E2 treatment; and (4) shPV22 (downregulation) mice, in which IPTG treatment at PND18, PND21, and PND24 reduced PV level to 50–60% of that in WT mice at PND25. PV expression profile (solid blue line) in WT ($PV^{+/+}$) mice is based on data obtained from protein extracts of mouse cerebellum (Collin et al., 2005). In $PV^{+/-}$ mice (red line), the level was assumed to be ∼50% that of WT mice at all time points. Treatment of $PV^{+/-}$ mice with E2 from PND5 to PND15 (green bar) results in a PV level that is ∼90% of that in WT mice at PND25 (green line). Treatment of transgenic shPV22 mice with IPTG at PND18, PND21, and PND24 (orange arrows) decreases PV level to ∼50% of that in WT mice at PND25 (orange line). As the precise course of PV expression in the three groups is not yet supported by experimental data, the lines are dashed. However, relative PV expression level at PND25 corresponds to the experimental data shown in **(A)**. As previously reported, IPTG treatment alone (at PND18, PND21, and PND24) had no effect on PV expression levels at PND25 as determined using the shTurboGFP control transgenic mouse line (Filice et al., 2019).

ASD-like phenotype, while PV restoration in constitutive $PV^{+/-}$ mice abrogates this phenotype. This strongly indicates that PV expression level is causally related to ASD-like behavior. In the next sections, mechanistic and anatomic evidence supporting this possibility are presented.

PV Affects Pvalb Neuron Targets and Inputs

Biophysical Considerations

The function of an intracellular Ca^{2+} buffer (better termed as a Ca^{2+}-signal modulator) like PV is simple in theory: binding Ca^{2+} ions at high intracellular Ca^{2+} concentration ($[Ca^{2+}]_i$) and releasing/unbinding Ca^{2+} when local Ca^{2+} concentration decreases. PV-specific biophysical properties include Ca^{2+} as well as Mg^{2+} affinity and kinetics. Only the most pertinent findings are discussed here; additional details can be found in Schwaller (2020). Data on the biophysical properties of PV were obtained from *in vitro* studies using purified recombinant PV. Rat PV contains two equivalent Ca^{2+}/Mg^{2+}-binding sites that are usually occupied by either of the two ions in a competitive manner, with dissociation constants (K_D) of 11 nM and 41 μM, respectively (Eberhard and Erne, 1994). Modeling studies investigating the effect of PV on depolarization-induced increases in $[Ca^{2+}]_i$ in isolated chromaffin cells revealed physiologically relevant parameters including binding kinetics (Lee et al., 2000) and apparent Ca^{2+} affinities (i.e., $K_{D,Ca[app]}$ values of 150–250 nM in an intracellular environment). Together with PV mobility determined in neuron somata [diffusion rate (D_{PV}), ∼40 $\mu m^2\ s^{-1}$; Table 1 in Schwaller (2020)], these parameters should enable accurate prediction of the effect of a given concentration of PV on Ca^{2+} signals in a particular neuron if all other parameters relevant to Ca^{2+} signaling are known, such as the "on" mechanisms that lead to an increase in $[Ca^{2+}]_i$ as well as the "off" mechanisms that reduce $[Ca^{2+}]_i$ to basal levels (Berridge et al., 2003). However, such information is currently unavailable for essentially all proteins—for example, for a single voltage-gated Ca^{2+} channel $Ca_V2.1$ (P/Q type; *CACNA1A*) or a plasma membrane calcium ATPase (e.g., PMCA1; *ATP2B1*) many splice variants exist, exhibiting distinct properties related to Ca^{2+} handling. All of these Ca^{2+} signaling components are present to varying degrees in different neuron subpopulations (some highly specific and others ubiquitous); even in supposedly homogeneous subpopulations such as cerebellar MLIs, PV expression levels vary considerably among individual neurons [average ∼570 μM; range, 55–1,788 μM (Eggermann and Jonas, 2012)]. Moreover, average PV concentrations in Pvalb neuron populations in different brain regions are highly heterogeneous, ranging from 10 μM in the hippocampus to ∼750 μM in TRN (Janickova et al., 2020). To further complicate matters, organelles previously assumed to be homogeneous such as mitochondria that are

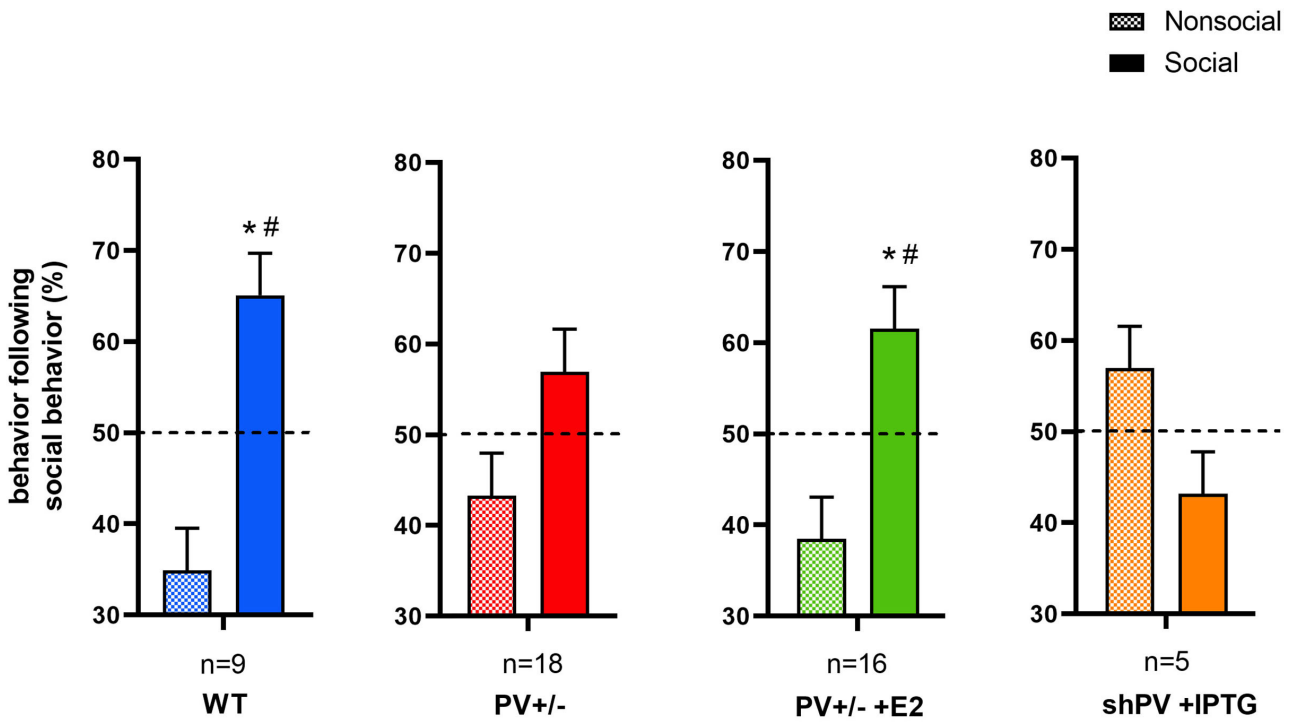

FIGURE 3 | In the reciprocal interaction assay, the type and duration of each behavior is recorded, yielding ethograms for mouse pairs (**Figure 1** in Wöhr et al., 2015). Behaviors classified as social include 1) facial and anogenital sniffing, 2) following, 3) social grooming, 4) pushing past, 5) crawling over-/under and 6) social inactive. Non-social behaviors include rearing, digging, and grooming. After each social-type interaction (independent of its duration) occurring during a 5 min observation period, the next interaction is either classified as social or non-social. From these data, the percentages of social and non-social interactions following a social interaction are calculated. In WT (blue bars) and E2-treated rescue $PV^{+/-}$ (green bars) mouse pairs, a social interaction is likely followed by another social interaction. This preference is not observed in constitutive $PV^{+/-}$ (red bars) or shPV mice, where parvalbumin (PV) is downregulated from PND18 to PND24 (orange bars); all mice were tested at PND25. It should be noted that the numbers shown (n) represent mouse pairs (i.e., the actual number of mice tested is 2n). Data for the first three groups are taken from Filice et al. (2018). Data for shPV mice is original. All other experimental details on breeding, testing, and data analysis can be found in Filice et al. (2018) and Wöhr et al. (2015) and briefly in **Supplementary Materials**. The dashed line indicates the 50% chance level. Filled and checkered bars represent social and non-social behaviors, respectively. $^{*}p < 0.05$ vs. non-social; $^{\#}p < 0.05$ vs. 50% chance level.

also involved in Ca^{2+} signaling/sequestration—especially in (pre)synaptic compartments (Devine and Kittler, 2018)—express a highly diverse set of proteins implicated in mitochondrial Ca^{2+} transport (Fecher et al., 2019), which is discussed in detail in *Effect of PV on Mitochondria, Oxidative Stress, and Pvalb Neuron Morphology: Link to NDDs*. Despite the complexity of the experimental data, certain global principles of neuronal Ca^{2+} signaling have been deduced.

The slow Ca^{2+}-binding kinetics of PV generally exclude an effect on the fast-rising phase of Ca^{2+} transients, for instance those elicited by the opening of voltage- or receptor-operated Ca^{2+} channels such as $Ca_V2.1$ (*CACNA1A*) or NMDA-type glutamate receptor (e.g., *GRIN1*). The same holds true for depolarization-evoked increases in $[Ca^{2+}]_i$ in PV-loaded chromaffin cells (Figure 7 in Lee et al., 2000). PV accelerates the initial rate of $[Ca^{2+}]_i$ decay, often transforming a monoexponential decay into a biexponential one with fast and slow decay components (τ_{fast} and τ_{slow}, respectively) (Collin et al., 2005; Muller et al., 2007). This property of PV prevents/delays the gradual buildup of presynaptic $[Ca^{2+}]_i$ (e.g., within a train of APs) that subsequently affects short-term modulation of synaptic plasticity. This has been observed in a model system based on PV-loaded chromaffin cells (Lee et al., 2000). The following aspects of PV function can be understood from this model: (1) buildup of residual $[Ca^{2+}]_i$ is delayed but not prevented; (2) the effect of PV is dependent on the time interval between stimuli and is strongest at the time point when the $[Ca^{2+}]_i$ decay curve with or without PV shows the largest difference; (3) if stimuli are long enough [i.e., all PV molecules are loaded with Ca^{2+} (last part of the rising phase in Figure 7 in Lee et al., 2000)], the maximum amplitude of the Ca^{2+} signal is independent of PV; and (4) $[Ca^{2+}]_i$ decay following such a train is slowed/prolonged by Ca^{2+}-loaded PV acting as a Ca^{2+} source ("on" mechanism). Evidence for a direct role of PV under these conditions is summarized below, although only a few selected examples are discussed; additional details can be found in the chapter on PV in Schwaller (2020).

Effect of PV on Synaptic Transmission

Higher residual Ca^{2+} in the absence of PV is the likely reason for increased paired-pulse facilitation (PPF) at the synapses between MLI and Purkinje cells (Caillard et al., 2000), hippocampal Pvalb neurons and CA1 pyramidal cells (Vreugdenhil et al., 2003),

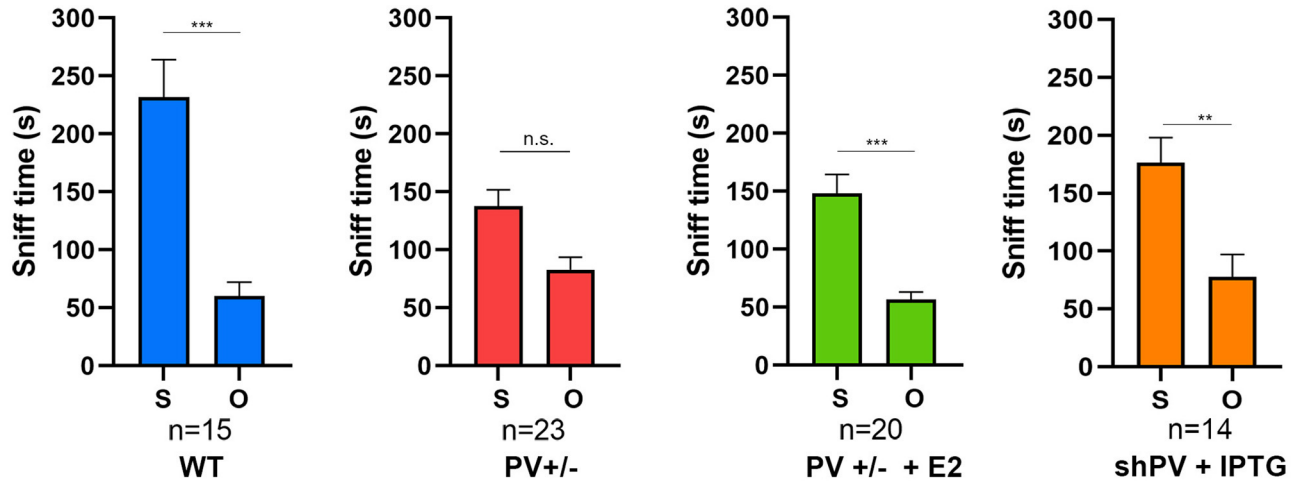

FIGURE 4 | In the three-chamber assay testing social preference during a 10 min (600 s) observation period, the sniffing time is longer with a stranger mouse (S) than with an empty cage (O) in WT mice, an effect that is lost in constitutive $PV^{+/-}$ mice (red bars). The preference for S is restored by upregulation of parvalbumin (PV) induced by E2 treatment (green bars). Data for the first three groups were previously reported (Filice et al., 2018). The preference for S is attenuated in shPV mice, in which PV is downregulated by isopropyl-β-D-thiogalactoside (IPTG) from PND18–24 (orange bars). Data for IPTG-treated shPV mice is original. All mice were tested at PND25. In the same shPV mice without IPTG treatment (sham-treated), the preference for S is similar to that of WT mice (data not shown). Data for the first three groups are from Filice et al. (2018). All other experimental details on breeding, testing, and data analysis can be found in Filice et al. (2018) and Wöhr et al. (2015). *Represents a significant preference for S over O. $^{**}p < 0.01$, $^{***}p < 0.001$; n.s., not significant.

striatal Pvalb neurons and medium spiny neurons (MSN) (Orduz et al., 2013), and at the calyx of Held, a glutamatergic synapse (Muller et al., 2007). The last of these examples is an exception, as most Pvalb neurons are GABAergic; nonetheless, it demonstrates that the inhibitory effect of PV on PPF is independent of neurotransmitter type. The prevention (reduction) of facilitation is a hallmark of PV. The PV-mediated effect size on PPF depends on many parameters but most importantly on PV concentration, stimulation frequency [interspike interval (ISI)], number of spikes, and Ca^{2+} on/off kinetics in Pvalb neurons. The role of PV as a delayed Ca^{2+} source has been investigated in less detail, although delayed release at GABAergic synapses has been observed (Lu and Trussell, 2000; Kirischuk and Grantyn, 2003). At MLI–MLI synapses, an MLI firing in bursts (10 APs) induces long-lasting asynchronous release for up to 2,400 ms after the train; the duration is much shorter (400 ms) in $PV^{-/-}$ MLIs (Collin et al., 2005). Interestingly, the IPSC integral of the delayed release in WT MLIs is greater than that of the signal generated during the AP train. Thus, the synaptic output of MLIs is random and almost constant during the interburst period; the mean signal intensity is essentially determined by the number of APs in the preceding burst. In summary, MLIs (and likely other Pvalb neurons, e.g., in the cortex) alternately adopt a phasic signaling mode during bursts and an integrating (tonic) signaling mode between bursts (Collin et al., 2005). PV has a different effect on sustained asynchronous release by layer 5 Pvalb neuron autapses in the SSC (Manseau et al., 2010). In the absence of PV, asynchronous release from the autaptic terminal is slightly but significantly increased; this decreases Pvalb neuron spike reliability and reduces the ability of pyramidal neurons to integrate incoming stimuli to produce precise firing. As each Pvalb neuron innervates multiple pyramidal neurons, asynchronous release from a single one may desynchronize a large portion of the local network and disrupt cortical information processing. While Pvalb autapses have been implicated in precise spike timing (required, for example, for synchronous oscillations) (Deleuze et al., 2019), asynchronous release reduces the spike precision and reliability of cortical neurons and thereby disrupts synchronous firing when the activity level surpasses a threshold value in order to prevent/decrease the generalized synchronous activity observed during epileptic discharges (Manseau et al., 2010). In the absence of PV (i.e., with increased asynchronous release), the onset of pentylenetetrazole-induced tonic–clonic seizures was found to be delayed in $PV^{-/-}$ mice, although the intensity of the subsequent generalized seizures was higher (Schwaller et al., 2004).

Yet another effect of PV may contribute to the modulation of intracellular Ca^{2+} signaling, especially in Pvalb neurons with high, near-millimolar PV concentrations such as MLIs (Eggermann and Jonas, 2012) and TRN neurons (Janickova et al., 2020). In these neurons, the large pool of Mg^{2+}-bound PV does not usually slow the effective Ca^{2+}-binding rate but instead contributes to the regeneration of metal-free (apo) PV that acts as a fast Ca^{2+} buffer. Therefore, Mg^{2+} binding/unbinding may serve as a metabuffering (buffering of buffering) mechanism that maintains the concentration of apo-PV during rapid, repetitive activity in fast-spiking Pvalb neurons (Eggermann and Jonas, 2012; Hu et al., 2014). While proteins including $K_V3.1b$ are a prerequisite for the fast afterhyperpolarization that characterizes Pvalb neurons, extracellular matrix molecules of the mostly negatively charged PNN components contribute to their rapid firing. PNNs are thought to establish local molecular gradients of

physiologically relevant ions such as Ca^{2+}, K^+, or Na^+ around Pvalb neuron somata (Morawski et al., 2015). Accordingly, treatment with chondroitinase ABC—a bacterial enzyme that cleaves polysaccharide chains of PNN components—significantly (∼50%) decreased Pvalb neuron firing frequency in cortical slices (Tewari et al., 2018).

PV influences spike reliability through asynchronous release and also during bursting activity. Besides the expected effect of increasing PPF at striatal Pvalb neuron–MSN synapses, the absence of PV leads to increased Pvalb neuron excitability and more regular spontaneous spiking within a train. Experimental (Orduz et al., 2013) and modeling (Bischop et al., 2012) data indicate that the likely cause of the latter is a change in the activation of small conductance (SK) Ca^{2+}-dependent K^+ channels. Thus, the presence of PV at the synapse induces arrhythmicity (i.e., increase in "jitter") by modulating intrinsic oscillations via SK channel activation (Orduz et al., 2013). The triad of SK channels, voltage-dependent Ca^{2+} channels, and sarco(endoplasmic) reticulum Ca^{2+} ATPase (SERCA) pumps enables the generation of Ca^{2+} signaling-dependent oscillatory activity in the TRN (Cueni et al., 2008); in striatal Pvalb neurons and likely in TRN Pvalb neurons, PV is a fourth component that contributes to this process by increasing the irregularity of the oscillatory spiking pattern (Orduz et al., 2013). How the absence of PV affects TRN Pvalb neuron function *in vivo* is discussed in *Striatum and TRN as a Hub in NDDs: Role of Pvalb Neurons*.

Functional phenotypes observed in $PV^{-/-}$ mice related to excitability, synaptic transmission, short-term modulation, firing properties, and network effects (e.g., oscillations) may represent the extreme end of decreased PV-induced changes because reduced but not complete loss of PV expression is usually observed in human NDDs and corresponding animal models. The functional consequences of a direct or indirect (i.e., secondary to NDD risk gene mutations) decrease in PV level are discussed here. A small hairpin (sh)RNA was used to assess the role of PV in cortical circuits of adolescent rats (PND34–38) (Caballero et al., 2020). PV level in the PFC was decreased by ∼25% at PND65, resembling the NDD rodent phenotype of lower PV expression at an older age (>PND60). In layer 5 pyramidal cells, the frequency of sIPSCs was reduced and PV deficiency was observed, which increased facilitation (i.e., a higher PPF ratio at an ISI of 50 ms). As sEPSC frequency was unchanged, the reduction in PV led to an increase in the E/I ratio in pyramidal cells. On the contrary, the frequency of sEPSCs was decreased in fast-spiking cortical Pvalb neurons. Hippocampal-evoked local field potential (LFP) responses in the PFC are affected by a lower PV level in a frequency-dependent manner: at 20 and 40 Hz, LFP facilitation occurs while control rats show LFP depression. In summary, higher PV expression is required for refinement of prefrontal GABAergic function, while its absence results in immature afferent processing and a hypofunctional state (Caballero et al., 2020).

Results from the above-described study cannot be directly compared to experiments carried out in $PV^{+/-}$ mice. Unlike in PV-shRNA rats, no data are available from $PV^{+/-}$ mice on LFPs in the PFC *in vivo* or IPSCs mediated by fast-spiking (Pvalb) neurons and EPSCs determined *ex vivo*. Moreover, behavioral data from PV-shRNA rats are sparse. In the trace fear conditioning and extinction test, acquisition of a cue-mediated fear response was unaffected by a reduction in PV level, while fear extinction was prolonged. Compared to controls, PV-shRNA rats showed increased freezing times lasting until the last trial of cue presentation (Caballero et al., 2020). Similar findings were obtained in the reward-based T-maze reversal learning assay carried out in $PV^{-/-}$ mice to assess behavioral inflexibility: while the initial learning phase was identical for WT and $PV^{-/-}$ mice, a large proportion of the latter exhibited a clear deficit in the ability to reverse their behavior in order to receive the reward (Wöhr et al., 2015). It will be interesting to determine whether PV-shRNA rats also exhibit repetitive and stereotyped ASD-like behaviors. Additionally, electrophysiological recordings of the PFC in $PV^{+/-}$ mice may reveal similarities between the two models in terms of neuronal firing properties and behavior.

Alterations in Synaptic Transmission in NDD Mouse Models Suggest PV Involvement

Mice lacking the ASD-associated gene *LMO4* (encoding an endogenous inhibitor of PTP1B phosphatase) specifically in Pvalb neurons [PV-*Lmo4* knockout (KO) mice] show increased Pvalb neuron-mediated perisomatic feedforward inhibition (likely by basket cells) onto pyramidal cells (Zhang et al., 2020a), as well as increased excitability of Pvalb neurons in the dorsal anterior cingulate cortex (dACC). Spontaneous inhibitory inputs (sIPSC amplitude) mostly from Pvalb neurons onto dACC layer 2/3 pyramidal cells are increased while excitatory inputs are less affected, resulting in a lower E/I ratio. Optogenetically induced activation of Pvalb neurons was shown to increase PPF. Differences between WT and KO mice were greatest at an ISI of around 20–50 ms, while short-term depression of IPSCs in a train (e.g., at 20 Hz) was reduced in KO mice. The broadened AP signal in PV-*Lmo4* KO mice may be attributable to a reduction in delayed rectifying potassium conductance (by $K_V1.2$ or K_V3) (Zhang et al., 2020a). Given the close association (coexpression) of PV and $K_V3.1b$ in most cortical Pvalb neurons (Chow et al., 1999), a decrease in $K_V3.1b$ is a potential mechanism for AP broadening. It is worth noting that, at the behavioral level, PV-*Lmo4*KO mice display typical ASD core symptoms of reduced social interaction and repetitive, stereotyped behaviors (**Table 1**).

As discussed above and shown in **Table 1**, PV expression is altered in several genetic and "environmental" mouse ASD models (*Animal NDD Models of ASD With Reduced PV Expression and/or Decreased Number/Altered Distribution of PV^+ Neurons*). Changes in proteins involved in synaptic transmission have been reported in these mice and are briefly summarized here. The level of *Kcnc1* transcript encoding the $K_v3.1b$ channel necessary for maintaining the fast-spiking phenotype of Pvalb neurons was decreased slightly in $PV^{-/-}$ mouse and significantly (−40%) in VPA mouse forebrain lysates (including neocortex, thalamus, and pallidus) (Lauber et al., 2016). The latter mice are characterized by reduced PV expression in the striatum (Lauber et al., 2016). In the cortex, $K_v3.1b$ shows near-perfect overlap with PV (99% of all PV^+ neurons are $K_v3.1b^+$ and vice versa) (Du et al., 1996; Chow et al., 1999; Lien and Jonas, 2003). The expression and function of hyperpolarization-activated cyclic

nucleotide-gated (HCN) channels responsible for I_h currents are important for regulating resting membrane potential, input resistance, dendritic integration, synaptic transmission, and neuronal excitability (Biel et al., 2009; Benarroch, 2013). These channels are altered in ASD mouse models, often in those with decreased PV expression. This is the case for Shank3B$^{-/-}$ mice expressing a lower level of PV in striatal Pvalb neurons (Filice et al., 2016). Cultures of developing hippocampal neurons derived from these mice show increased input resistance and excitability as well as drastically attenuated I_h currents and reduced expression of Hcn4 protein (Yi et al., 2016). Reduced *Hcn4* mRNA and PV levels are also seen in the striatum of Cntnap2$^{-/-}$ mice (Lauber et al., 2018). Moreover, *Hcn1* mRNA expression in the striatum was decreased slightly in PV$^{-/-}$ and significantly in Shank3B$^{-/-}$ mice at PND25 (Lauber et al., 2016). On the contrary, *Hcn1* mRNA and HCN1 protein levels were elevated (by ∼40%) in the forebrain of PND25 VPA mice that showed no difference in forebrain PV expression relative to the control (Lauber et al., 2016). Thus, brain region- and gene-specific (*Gad1*, *Pvalb*, *Kcnc1*, *Hcn1-4*, and *Kcnn1–4*) alterations may be responsible for (maladaptive) homeostatic mechanisms and are observed in several ASD models, mostly those with decreased PV level; some of these are likely cell autonomous and linked to Pvalb neuron hypofunction (e.g., *Gad1*, *Pvalb*, and *Kcnc1*), as are the downstream consequences of reduced (absent) PV expression such as increases in the number of mitochondria and dendritic branching (as discussed in *Effect of PV on Mitochondria, Oxidative Stress, and Pvalb Neuron Morphology: Link to NDDs*). Altered expression of HCN family members *Hcn1–4* or potassium calcium-activated channel subfamily N members 1–4 (SK channels) that are not specifically expressed in or even absent from Pvalb neurons reflect a Pvalb neuronal circuit phenotype caused by PV downregulation-mediated functional changes in Pvalb neurons. However, the putative changes (e.g., alterations in neuronal activity of one neuron subpopulation leading to parallel or hierarchical changes in others) have not been fully elucidated.

Adding yet another level of complexity, the absence of PV in striatal PV neurons has a presumed retrograde effect on the cortical glutamatergic inputs onto Pvalb neurons. In the time window (10–50 ms) when Pvalb neuron–MSN synapses show stronger facilitation in the absence of PV, PPF of EPSCs between cortical neurons and striatal Pvalb neurons—mostly mediated by AMPA receptors—is significantly reduced (Wöhr et al., 2015). The same effect is observed in PV$^{+/-}$ mice, in which a ∼50% reduction in PV level was sufficient to influence PPF at this corticostriatal synapse. Further experiments have suggested that changes in short-term plasticity at the cortical neuron–FSI synapse involve a presynaptic adaptation mechanism, possibly resulting from homeostatic plasticity in the cortical neuron caused by the absence/reduction in PV in the postsynaptic striatal Pvalb neuron. However, the lack of a direct link (synapse) between Pvalb neurons and their cortical inputs indicate a retrograde or circuit (network) effect. In summary, the removal/decrease in PV in Pvalb neurons has complex effects on intracellular Ca^{2+} signaling and synaptic transmission even without considering the changes induced at the morphological level (discussed in *Effect of PV on Mitochondria, Oxidative Stress, and Pvalb Neuron Morphology: Link to NDDs*).

Striatum and TRN as a Hub in NDDs: Role of Pvalb Neurons

Several brain regions and associated circuits have been investigated in the context of NDDs including the basal ganglia and thalamus, and especially the TRN. The basal ganglia are involved in motor learning, habit formation, and stimulus processing to generate appropriate responses; they are also implicated in mood, motivation, and decision making (goal-directed action). These processes involve the cortico–basal ganglia–thalamocortical loop in which cortical pyramidal cells project to the striatum, with striatal neurons giving rise to direct and indirect pathways. In the former, the neurons project to the internal segment of the globus pallidus, which sends efferents to the thalamus; projections from the thalamus to the cortex close the loop. In the indirect pathway, a fiber bundle from the striatum reaches the external segment of the external globus pallidus, which forms synapses with neurons of the subthalamic nucleus (STN). The STN projects to the thalamus and from there back to the cortex. The term "disclosed loop" has been used to describe a closed circuit that is open to outside influence at the initial stage of cortical input (Figure 8 in Shipp, 2017). Patients with a damaged striatum often show autistic traits (Damasio and Maurer, 1978; Maurer and Damasio, 1982) and stereotyped movements. In male mice, dorsal striatum-specific damage (by coablation of ∼40–50% Pvalb neurons and large cholinergic interneurons) results in spontaneous stereotypy and deficits in social interaction (Rapanelli et al., 2017). Restricted and repetitive behaviors are also linked to alterations in striatal and thalamic circuits (Farmer et al., 2013). Functional brain imaging studies have revealed the involvement of corticostriatal–thalamic circuits in ASD (Fuccillo, 2016), and morphological studies of the thalamus and striatum indicate differences such as a larger volume (Schuetze et al., 2016) and surface area and greater rostrocaudal variation in the shape of the thalamus in ASD patients compared to control subjects (Schuetze et al., 2019). ASD rodent models with striatal and thalamic alterations have been developed to investigate the mechanisms underlying such dysfunctions. Details on the striatal impairment in these mutant mice can be found in Table 1 of Li and Pozzo-Miller (2019).

Mutations in several ASD-associated genes affect corticostriatal connectivity (reviewed in Fuccillo, 2016; Li and Pozzo-Miller, 2019) or general striatal structure or function as observed in human ASD patients (Langen et al., 2007; Estes et al., 2011) and multiple ASD mouse models such as Fmr1$^{-/-}$ (Centonze et al., 2008), Shank3$^{-/-}$ (Peca et al., 2011), Cntnap2$^{-/-}$ (Penagarikano et al., 2011), and Cntnap4$^{-/-}$ (Karayannis et al., 2014). Another possible feature of corticostriatal dysfunction in ASD is abnormalities in Pvalb neurons, including decreased PV expression in striatal Pvalb neurons likely caused by mutations in ASD risk genes such as *CNTNAP2* and *SHANK3* (**Table 1**).

Although Pvalb neurons account for just 1% of striatal neurons (Tepper et al., 2010), they are responsible for ∼10%

of all striatal activity (Duhne et al., 2020). Striatal Pvalb neurons receive projections from different cortical regions (mainly primary motor cortex and primary SSC) as well as inhibitory input from TRN (Klug et al., 2018), which is often described as the "guardian of the gateway" (Crick, 1984), and selectively modulates the thalamocortical network, playing a critical role in sensorimotor and cognitive functions, sleep, and consciousness (Crick, 1984; Schmitt et al., 2017). It is unsurprising that abnormalities in the thalamocortical circuitry are associated with some of the sensory perceptual deficits typical of ASD; thus, TRN dysfunction is considered as a prototypical circuit endophenotype in NDDs (Krol et al., 2018). NDD risk genes associated with schizophrenia (*CACNA1I* and *GRM3*) and ASD (*CHD2* and *PTCHD1*) are strongly expressed in TRN, and as they are also thought to be linked to Pvalb neurons, results obtained in the mutant mice are discussed here. TRN neurons comprise two (mainly non-overlapping) populations characterized by expression of either PV (∼60% of neurons) or SST (∼40%) (Clemente-Perez et al., 2017; Steullet et al., 2017a). The cell types differ in terms of intrinsic membrane excitability and low-threshold Ca^{2+} current (I_T) mediated by $Ca_V3.2$ and $Ca_V3.3$ (Talley et al., 1999). Peak I_T density is higher in Pvalb neurons, suggesting that SST neurons have fewer and/or more dendritically located T-type calcium channels (Clemente-Perez et al., 2017). Hyperpolarization of TRN neurons leads to low-threshold Ca^{2+} spikes in the form of rebound bursts, each crowned by a series of APs. The maximal number of rebound bursts, number of APs after the first burst, and intraburst frequency are higher in Pvalb neurons than in SST cells (Clemente-Perez et al., 2017). $Ca_V3.3$ channels are required for TRN cell bursting and synchronized rhythmicity in the thalamic circuit. Absence of $Ca_V3.3$ channels (*Cacna1i*) in $Ca_V3.3^{-/-}$ mice decreases I_T by ∼80% and almost completely abolishes the bursting properties of TRN neurons (that likely express Pvalb) (Astori et al., 2011). A lack of $Ca_V3.3$ channels also reduces apamin-sensitive currents mediated by SK2 channels, indicating that $Ca_V3.3$/SK2 channel interactions are required for the proper functioning of the latter in TRN neurons (Cueni et al., 2008). Interestingly, KO mouse models of ASD and schizophrenia have shown similar findings with respect to TRN neuron function both *in vivo* and in slice cultures.

In vivo recordings of TRN Pvalb neurons in anesthetized $PV^{-/-}$ mice have revealed altered proportions of neurons with specific firing properties: medium-bursting (type II) neurons were more abundant than the long-bursting type (III), indicating a decrease in rebound bursting in the absence of PV. Additionally, the ISI within a burst was longer, while the number of spikes was unaffected (Alberi et al., 2013). These changes are likely associated with an altered distribution of $Ca_V3.2$ channels mediating I_T. $Ca_V3.2$ channels are more abundant at active axosomatic synapses of $PV^{-/-}$ TRN neurons as compared to WT TRN neurons, suggesting that the differential localization of $Ca_V3.2$ affects bursting dynamics. Notably, the distribution of $Ca_V3.3$ channels is similar in the two genotypes. TRN neurons express apamin-sensitive SK channels (Cueni et al., 2008), and the absence of PV is therefore presumed to have a similar effect on TRN neuron SK currents as in the striatum (Orduz et al., 2013). A cross-correlation analysis of neurons simultaneously recorded with the same electrode tip showed that ∼30% of neuron pairs tended to fire synchronously independent of PV expression. Hence, PV deficiency does not affect the functional connectivity between TRN neurons that are also coupled by chemical synapses (Zhang et al., 2020b), as is the case in cortical Pvalb neurons (Galarreta and Hestrin, 1999), but affects the distribution of $Ca_V3.2$ channels and dynamics of burst discharges in TRN cells, possibly by modulating SK channel activity. Other KO mouse models of Ca^{2+} signaling components (e.g., the schizophrenia risk gene *Disc1*) show a strong effect on the function of TRN neurons, which most likely involves SK channels (Delevich et al., 2020). In mice, patch-domain containing protein 1 (PTCHD1) is expressed almost exclusively in TRN neurons at PND0 and is still prominently expressed at PND15. $Ptchd1^{Y/-}$ mice with TRN neuron-specific deletion of the ASD- and intellectual disability-associated *Ptchd1* gene showed attention deficit and hyperactivity along with a 50% reduction in SK currents, which were rescued by a pharmacological treatment that restored SK channel function (Wells et al., 2016). Importantly, at all investigated membrane potentials of $Ptchd1^{Y/-}$ TRN neurons in cultured slices, the number of rebound bursts was smaller than in WT mice, whereas no difference was observed in I_T. Thus, the reduced bursting activity of $Ptchd1^{Y/-}$ TRN neurons is likely the result of decreased SK currents. Moreover, free $[Ca^{2+}]_i$ is significantly lower in $Ptchd1^{Y/-}$ TRN neurons, providing further evidence of altered intracellular Ca^{2+} handling.

Effect of PV on Mitochondria, Oxidative Stress, and Pvalb Neuron Morphology: Link to NDDs

The two major roles of mitochondria are the generation of ATP via oxidative phosphorylation and Ca^{2+} buffering. In neurons, these two processes occur not only globally but also locally—for example, in presynapses (reviewed in Devine and Kittler, 2018). The electrophysiological properties of Pvalb neurons require both fast presynaptic Ca^{2+} handling and sufficient energy production to sustain high-frequency firing. PV is a component of the Ca^{2+} signaling toolkit involved in the regulation of intracellular $[Ca^{2+}]_i$ (Berridge et al., 2003). A high firing rate of cortical GABAergic interneurons including Pvalb neurons is observed *in vivo*, which is more physiologically relevant than the fast-firing properties of Pvalb neurons that were mostly measured *in vitro*. Two-photon *in vivo* calcium imaging in the SSC of mice has revealed that GABAergic interneurons have higher activity than excitatory neurons, measured as event rate using the Ca^{2+} indicator GCaMP6 expressed in either neuron population (Chen et al., 2020). PV acting as a slow-onset Ca^{2+} buffer mostly serves as a "Ca^{2+} off" mechanism that reduces $[Ca^{2+}]_i$ after an initial increase in conjunction with two other essential "Ca^{2+} off" components—namely, SERCA pumps and PMCAs—that require ATP for this function. How the absence or partial downregulation of PV affects a cell expressing PV under physiological conditions remains an open question. A Ca^{2+} overlay blot with protein extracts of forebrain and cerebellum did not show upregulation of EF-hand Ca^{2+}-binding proteins similar to PV in the brain

of $PV^{-/-}$ mice (Schmidt et al., 2003). On the other hand, fast-twitch muscles of $PV^{-/-}$ mice are more resistant to fatigue as a result of increased fractional volume (density) of mitochondria (Chen et al., 2001). This inverse (antagonistic) regulation (i.e., PV downregulation and overexpression increasing and decreasing mitochondrial volume, respectively) occurs in all systems investigated to date including tissues/cells endogenously expressing PV such as fast-twitch muscle cells, kidney epithelial cells, and Pvalb neurons (Schwaller, 2020). The same mechanism exists in cells overexpressing PV including neurons of Thy-PV mice (Van Den Bosch et al., 2002; Maetzler et al., 2004), C2C12 muscle cells (Ducreux et al., 2012), MDCK kidney epithelial cells (Henzi and Schwaller, 2015), and CG4 oligodendrocyte-like cells (Lichvarova et al., 2019). Mitochondria are functionally similar to PV in terms of shaping intracellular Ca^{2+} transients: neither greatly affects the rising phase because of their slow-onset Ca^{2+}-buffering/Ca^{2+}-uptake properties but increases the rate of $[Ca^{2+}]_i$ decay, thus shortening Ca^{2+} transients, and both have anti-facilitating effects at presynaptic terminals—i.e., they accelerate recovery from synaptic depression (e.g., in the calyx of Held; Kim et al., 2005), thereby participating in the clearance of presynaptic Ca^{2+} and modulating neurotransmitter release (Billups and Forsythe, 2002). According to the notion of activity-dependent homeostatic changes/adaptations (Berridge et al., 2003), mitochondria are in the best position (with respect to Ca^{2+} signal modulation) to compensate for a loss/decrease in PV. Moreover, while SERCA pumps and PMCAs are not obviously upregulated in PV-deficient cells, they are presumed to contribute more extensively to Ca^{2+} removal in the absence of PV (although this has yet to be demonstrated). Thus, PV-deficient Pvalb neurons likely need to produce more ATP to accommodate the increased activity of Ca^{2+} extrusion systems. Ca^{2+} uptake by mitochondria is energetically costly and can only be maintained by increasing ATP production (Palmieri and Persico, 2010). Conversely, Ca^{2+} buffering by PV is an energy-saving process, as the small conformational changes in PV induced by Ca^{2+} binding/Ca^{2+} release require little energy and are independent of ATP levels.

Mitochondria were previously assumed to be homogeneous in terms of composition and function but are now known to be highly diverse within different organs (Mootha et al., 2003) and even in different cells of the brain, as demonstrated in cerebellar granule cells, Purkinje cells, and astrocytes (Fecher et al., 2019). This is also true of cell components involved in Ca^{2+} signaling, which show cell-type specific regulation (Fecher et al., 2019). Several experimental models with reduced PV expression show not only an increased mitochondrial volume but also elevated levels of mitochondrial proteins directly related to Ca^{2+} uptake. In epithelial cells of the distal convoluted tubule in mouse kidney, several genes implicated in mitochondrial Ca^{2+} uptake and generation of mitochondrial membrane potential including mitochondrial calcium uptake 1 *(Micu1)*, mitochondrial calcium uniporter regulator 1 (*Mcur1*), and mitochondrial cytochrome c oxidase subunit 1 (*mt-Co1*) are upregulated in $PV^{-/-}$ mice (Henzi and Schwaller, 2015). Levels of *COXI* and positive regulators of mitochondria biogenesis (*Ppargc1a*, *Nrf1*, and *Tfam*) are higher in PV-negative CG4 cells than in those overexpressing PV (Lichvarova et al., 2019). However, no differences are observed in the expression of mitochondrial genes directly linked to ATP synthesis such as F1-ATPase subunit (*Atp5Ff1b*) (reviewed in Schwaller, 2020), further suggesting that the increases in mitochondrial volume and protein expression likely enhance the slow Ca^{2+}-buffering capacity conferred by PV in WT cells. Additionally, transcript levels of mitochondrial uncoupler protein UCP2 (*Ucp2*) are elevated in control (PV^{-}) CG4 cells (similar to the condition in $PV^{-/-}$ mice) compared to PV-expressing CG4 cells (mimicking the condition in WT Pvalb neurons) (L. Janickova, unpublished). This is in line with RNA-seq results from cortical samples of ASD patients demonstrating that *UCP2* is among the most strongly upregulated transcripts (Parikshak et al., 2016; Schwede et al., 2018). Consistent with findings from $PV^{-/-}$ mice, transcript levels of several genes related to synaptic transmission and mitochondria are altered in ASD (Schwede et al., 2018), and expression-weighted cell type enrichment analysis of three mouse ASD and schizophrenia models revealed significant upregulation of mitochondrial genes in fast-firing inhibitory (presumably Pvalb) neurons, while mitochondrial protein levels showed a global downregulation in the cortex (Gordon et al., 2019).

The increase in the density of mitochondria is not homogeneous in the soma of Pvalb neurons and is mostly observed in the region adjacent to the plasma membrane in Purkinje cells (Chen et al., 2006) as well as in striatal and TRN Pvalb neurons (Janickova and Schwaller, 2020). Previously, it was unclear whether this is an on/off or precisely regulated mechanism. Analyses of nine different Pvalb neuron populations from five different brain regions (hippocampus, cortex, striatum, cerebellum, and TRN) selected based on moderate-to-strong PV staining revealed a strong positive correlation between the magnitude of the increase in mitochondrial density and estimated PV concentrations in Pvalb neurons of WT mice—i.e., a higher PV concentration was associated with a greater PV deficiency-induced increase in mitochondrial density (but not in the length of individual mitochondria). Such an increase exists not only in $PV^{-/-}$ Pvalb neuron somata but also in the dendrites (Janickova et al., 2020), confirming an earlier finding that mitochondrial density was higher in control CG4 (PV^{-}) cells than in those overexpressing PV (Lichvarova et al., 2019). In particular, more mitochondria are present at the end of elongating processes and near the growth cone in control CG4 cells, which likely promotes process branching similar to what is observed in $PV^{-/-}$ striatal and TRN Pvalb neurons (Janickova et al., 2020). Whether increased dendrite length and branching in the absence of PV results in local hyperconnectivity as observed in several ASD mouse models (Table 1 in Janickova et al., 2020) remains to be determined. More detailed information on mitochondria and branching can be found in the Discussion of Janickova et al. (2020).

The fast-firing property of Pvalb neurons is associated with their high energy demand (Kann et al., 2014; Kann et al., 2014); accordingly, Pvalb neurons contain significantly more mitochondria in their somata, dendrites, and axons than any other interneuron subtype or pyramidal cells. This makes Pvalb neurons especially vulnerable to metabolic stress and/or excessive

formation of reactive oxygen and nitrogen species (ROS and NOS, respectively) (Kann, 2016). ROS production increases with age in Pvalb neurons of WT mice and is highly correlated with PV concentration but not mitochondrial density, which is similar (∼8%) in all investigated Pvalb neurons (Janickova and Schwaller, 2020); that is, between the ages of 1 and 6 months, a higher PV concentration is associated with an age-dependent increase in ROS production. Importantly, in the absence of PV, ROS production is significantly higher in mice older than 1 month and the relative increase is approximately proportional to the PV concentration in WT Pvalb neurons (Janickova and Schwaller, 2020). An elevation in ROS levels causing an imbalance in redox homeostasis has been suggested as a pathophysiological mechanism of ASD (Tang et al., 2013; Pangrazzi et al., 2020). Increased ROS levels have also been observed in postmortem brain tissue of children with ASD (Siddiqui et al., 2016).

Increased mitochondrial ROS production and Pvalb neuron impairment (possibly linked to decreased PV level) have been causally linked to schizophrenia etiology and pathology (reviewed in Hardingham and Do, 2016; Steullet et al., 2016, 2017b). In $Gclm^{-/-}$ mice—a schizophrenia mouse model deficient in the glutamate cysteine ligase modifier subunit, the rate-limiting enzyme for glutathione biosynthesis (Cabungcal et al., 2019)—the number of PV^{+}/PNN^{+} neurons is decreased. This may be due to Pvalb neuron loss or a decrease in PV expression and altered molecular composition of PNNs, possibly as a result of neuron immaturity (Steullet et al., 2017a). In brain slices from $Gclm^{-/-}$ mice, most TRN neurons were shown to fire in a tonic mode at a membrane potential of −70 mV, whereas ∼80% neurons in WT mice exhibit bursting behavior. At more negative membrane potentials (−80 and −90 mV), no differences in bursting behavior existed between genotypes. While membrane potential-dependent differences in firing behavior of TRN neurons are correlated with decreased PV level in $Gclm^{-/-}$ TRN neurons, a causal relationship between these events has yet to be established. Notably, a decrease in the number of PV^{+} neurons in the TRN has been reported in other ASD models showing behavioral phenotypes such as the Engrailed-2 KO mice ($En2^{-/-}$) and abnormal spindle-like microcephaly-associated gene (Aspm1–7) mutants (Garrett et al., 2020; Pirone et al., 2020). Whether this is due to PV downregulation—and the electrophysiological consequences thereof—remains unclear.

Brain-development-dependent mitochondrial alterations (dysfunction) may trigger a cascade of events that leads to NDDs such as ASD or schizophrenia (Tang et al., 2013; Cabungcal et al., 2019). However, at least in 1 month-old $PV^{-/-}$ mice showing no increase in ROS production (Janickova and Schwaller, 2020) but exhibiting robust ASD-like behaviors, excessive oxidative stress can be excluded as the main contributor to the ASD phenotype. The onset of oxidative-stress-induced Pvalb neuron dysfunction may occur at a later age and result in a schizophrenia-like rather than an ASD-like phenotype, although this is speculative and must be tested in longitudinal studies using different NDD mouse models. Supporting the oxidative stress hypothesis of NDD, inhibiting oxidative stress in schizophrenia patients by treatment with the antioxidant N-acetyl-cysteine (NAC) significantly improved neurocognition and alleviated positive clinical symptoms (Klauser et al., 2018; Retsa et al., 2018). However, in young individuals with ASD, NAC treatment for 12 weeks boosted glutathione production but did not improve social interaction deficits (Wink et al., 2016). Meanwhile, symptoms of irritability were attenuated in children with ASD who were treated with NAC (Hardan et al., 2012). Additional studies are required to determine whether NAC can reduce ASD core symptoms.

CONCLUSIONS AND OUTLOOK

We have formulated the Parvalbumin Hypothesis of ASD based on experimental data (new and previously published) (**Figure 1**). This hypothesis pertaining to the etiology of ASD (and possibly schizophrenia) provides a framework for future research and allows the formulation of predictions that can be tested in human ASD postmortem brain samples or using the many existing animal models of ASD. This hypothesis does not hold true for all ASD cases and may even be restricted to a small number of cases with known genetic mutations or environmental perturbations in which downregulation of PV has been reported. The validation of a hub consisting of PV-expressing neurons in ASD is expected to facilitate the development of therapeutic strategies that restore brain function(s) in ASD and possibly other NDDs.

DATA AVAILABILITY STATEMENT

The raw data of novel experiments described in the article supporting the conclusions of this article will be made available by the authors, without undue reservation.

ETHICS STATEMENT

The animal study was reviewed and approved by the Cantonal Veterinary Office (Canton of Fribourg, Switzerland). Experiments were performed according to institutional guidelines of the present Swiss law and the European Communities Council Directive of 24 November 1986 (86/609/EEC). The authorization number for housing of mice is H-04.2012-Fr and for the experiments 2016_37_FR and 2019_24_FR.

AUTHOR CONTRIBUTIONS

FF, LJ, TH, AB, and BS contributed to data collection (literature research). FF, TH, and AB carried out the experiments and performed data analysis. BS conceived the concept of the article. All authors were involved in writing the paper and read and approved the final manuscript.

FUNDING

The experimental part of this study was supported by a Simons Foundation Autism Research Initiative (SFARI) Explorer award

(# 603695) to BS and by the Swiss National Science Foundation SNF grants # 155952 and 184668 to BS.

ACKNOWLEDGMENTS

We thank all investigators and collaborators in the many research labs (>35) worldwide (>10 countries) with whom we have had the privilege of collaborating and publishing many findings on the role of PV in the last two decades. The integration of results obtained in different transgenic mouse lines, various tissues and organs (brain, fast-twitch muscle, and kidney), and in cell-based systems allowed us to develop the Parvalbumin Hypothesis of ASD. Additionally, we thank Simone Eichenberger, Natascha Bersier, and Marie Bardet (University of Fribourg) for assistance in maintaining the mouse facility and Valerie Salicio, Marlene Sanchez, and Anne Oberson for technical assistance.

SUPPLEMENTARY MATERIAL

The Supplementary Material for this article can be found online at: https://www.frontiersin.org/articles/10.3389/fncel.2020.577525/full#supplementary-material

REFERENCES

Alberi, L., Lintas, A., Kretz, R., Schwaller, B., and Villa, A. E. (2013). The calcium-binding protein parvalbumin modulates the firing 1 properties of the reticular thalamic nucleus bursting neurons. *J. Neurophysiol.* 109, 2827–2841. doi: 10.1152/jn.00375.2012

Antoine, M. W., Langberg, T., Schnepel, P., and Feldman, D. E. (2019). Increased excitation-inhibition ratio stabilizes synapse and circuit excitability in four autism mouse models. *Neuron* 101, 648–661.e644. doi: 10.1016/j.neuron.2018.12.026

Ariza, J., Rogers, H., Hashemi, E., Noctor, S. C., and Martinez-Cerdeno, V. (2018). The number of chandelier and basket cells are differentially decreased in prefrontal cortex in autism. *Cereb. Cortex* 28, 411–420. doi: 10.1093/cercor/bhw349

Astori, S., Wimmer, R. D., Prosser, H. M., Corti, C., Corsi, M., Liaudet, N., et al. (2011). The Ca(V)3.3 calcium channel is the major sleep spindle pacemaker in thalamus. *Proc. Natl. Acad. Sci. U. S. A.* 108, 13823–13828. doi: 10.1073/pnas.1105115108

Balemans, M. C. M., Huibers, M. M. H., Eikelenboom, N. W. D., Kuipers, A. J., Van Summeren, R. C. J., Pijpers, M. M. C. A., et al. (2010). Reduced exploration, increased anxiety, and altered social behavior: autistic-like features of euchromatin histone methyltransferase 1 heterozygous knockout mice. *Behav. Brain Res.* 208, 47–55. doi: 10.1016/j.bbr.2009.11.008

Banerjee, A., Garcia-Oscos, F., Roychowdhury, S., Galindo, L. C., Hall, S., Kilgard, M. P., et al. (2013). Impairment of cortical GABAergic synaptic transmission in an environmental rat model of autism. *Int. J. Neuropsychopharmacol.* 16, 1309–1318. doi: 10.1017/S1461145712001216

Bayer, K. U., and Schulman, H. (2019). CaM kinase: still inspiring at 40. *Neuron* 103, 380–394. doi: 10.1016/j.neuron.2019.05.033

Ben-Ari, Y. (2002). Excitatory actions of gaba during development: the nature of the nurture. *Nat. Rev. Neurosci.* 3, 728–739. doi: 10.1038/nrn920

Ben-Ari, Y., Cherubini, E., Corradetti, R., and Gaiarsa, J. L. (1989). Giant synaptic potentials in immature rat CA3 hippocampal neurones. *J. Physiol.* 416, 303–325. doi: 10.1113/jphysiol.1989.sp017762

Benarroch, E. E. (2013). HCN channels: function and clinical implications. *Neurology* 80, 304–310. doi: 10.1212/WNL.0b013e31827dec42

Berridge, M. J., Bootman, M. D., and Roderick, H. L. (2003). Calcium signalling: dynamics, homeostasis and remodelling. *Nat. Rev. Mol. Cell Biol.* 4, 517–529. doi: 10.1038/nrm1155

Biel, M., Wahl-Schott, C., Michalakis, S., and Zong, X. (2009). Hyperpolarization-activated cation channels: from genes to function. *Physiol. Rev.* 89, 847–885. doi: 10.1152/physrev.00029.2008

Billups, B., and Forsythe, I. D. (2002). Presynaptic mitochondrial calcium sequestration influences transmission at mammalian central synapses. *J. Neurosci.* 22, 5840–5847. doi: 10.1523/JNEUROSCI.22-14-05840.2002

Bischop, D. P., Orduz, D., Lambot, L., Schiffmann, S. N., and Gall, D. (2012). Control of neuronal excitability by calcium binding proteins: a new mathematical model for striatal fast-spiking interneurons. *Front. Mol. Neurosci.* 5:78. doi: 10.3389/fnmol.2012.00078

Brielmaier, J., Matteson, P. G., Silverman, J. L., Senerth, J. M., Kelly, S., Genestine, M., et al. (2012). Autism-relevant social abnormalities and cognitive deficits in engrailed-2 knockout mice. *PLoS ONE* 7:e40914. doi: 10.1371/journal.pone.0040914

Butt, S. J., Stacey, J. A., Teramoto, Y., and Vagnoni, C. (2017). A role for GABAergic interneuron diversity in circuit development and plasticity of the neonatal cerebral cortex. *Curr. Opin. Neurobiol.* 43, 149–155. doi: 10.1016/j.conb.2017.03.011

Caballero, A., Flores-Barrera, E., Thomases, D. R., and Tseng, K. Y. (2020). Downregulation of parvalbumin expression in the prefrontal cortex during adolescence causes enduring prefrontal disinhibition in adulthood. *Neuropsychopharmacology* 45, 1527–1535. doi: 10.1038/s41386-020-0709-9

Cabungcal, J. H., Steullet, P., Kraftsik, R., Cuenod, M., and Do, K. Q. (2019). A developmental redox dysregulation leads to spatio-temporal deficit of parvalbumin neuron circuitry in a schizophrenia mouse model. *Schizophr. Res.* 213, 96–106. doi: 10.1016/j.schres.2019.02.017

Caillard, O., Moreno, H., Schwaller, B., Llano, I., Celio, M. R., and Marty, A. (2000). Role of the calcium-binding protein parvalbumin in short-term synaptic plasticity. *Proc. Natl. Acad. Sci. U. S. A.* 97, 13372–13377. doi: 10.1073/pnas.230362997

Calfa, G., Li, W., Rutherford, J. M., and Pozzo-Miller, L. (2015). Excitation/inhibition imbalance and impaired synaptic inhibition in hippocampal area CA3 of Mecp2 knockout mice. *Hippocampus* 25, 159–168. doi: 10.1002/hipo.22360

Cao, W., Lin, S., Xia, Q. Q., Du, Y. L., Yang, Q., Zhang, M. Y., et al. (2018). Gamma oscillation dysfunction in mPFC leads to social deficits in neuroligin 3 R451C knockin mice. *Neuron* 97, 1253–1260.e1257. doi: 10.1016/j.neuron.2018.02.001

Celio, M. R. (1990). Calbindin D-28k and parvalbumin in the rat nervous system. *Neuroscience* 35, 375–475. doi: 10.1016/0306-4522(90)90091-H

Celio, M. R., Spreafico, R., de Biasi, S., and Vitellaro-Zuccarello, L. (1998). Perineuronal nets: past and present. *Trends Neurosci.* 21, 510–515. doi: 10.1016/S0166-2236(98)01298-3

Centonze, D., Rossi, S., Mercaldo, V., Napoli, I., Ciotti, M. T., De Chiara, V., et al. (2008). Abnormal striatal GABA transmission in the mouse model for the fragile X syndrome. *Biol. Psychiatry* 63, 963–973. doi: 10.1016/j.biopsych.2007.09.008

Chao, H. T., Chen, H., Samaco, R. C., Xue, M., Chahrour, M., Yoo, J., et al. (2010). Dysfunction in GABA signalling mediates autism-like stereotypies and Rett syndrome phenotypes. *Nature* 468, 263–269. doi: 10.1038/nature09582

Chen, G., Carroll, S., Racay, P., Dick, J., Pette, D., Traub, I., et al. (2001). Deficiency in parvalbumin increases fatigue resistance in fast-twitch muscle and upregulates mitochondria. *Am. J. Physiol. Cell Physiol.* 281, C114–122. doi: 10.1152/ajpcell.2001.281.1.C114

Chen, G., Racay, P., Bichet, S., Celio, M. R., Eggli, P., and Schwaller, B. (2006). Deficiency in parvalbumin, but not in calbindin D-28k upregulates mitochondrial volume and decreases smooth endoplasmic reticulum surface selectively in a peripheral, subplasmalemmal region in the soma of Purkinje cells. *Neuroscience* 142, 97–105. doi: 10.1016/j.neuroscience.2006.06.008

Chen, L., and Toth, M. (2001). Fragile X mice develop sensory hyperreactivity to auditory stimuli. *Neuroscience* 103, 1043–1050. doi: 10.1016/S0306-4522(01)00036-7

Chen, Q., Deister, C. A., Gao, X., Guo, B., Lynn-Jones, T., Chen, N., et al. (2020). Dysfunction of cortical GABAergic neurons leads to sensory hyper-reactivity in a Shank3 mouse model of ASD. *Nat. Neurosci.* 23, 520–532. doi: 10.1038/s41593-020-0598-6

Chow, A., Erisir, A., Farb, C., Nadal, M. S., Ozaita, A., Lau, D., et al. (1999). K(+) channel expression distinguishes subpopulations of parvalbumin- and somatostatin-containing neocortical interneurons. *J. Neurosci.* 19, 9332–9345. doi: 10.1523/JNEUROSCI.19-21-09332.1999

Chow, M. L., Pramparo, T., Winn, M. E., Barnes, C. C., Li, H. R., Weiss, L., et al. (2012). Age-dependent brain gene expression and copy number anomalies in autism suggest distinct pathological processes at young versus mature ages. *PLoS Genet.* 8:e1002592. doi: 10.1371/journal.pgen.1002592

Clemente-Perez, A., Makinson, S. R., Higashikubo, B., Brovarney, S., Cho, F. S., Urry, A., et al. (2017). Distinct thalamic reticular cell types differentially modulate normal and pathological cortical rhythms. *Cell Rep* 19, 2130–2142. doi: 10.1016/j.celrep.2017.05.044

Cohen, S. M., Ma, H., Kuchibhotla, K. V., Watson, B. O., Buzsaki, G., Froemke, R. C., et al. (2016). Excitation-transcription coupling in parvalbumin-positive interneurons employs a novel CaM kinase-dependent pathway distinct from excitatory neurons. *Neuron* 90, 292–307. doi: 10.1016/j.neuron.2016.03.001

Collin, T., Chat, M., Lucas, M. G., Moreno, H., Racay, P., Schwaller, B., et al. (2005). Developmental changes in parvalbumin regulate presynaptic Ca^{2+} signaling. *J. Neurosci.* 25, 96–107. doi: 10.1523/JNEUROSCI.3748-04.2005

Crick, F. (1984). Function of the thalamic reticular complex: the searchlight hypothesis. *Proc. Natl. Acad. Sci. U. S. A.* 81, 4586–4590. doi: 10.1073/pnas.81.14.4586

Cueni, L., Canepari, M., Lujan, R., Emmenegger, Y., Watanabe, M., Bond, C. T., et al. (2008). T-type Ca^{2+} channels, SK2 channels and SERCAs gate sleep-related oscillations in thalamic dendrites. *Nat. Neurosci.* 11, 683–692. doi: 10.1038/nn.2124

Damasio, A. R., and Maurer, R. G. (1978). A neurological model for childhood autism. *Arch. Neurol.* 35, 777–786. doi: 10.1001/archneur.1978.00500360001001

Deleuze, C., Bhumbra, G. S., Pazienti, A., Lourenco, J., Mailhes, C., Aguirre, A., et al. (2019). Strong preference for autaptic self-connectivity of neocortical PV interneurons facilitates their tuning to gamma-oscillations. *PLoS Biol.* 17:e3000419. doi: 10.1371/journal.pbio.3000419

Delevich, K., Jaaro-Peled, H., Penzo, M., Sawa, A., and Li, B. (2020). Parvalbumin interneuron dysfunction in a thalamo-prefrontal cortical circuit in disc1 locus impairment mice. *eNeuro* 7:ENEURO.0496-19.2020. doi: 10.1523/ENEURO.0496-19.2020

Devine, M. J., and Kittler, J. T. (2018). Mitochondria at the neuronal presynapse in health and disease. *Nat. Rev. Neurosci.* 19, 63–80. doi: 10.1038/nrn.2017.170

Du, J., Zhang, L., Weiser, M., Rudy, B., and Mcbain, C. J. (1996). Developmental expression and functional characterization of the potassium-channel subunit Kv3.1b in parvalbumin-containing interneurons of the rat hippocampus. *J. Neurosci.* 16, 506–518. doi: 10.1523/JNEUROSCI.16-02-00506.1996

Ducreux, S., Gregory, P., and Schwaller, B. (2012). Inverse regulation of mitochondrial volume and the cytosolic Ca^{2+} buffer parvalbumin in muscle cells via SIRT-1/PGC-1α axis. *PLoS ONE* 7:e44837. doi: 10.1371/journal.pone.0044837

Duhne, M., Lara-Gonzalez, E., Laville, A., Padilla-Orozco, M., Avila-Cascajares, F., Arias-Garcia, M., et al. (2020). Activation of parvalbumin-expressing neurons reconfigures neuronal ensembles in murine striatal microcircuits. *Eur. J. Neurosci.* 1–16. doi: 10.1111/ejn.14670

Durand, S., Patrizi, A., Quast, K. B., Hachigian, L., Pavlyuk, R., Saxena, A., et al. (2012). NMDA receptor regulation prevents regression of visual cortical function in the absence of Mecp2. *Neuron* 76, 1078–1090. doi: 10.1016/j.neuron.2012.12.004

Eberhard, M., and Erne, P. (1994). Calcium and magnesium binding to rat parvalbumin. *Eur. J. Biochem.* 222, 21–26. doi: 10.1111/j.1432-1033.1994.tb18836.x

Ebert, D. H., and Greenberg, M. E. (2013). Activity-dependent neuronal signalling and autism spectrum disorder. *Nature* 493, 327–337. doi: 10.1038/nature11860

Eggermann, E., and Jonas, P. (2012). How the 'slow' Ca^{2+} buffer parvalbumin affects transmitter release in nanodomain-coupling regimes. *Nat. Neurosci.* 15, 20–22. doi: 10.1038/nn.3002

Estes, A., Shaw, D. W., Sparks, B. F., Friedman, S., Giedd, J. N., Dawson, G., et al. (2011). Basal ganglia morphometry and repetitive behavior in young children with autism spectrum disorder. *Autism Res.* 4, 212–220. doi: 10.1002/aur.193

Etherton, M., Foldy, C., Sharma, M., Tabuchi, K., Liu, X., Shamloo, M., et al. (2011). Autism-linked neuroligin-3 R451C mutation differentially alters hippocampal and cortical synaptic function. *Proc. Natl. Acad. Sci. U. S. A.* 108, 13764–13769. doi: 10.1073/pnas.1111093108

Farmer, C., Thurm, A., and Grant, P. (2013). Pharmacotherapy for the core symptoms in autistic disorder: current status of the research. *Drugs* 73, 303–314. doi: 10.1007/s40265-013-0021-7

Farre-Castany, M. A., Schwaller, B., Gregory, P., Barski, J., Mariethoz, C., Eriksson, J. L., et al. (2007). Differences in locomotor behavior revealed in mice deficient for the calcium-binding proteins parvalbumin, calbindin D-28k or both. *Behav. Brain Res.* 178, 250–261. doi: 10.1016/j.bbr.2007.01.002

Fecher, C., Trovo, L., Muller, S. A., Snaidero, N., Wettmarshausen, J., Heink, S., et al. (2019). Cell-type-specific profiling of brain mitochondria reveals functional and molecular diversity. *Nat. Neurosci.* 22, 1731–1742. doi: 10.1038/s41593-019-0479-z

Ferguson, B. R., and Gao, W. J. (2018). PV interneurons: critical regulators of e/i balance for prefrontal cortex-dependent behavior and psychiatric disorders. *Front. Neural Circuits* 12:37. doi: 10.3389/fncir.2018.00037

Filice, F., Blum, W., Lauber, E., and Schwaller, B. (2019). Inducible and reversible silencing of the Pvalb gene in mice: an *in vitro* and *in vivo* study. *Eur. J. Neurosci.* 50, 2694–2706. doi: 10.1111/ejn.14404

Filice, F., Lauber, E., Vorckel, K. J., Wöhr, M., and Schwaller, B. (2018). 17-beta estradiol increases parvalbumin levels in Pvalb heterozygous mice and attenuates behavioral phenotypes with relevance to autism core symptoms. *Mol. Autism* 9:15. doi: 10.1186/s13229-018-0199-3

Filice, F., Vorckel, K. J., Sungur, A. O., Wöhr, M., and Schwaller, B. (2016). Reduction in parvalbumin expression not loss of the parvalbumin-expressing GABA interneuron subpopulation in genetic parvalbumin and shank mouse models of autism. *Mol. Brain* 9:10. doi: 10.1186/s13041-016-0192-8

Frankland, P. W., Wang, Y., Rosner, B., Shimizu, T., Balleine, B. W., Dykens, E. M., et al. (2004). Sensorimotor gating abnormalities in young males with fragile X syndrome and Fmr1-knockout mice. *Mol. Psychiatry* 9, 417–425. doi: 10.1038/sj.mp.4001432

Frega, M., Selten, M., Mossink, B., Keller, J. M., Linda, K., Moerschen, R., et al. (2020). Distinct pathogenic genes causing intellectual disability and autism exhibit a common neuronal network hyperactivity phenotype. *Cell Rep.* 30, 173–186. doi: 10.1016/j.celrep.2019.12.002

Fuccillo, M. V. (2016). Striatal circuits as a common node for autism pathophysiology. *Front. Neurosci.* 10:27. doi: 10.3389/fnins.2016.00027

Fujimoto, N., Igarashi, K., Kanno, J., Honda, H., and Inoue, T. (2004). Identification of estrogen-responsive genes in the GH3 cell line by cDNA microarray analysis. *J. Steroid Biochem. Mol. Biol.* 91, 121–129. doi: 10.1016/j.jsbmb.2004.02.006

Gala, R., Budzillo, A., Baftizadeh, F., Miller, J., Gouwens, N., Arkhipov, A., et al. (2020). Consistent cross-modal identification of cortical neurons with coupled autoencoders. *bioRxiv* doi: 10.1101/2020.06.30.181065

Galarreta, M., and Hestrin, S. (1999). A network of fast-spiking cells in the neocortex connected by electrical synapses. *Nature* 402, 72–75. doi: 10.1038/47029

Gandal, M. J., Edgar, J. C., Ehrlichman, R. S., Mehta, M., Roberts, T. P., and Siegel, S. J. (2010). Validating gamma oscillations and delayed auditory responses as translational biomarkers of autism. *Biol. Psychiatry* 68, 1100–1106. doi: 10.1016/j.biopsych.2010.09.031

Gandal, M. J., Nesbitt, A. M., Mccurdy, R. M., and Alter, M. D. (2012). Measuring the maturity of the fast-spiking interneuron transcriptional program in autism, schizophrenia, and bipolar disorder. *PLoS ONE* 7:e41215. doi: 10.1371/journal.pone.0041215

Garbett, K., Ebert, P. J., Mitchell, A., Lintas, C., Manzi, B., Mirnics, K., et al. (2008). Immune transcriptome alterations in the temporal cortex of subjects with autism. *Neurobiol. Dis.* 30, 303–311. doi: 10.1016/j.nbd.2008.01.012

Garrett, L., Chang, Y. J., Niedermeier, K. M., Heermann, T., Enard, W., Fuchs, H., et al. (2020). A truncating Aspm allele leads to a complex cognitive phenotype

and region-specific reductions in parvalbuminergic neurons. *Transl. Psychiatry* 10:66. doi: 10.1038/s41398-020-0686-0

Gibson, J. R., Bartley, A. F., Hays, S. A., and Huber, K. M. (2008). Imbalance of neocortical excitation and inhibition and altered UP states reflect network hyperexcitability in the mouse model of fragile X syndrome. *J. Neurophysiol.* 100, 2615–2626. doi: 10.1152/jn.90752.2008

Gogolla, N., Leblanc, J. J., Quast, K. B., Sudhof, T. C., Fagiolini, M., and Hensch, T. K. (2009). Common circuit defect of excitatory-inhibitory balance in mouse models of autism. *J. Neurodev. Disord.* 1, 172–181. doi: 10.1007/s11689-009-9023-x

Gogolla, N., Takesian, A. E., Feng, G., Fagiolini, M., and Hensch, T. K. (2014). Sensory integration in mouse insular cortex reflects GABA circuit maturation. *Neuron* 83, 894–905. doi: 10.1016/j.neuron.2014.06.033

Gordon, A., Forsingdal, A., Klewe, I. V., Nielsen, J., Didriksen, M., Werge, T., et al. (2019). Transcriptomic networks implicate neuronal energetic abnormalities in three mouse models harboring autism and schizophrenia-associated mutations. *Mol. Psychiatry*. doi: 10.1038/s41380-019-0576-0

Gouwens, N. W., Sorensen, S. A., Baftizadeh, F., Budzillo, A., Lee, B. R., Jarsky, T., et al. (2020). Toward an integrated classification of neuronal cell types: morphoelectric and transcriptomic characterization of individual GABAergic cortical neurons. *Cell.* 183:935–953.e19. doi: 10.1016/j.cell.2020.09.057

Hardan, A. Y., Fung, L. K., Libove, R. A., Obukhanych, T. V., Nair, S., Herzenberg, L. A., et al. (2012). A randomized controlled pilot trial of oral N-acetylcysteine in children with autism. *Biol. Psychiatry* 71, 956–961. doi: 10.1016/j.biopsych.2012.01.014

Hardingham, G. E., and Do, K. Q. (2016). Linking early-life NMDAR hypofunction and oxidative stress in schizophrenia pathogenesis. *Nat. Rev. Neurosci.* 17, 125–134. doi: 10.1038/nrn.2015.19

Härtig, W., Brauer, K., and Bruckner, G. (1992). Wisteria floribunda agglutinin-labelled nets surround parvalbumin-containing neurons. *Neuroreport* 3, 869–872. doi: 10.1097/00001756-199210000-00012

Hashemi, E., Ariza, J., Rogers, H., Noctor, S. C., and Martinez-Cerdeno, V. (2017). The number of parvalbumin-expressing interneurons is decreased in the prefrontal cortex in autism. *Cereb. Cortex* 27, 1931–1943. doi: 10.1093/cercor/bhw021

Hashemi, E., Ariza, J., Rogers, H., Noctor, S. C., and Martinez-Cerdeno, V. (2018). The number of parvalbumin-expressing interneurons is decreased in the prefrontal cortex in autism. *Cereb. Cortex* 28:690. doi: 10.1093/cercor/bhx063

Henzi, T., and Schwaller, B. (2015). Antagonistic regulation of parvalbumin expression and mitochondrial calcium handling capacity in renal epithelial cells. *PLoS ONE* 10:e0142005. doi: 10.1371/journal.pone.0142005

Hodge, R. D., Bakken, T. E., Miller, J. A., Smith, K. A., Barkan, E. R., Graybuck, L. T., et al. (2019). Conserved cell types with divergent features in human versus mouse cortex. *Nature* 573, 61–68. doi: 10.1038/s41586-019-1506-7

Hu, H., Gan, J., and Jonas, P. (2014). Interneurons. Fast-spiking, parvalbumin(+) GABAergic interneurons: from cellular design to microcircuit function. *Science* 345:1255263. doi: 10.1126/science.1255263

Ito-Ishida, A., Ure, K., Chen, H., Swann, J. W., and Zoghbi, H. Y. (2015). Loss of MeCP2 in parvalbumin-and somatostatin-expressing neurons in mice leads to distinct rett syndrome-like phenotypes. *Neuron* 88, 651–658. doi: 10.1016/j.neuron.2015.10.029

Janickova, L., Rechberger, K. F., Wey, L., and Schwaller, B. (2020). Absence of parvalbumin increases mitochondria volume and branching of dendrites in Pvalb neurons *in vivo*: a point of convergence of autism spectrum disorder (ASD) risk gene phenotypes. *Mol. Autism* 11:47. doi: 10.1186/s13229-020-00323-8

Janickova, L., and Schwaller, B. (2020). Parvalbumin-deficiency accelerates the age-dependent ROS production in Pvalb neurons *in vivo*: link to neurodevelopmental disorders. *Front. Cell Neurosci.* 14:571216. doi: 10.3389/fncel.2020.571216

Jaramillo, T. C., Xuan, Z., Reimers, J. M., Escamilla, C. O., Liu, S., and Powell, C. M. (2020). Early restoration of Shank3 expression in Shank3 knockout mice prevents core ASD-like behavioural phenotypes. *eNeuro*. doi: 10.1523/ENEURO.0332-19.2020

Jurgensen, S., and Castillo, P. E. (2015). Selective dysregulation of hippocampal inhibition in the mouse lacking autism candidate gene CNTNAP2. *J. Neurosci.* 35, 14681–14687. doi: 10.1523/JNEUROSCI.1666-15.2015

Kann, O. (2016). The interneuron energy hypothesis: implications for brain disease. *Neurobiol. Dis.* 90, 75–85. doi: 10.1016/j.nbd.2015.08.005

Kann, O., Papageorgiou, I. E., and Draguhn, A. (2014). Highly energized inhibitory interneurons are a central element for information processing in cortical networks. *J. Cereb. Blood Flow Metab.* 34, 1270–1282. doi: 10.1038/jcbfm.2014.104

Karayannis, T., Au, E., Patel, J. C., Kruglikov, I., Markx, S., Delorme, R., et al. (2014). Cntnap4 differentially contributes to GABAergic and dopaminergic synaptic transmission. *Nature* 511, 236–240. doi: 10.1038/nature13248

Kawaguchi, Y., and Kubota, Y. (1997). GABAergic cell subtypes and their synaptic connections in rat frontal cortex. *Cereb. Cortex* 7, 476–486. doi: 10.1093/cercor/7.6.476

Kim, M. H., Korogod, N., Schneggenburger, R., Ho, W. K., and Lee, S. H. (2005). Interplay between Na^+/Ca^{2+} exchangers and mitochondria in Ca^{2+} clearance at the calyx of Held. *J. Neurosci.* 25, 6057–6065. doi: 10.1523/JNEUROSCI.0454-05.2005

Kim, Y., Yang, G. R., Pradhan, K., Venkataraju, K. U., Bota, M., Garcia Del Molino, L. C., et al. (2017). Brain-wide maps reveal stereotyped cell-type-based cortical architecture and subcortical sexual dimorphism. *Cell* 171, 456–469.e422. doi: 10.1016/j.cell.2017.09.020

Kirischuk, S., and Grantyn, R. (2003). Intraterminal Ca^{2+} concentration and asynchronous transmitter release at single GABAergic boutons in rat collicular cultures. *J. Physiol.* 548, 753–764. doi: 10.1113/jphysiol.2002.037036

Klauser, P., Xin, L., Fournier, M., Griffa, A., Cleusix, M., Jenni, R., et al. (2018). N-acetylcysteine add-on treatment leads to an improvement of fornix white matter integrity in early psychosis: a double-blind randomized placebo-controlled trial. *Transl. Psychiatry* 8:220. doi: 10.1038/s41398-018-0266-8

Klug, J. R., Engelhardt, M. D., Cadman, C. N., Li, H., Smith, J. B., Ayala, S., et al. (2018). Differential inputs to striatal cholinergic and parvalbumin interneurons imply functional distinctions. *Elife* 7:e35657. doi: 10.7554/eLife.35657.020

Krishnan, K., Wang, B. S., Lu, J., Wang, L., Maffei, A., Cang, J., et al. (2015). MeCP2 regulates the timing of critical period plasticity that shapes functional connectivity in primary visual cortex. *Proc. Natl. Acad. Sci. U. S. A.* 112, E4782–4791. doi: 10.1073/pnas.1506499112

Krol, A., Wimmer, R. D., Halassa, M. M., and Feng, G. (2018). Thalamic reticular dysfunction as a circuit endophenotype in neurodevelopmental disorders. *Neuron* 98, 282–295. doi: 10.1016/j.neuron.2018.03.021

Langen, M., Durston, S., Staal, W. G., Palmen, S. J., and Van Engeland, H. (2007). Caudate nucleus is enlarged in high-functioning medication-naive subjects with autism. *Biol. Psychiatry* 62, 262–266. doi: 10.1016/j.biopsych.2006.09.040

Lauber, E., Filice, F., and Schwaller, B. (2016). Prenatal valproate exposure differentially affects parvalbumin-expressing neurons and related circuits in the cortex and striatum of mice. *Front. Mol. Neurosci.* 9:150. doi: 10.3389/fnmol.2016.00150

Lauber, E., Filice, F., and Schwaller, B. (2018). Dysregulation of parvalbumin expression in the cntnap2-/- mouse model of autism spectrum disorder. *Front. Mol. Neurosci.* 11:262. doi: 10.3389/fnmol.2018.00262

Leblanc, J. J., and Fagiolini, M. (2011). Autism: a "critical period" disorder? *Neural Plast.* 2011:921680. doi: 10.1155/2011/921680

Lee, E., Lee, J., and Kim, E. (2017). Excitation/inhibition imbalance in animal models of autism spectrum disorders. *Biol. Psychiatry* 81, 838–847. doi: 10.1016/j.biopsych.2016.05.011

Lee, S. H., Schwaller, B., and Neher, E. (2000). Kinetics of Ca^{2+} binding to parvalbumin in bovine chromaffin cells: implications for $[Ca^{2+}]$ transients of neuronal dendrites. *J. Physiol.* (525 Pt 2), 419–432. doi: 10.1111/j.1469-7793.2000.t01-2-00419.x

Leonzino, M., Busnelli, M., Antonucci, F., Verderio, C., Mazzanti, M., and Chini, B. (2016). The timing of the excitatory-to-inhibitory GABA switch is regulated by the oxytocin receptor via KCC2. *Cell Rep.* 15, 96–103. doi: 10.1016/j.celrep.2016.03.013

Li, W., and Pozzo-Miller, L. (2019). Dysfunction of the corticostriatal pathway in autism spectrum disorders. *J. Neurosci. Res.* 98:2130–2147. doi: 10.1002/jnr.24560

Lichvarova, L., Blum, W., Schwaller, B., and Szabolcsi, V. (2019). Parvalbumin expression in oligodendrocyte-like CG4 cells causes a reduction in

mitochondrial volume, attenuation in reactive oxygen species production and a decrease in cell processes' length and branching. *Sci. Rep.* 9:10603. doi: 10.1038/s41598-019-47112-9

Lien, C. C., and Jonas, P. (2003). Kv3 potassium conductance is necessary and kinetically optimized for high-frequency action potential generation in hippocampal interneurons. *J. Neurosci.* 23, 2058–2068. doi: 10.1523/JNEUROSCI.23-06-02058.2003

Lim, L., Mi, D., Llorca, A., and Marin, O. (2018). Development and functional diversification of cortical interneurons. *Neuron* 100, 294–313. doi: 10.1016/j.neuron.2018.10.009

Lu, T., and Trussell, L. O. (2000). Inhibitory transmission mediated by asynchronous transmitter release. *Neuron* 26, 683–694. doi: 10.1016/S0896-6273(00)81204-0

Maetzler, W., Nitsch, C., Bendfeldt, K., Racay, P., Vollenweider, F., and Schwaller, B. (2004). Ectopic parvalbumin expression in mouse forebrain neurons increases excitotoxic injury provoked by ibotenic acid injection into the striatum. *Exp. Neurol.* 186, 78–88. doi: 10.1016/j.expneurol.2003.10.014

Manseau, F., Marinelli, S., Mendez, P., Schwaller, B., Prince, D. A., Huguenard, J. R., et al. (2010). Desynchronization of neocortical networks by asynchronous release of GABA at autaptic and synaptic contacts from fast-spiking interneurons. *PLoS Biol.* 8:e1000492. doi: 10.1371/journal.pbio.1000492

Marin, O. (2012). Interneuron dysfunction in psychiatric disorders. *Nat. Rev. Neurosci.* 13, 107–120. doi: 10.1038/nrn3155

Marino, M., Galluzzo, P., and Ascenzi, P. (2006). Estrogen signaling multiple pathways to impact gene transcription. *Curr. Genomics* 7, 497–508. doi: 10.2174/138920206779315737

Markram, K., Rinaldi, T., La Mendola, D., Sandi, C., and Markram, H. (2008). Abnormal fear conditioning and amygdala processing in an animal model of autism. *Neuropsychopharmacology* 33, 901–912. doi: 10.1038/sj.npp.1301453

Maurer, R. G., and Damasio, A. R. (1982). Childhood autism from the point of view of behavioral neurology. *J. Autism Dev. Disord.* 12, 195–205. doi: 10.1007/BF01531309

McFarlane, H. G., Kusek, G. K., Yang, M., Phoenix, J. L., Bolivar, V. J., and Crawley, J. N. (2008). Autism-like behavioral phenotypes in BTBR T+tf/J mice. *Genes Brain Behav.* 7, 152–163. doi: 10.1111/j.1601-183X.2007.00330.x

Mei, Y., Monteiro, P., Zhou, Y., Kim, J. A., Gao, X., Fu, Z., et al. (2016). Adult restoration of Shank3 expression rescues selective autistic-like phenotypes. *Nature* 530, 481–484. doi: 10.1038/nature16971

Modi, B., Pimpinella, D., Pazienti, A., Zacchi, P., Cherubini, E., and Griguoli, M. (2019). Possible implication of the CA2 hippocampal circuit in social cognition deficits observed in the neuroligin 3 knock-out mouse, a non-syndromic animal model of autism. *Front. Psychiatry* 10:513. doi: 10.3389/fpsyt.2019.00513

Mootha, V. K., Bunkenborg, J., Olsen, J. V., Hjerrild, M., Wisniewski, J. R., Stahl, E., et al. (2003). Integrated analysis of protein composition, tissue diversity, and gene regulation in mouse mitochondria. *Cell* 115, 629–640. doi: 10.1016/S0092-8674(03)00926-7

Morawski, M., Reinert, T., Meyer-Klaucke, W., Wagner, F. E., Troger, W., Reinert, A., et al. (2015). Ion exchanger in the brain: Quantitative analysis of perineuronally fixed anionic binding sites suggests diffusion barriers with ion sorting properties. *Sci. Rep.* 5:16471. doi: 10.1038/srep16471

Muller, M., Felmy, F., Schwaller, B., and Schneggenburger, R. (2007). Parvalbumin is a mobile presynaptic Ca^{2+} buffer in the calyx of held that accelerates the decay of Ca^{2+} and short-term facilitation. *J. Neurosci.* 27, 2261–2271. doi: 10.1523/JNEUROSCI.5582-06.2007

Negwer, M., Piera, K., Hesen, R., Lutje, L., Aarts, L., Schubert, D., et al. (2020). EHMT1 regulates Parvalbumin-positive interneuron development and GABAergic input in sensory cortical areas. *Brain Struct. Funct.* doi: 10.1007/s00429-020-02149-9

Nelson, S. B., and Valakh, V. (2015). Excitatory/inhibitory balance and circuit homeostasis in autism spectrum disorders. *Neuron* 87, 684–698. doi: 10.1016/j.neuron.2015.07.033

Nobili, A., Krashia, P., Cordella, A., La Barbera, L., Dell'acqua, M. C., Caruso, A., et al. (2018). Ambra1 shapes hippocampal inhibition/excitation balance: role in neurodevelopmental disorders. *Mol. Neurobiol.* 55, 7921–7940. doi: 10.1007/s12035-018-0911-5

Oblak, A. L., Rosene, D. L., Kemper, T. L., Bauman, M. L., and Blatt, G. J. (2011). Altered posterior cingulate cortical cyctoarchitecture, but normal density of neurons and interneurons in the posterior cingulate cortex and fusiform gyrus in autism. *Autism Res.* 4, 200–211. doi: 10.1002/aur.188

Okaty, B. W., Miller, M. N., Sugino, K., Hempel, C. M., and Nelson, S. B. (2009). Transcriptional and electrophysiological maturation of neocortical fast-spiking GABAergic interneurons. *J. Neurosci.* 29, 7040–7052. doi: 10.1523/JNEUROSCI.0105-09.2009

Orduz, D., Bischop, D. P., Schwaller, B., Schiffmann, S. N., and Gall, D. (2013). Parvalbumin tunes spike-timing and efferent short-term plasticity in striatal fast spiking interneurons. *J. Physiol.* 591, 3215–3232. doi: 10.1113/jphysiol.2012.250795

Palmieri, L., and Persico, A. M. (2010). Mitochondrial dysfunction in autism spectrum disorders: cause or effect? *Biochim. Biophys. Acta* 1797, 1130–1137. doi: 10.1016/j.bbabio.2010.04.018

Pangrazzi, L., Balasco, L., and Bozzi, Y. (2020). Oxidative stress and immune system dysfunction in autism spectrum disorders. *Int. J. Mol. Sci.* 21:3293. doi: 10.3390/ijms21093293

Parikshak, N. N., Swarup, V., Belgard, T. G., Irimia, M., Ramaswami, G., Gandal, M. J., et al. (2016). Genome-wide changes in lncRNA, splicing, and regional gene expression patterns in autism. *Nature* 540, 423–427. doi: 10.1038/nature20612

Patrizi, A., Awad, P. N., Chattopadhyaya, B., Li, C., Di Cristo, G., and Fagiolini, M. (2019). Accelerated hyper-maturation of parvalbumin circuits in the absence of MeCP2. *Cereb. Cortex*. 30, 256–268. doi: 10.1093/cercor/bhz085

Peca, J., Feliciano, C., Ting, J. T., Wang, W., Wells, M. F., Venkatraman, T. N., et al. (2011). Shank3 mutant mice display autistic-like behaviours and striatal dysfunction. *Nature* 472, 437–442. doi: 10.1038/nature09965

Penagarikano, O., Abrahams, B. S., Herman, E. I., Winden, K. D., Gdalyahu, A., Dong, H., et al. (2011). Absence of CNTNAP2 leads to epilepsy, neuronal migration abnormalities, and core autism-related deficits. *Cell* 147, 235–246. doi: 10.1016/j.cell.2011.08.040

Pietropaolo, S., Guilleminot, A., Martin, B., D'amato, F. R., and Crusio, W. E. (2011). Genetic-background modulation of core and variable autistic-like symptoms in Fmr1 knock-out mice. *PLoS ONE* 6:e17073. doi: 10.1371/journal.pone.0017073

Pirone, A., Viaggi, C., Cantile, C., Giannessi, E., Pardini, C., Vaglini, F., et al. (2020). Morphological alterations of the reticular thalamic nucleus in Engrailed-2 knockout mice. *J. Anat.* 236, 883–890. doi: 10.1111/joa.13150

Polepalli, J. S., Wu, H., Goswami, D., Halpern, C. H., Sudhof, T. C., and Malenka, R. C. (2017). Modulation of excitation on parvalbumin interneurons by neuroligin-3 regulates the hippocampal network. *Nat. Neurosci.* 20, 219–229. doi: 10.1038/nn.4471

Provenzano, G., Gilardoni, A., Maggia, M., Pernigo, M., Sgado, P., Casarosa, S., et al. (2020). Altered expression of GABAergic markers in the forebrain of young and adult Engrailed-2 knockout mice. *Genes* 11:384. doi: 10.3390/genes11040384

Rapanelli, M., Frick, L. R., Xu, M. Y., Groman, S. M., Jindachomthong, K., Tamamaki, N., et al. (2017). Targeted interneuron depletion in the dorsal striatum produces autism-like behavioral abnormalities in male but not female mice. *Biol. Psychiatry* 82, 194–203. doi: 10.1016/j.biopsych.2017.01.020

Reilly, M. P., Weeks, C. D., Topper, V. Y., Thompson, L. M., Crews, D., and Gore, A. C. (2015). The effects of prenatal PCBs on adult social behavior in rats. *Horm. Behav.* 73, 47–55. doi: 10.1016/j.yhbeh.2015.06.002

Retsa, C., Knebel, J. F., Geiser, E., Ferrari, C., Jenni, R., Fournier, M., et al. (2018). Treatment in early psychosis with N-acetyl-cysteine for 6months improves low-level auditory processing: Pilot study. *Schizophr. Res.* 191, 80–86. doi: 10.1016/j.schres.2017.07.008

Rothwell, P. E., Fuccillo, M. V., Maxeiner, S., Hayton, S. J., Gokce, O., Lim, B. K., et al. (2014). Autism-associated neuroligin-3 mutations commonly impair striatal circuits to boost repetitive behaviors. *Cell* 158, 198–212. doi: 10.1016/j.cell.2014.04.045

Rubenstein, J. L., and Merzenich, M. M. (2003). Model of autism: increased ratio of excitation/inhibition in key neural systems. *Genes Brain Behav.* 2, 255–267. doi: 10.1034/j.1601-183X.2003.00037.x

Satterstrom, F. K., Kosmicki, J. A., Wang, J. B., Breen, M. S., De Rubeis, S., An, J. Y., et al. (2020). Large-scale exome sequencing study implicates both developmental and functional changes in the neurobiology of autism. *Cell* 180:568. doi: 10.1016/j.cell.2019.12.036

Scattoni, M. L., Ricceri, L., and Crawley, J. N. (2011). Unusual repertoire of vocalizations in adult BTBR T+tf/J mice during three types of social encounters. *Genes Brain Behav.* 10, 44–56. doi: 10.1111/j.1601-183X.2010.00623.x

Schmidt, H., Stiefel, K. M., Racay, P., Schwaller, B., and Eilers, J. (2003). Mutational analysis of dendritic Ca^{2+} kinetics in rodent Purkinje cells: role of parvalbumin and calbindin D28k. *J. Physiol.* 551, 13–32. doi: 10.1113/jphysiol.2002.035824

Schmitt, L. I., Wimmer, R. D., Nakajima, M., Happ, M., Mofakham, S., and Halassa, M. M. (2017). Thalamic amplification of cortical connectivity sustains attentional control. *Nature* 545, 219–223. doi: 10.1038/nature22073

Schneider, T., and Przewlocki, R. (2005). Behavioral alterations in rats prenatally exposed to valproic acid: animal model of autism. *Neuropsychopharmacology* 30, 80–89. doi: 10.1038/sj.npp.1300518

Schuetze, M., Cho, I. Y. K., Vinette, S., Rivard, K. B., Rohr, C. S., Ten Eycke, K., et al. (2019). Learning with individual-interest outcomes in Autism spectrum disorder. *Dev. Cogn. Neurosci.* 38:100668. doi: 10.1016/j.dcn.2019.100668

Schuetze, M., Park, M. T., Cho, I. Y., Macmaster, F. P., Chakravarty, M. M., and Bray, S. L. (2016). Morphological alterations in the thalamus, striatum, and pallidum in autism spectrum disorder. *Neuropsychopharmacology* 41, 2627–2637. doi: 10.1038/npp.2016.64

Schwaller, B. (2020). Cytosolic Ca^{2+} buffers are inherently Ca^{2+} signal modulators. *Cold Spring Harb. Perspect. Biol.* 12:a035543. doi: 10.1101/cshperspect.a035543

Schwaller, B., Tetko, I. V., Tandon, P., Silveira, D. C., Vreugdenhil, M., Henzi, T., et al. (2004). Parvalbumin deficiency affects network properties resulting in increased susceptibility to epileptic seizures. *Mol. Cell. Neurosci.* 25, 650–663. doi: 10.1016/j.mcn.2003.12.006

Schwede, M., Nagpal, S., Gandal, M. J., Parikshak, N. N., Mirnics, K., Geschwind, D. H., et al. (2018). Strong correlation of downregulated genes related to synaptic transmission and mitochondria in post-mortem autism cerebral cortex. *J. Neurodev. Disord.* 10:18. doi: 10.1186/s11689-018-9237-x

Selby, L., Zhang, C., and Sun, Q. Q. (2007). Major defects in neocortical GABAergic inhibitory circuits in mice lacking the fragile X mental retardation protein. *Neurosci. Lett.* 412, 227–232. doi: 10.1016/j.neulet.2006.11.062

Selten, M., Van Bokhoven, H., and Nadif Kasri, N. (2018). Inhibitory control of the excitatory/inhibitory balance in psychiatric disorders. *F1000Res* 7:23. doi: 10.12688/f1000research.12155.1

Shipp, S. (2017). The functional logic of corticostriatal connections. *Brain Struct. Funct.* 222, 669–706. doi: 10.1007/s00429-016-1250-9

Siddiqui, M. F., Elwell, C., and Johnson, M. H. (2016). Mitochondrial dysfunction in autism spectrum disorders. *Autism Open Access* 6:1000190. doi: 10.4172/2165-7890.1000190

Soghomonian, J. J., Zhang, K., Reprakash, S., and Blatt, G. J. (2017). Decreased parvalbumin mRNA levels in cerebellar Purkinje cells in autism. *Autism Res.* 10, 1787–1796. doi: 10.1002/aur.1835

Somogyi, P., and Klausberger, T. (2005). Defined types of cortical interneurone structure space and spike timing in the hippocampus. *J. Physiol.* 562, 9–26. doi: 10.1113/jphysiol.2004.078915

Speed, H. E., Masiulis, I., Gibson, J. R., and Powell, C. M. (2015). Increased cortical inhibition in autism-linked neuroligin-3R451C mice is due in part to loss of endocannabinoid signaling. *PLoS ONE* 10:e0140638. doi: 10.1371/journal.pone.0140638

Stephenson, D. T., O'neill, S. M., Narayan, S., Tiwari, A., Arnold, E., Samaroo, H. D., et al. (2011). Histopathologic characterization of the BTBR mouse model of autistic-like behavior reveals selective changes in neurodevelopmental proteins and adult hippocampal neurogenesis. *Mol. Autism* 2:7. doi: 10.1186/2040-2392-2-7

Steullet, P., Cabungcal, J. H., Bukhari, S. A., Ardelt, M. I., Pantazopoulos, H., Hamati, F., et al. (2017a). The thalamic reticular nucleus in schizophrenia and bipolar disorder: role of parvalbumin-expressing neuron networks and oxidative stress. *Mol. Psychiatry.* 23, 2057–2065. doi: 10.1038/mp.2017.230

Steullet, P., Cabungcal, J. H., Coyle, J., Didriksen, M., Gill, K., Grace, A. A., et al. (2017b). Oxidative stress-driven parvalbumin interneuron impairment as a common mechanism in models of schizophrenia. *Mol. Psychiatry* 22, 936–943. doi: 10.1038/mp.2017.47

Steullet, P., Cabungcal, J. H., Monin, A., Dwir, D., O'donnell, P., Cuenod, M., et al. (2016). Redox dysregulation, neuroinflammation, and NMDA receptor hypofunction: a "central hub" in schizophrenia pathophysiology? *Schizophr. Res.* 176, 41–51. doi: 10.1016/j.schres.2014.06.021

Stoner, R., Chow, M. L., Boyle, M. P., Sunkin, S. M., Mouton, P. R., Roy, S., et al. (2014). Patches of disorganization in the neocortex of children with autism. *N. Engl. J. Med.* 370, 1209–1219. doi: 10.1056/NEJMoa1307491

Sztainberg, Y., Chen, H. M., Swann, J. W., Hao, S., Tang, B., Wu, Z., et al. (2015). Reversal of phenotypes in MECP2 duplication mice using genetic rescue or antisense oligonucleotides. *Nature* 528, 123–126. doi: 10.1038/nature16159

Tabuchi, K., Blundell, J., Etherton, M. R., Hammer, R. E., Liu, X., Powell, C. M., et al. (2007). A neuroligin-3 mutation implicated in autism increases inhibitory synaptic transmission in mice. *Science* 318, 71–76. doi: 10.1126/science.1146221

Takesian, A. E., Bogart, L. J., Lichtman, J. W., and Hensch, T. K. (2018). Inhibitory circuit gating of auditory critical-period plasticity. *Nat. Neurosci.* 21, 218–227. doi: 10.1038/s41593-017-0064-2

Talley, E. M., Cribbs, L. L., Lee, J. H., Daud, A., Perez-Reyes, E., and Bayliss, D. A. (1999). Differential distribution of three members of a gene family encoding low voltage-activated (T-type) calcium channels. *J. Neurosci.* 19, 1895–1911. doi: 10.1523/JNEUROSCI.19-06-01895.1999

Tang, G., Gutierrez Rios, P., Kuo, S. H., Akman, H. O., Rosoklija, G., Tanji, K., et al. (2013). Mitochondrial abnormalities in temporal lobe of autistic brain. *Neurobiol. Dis.* 54, 349–361. doi: 10.1016/j.nbd.2013.01.006

Tepper, J. M., Tecuapetla, F., Koos, T., and Ibanez-Sandoval, O. (2010). Heterogeneity and diversity of striatal GABAergic interneurons. *Front. Neuroanat.* 4:150. doi: 10.3389/fnana.2010.00150

Tewari, B. P., Chaunsali, L., Campbell, S. L., Patel, D. C., Goode, A. E., and Sontheimer, H. (2018). Perineuronal nets decrease membrane capacitance of peritumoral fast spiking interneurons in a model of epilepsy. *Nat. Commun.* 9:4724. doi: 10.1038/s41467-018-07113-0

Toledo-Rodriguez, M., Blumenfeld, B., Wu, C., Luo, J., Attali, B., Goodman, P., et al. (2004). Correlation maps allow neuronal electrical properties to be predicted from single-cell gene expression profiles in rat neocortex. *Cereb. Cortex* 14, 1310–1327. doi: 10.1093/cercor/bhh092

Toledo-Rodriguez, M., Goodman, P., Illic, M., Wu, C., and Markram, H. (2005). Neuropeptide and calcium-binding protein gene expression profiles predict neuronal anatomical type in the juvenile rat. *J. Physiol.* 567, 401–413. doi: 10.1113/jphysiol.2005.089250

Tripathi, P. P., Sgado, P., Scali, M., Viaggi, C., Casarosa, S., Simon, H. H., et al. (2009). Increased susceptibility to kainic acid-induced seizures in Engrailed-2 knockout mice. *Neuroscience* 159, 842–849. doi: 10.1016/j.neuroscience.2009.01.007

Van Den Bosch, L., Schwaller, B., Vleminckx, V., Meijers, B., Stork, S., Ruehlicke, T., et al. (2002). Protective effect of parvalbumin on excitotoxic motor neuron death. *Exp. Neurol.* 174, 150–161. doi: 10.1006/exnr.2001.7858

Vogt, D., Cho, K. K. A., Shelton, S. M., Paul, A., Huang, Z. J., Sohal, V. S., et al. (2018). Mouse Cntnap2 and human CNTNAP2 ASD alleles cell autonomously regulate pv+ cortical interneurons. *Cereb. Cortex* 28, 3868–3879. doi: 10.1093/cercor/bhx248

Voineagu, I., Wang, X., Johnston, P., Lowe, J. K., Tian, Y., Horvath, S., et al. (2011). Transcriptomic analysis of autistic brain reveals convergent molecular pathology. *Nature* 474, 380–384. doi: 10.1038/nature10110

Vreugdenhil, M., Jefferys, J. G., Celio, M. R., and Schwaller, B. (2003). Parvalbumin-deficiency facilitates repetitive IPSCs and gamma oscillations in the hippocampus. *J. Neurophysiol.* 89, 1414–1422. doi: 10.1152/jn.00576.2002

Wang, D., and Fawcett, J. (2012). The perineuronal net and the control of CNS plasticity. *Cell Tissue Res.* 349, 147–160. doi: 10.1007/s00441-012-1375-y

Wang, Y., Dye, C. A., Sohal, V., Long, J. E., Estrada, R. C., Roztocil, T., et al. (2010). Dlx5 and Dlx6 regulate the development of parvalbumin-expressing cortical interneurons. *J. Neurosci.* 30, 5334–5345. doi: 10.1523/JNEUROSCI.5963-09.2010

Wells, M. F., Wimmer, R. D., Schmitt, L. I., Feng, G., and Halassa, M. M. (2016). Thalamic reticular impairment underlies attention deficit in Ptchd1(Y/-) mice. *Nature* 532, 58–63. doi: 10.1038/nature17427

Wen, T. H., Lovelace, J. W., Ethell, I. M., Binder, D. K., and Razak, K. A. (2019). Developmental changes in EEG phenotypes in a mouse model of fragile X syndrome. *Neuroscience* 398, 126–143. doi: 10.1016/j.neuroscience.2018.11.047

Whitney, E. R., Kemper, T. L., Rosene, D. L., Bauman, M. L., and Blatt, G. J. (2009). Density of cerebellar basket and stellate cells in autism: evidence for a late developmental loss of Purkinje cells. *J. Neurosci. Res.* 87, 2245–2254. doi: 10.1002/jnr.22056

Wink, L. K., Adams, R., Wang, Z. M., Klaunig, J. E., Plawecki, M. H., Posey, D. J., et al. (2016). A randomized placebo-controlled pilot study of N-acetylcysteine in youth with autism spectrum disorder. *Mol. Autism* 7:26. doi: 10.1186/s13229-016-0088-6

Wöhr, M., Orduz, D., Gregory, P., Moreno, H., Khan, U., Vorckel, K. J., et al. (2015). Lack of parvalbumin in mice leads to behavioral deficits relevant to all human autism core symptoms and related neural morphofunctional abnormalities. *Transl. Psychiatry* 5:e525. doi: 10.1038/tp.2015.19

Ye, Q., and Miao, Q. L. (2013). Experience-dependent development of perineuronal nets and chondroitin sulfate proteoglycan receptors in mouse visual cortex. *Matrix Biol.* 32, 352–363. doi: 10.1016/j.matbio.2013.04.001

Yi, F., Danko, T., Botelho, S. C., Patzke, C., Pak, C., Wernig, M., et al. (2016). Autism-associated SHANK3 haploinsufficiency causes Ih channelopathy in human neurons. *Science* 352:aaf2669. doi: 10.1126/science.aaf2669

Zhang, L., Qin, Z., Ricke, K. M., Cruz, S. A., Stewart, A. F. R., and Chen, H. H. (2020a). Hyperactivated PTP1B phosphatase in parvalbumin neurons alters anterior cingulate inhibitory circuits and induces autism-like behaviors. *Nat. Commun.* 11:1017. doi: 10.1038/s41467-020-14813-z

Zhang, Y., Liu, C., Zhang, L., Zhou, W., Yu, S., Yi, R., et al. (2020b). Effects of propofol on electrical synaptic strength in coupling reticular thalamic GABAergic parvalbumin-expressing neurons. *Front. Neurosci.* 14:364. doi: 10.3389/fnins.2020.00364

Zikopoulos, B., and Barbas, H. (2013). Altered neural connectivity in excitatory and inhibitory cortical circuits in autism. *Front. Hum. Neurosci.* 7:609. doi: 10.3389/fnhum.2013.00609

Conflict of Interest: The authors declare that the research was conducted in the absence of any commercial or financial relationships that could be construed as a potential conflict of interest.

frontiers in Cellular Neuroscience

REVIEW
published: 13 January 2021
doi: 10.3389/fncel.2020.611379

Cell Adhesion Molecules Involved in Neurodevelopmental Pathways Implicated in 3p-Deletion Syndrome and Autism Spectrum Disorder

*Josan Gandawijaya[1], Rosemary A. Bamford[1], J. Peter H. Burbach[2] and Asami Oguro-Ando[1]**

[1] University of Exeter Medical School, University of Exeter, Exeter, United Kingdom, [2] Department of Translational Neuroscience, Brain Center Rudolf Magnus, University Medical Center Utrecht and Utrecht University, Utrecht, Netherlands

OPEN ACCESS

Edited by:
Yu-Chih Lin, Hussman Institute for Autism, United States

Reviewed by:
Deanna L. Benson, Icahn School of Medicine at Mount Sinai, United States
Xiaobing Yuan, East China Normal University, China
Vladimir Sytnyk, University of New South Wales, Australia

***Correspondence:**
Asami Oguro-Ando
A.Oguro-Ando@exeter.ac.uk

Specialty section:
This article was submitted to Cellular Neuropathology, a section of the journal Frontiers in Cellular Neuroscience

Received: *28 September 2020*
Accepted: *15 December 2020*
Published: *13 January 2021*

Citation:
Gandawijaya J, Bamford RA, Burbach JPH and Oguro-Ando A (2021) Cell Adhesion Molecules Involved in Neurodevelopmental Pathways Implicated in 3p-Deletion Syndrome and Autism Spectrum Disorder. Front. Cell. Neurosci. 14:611379. doi: 10.3389/fncel.2020.611379

Autism spectrum disorder (ASD) is characterized by impaired social interaction, language delay and repetitive or restrictive behaviors. With increasing prevalence, ASD is currently estimated to affect 0.5–2.0% of the global population. However, its etiology remains unclear due to high genetic and phenotypic heterogeneity. Copy number variations (CNVs) are implicated in several forms of syndromic ASD and have been demonstrated to contribute toward ASD development by altering gene dosage and expression. Increasing evidence points toward the p-arm of chromosome 3 (chromosome 3p) as an ASD risk locus. Deletions occurring at chromosome 3p result in 3p-deletion syndrome (Del3p), a rare genetic disorder characterized by developmental delay, intellectual disability, facial dysmorphisms and often, ASD or ASD-associated behaviors. Therefore, we hypothesize that overlapping molecular mechanisms underlie the pathogenesis of Del3p and ASD. To investigate which genes encoded in chromosome 3p could contribute toward Del3p and ASD, we performed a comprehensive literature review and collated reports investigating the phenotypes of individuals with chromosome 3p CNVs. We observe that high frequencies of CNVs occur in the 3p26.3 region, the terminal cytoband of chromosome 3p. This suggests that CNVs disrupting genes encoded within the 3p26.3 region are likely to contribute toward the neurodevelopmental phenotypes observed in individuals affected by Del3p. The 3p26.3 region contains three consecutive genes encoding closely related neuronal immunoglobulin cell adhesion molecules (IgCAMs): *Close Homolog of L1* (*CHL1*), *Contactin-6* (*CNTN6*), and *Contactin-4* (*CNTN4*). CNVs disrupting these neuronal IgCAMs may contribute toward ASD phenotypes as they have been associated with key roles in neurodevelopment. CHL1, CNTN6, and CNTN4 have been observed to promote neurogenesis and neuronal survival, and regulate neuritogenesis and synaptic function. Furthermore, there is evidence that these neuronal IgCAMs possess overlapping interactomes and participate in common signaling pathways regulating axon guidance. Notably, mouse models deficient for these neuronal IgCAMs do not display strong deficits in axonal migration or behavioral phenotypes, which is in contrast

to the pronounced defects in neuritogenesis and axon guidance observed *in vitro*. This suggests that when CHL1, CNTN6, or CNTN4 function is disrupted by CNVs, other neuronal IgCAMs may suppress behavioral phenotypes by compensating for the loss of function.

Keywords: 3p-deletion syndrome, autism spectrum disorder, copy number variation, IgCAM, neurogenesis, axon guidance, synaptic plasticity

INTRODUCTION

Autism Spectrum Disorder

Autism spectrum disorder (ASD) describes a group of neurodevelopmental disorders characterized by three core behavior domains: deficits in social interaction, delayed language development and repetitive or restrictive behaviors (American Psychiatric Association, 2013). ASD is currently estimated to affect 0.5–2.0% of the global population, with ever-increasing prevalence (Zablotsky et al., 2015; World Health Organization, 2019; Centers for Disease Control and Prevention, 2020; Maenner et al., 2020; May et al., 2020; Shaw et al., 2020). In addition to its phenotypic heterogeneity, several studies have reported associations between ASD and other neurodevelopmental and neuropsychiatric disorders, including but not limited to schizophrenia (Zheng et al., 2018; De Crescenzo et al., 2019), epilepsy (Besag, 2018), and major depressive disorder (Magnuson and Constantino, 2011). Individuals with ASD frequently present with intellectual and learning disabilities, demonstrating impaired cognitive function (Srivastava and Schwartz, 2014). Although ASD etiology remains unclear, several studies have demonstrated that ASD possesses a strong genetic component, with concordance rates in monozygotic twins as high as 95% (Abrahams and Geschwind, 2008; Sandin et al., 2014; Colvert et al., 2015; De La Torre-Ubieta et al., 2016; Ramaswami and Geschwind, 2018; Rylaarsdam and Guemez-Gamboa, 2019). The increased power of modern DNA sequencing technologies and number of ASD case-parent trio studies has allowed researchers to identify common inherited and rare *de novo* mutations that confer risk toward ASD development, and to date hundreds of ASD candidate genes have been reported (Rylaarsdam and Guemez-Gamboa, 2019).

Copy Number Variations and Their Contribution to Autism Spectrum Disorder Genetics

Copy number variations (CNVs) are structural genetic changes whereby segments of DNA on a chromosome – usually defined as greater than 1 kb in size – become deleted or duplicated through erroneous DNA replication (**Figure 1**). CNVs can be inherited or arise *de novo* and alter gene dosage (i.e., the number of copies of alleles of a given gene) and expression (i.e., the amount of a gene transcribed as RNA or translated into protein) (Gamazon and Stranger, 2015). Large CNVs (greater than 1 Mb) were among the first types of *de novo* genetic variation discovered in ASD and more recently, smaller CNVs have been associated with ASD as well (Ramaswami and Geschwind, 2018). Notably, individuals with ASD are observed to carry significantly more CNVs than their unaffected siblings or control subjects (Sebat et al., 2007; Pinto et al., 2010; Levy et al., 2011; Leppa et al., 2016). Multiple CNVs occurring at several loci including chromosomes 7q, 15q, 16p, 22q, and others have been implicated in ASD (Jacquemont et al., 2006; Marshall et al., 2008; Bucan et al., 2009; Glessner et al., 2009; Ramaswami and Geschwind, 2018). These CNVs cause clinically defined syndromes that are often comorbid with ASD, so called "syndromic" forms of ASD. Studying these rare genetic syndromes and how they overlap with ASD phenotypes will reveal candidate genes and convergent molecular pathways linking various forms of ASD. In this review, we will focus on CNVs occurring in the p-arm of chromosome 3 (henceforth referred to as chromosome 3p) and how they contribute toward ASD risk.

Copy Number Variations in Chromosome 3p26.3 as Risk Factors for ASD

There is increasing evidence that CNVs occurring at chromosome 3p contribute toward ASD risk. Deletions at chromosome 3p result in 3p-deletion syndrome (Del3p),

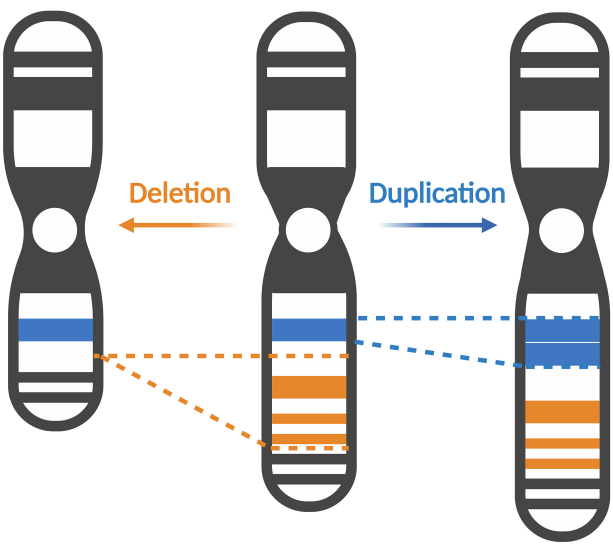

FIGURE 1 | Copy number variations alter gene dosage and expression. Copy number variations (CNVs) can manifest as deletions, where segments of DNA are removed (represented in orange), or duplications, where extra copies of a DNA segment are produced (represented in blue). CNVs can vary in size, affecting several exons in a gene, to multiple genes or even cytobands of a chromosome. Created with BioRender.com.

a rare genetic disorder characterized by developmental delay, intellectual disability, microcephaly, and various facial dysmorphisms and limb abnormalities (Verjaal and De Nef, 1978; Shuib et al., 2009; Peltekova et al., 2012; Kellogg et al., 2013). Cases of Del3p often present with neurodevelopmental and neuropsychiatric phenotypes, such as ASD, schizophrenia, and epilepsy (Schinzel, 1981; Drumheller et al., 1996; Fernandez et al., 2004; Bittel et al., 2006; Dijkhuizen et al., 2006; Malmgren et al., 2007; Roohi et al., 2009; Pohjola et al., 2010; Cottrell et al., 2011; Palumbo et al., 2013; Moghadasi et al., 2014; de la Hoz et al., 2015; Hu et al., 2015; Guo et al., 2017; Juan-Perez et al., 2018; Parmeggiani et al., 2018). Individuals affected by Del3p also tend to display neuroanatomical abnormalities as well (Malmgren et al., 2007; Pariani et al., 2009; Carr et al., 2010; Kellogg et al., 2013; Kuechler et al., 2015; Hajek et al., 2018; Parmeggiani et al., 2018). Although there are limited reports, duplications at chromosome 3p have been shown to present with ASD-associated phenotypes (Kashevarova et al., 2014; Li et al., 2016). Therefore, studying CNVs occurring in chromosome 3p could lead to the discovery of dosage-sensitive genes which are involved in molecular mechanisms that regulate neurodevelopmental processes. Genome-wide CNV studies in ASD cohorts have also detected ASD-specific and recurrent CNVs in the 3p26.3 cytoband, a region located at the distal end of the p-arm (**Figure 2**; Glessner et al., 2009; Levy et al., 2011; Guo et al., 2017). In a previous review of Del3p cases, Peltekova et al. (2012) noted that many of the cases of chromosome 3p CNVs that are comorbid with ASD occur at more distal cytobands of the p-arm. Furthermore, it is rare for individuals with a 3p26 deletion to display normal intelligence (Shuib et al., 2009). Therefore, it is likely that disruption of genes encoded in the 3p26.3 region play a role in the development of neurodevelopmental phenotypes in individuals with Del3p.

The 3p26.3 region contains three consecutive genes encoding closely related neuronal cell adhesion molecules of the immunoglobulin superfamily (IgCAMs), in order from the telomere: *Close Homolog of L1* (*CHL1*), *Contactin-6* (*CNTN6*), and *Contactin-4* (*CNTN4*) (**Figure 2**). Interestingly, the SFARI Gene database scores *CNTN6* and *CNTN4* as strong ASD candidate genes (Abrahams et al., 2013). These neuronal IgCAMs have been observed to play key roles in neurodevelopment, regulating axon guidance, neuronal migration and synaptic plasticity (Betancur et al., 2009; Sytnyk et al., 2017). Importantly, CNVs and other mutations affecting these neuronal IgCAMs have been reported in individuals with neurodevelopmental and neuropsychiatric phenotypes (**Table 1**). For example, CNVs in *CHL1* have been observed in individuals with ASD, intellectual disability and epilepsy, and are associated with speech delay, difficulties with expressive language, learning disabilities and cognitive impairment (Angeloni et al., 1999; Pohjola et al., 2010; Cuoco et al., 2011; Shoukier et al., 2013; Tassano et al., 2014; Li et al., 2016; Bitar et al., 2019; **Table 1**). CNVs in *CNTN6* have similarly been reported in individuals with ASD, schizophrenia, intellectual disability, bipolar disorder, and epilepsy (Kashevarova et al., 2014; Noor et al., 2014; Hu et al., 2015; Li et al., 2016; Mercati et al., 2017;

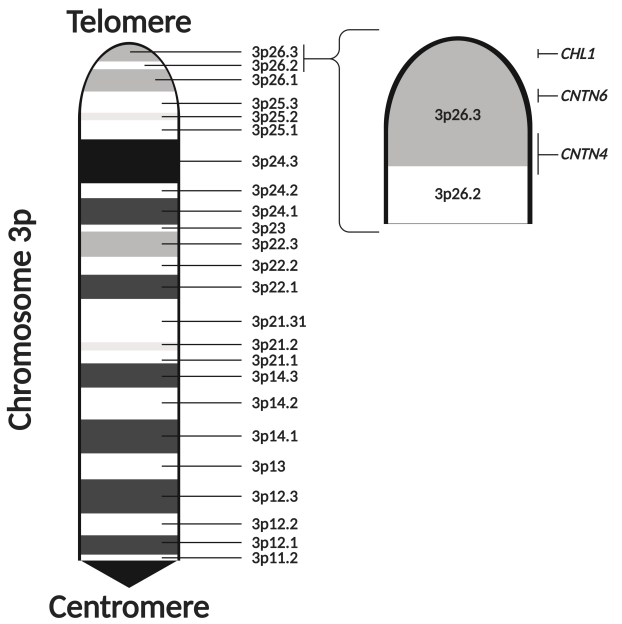

FIGURE 2 | The 3p26.3 region encodes three neuronal cell adhesion molecules of the immunoglobulin superfamily. The 3p26.3 region is located at the distal end of the p-arm of chromosome 3. It is the terminal cytoband, lying just before the telomeres and containing three genes (in order from the telomere): *Close Homolog of L1* (*CHL1*), *Contactin-6* (*CNTN6*), and *Contactin-4* (*CNTN4*). Figure adapted from the *Ensembl Genome Browser* (Yates et al., 2020). Created with BioRender.com.

TABLE 1 | Overview of phenotypes observed in individuals with CNVs in *CHL1*, *CNTN6*, and *CNTN4*.

CNV in Gene	Phenotypes Observed	References
CHL1	Autism spectrum disorder Epilepsy Intellectual disability Cognitive impairments and learning disabilities Speech delay and language difficulties	Angeloni et al., 1999; Pohjola et al., 2010; Cuoco et al., 2011; Shoukier et al., 2013; Tassano et al., 2014; Li et al., 2016; Bitar et al., 2019
CNTN6	Autism spectrum disorder Epilepsy Schizophrenia Bipolar disorder Intellectual disability	Kashevarova et al., 2014; Noor et al., 2014; Hu et al., 2015; Li et al., 2016; Mercati et al., 2017; Juan-Perez et al., 2018; Tassano et al., 2018; Repnikova et al., 2020
CNTN4	Autism spectrum disorder Speech delay and language difficulties Seizures	Fernandez et al., 2004; Fernandez T. et al., 2008; Fernandez T. V. et al., 2008; Dijkhuizen et al., 2006; Glessner et al., 2009; Roohi et al., 2009; Pinto et al., 2010; Cottrell et al., 2011; Poultney et al., 2013; Zhang et al., 2020

Further details on the coordinates and size of these CNVs, their de novo or inherited status and a more specific breakdown of behavior and developmental phenotypes can be found in ***Supplementary Table 1****.*

Juan-Perez et al., 2018; Tassano et al., 2018; Repnikova et al., 2020; **Table 1**). Finally, CNVs involving *CNTN4* have been observed in individuals with ASD, language delay, and seizures as well (Fernandez et al., 2004; Fernandez T. et al., 2008; Fernandez T. V. et al., 2008; Dijkhuizen et al., 2006; Glessner et al., 2009; Roohi et al., 2009; Pinto et al., 2010; Cottrell et al., 2011; Poultney et al., 2013; Zhang et al., 2020; **Table 1**). These observations suggest that the cellular pathways regulated by these neuronal IgCAMs are important contributors to the behavioral phenotypes of neurodevelopmental disorders such as ASD. Therefore, it is imperative to obtain a greater understanding of the functions of these neuronal IgCAMs, their interactors and how they modulate the cellular pathways underlying ASD etiology.

Notably, CNVs in the 3p26.3 region show a spectrum of phenotypic severity, and demonstrate incomplete penetrance for ASD and other neurodevelopmental phenotypes (elaborated upon in section "CNVs in the 3p26.3 Region Are Associated With Neurodevelopmental Behavior Phenotypes" of this review). However, larger CNVs affecting two or all three neuronal IgCAMs encoded in the 3p26.3 region are observed to produce more severe phenotypes, suggesting that disruptions to multiple members of these neuronal IgCAMs exert additive effects that contribute to phenotype severity. This would also explain the incomplete penetrance commonly observed with CNVs that only affect one of these genes, and why severe behavior phenotypes have not been observed in animal knockout models for *Chl1* or *Cntn4* (discussed later in section "Behavior Phenotypes of Animal Models" of this review). As such, this review aims to discuss our current understanding of the functions of CHL1, CNTN6, and CNTN4, examining their overlapping expression patterns and interactomes during neurodevelopment. We will discuss how these genes regulate neuronal migration and neurite outgrowth, how this alters synaptogenesis and synaptic plasticity and ultimately, behavior phenotypes in animal models.

COPY NUMBER VARIATIONS IN CHROMOSOME 3p26.3

CNVs in the 3p26.3 Region Are Associated With Neurodevelopmental Behavior Phenotypes

Using the online *PubMed* database, 195 studies investigating individuals with CNVs or chromosomal rearrangements in chromosome 3p were collected (**Supplementary Table 1**). In total, 894 individuals with a total of 907 CNVs were collated. Where available, CNV coordinates, properties (deletion or duplication), inheritance status, and ASD diagnoses were recorded (**Supplementary Table 1**). Additionally, any neurodevelopmental or neuropsychiatric phenotypes were also recorded, which included: the presence of autistic features (i.e., individuals displaying any or all of the core behavior domains of ASD but without an ASD diagnosis), Rett syndrome, Asperger syndrome, pervasive developmental disorder not otherwise specified (PDD-NOS), schizophrenia, Prader-Willi syndrome, attention deficit disorder or hyperactivity, bipolar disorder, intellectual disability, developmental delay, seizures or abnormal electroencephalogram, and any neuroanatomical abnormalities (as identified by magnetic resonance imaging) (**Supplementary Table 1**). Studies investigating chromosome 3p CNVs in cancerous tumors were excluded.

To identify which cytoband of chromosome 3p holds the largest burden for CNVs, the collated CNVs were mapped along the chromosome by the cytoband of their distal breakpoint (**Figure 3**). A significant portion of these CNVs (approximately 41.9%) are observed to occur in the 3p26.3 region, suggesting that mutations in genes encoded in this cytoband are important contributors to the neurodevelopmental phenotypes observed in individuals affected by Del3p. However, why is there such a high frequency of CNVs occurring at the 3p26.3 region? Although outside the scope of this review, the high frequency of CNVs in the 3p26.3 region could be explained by telomere attrition. Studies have previously reported higher frequency of ASD cases in individuals with shorter telomere lengths (Li et al., 2014), and that families at high-risk for ASD possess significantly shorter telomere lengths (Nelson et al., 2015). In spite of this, the high frequency of CNVs in the 3p26.3 region identifies this cytoband as a potential genetic risk locus for the ASD and ASD-associated phenotypes observed in individuals affected by Del3p.

It is important to acknowledge that just as ASDs present with a complex range of phenotypes (ranging from mild to severe), individuals affected by CNVs in chromosome 3p demonstrate a similar spectrum of phenotypic severity. Although the 3p26.3 region represents a promising candidate region for the neurodevelopmental phenotypes of Del3p, CNVs in the 3p26.3 region demonstrate incomplete penetrance for ASD and other neurodevelopmental phenotypes (Pohjola et al., 2010; Moghadasi et al., 2014). This suggests that depending on the location and magnitude of CNVs in chromosome 3p26.3, deletion or duplication of specific regions within the *CHL1*, *CNTN6*, and *CNTN4* genes may confer greater risk toward ASD development, and that these genes function as genetic modifiers to affect the severity of neurodevelopmental phenotypes. Interestingly, larger CNVs that encompass more genes appear to show higher penetrance and tend to result in more severe phenotypes. Guo et al. (2012) reported two cases of ASD with duplications affecting both *CNTN6* and *CNTN4*, which demonstrated striking deficits in social interaction and communication, in addition to markedly delayed development, seizures, speech delay and self-injurious behaviors. Other studies have also reported cases of CNVs affecting multiple neuronal IgCAMs in the 3p26.3 region in individuals diagnosed with ASD or those exhibiting pronounced autistic features (Schinzel, 1981; Drumheller et al., 1996; Angeloni et al., 1999; Fernandez et al., 2004; Malmgren et al., 2007; Pinto et al., 2010; van Daalen et al., 2011; Moghadasi et al., 2014; Weehi et al., 2014). These reports provide further evidence that mutations in the neuronal IgCAMs encoded at the 3p26.3 region produce additive deleterious effects that contribute to more severe phenotypes.

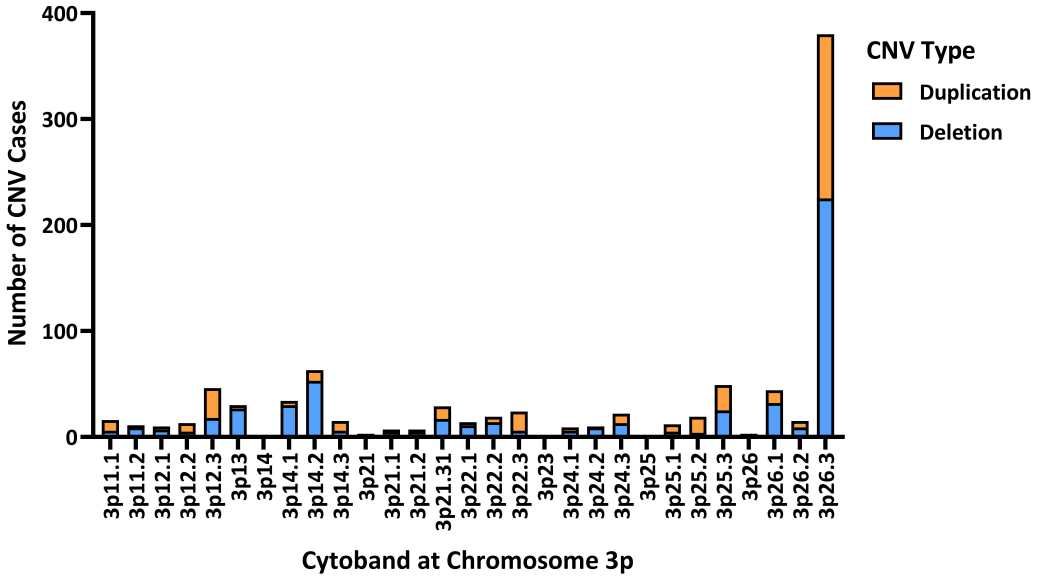

FIGURE 3 | The distribution of CNVs at chromosome 3p mapped by their distal breakpoint. Most deletions and duplications reported at chromosome 3p occur within the 3p26.3 region (380 of 907 CNVs; consisting of 225 deletions and 155 duplications), suggesting genes encoded in this region may be the molecular link between Del3p and ASD. Some studies were unable to provide high-resolution analysis of chromosomal breakpoints, only providing general coordinates (e.g., 3p26 rather than 3p26.1, 3p26.2, or 3p26.3). Additionally, cases of chromosomal translocations involving chromosome 3p have been included within the "Deletion" category for ease of visualization. In cases of inherited CNVs, if the phenotype of the parent is discussed, they have also been included as well. Figure created using GraphPad Prism 8.

Other Candidate Genes for Neurodevelopmental Phenotypes in Chromosome 3p

Although it is outside the scope of this review, other genes in chromosome 3p may also contribute to phenotypes observed in Del3p. Next to *CNTN4* in 3p26.2, three genes are present that are often lost in larger terminal 3p26.3 deletions: *Interleukin 5 Receptor Subunit Alpha* (*IL5RA*), *Transfer RNA Nucleotidyl Transferase 1* (*TRNT1*), and *Cereblon* (*CRBN*). *CRBN* in particular has been associated with autosomal recessive non-syndromic cognitive disability (Bavley et al., 2018), and disruptions to this gene by CNVs may contribute to the cognitive impairments observed in individuals affected by Del3p. Additionally, interstitial CNVs involving more proximal cytobands of the p-arm have also been associated with ASD (Harvard et al., 2005). CNVs affecting genes in these proximal cytobands have also been reported in individuals with ASD, PDD-NOS, language deficits, epilepsy, anxiety, and intellectual disability (Bittel et al., 2006; Ţuţulan-Cuniţă et al., 2012; Lesca et al., 2012; Riess et al., 2012; Schwaibold et al., 2013; Kellogg et al., 2013; Palumbo et al., 2013; Okumura et al., 2014; de la Hoz et al., 2015; Kuechler et al., 2015; Liu et al., 2015; Parmeggiani et al., 2018). A few genes encoded in chromosome 3p should be noted in relation to the neuronal IgCAMs at the 3p26.3 region – namely *Protein Tyrosine Receptor Phosphatase (PTPR) Type G* (*PTPRG*), *Fez Family Zinc Finger Protein 2* (*FEZF2*), and *Contactin-3* (*CNTN3*). *CNTN3* is encoded in the 3p12.3 region and belongs to the same subfamily of proteins as CNTN6 and CNTN4 and similarly, functions as a neuronal IgCAM to promote neurite outgrowth (Yoshihara et al., 1995). PTPRG is a protein tyrosine phosphatase that has previously been found to interact with CNTN3, CNTN4, and CNTN6 (Bouyain and Watkins, 2010a,b), and this interaction regulates neurite outgrowth (elaborated upon later in section "Axon Guidance, Neurite Outgrowth and Neuronal Migration" of this review) (Mercati et al., 2013). Furthermore, Parmeggiani et al. (2018) recently showed through a STRING protein interaction network analysis that FEZF2 interacts indirectly with PTPRG via CNTN4, placing these proteins in the same interactome network. This may explain why both interstitial and terminal CNVs in chromosome 3p result in similar phenotypes, as the affected genes participate in convergent neurodevelopmental pathways.

NEUROPHYSIOLOGICAL ROLES OF *CHL1*, *CNTN6*, AND *CNTN4*

Spatiotemporal Expression Patterns of CHL1, CNTN6, and CNTN4

The three neuronal IgCAMs encoded in the 3p26.3 region belong to the Immunoglobulin (Ig) CAM (IgCAM) superfamily (Holm et al., 1996; Fusaoka et al., 2006; Shimoda and Watanabe, 2009; Chatterjee et al., 2019). Within the IgCAM superfamily, CHL1 belongs to the L1 family, whilst CNTN6 and CNTN4 belong to the Contactin family (**Figure 4**). As such, they share a common extracellular domain comprised of six N-terminal Ig domains followed by five Fibronectin Type III (FNIII) domains

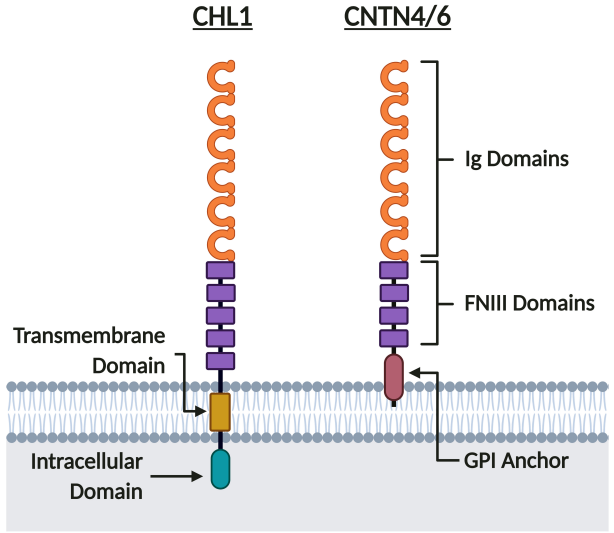

FIGURE 4 | CHL1, CNTN6, and CNTN4 share similar protein structure. CHL1, CNTN6, and CNTN4 are members of the IgCAM superfamily. These neuronal IgCAMs share similar extracellular domains composed of six Ig domains and five FNIII domains for CHL1, or four FNIII domains for CNTN6 and CNTN4. Whereas CNTN6 and CNTN4 are tethered to the membrane by a GPI anchor, CHL1 has both transmembrane and intracellular domains. Created with BioRender.com.

for CHL1 (Holm et al., 1996), or four FNIII domains for CNTN6 and CNTN4 (Shimoda and Watanabe, 2009; **Figure 4**). CHL1 contains a transmembrane and intracellular C-terminal domain, however CNTN6 and CNTN4 lack an intracellular domain and are instead tethered to the cell membrane by a C-terminal glycosylphosphatidylinositol (GPI) anchor (Holm et al., 1996; Maness and Schachner, 2007; Shimoda and Watanabe, 2009; **Figure 4**). As CNTN6 and CNTN4 do not have intracellular domains, they require interacting partners for intracellular signal transduction or act directly as ligands for receptors on opposing cells. Due to their structural similarity, it is likely that these neuronal IgCAMs interact with similar extracellular ligands during neurodevelopment (elaborated upon in sections "Axon Guidance, Neurite Outgrowth, and Neuronal Migration," "Synaptic Transmission and Plasticity," and "Behavior Phenotypes of Animal Models"). These neuronal IgCAMs also share some overlapping but distinct expression patterns, suggesting that they contribute to a combinatorial code (Yamagata et al., 2002). Previous studies within the rodent forebrain and cortex indicate that the temporal expression of all three neuronal IgCAMs follows a similar pattern – starting low during the final week of gestation and rising to peak expression levels during the first week of postnatal development (Yoshihara et al., 1995; Hillenbrand et al., 1999; Lee et al., 2000; Kaneko-Goto et al., 2008; Oguro-Ando et al., 2017). Post gestation, the expression of Chl1 and Cntn6 falls to a constant level (Hillenbrand et al., 1999; Lee et al., 2000), whereas the expression of Cntn4 continues to increase until a constant level that is maintained in adulthood (Yoshihara et al., 1995; Kaneko-Goto et al., 2008).

Cell-type-specific expression of these neuronal IgCAMs throughout neurodevelopment, from previously reported data in rodent models, is not so straightforward. Chl1 is reported to be strongly expressed in cortical layer V interneurons, hippocampal pyramidal cells of the Cornu Ammonis 1 and 3 (CA1 and CA3, respectively) regions, and in interneurons of the hippocampus proper and the hilar region of the dentate gyrus (DG) (Hillenbrand et al., 1999). Cntn6 is significantly expressed in the cortex within layer V interneurons, and within the CA1 hippocampus region, the DG and the hilar region of the DG (Lee et al., 2000; Zuko et al., 2016a,b). Cntn4 is strongly expressed within layer V cortical interneurons, and although weakly expressed in regions of the hippocampus, is specifically localized to granule cells of the DG (Chatterjee et al., 2019). Although Chl1, Cntn6, and Cntn4 are all expressed in layer V interneurons of the cortex, Cntn6 is more prominently expressed within layers Vb and VIb whereas Cntn4 is more strongly expressed in layers Vb and VIa (Oguro-Ando et al., 2017). Furthermore, while Cntn4 is extensively expressed in layers II–V of the cortex, Cntn6 expression is more confined to layers II, III, and V (Zuko et al., 2016b; Oguro-Ando et al., 2017). Although our knowledge of cell-type-specific expression of these neuronal IgCAMs is limited, these studies in rodent models suggest that Chl1, Cntn6, and Cntn4 display overlapping, though distinct, spatiotemporal expression patterns. Advances in single-cell transcriptomic profiling technology have provided greater insight into cell-type-specific expression patterns. For example, the *Allen Brain Atlas* has curated single-cell and single-nucleus RNA-sequencing data to produce a transcriptional profile of different regions of the human and mouse cortex and hippocampus (©2015 Allen Institute for Brain Science. Allen Cell Types Database. Available from https://celltypes.brain-map.org/). Single-cell transcriptomic datasets such as these are vital to improving our understanding of CHL1, CNTN6, and CNTN4 expression in the developing human brain.

In the human motor cortex, *CHL1* and *CNTN4* are, with a few exceptions, commonly expressed in most GABAergic interneuron and glutamatergic pyramidal neuron populations (©2015 Allen Institute for Brain Science). However, *CNTN6* demonstrates striking cell-type-specific expression, mainly being expressed in Vasoactive Intestinal Peptide (VIP), Somatostatin (SST), and Parvalbumin (PVALB) expressing interneurons, and Thymocyte Selection Associated (THEMIS), RAR-Related Orphan Receptor B (RORB) and FEZF2 expressing pyramidal neurons (©2015 Allen Institute for Brain Science). In the mouse hippocampus, the expression of these neuronal IgCAMs becomes more selective. Whilst *Cntn4* is expressed in the CA1, CA2, and CA3 regions, *Chl1* is only expressed in the CA1 and CA3, and *Cntn6* is only expressed in the CA3 (**Figure 5A**). In the DG, low levels of *Cntn6* and *Cntn4* can be detected, whilst *Chl1* is expressed in granule cells and GABAergic interneuron populations (Hochgerner et al., 2018; **Figure 5A**). This demonstrates that each of these neuronal IgCAMs has its own expression pattern independent from one other. The overlapping expression indicates that neurons can differ in combinations of *CHL1*, *CNTN6*, and *CNTN4* expression – these combinatorial patterns [suggest] that these IgCAMs are part

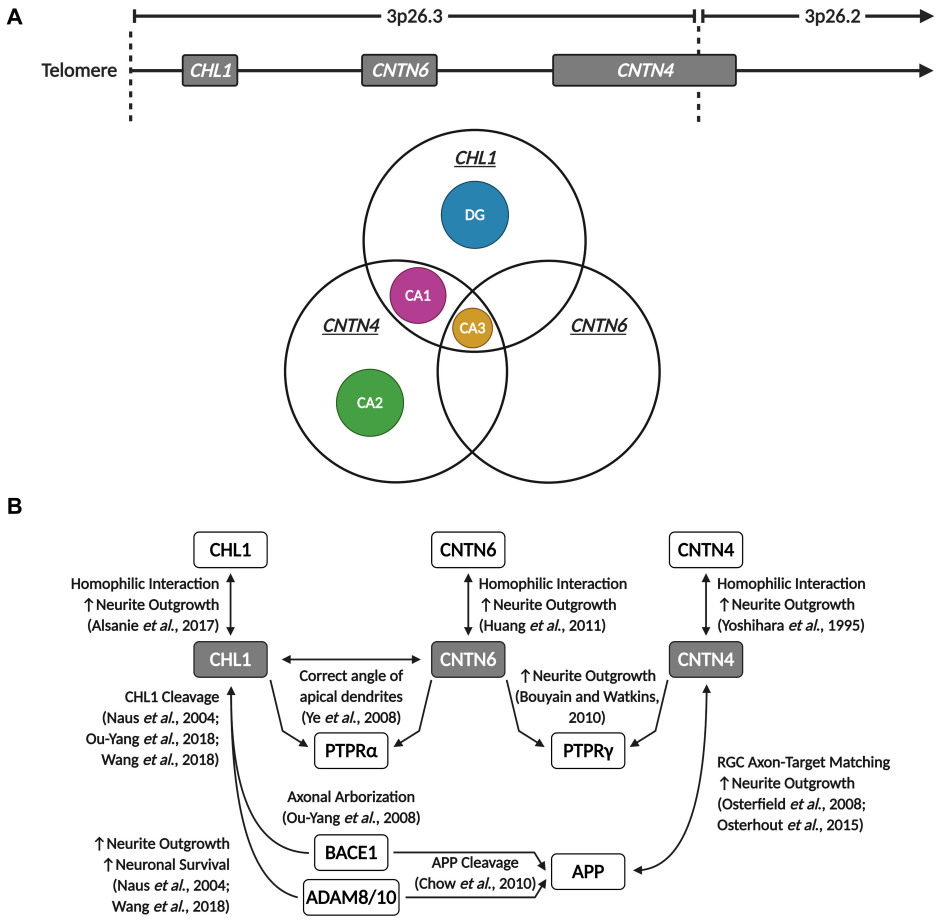

FIGURE 5 | *CHL1*, *CNTN6*, and *CNTN4* display overlapping expression in the hippocampus and participate in shared signaling pathways. **(A)** *Chl1*, *Cntn6*, and *Cntn4* demonstrate region-specific and overlapping expression patterns in the mouse hippocampus. The CA2 and DG only express *Cntn4* and *Chl1*, respectively, while all three neuronal IgCAMs are co-expressed in the CA3, and *Chl1* and *Cntn4* are co-expressed in the CA1. Data derived from the *Allen Brain Atlas* (©2015 Allen Institute for Brain Science. Allen Cell Types Database. Available from https://celltypes.brain-map.org/). **(B)** CHL1, CNTN6, and CNTN4 are capable of homophilic interactions that promote neurite outgrowth. These three neuronal IgCAMs commonly interact with members of the PTPR family – CHL1 interacts with CNTN6 to direct and maintain the correct angle of apical dendrites in cortical pyramidal neurons through PTPRα signaling, and both CNTN6 and CNTN4 are reported to interact with PTPRγ to promote neurite outgrowth. Additionally, CHL1 and CNTN4 interact with APP and enzymes involved in the proteolytic processing of APP – CNTN4 interacts with APP to promote neurite outgrowth and regulate retinal ganglion cell (RGC) axon-target matching in the development of visual pathways, and CHL1 cleavage by BACE1 and ADAM proteins is observed to promote neuronal survival, neurite outgrowth and regulate axonal arborization. Created with BioRender.com.

of a code, as has been suggested for Contactins in the retina (Yamagata and Sanes, 2012).

Regardless of their individual expression patterns, the common peak temporal expression during early postnatal development suggests that CHL1, CNTN6, and CNTN4 play key roles in synaptogenesis and the maintenance of neuronal networks within the developing brain. Their similar structure and partially overlapping spatial expression indicates that disruptions to the expression or function of these neuronal IgCAMs could produce additive deleterious effects. To understand the co-morbidities of these proteins in the brain, further investigations and confirmation of the developmental expression of *CHL1*, *CNTN6*, and *CNTN4* expression in the human brain is essential. In subsequent sections of this review, we will further discuss these neuronal IgCAMs and their functional role in neurons, including common interacting partners. In the case of overlapping interactomes, we will study their contribution toward ASD etiology.

Regulation of Neurogenesis and Neuronal Survival

Dysregulated neurogenesis and neuronal apoptosis are phenotypes that are associated with ASD – both in animal models and postmortem brains (Wegiel et al., 2010; Wei et al., 2014; Fan and Pang, 2017; Courchesne et al., 2019). The neuronal IgCAMs encoded in the 3p26.3 region have demonstrated roles in promoting neuronal survival and regulating neurogenesis. Chl1 has been observed to suppress apoptosis in primary cultures (Chen et al., 1999; Naus et al., 2004; Nishimune et al., 2005). Overexpression of Chl1 or its treatment in soluble or substrate form is hypothesized to exert anti-apoptotic effects by induction

of Phosphatidylinositol-3-Kinase (PI3K) and Mitogen-Activated Protein Kinase (MAPK) signaling (Nishimune et al., 2005) and by increasing the expression of B-Cell Lymphoma 2, an anti-apoptotic protein (Chen et al., 1999). Notably, altered PI3K and MAPK signaling is implicated in ASD and other neurodevelopmental disorders (Enriquez-Barreto and Morales, 2016; Baranova et al., 2020). Chl1 has also been observed to interact with the Patched-1 hedgehog receptor in regulation of neuronal survival, as inhibitors of Smoothened and RhoA and Rho-Associated Kinases 1 and 2 are able to inhibit Chl1-mediated survival of cerebellar Purkinje and granule cells (Katic et al., 2017). Studies in Chl1-deficient mice have also revealed increased apoptosis, loss of PVALB-positive (PV+) neurons and decreased precursor cell proliferation in the CA1 region of the hippocampus and cerebellum (Jakovcevski et al., 2009; Schmalbach et al., 2015). Interestingly, the loss of PV+ interneurons in the hippocampus is correlated with increased microglial activation and enhanced IL-6 secretion in the hippocampus (Schmalbach et al., 2015). Although it is outside the scope of this review, dysregulated neurogenesis as a result of neuroinflammation has also been observed in ASD (Fan and Pang, 2017), suggesting a mechanism exists by which Chl1 and other neuronal IgCAMs may regulate inflammatory signaling in the brain.

Although there are limited studies, Cntn6 and Cntn4 are also reported to play roles in regulating neuronal survival. Cntn6 regulates neuronal survival and morphology through its interaction with Latrophilin-1 (Lphn1) (Zuko et al., 2016a). Neurons overexpressing Lphn1 display morphological defects including reduced neurite branching points, soma size, total neurite length, and longest branch length (Zuko et al., 2016a). Increased Caspase-3 immunoreactivity was also observed in the Cntn6-deficient visual cortex (Zuko et al., 2016a). Interestingly, Lphn1 is known to interact with Neurexin-1, another neuronal IgCAM whose disruption is also associated with ASD (Kim et al., 2008; Moreno-Salinas et al., 2019). These interactions between Lphn1, Cntn6, and other neuronal IgCAMs may point toward a common cellular pathway implicated in ASD etiology.

Axon Guidance, Neurite Outgrowth, and Neuronal Migration

Deficits in neuronal migration and axon guidance are a characteristic commonly observed in ASD (Wegiel et al., 2010; Pan et al., 2019). In Chl1-deficient mice, impairments in neuritogenesis and axonal guidance can be observed. In the hippocampus, mossy fibers of the CA3 region display unorganized projections that invade into the pyramidal cell layer, rather than forming the supra- and infra-pyramidal bundles parallel to the pyramidal cell layer observed in wild-type mice (Montag-Sallaz et al., 2002; Frints et al., 2003; Heyden et al., 2008). Additionally, Chl1-deficient mice display aberrant arborization of olfactory sensory neuron axons (Montag-Sallaz et al., 2002; Heyden et al., 2008). Chl1 is further reported to stimulate neurite outgrowth in primary neuronal cultures (Chen et al., 1999; Hillenbrand et al., 1999; Dong et al., 2002), and may promote neurite outgrowth via multiple pathways. For example, the intracellular domain of Chl1 interacts with Ezrin, a member of the Ezrin-Radixin-Moesin (ERM) family of Actin-binding proteins, to modulate Actin dynamics and facilitate F-Actin remodeling (Schlatter et al., 2008). The Chl1-Ezrin interaction also plays a role in axonal repulsion by mediating the growth cone collapsing activity of the chemorepellent Semaphorin-3A (Sema3a) (Schlatter et al., 2008), and insufficient Sema3a-mediated repulsion in CHL1-deficient mice is observed to alter the positioning of axons projecting toward the cortex from the ventral telencephalon and basal complex (Wright et al., 2007). Chl1 binding to Sema3a triggers Chl1 cleavage by β-Site Amyloid-Precursor Protein-Cleaving Enzyme 1 (Bace1), which generates an active membrane-bound Chl1 fragment that interacts with Ezrin to relay the Sema3a signal to the Actin cytoskeleton (Barão et al., 2015). In addition to Sema3a, Chl1 also interacts with other molecules in the growth cone to regulate axon targeting and neurite outgrowth, including the Ephrin A7 Receptor (Demyanenko et al., 2011) and Disrupted in Schizophrenia 1 (Ren et al., 2016). Chl1 may also promote neuronal migration and neurite outgrowth by interacting with β1 Integrins and recruiting the Actin-binding protein Ankyrin to the cell membrane, triggering activation of c-Src, PI3K, and MAPK cascades (Buhusi et al., 2003; Demyanenko et al., 2004; Katic et al., 2014). More recently, homophilic Chl1–Chl1 interactions have also been observed to regulate neurite outgrowth during the development of ventral midbrain dopaminergic pathways (Alsanie et al., 2017).

Interestingly, Chl1 was observed to interact with Cntn6, and this interaction is responsible for maintaining the correct angle of apical dendrites in cortical pyramidal neurons through Ptpr-Alpha (Ptpra) signaling (Ye et al., 2008). Notably, compound heterozygous mice for both Chl1 and Cntn6 display an additive deleterious phenotype – these compound heterozygous mice showed more severe misoriented dendrites compared to single heterozygous Chl1 or Cntn6 mice and wild-type littermates (Ye et al., 2008). This suggests that Chl1 and Cntn6 may partially compensate for one another, and places Cntn6 directly within Chl1's interactome. Although no studies have validated this further, it is possible Cntn6 could interact with the same binding partners as Chl1 as well, thereby participating in shared intracellular pathways (Zuko et al., 2013). It is worthwhile to note that *Chl1* and *Cntn6* are both expressed in the CA3 region of the hippocampus (**Figure 5A**), and that Cntn6-deficient mice also display a larger suprapyramidal bundle (Zuko et al., 2016b), a phenotype similar to that observed in the hippocampus of Chl1-deficient mice (Montag-Sallaz et al., 2002; Frints et al., 2003; Heyden et al., 2008). In addition to its interaction with Chl1, Cntn6 is also reported to regulate neurite outgrowth in primary neuronal cultures through Ptprg signaling (Takeda et al., 2003; Bouyain and Watkins, 2010b; Mercati et al., 2013). Importantly, Cntn4 has been observed to interact with Ptprg, and this interaction promotes neurite extension (Bouyain and Watkins, 2010b; Cottrell et al., 2011). Therefore, at least within the context of neuritogenesis, these three neuronal IgCAMs share an overlapping interactome, as they interact with each other and with similar binding partners (**Figure 5B**). This suggests that these neuronal IgCAMs participate in common

neurodevelopmental pathways and may display some functional redundancy, leading to additive deleterious phenotypes with loss-of-function mutations. Additionally, similar to Chl1, Cntn6 is capable of promoting neurite outgrowth through homophilic Cntn6–Cntn6 interactions (Huang et al., 2011). As well as promoting neuritogenesis, Cntn6 is also observed to play roles in axon guidance, particularly in the establishment of the corticospinal tract (Huang et al., 2012). Cntn6-deficient mice display a delay in the development of projections of corticospinal tract axons during prenatal and neonatal development (Huang et al., 2012).

Contactin-4 is observed to play roles in regulating axon guidance and neurite extension, for example promoting neurite outgrowth in primary cortical neurons (Yoshihara et al., 1995; Mercati et al., 2013). Similar to Cntn6, Cntn4 may interact with Chl1 or other members of the L1 family, and both heterophilic and homophilic Cntn4 interactions may promote neurite extension (Yoshihara et al., 1995; Mercati et al., 2013). Cntn4's role in axon guidance has been extensively explored in multiple species in the development of olfactory and visual pathways (Kaneko-Goto et al., 2008; Osterfield et al., 2008). In the olfactory system, Cntn4 expression in axon terminals guides individual axons from odorant receptors to distinct olfactory bulb glomeruli, suggesting Cntn4 promotes the formation and maintenance of odor maps, possibly via interaction with Ephrin-A5 (Kaneko-Goto et al., 2008). Similar to Chl1, Cntn4-deficient olfactory sensory neurons display aberrant projections toward multiple olfactory bulb glomeruli (Kaneko-Goto et al., 2008). This shared axon guidance deficit observed between Chl1- and Cntn4-deficient mice further supports the possibility that these neuronal IgCAMs participate in common signaling pathways during neurodevelopment. Osterfield et al. (2008) identified extracellular binding partners of Amyloid Precursor Protein (App) in retinal axons growing on the optical tectum, which is a well characterized model of axon development (McLaughlin and O'Leary, 2005; Flanagan, 2006). In retinal ganglion cells, Cntn4 is suitably placed to interact with App during the developing retinotectal system in order to mediate axon outgrowth and axon-target matching. Cntn4-deficiency results in defects in retinal ganglion cell axon-target matching, arborization and outgrowth (Osterfield et al., 2008; Osterhout et al., 2015). This system is clearly sensitive to axon guidance defects or to absence of certain CAMs, as was demonstrated in Bace1-knockout mice (Hitt et al., 2012). Although axon guidance deficits in the hippocampus of Cntn4-deficient mice have not yet been explored, it would be interesting to see if Cntn4-deficient mice also display abnormal mossy fiber projections similar to Chl1- and Cntn6-deficient mice, as *Cntn4* is expressed in the CA3 region as well (**Figure 5A**).

Interestingly, cleavage of these neuronal IgCAMs by specific enzymes may also be key to their functions in axon guidance and promoting neurite outgrowth. For example, Chl1 cleavage by Bace1 has been demonstrated to be involved in axonal organization, as reduced Bace1-mediated Chl1 cleavage is reported to contribute toward defective axonal organization in Bace1-deficient mice (Ou-Yang et al., 2018). Notably, Bace1-deficient mice display axon guidance defects in the olfactory bulb and hippocampus similar to Chl1 and Cntn4-deficient mice (Hitt et al., 2012). BACE1, together with proteins of the Disintegrin and Metalloproteinase Domain-Containing Protein (ADAM) family, are key enzymes in APP processing (Sinha et al., 1999; Vassar et al., 1999). APP cleavage by ADAM family proteins (α-secretase activity) or BACE1 (β-secretase activity) produces a secreted APP (sAPP) fragment and a membrane-bound carboxyl terminal fragment (CTF) – these fragments are referred to as sAPPα/β and CTFα/β depending on their generation via α- or β-secretase activity (Chow et al., 2010). In addition to its interaction with APP, CNTN4 may also play a modulatory role in APP processing, as co-expression of CNTN4 with APP in transfected HEK-293T cells resulted in an increase production of CTFα (Osterfield et al., 2008). It is unknown if CNTN4 also regulates the activity of or is cleaved by ADAM proteins, but these findings suggest that CHL1 and CNTN4 may play similar roles in an overlapping pathway regulating APP processing. Other studies have also reported that Adam8 cleaves Chl1 to release an extracellular fragment that promotes neuronal survival and neurite outgrowth *in vitro* (Naus et al., 2004), and Adam10 interacts with Bace1 to regulate Chl1 cleavage (Wang et al., 2018). The Adam10-Bace1 interaction may be important for neuritogenesis in primary neuronal cultures and importantly, APP is reported to promote neuronal migration and neurite outgrowth (Billnitzer et al., 2013; Nicolas and Hassan, 2014; Wang et al., 2017). Increased levels of sAPPα are also associated with ASD, hinting toward dysregulated APP processing as a convergent pathway in ASD etiology (Ray et al., 2011; Sokol et al., 2019).

Synaptic Transmission and Plasticity

Neuronal IgCAMs have been found to influence synapse formation, maintenance and plasticity (Betancur et al., 2009; Sytnyk et al., 2017). L1 and Contactin family neuronal IgCAMs perform important functions at neuronal synapses, forming homodimer and heterodimer *trans* complexes with other neuronal IgCAMs or receptors. As discussed in section "Axon Guidance, Neurite Outgrowth, and Neuronal Migration," these neuronal IgCAM interactions are important for axon guidance, target-matching, and arborization, but they also anchor, organize, and bridge the synaptic cleft (Missler et al., 2012; Yang et al., 2014; Chatterjee et al., 2019). In this section we focus on the reported non-adhesion functions of CHL1, CNTN6, and CNTN4 in synaptic transmission and how they may influence synaptic plasticity.

In addition to promoting the formation and stabilization of synapses (Ashrafi et al., 2014), CHL1 is reported to play multiple non-adhesion roles that modulate synaptic activity. The intracellular domain of Chl1 regulates synaptic vesicle recycling by interacting with the 70 kDa Heat Shock Cognate (Hsc70) synaptic chaperone protein and regulating the un-coating of Clathrin-coated synaptic vesicles in the Clathrin-dependent recycling pathway (Leshchyns'ka et al., 2006). Chl1 localizes primarily in the presynaptic terminals of axons of both excitatory and inhibitory neurons, co-localizing with Hsc70 and the synaptic vesicle marker Sv2 (Leshchyns'ka et al., 2006). Chl1 also modulates the refolding of Soluble N-Ethylmaleimide-Sensitive Factor Attachment Protein Receptor (SNARE) complex

proteins to maintain the vesicle recycling machinery during periods of continuous synaptic activity (Andreyeva et al., 2010). Interestingly, Chl1 was recently reported to interact with Dopamine Receptor D2 (DRD2), regulating its internalization at the presynaptic environment (Kotarska et al., 2020). This suggests that Chl1 may regulate dopaminergic signaling in neurons, and also the density of neurotransmitter receptors on the surface of axon terminals, which can influence how the presynaptic environment responds to modulatory signals from axo-axonic synapses. Chl1 has also been observed to play roles in Serotonin-2C Receptor (5-ht2cr) signaling in hippocampal GABAergic neurons – its deficiency impairs 5-ht2cr phosphorylation and 5-ht2cr association with Phosphatase and Tensin Homolog (Pten) and Arrestin Beta-2 (Arrb2) (Kleene et al., 2015). Notably, *PTEN* and *ARRB2* are both implicated in ASD etiology as well (Varga et al., 2009; Thompson and Dulawa, 2019). Genetic variants in *CHL1*, *ITGB1*, and *ITGB3* have also been identified as predictors of treatment-resistant depression and responsiveness to selective serotonin reuptake inhibitors (SSRIs), suggesting that the Chl1-Integrin interactions that regulate neuronal migration have further roles in serotonergic signaling (Morag et al., 2011; Oved et al., 2013, 2017; Fabbri et al., 2015, 2017; Probst-Schendzielorz et al., 2015). Several studies have also observed long-term potentiation (LTP) deficits at synapses between the CA3 and CA1 region of the hippocampus that could be rescued by application of $GABA_AR$ modulators, indicating that Chl1 may play a role in the establishment of synaptic plasticity as well (Nikonenko et al., 2006; Schmalbach et al., 2015). Taken altogether, these studies demonstrate that CHL1 and its interactors regulate a complex array of synaptic functions, ranging from synaptic vesicle recycling to neurotransmitter receptor internalization and downstream signaling.

As Chl1 has been observed to interact with Cntn6 within cortical neurons (Ye et al., 2008), and both neuronal IgCAMs share overlapping expression patterns in certain brain regions and neuronal populations, it is also possible Cntn6 may participate in similar functions to Chl1 in the presynaptic environment. Although there have been no direct studies investigating the role of Cntn6 in vesicular recycling, Cntn6 is expressed in the presynaptic terminals of glutamatergic synapses in the hippocampus where it interacts with Vglut1 and Vglut2, transporters that regulate glutamate uptake into presynaptic vesicles (Sakurai et al., 2009, 2010). Cntn6-deficiency is observed to reduce Vglut1 and Vglut2 expression in the hippocampal formation, suggesting that Cntn6 participates in the formation and maintenance of glutamatergic synapses (Sakurai et al., 2010). These studies point toward Cntn6's involvement in a shared pathway regulating vesicle processing at the presynapse with Chl1. Similar to the regulation of apical dendrites in pyramidal neurons (Ye et al., 2008), this could be another mechanism by which Cntn6 can compensate for Chl1 deficiency, and future studies should investigate if Cntn6 regulates vesicular recycling in a similar manner to Chl1. Interestingly, Cntn6-deficiency is also observed to cause a decrease in the number of PV+ GABAergic interneurons in the visual cortex (Zuko et al., 2016a). These studies indicate that Cntn6 may be a regulator of synaptic transmission in both excitatory and inhibitory neuron populations within the brain. It would therefore be interesting investigate if the effects of Cntn6 deficiency in cortical and hippocampal neurons translates to a shift in excitation-inhibition (E/I) ratios and changes in synaptic plasticity, as increases in E/I ratios due to reduced GABAergic signaling have been associated with deficits in social interaction and other neuropsychiatric phenotypes (Yizhar et al., 2011).

A recent study observed that Cntn4-deficient mice display altered cell-surface expression of glutamate and GABA receptors (GABARs) in ASD-related brain regions (Heise et al., 2018). Cntn4-deficient mice show reduced cell-surface glutamate and $GABA_AR\alpha1$ receptor levels in the cerebral cortex and hippocampus, suggesting Cntn4 can modulate synaptic transmission by altering the density of cell-surface neurotransmitter receptors (Heise et al., 2018). However, whether Cntn4 deficiency impairs glutamatergic or GABAergic signaling within cortical and hippocampal neurons, and subsequently whether these changes in cell-surface receptor expression result in altered E/I ratios or changes in LTP remains to be fully determined. *Cntn4* is expressed in both the CA1 and CA3 regions (**Figure 5A**), so it would be interesting to see if Cntn4-deficient mice display decreased PV+ neurons in the CA1 region and LTP deficits at CA3-CA1 synapses, similar to Chl1-deficient mice (Nikonenko et al., 2006; Schmalbach et al., 2015). Additionally, due to its high structural similarity with Cntn6, and shared binding partners with Cntn6, it is likely Cntn4 may perform similar functions to Cntn6 or even Chl1 at neuronal synapses. Therefore, it is possible these neuronal IgCAMs can compensate for each other's loss of function, and that disruptions to multiple genes can produce additive deleterious phenotypes.

Members of the Contactin-Associated Protein (CASPR) family interact and modulate the activity of Contactins (Murai et al., 2002; Gollan et al., 2003; Ashrafi et al., 2014; Rubio-Marrero et al., 2016). Importantly, several CASPR proteins have been reported to regulate the function of neurotransmitter receptors. CASPR1 and CASPR2 are observed to disrupt α-Amino-3-Hydroxy-5-Methyl-4-Isoxazolepropionic Acid receptor (AMPAR) function, causing synaptic abnormalities and regulating trafficking to the synapse (Santos et al., 2012; Fernandes et al., 2019; Gao et al., 2019). This presents a hypothesis that neuronal IgCAMs such as CNTN6 and CNTN4 could form complexes whose interactions regulate AMPAR and GABAR function and synaptic plasticity. Heise et al. (2018) suggests that CNTN4 may act as a molecular chaperone for cell surface expression of neurotransmitter receptors. It is worthwhile to note that CNTN6 has been observed to perform a similar role as well (Ye et al., 2011). Considering that Contactins lack intracellular signaling domains, it is likely that in certain cells CNTN6 and CNTN4 act as part of a larger complex of proteins, serving as chaperones or as ligands to initiate and inhibit molecular pathways. A similar situation may be the case between CHL1 and BACE1 (Hitt et al., 2012; Ou-Yang et al., 2018). Taking into account that CHL1 and CNTN6 interact with each other, the formation of a protein complex comprised of CHL1, CNTN6, and various CASPR proteins could regulate a range of synaptic functions. Ashrafi et al. (2014) demonstrated an example of such a complex in the mouse spinal cord, in

which a Chl1-Nrcam heterodimer interacts in *trans* with a Cntn5-Caspr4 heterodimer to promote the formation of and stabilize axo-axonic synapses. These collective interactions merit further investigation to decipher the heterodimeric complexes and signaling pathways CHL1, CNTN6, and CNTN4 are involved in at the synapse.

Behavior Phenotypes of Animal Models

The use of validated neurobehavioral tests for rodents provides an avenue for researchers to understand how specific genetic alterations impact molecular pathways that alter neuronal development and synaptogenesis. Understanding how these alterations affect brain connectivity and function is essential to improve our understanding of the core behavioral features of ASD (Zerbi et al., 2018). To model the behavior phenotypes of Del3p, it important to note that the 3p26.3 cytoband encoding *CHL1-CNTN6-CNTN4* is syntenic to the mouse chromosome 6qE1. Several studies have extensively characterized the phenotype of Chl1-deficient mice (**Table 2**). The use of SHIRPA behavior test batteries (Rogers et al., 1997, 2001) has revealed that Chl1-deficient mice display altered exploratory behavior, reduced behavior flexibility and novelty detection, impaired motor coordination, and altered social interaction and spatial information processing. Chl1-deficient mice are consistently observed to exhibit altered exploratory behavior and reduced anxiety in tests such as the open-field test, elevated-plus maze, light-dark transition test, and the Morris water maze (Montag-Sallaz et al., 2002; Frints et al., 2003; Pratte et al., 2003; Pratte and Jamon, 2009). This altered exploratory behavior may be due to impaired spatial and object novelty detection (Pratte et al., 2003; Morellini et al., 2007; Pratte and Jamon, 2009). Furthermore, Chl1-deficient mice are observed to have deficits in motor coordination, struggling to remain balanced in the rotarod test (Pratte et al., 2003). Chl1-deficient mice also display increased passivity and reduced aggressiveness, including reduced stress responses associated with transfer arousal, touch escape and irritability (Frints et al., 2003; Pratte et al., 2003; Morellini et al., 2007). Importantly, Chl1-deficient mice display altered social preference, increased behavioral inflexibility, and deficits in integrating spatial and temporal information in the hippocampus (Montag-Sallaz et al., 2002; Frints et al., 2003; Morellini et al., 2007; Buhusi et al., 2013). These are phenotypes that have been observed in certain mouse models for ASD such as the Fmr1-, Shank3-, Nlgn4-, Caspr2-, and Pten-deficient mice (Kwon et al., 2006; Jamain et al., 2008; Peñagarikano et al., 2011; Duffney et al., 2015; Kazdoba et al., 2016; Ricceri et al., 2016; Gurney et al., 2017; Verma et al., 2019).

In contrast to Chl1, the behavioral impacts of Cntn6 deficiency have not yet been well characterized (**Table 2**) and very few studies have examined the ASD-related behavioral effects of Cntn6 deficiency. Cntn6 deficiency was observed to result in deficits in spatial learning and memory in the Morris water maze task (Mu et al., 2018). In particular, male Cntn6-deficient mice exhibited slower spatial learning, which was attributed to altered hippocampal development (Mu et al., 2018). Another study investigated the effect of Cntn6 deficiency on motor coordination and observed that similar to Chl1-deficient mice, Cntn6-deficient mice display impaired motor coordination as well (Takeda et al., 2003). When subjected to the rotarod and horizontal rod tests, Cntn6-deficient mice struggled to stay and walk on the rods, indicating impaired balance control, despite muscle strength being unaffected (Takeda et al., 2003). Takeda et al. (2003) hypothesized that these defects in motor coordination were due to Cntn6 deficiency in the cerebellum, which leads to neuronal dysfunction. Notably, other studies have also reported that Chl1 plays an important role in cerebellar development, being expressed on the Bergmann glial cells that guide neuronal migration and synaptogenesis (Ango et al., 2008), and Chl1-deficient mice display increased neuronal apoptosis in the cerebellum (Jakovcevski et al., 2009). Importantly, cerebellar dysfunction has been previously associated with ASD (Wang et al., 2014; Hampson and Blatt, 2015; Mosconi et al., 2015). Zuko et al. (2016a) also hypothesized that as Cntn6-deficient mice display reduced numbers of PV+ GABAergic interneurons in the visual cortex, this shift in interneuron populations could lead to changes in E/I ratios in the cortex and affect behavior. Future studies into the behavioral impact of Cntn6-deficiency are clearly warranted.

Molenhuis et al. (2016) analyzed the development of neurological phenotypes in Cntn4-deficient mice at various developmental ages through an extended SHIRPA battery of tests. This study also included assessments for ASD-related behaviors such as the juvenile social interaction test, three-chamber social interaction test, novel object investigation task and the Barnes maze; however, Cntn4-deficiency was not observed to affect ASD-related behaviors (Molenhuis et al., 2016). Compared to wild-type littermates, Cntn4-deficient mice did not show any further changes in grooming behavior, social interaction, sensorimotor coordination, or cognitive flexibility (Molenhuis et al., 2016). No defects in olfaction were observed in Cntn4-deficient mice, which is unexpected since Cntn4 has been found to play a role in the establishment of odor maps (Kaneko-Goto et al., 2008). However, Cntn4-deficient mice do demonstrate enhanced spatial learning in the Barnes maze and a consistently increased startle response to auditory stimuli at high amplitudes (Molenhuis et al., 2016). Based on these findings, Molenhuis et al. (2016) concluded that Cntn4-deficiency does not affect ASD-specific phenotypes, but rather results in subtle non-ASD-specific changes in responsiveness to stimuli and cognitive performance. Notably, hyper-responsiveness to acoustic stimuli is a phenotype that has been associated with ASD and other neuropsychiatric disorders (Baranek et al., 2013; Green et al., 2013; Acevedo et al., 2018; Dakopolos and Jahromi, 2019; Hornix et al., 2019).

Overall, the lack of any strong phenotypes in Cntn4-deficient mice supports the idea that Cntn4 deficiency may be compensated for by other neuronal IgCAMs. As discussed in sections "Axon Guidance, Neurite Outgrowth, and Neuronal Migration" and "Synaptic Transmission and Plasticity," Cntn4 regulates neurite outgrowth, axon guidance, dendritic spine morphology, and cell-surface neurotransmitter receptor expression. This discrepancy between the subtle behavior reported and phenotypes observed in *ex vivo* or *in vitro* cultures suggest other neuronal IgCAMs exhibit a degree of functional redundancy that can compensate for deficits in neuronal

TABLE 2 | Behavior phenotypes observed in animal models for CHL1, CNTN6, and CNTN4 deficiency.

Mouse Model	Cognitive Domain	Task (If Applicable)	Phenotype	References
Chl1$^{-/-}$ mouse	Aggressiveness	Resident-intruder test	Reduced	Frints et al., 2003; Morellini et al., 2007
			Reduced social urine marking behavior	Morellini et al., 2007
	Anxiety	Open-field test	Reduced	Montag-Sallaz et al., 2002
		Elevated-plus maze	Reduced	Montag-Sallaz et al., 2002
		Light/dark avoidance test	Unaffected	Montag-Sallaz et al., 2002; Pratte et al., 2003
	Behavioral or cognitive flexibility	Morris water maze	Reduced	Montag-Sallaz et al., 2002; Frints et al., 2003
	Exploratory behavior	Open-field test	Altered	Montag-Sallaz et al., 2002; Pratte et al., 2003; Pratte and Jamon, 2009
		Morris water maze	Altered	Montag-Sallaz et al., 2002; Frints et al., 2003
	Learning and memory	Radial-arm maze	Deficits in integrating spatial and temporal information	Buhusi et al., 2013
	Motor coordination	Rotarod test	Impaired	Pratte et al., 2003
	Novelty detection	Open-field test	Impaired	Pratte et al., 2003; Morellini et al., 2007; Pratte and Jamon, 2009
		Elevated-plus maze	Impaired	Morellini et al., 2007
		Novel object test	Impaired	Morellini et al., 2007
	Olfactory function		Unaffected	Morellini et al., 2007
	Social interaction	Social preference test	Delayed reactivity to initiate social investigation and preference for familiar animals	Morellini et al., 2007
	Stress response		Reduced stress associated with transfer arousal, touch escape, and irritability	Pratte et al., 2003
Cntn6$^{-/-}$ mouse	Motor coordination	Rotarod test	Impaired	Takeda et al., 2003
	Learning and memory	Morris water maze	Impaired spatial learning	Mu et al., 2018
Cntn4$^{-/-}$ mouse	Anxiety	Open-field test	Unaffected	Molenhuis et al., 2016
		Elevated-plus maze	Unaffected	Molenhuis et al., 2016
	Behavioral or cognitive flexibility	Barnes maze	Unaffected	Molenhuis et al., 2016
		Set-shifting task	Unaffected	Molenhuis et al., 2016
	Exploratory behavior	Open-field test	Unaffected	Molenhuis et al., 2016
		Elevated-plus maze	Unaffected	Molenhuis et al., 2016
	Learning and memory	Barnes maze	Enhanced spatial learning	Molenhuis et al., 2016
	Motor coordination	Rotarod test	Unaffected	Molenhuis et al., 2016
	Olfactory function	Buried food test	Unaffected	Molenhuis et al., 2016
	Repetitive behavior		No effect on time spent grooming	Molenhuis et al., 2016
	Responsiveness to stimuli		Increased startle response to auditory stimuli	Molenhuis et al., 2016
	Social interaction	Juvenile social interaction test	No effect on social sniffing, anogenital sniffing, or social grooming	Molenhuis et al., 2016
		Three-chamber social interaction test	No effect on social preference	Molenhuis et al., 2016
		Social discrimination test	No effect on social exploration or recognition	Molenhuis et al., 2016

migration and neurite outgrowth. Indeed, Cntn4 deficiency is mainly reported to only cause mild abnormalities in gross cortical development and axon guidance in the olfactory bulb. Similarly, the effects of Chl1 and Cntn6 deficiency on neurite outgrowth are more pronounced within primary neuronal cultures, and milder phenotypes are observed in animal models. Studies in other CAMs, such as Neural Cell Adhesion Molecule 1 (Ncam1), L1 Cell Adhesion Molecule (L1cam) and several members of the Cadherin family have also indicated similar findings (reviewed in Hortsch, 1996; Colman and Filbin, 1999; Halbleib and Nelson, 2006; Dalva et al., 2007; Niessen et al., 2011; Lin et al., 2016). Ncam1- and L1cam-deficiency results in pronounced defects in neuronal migration and neurite outgrowth in culture, however, only subtle neuronal migration and behavior phenotypes are observed in Ncam1- and L1cam-knockout mice (Hortsch, 1996; Colman and Filbin, 1999). This may explain the highly variable severity of phenotypes in humans caused by CNVs in the 3p26.3 region and further suggests that

multiple neuronal IgCAMs and their signaling pathways may interact with one another. When one gene is disrupted, others may act to suppress the behavioral phenotype by compensating for the loss of function.

Considering the region-specific expression patterns of *Chl1*, *Cntn6*, and *Cntn4*, such as in the hippocampus (discussed in section "Spatiotemporal Expression Patterns of CHL1, CNTN6, and CNTN4") (**Figure 5A**), how can shared signaling pathways exist between these neuronal IgCAMs? For example, if certain axon guidance deficits in the hippocampus could be compensated for by different combinations of these neuronal IgCAMs, this can only occur in regions where co-expression of these neuronal IgCAMs does exist, e.g., in the CA1 and CA3 (**Figure 5A**). Yet, other regions remain unaccounted for, e.g., the CA2 and DG only express *Cntn4* and *Chl1*, respectively (**Figure 5A**), so how can common signaling pathways exist in these regions in order to compensate for axon guidance deficits? It is important to consider two factors: (1) the high structural similarity and shared binding partners among the Contactin family members (Shimoda and Watanabe, 2009; Bouyain and Watkins, 2010a); and (2) the capability of Chl1 to form large complexes through heterodimerization in *cis* and *trans* with other neuronal IgCAMs of the Contactin and CASPR families (Ashrafi et al., 2014). Other members of the L1, Contactin, and CASPR families should also be considered to be participating in regulating compensatory effects as a high degree of functional redundancy may exist between these neuronal IgCAMs. Some of these family members demonstrate region-specific expression as well. For example, *Cntn3* is expressed in the CA2 and not the DG, whilst *Cntn5*, *Caspr1*, *Caspr5*, and *L1cam* are expressed in the DG and not the CA2 region (©2015 Allen Institute for Brain Science; Hochgerner et al., 2018). Certain genes, such as *Cntn1*, *Caspr2*, *Caspr5*, and *Nrcam* are also commonly expressed in both the CA2 and DG (©2015 Allen Institute for Brain Science; Hochgerner et al., 2018). As interactors of Chl1 (Ashrafi et al., 2014), Cntn5 and Nrcam may initiate signaling pathways to compensate for Chl1 deficiency in the DG. Additionally, Cntn3 and Cntn5 are particularly interesting as, similar to Cntn6 and Cntn4, they are reported to interact with PTPRG to regulate neurite outgrowth (Bouyain and Watkins, 2010a,b). Notably, PTPRG is expressed in the CA1, CA2, CA3, and DG (©2015 Allen Institute for Brain Science; Hochgerner et al., 2018) – it is possible that interactors shared among these different neuronal IgCAMs such as PTPRG act as hub proteins to facilitate axon guidance in regions such as the hippocampus, allowing for compensation during instances where the expression or function of certain neuronal IgCAMs are disrupted. Therefore, not every member of the L1 and Contactin families need to be expressed in all cells of the hippocampus – rather, alternate family members form complex networks of interactomes to compensate for axon guidance deficits. In fact, the specific blend of these molecules in different neurons may bestow a combinatorial code upon different populations of neurons. It would also be pertinent to monitor the expression of other neuronal IgCAMs in Chl1-, Cntn6-, and Cntn4-deficient models to see if other family members are being upregulated to compensate for each other's deficiency. Examples of this have been observed in other ASD models such as the Shank3 mutant mouse, where upregulation of Shank1 and Shank2 are observed to partially compensate for synaptic defects (Zhou et al., 2016). However, shared interactions such as PTPRG between the Contactins also raise the question of whether certain neuronal IgCAMs act as core components for axon guidance regulation and if others exhibit higher degrees of functional redundancy? At this point further research is still required to answer this question.

FUTURE DIRECTIONS

Our understanding of the function of neuronal IgCAMs, *CHL1, CNTN6,* and *CNTN4,* encoded within the 3p26.3 region in neurodevelopment has greatly advanced over recent decades. Evidence has shown a genetic link between these genes, Del3p and ASD. In particular, there are specific CNVs reported in these genes (**Supplementary Table 1**). Through clinical reports and patient genetics, we are beginning to understand the link between CNVs in *CHL1, CNTN6,* and *CNTN4*, and the severity of Del3p and ASD phenotypes. CNVs occurring in these neuronal IgCAMs may affect the severity of ASD phenotypes through multiple molecular pathways. We hypothesize that disruption or imbalance of these pathways can contribute toward the ASD phenotype. However, the high variability of these CNVs makes it difficult to currently predict the effects of these mutations on gene dosage and their consequence on neurodevelopment. Further studies should aim to establish a link between CNV length, magnitude and location within a gene with the severity of ASD phenotypes reported in the patient in order to further elucidate genotype-phenotype relationships.

Disrupting the functions of CHL1, CNTN6, and CNTN4 and their signaling pathways may contribute to ASD via three main routes. Firstly, these neuronal IgCAMs participate in signaling pathways that regulate neurogenesis and neuronal survival. Chl1 induces activation of the PI3K, MAPK, and hedgehog signaling pathways (Nishimune et al., 2005; Katic et al., 2017), and Cntn6 modulates neuronal apoptosis by inhibiting the neurotoxic effects of Lphn1 (Zuko et al., 2016a). Cntn6 modulates activity of Lphn1 by direct binding, however, in regions of the brain Lphn1 may be regulated by other binding partners, since Cntn6 has a range of interactors (a common theme in the Contactin family) (Zuko et al., 2013). Secondly, these neuronal IgCAMs have been shown to interact with each other and with similar binding partners in the context of axon guidance, neuritogenesis and synapse formation likely participating in common signaling pathways and sequestering each other's binding partners (**Figure 5B**). Chl1-Cntn6 interactions are important in regulating dendritic morphology (Ye et al., 2008), and Cntn6 and Cntn4 interact with Ptprg to promote neurite extension (Bouyain and Watkins, 2010b; Cottrell et al., 2011; Mercati et al., 2013). Additionally, CHL1 and CNTN4 may regulate axon guidance and arborization via direct heterodimerization and perhaps an overlapping pathway of APP processing (Osterfield et al., 2008; Osterhout et al., 2015; Ou-Yang et al., 2018). CNTN4 is shown to be an extracellular binding partner of the E1 domain of APP, although this interaction leaves the Ig domains of CNTN4 available for other binding partners. This is important since not only is APP linked with neurodegeneration but also neurodevelopment

(Steinbach et al., 1998; Magara et al., 1999; Osterfield et al., 2008). Furthermore, the E1 domain of APP is important for neural stem cell differentiation (Ohsawa et al., 1999), synaptogenesis (Morimoto, 1998), and neurite outgrowth (Small et al., 1994; Ohsawa et al., 1997). The CNTN4-APP interaction has been observed in the olfactory bulb and retinal axons of the retinotectal system, which are regions where the development of axon–axon and axon-target contacts is crucial (Osterhout et al., 2015). Alterations in CNTN4 expression have been implicated to negatively affect the proteolytic processing of APP, which contributes to impairments in axon guidance and synaptic plasticity, reduced neuronal survival, and ultimately results in cognitive impairments (Bamford et al., 2020). Finally, deficiencies in CHL1, CNTN6, and CNTN4 may impair the formation and stabilization of synapses due to their role as synaptic adhesion molecules. Dysregulation of CHL1, CNTN6, and CNTN4 signaling is observed to alter synaptic function, causing impairments in synaptic plasticity and shifting the E/I balance in neuronal circuits. CHL1 and CNTN6 in particular play important roles in vesicular recycling at the presynapse (Leshchyns'ka et al., 2006; Sakurai et al., 2009, 2010; Andreyeva et al., 2010), and their deficiency alters both glutamatergic and GABAergic transmission and causes synaptic loss (Nikonenko et al., 2006; Sakurai et al., 2009, 2010; Schmalbach et al., 2015; Zuko et al., 2016b). CNTN4 deficiency is also observed to alter cell-surface expression of neurotransmitter receptors (Heise et al., 2018). Taken altogether, we hypothesize that disruptions to CHL1, CNTN6, and CNTN4 pathways impacts neurogenesis, neuronal survival and axon guidance. Disruptions to these neuronal IgCAMs can also lead to impairments in synaptic function by directly disrupting synapse formation and stabilization, or through altering synaptic transmission and plasticity. These impairments in turn can contribute to the cognitive and behavior phenotypes observed in Del3p and ASD.

Evidence from animal studies have also shown a potential involvement of these neuronal IgCAMs in the development of ASD-associated behaviors (**Table 2**), but importantly suggest that the deficiency of these molecules can be compensated for by other neuronal IgCAMs. The lack of strong behavioral phenotypes, as opposed to the pronounced defects in neuronal migration and neuritogenesis in culture, indicate that loss of function in CHL1, CNTN6, and CNTN4 may be compensated for by other neuronal IgCAMs which act to suppress the behavior phenotype. To better understand how these genes interact with one another, multi-gene models may be more appropriate than single-gene knockout studies. We hypothesize that a more severe phenotype will be observed when all three neuronal IgCAMs encoded in the 3p26.3 region are disrupted. A model in which all three genes have been disrupted will help to increase our understanding of how defects in multiple genes cause developmental syndromes such as Del3p. Such a model will also allow for further investigation into the formation of neuronal IgCAM complexes in different brain regions and the role they play in neurodevelopment.

AUTHOR CONTRIBUTIONS

AO-A: concept, research design, editing figures and artwork, and manuscript writing and editing. JG: research, generating figures and artwork, and manuscript writing. RB: formatting corrections and manuscript writing and editing. JB: critical input and manuscript editing. All authors read and approved the final manuscript.

ACKNOWLEDGMENTS

The authors acknowledge the insightful discussions with Drs. Rebecca G. Smith, Ehsan Pishva, and Miss. Charli Stoneman. We also thank Dr. Amila Zuko for critical reading of the manuscript and helpful suggestions.

SUPPLEMENTARY MATERIAL

The Supplementary Material for this article can be found online at: https://www.frontiersin.org/articles/10.3389/fncel.2020.611379/full#supplementary-material

REFERENCES

Abrahams, B. S., and Geschwind, D. H. (2008). Advances in autism genetics: on the threshold of a new neurobiology. *Nat. Rev. Genet.* 9, 341–355. doi: 10.1038/nrg2346

Abrahams, B. S., Arking, D. E., Campbell, D. B., Mefford, H. C., Morrow, E. M., Weiss, L. A., et al. (2013). SFARI Gene 2.0: a community-driven knowledgebase for the autism spectrum disorders (ASDs). *Mol. Autism* 4:36. doi: 10.1186/2040-2392-4-36

Acevedo, B., Aron, E., Pospos, S., and Jessen, D. (2018). The functional highly sensitive brain: a review of the brain circuits underlying sensory processing sensitivity and seemingly related disorders. *Philos. Trans. R. Soc. B Biol. Sci.* 373:20170161. doi: 10.1098/rstb.2017.0161

Alsanie, W. F., Penna, V., Schachner, M., Thompson, L. H., and Parish, C. L. (2017). Homophilic binding of the neural cell adhesion molecule CHL1 regulates development of ventral midbrain dopaminergic pathways. *Sci. Rep.* 7:9368. doi: 10.1038/s41598-017-09599-y

American Psychiatric Association (2013). *Diagnostic and Statistical Manual of Mental Disorders*, 5th Edn. Washington, DC: American Psychiatric Association, doi: 10.1176/appi.books.9780890425596

Andreyeva, A., Leshchyns'ka, I., Knepper, M., Betzel, C., Redecke, L., Sytnyk, V., et al. (2010). CHL1 is a selective organizer of the presynaptic machinery chaperoning the SNARE complex. *PLoS One* 5:e12018. doi: 10.1371/journal.pone.0012018

Angeloni, D., Lindor, N. M., Pack, S., Latif, F., Wei, M., and Lerman, M. I. (1999). CALL gene is haploinsufficient in a 3p- syndrome patient. *Am. J. Med. Genet.* 86, 482–485. doi: 10.1002/(SICI)1096-8628(19991029)86:5<482::AID-AJMG15<3.0.CO;2-L

Ango, F., Wu, C., Van Der Want, J. J., Wu, P., Schachner, M., and Huang, Z. J. (2008). Bergmann glia and the recognition molecule CHL1 organize GABAergic axons and direct innervation of Purkinje cell dendrites. *PLoS Biol.* 6:e103. doi: 10.1371/journal.pbio.0060103

Ashrafi, S., Betley, J. N., Comer, J. D., Brenner-Morton, S., Bar, V., Shimoda, Y., et al. (2014). Neuronal Ig/Caspr recognition promotes the formation of

axoaxonic synapses in mouse spinal cord. *Neuron* 81, 120–129. doi: 10.1016/j.neuron.2013.10.060

Bamford, R. A., Widagdo, J., Takamura, N., Eve, M., Anggono, V., and Oguro-Ando, A. (2020). The interaction between contactin and amyloid precursor protein and its role in Alzheimer's disease. *Neuroscience* 424, 184–202. doi: 10.1016/j.neuroscience.2019.10.006

Baranek, G. T., Watson, L. R., Boyd, B. A., Poe, M. D., David, F. J., and McGuire, L. (2013). Hyporesponsiveness to social and nonsocial sensory stimuli in children with autism, children with developmental delays, and typically developing children. *Dev. Psychopathol.* 25, 307–320. doi: 10.1017/S0954579412001071

Baranova, J., Dragunas, G., Botellho, M. C. S., Ayub, A. L. P., Bueno-Alves, R., Alencar, R. R., et al. (2020). Autism spectrum disorder: signaling pathways and prospective therapeutic targets. *Cell. Mol. Neurobiol.* doi: 10.1007/s10571-020-00882-7 [Epub ahead of print].

Barão, S., Gärtner, A., Leyva-Díaz, E., Demyanenko, G., Munck, S., Vanhoutvin, T., et al. (2015). Antagonistic effects of BACE1 and APH1B-γ-secretase control axonal guidance by regulating growth cone collapse. *Cell Rep.* 12, 1367–1376. doi: 10.1016/j.celrep.2015.07.059

Bavley, C. C., Rice, R. C., Fischer, D. K., Fakira, A. K., Byrne, M., Kosovsky, M., et al. (2018). Rescue of learning and memory deficits in the human nonsyndromic intellectual disability cereblon knock-out mouse model by targeting the amp-activated protein kinase–mtorc1 translational pathway. *J. Neurosci.* 38, 2780–2795. doi: 10.1523/JNEUROSCI.0599-17.2018

Besag, F. M. C. (2018). Epilepsy in patients with autism: links, risks and treatment challenges. *Neuropsychiatr. Dis. Treat.* 14, 1–10. doi: 10.2147/NDT.S120509

Betancur, C., Sakurai, T., and Buxbaum, J. D. (2009). The emerging role of synaptic cell-adhesion pathways in the pathogenesis of autism spectrum disorders. *Trends Neurosci.* 32, 402–412. doi: 10.1016/j.tins.2009.04.003

Billnitzer, A. J., Barskaya, I., Yin, C., and Perez, R. G. (2013). APP independent and dependent effects on neurite outgrowth are modulated by the receptor associated protein (RAP). *J. Neurochem.* 124, 123–132. doi: 10.1111/jnc.12051

Bitar, T., Hleihel, W., Marouillat, S., Vonwill, S., Vuillaume, M. L., Soufia, M., et al. (2019). Identification of rare copy number variations reveals PJA2, APCS, SYNPO, and TAC1 as novel candidate genes in Autism Spectrum Disorders. *Mol. Genet. Genomic Med.* 7:e786. doi: 10.1002/mgg3.786

Bittel, D. C., Kibiryeva, N., Dasouki, M., Knoll, J. H. M., and Butler, M. G. (2006). A 9-year-old male with a duplication of chromosome 3p25.3p26.2: clinical report and gene expression analysis. *Am. J. Med. Genet. A* 140, 573–579. doi: 10.1002/ajmg.a.31132

Bouyain, S., and Watkins, D. J. (2010a). Identification of tyrosine phosphatase ligands for contactin cell adhesion molecules. *Commun. Integr. Biol.* 3, 284–286. doi: 10.4161/cib.3.3.11656

Bouyain, S., and Watkins, D. J. (2010b). The protein tyrosine phosphatases PTPRZ and PTPRG bind to distinct members of the contactin family of neural recognition molecules. *Proc. Natl. Acad. Sci. U.S.A.* 107, 2443–2448. doi: 10.1073/pnas.0911235107

Bucan, M., Abrahams, B. S., Wang, K., Glessner, J. T., Herman, E. I., Sonnenblick, L. I., et al. (2009). Genome-wide analyses of exonic copy number variants in a family-based study point to novel autism susceptibility genes. *PLoS Genet.* 5:e1000536. doi: 10.1371/journal.pgen.1000536

Buhusi, M., Midkiff, B. R., Gates, A. M., Richter, M., Schachner, M., and Maness, P. F. (2003). Close homolog of L1 is an enhancer of integrin-mediated cell migration. *J. Biol. Chem.* 278, 25024–25031. doi: 10.1074/jbc.M303084200

Buhusi, M., Scripa, I., Williams, C. L., and Buhusi, C. V. (2013). Impaired interval timing and spatial-temporal integration in mice deficient in CHL1, a gene associated with schizophrenia. *Timing Time Percept.* 1, 21–38. doi: 10.1163/22134468-00002003

Carr, C. W., Moreno-De-Luca, D., Parker, C., Zimmerman, H. H., Ledbetter, N., Martin, C. L., et al. (2010). Chiari I malformation, delayed gross motor skills, severe speech delay, and epileptiform discharges in a child with FOXP1 haploinsufficiency. *Eur. J. Hum. Genet.* 18, 1216–1220. doi: 10.1038/ejhg.2010.96

Centers for Disease Control and Prevention (2020). *Data & Statistics on Autism Spectrum Disorder*. Available online at: https://www.cdc.gov/ncbddd/autism/data.html (accessed April 8, 2020).

Chatterjee, M., Schild, D., and Teunissen, C. E. (2019). Contactins in the central nervous system: role in health and disease. *Neural Regen. Res.* 14, 206–216. doi: 10.4103/1673-5374.244776

Chen, S., Mantei, N., Dong, L., and Schachner, M. (1999). Prevention of neuronal cell death by neural adhesion molecules L1 and CHL1. *J. Neurobiol.* 38, 428–439. doi: 10.1002/(SICI)1097-4695(19990215)38:3<428::AID-NEU10<3.0.CO;2-6

Chow, V. W., Mattson, M. P., Wong, P. C., and Gleichmann, M. (2010). An overview of APP processing enzymes and products. *Neuromolecular Med.* 12, 1–12. doi: 10.1007/s12017-009-8104-z

Colman, D. R., and Filbin, M. T. (1999). "Cell adhesion molecules and axonal outgrowth," in *Basic Neurochemistry: Molecular, Cellular and Medical Aspects*, eds G. J. Siegel, B. W. Agranoff, R. W. Albers, S. K. Fisher, and M. D. Uhler (Philadelphia, PA: Lippincott-Raven).

Colvert, E., Tick, B., McEwen, F., Stewart, C., Curran, S. R., Woodhouse, E., et al. (2015). Heritability of autism spectrum disorder in a UK population-based twin sample. *JAMA Psychiatry* 72, 415–423. doi: 10.1001/jamapsychiatry.2014.3028

Cottrell, C. E., Bir, N., Varga, E., Alvarez, C. E., Bouyain, S., Zernzach, R., et al. (2011). Contactin 4 as an autism susceptibility locus. *Autism Res.* 4, 189–199. doi: 10.1002/aur.184

Courchesne, E., Pramparo, T., Gazestani, V. H., Lombardo, M. V., Pierce, K., and Lewis, N. E. (2019). The ASD Living Biology: from cell proliferation to clinical phenotype. *Mol. Psychiatry* 24, 88–107. doi: 10.1038/s41380-018-0056-y

Cuoco, C., Ronchetto, P., Gimelli, S., Béna, F., Divizia, M. T., Lerone, M., et al. (2011). Microarray based analysis of an inherited terminal 3p26.3 deletion, containing only the CHL1 gene, from a normal father to his two affected children. *Orphanet J. Rare Dis.* 6:12. doi: 10.1186/1750-1172-6-12

Dakopolos, A. J., and Jahromi, L. B. (2019). Differences in sensory responses among children with autism spectrum disorder and typical development: links to joint attention and social competence. *Infant Child Dev.* 28:e2117. doi: 10.1002/icd.2117

Dalva, M. B., McClelland, A. C., and Kayser, M. S. (2007). Cell adhesion molecules: signalling functions at the synapse. *Nat. Rev. Neurosci.* 8, 206–220. doi: 10.1038/nrn2075

De Crescenzo, F., Postorino, V., Siracusano, M., Riccioni, A., Armando, M., Curatolo, P., et al. (2019). Autistic symptoms in schizophrenia spectrum disorders: a systematic review and meta-analysis. *Front. Psychiatry* 10:78. doi: 10.3389/fpsyt.2019.00078

de la Hoz, A. B., Maortua, H., García-Rives, A., Martínez-González, M. J., Ezquerra, M., and Tejada, M.-I. (2015). 3p14 de novo interstitial microdeletion in a patient with intellectual disability and autistic features with language impairment: a comparison with similar cases. *Case Rep. Genet.* 2015:876348. doi: 10.1155/2015/876348

De La Torre-Ubieta, L., Won, H., Stein, J. L., and Geschwind, D. H. (2016). Advancing the understanding of autism disease mechanisms through genetics. *Nat. Med.* 22, 345–361. doi: 10.1038/nm.4071

Demyanenko, G. P., Schachner, M., Anton, E., Schmid, R., Feng, G., Sanes, J., et al. (2004). Close homolog of L1 modulates area-specific neuronal positioning and dendrite orientation in the cerebral cortex. *Neuron* 44, 423–437. doi: 10.1016/j.neuron.2004.10.016

Demyanenko, G., Siesser, P., Wright, A., Brennaman, L., Bartsch, U., Schachner, M., et al. (2011). L1 and CHL1 cooperate in thalamocortical axon targeting. *Cereb. Cortex* 21, 401–412. doi: 10.1093/cercor/bhq115

Dijkhuizen, T., van Essen, T., van der Vlies, P., Verheij, J. B. G. M., Sikkema-Raddatz, B., van der Veen, A. Y., et al. (2006). FISH and array-CGH analysis of a complex chromosome 3 aberration suggests that loss of CNTN4 and CRBN contributes to mental retardation in 3pter deletions. *Am. J. Med. Genet. A* 140, 2482–2487. doi: 10.1002/ajmg.a.31487

Dong, L., Chen, S., Richter, M., and Schachner, M. (2002). Single-chain variable fragment antibodies against the neural adhesion molecule CHL1 (close homolog of L1) enhance neurite outgrowth. *J. Neurosci. Res.* 69, 437–447. doi: 10.1002/jnr.10250

Drumheller, T., McGillivray, B. C., Behrner, D., MacLeod, P., McFadden, D. E., Roberson, J., et al. (1996). Precise localisation of 3p25 breakpoints in four patients with the 3p-syndrome. *J. Med. Genet.* 33, 842–847. doi: 10.1136/jmg.33.10.842

Duffney, L. J., Zhong, P., Wei, J., Matas, E., Cheng, J., Qin, L., et al. (2015). Autism-like deficits in Shank3-deficient Mice are rescued by targeting actin regulators. *Cell Rep.* 11, 1400–1413. doi: 10.1016/j.celrep.2015.04.064

Enriquez-Barreto, L., and Morales, M. (2016). The PI3K signaling pathway as a pharmacological target in Autism related disorders and Schizophrenia. *Mol. Cell. Ther.* 4:2. doi: 10.1186/s40591-016-0047-9

Fabbri, C., Crisafulli, C., Calati, R., Albani, D., Forloni, G., Calabrò, M., et al. (2017). Neuroplasticity and second messenger pathways in antidepressant efficacy: pharmacogenetic results from a prospective trial investigating treatment resistance. *Eur. Arch. Psychiatry Clin. Neurosci.* 267, 723–735. doi: 10.1007/s00406-017-0766-1

Fabbri, C., Crisafulli, C., Gurwitz, D., Stingl, J., Calati, R., Albani, D., et al. (2015). Neuronal cell adhesion genes and antidepressant response in three independent samples. *Pharmacogenomics J.* 15, 538–548. doi: 10.1038/tpj.2015.15

Fan, L.-W., and Pang, Y. (2017). Dysregulation of neurogenesis by neuroinflammation: key differences in neurodevelopmental and neurological disorders. *Neural Regen. Res.* 12, 366–371. doi: 10.4103/1673-5374.202926

Fernandes, D., Santos, S. D., Coutinho, E., Whitt, J. L., Beltrão, N., Rondão, T., et al. (2019). Disrupted AMPA receptor function upon genetic- or antibody-mediated loss of Autism-associated CASPR2. *Cereb. Cortex* 29, 4919–4931. doi: 10.1093/cercor/bhz032

Fernandez, T. V., García-González, I. J., Mason, C. E., Hernández-Zaragoza, G., Ledezma-Rodríguez, V. C., Anguiano-Alvarez, V. M., et al. (2008). Molecular characterization of a patient with 3p deletion syndrome and a review of the literature. *Am. J. Med. Genet. A* 146A, 2746–2752. doi: 10.1002/ajmg.a.32533

Fernandez, T., Morgan, T., Davis, N., Klin, A., Morris, A., Farhi, A., et al. (2004). Disruption of contactin 4 (CNTN4) results in developmental delay and other features of 3p deletion syndrome. *Am. J. Hum. Genet.* 74, 1286–1293. doi: 10.1086/421474

Fernandez, T., Morgan, T., Davis, N., Klin, A., Morris, A., Farhi, A., et al. (2008). Disruption of contactin 4 (CNTN4) results in developmental delay and other features of 3p deletion syndrome. *Am. J. Hum. Genet.* 82:1385. doi: 10.1016/j.ajhg.2008.04.021

Flanagan, J. G. (2006). Neural map specification by gradients. *Curr. Opin. Neurobiol.* 16, 59–66. doi: 10.1016/j.conb.2006.01.010

Frints, S. G. M., Marynen, P., Hartmann, D., Fryns, J.-P., Steyaert, J., Schachner, M., et al. (2003). CALL interrupted in a patient with non-specific mental retardation: gene dosage-dependent alteration of murine brain development and behavior. *Hum. Mol. Genet.* 12, 1463–1474. doi: 10.1093/hmg/ddg165

Fusaoka, E., Inoue, T., Mineta, K., Agata, K., and Takeuchi, K. (2006). Structure and function of primitive immunoglobulin superfamily neural cell adhesion molecules: a lesson from studies on planarian. *Genes Cells* 11, 541–555. doi: 10.1111/j.1365-2443.2006.00962.x

Gamazon, E. R., and Stranger, B. E. (2015). The impact of human copy number variation on gene expression. *Brief. Funct. Genomics* 14, 352–357. doi: 10.1093/bfgp/elv017

Gao, R., Zaccard, C. R., Shapiro, L. P., Dionisio, L. E., Martin-de-Saavedra, M. D., Piguel, N. H., et al. (2019). The CNTNAP2-CASK complex modulates GluA1 subcellular distribution in interneurons. *Neurosci. Lett.* 701, 92–99. doi: 10.1016/j.neulet.2019.02.025

Glessner, J. T., Wang, K., Cai, G., Korvatska, O., Kim, C. E., Wood, S., et al. (2009). Autism genome-wide copy number variation reveals ubiquitin and neuronal genes. *Nature* 459, 569–573. doi: 10.1038/nature07953

Gollan, L., Salomon, D., Salzer, J. L., and Peles, E. (2003). Caspr regulates the processing of contactin and inhibits its binding to neurofascin. *J. Cell Biol.* 163, 1213–1218. doi: 10.1083/jcb.200309147

Green, S. A., Rudie, J. D., Colich, N. L., Wood, J. J., Shirinyan, D., Hernandez, L., et al. (2013). Overreactive brain responses to sensory stimuli in youth with autism spectrum disorders. *J. Am. Acad. Child Adolesc. Psychiatry* 52, 1158–1172. doi: 10.1016/j.jaac.2013.08.004

Guo, H., Peng, Y., Hu, Z., Li, Y., Xun, G., Ou, J., et al. (2017). Genome-wide copy number variation analysis in a Chinese autism spectrum disorder cohort. *Sci. Rep.* 7:44155. doi: 10.1038/srep44155

Guo, H., Xun, G., Peng, Y., Xiang, X., Xiong, Z., Zhang, L., et al. (2012). Disruption of contactin 4 in two subjects with autism in Chinese population. *Gene* 505, 201–205. doi: 10.1016/J.GENE.2012.06.051

Gurney, M. E., Cogram, P., Deacon, R. M., Rex, C., and Tranfaglia, M. (2017). Multiple behavior phenotypes of the fragile-X syndrome mouse model respond to chronic inhibition of phosphodiesterase-4D (PDE4D). *Sci. Rep.* 7:14653. doi: 10.1038/s41598-017-15028-x

Hajek, C. A., Ji, J., and Saitta, S. C. (2018). Interstitial chromosome 3p13p14 deletions: an update and review. *Mol. Syndromol.* 9, 122–133. doi: 10.1159/000488168

Halbleib, J. M., and Nelson, W. J. (2006). Cadherins in development: cell adhesion, sorting, and tissue morphogenesis. *Genes Dev.* 20, 3199–3214. doi: 10.1101/gad.1486806

Hampson, D. R., and Blatt, G. J. (2015). Autism spectrum disorders and neuropathology of the cerebellum. *Front. Neurosci.* 9:420. doi: 10.3389/fnins.2015.00420

Harvard, C., Malenfant, P., Koochek, M., Creighton, S., Mickelson, E., Holden, J., et al. (2005). A variant Cri du Chat phenotype and autism spectrum disorder in a subject with de novo cryptic microdeletions involving 5p15.2 and 3p24.3-25 detected using whole genomic array CGH. *Clin. Genet.* 67, 341–351. doi: 10.1111/j.1399-0004.2005.00406.x

Heise, C., Preuss, J. M., Schroeder, J. C., Battaglia, C. R., Kolibius, J., Schmid, R., et al. (2018). Heterogeneity of cell surface glutamate and GABA receptor expression in shank and CNTN4 autism mouse models. *Front. Mol. Neurosci.* 11:212. doi: 10.3389/fnmol.2018.00212

Heyden, A., Angenstein, F., Sallaz, M., Seidenbecher, C., and Montag, D. (2008). Abnormal axonal guidance and brain anatomy in mouse mutants for the cell recognition molecules close homolog of L1 and NgCAM-related cell adhesion molecule. *Neuroscience* 155, 221–233. doi: 10.1016/j.neuroscience.2008.04.080

Hillenbrand, R., Molthagen, M., Montag, D., and Schachner, M. (1999). The close homologue of the neural adhesion molecule L1 (CHL1): patterns of expression and promotion of neurite outgrowth by heterophilic interactions. *Eur. J. Neurosci.* 11, 813–826. doi: 10.1046/j.1460-9568.1999.00496.x

Hitt, B., Riordan, S. M., Kukreja, L., Eimer, W. A., Rajapaksha, T. W., and Vassar, R. (2012). β-Site amyloid precursor protein (APP)-cleaving enzyme 1 (BACE1)-deficient mice exhibit a close homolog of L1 (CHL1) loss-of-function phenotype involving axon guidance defects. *J. Biol. Chem.* 287, 38408–38425. doi: 10.1074/jbc.M112.415505

Hochgerner, H., Zeisel, A., Lönnerberg, P., and Linnarsson, S. (2018). Conserved properties of dentate gyrus neurogenesis across postnatal development revealed by single-cell RNA sequencing. *Nat. Neurosci.* 21, 290–299. doi: 10.1038/s41593-017-0056-2

Holm, J., Hillenbrand, R., Steuber, V., Bartsch, U., Moos, M., Lübbert, H., et al. (1996). Structural features of a close homologue of L1 (CHL1)in the mouse: a new member of the L1 family of neural recognition molecules. *Eur. J. Neurosci.* 8, 1613–1629. doi: 10.1111/j.1460-9568.1996.tb01306.x

Hornix, B. E., Havekes, R., and Kas, M. J. H. (2019). Multisensory cortical processing and dysfunction across the neuropsychiatric spectrum. *Neurosci. Biobehav. Rev.* 97, 138–151. doi: 10.1016/j.neubiorev.2018.02.010

Hortsch, M. (1996). The L1 family of neural cell adhesion molecules: old proteins performing new tricks. *Neuron* 17, 587–593. doi: 10.1016/S0896-6273(00)80192-0

Hu, J., Liao, J., Sathanoori, M., Kochmar, S., Sebastian, J., Yatsenko, S. A., et al. (2015). CNTN6 copy number variations in 14 patients: a possible candidate gene for neurodevelopmental and neuropsychiatric disorders. *J. Neurodev. Disord.* 7:26. doi: 10.1186/s11689-015-9122-9

Huang, X., Sun, J., Zhao, T., Wu, K. W., Watanabe, K., Xiao, Z. C., et al. (2011). Loss of NB-3 aggravates cerebral ischemia by impairing neuron survival and neurite growth. *Stroke* 42, 2910–2916. doi: 10.1161/strokeaha.110.609560

Huang, Z., Yu, Y., Shimoda, Y., Watanabe, K., and Liu, Y. (2012). Loss of neural recognition molecule NB-3 delays the normal projection and terminal branching of developing corticospinal tract axons in the mouse. *J. Comp. Neurol.* 520, 1227–1245. doi: 10.1002/cne.22772

Jacquemont, M.-L., Sanlaville, D., Redon, R., Raoul, O., Cormier-Daire, V., Lyonnet, S., et al. (2006). Array-based comparative genomic hybridisation identifies high frequency of cryptic chromosomal rearrangements in patients with syndromic autism spectrum disorders. *J. Med. Genet.* 43, 843–849. doi: 10.1136/jmg.2006.043166

Jakovcevski, I., Siering, J., Hargus, G., Karl, N., Hoelters, L., Djogo, N., et al. (2009). Close homologue of adhesion molecule L1 promotes survival of purkinje and granule cells and granule cell migration during murine cerebellar development. *J. Comp. Neurol.* 513, 496–510. doi: 10.1002/cne.21981

Jamain, S., Radyushkin, K., Hammerschmidt, K., Granon, S., Boretius, S., Varoqueaux, F., et al. (2008). Reduced social interaction and ultrasonic communication in a mouse model of monogenic heritable autism. *Proc. Natl. Acad. Sci. U.S.A.* 105, 1710–1715. doi: 10.1073/pnas.0711555105

Juan-Perez, C., Farrand, S., and Velakoulis, D. (2018). Schizophrenia and epilepsy as a result of maternally inherited CNTN6 copy number variant. *Schizophr. Res.* 202, 111–112. doi: 10.1016/j.schres.2018.06.062

Kaneko-Goto, T., Yoshihara, S. I., Miyazaki, H., and Yoshihara, Y. (2008). BIG-2 mediates olfactory axon convergence to target glomeruli. *Neuron* 57, 834–846. doi: 10.1016/j.neuron.2008.01.023

Kashevarova, A. A., Nazarenko, L. P., Schultz-Pedersen, S., Skryabin, N. A., Salyukova, O. A., Chechetkina, N. N., et al. (2014). Single gene microdeletions and microduplication of 3p26.3 in three unrelated families: CNTN6 as a new candidate gene for intellectual disability. *Mol. Cytogenet.* 7:97. doi: 10.1186/s13039-014-0097-0

Katic, J., Loers, G., Kleene, R., Karl, N., Schmidt, C., Buck, F., et al. (2014). Interaction of the cell adhesion molecule CHL1 with vitronectin, integrins, and the plasminogen activator inhibitor-2 promotes CHL1-induced neurite outgrowth and neuronal migration. *J. Neurosci.* 34, 14606–14623. doi: 10.1523/JNEUROSCI.3280-13.2014

Katic, J., Loers, G., Tosic, J., Schachner, M., and Kleene, R. (2017). The cell adhesion molecule CHL1 interacts with patched-1 to regulate apoptosis during postnatal cerebellar development. *J. Cell Sci.* 130, 2606–2619. doi: 10.1242/jcs.194563

Kazdoba, T. M., Leach, P. T., Yang, M., Silverman, J. L., Solomon, M., and Crawley, J. N. (2016). Translational mouse models of autism: advancing toward pharmacological therapeutics. *Curr. Top. Behav. Neurosci.* 28, 1–52. doi: 10.1007/7854_2015_5003

Kellogg, G., Sum, J., and Wallerstein, R. (2013). Deletion of 3p25.3 in a patient with intellectual disability and dysmorphic features with further definition of a critical region. *Am. J. Med. Genet. A* 161A, 1405–1408. doi: 10.1002/ajmg.a.35876

Kim, H. G., Kishikawa, S., Higgins, A. W., Seong, I. S., Donovan, D. J., Shen, Y., et al. (2008). Disruption of neurexin 1 associated with autism spectrum disorder. *Am. J. Hum. Genet.* 82, 199–207. doi: 10.1016/j.ajhg.2007.09.011

Kleene, R., Chaudhary, H., Karl, N., Katic, J., Kotarska, A., Guitart, K., et al. (2015). Interaction between CHL1 and serotonin receptor 2c regulates signal transduction and behavior in mice. *J. Cell Sci.* 128, 4642–4652. doi: 10.1242/jcs.176941

Kotarska, A., Fernandes, L., Kleene, R., and Schachner, M. (2020). Cell adhesion molecule close homolog of L1 binds to the dopamine receptor D2 and inhibits the internalization of its short isoform. *FASEB J.* 34, 4832–4851. doi: 10.1096/fj.201900577RRRR

Kuechler, A., Zink, A. M., Wieland, T., Lüdecke, H.-J., Cremer, K., Salviati, L., et al. (2015). Loss-of-function variants of SETD5 cause intellectual disability and the core phenotype of microdeletion 3p25.3 syndrome. *Eur. J. Hum. Genet.* 23, 753–760. doi: 10.1038/ejhg.2014.165

Kwon, C. H., Luikart, B. W., Powell, C. M., Zhou, J., Matheny, S. A., Zhang, W., et al. (2006). Pten regulates neuronal arborization and social interaction in mice. *Neuron* 50, 377–388. doi: 10.1016/j.neuron.2006.03.023

Lee, S., Takeda, Y., Kawano, H., Hosoya, H., Nomoto, M., Fujimoto, D., et al. (2000). Expression and regulation of a gene encoding neural recognition molecule NB-3 of the contactin/F3 subgroup in mouse brain. *Gene* 245, 253–266. doi: 10.1016/S0378-1119(00)00031-7

Leppa, V. M., Kravitz, S. N., Martin, C. L., Andrieux, J., Le Caignec, C., Martin-Coignard, D., et al. (2016). Rare inherited and de novo CNVs reveal complex contributions to ASD risk in multiplex families. *Am. J. Hum. Genet.* 99, 540–554. doi: 10.1016/j.ajhg.2016.06.036

Lesca, G., Rudolf, G., Labalme, A., Hirsch, E., Arzimanoglou, A., Genton, P., et al. (2012). Epileptic encephalopathies of the Landau-Kleffner and continuous spike and waves during slow-wave sleep types: genomic dissection makes the link with autism. *Epilepsia* 53, 1526–1538. doi: 10.1111/j.1528-1167.2012.03559.x

Leshchyns'ka, I., Sytnyk, V., Richter, M., Andreyeva, A., Puchkov, D., and Schachner, M. (2006). The adhesion molecule CHL1 regulates uncoating of clathrin-coated synaptic vesicles. *Neuron* 52, 1011–1025. doi: 10.1016/j.neuron.2006.10.020

Levy, D., Ronemus, M., Yamrom, B., Lee, Y., Leotta, A., Kendall, J., et al. (2011). Rare de novo and transmitted copy-number variation in autistic spectrum disorders. *Neuron* 70, 886–897. doi: 10.1016/j.neuron.2011.05.015

Li, C., Liu, C., Zhou, B., Hu, C., and Xu, X. (2016). Novel microduplication of CHL1 gene in a patient with autism spectrum disorder: a case report and a brief literature review. *Mol. Cytogenet.* 9:51. doi: 10.1186/s13039-016-0261-9

Li, Z., Tang, J., Li, H., Chen, S., He, Y., Liao, Y., et al. (2014). Shorter telomere length in peripheral blood leukocytes is associated with childhood autism. *Sci. Rep.* 4:7073. doi: 10.1038/srep07073

Lin, Y. C., Frei, J. A., Kilander, M. B. C., Shen, W., and Blatt, G. J. (2016). A subset of autism-associated genes regulate the structural stability of neurons. *Front. Cell. Neurosci.* 10:263. doi: 10.3389/fncel.2016.00263

Liu, Y., Zhang, Y., Zhao, D., Dong, R., Yang, X., Tammimies, K., et al. (2015). Rare de novo deletion of metabotropic glutamate receptor 7 (GRM7) gene in a patient with autism spectrum disorder. *Am. J. Med. Genet. Part B Neuropsychiatr. Genet.* 168, 258–264. doi: 10.1002/ajmg.b.32306

Maenner, M. J., Shaw, K. A., Baio, J., Washington, A., Patrick, M., DiRienzo, M., et al. (2020). Prevalence of Autism Spectrum Disorder Among Children Aged 8 Years — Autism and Developmental Disabilities Monitoring Network, 11 Sites, United States, 2016. *MMWR. Surveill. Summ.* 69, 1–12. doi: 10.15585/mmwr.ss6904a1

Magara, F., Müller, U., Li, Z. W., Lipp, H. P., Weissmann, C., Stagljar, M., et al. (1999). Genetic background changes the pattern of forebrain commissure defects in transgenic mice underexpressing the beta-amyloid-precursor protein. *Proc. Natl. Acad. Sci. U.S.A.* 96, 4656–4661. doi: 10.1073/PNAS.96.8.4656

Magnuson, K. M., and Constantino, J. N. (2011). Characterization of depression in children with autism spectrum disorders. *J. Dev. Behav. Pediatr.* 32, 332–340. doi: 10.1097/DBP.0b013e318213f56c

Malmgren, H., Sahlén, S., Wide, K., Lundvall, M., and Blennow, E. (2007). Distal 3p deletion syndrome: detailed molecular cytogenetic and clinical characterization of three small distal deletions and review. *Am. J. Med. Genet. Part A* 143A, 2143–2149. doi: 10.1002/ajmg.a.31902

Maness, P. F., and Schachner, M. (2007). Neural recognition molecules of the immunoglobulin superfamily: signaling transducers of axon guidance and neuronal migration. *Nat. Neurosci.* 10, 19–26. doi: 10.1038/nn1827

Marshall, C. R., Noor, A., Vincent, J. B., Lionel, A. C., Feuk, L., Skaug, J., et al. (2008). Structural variation of chromosomes in autism spectrum disorder. *Am. J. Hum. Genet.* 82, 477–488. doi: 10.1016/j.ajhg.2007.12.009

May, T., Brignell, A., and Williams, K. (2020). Autism spectrum disorder prevalence in children aged 12–13 years from the longitudinal study of Australian children. *Autism Res.* 13, 821–827. doi: 10.1002/aur.2286

McLaughlin, T., and O'Leary, D. D. M. (2005). Molecular gradients and development of retinotopic maps. *Annu. Rev. Neurosci.* 28, 327–355. doi: 10.1146/annurev.neuro.28.061604.135714

Mercati, O., Danckaert, A., André-Leroux, G., Bellinzoni, M., Gouder, L., Watanabe, K., et al. (2013). Contactin 4, -5 and -6 differentially regulate neuritogenesis while they display identical PTPRG binding sites. *Biol. Open* 2, 324–334. doi: 10.1242/bio.20133343

Mercati, O., Huguet, G., Danckaert, A., André-Leroux, G., Maruani, A., Bellinzoni, M., et al. (2017). CNTN6 mutations are risk factors for abnormal auditory sensory perception in autism spectrum disorders. *Mol. Psychiatry* 22, 625–633. doi: 10.1038/mp.2016.61

Missler, M., Südhof, T. C., and Biederer, T. (2012). Synaptic cell adhesion. *Cold Spring Harb. Perspect. Biol.* 4, 5694–5695. doi: 10.1101/cshperspect.a005694

Moghadasi, S., van Haeringen, A., Langendonck, L., Gijsbers, A. C. J., and Ruivenkamp, C. A. L. (2014). A terminal 3p26.3 deletion is not associated with dysmorphic features and intellectual disability in a four-generation family. *Am. J. Med. Genet. Part A* 164, 2863–2868. doi: 10.1002/ajmg.a.36700

Molenhuis, R. T., Bruining, H., Remmelink, E., de Visser, L., Loos, M., Burbach, J. P. H., et al. (2016). Limited impact of Cntn4 mutation on autism-related traits in developing and adult C57BL/6J mice. *J. Neurodev. Disord.* 8:6. doi: 10.1186/s11689-016-9140-2

Montag-Sallaz, M., Schachner, M., and Montag, D. (2002). Misguided axonal projections, neural cell adhesion molecule 180 mRNA upregulation, and altered behavior in mice deficient for the close homolog of L1. *Mol. Cell. Biol.* 22, 7967–7981. doi: 10.1128/mcb.22.22.7967-7981.2002

Morag, A., Pasmanik-Chor, M., Oron-Karni, V., Rehavi, M., Stingl, J. C., and Gurwitz, D. (2011). Genome-wide expression profiling of human lymphoblastoid cell lines identifies CHL1 as a putative SSRI antidepressant response biomarker. *Pharmacogenomics* 12, 171–184. doi: 10.2217/pgs.10.185

Morellini, F., Lepsveridze, E., Kähler, B., Dityatev, A., and Schachner, M. (2007). Reduced reactivity to novelty, impaired social behavior, and enhanced basal synaptic excitatory activity in perforant path projections to the dentate gyrus

in young adult mice deficient in the neural cell adhesion molecule CHL1. *Mol. Cell. Neurosci.* 34, 121–136. doi: 10.1016/J.MCN.2006.10.006

Moreno-Salinas, A. L., Avila-Zozaya, M., Ugalde-Silva, P., Hernández-Guzmán, D. A., Missirlis, F., and Boucard, A. A. (2019). Latrophilins: a neuro-centric view of an evolutionary conserved adhesion g protein-coupled receptor subfamily. *Front. Neurosci.* 13:700. doi: 10.3389/fnins.2019.00700

Morimoto, T. (1998). Novel domain-specific actions of amyloid precursor protein on developing synapses. *J. Neurosci.* 18, 9386–9393. doi: 10.1523/jneurosci.18-22-09386.1998

Mosconi, M. W., Wang, Z., Schmitt, L. M., Tsai, P., and Sweeney, J. A. (2015). The role of cerebellar circuitry alterations in the pathophysiology of autism spectrum disorders. *Front. Neurosci.* 9:296. doi: 10.3389/fnins.2015.00296

Mu, D., Xu, Y., Zhao, T., Watanabe, K., Xiao, Z. C., and Ye, H. (2018). Cntn6 deficiency impairs allocentric navigation in mice. *Brain Behav.* 8:e00969. doi: 10.1002/brb3.969

Murai, K. K., Misner, D., and Ranscht, B. (2002). Contactin supports synaptic plasticity associated with hippocampal long-term depression but not potentiation. *Curr. Biol.* 12, 181–190. doi: 10.1016/s0960-9822(02)00680-2

Naus, S., Richter, M., Wildeboer, D., Moss, M., Schachner, M., and Bartsch, J. W. (2004). Ectodomain shedding of the neural recognition molecule CHL1 by the metalloprotease-disintegrin ADAM8 promotes neurite outgrowth and suppresses neuronal cell death. *J. Biol. Chem.* 279, 16083–16090. doi: 10.1074/jbc.M400560200

Nelson, C. A., Varcin, K. J., Coman, N. K., DeVivo, I., and Tager-Flusberg, H. (2015). Shortened telomeres in families with a propensity to autism. *J. Am. Acad. Child Adolesc. Psychiatry* 54, 588–594. doi: 10.1016/j.jaac.2015.04.006

Nicolas, M., and Hassan, B. A. (2014). Amyloid precursor protein and neural development. *Development* 141, 2543–2548. doi: 10.1242/dev.108712

Niessen, C. M., Leckband, D., and Yap, A. S. (2011). Tissue organization by cadherin adhesion molecules: dynamic molecular and cellular mechanisms of morphogenetic regulation. *Physiol. Rev.* 91, 691–731. doi: 10.1152/physrev.00004.2010

Nikonenko, A. G., Sun, M., Lepsveridze, E., Apostolova, I., Petrova, I., Irintchev, A., et al. (2006). Enhanced perisomatic inhibition and impaired long-term potentiation in the CA1 region of juvenile CHL1-deficient mice. *Eur. J. Neurosci.* 23, 1839–1852. doi: 10.1111/j.1460-9568.2006.04710.x

Nishimune, H., Bernreuther, C., Carroll, P., Chen, S., Schachner, M., and Henderson, C. E. (2005). Neural adhesion molecules L1 and CHL1 are survival factors for motoneurons. *J. Neurosci. Res.* 80, 593–599. doi: 10.1002/jnr.20517

Noor, A., Lionel, A. C., Cohen-Woods, S., Moghimi, N., Rucker, J., Fennell, A., et al. (2014). Copy number variant study of bipolar disorder in Canadian and UK populations implicates synaptic genes. *Am. J. Med. Genet. Part B Neuropsychiatr. Genet.* 165, 303–313. doi: 10.1002/ajmg.b.32232

Oguro-Ando, A., Zuko, A., Kleijer, K. T. E., and Burbach, J. P. H. (2017). A current view on contactin-4, -5, and -6: implications in neurodevelopmental disorders. *Mol. Cell. Neurosci.* 81, 72–83. doi: 10.1016/J.MCN.2016.12.004

Ohsawa, I., Takamura, C., and Kohsaka, S. (1997). The amino-terminal region of amyloid precursor protein is responsible for neurite outgrowth in rat neocortical explant culture. *Biochem. Biophys. Res. Commun.* 236, 59–65. doi: 10.1006/bbrc.1997.6903

Ohsawa, I., Takamura, C., Morimoto, T., Ishiguro, M., and Kohsaka, S. (1999). Amino-terminal region of secreted form of amyloid precursor protein stimulates proliferation of neural stem cells. *Eur. J. Neurosci.* 11, 1907–1913. doi: 10.1046/j.1460-9568.1999.00601.x

Okumura, A., Yamamoto, T., Miyajima, M., Shimojima, K., Kondo, S., Abe, S., et al. (2014). 3p interstitial deletion including PRICKLE2 in identical twins with autistic features. *Pediatr. Neurol.* 51, 730–733. doi: 10.1016/j.pediatrneurol.2014.07.025

Osterfield, M., Egelund, R., Young, L. M., and Flanagan, J. G. (2008). Interaction of amyloid precursor protein with contactins and NgCAM in the retinotectal system. *Development* 135, 1189–1199. doi: 10.1242/dev.007401

Osterhout, J. A., Stafford, B. K., Nguyen, P. L., Yoshihara, Y., and Huberman, A. D. (2015). Contactin-4 mediates axon-target specificity and functional development of the accessory optic system. *Neuron* 86, 985–999. doi: 10.1016/j.neuron.2015.04.005

Ou-Yang, M.-H., Kurz, J. E., Nomura, T., Popovic, J., Rajapaksha, T. W., Dong, H., et al. (2018). Axonal organization defects in the hippocampus of adult conditional BACE1 knockout mice. *Sci. Transl. Med.* 10:eaao5620. doi: 10.1126/scitranslmed.aao5620

Oved, K., Farberov, L., Gilam, A., Israel, I., Haguel, D., Gurwitz, D., et al. (2017). MicroRNA-mediated regulation of ITGB3 and CHL1 is implicated in SSRI action. *Front. Mol. Neurosci.* 10:355. doi: 10.3389/fnmol.2017.00355

Oved, K., Morag, A., Pasmanik-Chor, M., Rehavi, M., Shomron, N., and Gurwitz, D. (2013). Genome-wide expression profiling of human lymphoblastoid cell lines implicates integrin beta-3 in the mode of action of antidepressants. *Transl. Psychiatry* 3:e313. doi: 10.1038/tp.2013.86

Palumbo, O., D'Agruma, L., Minenna, A. F., Palumbo, P., Stallone, R., Palladino, T., et al. (2013). 3p14.1 de novo microdeletion involving the FOXP1 gene in an adult patient with autism, severe speech delay and deficit of motor coordination. *Gene* 516, 107–113. doi: 10.1016/j.gene.2012.12.073

Pan, Y. H., Wu, N., and Yuan, X. B. (2019). Toward a better understanding of neuronal migration deficits in autism spectrum disorders. *Front. Cell Dev. Biol.* 7:205. doi: 10.3389/fcell.2019.00205

Pariani, M. J., Spencer, A., Graham, J. M., and Rimoin, D. L. (2009). A 785 kb deletion of 3p14.1p13, including the FOXP1 gene, associated with speech delay, contractures, hypertonia and blepharophimosis. *Eur. J. Med. Genet.* 52, 123–127. doi: 10.1016/j.ejmg.2009.03.012

Parmeggiani, G., Buldrini, B., Fini, S., Ferlini, A., and Bigoni, S. (2018). A new 3p14.2 microdeletion in a patient with intellectual disability and language impairment: case report and review of the literature. *Mol. Syndromol.* 9, 175–181. doi: 10.1159/000489842

Peltekova, I. T., Macdonald, A., and Armour, C. M. (2012). Microdeletion on 3p25 in a patient with features of 3p deletion syndrome. *Am. J. Med. Genet. Part A* 158A, 2583–2586. doi: 10.1002/ajmg.a.35559

Peñagarikano, O., Abrahams, B. S., Herman, E. I., Winden, K. D., Gdalyahu, A., Dong, H., et al. (2011). Absence of CNTNAP2 leads to epilepsy, neuronal migration abnormalities, and core autism-related deficits. *Cell* 147, 235–246. doi: 10.1016/j.cell.2011.08.040

Pinto, D., Pagnamenta, A. T., Klei, L., Anney, R., Merico, D., Regan, R., et al. (2010). Functional impact of global rare copy number variation in autism spectrum disorders. *Nature* 466, 368–372. doi: 10.1038/nature09146

Pohjola, P., de Leeuw, N., Penttinen, M., and Kääriäinen, H. (2010). Terminal 3p deletions in two families-Correlation between molecular karyotype and phenotype. *Am. J. Med. Genet. Part A* 152A, 441–446. doi: 10.1002/ajmg.a.33215

Poultney, C. S., Goldberg, A. P., Drapeau, E., Kou, Y., Harony-Nicolas, H., Kajiwara, Y., et al. (2013). Identification of small exonic CNV from whole-exome sequence data and application to autism spectrum disorder. *Am. J. Hum. Genet.* 93, 607–619. doi: 10.1016/j.ajhg.2013.09.001

Pratte, M., and Jamon, M. (2009). Impairment of novelty detection in mice targeted for the Chl1 gene. *Physiol. Behav.* 97, 394–400. doi: 10.1016/J.PHYSBEH.2009.03.009

Pratte, M., Rougon, G., Schachner, M., and Jamon, M. (2003). Mice deficient for the close homologue of the neural adhesion cell L1 (CHL1) display alterations in emotional reactivity and motor coordination. *Behav. Brain Res.* 147, 31–39. doi: 10.1016/S0166-4328(03)00114-1

Probst-Schendzielorz, K., Scholl, C., Efimkina, O., Ersfeld, E., Viviani, R., Serretti, A., et al. (2015). CHL1, ITGB3 and SLC6A4 gene expression and antidepressant drug response: results from the Munich Antidepressant Response Signature (MARS) study. *Pharmacogenomics* 16, 689–701. doi: 10.2217/pgs.15.31

Ramaswami, G., and Geschwind, D. H. (2018). Genetics of autism spectrum disorder. *Handb. Clin. Neurol.* 147, 321–329. doi: 10.1016/B978-0-444-63233-3.00021-X

Ray, B., Long, J. M., Sokol, D. K., and Lahiri, D. K. (2011). Increased secreted amyloid precursor protein-α (sappα) in severe autism: proposal of a specific, anabolic pathway and putative biomarker. *PLoS One* 6:e20405. doi: 10.1371/journal.pone.0020405

Ren, J., Zhao, T., Xu, Y., and Ye, H. (2016). Interaction between DISC1 and CHL1 in regulation of neurite outgrowth. *Brain Res.* 1648, 290–297. doi: 10.1016/j.brainres.2016.06.033

Repnikova, E. A., Lyalin, D. A., McDonald, K., Astbury, C., Hansen-Kiss, E., Cooley, L. D., et al. (2020). CNTN6 copy number variations: uncertain clinical significance in individuals with neurodevelopmental disorders. *Eur. J. Med. Genet.* 63:103636. doi: 10.1016/j.ejmg.2019.02.008

Ricceri, L., Michetti, C., and Scattoni, M. L. (2016). "Mouse behavior and models for autism spectrum disorders," in *Neuronal and Synaptic Dysfunction in Autism Spectrum Disorder and Intellectual Disability*, eds C. Sala and C. Verpelli (Cambridge, MA: Elsevier Inc.), 269–293. doi: 10.1016/B978-0-12-800109-7.00017-0

Riess, A., Grasshoff, U., Schäferhoff, K., Bonin, M., Riess, O., Horber, V., et al. (2012). Interstitial 3p25.3-p26.1 deletion in a patient with intellectual disability. *Am. J. Med. Genet. Part A* 158A, 2587–2590. doi: 10.1002/ajmg.a.35562

Rogers, D. C., Fisher, E. M. C., Brown, S. D. M., Peters, J., Hunter, A. J., and Martin, J. E. (1997). Behavioral and functional analysis of mouse phenotype: SHIRPA, a proposed protocol for comprehensive phenotype assessment. *Mamm. Genome* 8, 711–713. doi: 10.1007/s003359900551

Rogers, D. C., Peters, J., Martin, J. E., Ball, S., Nicholson, S. J., Witherden, A. S., et al. (2001). SHIRPA, a protocol for behavioral assessment: validation for longitudinal study of neurological dysfunction in mice. *Neurosci. Lett.* 306, 89–92. doi: 10.1016/S0304-3940(01)01885-7

Roohi, J., Montagna, C., Tegay, D. H., Palmer, L. E., DeVincent, C., Pomeroy, J. C., et al. (2009). Disruption of contactin 4 in three subjects with autism spectrum disorder. *J. Med. Genet.* 46, 176–182. doi: 10.1136/jmg.2008.057505

Rubio-Marrero, E. N., Vincelli, G., Jeffries, C. M., Shaikh, T. R., Pakos, I. S., Ranaivoson, F. M., et al. (2016). Structural characterization of the extracellular domain of CASPR2 and insights into its association with the novel ligand Contactin 1. *J. Biol. Chem.* 291, 5788–5802. doi: 10.1074/jbc.M115.705681

Rylaarsdam, L., and Guemez-Gamboa, A. (2019). Genetic causes and modifiers of autism spectrum disorder. *Front. Cell. Neurosci.* 13:385. doi: 10.3389/fncel.2019.00385

Sakurai, K., Toyoshima, M., Takeda, Y., Shimoda, Y., and Watanabe, K. (2010). Synaptic formation in subsets of glutamatergic terminals in the mouse hippocampal formation is affected by a deficiency in the neural cell recognition molecule NB-3. *Neurosci. Lett.* 473, 102–106. doi: 10.1016/j.neulet.2010.02.027

Sakurai, K., Toyoshima, M., Ueda, H., Matsubara, K., Takeda, Y., Karagogeos, D., et al. (2009). Contribution of the neural cell recognition molecule NB-3 to synapse formation between parallel fibers and Purkinje cells in mouse. *Dev. Neurobiol.* 69, 811–824. doi: 10.1002/dneu.20742

Sandin, S., Lichtenstein, P., Kuja-Halkola, R., Larsson, H., Hultman, C. M., and Reichenberg, A. (2014). The familial risk of autism. *JAMA* 311:1770. doi: 10.1001/jama.2014.4144

Santos, S. D., Iuliano, O., Ribeiro, L., Veran, J., Ferreira, J. S., Rio, P., et al. (2012). Contactin-associated protein 1 (Caspr1) regulates the traffic and synaptic content of α-amino-3-hydroxy-5-methyl-4-isoxazolepropionic acid (AMPA)-type glutamate receptors. *J. Biol. Chem.* 287, 6868–6877. doi: 10.1074/jbc.M111.322909

Schinzel, A. (1981). Duplication-deletion with partial trisomy 1q and partial monosomy 3p resulting from a maternal reciprocal translocation rcp(1;3)(q32;p25). *J. Med. Genet.* 18, 64–68. doi: 10.1136/jmg.18.1.64

Schlatter, M. C., Buhusi, M., Wright, A. G., and Maness, P. F. (2008). CHL1 promotes Sema3A-induced growth cone collapse and neurite elaboration through a motif required for recruitment of ERM proteins to the plasma membrane. *J. Neurochem.* 104, 731–744. doi: 10.1111/j.1471-4159.2007.05013.x

Schmalbach, B., Lepsveridze, E., Djogo, N., Papashvili, G., Kuang, F., Leshchyns'Ka, I., et al. (2015). Age-dependent loss of parvalbumin-expressing hippocampal interneurons in mice deficient in CHL1, a mental retardation and schizophrenia susceptibility gene. *J. Neurochem.* 135, 830–844. doi: 10.1111/jnc.13284

Schwaibold, E. M. C., Zoll, B., Burfeind, P., Hobbiebrunken, E., Wilken, B., Funke, R., et al. (2013). A 3p interstitial deletion in two monozygotic twin brothers and an 18-year-old man: further characterization and review. *Am. J. Med. Genet. Part A* 161, 2634–2640. doi: 10.1002/ajmg.a.36129

Sebat, J., Lakshmi, B., Malhotra, D., Troge, J., Lese-Martin, C., Walsh, T., et al. (2007). Strong association of de novo copy number mutations with autism. *Science* 316, 445–449. doi: 10.1126/science.1138659

Shaw, K. A., Maenner, M. J., Baio, J., Washington, A., Christensen, D. L., Wiggins, L. D., et al. (2020). Early identification of autism spectrum disorder among children aged 4 years – early autism and developmental disabilities monitoring network, six sites, United States, 2016. *MMWR. Surveill. Summ.* 69, 1–11. doi: 10.15585/mmwr.ss6903a1

Shimoda, Y., and Watanabe, K. (2009). Contactins: emerging key roles in the development and function of the nervous system. *Cell Adh. Migr.* 3, 64–70. doi: 10.4161/cam.3.1.7764

Shoukier, M., Fuchs, S., Schwaibold, E., Lingen, M., Gärtner, J., Brockmann, K., et al. (2013). Microduplication of 3p26.3 in nonsyndromic intellectual disability indicates an important role of CHL1 for normal cognitive function. *Neuropediatrics* 44, 268–271. doi: 10.1055/s-0033-1333874

Shuib, S., McMullan, D., Rattenberry, E., Barber, R. M., Rahman, F., Zatyka, M., et al. (2009). Microarray based analysis of 3p25-p26 deletions (3p-syndrome). *Am. J. Med. Genet. Part A* 149A, 2099–2105. doi: 10.1002/ajmg.a.32824

Sinha, S., Anderson, J. P., Barbour, R., Basi, G. S., Caccaveffo, R., Davis, D., et al. (1999). Purification and cloning of amyloid precursor protein β-secretase from human brain. *Nature* 402, 537–540. doi: 10.1038/990114

Small, D. H., Nurcombe, V., Reed, G., Clarris, H., Moir, R., Beyreuther, K., et al. (1994). A heparin-binding domain in the amyloid protein precursor of Alzheimer's disease is involved in the regulation of neurite outgrowth. *J. Neurosci.* 14, 2117–2127. doi: 10.1523/jneurosci.14-04-02117.1994

Sokol, D. K., Maloney, B., Westmark, C. J., and Lahiri, D. K. (2019). Novel contribution of secreted amyloid-β precursor protein to white matter brain enlargement in autism spectrum disorder. *Front. Psychiatry* 10:165. doi: 10.3389/fpsyt.2019.00165

Srivastava, A. K., and Schwartz, C. E. (2014). Intellectual disability and autism spectrum disorders: causal genes and molecular mechanisms. *Neurosci. Biobehav. Rev.* 46, 161–174. doi: 10.1016/j.neubiorev.2014.02.015

Steinbach, J. P., Müller, U., Leist, M., Li, Z.-W., Nicotera, P., and Aguzzi, A. (1998). Hypersensitivity to seizures in β-amyloid precursor protein deficient mice. *Cell Death Differ.* 5, 858–866. doi: 10.1038/sj.cdd.4400391

Sytnyk, V., Leshchyns'ka, I., and Schachner, M. (2017). Neural cell adhesion molecules of the immunoglobulin superfamily regulate synapse formation, maintenance, and function. *Trends Neurosci.* 40, 295–308. doi: 10.1016/j.tins.2017.03.003

Takeda, Y., Akasaka, K., Lee, S., Kobayashi, S., Kawano, H., Murayama, S., et al. (2003). Impaired motor coordination in mice lacking neural recognition molecule NB-3 of the contactin/F3 subgroup. *J. Neurobiol.* 56, 252–265. doi: 10.1002/neu.10222

Tassano, E., Biancheri, R., Denegri, L., Porta, S., Novara, F., Zuffardi, O., et al. (2014). Heterozygous deletion of CHL1 gene: detailed array-CGH and clinical characterization of a new case and review of the literature. *Eur. J. Med. Genet.* 57, 626–629. doi: 10.1016/j.ejmg.2014.09.007

Tassano, E., Uccella, S., Giacomini, T., Severino, M., Fiorio, P., Gimelli, G., et al. (2018). Clinical and molecular characterization of two patients with CNTN6 copy number variations. *Cytogenet. Genome Res.* 156, 144–149. doi: 10.1159/000494152

Thompson, S. L., and Dulawa, S. C. (2019). Dissecting the roles of β-arrestin2 and GSK-3 signaling in 5-HT1BR-mediated perseverative behavior and prepulse inhibition deficits in mice. *PLoS One* 14:e0211239. doi: 10.1371/journal.pone.0211239

Ţuţulan-Cuniţă, A. C., Papuc, S. M., Arghir, A., Rötzer, K. M., Deshpande, C., Lungeanu, A., et al. (2012). 3p interstitial deletion: novel case report and review. *J. Child Neurol.* 27, 1062–1066. doi: 10.1177/0883073811431016

van Daalen, E., Kemner, C., Verbeek, N. E., van der Zwaag, B., Dijkhuizen, T., Rump, P., et al. (2011). Social responsiveness scale-aided analysis of the clinical impact of copy number variations in autism. *Neurogenetics* 12, 315–323. doi: 10.1007/s10048-011-0297-2

Varga, E. A., Pastore, M., Prior, T., Herman, G. E., and McBride, K. L. (2009). The prevalence of PTEN mutations in a clinical pediatric cohort with autism spectrum disorders, developmental delay, and macrocephaly. *Genet. Med.* 11, 111–117. doi: 10.1097/GIM.0b013e31818fd762

Vassar, R., Bennett, B. D., Babu-Khan, S., Kahn, S., Mendiaz, E. A., Denis, P., et al. (1999). β-Secretase cleavage of Alzheimer's amyloid precursor protein by the transmembrane aspartic protease BACE. *Science* 286, 735–741. doi: 10.1126/science.286.5440.735

Verjaal, M., and De Nef, M. B. (1978). A patient with a partial deletion of the short arm of chromosome 3. *Am. J. Dis. Child.* 132, 43–45. doi: 10.1001/archpedi.1978.02120260045012

Verma, V., Paul, A., Vishwanath, A. A., Vaidya, B., and Clement, J. P. (2019). Understanding intellectual disability and utism spectrum disorders from

common mouse models: synapses to behaviour. *Open Biol.* 9:180265. doi: 10.1098/rsob.180265

Wang, B., Li, H., Mutlu, S. A., Bowser, D. A., Moore, M. J., Wang, M. C., et al. (2017). The amyloid precursor protein is a conserved receptor for slit to mediate axon guidance. *eNeuro* 4. doi: 10.1523/ENEURO.0185-17.2017

Wang, S. S. H., Kloth, A. D., and Badura, A. (2014). The cerebellum, sensitive periods, and autism. *Neuron* 83, 518–532. doi: 10.1016/j.neuron.2014.07.016

Wang, X., Wang, C., and Pei, G. (2018). α-secretase ADAM10 physically interacts with β-secretase BACE1 in neurons and regulates CHL1 proteolysis. *J. Mol. Cell Biol.* 10, 411–422. doi: 10.1093/jmcb/mjy001

Weehi, L. T., Maikoo, R., Cormack, A. M., Mazzaschi, R., Ashton, F., Zhang, L., et al. (2014). Microduplication of 3p26.3 implicated in cognitive development. *Case Rep. Genet.* 2014:295359. doi: 10.1155/2014/295359

Wegiel, J., Kuchna, I., Nowicki, K., Imaki, H., Wegiel, J., Marchi, E., et al. (2010). The neuropathology of autism: defects of neurogenesis and neuronal migration, and dysplastic changes. *Acta Neuropathol.* 119, 755–770. doi: 10.1007/s00401-010-0655-4

Wei, H., Alberts, I., and Li, X. (2014). The apoptotic perspective of autism. *Int. J. Dev. Neurosci.* 36, 13–18. doi: 10.1016/j.ijdevneu.2014.04.004

World Health Organization (2019). *Autism Spectrum Disorders*. Available online at: https://www.who.int/news-room/fact-sheets/detail/autism-spectrum-disorders (accessed April 8, 2020).

Wright, A. G., Demyanenko, G. P., Powell, A., Schachner, M., Enriquez-Barreto, L., Tran, T. S., et al. (2007). Close homolog of L1 and neuropilin 1 mediate guidance of thalamocortical axons at the ventral telencephalon. *J. Neurosci.* 27, 13667–13679. doi: 10.1523/JNEUROSCI.2888-07.2007

Yamagata, M., and Sanes, J. R. (2012). Expanding the Ig superfamily code for laminar specificity in retina: expression and role of contactins. *J. Neurosci.* 32, 14402–14414. doi: 10.1523/JNEUROSCI.3193-12.2012

Yamagata, M., Weiner, J. A., and Sanes, J. R. (2002). Sidekicks: synaptic adhesion molecules that promote lamina-specific connectivity in the retina. *Cell* 110, 649–660. doi: 10.1016/S0092-8674(02)00910-8

Yang, X., Hou, D., Jiang, W., and Zhang, C. (2014). Intercellular protein-protein interactions at synapses. *Protein Cell* 5, 420–444. doi: 10.1007/s13238-014-0054-z

Yates, A. D., Achuthan, P., Akanni, W., Allen, J., Allen, J., Alvarez-Jarreta, J., et al. (2020). Ensembl 2020. *Nucleic Acids Res.* 48, D682–D688.

Ye, H., Tan, Y. L. J., Ponniah, S., Takeda, Y., Wang, S.-Q., Schachner, M., et al. (2008). Neural recognition molecules CHL1 and NB-3 regulate apical dendrite orientation in the neocortex via PTP alpha. *EMBO J.* 27, 188–200. doi: 10.1038/sj.emboj.7601939

Ye, H., Zhao, T., Tan, Y. L. J., Liu, J., Pallen, C. J., and Xiao, Z.-C. (2011). Receptor-like protein-tyrosine phosphatase α enhances cell surface expression of neural adhesion molecule NB-3. *J. Biol. Chem.* 286, 26071–26080.

Yizhar, O., Fenno, L. E., Prigge, M., Schneider, F., Davidson, T. J., Ogshea, D. J., et al. (2011). Neocortical excitation/inhibition balance in information processing and social dysfunction. *Nature* 477, 171–178. doi: 10.1038/nature10360

Yoshihara, Y., Kawasaki, M., Tamada, A., Nagata, S., Kagamiyama, H., and Mori, K. (1995). Overlapping and differential expression of BIG-2, BIG-1, TAG-1, and F3: four members of an axon-associated cell adhesion molecule subgroup of the immunoglobulin superfamily. *J. Neurobiol.* 28, 51–69. doi: 10.1002/neu.480280106

Zablotsky, B., Black, L. I., Maenner, M. J., Schieve, L. A., and Blumberg, S. J. (2015). Estimated prevalence of autism and other developmental disabilities following questionnaire changes in the 2014 national health interview survey. *Natl. Health Stat. Report.* 2015, 1–20.

Zerbi, V., Ielacqua, G. D., Markicevic, M., Haberl, M. G., Ellisman, M. H., Bhaskaran, A. A., et al. (2018). Dysfunctional autism risk genes cause circuit-specific connectivity deficits with distinct developmental trajectories. *Cereb. Cortex* 28, 2495–2506. doi: 10.1093/cercor/bhy046

Zhang, S. Q., Fleischer, J., Al-Kateb, H., Mito, Y., Amarillo, I., and Shinawi, M. (2020). Intragenic CNTN4 copy number variants associated with a spectrum of neurobehavioral phenotypes. *Eur. J. Med. Genet.* 63:103736. doi: 10.1016/j.ejmg.2019.103736

Zheng, Z., Zheng, P., and Zou, X. (2018). Association between schizophrenia and autism spectrum disorder: a systematic review and meta-analysis. *Autism Res.* 11, 1110–1119. doi: 10.1002/aur.1977

Zhou, Y., Kaiser, T., Monteiro, P., Zhang, X., Van der Goes, M. S., Wang, D., et al. (2016). Mice with Shank3 mutations associated with ASD and schizophrenia display both shared and distinct defects. *Neuron* 89, 147–162. doi: 10.1016/j.neuron.2015.11.023

Zuko, A., Kleijer, K. T. E., Oguro-Ando, A., Kas, M. J. H., van Daalen, E., van der Zwaag, B., et al. (2013). Contactins in the neurobiology of autism. *Eur. J. Pharmacol.* 719, 63–74. doi: 10.1016/j.ejphar.2013.07.016

Zuko, A., Oguro-Ando, A., Post, H., Taggenbrock, R. L. R. E., van Dijk, R. E., Altelaar, A. F. M., et al. (2016a). Association of cell adhesion molecules contactin-6 and latrophilin-1 regulates neuronal apoptosis. *Front. Mol. Neurosci.* 9:143. doi: 10.3389/fnmol.2016.00143

Zuko, A., Oguro-Ando, A., van Dijk, R., Gregorio-Jordan, S., van der Zwaag, B., and Burbach, J. P. H. (2016b). Developmental role of the cell adhesion molecule Contactin-6 in the cerebral cortex and hippocampus. *Cell Adh. Migr.* 10, 378–392. doi: 10.1080/19336918.2016.1155018

Conflict of Interest: The authors declare that the research was conducted in the absence of any commercial or financial relationships that could be construed as a potential conflict of interest.

frontiers in Cellular Neuroscience

REVIEW
published: 14 January 2021
doi: 10.3389/fncel.2020.592710

Neural Mechanisms Underlying Repetitive Behaviors in Rodent Models of Autism Spectrum Disorders

Tanya Gandhi and Charles C. Lee*

Department of Comparative Biomedical Sciences, Louisiana State University School of Veterinary Medicine, Baton Rouge, LA, United States

Autism spectrum disorder (ASD) is comprised of several conditions characterized by alterations in social interaction, communication, and repetitive behaviors. Genetic and environmental factors contribute to the heterogeneous development of ASD behaviors. Several rodent models display ASD-like phenotypes, including repetitive behaviors. In this review article, we discuss the potential neural mechanisms involved in repetitive behaviors in rodent models of ASD and related neuropsychiatric disorders. We review signaling pathways, neural circuits, and anatomical alterations in rodent models that display robust stereotypic behaviors. Understanding the mechanisms and circuit alterations underlying repetitive behaviors in rodent models of ASD will inform translational research and provide useful insight into therapeutic strategies for the treatment of repetitive behaviors in ASD and other neuropsychiatric disorders.

Keywords: autism models, repetitive behavior, neural mechanisms, signaling, circuitry, neuroanatomical alterations

OPEN ACCESS

Edited by:
Yu-Chih Lin,
Hussman Institute for Autism, United States

Reviewed by:
Mark H. Lewis,
University of Florida, United States
Christina Gross,
Cincinnati Children's Hospital Medical Center, United States

****Correspondence:***
Tanya Gandhi
tgandh1@lsu.edu

Specialty section:
This article was submitted to Cellular Neuropathology, a section of the journal Frontiers in Cellular Neuroscience

Received: *07 August 2020*
Accepted: *09 December 2020*
Published: *14 January 2021*

Citation:
Gandhi T and Lee CC (2021) Neural Mechanisms Underlying Repetitive Behaviors in Rodent Models of Autism Spectrum Disorders. Front. Cell. Neurosci. 14:592710. doi: 10.3389/fncel.2020.592710

INTRODUCTION

Autism spectrum disorder (ASD) consists of a group of neurodevelopmental disorders with shared, yet heterogeneous, behaviors. With the introduction of improved diagnostic criteria, there has been a substantial rise in the prevalence of autistic cases in the last few decades, reported between three and six children per 1,000 worldwide (Kassim and Mohamed, 2019; Lord et al., 2020) and 1 in 54 children in the US (Zablotsky et al., 2019; Maenner et al., 2020). The variability in global prevalence is largely due to differences in methodological assessment and environmental and/or geographical factors (Chiarotti and Venerosi, 2020; Lord et al., 2020). Both genetic and environmental factors influence the development of ASD and may converge on similar neural outcomes, such as altered connectivity, excitation/inhibition imbalance, and signaling system alterations (Muhle et al., 2004; Satterstrom et al., 2020). Several candidate genes have been associated with the development of ASD (Levitt and Campbell, 2009; Yuen et al., 2017; Feliciano et al., 2019; Grove et al., 2019; Guo et al., 2019); siblings born in families with ASD are particularly high risk indicating a strong genetic basis (Stubbs et al., 2016). Environmental factors involved in the development of ASD include prenatal and postnatal complications, viral infections and nutrient deficiencies (Grabrucker, 2013; Sealey et al., 2016; Karimi et al., 2017; Modabbernia et al., 2017). Understanding these environmental and genetic interactions in autism risk will help guide treatment strategies for ASD (Chaste and Leboyer, 2012; LaSalle, 2013; Tordjman et al., 2014; Kim and Leventhal, 2015; Nardone and Elliott, 2016).

Children with ASD are characterized by social and communication challenges and restricted, repetitive behaviors (Baranek, 1999; Lord et al., 2000). These core behaviors are often accompanied by comorbidities such as epilepsy, anxiety, hyperactivity, and aggression (Richler et al., 2007; King et al., 2009). The restricted, repetitive behaviors (RRBs) in ASD are clustered into two categories. The repetitive behaviors include stereotypic motor movements, repetitive use of objects, self-injurious behaviors, and the circumscribed behaviors include compulsions, desire for sameness, rituals, and restricted interests (Zandt et al., 2007; Whitehouse and Lewis, 2015). The restricted, repetitive behaviors in ASD share similarities with obsessive-compulsive disorder (OCD) and other neuropsychiatric and neurodevelopmental disorders (Scahill and Challa, 2016; Jiujias et al., 2017; Gulisano et al., 2020). Currently, behavioral and pharmacological interventions target specific symptoms and/or associated comorbidities, which are personalized according to individual needs (Eissa et al., 2018; Chahin et al., 2020). Yet, more robust therapeutic interventions have been required that target the underlying neural mechanisms that govern these core autistic symptoms.

Behavioral approaches are typically used to treat repetitive behaviors in ASD and related neurodevelopmental disorders. Behavioral approaches usually employ reinforcement procedures, altering the environment, and promoting variability and flexibility in behavior (Boyd et al., 2012). Pharmacological interventions for irritability and some forms of repetitive behavior, such as self-injurious behavior include selective serotonin reuptake inhibitors (SSRIs) like Fluoxetine and antipsychotics such as haloperidol (typical) and Risperidone (atypical) (Gencer et al., 2008; Miral et al., 2008; Malone and Waheed, 2009; Doyle and McDougle, 2012; DeFilippis and Wagner, 2016; Masi et al., 2017; Maneeton et al., 2018). Risperidone is a second-generation antipsychotic medication that has been FDA approved for the treatment of irritability in children and adolescents (McDougle et al., 2005, 2008; Scahill et al., 2007, 2012; Aman et al., 2009). It is an antagonist at the serotonin 2A and dopamine D2 receptors and is useful in alleviating irritability, aggression, and self-injurious behavior in young ASD subjects (McCracken et al., 2002; Shea et al., 2004; Chavez et al., 2006; Kent et al., 2013; Fung et al., 2016; Maneeton et al., 2018). Besides, in controlled clinical trials, some of these pharmacological medications also reduce repetitive behaviors, but with potential side-effects that limit the widespread usage of these drugs in the treatment of ASD and as such is not approved by the FDA for repetitive disorders (McPheeters et al., 2011; Sharma and Shaw, 2012; Whitehouse and Lewis, 2015). Additionally, the benefits of pharmacological medications in improving ASD behavior are highly variable across studies and clinical populations. There is also a paucity of long-term clinical trials with a large sample size on pharmacological interventions against restricted/repetitive behavior in ASD (Yu et al., 2020; Zhou et al., 2020). Furthermore, there is a lack of evidence-based treatment strategies targeting diverse repetitive/restricted behaviors in ASD. Hence, novel treatment strategies are required that target core autistic deficits, while limiting the detrimental side effects of such medications. In this review article, we have discussed preclinical studies demonstrating the efficacy of the pharmacological treatments on restricted/repetitive behaviors, which are still under development for targeting repetitive/restricted behaviors in a clinical population. Besides, we have also reviewed studies pointing in the direction of circuit-based strategies for targeting repetitive/restricted behaviors in rodent models of ASD.

As an approach to developing new therapeutics, several rodent models of ASD have been generated with good construct validity that recapitulates many of the behavioral phenotypes observed in autistic individuals. The behavioral tasks assessing repetitive behaviors are more developed than behavioral tasks assaying resistance to change or restricted behaviors (Lewis et al., 2007). The studies we will review mainly discuss rodent models primarily displaying lower-order stereotyped motor behaviors, which are generally better characterized and easier to model than models of insistence on sameness or restricted behaviors (higher-order). Nevertheless, in this review article, we have also discussed a few rodent models that show both the repetitive and restricted behavioral phenotypes. The repetitive behaviors observed in rodent models of autism are complex and diverse, including self-grooming, jumping, circling, marble burying, hanging, rearing, and forelimb movements and involve several molecular and neural pathways (Whitehouse and Lewis, 2015; Kim et al., 2016). Also, complex restricted behaviors such as resistance to change and narrow interests represent cognitive rigidity to routines and obsessions that correspond with executive function deficits (Lopez et al., 2005). Behavioral assays for resistance to change or cognitive inflexibility in rodents include response extinction, reversal learning, and set-shifting tasks, assessing the inability to change the developed spatial habit (Colacicco et al., 2002; Roullet and Crawley, 2011). Understanding of the complex neural mechanisms underlying repetitive behaviors in these models is expected to boost translational research and provide valuable insight into potential treatments for repetitive behaviors observed in ASD. Therefore, in this review article, we will discuss the underlying mechanisms that mediate the complex motor activities and consequent repetitive behavioral repertoire in different rodent models of ASD.

RODENT MODELS OF AUTISM: GENETIC MUTATIONS, ENVIRONMENTAL RISK FACTORS, AND SOME INBRED STRAINS DISPLAYING REPETITIVE/RESTRICTED BEHAVIORS

Genetic mutations account for a significant proportion of ASD risk (Ronemus et al., 2014). Genetic mutations in ASD are complex and diverse depending on structure type [i.e., large-scale chromosome abnormalities, small scale insertions, deletions, substitutions, copy number variation (CNV) and single nucleotide variation (SNV)], inheritance type [i.e., germline, somatic, *de novo* mutation (non-inherited)], frequencies (i.e., common, rare and very rare) and protein sequence affected (i.e., frameshift

mutation, point substitution (De Rubeis and Buxbaum, 2015; De La Torre-Ubieta et al., 2016; Ramaswami and Geschwind, 2018). Over the last decade, with the advancement of sequencing technology, many genes have been implicated in autism pathogenesis (Geschwind and State, 2015). This review covers many of the most common of these factors, which underscores the range of molecular and cellular factors implicated in ASD. Such diversity of neurobiological factors in ASD further highlights the challenges of treatment development, where seemingly divergent neural factors may converge on similar behavioral outcomes, i.e., restrictive and repetitive behaviors. When possible, we have attempted to highlight some of these similarities and differences in risk factors (**Figure 1**), which remains a major challenge for the field to define and address.

Many genes are linked to syndromic ASD, in which monogenic syndromes exhibit phenotypic overlap with ASDs (i.e., ASD is secondary to a known genetic cause and disorder with clinically defined presentation) (Walsh et al., 2008; Schaefer and Mendelsohn, 2013; Ramaswami and Geschwind, 2018). Monogenic disorders accounted for in ASD include Fragile X

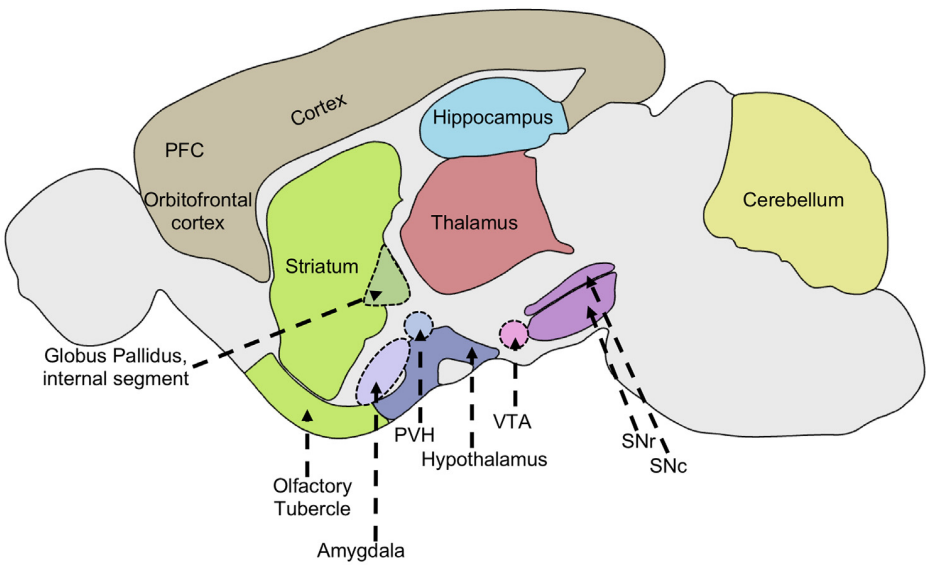

BTBR, Cntnap2$^{-/-}$, Deer, FMR1$^{-/-}$, Hoxb8, KCNQ2$^{+/-}$, MeCP2, Ninj1, NL2, NL3^{R451C}, Pak2$^{+/-}$, PV$^{-/-}$, Scn1a$^{+/-}$, VPA, 16p11$^{+/-}$

BTBR, Cntnap2$^{-/-}$, C58/J, Deer, DGLa, FMR1$^{-/-}$, MeCP2, NL1$^{-/-}$, NL3$^{-/-}$, NL3^{R451C}, Oxtr$^{-/-}$, Pcdh19 X^{LacZ}/Y, Sapap3$^{-/-}$, Shank2$^{-/-}$, Shank3A^{e4-9}, Shank3b$^{-/-}$, 16p11$^{+/-}$

BTBR, Cntnap2$^{-/-}$, DGLa, FMR1$^{-/-}$, Gabrb3$^{-/-}$, Hoxb8, Itgb3$^{-/-}$, KCNQ2$^{+/-}$, Kirrel3$^{-/-}$, Lrrc4$^{-/-}$, MeCP2, NL1$^{-/-}$, NL3^{R451C}, NRXN1a$^{-/-}$, Pak2$^{+/-}$, Pten$^{+/-}$, Shank2$^{-/-}$, Shank3^{e4-22}, Shank3A^{e4-9}, Shank3b$^{-/-}$, Sh3rf2$^{+/-}$, Ube3A$^{m-/p+}$, VPA, 5Ko

BTBR, FMR1$^{-/-}$, Gabrb3$^{-/-}$, Itgb3$^{-/-}$, MeCP2, PV$^{-/-}$, Tsc2f/-;Cre, Ube3A,

BTBR, Cntnap2$^{-/-}$, MeCP2, Ninj1

Itgb3$^{-/-}$, NL3^{R451C}

16p11$^{+/-}$

FIGURE 1 | Implicated brain regions in mouse models of autism. Different mouse models of autism exhibit alterations in various brain areas such as the striatum, cortex, thalamus, hippocampus, cerebellum, hypothalamus, and amygdala. These brain regions are involved in cortico-striatal and limbic circuitry. Molecular and/or neuroanatomical changes in these structures are correlated with the pathophysiology of repetitive behaviors. Some mice models implicate multiple brain regions in the pathology of restricted/repetitive behaviors. PFC, prefrontal cortex; VTA, ventral tegmental area; SNc, substantia nigra pars compacta; SNr, substantia nigra pars reticulata; PVH, paraventricular nucleus of hypothalamus; Cntnap2, Contactin Associated Protein-like 2 gene; FMR1, Fragile X mental retardation 1; Gabrb3, Gamma-aminobutyric acid receptor subunit beta-3; Hoxb8, Homeobox protein; Itgb3, Integrin beta-3; KCNQ, Potassium voltage-gated channel subfamily; Kirrel3, Kin of Irregular Chiasm-like 3; Lrrc4, Leucine-rich repeat-containing 4; MeCP2, Methyl CpG binding protein 2; Ninj1, Nerve injury-induced protein-1; NL, Neuroligin; NRXN1a, Neurexin 1a; Oxtr, Oxytocin receptor; Pcdh19, Protocadherin-19; PV, Parvalbumin; Pak2, p21 activated kinase 2; Pten, Phosphatase and tensin homolog; Sapap3, Synapse-associated protein 90/postsynaptic density protein 95 associated protein 3; Shank, SH3 and multiple ankyrin repeat domains 3; Sh3rf2, SH3 Domain Containing Ring Finger 2; Scn1, Sodium Voltage-Gated Channel Alpha Subunit 1; Tsc2, Tuberous Sclerosis Complex 2; Ube3A, Ubiquitin Protein Ligase E3A; VPA, Valproic acid; 5Ko, 5 kainate receptor subunit.

Syndrome (FMR1), Tuberous Sclerosis (TSC1, TSC2), Angelman and Prader-Willi Syndromes (15q11–q13 deletion/UBE3A and GABRB3 deletion), Rett Syndrome (MECP2), Phelan-McDermid syndrome (PMS; 22q13.3 deletion/SHANK3 mutation), Smith-Lemli-Opitz Syndrome (DHCR7), Neurofibromatosis (NF1), Timothy Syndrome (CACNA1C), et cetera (Muhle et al., 2004; Moss and Howlin, 2009; Geschwind, 2011; Ramaswami and Geschwind, 2018). Whereas in idiopathic autism, the cause is unknown.

Susceptibility genes linked with non-syndromic autism involve multiple common and rare variants (CNVs), and *de novo* mutations. This genetic heterogeneity is associated with idiopathic ASD and accounts for a substantial fraction of autism risk, indicating the involvement of multiple genetic pathways in its etiology (Swanwick et al., 2011; Devlin and Scherer, 2012). Multiple genes with different functions implicated in ASD include SHANK1, 2, CNTNAP2, NLGN, NRXN, 16p11.2 microdeletion/microduplication, SCN1A, et cetera (Cook and Scherer, 2008; Geschwind and State, 2015; Ramaswami and Geschwind, 2018; Sultana et al., 2018). Most ASD related genes affect neural circuit structure and function, with defects in either a single neural circuit component (localized) or multiple neural systems (distributed) impacting overall network activity (**Figure 1**) (Rubenstein, 2010). These neurodevelopmental defects can lead to abnormal neural structure and connectivity, as well as alterations to neurotransmitter systems and their receptors.

Animal models of repetitive and restricted behaviors are classified into different categories by causal factors. The categories of models of repetitive and restricted behavior include: (1) after CNS insult (e.g., specific genetic mutations, lesions or environmental factors); (2) caused by pharmacological agents [e.g., apomorphine (dopamine agonist), amphetamine, cocaine, NMDA (glutamate receptor ligand)]; (3) resulting from restricted housing (e.g., laboratory cage, social deprivation); and (4) linked with particular inbred rodent strains (BTBR, C58) (Lewis et al., 2007; Bechard and Lewis, 2012).

Many of the genetic and environmental factors implicated in the etiology of autism have been modeled using rodents. However, not all rodent models of ASD manifest repetitive behavior. For example, mice with knockout of neuroligin-2 and -4 genes or mutations of the Scn2a ($Scn2a^{+/-}$) gene do not exhibit alterations in intensity or frequency of repetitive behavior (El-Kordi et al., 2013; Wöhr et al., 2013; Shin et al., 2019; Cao et al., 2020). Hence, we will review preclinical studies with particular emphasis on rodent models displaying robust stereotypic behavior (**Table 1**), as discussed below.

Fragile X syndrome (FXS) is caused by an expansion of a single trinucleotide sequence (CGG) resulting in silencing of FMR1, an X-linked gene coding for fragile X mental retardation protein (FMRP). FMR-1 protein, an RNA binding protein plays an important role in regulating synaptic proteins *via* mRNA translation and the development of neural synapses. In addition to mRNA binding, FMRP protein has diverse functions including protein-protein interactions, DNA damage repair *via* chromatin binding, regulation of Ca^{2+} signaling, and neuronal excitation/inhibition balance (Brown et al., 2010; Alpatov et al., 2014; Davis and Broadie, 2017; Filippini et al., 2017; Zhou et al., 2017). Hence, failure to express the FMR-1 protein results in the development of autistic symptoms such as repetitive and restricted behavior (Turner et al., 1996; Mazzocco et al., 1998; Spencer et al., 2005). Fragile X mutant models exhibit increased marble burying (Thomas et al., 2012; Gandhi et al., 2014), resistance to change in an operant task (Moon et al., 2006), learning deficits on water maze task, hyperactivity, anxiety, and inadequate pre-pulse inhibition of acoustic startle (D'Hooge et al., 1997; Peier et al., 2000; Spencer et al., 2005; Lauterborn et al., 2007; Errijgers et al., 2008). Fmr-1 null mice exhibit altered spine density and morphology on apical dendrites of occipital cortical layer 5 pyramidal cells (Comery et al., 1997; Beckel-Mitchener and Greenough, 2004). Also, Fmr1 knockout mice exhibit dysfunctional cortico-striatal circuitry, reduced long-term potentiation (LTP), and decrease in levels of synaptic proteins like NMDAR subunits NR1, NR2A, and NR2B in the medial prefrontal cortex (Lauterborn et al., 2007; Krueger et al., 2011; Zerbi et al., 2018). Gene therapy using human *FRM1* alleviates the low pre-pulse inhibition, hyperactivity, and anxiety behaviors in Fmr1-KO mice (Peier et al., 2000; Paylor et al., 2008; Spencer et al., 2008; Gholizadeh et al., 2014). Application of brain-derived neurotrophic factor (BDNF), mGluR5 antagonists, anti-purinergic therapy (suramin), minocycline, phosphodiesterase-4D negative allosteric modulator (BPN14770) and PI3K antagonist [GSK2702926A (GSK6A)] attenuates dendritic spine development aberrations, LTP impairments, and behavioral abnormalities in *Fmr1* mutant mice (Dölen et al., 2007; Lauterborn et al., 2007; Dölen and Bear, 2008; Bilousova et al., 2009; Naviaux et al., 2015; Gurney et al., 2017; Yau et al., 2018; Gross et al., 2019).

Angelman syndrome involves chromosome 15 deletions, particularly the q11–13 region, comprising the $GABA_A$ receptor beta 3 subunit (GABRB3) and ubiquitin ligase (UBE3A) genes. GABRB3 and UBE3A genes play a role in regulating protein synthesis and synaptic plasticity (Weeber et al., 2003; Moy et al., 2006; Mardirossian et al., 2009). Mouse models of GABRB3 and UBE3A deletions exhibit ASD phenotype including developmental delay, hyperactivity, epilepsy, impaired motor function, learning deficits, and anxiety-related behaviors (DeLorey et al., 1998; Jiang et al., 2010; Tanaka et al., 2012). Mice with a mutation in $Ube3A^{m-/p+}$ (maternal null mutation) exhibit deficits in LTP and changes in calcium-dependent CaMKII activity in the hippocampus (Weeber et al., 2003). The $Ube3A^{m-/p+}$ mice show decreased marble burying, rearing behavior, and reversal-learning deficits in the Morris water maze (MWM) (Huang et al., 2013). Additionally, Gabrb3 deletions cause neuronal dysfunction *via* alterations in protein synthesis and GABA-A receptor-mediated synaptic transmission. The $Gabrb3^{-/-}$ mice also exhibit repetitive circling behavior (Mercer et al., 2016; Orefice et al., 2016).

Another condition, tuberous sclerosis (TSC), involves mutation of either TSC1 and TSC2 genes that codes for proteins hamartin and tuberin, which act as tumor suppressors that regulate cell growth and the mTORC1 complex (Astrinidis and Henske, 2005; Inoki et al., 2005; Curatolo and Bombardieri, 2007). mTOR is a crucial part of signaling pathways involved

TABLE 1 | Neural alterations underlying repetitive behaviors and rescue of repetitive behaviors in rodent models of autism spectrum disorders (ASDs).

Model	Repetitive and related behaviors	Neural alterations	Rescue of repetitive behaviors	References
BTBR T+tf/J	• Repetitive self-grooming • Increased marble-burying behavior • Reversal learning deficit in Morris water maze (MWM)	• Reduced GABAergic inhibitory transmission • Upregulation of serotonin $5HT_{2A}$ receptor density and activity • Increased in glutamatergic transmission in cortico-striatal circuitry • Impaired dopamine D2 receptor function • Reduced expression of BDNF in hippocampus and cortex • Absence of corpus callosum, lack of hippocampal commissure • Reduced cortical thickness • Reduced cerebral white and gray matter • Impaired cortico-thalamic function • Altered volumes of cerebellum, brainstem, striatum, and hippocampus	• mGluR5 receptor antagonist (MPEP) • Selective $GABA_b$ receptor agonist (R-baclofen) • Dorsomedial striatal injection of selective $5HT_{2A}$ receptor antagonist (M100907) • Risperidone • Muscarinic receptor (mAChR) agonist (Oxotremorine) • Nicotinic receptor (nAChR) agonist (nicotine) • Acetylcholinesterase inhibitor (AChEI; Donepezil) reduced behavioral rigidity in water T-maze task • Retinoic acid receptor-related orphan receptor alpha (ROR a) agonist (SR1078)	Wahlsten et al. (2003), Moy et al. (2007), McFarlane et al. (2008), Silverman et al. (2010, 2012), Gould et al. (2011), Wöhr et al. (2011), Amodeo et al. (2012), Burket et al. (2013), Dodero et al. (2013); Ellegood et al. (2013), Reynolds et al. (2013), Han et al. (2014), Karvat and Kimchi (2014), Wang et al. (2015), Wang Y. et al. (2016), and Meyza and Blanchard (2017)
Cntnap2$^{-/-}$	• Repetitive self-grooming and digging • Reversal learning deficit (MWM) • Hyperactivity • Seizures	• A decrease in parvalbumin-positive interneurons in striatum resulting in altered activity of the cortico-striatal-thalamic pathway • Cortical migration abnormalities	• Dopamine D2 receptor antagonist (Risperidone)	Peñagarikano et al. (2011) and Lauber et al. (2018)
C58/J	• Repetitive self-grooming • Hind limb jumping • Backflips • Decreased exploratory behavior • Reversal learning deficit	• Increased mGluR5 signaling • NMDA receptor hyperfunction • Reduced GABAergic signaling • Reduced dendritic spines • Increased dopaminergic function and cortical activation • Aberrant hippocampal and cortical activity	• mGluR5 negative allosteric modulator (GRN-529) • Selective $GABA_b$ receptor agonist (R-baclofen) • Environmental enrichment	Moy et al. (2008b), Ryan et al. (2010), Muehlmann et al. (2012), Silverman et al. (2012), and Whitehouse et al. (2017)
Deer	• Repetitive hindlimb jumping and backflips • Perseverative behavior in a reversal-learning task (T-maze)	• Enhanced Cortico-striatal glutamatergic projections • Decrease density of serotonin transporters in the striatum • Reduced indirect basal ganglia pathway activity • Dorsomedial striatum alterations	• Striatal injections of NMDA receptor antagonist (MK-801) • Dopamine D1 receptor antagonist (SCH23390) • Co-administration of adenosine A_{2A} receptor agonist (CGS21680) and A_1 receptor agonist (CPA) • Selective SSRI (Escitalopram) • Triple drug cocktail (D2R antagonist L-741, 626 + Adenosine A_{2A}R agonist CGS21680 + mGluR5 positive allosteric modulator CDPPB) • Environmental enrichment (EE)	Presti et al. (2003); Tanimura Y. et al. (2010), Tanimura et al. (2008, 2011), Wolmarans et al. (2013), Bechard et al. (2017), and Lewis et al. (2019)

(Continued)

TABLE 1 | Continued

Model	Repetitive and related behaviors	Neural alterations	Rescue of repetitive behaviors	References
DGLa$^{flx/flx}$	• Repetitive self-grooming	• Reduced levels of 2-acyl glycerol in the striatum • Excessive glutamatergic drive in direct-pathway MSNs		Shonesy et al. (2014, 2018)
EphA2/A3 double KO	• Stereotypic facial grooming • Reduced locomotor activity • Increased pre-pulse inhibition of acoustic startle	• Sensorimotor gating abnormalities • Altered excitability of forebrain pathways		Qiu et al. (2012) and Wurzman et al. (2015)
FMR1$^{-/-}$	• Repetitive self-grooming • Increased/decreased marble-burying • A deficit in novelty preference (T-maze spontaneous alternation) • Learning task deficits • Hyperactivity • Anxiety • Reduced motor learning • Olfactory learning deficits	• Increased mGluR-LTD in hippocampal CA1 and cerebellum • Increased endocannabinoid mediated transmission at GABAergic synapses of the hippocampus and dorsal striatum • Dysfunctional cortico-striatal circuitry • Decrease activity of fast-spiking interneurons in cortical areas (hyperexcitability) • Abnormal sensorimotor gating • Altered dendritic spine density and morphology • Impaired long-term potentiation • PSD-95 protein deficits • PI3K/AKT pathway abnormal activity • AMPAR and NMDAR dysfunction • Purinergic signaling alteration • Altered cerebellar and striatal volumes	• Selective GABA-B receptor agonist (R-baclofen) • mGluR5 receptor antagonist (MPEP) • Minocycline (antibiotic inhibiting MMP9) • Antipurinergic therapy (suramin) • CB1R antagonist (rimonabant) • Small-molecule PAK [p21-activated kinase regulates actin cytoskeleton dynamics] inhibitor (FRAX486) • BDNF application • Gene therapy with human FMR1 • Delta-subunit containing extrasynaptic GABA-A receptors agonist (Gaboxadol) • Intracranial injection of CRISPR-Gold targeting mGluR5 • Chronic application of Bryostatin-1 (Protein Kinase C potent activator) • eFT508, MNK (mitogen-activated protein kinase interacting protein kinase) inhibitor • BPN14770, phosphodiesterase-4D negative allosteric modulator (PDE4DNAM) • GSK6A (PI3K antagonist) • FS-115, S6KI (mTORC1-p70 ribosomal S6 kinase 1) inhibitor	Peier et al. (2000), Spencer et al. (2005, 2008), Lauterborn et al. (2007), Dölen and Bear (2008), Errijgers et al. (2008), McNaughton et al. (2008), Paylor et al. (2008), Bilousova et al. (2009), Zhang and Alger (2010), Pietropaolo et al. (2011), Henderson et al. (2012), Jung et al. (2012), Thomas et al. (2012), Busquets-Garcia et al. (2013), Dolan et al. (2013), Berry-Kravis (2014), Gandhi et al. (2014), Naviaux et al. (2015), Tang and Alger (2015), Bhattacharya et al. (2016), Gurney et al. (2017), Sinclair et al. (2017), Lee et al. (2018), Nolan and Lugo (2018), Yau et al. (2018), Zerbi et al. (2018), Cogram et al. (2019, 2020), Gross et al. (2019), and Shukla et al. (2020)
Gabrb3$^{-/-}$	• Repetitive circling • Hyperactivity	• Cerebellar vermis hypoplasia • Abnormal GABA-A receptor function in the hippocampus • Altered GABA-A receptor-mediated neurotransmission		DeLorey et al. (1998, 2008), Mercer et al. (2016), and Orefice et al. (2016)
Hoxb8 KO in microglia	• Increased grooming • Anxiety-like behavior	• Increased cortical dendritic spine density • Increased dendritic spines in the striatum • Defects in LTP, miniature postsynaptic currents	• Fluoxetine (SSRI)	Greer and Capecchi (2002), Chen et al. (2010), and Nagarajan et al. (2018)

(Continued)

TABLE 1 | Continued

Model	Repetitive and related behaviors	Neural alterations	Rescue of repetitive behaviors	References
Itgb3$^{-/-}$	• Increased grooming in a novel environment	• Alterations in axon/dendrite outgrowth, cell adhesion, and synapse formation • The reduced corpus callosum, hippocampus, striatum, and cerebellum • Increased amygdala volume		De Arcangelis and Georges-Labouesse (2000), Clegg et al. (2003), Carter et al. (2011), and Ellegood et al. (2012)
KCNQ2$^{+/-}$	• Repetitive grooming • Hyperactivity • Increased locomotor activity	• Increased neuronal excitability		Yue and Yaari (2006), Shah et al. (2008), Brown and Passmore (2009), and Kim et al. (2020)
Kirrel3$^{-/-}$	• Repetitive rearing behavior • Increased locomotor activity • Hypersensitivity to acoustic startle (acoustic startle test) • Hyperactivity	• Abnormal hippocampal mossy fiber synapse formation • Increased CA3 neuron activity during development • Abnormal neuronal migration		Gerke et al. (2006), Serizawa et al. (2006), Nishida et al. (2011), Prince et al. (2013), Martin et al. (2015), Choi et al. (2015), and Hisaoka et al. (2018)
Lrrc4$^{-/-}$	• Repetitive self-grooming • Impaired spatial learning (MWM)	• Reduced NMDA receptor-mediated synaptic plasticity • Abnormal synaptic transmission	• NMDA receptor agonist (D-cycloserine)	DeNardo et al. (2012), Soto et al. (2013, 2018), and Um et al. (2018)
MeCP2	• Repeated forelimb movements • Deficits in motor coordination and motor learning • Memory deficits	• Decreased levels of dopamine transporter (DAT) and tyrosine hydroxylase (TH) in the striatum • Altered cortical and cerebellar volumes • Cortical LTP deficit • Decreased cortical BDNF levels • Impaired PI3K/AKT/mTOR pathway • Upregulated CB1 and CB2 receptor levels • Hippocampal circuit dysfunction		Shahbazian et al. (2002), Moretti et al. (2005), Lonetti et al. (2010), Lu et al. (2016), Allemang-Grand et al. (2017), and Zamberletti et al. (2019)
Ninj1	• Excessive grooming inducing hair loss and lesions • Increased anxiety-like behavior	• Altered synaptic function in thalamocortical neurons • Increased expression of ionotropic glutamate receptor • The increased amplitude of miniature EPSCs	• Fluoxetine (SSRI)	Le et al. (2017)
NL1$^{-/-}$	• Repetitive self-grooming • Spatial learning deficits	• Reduced NMDA/AMPA receptor ratio in the hippocampus and dorsal striatum • Reduced hippocampal LTP • Abnormal function of dopamine D1 MSNs • Reduced GluN2A containing NMDARs expression in direct-pathway MSNs • Reduced frequency of miniature excitatory neurotransmission in indirect-pathway MSNs	• NMDA receptor partial co-agonist (D-cycloserine)	Blundell et al. (2010) and Espinosa et al. (2015)

(Continued)

TABLE 1 | Continued

Model	Repetitive and related behaviors	Neural alterations	Rescue of repetitive behaviors	References
NL2 overexpression	• Repetitive Jumping	• Reduced E/I balance in PFC		Hines et al. (2008)
NL3$^{-/-}$	• Repetitive motor routine • Hyperactivity	• Reduced striatal synaptic function in nucleus accumbens/ventral striatum • Abnormal function of dopamine D1 MSNs • Altered GABAergic signaling and E/I balance in CA2 hippocampal area • Altered synaptic activity in the hippocampus, somatosensory cortex, and basolateral amygdala • Increased AMPA mediated neurotransmission and LTP in the hippocampus		Radyushkin et al. (2009), Rothwell et al. (2014), Modi et al. (2019), Burrows et al. (2015), Hosie et al. (2018), and Matta et al. (2020)
NL3^{R451C}	• Repetitive behavior (object exploration task) • Aggression	• Smaller striatal volume • Increased striatal postsynaptic density 95 (PSD-95) protein levels	• Risperidone, CB1 receptor agonist (WIN55, 212–2) targeting aggression	Tabuchi et al. (2007), Etherton et al. (2011), and Kumar et al. (2014)
NRXN1a$^{-/-}$	• Repetitive self-grooming • Altered nest building • Impaired prepulse inhibition • Aggressive behaviors • Mild anxiety-like behavior	• A decrease in miniature excitatory postsynaptic current frequency in the hippocampus • Impaired excitatory synaptic transmission in the hippocampus • Sensorimotor gating impairments • Increased cortical volume and decreased cerebellar volume		Etherton et al. (2009) and Grayton et al. (2013)
Oxtr$^{-/-}$	• Cognitive inflexibility in the reversal phase in T—maze • Increased aggression	• Alterations in excitatory synaptic markers (PSD-95, gephyrin scaffolding proteins) • Altered glutamatergic and GABAergic receptors		Sala et al. (2011), Pobbe et al. (2012), and Leonzino et al. (2019)
Pak2$^{+/-}$	• Repetitive self-grooming behavior • Increased marble-burying behavior	• Changes in striatal dendritic spines • Reduced spine density in cortex and hippocampus • Impaired LTP in CA1 hippocampal region • Reduced actin polymerization and perturbation of actin network		Wang Y. et al. (2018)
Pcdh19 X^{LacZ}*/Y*	• Repetitive grooming behavior • Increased rearing behavior	• Impaired migration and dendritic arborization of hippocampal CA1 neurons • Decreased GABA-A receptor surface expression and transmission		Bassani et al. (2018) and Lim et al. (2019)
Pten$^{+/-}$	• Repetitive digging and increased marble-burying behavior • Reduced sensorimotor gating • Increased depression-like behavior	• Increased mTOR signaling • Alterations in the serotonin system • Altered synaptic scaffolding proteins (PSD-95, sapap1, sap-102)		Page et al. (2009), Clipperton-Allen and Page (2014, 2015), Lugo et al. (2014), and Rademacher and Eickholt (2019)

(Continued)

TABLE 1 | Continued

Model	Repetitive and related behaviors	Neural alterations	Rescue of repetitive behaviors	References
		• Decreased mGluR in the hippocampus • Structural aberrations in Purkinje cells dendrites and axons		
PV$^{-/-}$	• Higher-order reversal learning in T-maze	• Decreased parvalbumin levels • Altered excitatory and inhibitory synaptic transmission • Decreased inhibition of pyramidal neuron output • Loss of inhibitory synapses resulting in hyperexcitation of cortical circuits • Reduced cortical volume, increased cerebellar volume	• 17-beta estradiol	Filice et al. (2018)
Sapap3$^{-/-}$	• Compulsive self-grooming	• Glutamatergic transmission defects at cortico-striatal synapses • Elevated mGluR5 signaling	• Sapap3 re-expression in the striatum • Optogenetic stimulation of the lateral orbitofrontal cortex • mGluR5 inhibition • Serotonin uptake inhibitor (fluoxetine)	Welch et al. (2007), Bienvenu et al. (2009), and Burguière et al. (2013)
Scn1a$^{+/-}$	• Repetitive self-grooming and circling • Hyperactivity	• Increased PFC excitation • Altered GABAergic activity in PFC		Han et al. (2012)
Shank1$^{+/-}$, *Shank1*$^{-/-}$	• Repetitive self-grooming • increased acquisition of spatial memory • motor deficits • mild anxiety-like phenotype • Reduced exploratory locomotion	• A decrease in mEPSC, altered glutamatergic synapse • Altered maturation of postsynaptic dendritic spines • Reduced density of CA1 pyramidal neurons dendritic spines		Hung et al. (2008), Silverman et al. (2011), Sungur et al. (2014), and Sala et al. (2015)
Shank2$^{-/-}$ (*exon 7 deletion*)	• Repetitive grooming • Hyperactivity • Anxiety-like behavior • Increased locomotor activity	• Increased NMDAR-dependent LTP and altered NMDAR-mediated synaptic transmission • Reduced spine density • Increased levels of GluN2A, GluN1, GluN2B, GluA2 glutamate receptor subunits in hippocampus and striatum		Schmeisser et al. (2012)
Shank2 (*exons 6, 7 deletions and frameshift affecting both splice variants Shank2a and Shank2b*)	• Stereotypic jumping • Impaired spatial learning and memory (Morris water maze) • Impaired nesting behavior • Hyperactivity • Anxiety-like behavior • Increased grooming in the novel object recognition area	• Reduced activity of glutamatergic NMDA receptors • Impaired LTP and LTD at Schaffer-collateral-CA1-pyramidal (SC-CA1) synapses • Reduced NMDA/AMPA ratio at SC-CA1 synapses • Decreased NMDAR-mediated synaptic transmission		Won et al. (2012)

(Continued)

TABLE 1 | Continued

Model	Repetitive and related behaviors	Neural alterations	Rescue of repetitive behaviors	References
Shank3 (*exon 21 deletions including Homer binding domain*)	• Repetitive grooming in older mice • A deficit in spatial learning and memory • Impaired motor coordination • Aberrant locomotor response to novelty • Increased novel object avoidance (in marble-burying test)	• Decreased excitatory postsynaptic NMDA/AMPA current ratio in the hippocampal CA1 region • Reduced LTP in CA1 hippocampus • Increased mGluR5 levels in synaptic fractions		Kouser et al. (2013)
Shank3^{e4-22} (*exons 4–22 deletion*)	• Excessive Repetitive self-grooming • Reduced locomotion • Deficient motor performance • Anxiety-like behavior • Impaired striatal learning	• Impaired postsynaptic SAPAP, mGluR5-Homer scaffolding proteins, and mGluR5 signaling in striatal neurons • Impaired striatal LTD and synaptic plasticity • Decreased neurotransmission in corticostriatal circuits • Reduced striatal spine density	• mGluR5 antagonist (MPEP)	Wang X. et al. (2016)
Shank3A^{e4-9} *heterozygous and knockout (exons 4–9 deletion encoding ANK domain)*	• Repetitive self-grooming • An enhanced head pokes (hole board test) • Mild motor abnormalities including difficulty in motor coordination in KO mice • Motor learning deficits in KO mice • Impaired novel and spatial object recognition learning and memory	• Reduced Homer1b/c, GKAP, and AMPAR subunit GluA1, GluA2, GluA3 levels at PSD in KO mice indicating altered synaptic scaffolding proteins and receptor subunits • Reduced spine density and increased spine length in CA1 hippocampus • Impaired hippocampal LTP (in both KO and HTZ), glutamatergic synaptic transmission, and synaptic plasticity in knockout mice • Reduced NMDA/AMPA ratio at excitatory synapses onto striatal MSNs (in both KO and HTZ)		Bozdagi et al. (2010), Wang et al. (2011), Yang et al. (2012), Drapeau et al. (2014), and Jaramillo et al. (2016)
Shank3b$^{-/-}$	• Repetitive self-grooming • Attention-deficit	• Functionally impaired AMPA and NMDA receptors • Decreased D2 MSNs AMPA receptor responses • Deficits of hippocampal synaptic plasticity and its association with the impaired remodeling of the actin cytoskeleton	• Enhancing the activity of the indirect striatopallidal pathway • Subthalamic nucleus stimulation • Partial 5-HT1A receptor agonist (tandospirone) in Shank3B$^{+/-}$	Bozdagi et al. (2010), Peça et al. (2011), Wang et al. (2011), Schmeisser et al. (2012), Duffney et al. (2013), Sala et al. (2015), Chang et al. (2016), Peixoto et al. (2016), Harony-Nicolas et al. (2017), and Dunn et al. (2020)
Shank3B$^{-/-}$ (*PDZ domain deletion*)	• Excessive and self-injurious self-grooming • Anxiety-like behavior	• Reduced levels of synaptic scaffolding proteins SAPAP3, Homer-1b/c, PSD93 and glutamate receptor subunits GluR2, NR2A, and NR2B at PSD • Neuronal hypertrophy • Reduced dendritic spine density		Peça et al. (2011)

(Continued)

TABLE 1 | Continued

Model	Repetitive and related behaviors	Neural alterations	Rescue of repetitive behaviors	References
		• Increased caudate volume • Decreased C-S circuits neurotransmission		
Sh3rf2$^{+/-}$	• Increased jumping and rearing behavior • Increased marble burying and digging • Hyperactivity	• Abnormal dendritic spine development in the hippocampus • Changes in the composition of glutamate receptor subunits NR2A and GluR2 • Altered AMPA receptor-mediated synaptic transmission in CA1 hippocampus		Wang S. et al. (2018)
Tsc2f/−;Cre (Tsc2 deletion in cerebellar Purkinje cells)	• Increase marble-burying	• Cerebellar GABAergic Purkinje cell loss • Abnormalities in axonal pathfinding		Reith et al. (2013)
Ube3A$^{m-/p+}$	• Decrease marble burying and rearing • Reversal learning deficit (MWM) • Impaired motor coordination	• Reduced mGluR-LTD • Altered mGluR signaling • Changes in calcium-dependent CAMKII activity in the hippocampus		Weeber et al. (2003), Huang et al. (2013), and Pignatelli et al. (2014)
VPA	• Repetitive self-grooming • Marble burying • Decrease pre-pulse inhibition • Reduced social behaviors	• Increased glutamatergic excitatory signaling • Hyperexcitable local connectivity • A decrease in parvalbumin-positive inhibitory interneurons • Elevated brain serotonin levels • Apical dendritic arborization complexity • Decreased PTEN expression and increased p-AKT protein levels in hippocampus and cortex	• mGluR5 receptor antagonist, MPEP • Environmental enrichment • Betaine (methyl group donor in homocysteine metabolism, prevents homocysteine accumulation) • NMDA receptor antagonist (agmatine)	Schneider and Przewocki (2005), Schneider et al. (2006), Rinaldi et al. (2007), Tsujino et al. (2007), Snow et al. (2008), Mehta et al. (2011), Choi et al. (2016), Kim et al. (2017), Mahmood et al. (2018), and Huang et al. (2019)
16p11$^{+/-}$	• Repetitive circling and climbing • Hyperactivity • Increased locomotion	• Increased dopamine D2 receptor-expressing striatal neurons • Decreased dopamine D2 receptor-expressing cortical neurons • Synaptic function defects • Volumetric alterations in striatum, hypothalamus, and midbrain area		Horev et al. (2011) and Portmann et al. (2014)
5Ko (deletion of 5 kainate receptor subunits)	• Elevated self-grooming • Increased marble burying and digging • Increased perseverative behavior (Y-maze) • Motor problems	• Impaired corticostriatal synaptic transmission in the dorsal striatum • Altered NMDA/AMPA ratio • Reduced mEPSC frequencies • Reduced spine density of spiny projections neurons in the dorsal striatum		Xu et al. (2017)

Treatment strategies discussed are from preclinical studies in rodent models targeting behavioral abnormalities including stereotypic behaviors.

in cell growth, protein synthesis, and axon formation (Choi et al., 2008; Huang and Manning, 2008). $Tsc2^{+/-}$ mice with heterozygous TSC2 gene mutations exhibit learning, and memory deficits associated with aberrant mTOR signaling mediated LTP in the hippocampal CA1 region (Ehninger et al., 2008). Mice with *Tsc2* loss in cerebellar Purkinje cells (Tsc2f/−; Cre mice) display ASD-like behaviors, including social deficits and repetitive behavior (Reith et al., 2013). Further, Tsc2 mutant mice with *Tsc2* gene deletion from radial glial progenitor cells exhibit lamination aberrations, enlargement of neurons and glia, myelination defects, and astrocytosis (Way et al., 2009). Also, mice with ablated TSC1 expression in neurons show seizures and neuropathological aberrations including enlarged, ectopic neurons in the hippocampus, cortical, thalamic brain areas, alterations in glutamatergic synapses, abnormalities in cortical lamination, cytoskeleton, dendritic spine structure, and myelination (Tavazoie et al., 2005; Meikle et al., 2007). Application of mTORC1 inhibitors rapamycin and RAD001 [40-O-(2-hydroxyethyl)-rapamycin] ameliorates synaptic, cognitive, and behavioral deficits in a mouse model of tuberous sclerosis (Ehninger et al., 2008; Meikle et al., 2008; Zeng et al., 2008; Ehninger and Silva, 2011; Bateup et al., 2013).

Rett syndrome (RTT) is caused by mutations in the MECP2 gene located on the X-chromosome, which encodes for methyl-CpG-binding protein 2 (MeCP2) and affects brain development mostly in females (Ghidoni, 2007). Several mouse models of autism have been developed to study the effects of MeCP2 mutations (Chahrour and Zoghbi, 2007; Samaco et al., 2008). Mutant mice with truncated MeCP2 protein show repeated forelimb motions similar to repetitive hand movements in individuals with Rett syndrome (**Table 1**) (Shahbazian et al., 2002; Moretti et al., 2005). Dopaminergic deficits are implicated in RTT, such as decreased levels of dopamine transporter (DAT) (Wong et al., 1998), the altered density of dopamine D2 receptors in the striatum (Chiron et al., 1993), and reduced levels of tyrosine hydroxylase (TH), dopamine synthetic enzyme, in the striatum (Panayotis et al., 2011), suggesting striatal dysfunction in RTT individuals. Additionally, MeCP2 null mice exhibit deficits in motor coordination and motor learning along with memory deficits in the MWM. Environmental enrichment alters excitatory synaptic density in cortex and cerebellum, LTP deficit, increased BDNF levels in cortex, and rescued motor learning deficits (Lonetti et al., 2010).

Autism susceptibility genes, such as neuroligin genes (NL1, 2, 3, 4) encode the eponymous members of postsynaptic cell surface adhesion proteins that are crucial for synapse formation and maintenance (Südhof, 2008). Deletion and point mutation of neuroligin-3 (NL3) are associated with autistic behavioral phenotypes (Jamain et al., 2003; Levy et al., 2011). Overexpression of neuroligin-2 (NL2) in PFC leads to repetitive jumping behavior in mice (**Table 1**) (Hines et al., 2008). Moreover, deficits in neurexins, which are presynaptic cell adhesion proteins that serve as ligands for neuroligins and modulates synapse differentiation and maturation, control transmitter release, result in stereotypic grooming and altered nest-building behaviors in neurexin1a mutant mice (Etherton et al., 2009; Li and Pozzo-Miller, 2020).

SH3 and multiple ankyrin repeat domains 1, 2, and 3 (SHANK1, SHANK2, and SHANK3) are postsynaptic scaffolding proteins present in excitatory synapses that are important for synaptic development and function (Grabrucker et al., 2011; Guilmatre et al., 2014). The Shank3 protein contains multiple conserved motifs, comprising an ANK repeat, PDZ, and SAM domains, a proline-rich cluster, and SH3 (Gundelfinger et al., 2006; Kreienkamp, 2008). The SHANK proteins also regulate spine morphology and receptor endocytosis, promote interaction of signaling pathways and facilitate synaptic plasticity, crucial for the process of learning and memory (Ehlers, 1999; Sheng and Kim, 2000; Monteiro and Feng, 2017). Mutations in Shank genes are implicated in ASD (Schmeisser, 2015). In particular, PMS or 22q13.3 deletion syndrome is characterized by developmental and speech delays, intellectual disability, reduced motor function, and ASD. PMS is caused by loss of function of the *SHANK3* gene resulting in reduced expression of SHANK3 protein, affecting synaptic transmission and plasticity (Costales and Kolevzon, 2015). SH3 and multiple ankyrin repeat domains 3b mutant mice ($Shank3b^{-/-}$) show repetitive grooming behavior (**Table 1**) (Peça et al., 2011; Schmeisser et al., 2012). Moreover, Shank3B mutant mice manifest functionally impaired AMPA and NMDA receptors (Peça et al., 2011; Sala et al., 2015; Peixoto et al., 2016) (**Figure 2**). $Shank1^{+/-}$ mice display increased self-grooming behavior during adulthood (Sungur et al., 2014), while $Shank2^{-/-}$ mice manifest hyperactivity and repetitive jumping behavior along with the reduced activity of NMDA receptors (**Table 1**) (Schmeisser et al., 2012; Won et al., 2012). In contrast, Shank1 genotypes ($Shank1^{+/+}$, $Shank1^{+/-}$ and $Shank1^{-/-}$) exhibit high self-grooming behaviors, but which are confounded by behavioral testing or housing conditions. Shank1 null mutant mice show decreased transitions in the light-dark test, suggesting anxiety-related phenotypes and reduced motor abilities (Silverman et al., 2011).

Contactin associated protein-like 2 (CASPR-2) transmembrane protein is encoded by the CNTNAP2 gene of the neurexin superfamily that primarily mediates cell-cell adhesions in the nervous system (Rodenas-Cuadrado et al., 2014). Also, the CNTNAP2 gene plays an important role in the formation of dendritic spines and dendritic arborization (Anderson et al., 2012). Cntnap2 KO mice exhibit neuronal migration abnormalities, decreased cortical interneurons number, and aberrant hippocampal and cortical network activity (Peñagarikano et al., 2011). Also, the Cntnap2 mutant mice show reduced densities of dendritic spines along with decreased levels of AMPA receptors (AMPAR) subunit GluA1 in the spines (Gdalyahu et al., 2015; Varea et al., 2015; Gao et al., 2019). Further, the decreased number of parvalbumin-positive interneurons in the striatum results in altered activity of the cortico-striatal-thalamic pathway underlying repetitive behaviors (Lauber et al., 2018). Mice with the CNTNAP2 mutation display repetitive self-grooming behavior, rescued by risperidone, a dopamine D2 receptor antagonist (**Table 1**) (Peñagarikano et al., 2011), thereby, decreasing dopaminergic function and cortical activation (Parr-Brownlie and Hyland, 2005).

In addition to the above autism susceptibility genes, many other genes implicated in autistic phenotypes have been investigated in preclinical studies. Mutations in protocadherin 19 (*PCDH19*) chromosome X-linked gene, leads to Epilepsy in Females with Mental Retardation (EFMR) disease, cognitive impairments, and autistic phenotype (Ryan et al., 1997; Dibbens et al., 2008; Hynes et al., 2010; Specchio et al., 2011). *PCDH19* gene encodes PCDH19 protein which is a cell-adhesion protein. PCDH19 regulates hippocampal neurons maturation, migration, and GABAergic transmission *via* binding with GABA-A receptor alpha subunit (Bassani et al., 2018). Additionally, PCDH19 interacts with intracellular protein NONO, involved in the modulation of steroid hormone receptors (Pham et al., 2017). Male mice with *Pcdh19* knockout (*Pcdh19* X^{LacZ}/Y) exhibit increased rearing and stereotypic grooming behaviors (Lim et al., 2019).

Ephrins are membrane-bound proteins acting as ligands of ephrin receptors, belonging to receptor tyrosine kinases (RTKs) family which are transmembrane proteins. They serve important functions including angiogenesis, axon guidance, cell migration, tissue border formation, and synaptic plasticity (Chin-Sang et al., 1999; Kullander and Klein, 2002; Martínez and Soriano, 2005; Héroult et al., 2006; Aoto and Chen, 2007; Klein, 2009). In CNS, ephrins and Eph receptors are involved in axon pathfinding, topographic development of different brain regions and connectivity, neuronal migration, dendritic spine maturation, synapse formation, and plasticity (Gao et al., 1996; Dalva et al., 2000; Ethell et al., 2001; Grunwald et al., 2001, 2004; Henkemeyer et al., 2003; Murai et al., 2003; Palmer and Klein, 2003; Bolz et al., 2004; Klein, 2004; Yamaguchi and Pasquale, 2004; Egea and Klein, 2007; Akaneya et al., 2010; Triplett and Feldheim, 2012). Deletion of ephrin-A2 in mice exhibits impairment of behavioral flexibility in visual discrimination reversal-learning task (Arnall et al., 2010). Mice with a double knockout of ephrin-A2 and ephrin-A3 manifest excessive stereotypic facial grooming behaviors, resulting in face lesions. Also, they show reduced locomotor activity, shift towards grooming in the marble-burying assay, and increased pre-pulse inhibition of acoustic startle (Wurzman et al., 2015). The repetitive grooming behavior in double knockout mice suggests abnormalities in sensorimotor gating (Ben-Sasson et al., 2007; Perry et al., 2007; Wurzman et al., 2015). Ephrin-A2 and ephrin-A3 are located at excitatory synapses in multiple brain regions. Their deletions may result in altered excitability of forebrain networks suggesting defective processing of sensory information (Qiu et al., 2012; Wurzman et al., 2015).

Phosphoinositide signaling is important for cell survival and proliferation. Phosphoinositide 3-kinase (PI3K), Akt (serine/threonine kinase), and mammalian target of rapamycin (mTOR) are important interlinks in the PI3K pathway and are activated by upstream receptor tyrosine kinases (RTKs) and regulates protein synthesis for cell growth and proliferation (Cantley, 2002). Phosphatase and tensin homolog deleted on chromosome 10 (PTEN), a tumor suppressor gene is a negative regulator of the PI3K/AKT/mTOR signaling pathway (Ali et al., 1999; Sansal and Sellers, 2004). *Pten* is an ASD candidate risk gene and its mutation is reported in a subset of autistic cases with macrocephaly (Butler et al., 2005; Herman et al., 2007; Varga et al., 2009). Mice with PTEN deletions in cortical and hippocampal neurons show macrocephaly and ASD behavioral deficits, including seizures, increased anxiety, and learning deficits. The conditional *Pten* mutant mice exhibit neuronal hypertrophy associated with abnormal activation of the Akt/mTOR pathway and Gsk3b inactivation (Kwon et al., 2006). Additionally, conditional *Pten* knockout in astrocytes results in increases in their size (Fraser et al., 2004). Further, *Pten* conditional KO mice exhibit increased spine number, myelination defects, and changes in synaptic structure and transmission (Fraser et al., 2008). Germline $Pten^{+/-}$ male mice also exhibit increased marble burying and digging, suggesting repetitive behavioral phenotype (Clipperton-Allen and Page, 2014, 2015). Deletion of PTEN causes changes in synaptic scaffolding proteins (PSD-95, Sapap1, sap-102) and reduced mGluR expression in the hippocampus (Lugo et al., 2014). PTEN also exhibits critical functions during development, with significant implications for autism and neurodevelopmental disorders (Rademacher and Eickholt, 2019). Hence, PTEN dysfunction in neurons has profound effects on neuronal morphology and connectivity resulting in ASD-like behaviors.

Additionally, the Homeobox protein (Hoxb8) protein is encoded by the HOXB8 gene, a member of the homeobox-containing group of transcription factors, involved in developmental processes such as positioning along the anterior-posterior axis and other physiological functions. *Hoxb8* mutant mice display excessive grooming behavior resulting in skin lesions and anxiety-like behavior (Greer and Capecchi, 2002). In mouse brains, Hoxb8 cell lineage is present in the microglia. *Hoxb*8 mutant mice with Hoxb8 mutations in microglia, exhibit increased cortical dendritic spine density and dendritic spines in the striatum, defects in synapse structure, LTP, and miniature postsynaptic currents. Long-term application of fluoxetine (SSRI) attenuates excessive grooming and hyperactivity in *Hoxb8* mutant mice. Hence, Hoxb8 in microglia may play role in the modulation of cortico-striatal circuits and associated grooming behavior (Chen et al., 2010; Nagarajan et al., 2018).

KCNQ/K_v7 channels mediate voltage-dependent outward potassium currents regulating resting membrane potential and decreasing neuronal excitability. KCNQ2 encodes subunits of neuronal KCNQ/K_V7- K^+ channels, K_V7.2, which are present in the hippocampus and cortex. Mutations in K_V7.2 are associated with developmental delay and autism (Cooper et al., 2001; Yue and Yaari, 2006; Shah et al., 2008; Brown and Passmore, 2009). Mice with heterozygous null mutations in the KCNQ2 gene ($KCNQ2^{+/-}$) exhibit elevated locomotor activity, hyperactivity, exploratory and repetitive grooming, suggesting loss of K_V7.2 is linked to ASD behavioral abnormalities (Kim et al., 2020).

Kin of Irregular Chiasm-like 3 (*KIRREL3*) gene mutations are linked with neurodevelopmental disorders including autism and intellectual disability (Bhalla et al., 2008; Iossifov et al., 2012; Baig et al., 2017). The KIRREL3 gene encodes the Kin of IRRE-like protein 1 (KIRREL3), also called NEPH2 (Sellin et al., 2003). KIRREL3 (NEPH2) is a member of the KIRREL protein family of transmembrane proteins that includes KIRREL (NEPH1) and KIRREL2 (NEPH3). KIRREL3 plays a role in kidney

blood filtration function and is a synaptic cell-cell adhesion molecule (Gerke et al., 2006; Neumann-Haefelin et al., 2010). Kirrel3 in mice is present in the developing cochlea, retina, and olfactory neuroepithelial regions and in the adult nervous system comprising sensory regions (Morikawa et al., 2007). Disruption of the function of the KIRREL3 gene is associated with alterations in brain function. The gene is implicated in neural circuit development including neuronal migration, axonal fasciculation, and synapse formation (Serizawa et al., 2006; Nishida et al., 2011; Prince et al., 2013). KIRREL3 gene knockout in mice leads to alterations in synapses connecting dentate gyrus (DG) neurons to GABAergic neurons but no changes were observed in synapses linking DG neurons to CA3 neurons. This resulted in the disruption of DG synaptic activity and overactivation of CA3 neurons (Martin et al., 2015). KIRREL3 KO mice display increased rearing repetitive behavior, hyperactivity, impaired novel object recognition, and sensory abnormalities (Choi et al., 2015; Hisaoka et al., 2018).

Furthermore, Integrin-beta3 gene encodes integrin beta-3 protein which is a cell-surface protein (a member of alpha/beta heterodimeric receptors) and is involved in various functions including cell adhesion/migration, cell-extracellular matrix interactions, and axon/dendrite outgrowth (Sosnoski et al., 1988; De Arcangelis and Georges-Labouesse, 2000; Clegg et al., 2003). Increased integrin-beta3 activity leads to elevated SERT transport of 5-HT and increased blood serotonin levels which are reported in autistic individuals (Carneiro et al., 2008). Mice with a mutation in the integrin-beta3 gene exhibit elevated grooming in novel environments with no changes in activity in the open field test. Disruption of integrin-beta3 protein impairs platelet aggregation resulting in increased bleeding times and hemorrhages. Additional studies are required to ascertain behavioral abnormalities in integrin-beta3 deficient mice (Carter et al., 2011).

Netrin-G ligand 2 (NGL-2)/LRRC4 is a leucine-rich repeat comprising postsynaptic cell adhesion molecule which interacts with PSD-95, excitatory postsynaptic scaffolding protein, and netrin-G2, a presynaptic cell adhesion molecule (Lin et al., 2003; Kim et al., 2006; Woo et al., 2009; Matsukawa et al., 2014). NGL-2 is implicated in intellectual disability and ASD (Jiang et al., 2013; Sangu et al., 2017). NGL-2 is involved in the regulation of glutamatergic synapse development and excitatory transmission (DeNardo et al., 2012). Mice with mutations in NGL-2 (*Lrrc4*$^{-/-}$) exhibit reduced hippocampal NMDA receptor synaptic plasticity (Soto et al., 2013, 2018; Um et al., 2018). Lrrc4$^{-/-}$ mice show repetitive self-grooming behavior which is rescued by D-cycloserine, the NMDAR agonist. Also, Lrrc4$^{-/-}$ mice exhibit impaired spatial learning in the MWM test and mild anxiety-like behavior (Um et al., 2018).

Similarly, Nerve injury-induced protein 1 (Ninjurin1/Ninj1), is a cell-adhesion molecule involved in nerve regeneration, angiogenesis, inflammation, and cancer (Araki and Milbrandt, 1996; Ifergan et al., 2011; Matsuki et al., 2015; Jang et al., 2016). Ninj1 is expressed in cortico-thalamic circuits and is implicated in the regulation of synaptic transmission. Mutation in Ninjurin1 (Ninj1) in mice leads to excessive grooming to the point of inducing hair loss and lesions and increased anxiety-like behavior. Also, Ninj1 mutant mice exhibit glutamatergic alterations in the brain, including elevated ionotropic glutamate receptors synaptic expression and mEPSCs amplitude. Stereotypic grooming in these mice is alleviated by fluoxetine (SSRI), correlating with direct inhibitory effects of fluoxetine on NMDA receptors (Le et al., 2017).

SH3RF2 gene present in the 1.8 Mb microdeletion at 5q32 is implicated in autism (Gau et al., 2012; Yuen et al., 2017). It plays a role as an anti-apoptotic regulator of the JNK pathway *via* degrading SH3RF1 protein that activates the JNK pathway (Wilhelm et al., 2012; Kim et al., 2014). Mice with haploinsufficiency of Sh3rf2 (Sh3rf2$^{+/-}$) show increased jumping, rearing behavior, bury more marbles in the marble-burying test correlating with elevated digging behavior and hyperactivity. Abnormalities in dendritic spine development in the hippocampus, AMPAR-mediated excitatory synaptic transmission in CA1 hippocampus, altered hippocampal pyramidal neurons membrane properties, and increases in NR2A and GluR2 glutamate receptor subunits in the hippocampus are observed in Sh3rf2$^{+/-}$ mutant mice (Wang S. et al., 2018).

Additionally, the p21-activated kinase 2 (*PAK2*), a serine/threonine kinase, activated by Rho GTPases plays a crucial role in regulating cytoskeleton remodeling, dynamics, the formation of postsynaptic dendritic spines, and cortical neuronal migration (Bokoch, 2003; Boda et al., 2006; Asrar et al., 2009; Causeret et al., 2009; De La Torre-Ubieta et al., 2010). Mutations in the *PAK2* gene are implicated in ASD (Willatt et al., 2005; Quintero-Rivera et al., 2010; Sagar et al., 2013). Haploinsufficiency of Pak2 leads to reduced spine densities in cortex and hippocampus, impaired hippocampal CA1 LTP, decreased phosphorylation of actin regulators LIMK1, cofilin, and reduced actin polymerization. Pak2$^{+/-}$ mice show repetitive grooming behavior and bury more marbles in the marble-burying test (Wang Y. et al., 2018). This suggests PAK2 is critical in brain development and its mutation contributes to autistic phenotypes.

The SCN1A gene heterozygous loss of function mutation results in Dravet Syndrome. Haploinsufficiency of the SCN1A gene affects the α subunit of the voltage-gated sodium channel ($Na_V1.1$) in mice leading to autistic behavioral phenotypes, including hyperactivity and stereotypic behaviors such as self-grooming and circling behaviors. Scn1a$^{+/-}$ mouse model of autism exhibit increased excitation in the prefrontal cortex (PFC). Deletion of sodium channels ($Na_v1.1$) in cortical interneurons causes reduced sodium (Na^+) currents and neurotransmission of GABAergic interneurons resulting in altered GABAergic activity, hyperexcitability, and behavioral impairments in the mutant mice (**Table 1**) (Han et al., 2012).

Mutations in receptor proteins are also involved in autistic phenotypes. Oxytocin is a peptide produced in the brain, particularly in the paraventricular nuclei and hypothalamic supraoptic. It is secreted primarily by the posterior pituitary gland into the circulation (Lee et al., 2009). Oxytocin facilitates biological effects by binding to the oxytocin receptor (Oxtr). The oxytocin receptor is mainly found in the amygdala, hippocampus, olfactory lobe, and hypothalamus areas of the brain (Gould and Zingg, 2003). *Oxtr*$^{-/-}$ mice exhibit autistic-like

phenotypes, increased self-grooming behavior in a visible burrow system (VBS) (Pobbe et al., 2012). *Oxtr*$^{-/-}$ mice also exhibit cognitive inflexibility during the reversal phase in the T-maze test and increased aggression. *Oxtr*$^{-/-}$ mice exhibit alterations in excitatory synaptic markers including PSD95, gephyrin scaffolding proteins, and glutamatergic, GABAergic receptors along with changes in striatal dendritic spines, indicating striatal dysfunction (Sala et al., 2011; Leonzino et al., 2019).

Environmentally induced alterations to the developing nervous system, such as through specific teratogenic agents or restricted housing also contribute to the etiology of ASD. *In utero* valproic acid (VPA), an antiepileptic drug, exposed mice and rats show increased repetitive behaviors, such as self-grooming along with reduced social interactions and communication dysfunction (Schneider and Przewocki, 2005; Bromley et al., 2008).

C58/J, an inbred mice strain, show social deficits, repetitive backward somersaulting and hind limb jumping behaviors, restricted novel hole-board exploration, and reversal-learning deficits in the appetitive operant task (Moy et al., 2008b; Ryan et al., 2010; Muehlmann et al., 2012; Whitehouse et al., 2017). The hole-board test measures the number of nose-pokes (head-dipping) into holes in the floor arena as a measure of exploratory behavior (Moy et al., 2008a). Moreover, BTBR, an inbred mouse strain, shows ASD-like behavioral phenotype including social, communication deficits and stereotypic behaviors (McFarlane et al., 2008; Silverman et al., 2010; Wöhr et al., 2011). Balb/c mice, another inbred strain shows ASD-like behaviors, such as sociability deficits and stereotypic behaviors. Functional alterations in NMDAR mediated activity and elicitation of jumping and circling behavior by NMDAR antagonist MK-801 application is described in Balb/c strain (Deutsch et al., 1997; Burket et al., 2010).

Deer mice belong to a diverse *Peromyscus* genus of Cricetidae rodent family that is native to North America and utilized as a laboratory animal model for basic and applied research (Joyner et al., 1998; Crossland and Lewandowski, 2006). Deer mice exhibit repetitive behavior including hindlimb jumping and backward somersaulting upon being maintained in standard laboratory housing. The repetitive behaviors showed by deer mice occur at an increased rate, apparent during initial development and continuing across the lifespan. Deer mice also display reversal learning deficits in a procedural learning behavioral task involving learning to change spatial habits upon relocation of reinforcement in a T-maze (Hadley et al., 2006). Hence, deer mice are used as animal models of repetitive/restricted behaviors in autism (Powell et al., 2000; Lewis et al., 2007; Bechard et al., 2017).

GLUTAMATERGIC AND GABAERGIC SIGNALING

The normal balance of excitation and inhibition (E/I) in the forebrain is maintained by excitatory glutamatergic neurons and inhibitory GABAergic interneurons. The major excitatory neurotransmitter in the cortex is glutamate, which activates two types of receptors, i.e., ionotropic and metabotropic G-protein coupled receptors (Mehta et al., 2011). Increased excitatory signaling, hyper-excitable local connectivity, and decreases in inhibitory interneurons accompany repetitive behavioral changes in the brains of ASD animals (Rinaldi et al., 2007; Gogolla et al., 2009). Interestingly, these behaviors are ameliorated by environmental enrichment, correlating to functional alterations in neural circuitry by modifying cortical excitatory and inhibitory synaptic density, LTP, increasing BDNF expression and synaptic plasticity in the cortical network (Schneider et al., 2006; Baroncelli et al., 2010; Lonetti et al., 2010; Reynolds et al., 2013; Jung and Herms, 2014).

Glutamatergic signaling plays a crucial role in the modulation of repetitive behaviors. On the one hand, NMDA receptors play important roles in the regulation of neurotransmitter release such as glutamate affecting excitatory neural pathways. For instance, intra-striatal injections of NMDA, glutamate receptor ligand, induces repetitive behaviors caused by elevated glutamatergic activity in the basal ganglia motor circuits (Karler et al., 1997). Deer mice exhibit repetitive behaviors, such as excessive jumping and backward flips, attenuated by interrupting cortico-striatal glutamatergic projections *via* striatal injection of NMDA receptor antagonist MK-801 (dizocilpine) (Presti et al., 2003). Mice with astrocyte-specific inducible deletion of GLT-1 (GLAST$^{CreERT2/+}$/GLT1$^{flox/flox}$, iKO) manifesting stereotypic grooming behavior is alleviated by memantine, NMDA receptor antagonist (Aida et al., 2015).

On the other hand, NMDA receptors are also expressed on the surface of GABAergic neurons modulating their inhibitory tone and controlling oscillations of pyramidal neurons involved in the regulation of neuronal rhythms and activity (Benes, 2010; Deutsch et al., 2010). For instance, systemic application of anti-glutamatergic agents, phencyclidine (PCP), an NMDA receptor antagonist, evokes stereotypic behaviors, including self-grooming in rodents. NMDA antagonist application might inhibit excitation of GABAergic inputs onto pyramidal neurons causing disinhibitory (i.e., hyperexcitation of pyramidal neurons) increase in glutamate efflux and glutamatergic neurotransmission *via* AMPA and non-NMDA receptors in the PFC, activating motor pathways (Liu and Moghaddam, 1995). This PCP or non-NMDA receptor-induced stereotypic grooming is alleviated by blocking AMPAR (non-NMDAR) mediated glutamatergic transmission between the prefrontal cortex (PFC) and ventral tegmental area (VTA) (Takahata and Moghaddam, 2003; Audet et al., 2006) (**Figure 2**). Also, neuroligin-1 (NL1) knockout mice exhibit a reduced NMDA/AMPA ratio in the dorsal striatum that correlates with repetitive grooming behavior, which is rescued by systemic administration of D-cycloserine, an NMDA receptor partial co-agonist (Blundell et al., 2010). Shank2$^{-/-}$ mice manifest reduced NMDA receptor function and social deficits, normalized by application of D-cycloserine (Won et al., 2012). D-cycloserine is also revealed to improve sociability deficits and stereotypies in BTBR and Balb/c inbred mouse strains of ASDs (Deutsch et al., 1997, 2011a,b; Burket et al., 2013).

Dysfunction of glutamatergic signaling at the metabotropic glutamate receptor 5 (mGluR5) is implicated in neuropsychiatric

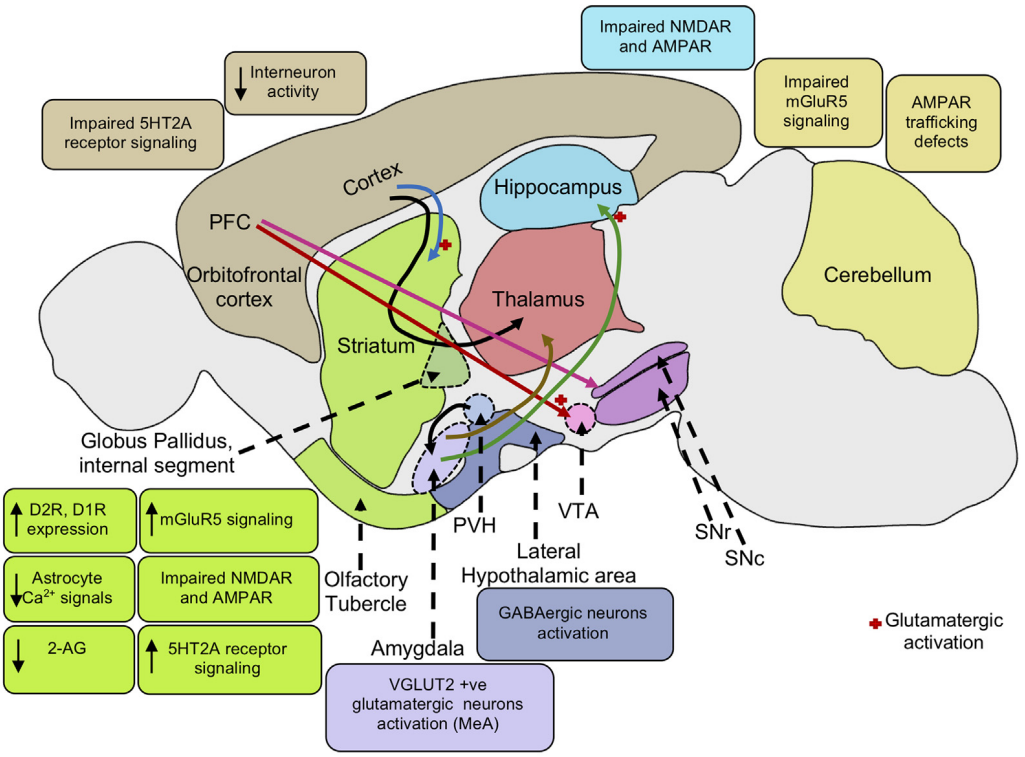

FIGURE 2 | Neural mechanisms underlying repetitive behaviors. Increased mGluR5 signaling activates the striatal direct pathway leading to heightened motor cortex activity inducing repetitive behaviors. Impaired NMDA and AMPA receptors in the striatum and hippocampus also mediates stereotypic behaviors. Cortico-striatal and PFC-VTA glutamatergic projections induce repetitive behavior. PFC projections to the SNc causes striatal dopaminergic release promoting movement. The decrease in interneuron activity in the cortex and increase in dopamine D2, D1 receptor expression in the striatum leads to reduced GABAergic signaling in the cortex, enhancing motor cortical activity, and repetitive behaviors. Elevation of serotonin $5HT_{2A}$ receptor signaling in the dorsomedial striatum gives rise to stereotypic behaviors. Activation of VGLUT-positive glutamatergic neurons in the amygdala nucleus, MeA also results in stereotypic behaviors. Activation of glutamatergic projection from BLA to the ventral hippocampus leads to an increase in locomotor activity. Further, activation of lateral hypothalamic GABAergic neurons mediates an increase in locomotor activity and repetitive behaviors. Reduction in endocannabinoid 2-AG signaling in the striatum leads to an increase in glutamatergic output, enhancing motor cortex activity resulting in repetitive behaviors. Low astrocytic Ca^{2+} signals in the striatum elevate membrane GAT-3 expression that modulates striatal MSN activity *via* reduced ambient GABA levels inducing repetitive behavior. mGluR5, metabotropic glutamate receptor 5; NMDA, *N*-Methyl-d-aspartate; AMPA, α-amino-3-hydroxy-5-methyl-4-isoxazolepropionic acid; PFC, prefrontal cortex; VTA, ventral tegmental area; SNc, substantia nigra pars compacta; SNr, substantia nigra pars reticulata; PVH, paraventricular nucleus of the hypothalamus; GABA, gamma-aminobutyric acid; D2R, dopamine receptor D2; D1R, dopamine receptor D1; $5HT_{2A}$, 5-hydroxy-tryptamine receptor 2A subtype; VGAT, vesicular GABA transporter; MeA, medial nucleus of the amygdala; BLA, basolateral amygdala; 2-AG, 2-arachidonoyl glycerol; GAT-3, GABA transporter 3; MSN, and medium spiny neuron.

disorders such as autism (Carlson, 2012) (**Figure 2**). As noted above, Fragile X Syndrome is a genetic disorder associated with autism and mental retardation. This disorder is caused by a loss of FMRP (Hagerman et al., 2017; Niu et al., 2017). The "mGluR theory of fragile X" suggests that FMRP and Group I metabotropic glutamate receptors (mGluRs) regulate protein synthesis at the synapse in an antagonist manner. mRNA translation at the synapse is activated by mGluRs and repressed by FMRP (Bear et al., 2004; Bear, 2005; Dölen and Bear, 2008). Fmr1-KO mice manifest increased expression of mGluR-dependent long-term depression (LTD) in the hippocampus, which is likely associated with alterations in mGluR signaling that contribute to repetitive behaviors in mutant mice (**Table 1**) (Yan et al., 2005; Nosyreva and Huber, 2006; Dölen and Bear, 2008; McNaughton et al., 2008; Pietropaolo et al., 2011). Also, $Shank3^{\Delta e4-22-/-}$ mice (exons 4–22 deletion) exhibit excessive grooming and have reduced striatal postsynaptic mGluR5-Homer scaffolding proteins, altered mGluR5 signaling in the striatum and cortico-striatal circuit abnormalities (Wang X. et al., 2016). Interestingly, in the $Ube3A^{m-/p+}$ (maternal null mutation) mouse model of Angelman Syndrome, mGluR-dependent LTD and coupling of mGluR5 to Homer proteins in the hippocampus is enhanced (Pignatelli et al., 2014). A mouse model of Tuberous Sclerosis $Tsc2^{+/-}$ exhibits reduced mGluR-LTD (LTD) in the hippocampus and altered levels of mGluR signaling Arc (activity-regulated cytoskeleton-associated) protein, which is crucial for AMPAR internalization in cerebellar LTD (Auerbach et al., 2011). This suggests that altered mGluR5 function may underlie cognitive and behavioral impairments in mutant mice models (**Table 1**) (Auerbach et al., 2011; Pignatelli et al., 2014).

Several studies have demonstrated the therapeutic efficacy of the mGluR5 receptor antagonist, 2-methyl-6-phenyethyl-pyrididine (MPEP), on core behavioral deficits of autism. MPEP reduces repetitive and stereotypic behaviors in the VPA and BTBR mouse models of autism (Silverman et al., 2010; Mehta et al., 2011) (**Figure 3**). Additionally, MPEP application decreases marble burying stereotypic behavior in Fmr1 KO mice and excessive repetitive grooming in Shank3$^{\Delta e4-22-/-}$ mice *via* modulation of mGluR5 signaling (Thomas et al., 2012; Gandhi et al., 2014; Wang X. et al., 2016). Also, in C58/J mice that exhibit stereotypic jumping behavior, backflips, and decreased exploratory behavior, blocking mGluR5 signaling *via* GRN-529, a mGluR5 negative allosteric modulator, rescues normal behavior (Silverman et al., 2012). The suppression of mGluR5 activity may modify NMDA receptor activity, since they are close associates at the postsynaptic density, suggesting NMDA receptor hyperfunction underlies jumping behavior in C58/J mice (Kim et al., 2016). Also, repetitive behavior and reversal learning deficits were attenuated by environmental enrichment in C58/J mice (Muehlmann et al., 2012; Whitehouse et al., 2017).

GABAergic signaling also plays a critical role in the regulation of stereotypic behaviors. For example, the application of GABA-enhancing drugs reduces self-grooming behavior in rodents (Silverman et al., 2015). Administration of R-baclofen, a selective $GABA_B$ receptors agonist, alleviates repetitive self-grooming behavior in several ASD models, including the BTBR, Fragile X, C58/J, and idiopathic mice models (Han et al., 2014; Silverman et al., 2015). Also, the application of a $GABA_A$ receptor-selective agonist, muscimol, into the bed nucleus of the stria terminalis (BNST) decreases self-grooming behavior induced by exposure to cat urine (Xu et al., 2012). Additionally, GABRB-3 knockout mice show hyperactivity and stereotypic behaviors such as circling (Moy et al., 2006). GABA also plays an important role in regulating stress and anxiety-related behaviors, with increased GABAergic signaling exerting anxiolytic effects and inhibition of stress and anxiety-induced grooming behaviors (Chao et al., 2010).

GABA receptor agonists regulate excitation and inhibition (E/I) balance, resulting in minimizing elevated excitation in motor cortical areas and parts of basal ganglia-thalamic circuitry (Lewis and Kim, 2009; Kim et al., 2016) (**Figure 3**). For instance, stereotypic behaviors evoked by amphetamine are diminished by the application of GABA receptor agonists (Lewis and Kim, 2009). Likewise, the application of $GABA_A$ receptor antagonist, bicuculline, in the VTA enhances self-grooming in mice induced by alpha-melanocyte-stimulating hormone (MSH; De Barioglio et al., 1991). Also, muscimol injections into the substantia nigra pars reticulata (SNr) evoke repeated circling behavior in rats (Velíšek et al., 2005). Thus, altered GABA levels may modify basal ganglia activity by affecting dopaminergic neurons, leading to repetitive behaviors in rodents, as discussed further below (De Barioglio et al., 1991; Kim et al., 2016). Antidepressants/anxiolytics like fluvoxamine, bupropion, and diazepam alleviate repetitive digging behaviors (Hayashi et al., 2010). Moreover, Fmr1$^{-/-}$ mice, discussed above, exhibit hyperexcitability due to reduced activity of fast-spiking interneurons (FSI) in the somatosensory and barrel cortex (**Figure 2**). GABA-receptor agonists decrease marble-burying behavior in these Fmr1 knockout mice (Draper et al., 2014). Hence, altered neural signaling and E/I balance underlie repetitive behaviors associated with ASD. Enhanced GABAergic function results in reduced cortical excitation and alleviates repetitive self-grooming behavior (Kalueff et al., 2016).

SEROTONERGIC SIGNALING

Serotonergic $5HT_{2A}$ receptors are found mainly in prefrontal cortical and striatal brain regions (Xu and Pandey, 2000), which are associated with repetitive behaviors in ASD (Di Martino et al., 2011; Langen et al., 2012; Delmonte et al., 2013). Differences in serotonergic components in the basal ganglia are associated with repetitive behaviors (Di Giovanni et al., 2006). For instance, deer mice exhibit a decreased density of serotonin transporters in the striatum (Wolmarans et al., 2013). And, injection of escitalopram, a selective serotonergic reuptake inhibitor (SSRI) alleviates some of the repetitive movements in deer mice, but with no effect on jumping behavior (Wolmarans et al., 2013). Additionally, optogenetic repetitive stimulation of the medial orbitofrontal cortex-ventromedial striatum pathway in mice leads to abnormal grooming behavior, which is rescued by fluoxetine administration, also an SSRI (Schmeisser et al., 2012). Family-based genetic association studies demonstrate linkages between serotonin transporter locus (SLC6A4) variants and rigid compulsive behavior (Sutcliffe et al., 2005), with the serotonin transporter gene (SLC6A4) subtype, 5HTTLPR, consistently associated with repetitive sensory and motor behaviors (Brune et al., 2006). Also, depleting tryptophan, a precursor of serotonin augments repetitive motor behaviors in autistic adults (McDougle et al., 1996).

Clinical and preclinical studies have implicated alterations in serotonin receptor activity, particularly $5HT_{2A}$ receptor signaling, in ASD symptomology (McBride et al., 1989; Veenstra-VanderWeele et al., 2012) (**Figure 2**). Systemic treatment with a serotonin $5HT_{2A}$ receptor antagonist decreases repetitive behaviors in the BTBR mouse model of autism, an inbred strain that shows similar ASD-like behavioral deficits to an idiopathic mouse model of autism (McFarlane et al., 2008; Amodeo et al., 2012, 2014, 2016). Further, infusion of M100907, a highly selective antagonist for $5HT_{2A}$ receptors into the dorsomedial striatum reduces grooming behavior and reversal learning deficits in BTBR mice. This regulation of reversal learning and grooming behavior by $5HT_{2A}$ receptor antagonist infusion into the dorsomedial striatum may be associated with a reduction in striatal direct pathway activation (Reiner and Anderson, 1990; Amodeo et al., 2017). However, $5HT_{2A}$ receptor antagonist infusion into the orbitofrontal cortex results in increased grooming behavior and perseveration in reversal learning (Amodeo et al., 2017). This altered grooming behavior by blocking

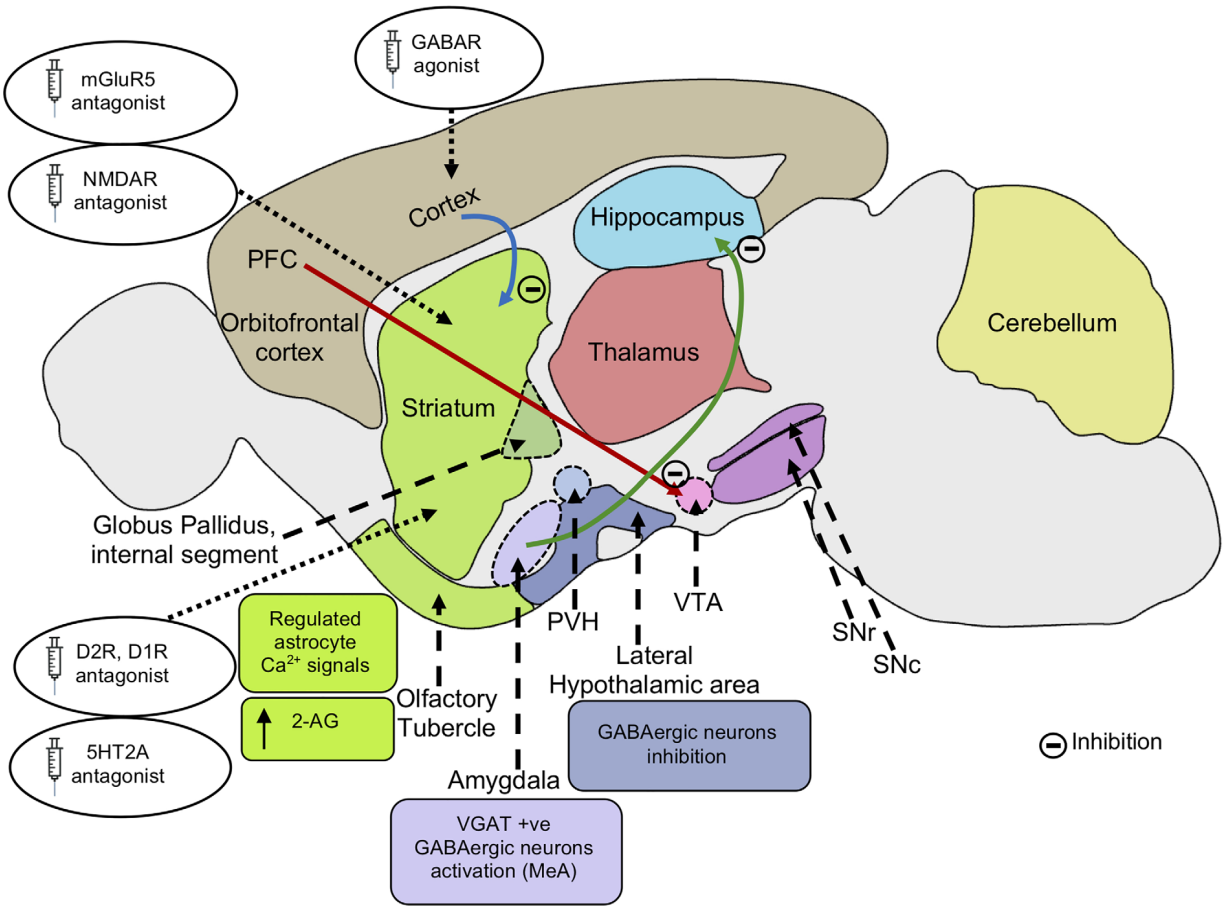

FIGURE 3 | Possible mechanisms alleviating repetitive behaviors. Inhibition of mGluR5 signaling inhibits striatal direct pathway *via* suppressing dopamine D1 receptor signaling. The reduced D1R signaling results in decreased motor cortex activity. Inhibition of cortico-striatal and PFC-VTA glutamatergic projections alleviate repetitive behaviors. Application of GABA agonists in the cortex and dopamine D2R, D1R antagonist in the striatum leads to an increase in GABAergic signaling in the cortex, reducing motor cortical activity and repetitive behaviors. Application of serotonin $5HT_{2A}$ antagonist in the dorsomedial striatum also results in the rescue of repetitive behavior. Activation of VGAT-positive GABAergic neurons in the amygdala nucleus, MeA reduces repetitive behaviors. Inhibition of glutamatergic projection from BLA to the ventral hippocampus results in decreased locomotor activity. Inhibition of lateral hypothalamic GABAergic neurons leads to a decrease in locomotor activity and repetitive behaviors. Endocannabinoid 2-AG signaling in the striatum leads to reduced glutamatergic output, decreasing repetitive behaviors. Regulated astrocytes Ca^{2+} signals in the striatum modulate GAT-3 activity which maintains synaptic GABA levels, regulating striatal MSN activity and associated repetitive behavior. mGluR5, metabotropic glutamate receptor 5; NMDA, *N*-Methyl-d-aspartate; AMPA, α-amino-3-hydroxy -5-methyl-4-isoxazolepropionic acid; PFC, prefrontal cortex; VTA, ventral tegmental area; SNc, substantia nigra pars compacta; SNr, substantia nigra pars reticulata; PVH, paraventricular nucleus of the hypothalamus; GABA, gamma-aminobutyric acid; D2R, dopamine receptor D2; D1R, dopamine receptor D1; $5HT_{2A}$, 5-hydroxy-tryptamine receptor 2A subtype; VGAT, vesicular GABA transporter; MeA, medial nucleus of the amygdala; BLA, basolateral amygdala; 2-AG, 2-arachidonoyl glycerol; GAT-3, GABA transporter 3; MSN, the medium spiny neuron.

of $5HT_{2A}$ receptor activity in the orbitofrontal cortex may be associated with an increased output by the orbitofrontal cortex *via* reduced interneuron activity, as the orbitofrontal infusion of GABA receptor agonist, muscimol, results in decreased grooming behavior in BTBR mice (Amodeo et al., 2017) (**Figure 3**).

Thus, elevated serotonin $5HT_{2A}$ receptor signaling in the dorsomedial striatum plays a critical role in the development of stereotyped behaviors, whereas normal $5HT_{2A}$ receptor activity in the orbitofrontal cortex contributes to attenuation of stereotyped behaviors in BTBR mice. Hence, abnormal serotonin receptor activity in various brain regions may contribute to restricted and repetitive behaviors.

DOPAMINERGIC SIGNALING AND BASAL GANGLIA CIRCUITRY

The cortico-basal ganglia-thalamic pathway implements motor patterned behaviors and is implicated in repetitive behaviors (Haber and Calzavara, 2009; Kalueff et al., 2016). Sequential patterns of behaviors, such as stereotyped sequential grooming movements, also called grooming chains, are carried out by these circuits in rodents (Berridge et al., 2005; Denys et al., 2013). Striatal lesions, particularly in the anterior dorsolateral region of the striatum, resulting in an inability to complete sequential grooming movements. Additionally, lesions of the ventral pallidum and globus pallidus result in disruption of

grooming movements (Cromwell and Berridge, 1996), further underscoring their role in the regulation of complex and mechanistic sequenced behaviors.

Enhanced activity of basal ganglia circuitry results in increased hyperactivity and repetitive behaviors (Kim et al., 2015). In particular, the prefrontal cortical (PFC) projection to the substantia nigra pars compacta (SNc), leads to a dopaminergic release in the striatum, which promotes movement through opposing actions on direct and indirect basal ganglia pathways. Dopamine through D1 receptors is involved in the activation of the direct pathway, which in turn activates the motor cortex, resulting in movement. In contrast, dopamine through D2 receptors on neurons present in the indirect pathway, results in inhibition of the indirect pathway, also promoting movement (Gerfen et al., 1990; Gerfen, 1995). For example, amphetamine pretreated rats, when injected with a dopamine D2, D3 receptor antagonist, sulpiride, or the GABA antagonist, bicuculine, leads to repetitive behavior (Morency et al., 1985; Karler et al., 1998; Kiyatkin and Rebec, 1999). Further, these circuits are disrupted in autistic mouse models, which display PFC abnormalities. Namely, mice with mutations in the SCN1A gene leads to autistic-like phenotypes, including hyperactivity and stereotypic self-grooming and circling behaviors and increased excitation in the PFC (Han et al., 2012).

Dopamine plays a major role in modulating striatal pathways resulting in locomotion and repetitive motor behaviors. Application of Risperidone, which acts on different molecular receptors, including blocking of dopamine D2 receptors, leads to decreases in repetitive self-grooming behavior, perseveration, hyperactivity and rescues nesting deficits in Cntnap2$^{-/-}$ mice. Similarly, systemic administration of haloperidol, a dopamine D2 receptor antagonist decreases motor cortex activity, thereby impeding locomotor movements in rats (Parr-Brownlie and Hyland, 2005). Interestingly, increased striatal dopamine D2 receptor expression leads to deficits in GABAergic activity, thereby enhancing prefrontal cortical (PFC) excitation (Li et al., 2011) (**Figure 3**). Hence, reduced repetitive and locomotory behavior caused by altered dopamine D2 receptor expression may be linked to heightened cortical GABAergic function and reduced PFC excitability.

Manipulation of the nigrostriatal dopamine pathway is sufficient for modulating many stereotyped behaviors (Lewis and Bodfish, 1998). Altered striatal dopamine activity is implicated in repetitive circling behaviors, which are observed in several mouse models of ASD (Vaccarino and Franklin, 1982; Ishiguro et al., 2007). Systemic administration of a dopamine precursor, L-DOPA, and a non-selective dopamine agonist, apomorphine into the striatum induces stereotyped behaviors in rodents (Ernst and Smelik, 1966; Presti et al., 2004). Likewise, injection of dopamine D1 receptor agonists evokes stereotypic and rigid behavioral phenotype in rodents (Berridge and Aldridge, 2000a,b). Furthermore, deer mice exhibit stereotyped behaviors, such as excessive jumping and backward flips, which are attenuated by intrastriatal injection of dopamine D1 receptor antagonist, SCH23390 (Presti et al., 2003) (**Figure 3**). Spontaneous motor stereotypies observed in deer mice exhibit a negative association with neuropeptide enkephalin expression, a marker of striatopallidal neurons, and is attenuated by combined administration of adenosine A2A receptor agonist CGS21680 and A1 receptor agonist CPA in a dose-dependent manner, indicating altered striatal pathway activity (Tanimura Y. et al., 2010). Environmental enrichment attenuates repetitive behavior by increasing activation through the indirect basal ganglia pathway, which also results in changes in dendritic spine density in the subthalamic nucleus (STN) and globus pallidus (GP) (Bechard et al., 2016).

Several ASD mice models exhibit alterations to dopaminergic nigrostriatal signaling. Mutant mice with heterozygous deletion of the syntenic region on chromosome 7F3 (16p11$^{+/-}$) display decreased self-grooming behavior along with hyperactivity and increased stereotypic circling behavior. Neuroanatomically, these mice have increased numbers of dopamine D2 receptor-expressing neurons in the striatum, reduced number of cortical neurons manifesting dopamine D1 receptors, and synaptic function defects (Portmann et al., 2014) (**Figure 2**). Mice deficient in the DAT have elevated levels of dopamine and increased stereotypic sequential grooming behavior. Dopamine D1A receptor-deficient mice manifest disrupted and shorter duration grooming bouts (Cromwell et al., 1998). Neuroligin NL3 mutations result in a selective decrease of synaptic inhibition onto dopamine D1-expressing medium spiny neurons (MSNs) in the nucleus accumbens (NAc) and result in behavioral changes in mutant mice *via* reduced selective striatal synaptic function in the nucleus accumbens/ventral striatum (Rothwell et al., 2014). Apart from this, neuroligin-1 and 3 mutant mice show the abnormal function of dopamine D1 MSNs leading to autistic-like repetitive behaviors (Rothwell et al., 2014; Espinosa et al., 2015). In the Shank3 gene deletion mouse model, striatopallidal D2 MSNs show postsynaptic defects and decreased AMPAR responses (Mei et al., 2016; Zhou et al., 2016). Repetitive grooming in Shank3B mutant mice is rescued by enhancing indirect striatopallidal pathway activity (Wang et al., 2017). Additionally, synaptic plasticity is impaired in dorsolateral striatal medium spiny neurons (MSN) in mutant mice carrying full Shank3 deletion in exons 4–22 (Δe4–22$^{-/-}$), which also exhibit decreased striatal spine density and altered striatal synapse postsynaptic density (Peça et al., 2011; Sala et al., 2015; Peixoto et al., 2016; Wang X. et al., 2016). Finally, BTBR T + Itpr3tf/J mice show impairments in mesolimbic and striatal synaptic dopamine D2 receptor signaling resulting in reduced dopamine neurotransmission. Reductions in pre-and post-synaptic adenosine A2A receptor function also indicate associations with altered dopamine neurotransmission (Squillace et al., 2014).

Overall, dopaminergic circuitry in the basal ganglia mediates rigid and sequential behavioral phenotypes associated with ASD. As dopamine-containing neurons and pathways are crucial in movement and sequencing behaviors, the regulation of the dopaminergic system may provide a valuable tool for modulating repetitive behaviors. Hence, basal ganglia circuits play an instrumental role in the regulation of

compulsive and repetitive behavioral phenotype associated with ASD.

GLUTAMATERGIC SIGNALING AT CORTICO-STRIATAL SYNAPSES

Striatal glutamatergic synapses express synapse-associated protein 90/postsynaptic density protein 95 (SAP90/PSD95) associated proteins (SAPAP), which form scaffolding protein complexes involved in the regulation of neurotransmitters trafficking and targeting to the post-synaptic membrane (Wu et al., 2012). Mutations in synapse-associated protein 90/postsynaptic density protein 95-associated protein 3 (SAPAP3) that also binds to SHANK3 postsynaptic scaffolding protein is associated with stereotypic behaviors in mice (Sapap3$^{-/-}$), such as compulsive self-grooming to the point of inducing lesions, which is rescued by Sapap3 re-expression in the striatum and optogenetic stimulation of lateral orbitofrontal cortex (Welch et al., 2007; Bienvenu et al., 2009; Burguière et al., 2013).

Sapap3 mutant mice exhibit glutamatergic transmission defects at cortico-striatal synapses and elevated mGluR5 signaling, leading to abnormal striatal output and stereotyped behavior, which is alleviated by mGluR5 inhibition (Ade et al., 2016). This suppression of mGluR5 possibly inhibits the direct basal ganglia pathway resulting in reduced repetitive behaviors (Conn et al., 2005). NMDA and AMPAR-dependent cortico-striatal synaptic transmission is also altered. Intriguingly, systemic administration of fluoxetine, a serotonin uptake inhibitor attenuates obsessive grooming in mutant mice (Welch et al., 2007).

ENDOCANNABINOID SIGNALING IN STRIATAL SYNAPSES

Endocannabinoid signaling plays a crucial part in modulating striatal synaptic transmission and in regulating stereotypic behaviors (Chen et al., 2011; Gremel et al., 2016). The abundant endocannabinoid, 2-arachidonoyl glycerol (2-AG), activates cannabinoid-1 receptor (CB1R), mediating suppression of glutamatergic release *via* feedback inhibition at direct and indirect medium spiny neuron (MSN) synapses (Kano et al., 2009). Synthesis of 2-AG in the postsynaptic neuron is mediated by diacylglycerol lipase alpha (DGLα) (Gao et al., 2010; Tanimura A. et al., 2010; Shonesy et al., 2014). Mice with DGLα knockout in direct-pathway MSN exhibit reduced levels of 2-AG in the striatum and absence of feedback inhibition mediated by 2-AG at glutamatergic direct-pathway MSN synapses, resulting in excessive glutamatergic drive in direct-pathway MSNs (**Figure 3**). In addition, DGLα deletion in direct-pathway MSNs does not change GABAergic synaptic transmission, suggesting that alterations to excitation/inhibition balance may contribute to increased direct-pathway MSN output, resulting in excessive grooming behavior (**Figure 4**). Furthermore, mice with regional DGLα deletions in the ventral striatum (nucleus accumbens) exhibit repetitive grooming behavior (Shonesy et al., 2018). Thus, 2-AG signaling impairment in direct pathway MSNs leads to circuit alterations and ASD behavioral phenotypes, such as repetitive self-grooming behavior (**Figure 2**).

Group1 mGluRs play a role in mobilizing endocannabinoids in the hippocampus, contributing to increased excitability. In FMR1 null mice, mGluR5 dependent LTD is absent at excitatory synapses of PFC and ventral striatum, which is moderated by endocannabinoid 2-arachidonoylglycerol (2-AG). The Homer scaffolding complex linking mGluR5 to DGLα is disrupted resulting in impairment of endocannabinoid mediated LTD at excitatory synapses. Application of CB1R antagonist rimonabant improves cognitive deficits in Fmr1 KO mice (Busquets-Garcia et al., 2013). Hence, endocannabinoid signaling contributes to increased excitability in FXS (Jung et al., 2012; Tang and Alger, 2015). Intriguingly, CB1, and CB2 receptor expression is upregulated in the brain of MeCP2 mutant mice. Treatment with cannabinoid cannabidivarin (CBDV) ameliorates memory deficits in MeCP2 mutant mice. CBDV also regulates BDNF, CB1, CB2 receptor levels, and PI3K/AKT/mTOR pathway which is dysregulated in MeCP2 deficient mice (Zamberletti et al., 2019). Hence, altered endocannabinoid signaling is associated with behavioral abnormalities in neurodevelopmental disorders.

ASTROCYTIC CALCIUM SIGNALING REGULATING STRIATAL CIRCUITRY

Astrocytes perform numerous functions, including maintenance of the blood-brain barrier, extracellular ion homeostasis, synapse formation, and regulation of synaptic transmission (Khakh and Sofroniew, 2015). Astrocytes also propagate intercellular Ca^{2+} waves upon stimulation and modulate neuronal function through Ca^{2+} dependent signaling (Bazargani and Attwell, 2016). Astrocytic Ca^{2+} signaling stimulates the release of gliotransmitters such as glutamate, GABA, ATP, and D-serine that regulate neuronal activity (Bazargani and Attwell, 2016). Astrocytes regulate extracellular levels of glutamate *via* transporters like GLT1, hence influencing excitatory and inhibitory neuronal balance (Wu et al., 2012). High levels of glutamate in the extracellular space lead to over-activation of glutamate receptors, i.e., neuronal excitotoxicity. Astrocytes protect against neurotoxicity by mediating glutamate clearance from synaptic space *via* glutamate uptake transporters, thereby modulating neuronal activity. Astrocytes also supply ATP that is crucial for the process of glutamate uptake. In astrocytes, glutamate is converted to glutamine which acts as a precursor for the resynthesis of neurotransmitters like glutamate/GABA in neurons. Further, glutamate in the synapse induces astrocytic Ca^{2+} increase that results in release of glutamate from astrocytes to adjoining neurons, stimulating NMDA receptors and iGluRs (ionotropic glutamate receptors), modulating their activity. Therefore, astrocytes have dual roles in maintaining glutamate release and uptake (Bazargani and Attwell, 2016; Mahmoud et al., 2019). Astrocytes also modulate synaptic GABA levels *via* GABA transporters (GAT) that mediates GABA uptake. Expression of synaptic GAT1 regulates GABA levels in the synapses, thereby modulating neuronal excitability. The rise in astroglial Ca^{2+} signaling leads to inhibition of neuronal

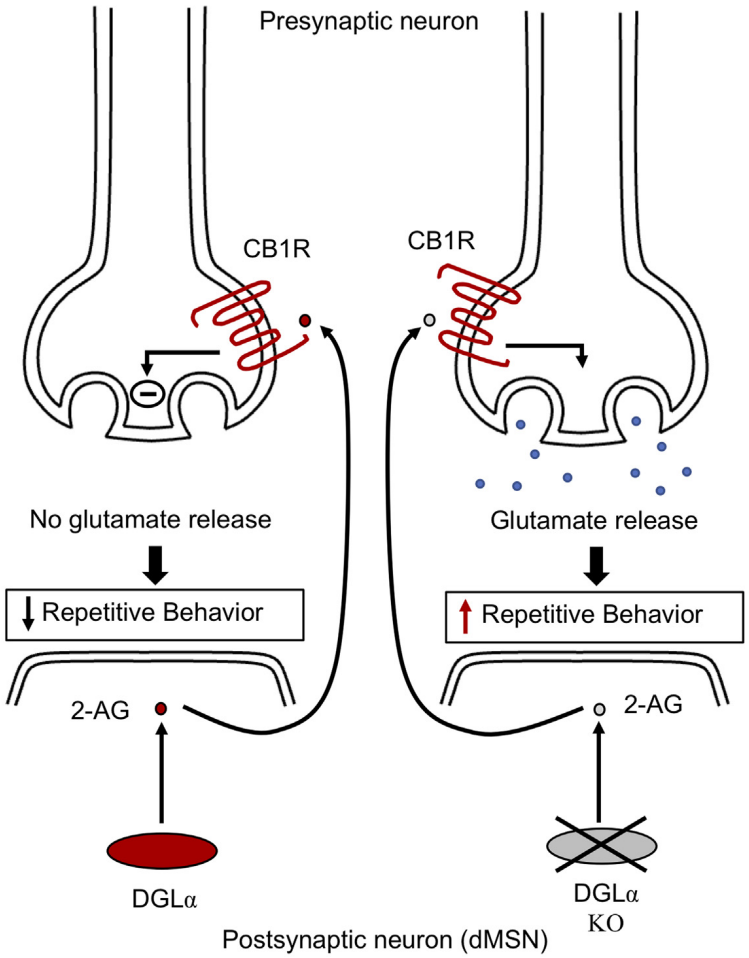

FIGURE 4 | Endocannabinoid signaling in striatal neurons. DGLα synthesizes 2-AG in the postsynaptic neuron. Postsynaptic 2-AG activates presynaptic cannabinoid-1 receptor (CB1R). The activated CB1 receptor *via* feedback inhibition leads to suppression of glutamate release at MSN synapses, thereby relieving repetitive behavior. However, mice with knockout of DGLα exhibit decreased striatal 2-AG levels, resulting in unrestricted synaptic glutamate release *via* an absence of feedback inhibition, thereby leading to elevated grooming behavior in mice. Impaired endocannabinoid signaling is involved in the alteration of striatal activity, contributing to the development of repetitive behavior. CB1R, cannabinoid type 1 receptor; DGLα, diacylglycerol lipase alpha; 2-AG, 2-arachidonoyl glycerol; dMSN, direct pathway medium spiny neurons.

activity. This is associated with elevated GABA levels in the synapse caused by decreases in astroglial membrane GAT levels *via* endocytosis into astrocytes. The membrane trafficking of GAT is regulated by Rab11, Rab family small GTPases. Rab11 suppression counteracts the decrease in neuronal activity by elevated astroglial Ca^{2+} levels *via* repressing GAT endocytosis. Therefore, astrocytes regulate activity of neuronal circuits (Zhang et al., 2017). Alterations in astroglial uptake processes or gliotransmitters release is implicated in the pathogenesis of neurological disorders including epilepsy and may contribute to the development of behavioral impairments in these disorders (Mahmoud et al., 2019).

Also, astrocytic dysfunction is implicated in stereotypic behaviors associated with neuropsychiatric disorders (Molofsky et al., 2012; Aida et al., 2015; Yu et al., 2018). Mutant mice with GLT-1 inducible deletion in astrocytes ($GLAST^{CreERT2/+}/GLT1^{flox/flox}$, iKO) display excessive self-grooming repetitive behavior resulting in self-induced injury. The knockout of astroglial GLT1 leads to alteration in the cortico-striatal synapse, suggesting glial dysfunction involvement in the pathophysiology of repetitive behaviors (Aida et al., 2015). In wild-type C57BL/6NTac mice, decreased astrocyte Ca^{2+} signaling in the striatum leads to increased stereotypic grooming behavior (**Figure 2**). In these experiments, wild-type C57BL/6NTac mice were injected with hPMCA2w/b construct to impair striatal astrocytic Ca^{2+} signals. The hPMCA2w/b construct consists of a w/b splice variant in human plasma membrane Ca^{2+}-ATPases pump (hPMCA2) deficient in the cytosolic interaction domains (Yu et al., 2018). Membrane targeting of PMCA2 is determined by alternative splicing of protein cytosolic loop, in which "w" form (w splice variant) containing 45 amino acid residue

insertion, display membrane localization of PMCA2. The b splice variant is generated at the COOH terminal site of the protein, an important regulatory region of the pump and its terminal sequence interacts with PDZ proteins (Chicka and Strehler, 2003). Astrocytes express the plasma membrane Ca^{2+} pump (PMCA2) that function to expel cytosolic Ca^{2+}. The generated hPMCA2w/b mice exhibit excessive repetitive self-grooming behavior. Reduced astrocyte Ca^{2+} signaling decreases ambient GABA levels *via* enhanced GABA transporter 3 (GAT-3) activity (**Figure 5**). Also, Rab11a gene downregulation leads to increased GAT-3 functional activity, thereby reducing inhibition of MSNs in the striatum. The elevated self-grooming behavior is also observed in a mouse model of Huntington's disease, R6/2 that is associated with decreases in astrocytic Ca^{2+} signals and alleviated by blocking astrocytic GAT-3. Hence, attenuated astrocytic Ca^{2+} signaling decreases striatal MSN inhibition, *via* altered GABA levels resulting in repetitive behavior (Yu et al., 2018) (**Figure 5**). Moreover, astrocytic GLT1 deficient mice show increased grooming, rearing, and jumping behavior, suggesting reduced synaptic glutamate clearance resulting in glutamatergic dysfunction underlying these behaviors (Jia et al., 2021). Hence, astrocytes regulate striatal activity and associated stereotypic behavior.

Further, mice with inactivation of *Tsc1* gene in astrocytes ($Tsc1^{GFAP}$CKO) displays epilepsy, learning deficits, reduced GLT-1 protein expression, elevated levels of glutamate in the hippocampus, and impairment of hippocampus-LTP suggesting altered glutamate homeostasis and synaptic plasticity in a mouse model of Tuberous Sclerosis (Wong et al., 2003; Zeng et al., 2007).

Glial ephrin-A3 also plays an important role in modulating hippocampal activity. In the adult hippocampus, dendritic spines of pyramidal neurons express EphA4 tyrosine kinase receptor, the activation of which is dependent on ligand ephrin-A3, present in the perisynaptic processes of astrocytes, is involved in the regulation of dendritic spine morphology and synapse formation (Murai et al., 2003; Klein, 2009). Mice with a knockout of ephrin-A3 or EphA4 exhibits spine irregularities and results in increased expression of astroglial glutamate transporters GLT-1 and GLAST in the hippocampus. Hence, bidirectional signals between neuronal EphA4 and astroglial ephrin-A3 regulate spine morphology, glutamate transport, and excitatory synaptic function (Carmona et al., 2009; Filosa et al., 2009).

Neural circuit refinement is associated with experience-dependent synaptic pruning. In the cortex of ephrin-A2 knockout mice, experience-dependent removal of postsynaptic dendritic spines was mediated by activation of NMDA glutamate receptors, thereby leading to changes in adult neural circuits. Ephrin-A2 null mice also showed reduced glutamate transporters, contributing to increasing synaptic glutamate and promoting spine elimination (Yu et al., 2013).

Hence, astroglial expressed ephrin-A3 and ephrin-A2 in the hippocampus and cortex, respectively, have opposite effects on the modulation of glutamate transporters and spine morphology. Treatment interventions targeting astroglial ephrin-A3/A2 signaling may alter the expression of glutamate transporters and protect against glutamate excitotoxicity, maintaining the synapse structure and dynamics.

AMYGDALA AND LIMBIC CIRCUITRY IN REPETITIVE BEHAVIORS

The amygdala is involved in the regulation of emotions, anxiety, and fear, as well as regulating repetitive behaviors. High levels of anxiety in rodents are accompanied by increased self-grooming behaviors, rescued by anxiolytic treatments (Kalueff and Tuohimaa, 2004a; Ahmari and Dougherty, 2015). Anxiety-related behavior in rats is correlated with reduced dopamine release in the amygdala and increased grooming episodes. In the medial nucleus of the amygdala (MeA), activation of vesicular glutamate transporter 2 (vGLUT2) expressing glutamatergic neurons increases repetitive self-grooming behavior (**Figure 2**), whereas activation of vesicular GABA transporter (VGAT)-positive GABAergic neurons represses self-grooming behavior in mice (**Figure 3**) (Hong et al., 2014). Also, injections of Orexin-B, a neuropeptide that regulates food intake, mood, and wakefulness in the central nucleus of the amygdala (CeA), lead to enhanced grooming frequency in hamsters. Orexin-B-induced grooming behavior is potentiated by infusion of NMDA receptor agonists (Alò et al., 2015). In the lateral amygdala, the Fmr1 KO mouse model shows synaptic defects including impaired mGluR-dependent LTP, and reduced AMPAR subunit, GluR1 surface expression (Suvrathan et al., 2010).

The basolateral nucleus of the amygdala (BLA) sends projections to the hippocampus and the prefrontal cortex (PFC; Obeso and Lanciego, 2011). Activation of glutamatergic projections from the basolateral amygdala (BLA) to the ventral hippocampus heightens self-grooming in mice (Felix-Ortiz and Tye, 2014) (**Figure 2**), while its inhibition leads to reduced locomotor activity, suggesting a crucial role for the ventral hippocampus in repetitive behaviors (**Figure 3**) (Bast et al., 2001; Zhang et al., 2002). Shank3 deficient rats show attention deficit and decreased synaptic plasticity in the hippocampal-medial prefrontal cortex pathway. Mouse models of Shank3 deletion also exhibit impaired synaptic plasticity in the hippocampus, associated with deficits in actin cytoskeleton remodeling, along with changes in NMDA glutamatergic receptors and mGluR-Homer scaffolding complex, resulting in abnormalities in cortico-striatal circuits underlying repetitive behaviors (Bozdagi et al., 2010; Duffney et al., 2013; Kouser et al., 2013; Wang X. et al., 2016). In addition, the Shank postsynaptic protein scaffold helps regulate synaptic transmission at hippocampal Schaffer Collateral-CA1 synapses (Shi et al., 2017). Further, altered synaptic transmission at thalamo-amygdala circuits is associated with obsessive self-grooming behavior in rodents (Ullrich et al., 2018).

The hypothalamus is another limbic brain region involved in regulating numerous behaviors, including self-grooming in rodents (Qualls-Creekmore and Münzberg, 2018). The hypothalamic paraventricular nucleus and the dorsal hypothalamus are associated with grooming behavior observed by local electrical stimulation in the hypothalamus that induces

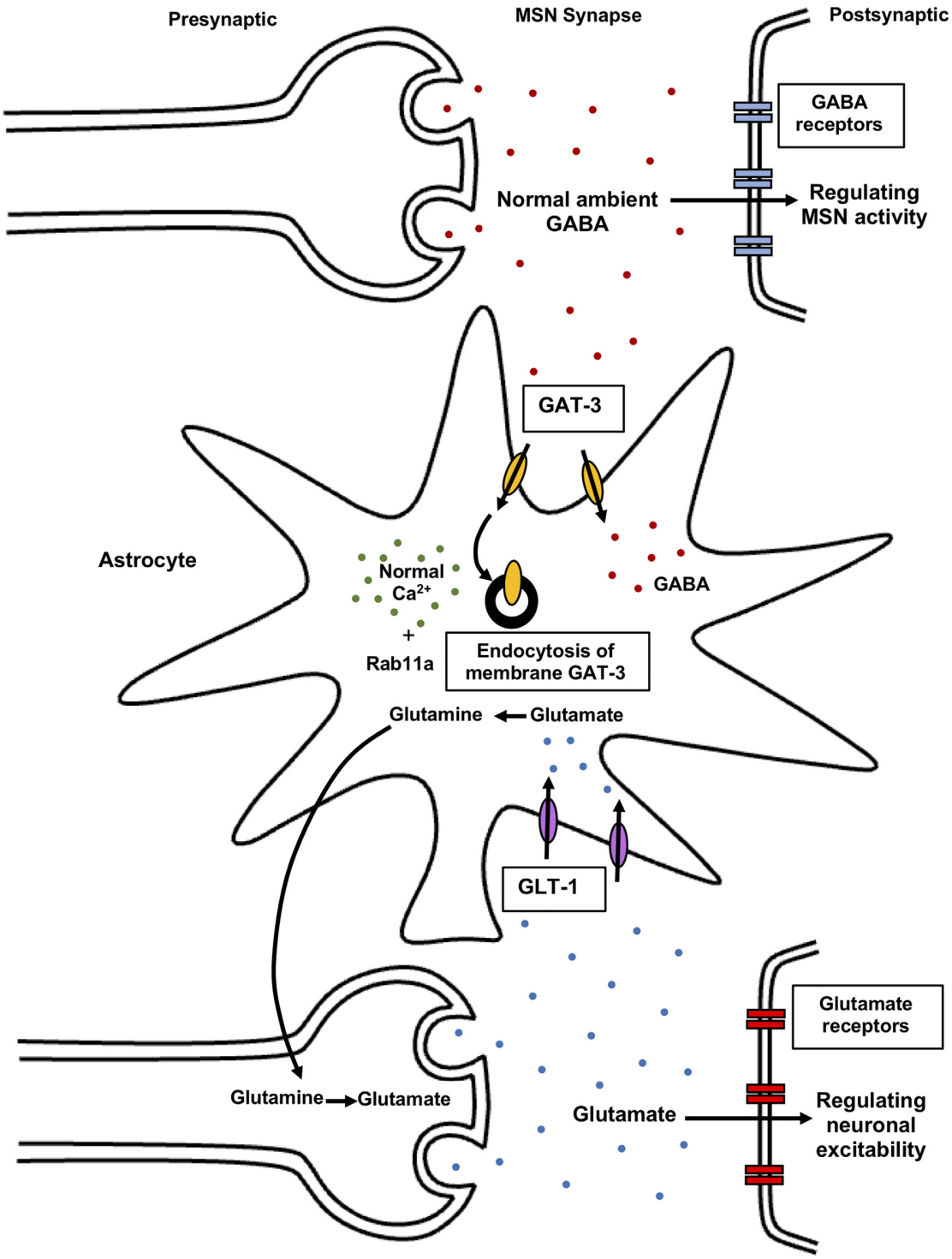

FIGURE 5 | Astrocytic regulation of synaptic glutamate and GABA levels. Normal astrocytic Ca^{2+} signals modulate GAT-3 levels in the presence of Rab11a GTPase mediating GAT-3 endocytosis. As a result, controlled ambient GABA levels in the synapses regulate striatal MSNs activity, resulting in normal behavior. Reduced striatal astrocyte Ca^{2+} signaling contributes to elevated self-grooming behavior *via* altered striatal MSN activity. Astrocytes also regulate synaptic glutamate levels *via* transporters like GLT-1. Elevated glutamate levels in the extracellular space induce over-activation of glutamate receptors resulting in excitotoxicity. Astrocytes protect against this excitotoxicity by clearance of synaptic glutamate *via* glutamate uptake transporters. In astrocytes, glutamate is converted to glutamine which acts as a precursor for re-synthesis of glutamate in neurons, mediating both uptake and release of glutamate. Astrocytes regulate glutamate and GABA in the synapse, thereby modulating neuronal activity and behavior. GABA, gamma-aminobutyric acid; GAT-3, GABA transporter 3; GLT-1, glutamate transporter 1; Rab, small Rab GTPase.

self-grooming in rats. The paraventricular nucleus projects to the posterior dorsal part of the medial amygdala (MeApd) which is involved in self-grooming behavior (Roeling et al., 1993). Lateral hypothalamic glutamatergic neurons adjacent to the MeApd play roles in repetitive self-grooming behaviors in mice (**Figure 3**). Moreover, MeApd also projects to the medial hypothalamus (Hong et al., 2014). Finally, the central nucleus of the amygdala (CeA) and MeA projects to the BNST that connects the amygdala and hypothalamus (Heimer et al., 2007). Hence, the limbic system, incorporating the amygdala, hippocampus, hypothalamus, and basal ganglia regions, play important roles in regulating repetitive behaviors.

NEUROANATOMY OF ASD

Magnetic resonance imaging (MRI) studies in humans have contributed to the understanding of the neuroanatomical basis of ASD, such as a period of early brain overgrowth in autism, particularly in frontal, temporal and cingulate cortices, hippocampus, cerebellum, and amygdala (Palmen and van Engeland, 2004; Bauman and Kemper, 2005; Courchesne et al., 2007; Amaral et al., 2008). Further, atypical functional connectivity between caudate and cortical areas has been observed in autistic subjects (Turner et al., 2006). These findings match neuroanatomical alterations observed in several of the mice models discussed above, which also show alterations to the hippocampal commissure, decreased frontal-cortical, occipital, and thalamic gray matter volume along with reduced cortical thickness (Wahlsten et al., 2003).

Neuroimaging studies also suggest an association of repetitive behaviors, with the volume of basal ganglia areas, such as the caudate-putamen (Sears et al., 1999; Calderoni et al., 2014). Autistic individuals show significantly larger right caudate and putamen volumes compared to matched controls. Moreover, total putamen and right caudate volumes reveal a positive association with ADI-C domain repetitive behavior scores (Hollander et al., 2005). Neuroimaging of individuals with fragile X syndrome (FXS) also exhibit altered gray matter volume in the caudate and white matter of the ventral frontostriatal pathway (Haas et al., 2009; Hallahan et al., 2011). Moreover, imaging studies of RTT individuals show reduced caudate nucleus and midbrain volumes (Casanova et al., 1991; Reiss et al., 1993; Subramaniam et al., 1997).

The medial frontal gyri, right fusiform gyrus, and left hippocampal volumes are also enlarged in autistic groups (Rojas et al., 2006; Verhoeven et al., 2010). The increased regional brain volumes show a positive correlation with stereotypic behaviors; however, the decreased volume of the cerebellum in autistic subjects shows a negative correlation with repetitive behavioral measures (Rojas et al., 2006). One study on autistic children demonstrated a positive association of repetitive behavior and frontal lobe volume and a negative association with cerebellar vermis volume (Pierce and Courchesne, 2001). Also, developmental studies in rodents and non-human primates show that damage to the amygdala, hippocampus, and temporal cortex induces ASD-like behaviors such as stereotypies (Bachevalier and Loveland, 2006). Early in life, amygdala and hippocampal lesions result in self-directed and stereotypic head twisting behaviors in juvenile monkeys (Bauman et al., 2008).

The anterior cingulate cortex (ACC) is also implicated in repetitive behaviors in ASD (Thakkar et al., 2008). An fMRI study in high-functioning autistic individuals revealed a negative correlation of repetitive/restricted behaviors with ACC and posterior parietal activation implicating frontal-striatal circuitry in stereotyped behaviors (Shafritz et al., 2008). Additional consistent neuroimaging findings are required to understand the neural circuitry of stereotypic behaviors in neurodevelopmental disorders.

Imaging studies in preclinical animal models are limited and research in this area is still ongoing (Wilkes and Lewis, 2018). There are a few MRI studies that have utilized diffusion tensor imaging (DTI) and functional MRI (fMRI) in animal models of repetitive behaviors (Ellegood et al., 2010, 2013; Dodero et al., 2013; Squillace et al., 2014; Haberl et al., 2015; Allemang-Grand et al., 2017). Mice with hemizygous (−/Y), heterozygous (−/+) and homozygous (−/−) *Mecp2* mutation show enlarged cerebellar volume, including the vermis, cerebellar cortex region, and smaller cortical volumes including somatosensory, frontal, motor, and cingulate regions. Also, *Mecp2* hemizygous male mice (−/Y) exhibit increased brainstem volume and reduced volumes in the striatum, thalamus, frontal cortex, and corpus callosum. These studies correlate with imaging findings in individuals with Rett syndrome (Dunn et al., 2002; Carter et al., 2008; Ellegood et al., 2015; Allemang-Grand et al., 2017).

MRI imaging in *Fmr1* KO mice reveals decreased cerebellar nuclei and striatal volumes (Ellegood et al., 2010). Also, diffusion tensor MRI and functional MRI (fMRI) studies show changes in structural connectivity of the corpus callosum and functional connectivity between cortical regions such as visual, somatosensory, auditory, and motor regions (Haberl et al., 2015). MRI analysis of 16p11.2 CNV mice demonstrates volumetric alterations in brain regions including basal forebrain, hypothalamus, midbrain, and superior colliculus (Horev et al., 2011). Additionally, $16p11^{+/-}$ pups show reduced brain volume at postnatal day 7, while the relative volume i.e., normalized to total brain volume of nucleus accumbens (NAc) and globus pallidus (GP) regions is increased. Structural abnormalities in cortical areas are also observed in $16p11^{+/-}$ pups (Portmann et al., 2014). Adult heterozygous 16p11.2 mice after controlling for total brain volume show neuroanatomical alterations in different brain regions including increased midbrain, hypothalamus, superior colliculus volumes, and reduced striatal volume (Ellegood et al., 2015). Mice with chromosome 15 mutations, particularly with duplication of the 15q11–13 region show reduced relative volumes for different brain areas like basal forebrain, midbrain, hypothalamus, and thalamus (Ellegood et al., 2015).

Decreases in parvalbumin-containing interneurons in the medial prefrontal cortex are observed in ASD individuals (Hashemi et al., 2017). *Parvalbumin* knockout mice show ASD behavioral phenotypes, such as deficits in social

interaction behaviors, ultrasonic vocalizations, and higher-order reversal learning in the T-maze assay (Wöhr et al., 2015). An MRI study of juvenile *Parvalbumin* knockout mice revealed reduced cortical volume and increased cerebellar volume. However, these anatomical alterations are not consistent in adult *Parvalbumin* knockout mice (Wöhr et al., 2015). Additional studies are required for elucidating other repetitive behaviors and brain region structural alterations in this mouse model. *In utero* VPA exposed rats exhibit decreased total brain volume, relative cortical and brainstem volumes, and hippocampus volume (Frisch et al., 2009; Petrenko et al., 2013).

BTBR mice exhibit reduced cerebral white and gray matter, ventricular volumes, and larger olfactory, brainstem, and cerebellum volumes compared to C67BL/6 mice (Ellegood et al., 2013). An fMRI study of BTBR mice showed decreased bilateral functional connectivity for cingulate, striatum, insular, motor cortex, and reduced striatal-thalamic connectivity. However, hippocampus, temporal and occipital areas show increased interhemispheric connectivity in BTBR mice (Sforazzini et al., 2016).

Molecularly, scaffolding proteins, glutamate receptor-interacting proteins 1/2 (Grip1/2), plays a role in AMPAR trafficking and its absence contributes to cerebellar LTD deficit in cultured Purkinje cells and social preference changes in cell-specific Grip1/2 mutant mice (Takamiya et al., 2008; Mejias et al., 2011). Grip1/2 KO mice exhibit repetitive grooming with no changes in social interaction and anxiety, normal mEPSCs but weakened mGluR-LTD at the parallel fiber-PC synapses and altered expression of arc, mGluR5, phosphorylated P38 and AKT in the Purkinje cells. So, defects in Grip1/2 mediating AMPAR trafficking at cerebellar Purkinje cells along with impaired mGluR5 signaling in cerebellum results in the pathogenesis of repetitive behaviors (Mejias et al., 2019). Mice with conditional *Pten* inactivation in Purkinje cells show stereotyped jumping and decreased motor learning with a structural aberration in PC dendrites, axons, reduced excitability, altered parallel fiber and climbing fiber synapses (Cupolillo et al., 2016). Further, the mouse model of Tuberous Sclerosis with *Tsc2* loss in Purkinje cells (Tsc2f/−; Cre mice) displays increased marble burying repetitive behavior and Purkinje cell dysfunction, suggesting Purkinje cell loss contribution to ASD phenotype (Reith et al., 2013). Therefore, the cerebellum, particularly Purkinje cells and associated signaling pathways play important role in the regulation of repetitive behaviors.

Post-mortem studies of autistic cases have also implicated many of these same brain regions. Purkinje cells (PC) in the cerebellum are consistently altered in neuropathological analyses of ASD brain samples (Fatemi et al., 2002; Palmen and van Engeland, 2004; Whitney et al., 2008). However, the limitation of imaging studies includes poor tissue quality and small sample sizes, as well as an analysis of samples from adult brains which does not provide information regarding development (Amaral et al., 2008).

Overall, neuroanatomical alterations are largely found in frontal, temporal cortical regions, basal ganglia areas, and cerebellum in human studies and mouse models showing repetitive behaviors (Ellegood et al., 2010, 2013, 2015; Portmann et al., 2014; Haberl et al., 2015; Wöhr et al., 2015). Basal ganglia areas such as striatum and globus pallidus show volumetric alterations related to stereotyped behaviors (Ellegood et al., 2010, 2013, 2015; Portmann et al., 2014). Associations between repetitive behavioral phenotypes and changes in specific brain region structural and functional aspects require additional studies in animal models of ASD and other neurodevelopmental disorders.

ANXIETY AND REPETITIVE BEHAVIORS

ASD is associated with anxiety disorders and the prevalence estimates of anxiety in ASD individuals vary widely from 22% to 84% (van Steensel et al., 2011; Lai et al., 2014; Vasa and Mazurek, 2015; Lever and Geurts, 2016; Russell et al., 2016; Nimmo-Smith et al., 2020). There is also a significant relationship between anxiety and restricted/repetitive behaviors in the ASD population (Gotham et al., 2013; Stratis and Lecavalier, 2013; Postorino et al., 2017; Russell et al., 2019; Baribeau et al., 2020). Association of anxiety with ritualistic behaviors is related to abnormal sensory gating suggesting altered sensory processing (Green et al., 2012; Mazurek et al., 2013; Lidstone et al., 2014).

Grooming behavior reflects repetitive, stress-coping behavior and complex interplay with anxiety and motor activity in rodents (Kalueff and Tuohimaa, 2005a; Lewis et al., 2007; O'Leary et al., 2013). Some ASD mouse models demonstrate both anxiety and repetitive behaviors. In a mouse model of Rett syndrome, deletion of MeCP2 in the basolateral amygdala causes increases anxiety and learning deficits (Adachi et al., 2009). The increased grooming behavior in EphrinA2/A3 double KO mice may correlate with sensorimotor gating deficits and abnormal sensory processing as a result of exposure to novel environments (Wurzman et al., 2015). The Shank1 mice model of ASD manifests mild anxiety and repetitive behavior (Hung et al., 2008). ASD mice models with FMR1, PTEN, UBE3A, and GABRB3 mutations exhibit learning deficits, stereotypic behaviors, and anxiety phenotypes (Jiang et al., 2010; Tanaka et al., 2012; Gandhi et al., 2014; Clipperton-Allen and Page, 2015; Zieba et al., 2019). Additionally, the BTBR mouse model of autism displays anxiety traits and repetitive behaviors (McFarlane et al., 2008; Pobbe et al., 2011). In contrast, some mouse models exhibiting repetitive behaviors do not show anxiety-like behaviors or are not reported in some cases. Mouse models including mutations in CNTNAP2, neuroligin1, the oxytocin receptor, and 16p11.2 chromosomal deletions do not display anxiety behaviors or are not reported in some studies (Peñagarikano et al., 2011; Crawley, 2012; Kazdoba et al., 2016). Thus, future studies are required to elucidate the anxiety phenotype along with the repetitive behavior in different rodent models of ASD.

Acute and chronic stress plays a role in alterations of grooming activity (Katz and Roth, 1979; Fentress, 1988; Kalueff and Tuohimaa, 2004b; Komorowska and Pellis, 2004). For instance, C57BL/6J male mice following chronic social defeat stressors, display disorganized cephalo-caudal grooming

patterning and induces anxiety (Veenema et al., 2003; Kinsey et al., 2007; Denmark et al., 2010). Additionally, Wistar rats exposed to the lightbox show increased grooming frequency and duration as compared to rats exposed to the dark box. The light-dark paradigm helps in assessing stress levels in rats *via* counting the number of defecation boli and urination spots, indicating more anxiety in rats exposed to the lightbox. This may suggest that stress and anxiety may affect grooming activity and its microstructure in rodents (Kalueff and Tuohimaa, 2005b, 2004b). Surprisingly, some inbred mouse strains demonstrate high or low grooming in response to anxiety. The BALB/c mice show increased grooming compared to 129S1 mice. The high grooming in BALB/c mice may correlate with increased anxiety as assessed by high defecation boli scores, one of the stress markers in rodents. In contrast, 129S1 mice show low-grooming and high anxiety levels, indicating that different rodent strains exhibit variation in anxiety-induced behaviors (Kalueff and Tuohimaa, 2004a, 2005a). Anxiolytics like bupropion (noradrenaline and dopamine reuptake inhibitor), fluvoxamine (SSRI), diazepam (benzodiazepine), and imipramine (tricyclic antidepressant) decreased marble burying and digging behavior in mice (Hayashi et al., 2010). Further, minocycline ameliorates marble-burying behavior and correlates with proper dendritic spines maturation in Fmr1 KO mice (Dansie et al., 2013). Studies on marble-burying are controversial as some indicate that marble-burying correlates with anxiety whereas others indicate that it reflects repetitive digging (Njung'e and Handley, 1991; Thomas et al., 2009; Taylor et al., 2017; de Brouwer et al., 2019). Minocycline also alleviates aberrant grooming behavior and modulates hippocampal GABA levels in rats (Zhang et al., 2019).

Neuropsychiatric and neurodevelopmental disorders including autism, OCD, schizophrenia, and anxiety share some symptoms and overlap in common pathological genes, circuits, and mechanisms (Shavitt et al., 2006; Kalueff and Nutt, 2007; Kalueff et al., 2008; Szechtman et al., 2017). For instance, GABAergic activity alterations are associated with anxiety, depression, and autistic phenotypes, indicating common underlying neural pathology (Persico and Bourgeron, 2006; Kalueff and Nutt, 2007). Altered GABA receptor activity by anxiolytic (GABA enhancing) and anxiogenic (GABA inhibiting) drugs correlates with a decrease and increase in stress-induced grooming behavior. This may indicate that these drugs regulate the strength of the anxiogenic stimuli perception and grooming behavior (Kalueff and Tuohimaa, 2005c; Nin et al., 2012; Xu et al., 2012; Kalueff et al., 2016). Similarly, BDNF and serotonin transporter (SERT) gene has been linked to cognitive deficits, anxiety, depression, schizophrenia, OCD, and autism (Devlin et al., 2005; Hu et al., 2006; Kaufman et al., 2006; Kalueff et al., 2007; Kas et al., 2007; Moy and Nadler, 2008). Rodents manifest heightened grooming behavior in response to changes in the environment by stressful and/or anxiogenic stimuli (Gispen and Isaacson, 1981; Florijn et al., 1993; Gargiulo and Donoso, 1996). Dopaminergic activity in the basal ganglia pathways likely mediates the stress-coping grooming behavior (Spruijt et al., 1986, 1992; Cools et al., 1988; Kametani, 1988; Reis-Silva et al., 2019). Anxiety-like behaviors correlate with decreased dopamine release in PFC, substantia nigra, and amygdala of rats spending more time self-grooming induced by stress on exposure to the elevated plus-maze (EPM). This suggests that self-grooming is associated with reward systems and may be reflective of de-arousal activity instead of a direct response to anxiety (Homberg et al., 2002). Additionally, serotonin plays a role in regulating stress-coping behavior such as self-grooming (Houwing et al., 2019). Hence, rodent grooming may represent one method for stress reduction or de-arousal, instead of directly involved in the stress response (Estanislau et al., 2013, 2019).

Also, several common brain regions have been associated with anxiety and repetitive behavioral disorders, particularly the amygdala and PFC. For instance, muscimol (GABA agonist) infusion into the basolateral nucleus of the amygdala and PFC decreases anxiety in rats (Shah et al., 2004; Bueno et al., 2005). Intriguingly, muscimol injection into BNST (extended amygdala), a region that regulates innate fear responses leads to decreased self-grooming behavior in rats (Xu et al., 2012). Additionally, GABAergic neurons in the MeApD region reduce self-grooming behavior (Hong et al., 2014). Further, injections of GABA-A receptor antagonist bicuculline into the basolateral amygdala increases anxiety in rats (Sajdyk and Shekhar, 2000). In the MeApD region, glutamatergic neurons promote stereotypic self-grooming (Hong et al., 2014). Alterations in GABA, serotonin, kainate, and glutamate receptor densities in various amygdala nuclei correlate with anxiety-like behavior in some inbred mouse strains (Yilmazer-Hanke et al., 2003; Caldji et al., 2004). Amygdala stimulation leads to increases in anxiety and facilitates compulsive behaviors (McGrath et al., 1999). In the case of OCD, basolateral amygdala projections to medial PFC modulate repetitive checking behavior in rodents (Sun et al., 2019). One of the brain regions involved in stress coping responses, the periaqueductal gray (PAG) and its pathways, influences self-grooming behavior (Bandler et al., 2000). Alteration in striatal neurons, CeA and mPFC projections to the PAG region may affect self-grooming behavior (Spruijt et al., 1992; Floyd et al., 2000). Increased expression of c-fos is observed in the hippocampus, hypothalamus, PFC after administration of anxiogenic drugs, and hypothalamic injection of GABAergic anxiolytic drugs reduces anxiety in rats (Jardim and Guimarães, 2001; Singewald et al., 2003). Hence, regulated GABAergic activity and consequent excitatory neurotransmission in these brain regions are critical for the modulation of anxiety and repetitive behaviors, indicating overlapping circuits in anxiety and repetitive behaviors.

However, further studies are required to ascertain regional and circuit differences between anxiety-induced and repetitive self-grooming behavior. Investigations of animal models displaying both anxiety and repetitive behavior simultaneously or induction of one disorder by another will help in providing innovative insight into the common and specific neural alterations underlying these disorders.

SUMMARY

Animal models of neuropsychiatric and neurodevelopmental disorders such as autism have provided relevant knowledge

on the neuronal circuitry and receptor targets implicated in the etiology and pathophysiology of repetitive behaviors. Several brain regions and neural circuits including cortico-basal ganglia-thalamic circuits, limbic circuits, prefrontal cortex, cerebellum, hypothalamus, and striatum are involved in the regulation of core autistic behaviors. Genetic mutations and environmental risk factors resulting in the presentation of repetitive behaviors in rodent models involve multiple cellular, molecular, and network factors. The majority of ASD alterations involve excitatory glutamatergic, inhibitory GABAergic, serotonergic and dopaminergic neurons, receptors, neurotransmitters, neuronal migration, and spine densities resulting in changes in signaling pathways and synaptic activity which may converge on common neural circuits (Golden et al., 2018).

Genome-wide association studies (GWAS) have indicated various ASD risk genes including neuronal cell adhesion molecules (neurexins, neuroligins, CNTNAP), postsynaptic scaffolding proteins (Shanks, SAPAP), neurotransmitter signaling and trafficking (Glutamate, GABA, EphA3), and molecules involved in protein synthesis in the brain (Fmr1, TSC, MeCP2) (Stearns et al., 2007; Tabuchi et al., 2007; Hung et al., 2008; Samaco et al., 2008; Etherton et al., 2009; Radyushkin et al., 2009; Peñagarikano et al., 2011; Peça et al., 2011; Silverman et al., 2011; Casey et al., 2012; Eadie et al., 2012; Schmeisser et al., 2012; Grayton et al., 2013; Monteiro and Feng, 2017; Wang et al., 2017; Zerbi et al., 2018). Many of the autism risk genes encode for proteins involved in excitatory glutamatergic signaling, converging at excitatory synapses (Peça et al., 2011; Qiu et al., 2012). For instance, Shank3 forms a scaffolding complex comprised of SAPAP that also interconnects with ephrins/Ephs and neurexin/neuroligin complexes (Qiu et al., 2012). This suggests that alterations in these molecules may converge on common synaptic and circuit mechanisms underlying autistic behavioral phenotypes. Understanding the mechanisms by which these factors affect neuronal circuits will provide insight into relevant targets of sensorimotor repetitive behaviors.

Although ASD etiological heterogeneity leads to complex and sometimes divergent behavioral outcomes in affected populations, a large literature exists, including neuroimaging studies, that have determined the crucial role of cortico-basal ganglia and limbic circuit alterations in mediating stereotypic behaviors. Altogether, common neural modifications in specific pathways and neural circuits lead to the emergence of repetitive behaviors in ASD. Inconsistencies in some studies and factors influencing generality of the repetitive behavioral findings may be related to sample, environment, and experimental heterogeneity. Future research integrating disparate findings hold immense potential to ascertain the involvement of common neural changes converging at the level of circuit alterations in neurodevelopmental disorders. More detailed work with additional animal models is required to dissect the molecular and neuroanatomical alterations in other pathways and brain regions implicated in repetitive behavioral phenotypes, to identify potential targets and treatment strategies for attenuating repetitive behaviors in affected individuals. Finally, early interventions for repetitive behaviors hold great promise for improving the quality of life for affected individuals.

FUTURE DIRECTIONS AND LIMITATIONS

The scope of this review is narrowed to neural mechanisms underlying lower-order repetitive behaviors in rodent models of ASD. Most of the literature in rodent models of ASD discusses lower-order stereotyped sensory-motor behaviors. However, some studies address higher-order insistence on sameness behaviors, such as circumscribed interests and resistance to change in a few rodent models. Future studies are required to evaluate common underlying molecular and circuit alterations in repetitive and restricted behaviors in autism. Further, characterization of both repetitive motor behaviors and insistence on sameness behaviors should be performed in different rodent models of ASD and other neurodevelopmental disorders to increase their translational value and to identify overlapping neurobiological alterations underlying these behaviors.

Although the studies reviewed here contribute to our understanding of the underlying neural alterations in rodent models displaying robust repetitive behaviors, the relation of such alterations with repetitive behavioral expression is unresolved. A focus of most investigations has been on the pathophysiology of mutations resulting in the expression of general ASD phenotype and rescuing the core ASD behavioral deficits rather than focusing exclusively on repetitive behaviors. Future findings targeting specific brain regions and focusing on neural alterations elemental to repetitive behaviors solely, while controlling for other behaviors, will provide a better understanding of how individual genetic and environmental changes converge at molecular and circuit levels to mediate repetitive behaviors. Alternatively, the generation of mutant rodent models with a targeted knockout of susceptibility genes in circumscribed brain regions may help in clarifying particular behavioral phenotypes. For instance, in NL3 mice, inhibition is elevated in the somatosensory cortex, whereas AMPAR mediated excitation is heightened in the CA1 hippocampal region (Etherton et al., 2011). Consequently, the specific neural circuitry associated with particular cognitive and behavioral components in ASD remains to be fully dissected. Regardless of these challenges, common circuits and molecular alterations provide a basis for understanding ASD etiological factors and behavioral abnormalities.

Also, very few studies have incorporated different methodological approaches to elucidate changes fundamental in mediating repetitive behaviors in rodents (Squillace et al., 2014; Wöhr et al., 2015; Sforazzini et al., 2016). A combination of different methodological approaches such as neuroimaging, histological and molecular analysis may provide a more comprehensive understanding of alterations in specific brain regions and their neural projections primarily mediating repetitive behaviors in rodent models of ASD. Also, future studies incorporating both male and female rodent models may help in elucidating any gender differences

in brain structure and function associated with repetitive behaviors. Another important requirement is to evaluate molecular and circuit modifications fundamental to repetitive behaviors in other neurodevelopmental and neuropsychiatric disorders. Corroboration of findings across varied rodent models displaying repetitive behaviors may illuminate similar and dissimilar changes in brain pathways underlying these disorders.

A somewhat underexplored therapeutic avenue in rodent models is environmental enrichment (EE), which attenuates the repetitive behaviors in models of ASD. The EE reduces repetitive behaviors in deer mice by elevating indirect basal ganglia pathway function *via* increasing neuronal activation and dendritic spine densities in the subthalamic nucleus (STN) and globus pallidus (GP) (Bechard et al., 2016). However, mechanisms by which environmental enrichment alters repetitive behavior and correlations with structural, functional, and molecular modifications in brain regions demand a detailed investigation. Also, investigations of the effectiveness of environmental enrichment in attenuating repetitive behaviors should be extended to different rodent models of repetitive behavioral and neurodevelopmental disorders. This may help in probing the efficacy of environmental enrichment concerning repetitive behaviors.

Pharmacologically, systemic and local applications of glutamatergic inhibitors, GABAergic, serotonergic and dopaminergic agents have varied effects in different brain regions and circuits mediating repetitive behaviors. However, it remains to be determined whether these agents are applicable for alleviating behaviors beyond lower-order motor stereotypies in rodent models. Further research is required to ascertain if these various receptor agents also play a role in higher-order stereotypies in rodent models. Also, investigating the cross-over effects of these agents in different neural pathways may help to understand the underlying cellular and molecular pathologies concerning repetitive behaviors.

Also, future research studying overlapping or common pathways underlying stress, anxiety, and repetitive behaviors may provide some critical insight into targets directed towards these behavioral domains.

This review summarizes findings on molecular, signaling pathways, circuit, and neuroanatomical alterations in rodent models of ASD displaying robust repetitive behaviors. These findings emphasize important molecular, structural, and functional connectivity changes in brain regions like the prefrontal cortex, basal ganglia structures, limbic areas, and cerebellum, suggesting a major role of cortical-basal ganglia circuits. Besides, signaling pathways involving different neurotransmitters and their receptors such as glutamate, GABA, serotonin, and dopamine are also involved in the pathophysiology of stereotypic motor behaviors. Understanding the hierarchy of changes in different brain regions molecular, structure, function, and connectivity aspects mediating repetitive behaviors in rodent models will provide an important platform for translational study.

Last, comparative research involving human clinical population and animal models of ASD and other neurodevelopmental disorders holds enormous potential for unraveling the underlying neural alterations mediating repetitive behaviors and identifying directed pharmacological and circuit-based targets for treatment interventions.

AUTHOR CONTRIBUTIONS

TG and CL wrote the review article. All authors contributed to the article and approved the submitted version.

REFERENCES

Adachi, M., Autry, A. E., Covington, H. E. III., and Monteggia, L. M. (2009). MeCP2-mediated transcription repression in the basolateral amygdala may underlie heightened anxiety in a mouse model of Rett syndrome. *J. Neurosci.* 29, 4218–4227. doi: 10.1523/JNEUROSCI.4225-08.2009

Ade, K. K., Wan, Y., Hamann, H. C., O'Hare, J. K., Guo, W., Quian, A., et al. (2016). Increased metabotropic glutamate receptor 5 signaling underlies obsessive-compulsive disorder-like behavioral and striatal circuit abnormalities in mice. *Biol. Psychiatry* 80, 522–533. doi: 10.1016/j.biopsych.2016.04.023

Ahmari, S. E., and Dougherty, D. D. (2015). Dissecting OCD circuits: from animal models to targeted treatments. *Depress. Anxiety* 32, 550–562. doi: 10.1002/da.22367

Aida, T., Yoshida, J., Nomura, M., Tanimura, A., Iino, Y., Soma, M., et al. (2015). Astroglial glutamate transporter deficiency increases synaptic excitability and leads to pathological repetitive behaviors in mice. *Neuropsychopharmacology* 40, 1569–1579. doi: 10.1038/npp.2015.26

Akaneya, Y., Sohya, K., Kitamura, A., Kimura, F., Washburn, C., Zhou, R., et al. (2010). Ephrin-A5 and EphA5 interaction induces synaptogenesis during early hippocampal development. *PLoS One* 5:e12486. doi: 10.1371/journal.pone.0012486

Ali, I. U., Schriml, L. M., and Dean, M. (1999). Mutational spectra of PTEN/MMAC1 gene: a tumor suppressor with lipid phosphatase activity. *J. Natl. Cancer Inst.* 91, 1922–1932. doi: 10.1093/jnci/91.22.1922

Allemang-Grand, R., Ellegood, J., Noakes, L. S., Ruston, J., Justice, M., Nieman, B. J., et al. (2017). Neuroanatomy in mouse models of Rett syndrome is related to the severity of Mecp2 mutation and behavioral phenotypes. *Mol. Autism* 8:32. doi: 10.1186/s13229-017-0138-8

Alò, R., Avolio, E., Mele, M., Di Vito, A., and Canonaco, M. (2015). Central amygdalar nucleus treated with orexin neuropeptides evoke differing feeding and grooming responses in the hamster. *J. Neurol. Sci.* 351, 46–51. doi: 10.1016/j.jns.2015.02.030

Alpatov, R., Lesch, B. J., Nakamoto-Kinoshita, M., Blanco, A., Chen, S., Stützer, A., et al. (2014). A chromatin-dependent role of the fragile X mental retardation protein FMRP in the DNA damage response. *Cell* 157, 869–881. doi: 10.1016/j.cell.2014.03.040

Aman, M. G., McDougle, C. J., Scahill, L., Handen, B., Arnold, L. E., Johnson, C., et al. (2009). Medication and parent training in children with pervasive developmental disorders and serious behavior problems: results from a randomized clinical trial. *J. Am. Acad. Child Adolesc. Psychiatry* 48, 1143–1154. doi: 10.1097/CHI.0b013e3181bfd669

Amaral, D. G., Schumann, C. M., and Nordahl, C. W. (2008). Neuroanatomy of autism. *Trends Neurosci.* 31, 137–145. doi: 10.1016/j.tins.2007.12.005

Amodeo, D. A., Jones, J. H., Sweeney, J. A., and Ragozzino, M. E. (2012). Differences in BTBR T+ tf/J and C57BL/6J mice on probabilistic reversal learning and stereotyped behaviors. *Behav. Brain Res.* 227, 64–72. doi: 10.1016/j.bbr.2011.10.032

Amodeo, D. A., Jones, J. H., Sweeney, J. A., and Ragozzino, M. E. (2014). Risperidone and the $5HT_{2A}$ receptor antagonist M100907 improve

probabilistic reversal learning in BTBR T+ tf/J mice. *Autism Res.* 7, 555–567. doi: 10.1002/aur.1395

Amodeo, D. A., Rivera, E., Cook, E. Jr., Sweeney, J. A., and Ragozzino, M. E. (2017). $5HT_{2A}$ receptor blockade in dorsomedial striatum reduces repetitive behaviors in BTBR mice. *Genes Brain Behav.* 16, 342–351. doi: 10.1111/gbb.12343

Amodeo, D. A., Rivera, E., Dunn, J. T., and Ragozzino, M. E. (2016). M100907 attenuates elevated grooming behavior in the BTBR mouse. *Behav. Brain Res.* 313, 67–70. doi: 10.1016/j.bbr.2016.06.064

Anderson, G. R., Galfin, T., Xu, W., Aoto, J., Malenka, R. C., and Südhof, T. C. (2012). Candidate autism gene screen identifies critical role for cell-adhesion molecule CASPR2 in dendritic arborization and spine development. *Proc. Natl. Acad. Sci. U S A* 109, 18120–18125. doi: 10.1073/pnas.1216398109

Aoto, J., and Chen, L. (2007). Bidirectional ephrin/Eph signaling in synaptic functions. *Brain Res.* 1184, 72–80. doi: 10.1016/j.brainres.2006.11.033

Araki, T., and Milbrandt, J. (1996). Ninjurin, a novel adhesion molecule, is induced by nerve injury and promotes axonal growth. *Neuron* 17, 353–361. doi: 10.1016/s0896-6273(00)80166-x

Arnall, S., Cheam, L., Smart, C., Rengel, A., Fitzgerald, M., Thivierge, J., et al. (2010). Abnormal strategies during visual discrimination reversal learning in ephrin-$A2^{-/-}$ mice. *Behav. Brain Res.* 209, 109–113. doi: 10.1016/j.bbr.2010.01.023

Asrar, S., Meng, Y., Zhou, Z., Todorovski, Z., Huang, W. W., and Jia, Z. (2009). Regulation of hippocampal long-term potentiation by p21-activated protein kinase 1 (PAK1). *Neuropharmacology* 56, 73–80. doi: 10.1016/j.neuropharm.2008.06.055

Astrinidis, A., and Henske, E. P. (2005). Tuberous sclerosis complex: linking growth and energy signaling pathways with human disease. *Oncogene* 24, 7475–7481. doi: 10.1038/sj.onc.1209090

Audet, M.-C., Goulet, S., and Doré, F. Y. (2006). Repeated subchronic exposure to phencyclidine elicits excessive atypical grooming in rats. *Behav. Brain Res.* 167, 103–110. doi: 10.1016/j.bbr.2005.08.026

Auerbach, B. D., Osterweil, E. K., and Bear, M. F. (2011). Mutations causing syndromic autism define an axis of synaptic pathophysiology. *Nature* 480, 63–68. doi: 10.1038/nature10658

Bachevalier, J., and Loveland, K. A. (2006). The orbitofrontal-amygdala circuit and self-regulation of social-emotional behavior in autism. *Neurosci. Biobehav. Rev.* 30, 97–117. doi: 10.1016/j.neubiorev.2005.07.002

Baig, D. N., Yanagawa, T., and Tabuchi, K. (2017). Distortion of the normal function of synaptic cell adhesion molecules by genetic variants as a risk for autism spectrum disorders. *Brain Res. Bull.* 129, 82–90. doi: 10.1016/j.brainresbull.2016.10.006

Bandler, R., Keay, K. A., Floyd, N., and Price, J. (2000). Central circuits mediating patterned autonomic activity during active vs. passive emotional coping. *Brain Res. Bull.* 53, 95–104. doi: 10.1016/s0361-9230(00)00313-0

Baranek, G. T. (1999). Autism during infancy: a retrospective video analysis of sensory-motor and social behaviors at 9–12 months of age. *J. Autism Dev. Disord.* 29, 213–224. doi: 10.1023/a:1023080005650

Baribeau, D. A., Vigod, S., Pullenayegum, E., Kerns, C. M., Mirenda, P., Smith, I. M., et al. (2020). Repetitive behavior severity as an early indicator of risk for elevated anxiety symptoms in autism spectrum disorder. *J. Am. Acad. Child Adolesc. Psychiatry* 59, 890.e3–899.e3. doi: 10.1016/j.jaac.2019.08.478

Baroncelli, L., Braschi, C., Spolidoro, M., Begenisic, T., Sale, A., and Maffei, L. (2010). Nurturing brain plasticity: impact of environmental enrichment. *Cell Death Differ.* 17, 1092–1103. doi: 10.1038/cdd.2009.193

Bassani, S., Cwetsch, A. W., Gerosa, L., Serratto, G. M., Folci, A., Hall, I. F., et al. (2018). The female epilepsy protein PCDH19 is a new $GABA_AR$-binding partner that regulates GABAergic transmission as well as migration and morphological maturation of hippocampal neurons. *Hum. Mol. Genet.* 27, 1027–1038. doi: 10.1093/hmg/ddy019

Bast, T., Zhang, W.-N., and Feldon, J. (2001). The ventral hippocampus and fear conditioning in rats. *Exp. Brain Res.* 139, 39–52. doi: 10.1007/s002210100746

Bateup, H. S., Johnson, C. A., Denefrio, C. L., Saulnier, J. L., Kornacker, K., and Sabatini, B. L. (2013). Excitatory/inhibitory synaptic imbalance leads to hippocampal hyperexcitability in mouse models of tuberous sclerosis. *Neuron* 78, 510–522. doi: 10.1016/j.neuron.2013.03.017

Bauman, M. L., and Kemper, T. L. (2005). Neuroanatomic observations of the brain in autism: a review and future directions. *Int. J. Dev. Neurosci.* 23, 183–187. doi: 10.1016/j.ijdevneu.2004.09.006

Bauman, M. D., Toscano, J., Babineau, B., Mason, W., and Amaral, D. G. (2008). Emergence of stereotypies in juvenile monkeys (*Macaca mulatta*) with neonatal amygdala or hippocampus lesions. *Behav. Neurosci.* 122:1005. doi: 10.1177/2398212820972599

Bazargani, N., and Attwell, D. (2016). Astrocyte calcium signaling: the third wave. *Nat. Neurosci.* 19, 182–189. doi: 10.1038/nn.4201

Bear, M. F. (2005). Therapeutic implications of the mGluR theory of fragile X mental retardation. *Genes Brain Behav.* 4, 393–398. doi: 10.1111/j.1601-183X.2005.00135.x

Bear, M. F., Huber, K. M., and Warren, S. T. (2004). The mGluR theory of fragile X mental retardation. *Trends Neurosci.* 27, 370–377. doi: 10.1016/j.tins.2004.04.009

Bechard, A. R., Bliznyuk, N., and Lewis, M. H. (2017). The development of repetitive motor behaviors in deer mice: effects of environmental enrichment, repeated testing and differential mediation by indirect basal ganglia pathway activation. *Dev. Psychobiol.* 59, 390–399. doi: 10.1002/dev.21503

Bechard, A. R., Cacodcar, N., King, M. A., and Lewis, M. H. (2016). How does environmental enrichment reduce repetitive motor behaviors? Neuronal activation and dendritic morphology in the indirect basal ganglia pathway of a mouse model. *Behav. Brain Res.* 299, 122–131. doi: 10.1016/j.bbr.2015.11.029

Bechard, A., and Lewis, M. (2012). Modeling restricted repetitive behavior in animals. *Autism* 6:2. doi: 10.4172/2165-7890.s1-006

Beckel-Mitchener, A., and Greenough, W. T. (2004). Correlates across the structural, functional, and molecular phenotypes of fragile X syndrome. *Ment. Retard. Dev. Disabil. Res. Rev.* 10, 53–59. doi: 10.1002/mrdd.20009

Benes, F. M. (2010). Amygdalocortical circuitry in schizophrenia: from circuits to molecules. *Neuropsychopharmacology* 35, 239–257. doi: 10.1038/npp.2009.116

Ben-Sasson, A., Cermak, S. A., Orsmond, G. I., Tager-Flusberg, H., Carter, A. S., Kadlec, M. B., et al. (2007). Extreme sensory modulation behaviors in toddlers with autism spectrum disorders. *Am. J. Occup. Ther.* 61, 584–592. doi: 10.5014/ajot.61.5.584

Berridge, K. C., and Aldridge, J. W. (2000a). Super-stereotypy I: enhancement of a complex movement sequence by systemic dopamine D1 agonists. *Synapse* 37, 194–204. doi: 10.1002/1098-2396(20000901)37:3<194::AID-SYN3>3.0.CO;2-A

Berridge, K. C., and Aldridge, J. W. (2000b). Super-stereotypy II: enhancement of a complex movement sequence by intraventricular dopamine D1 agonists. *Synapse* 37, 205–215. doi: 10.1002/1098-2396(20000901)37:3<205::AID-SYN4>3.0.CO;2-A

Berridge, K. C., Aldridge, J. W., Houchard, K. R., and Zhuang, X. (2005). Sequential super-stereotypy of an instinctive fixed action pattern in hyper-dopaminergic mutant mice: a model of obsessive compulsive disorder and Tourette's. *BMC Biol.* 3:4. doi: 10.1186/1741-7007-3-4

Berry-Kravis, E. (2014). Mechanism-based treatments in neurodevelopmental disorders: fragile X syndrome. *Pediatr. Neurol.* 50, 297–302. doi: 10.1016/j.pediatrneurol.2013.12.001

Bhalla, K., Luo, Y., Buchan, T., Beachem, M. A., Guzauskas, G. F., Ladd, S., et al. (2008). Alterations in CDH15 and KIRREL3 in patients with mild to severe intellectual disability. *Am. J. Hum. Genet.* 83, 703–713. doi: 10.1016/j.ajhg.2008.10.020

Bhattacharya, A., Mamcarz, M., Mullins, C., Choudhury, A., Boyle, R. G., Smith, D. G., et al. (2016). Targeting translation control with p70 S6 kinase 1 inhibitors to reverse phenotypes in fragile X syndrome mice. *Neuropsychopharmacology* 41, 1991–2000. doi: 10.1038/npp.2015.369

Bienvenu, O. J., Wang, Y., Shugart, Y., Welch, J., Grados, M., Fyer, A., et al. (2009). Sapap3 and pathological grooming in humans: results from the OCD collaborative genetics study. *Am. J. Med. Genet. B Neuropsychiatr. Genet.* 150, 710–720. doi: 10.1002/ajmg.b.30897

Bilousova, T., Dansie, L., Ngo, M., Aye, J., Charles, J. R., Ethell, D. W., et al. (2009). Minocycline promotes dendritic spine maturation and improves behavioural performance in the fragile X mouse model. *J. Med. Genet.* 46, 94–102. doi: 10.1136/jmg.2008.061796

Blundell, J., Blaiss, C. A., Etherton, M. R., Espinosa, F., Tabuchi, K., Walz, C., et al. (2010). Neuroligin-1 deletion results in impaired spatial memory and increased

repetitive behavior. *J. Neurosci.* 30, 2115–2129. doi: 10.1523/JNEUROSCI.4517-09.2010

Boda, B., Nikonenko, I., Alberi, S., and Muller, D. (2006). Central nervous system functions of PAK protein family. *Mol. Neurobiol.* 34, 67–80. doi: 10.1385/mn:34:1:67

Bokoch, G. M. (2003). Biology of the p21-activated kinases. *Annu. Rev. Biochem.* 72, 743–781. doi: 10.1146/annurev.biochem.72.121801.161742

Bolz, J., Uziel, D., Mühlfriedel, S., Güllmar, A., Peuckert, C., Zarbalis, K., et al. (2004). Multiple roles of ephrins during the formation of thalamocortical projections: maps and more. *J. Neurobiol.* 59, 82–94. doi: 10.1002/neu.10346

Boyd, B. A., McDonough, S. G., and Bodfish, J. W. (2012). Evidence-based behavioral interventions for repetitive behaviors in autism. *J. Autism Dev. Disord.* 42, 1236–1248. doi: 10.1007/s10803-011-1284-z

Bozdagi, O., Sakurai, T., Papapetrou, D., Wang, X., Dickstein, D. L., Takahashi, N., et al. (2010). Haploinsufficiency of the autism-associated Shank3 gene leads to deficits in synaptic function, social interaction, and social communication. *Mol. Autism* 1:15. doi: 10.1186/2040-2392-1-15

Bromley, R., Mawer, G., Clayton-Smith, J., and Baker, G. (2008). Autism spectrum disorders following *in utero* exposure to antiepileptic drugs. *Neurology* 71, 1923–1924. doi: 10.1212/01.wnl.0000339399.64213.1a

Brown, M. R., Kronengold, J., Gazula, V.-R., Chen, Y., Strumbos, J. G., Sigworth, F. J., et al. (2010). Fragile X mental retardation protein controls gating of the sodium-activated potassium channel Slack. *Nat. Neurosci.* 13, 819–821. doi: 10.1038/nn.2563

Brown, D. A., and Passmore, G. M. (2009). Neural KCNQ (kv7) channels. *Br. J. Pharmacol.* 156, 1185–1195. doi: 10.1111/j.1476-5381.2009.00111.x

Brune, C. W., Kim, S.-J., Salt, J., Leventhal, B. L., Lord, C., Cook, M. Jr., et al. (2006). 5-HTTLPR genotype-specific phenotype in children and adolescents with autism. *Am. J. Psychiatry* 163, 2148–2156. doi: 10.1176/ajp.2006.163.12.2148

Bueno, C. H., Zangrossi, H. Jr., and Viana, M. B. (2005). The inactivation of the basolateral nucleus of the rat amygdala has an anxiolytic effect in the elevated T-maze and light/dark transition tests. *Braz. J. Med. Biol. Res.* 38, 1697–1701. doi: 10.1590/s0100-879x2005001100019

Burguière, E., Monteiro, P., Feng, G., and Graybiel, A. M. (2013). Optogenetic stimulation of lateral orbitofronto-striatal pathway suppresses compulsive behaviors. *Science* 340, 1243–1246. doi: 10.1126/science.1232380

Burket, J. A., Benson, A. D., Tang, A. H., and Deutsch, S. I. (2013). D-Cycloserine improves sociability in the BTBR T+ Itpr3tf/J mouse model of autism spectrum disorders with altered Ras/Raf/ERK1/2 signaling. *Brain Res. Bull.* 96, 62–70. doi: 10.1016/j.brainresbull.2013.05.003

Burket, J. A., Cannon, W. R., Jacome, L. F., and Deutsch, S. I. (2010). MK-801, a noncompetitive NMDA receptor antagonist, elicits circling behavior in the genetically inbred Balb/c mouse strain. *Brain Res. Bull.* 83, 337–339. doi: 10.1016/j.brainresbull.2010.08.014

Burrows, E. L., Laskaris, L., Koyama, L., Churilov, L., Bornstein, J. C., Hill-Yardin, E. L., et al. (2015). A neuroligin-3 mutation implicated in autism causes abnormal aggression and increases repetitive behavior in mice. *Mol. Autism* 6:62. doi: 10.1186/s13229-015-0055-7

Busquets-Garcia, A., Gomis-González, M., Guegan, T., Agustín-Pavón, C., Pastor, A., Mato, S., et al. (2013). Targeting the endocannabinoid system in the treatment of fragile X syndrome. *Nat. Med.* 19, 603–607. doi: 10.1038/nm.3127

Butler, M. G., Dasouki, M. J., Zhou, X.-P., Talebizadeh, Z., Brown, M., Takahashi, T. N., et al. (2005). Subset of individuals with autism spectrum disorders and extreme macrocephaly associated with germline PTEN tumour suppressor gene mutations. *J. Med. Genet.* 42, 318–321. doi: 10.1136/jmg.2004.024646

Calderoni, S., Bellani, M., Hardan, A., Muratori, F., and Brambilla, P. (2014). Basal ganglia and restricted and repetitive behaviours in autism spectrum disorders: current status and future perspectives. *Epidemiol. Psychiatr. Sci.* 23, 235–238. doi: 10.1017/S2045796014000171

Caldji, C., Diorio, J., Anisman, H., and Meaney, M. J. (2004). Maternal behavior regulates benzodiazepine/$GABA_A$ receptor subunit expression in brain regions associated with fear in BALB/c and C57BL/6 mice. *Neuropsychopharmacology* 29, 1344–1352. doi: 10.1038/sj.npp.1300436

Cantley, L. C. (2002). The phosphoinositide 3-kinase pathway. *Science* 296, 1655–1657. doi: 10.1126/science.296.5573.1655

Cao, F., Liu, J. J., Zhou, S., Cortez, M. A., Snead, O. C., Han, J., et al. (2020). Neuroligin 2 regulates absence seizures and behavioral arrests through GABAergic transmission within the thalamocortical circuitry. *Nat. Commun.* 11, 1–15. doi: 10.1038/s41467-020-17560-3

Carlson, G. C. (2012). Glutamate receptor dysfunction and drug targets across models of autism spectrum disorders. *Pharmacol. Biochem. Behav.* 100, 850–854. doi: 10.1016/j.pbb.2011.02.003

Carmona, M. A., Murai, K. K., Wang, L., Roberts, A. J., and Pasquale, E. B. (2009). Glial ephrin-A3 regulates hippocampal dendritic spine morphology and glutamate transport. *Proc. Natl. Acad. Sci. U S A* 106, 12524–12529. doi: 10.1073/pnas.0903328106

Carneiro, A. M. D., Cook, E. H., Murphy, D. L., and Blakely, R. D. (2008). Interactions between integrin αIIbβ3 and the serotonin transporter regulate serotonin transport and platelet aggregation in mice and humans. *J. Clin. Invest.* 118, 1544–1552. doi: 10.1172/JCI33374

Carter, J., Lanham, D., Pham, D., Bibat, G., Naidu, S., and Kaufmann, W. E. (2008). Selective cerebral volume reduction in Rett syndrome: a multiple-approach MR imaging study. *Am. J. Neuroradiol.* 29, 436–441. doi: 10.3174/ajnr.A0857

Carter, M. D., Shah, C. R., Muller, C. L., Crawley, J. N., Carneiro, A. M., and Veenstra-VanderWeele, J. (2011). Absence of preference for social novelty and increased grooming in integrin β3 knockout mice: initial studies and future directions. *Autism Res.* 4, 57–67. doi: 10.1002/aur.180

Casanova, M., Naidu, S., Goldberg, T., Moser, H., Khoromi, S., Kumar, A., et al. (1991). Quantitative magnetic resonance imaging in Rett syndrome. *J. Neuropsychiatry Clin. Neurosci.* 3, 66–72. doi: 10.1176/jnp.3.1.66

Casey, J. P., Magalhaes, T., Conroy, J. M., Regan, R., Shah, N., Anney, R., et al. (2012). A novel approach of homozygous haplotype sharing identifies candidate genes in autism spectrum disorder. *Hum. Genet.* 131, 565–579. doi: 10.1007/s00439-011-1094-6

Causeret, F., Terao, M., Jacobs, T., Nishimura, Y. V., Yanagawa, Y., Obata, K., et al. (2009). The p21-activated kinase is required for neuronal migration in the cerebral cortex. *Cereb. Cortex* 19, 861–875. doi: 10.1093/cercor/bhn133

Chahin, S. S., Apple, R. W., Kuo, K. H., and Dickson, C. A. (2020). Autism spectrum disorder: psychological and functional assessment and behavioral treatment approaches. *Transl. Pediatr.* 9:S66. doi: 10.21037/tp.2019.11.06

Chahrour, M., and Zoghbi, H. Y. (2007). The story of Rett syndrome: from clinic to neurobiology. *Neuron* 56, 422–437. doi: 10.1016/j.neuron.2007.10.001

Chang, A. D., Berges, V. A., Chung, S. J., Fridman, G. Y., Baraban, J. M., and Reti, I. M. (2016). High-frequency stimulation at the subthalamic nucleus suppresses excessive self-grooming in autism-like mouse models. *Neuropsychopharmacology* 41, 1813–1821. doi: 10.1038/npp.2015.350

Chao, H.-T., Chen, H., Samaco, R. C., Xue, M., Chahrour, M., Yoo, J., et al. (2010). Dysfunction in GABA signalling mediates autism-like stereotypies and Rett syndrome phenotypes. *Nature* 468, 263–269. doi: 10.1038/nature09582

Chaste, P., and Leboyer, M. (2012). Autism risk factors: genes, environment, and gene-environment interactions. *Dialogues Clin. Neurosci.* 14:281. doi: 10.31887/DCNS.2012.14.3/pchaste

Chavez, B., Chavez-Brown, M., and Rey, J. A. (2006). Role of risperidone in children with autism spectrum disorder. *Ann. Pharmacother.* 40, 909–916. doi: 10.1345/aph.1G389

Chen, S.-K., Tvrdik, P., Peden, E., Cho, S., Wu, S., Spangrude, G., et al. (2010). Hematopoietic origin of pathological grooming in Hoxb8 mutant mice. *Cell* 141, 775–785. doi: 10.1016/j.cell.2010.03.055

Chen, M., Wan, Y., Ade, K., Ting, J., Feng, G., and Calakos, N. (2011). Sapap3 deletion anomalously activates short-term endocannabinoid-mediated synaptic plasticity. *J. Neurosci.* 31, 9563–9573. doi: 10.1523/JNEUROSCI.1701-11.2011

Chiarotti, F., and Venerosi, A. (2020). Epidemiology of autism spectrum disorders: a review of worldwide prevalence estimates since 2014. *Brain Sci.* 10:274. doi: 10.3390/brainsci10050274

Chicka, M. C., and Strehler, E. E. (2003). Alternative splicing of the first intracellular loop of plasma membrane Ca^{2+}-ATPase isoform 2 alters its membrane targeting. *J. Biol. Chem.* 278, 18464–18470. doi: 10.1074/jbc.M301482200

Chin-Sang, I. D., George, S. E., Ding, M., Moseley, S. L., Lynch, A. S., and Chisholm, A. D. (1999). The ephrin VAB-2/EFN-1 functions in neuronal signaling to regulate epidermal morphogenesis in *C. elegans*. *Cell* 99, 781–790. doi: 10.1016/s0092-8674(00)81675-x

Chiron, C., Bulteau, C., Loc'h, C., Raynaud, C., Garreau, B., Syrota, A., et al. (1993). Dopaminergic D2 receptor SPECT imaging in Rett syndrome: increase of specific binding in striatum. *J. Nucl. Med.* 34, 1717–1721.

Choi, Y.-J., Di Nardo, A., Kramvis, I., Meikle, L., Kwiatkowski, D. J., Sahin, M., et al. (2008). Tuberous sclerosis complex proteins control axon formation. *Genes Dev.* 22, 2485–2495. doi: 10.1101/gad.1685008

Choi, C. S., Gonzales, E. L., Kim, K. C., Yang, S. M., Kim, J.-W., Mabunga, D. F., et al. (2016). The transgenerational inheritance of autism-like phenotypes in mice exposed to valproic acid during pregnancy. *Sci. Rep.* 6:36250. doi: 10.1038/srep36250

Choi, S.-Y., Han, K., Cutforth, T., Chung, W., Park, H., Lee, D., et al. (2015). Mice lacking the synaptic adhesion molecule Neph2/Kirrel3 display moderate hyperactivity and defective novel object preference. *Front. Cell. Neurosci.* 9:283. doi: 10.3389/fncel.2015.00283

Clegg, D. O., Wingerd, K. L., Hikita, S. T., and Tolhurst, E. C. (2003). Integrins in the development, function and dysfunction of the nervous system. *Front. Biosci.* 8:d723-50. doi: 10.2741/1020

Clipperton-Allen, A. E., and Page, D. T. (2014). Pten haploinsufficient mice show broad brain overgrowth but selective impairments in autism-relevant behavioral tests. *Hum. Mol. Genet.* 23, 3490–3505. doi: 10.1093/hmg/ddu057

Clipperton-Allen, A. E., and Page, D. T. (2015). Decreased aggression and increased repetitive behavior in Pten haploinsufficient mice. *Genes Brain Behav.* 14, 145–157. doi: 10.1111/gbb.12192

Cogram, P., Alkon, D. L., Crockford, D., Deacon, R. M., Hurley, M. J., Altimiras, F., et al. (2020). Chronic bryostatin-1 rescues autistic and cognitive phenotypes in the fragile X mice. *Sci. Rep.* 10:18058. doi: 10.1038/s41598-020-74848-6

Cogram, P., Deacon, R. J., Warner-Schmidt, J., von Schimmelmann, M. J., Abrahams, B. S., and During, M. J. (2019). Gaboxadol normalizes behavioral abnormalities in a mouse model of fragile X syndrome. *Front. Behav. Neurosci.* 13:141. doi: 10.3389/fnbeh.2019.00141

Colacicco, G., Welzl, H., Lipp, H.-P., and Würbel, H. (2002). Attentional set-shifting in mice: modification of a rat paradigm and evidence for strain-dependent variation. *Behav. Brain Res.* 132, 95–102. doi: 10.1016/s0166-4328(01)00391-6

Comery, T. A., Harris, J. B., Willems, P. J., Oostra, B. A., Irwin, S. A., Weiler, I. J., et al. (1997). Abnormal dendritic spines in fragile X knockout mice: maturation and pruning deficits. *Proc. Natl. Acad. Sci. U S A* 94, 5401–5404. doi: 10.1073/pnas.94.10.5401

Conn, P. J., Battaglia, G., Marino, M. J., and Nicoletti, F. (2005). Metabotropic glutamate receptors in the basal ganglia motor circuit. *Nat. Rev. Neurosci.* 6, 787–798. doi: 10.1038/nrn1763

Cook, E. H. Jr., and Scherer, S. W. (2008). Copy-number variations associated with neuropsychiatric conditions. *Nature* 455, 919–923. doi: 10.1038/nature07458

Cools, A. R., Spruijt, B. M., and Ellenbroek, B. A. (1988). Role of central dopamine in ACTH-induced grooming behavior in rats. *Ann. N Y Acad. Sci.* 525, 338–349. doi: 10.1111/j.1749-6632.1988.tb38618.x

Cooper, E. C., Harrington, E., Jan, Y. N., and Jan, L. Y. (2001). M channel KCNQ2 subunits are localized to key sites for control of neuronal network oscillations and synchronization in mouse brain. *J. Neurosci.* 21, 9529–9540. doi: 10.1523/JNEUROSCI.21-24-09529.2001

Costales, J. L., and Kolevzon, A. (2015). Phelan-McDermid syndrome and SHANK3: implications for treatment. *Neurotherapeutics* 12, 620–630. doi: 10.1007/s13311-015-0352-z

Courchesne, E., Pierce, K., Schumann, C. M., Redcay, E., Buckwalter, J. A., Kennedy, D. P., et al. (2007). Mapping early brain development in autism. *Neuron* 56, 399–413. doi: 10.1016/j.neuron.2007.10.016

Crawley, J. N. (2012). Translational animal models of autism and neurodevelopmental disorders. *Dialogues Clin. Neurosci.* 14:293. doi: 10.31887/DCNS.2012.14.3/jcrawley

Cromwell, H. C., and Berridge, K. C. (1996). Implementation of action sequences by a neostriatal site: a lesion mapping study of grooming syntax. *J. Neurosci.* 16, 3444–3458. doi: 10.1523/JNEUROSCI.16-10-03444.1996

Cromwell, H. C., Berridge, K. C., Drago, J., and Levine, M. S. (1998). Action sequencing is impaired in D1A-deficient mutant mice. *Eur. J. Neurosci.* 10, 2426–2432. doi: 10.1046/j.1460-9568.1998.00250.x

Crossland, J., and Lewandowski, A. (2006). Peromyscus—a fascinating laboratory animal model. *Techtalk* 11, 1–2.

Cupolillo, D., Hoxha, E., Faralli, A., De Luca, A., Rossi, F., Tempia, F., et al. (2016). Autistic-like traits and cerebellar dysfunction in purkinje cell PTEN knock-out mice. *Neuropsychopharmacology* 41, 1457–1466. doi: 10.1038/npp.2015.339

Curatolo, P., and Bombardieri, R. (2007). Tuberous sclerosis. *Handb. Clin. Neurol.* 87, 129–151. doi: 10.1016/S0072-9752(07)87009-6

Dalva, M. B., Takasu, M. A., Lin, M. Z., Shamah, S. M., Hu, L., Gale, N. W., et al. (2000). EphB receptors interact with NMDA receptors and regulate excitatory synapse formation. *Cell* 103, 945–956. doi: 10.1016/s0092-8674(00)00197-5

Dansie, L. E., Phommahaxay, K., Okusanya, A. G., Uwadia, J., Huang, M., Rotschafer, S. E., et al. (2013). Long-lasting effects of minocycline on behavior in young but not adult Fragile X mice. *Neuroscience* 246, 186–198. doi: 10.1016/j.neuroscience.2013.04.058

Davis, J. K., and Broadie, K. (2017). Multifarious functions of the fragile X mental retardation protein. *Trends Genet.* 33, 703–714. doi: 10.1016/j.tig.2017.07.008

De Arcangelis, A., and Georges-Labouesse, E. (2000). Integrin and ECM functions: roles in vertebrate development. *Trends Genet.* 16, 389–395. doi: 10.1016/s0168-9525(00)02074-6

De Barioglio, S. R., Lezcano, N., and Celis, M. E. (1991). Alpha MSH-induced excessive grooming behavior involves a GABAergic mechanism. *Peptides* 12, 203–205. doi: 10.1016/0196-9781(91)90189-v

de Brouwer, G., Fick, A., Harvey, B. H., and Wolmarans, W. (2019). A critical inquiry into marble-burying as a preclinical screening paradigm of relevance for anxiety and obsessive-compulsive disorder: mapping the way forward. *Cogn. Affect. Behav. Neurosci.* 19, 1–39. doi: 10.3758/s13415-018-00653-4

De La Torre-Ubieta, L., Gaudillière, B., Yang, Y., Ikeuchi, Y., Yamada, T., DiBacco, S., et al. (2010). A FOXO-Pak1 transcriptional pathway controls neuronal polarity. *Genes Dev.* 24, 799–813. doi: 10.1101/gad.1880510

De La Torre-Ubieta, L., Won, H., Stein, J. L., and Geschwind, D. H. (2016). Advancing the understanding of autism disease mechanisms through genetics. *Nat. Med.* 22, 345–361. doi: 10.1038/nm.4071

De Rubeis, S., and Buxbaum, J. D. (2015). Genetics and genomics of autism spectrum disorder: embracing complexity. *Hum. Mol. Genet.* 24, R24–R31. doi: 10.1093/hmg/ddv273

DeFilippis, M., and Wagner, K. D. (2016). Treatment of autism spectrum disorder in children and adolescents. *Psychopharmacol. Bull.* 46, 18–41.

Delmonte, S., Gallagher, L., O'Hanlon, E., Mc Grath, J., and Balsters, J. H. (2013). Functional and structural connectivity of frontostriatal circuitry in autism spectrum disorder. *Front. Hum. Neurosci.* 7:430. doi: 10.3389/fnhum.2013.00430

DeLorey, T., Handforth, A., Anagnostaras, S., Homanics, G., Minassian, B., Asatourian, A., et al. (1998). Mice lacking the β3 subunit of the $GABA_A$ receptor have the epilepsy phenotype and many of the behavioral characteristics of Angelman syndrome. *J. Neurosci.* 18, 8505–8514. doi: 10.1523/JNEUROSCI.18-20-08505.1998

DeLorey, T. M., Sahbaie, P., Hashemi, E., Homanics, G. E., and Clark, J. D. (2008). Gabrb3 gene deficient mice exhibit impaired social and exploratory behaviors, deficits in non-selective attention and hypoplasia of cerebellar vermal lobules: a potential model of autism spectrum disorder. *Behav. Brain Res.* 187, 207–220. doi: 10.1016/j.bbr.2007.09.009

DeNardo, L. A., de Wit, J., Otto-Hitt, S., and Ghosh, A. (2012). NGL-2 regulates input-specific synapse development in CA1 pyramidal neurons. *Neuron* 76, 762–775. doi: 10.1016/j.neuron.2012.10.013

Denmark, A., Tien, D., Wong, K., Chung, A., Cachat, J., Goodspeed, J., et al. (2010). The effects of chronic social defeat stress on mouse self-grooming behavior and its patterning. *Behav. Brain Res.* 208, 553–559. doi: 10.1016/j.bbr.2009.12.041

Denys, D., de Vries, F., Cath, D., Figee, M., Vulink, N., Veltman, D. J., et al. (2013). Dopaminergic activity in Tourette syndrome and obsessive-compulsive disorder. *Eur. Neuropsychopharmacol.* 23, 1423–1431. doi: 10.1016/j.euroneuro.2013.05.012

Deutsch, S. I., Burket, J. A., Jacome, L. F., Cannon, W. R., and Herndon, A. L. (2011a). D-Cycloserine improves the impaired sociability of the Balb/c mouse. *Brain Res. Bull.* 84, 8–11. doi: 10.1016/j.brainresbull.2010.10.006

Deutsch, S. I., Burket, J. A., Urbano, M. R., Herndon, A. L., and Winebarger, E. E. (2011b). "Impaired sociability of the Balb/c mouse, an animal model of autism spectrum disorders, is attenuated by NMDA receptor agonist interventions: clinical implications," in *A Comprehensive Book on Autism Spectrum Disorders*, ed M. A. Mohammadi (London: IntechOpen), 323–342.

Deutsch, S. I., Rosse, R. B., Paul, S. M., Riggs, R. L., and Mastropaolo, J. (1997). Inbred mouse strains differ in sensitivity to "popping" behavior elicited by MK-801. *Pharmacol. Biochem. Behav.* 57, 315–317. doi: 10.1016/s0091-3057(96)00347-4

Deutsch, S. I., Rosse, R. B., Schwartz, B. L., Mastropaolo, J., Burket, J. A., and Weizman, A. (2010). Regulation of intermittent oscillatory activity of pyramidal cell neurons by GABA inhibitory interneurons is impaired in schizophrenia: rationale for pharmacotherapeutic GABAergic interventions. *Isr. J. Psychiatry Relat. Sci.* 47, 17–26.

Devlin, B., and Scherer, S. W. (2012). Genetic architecture in autism spectrum disorder. *Curr. Opin. Genet. Dev.* 22, 229–237. doi: 10.1016/j.gde.2012.03.002

Devlin, B., Cook, E. H. Jr., Coon, H., Dawson, G., Grigorenko, E., McMahon, W., et al. (2005). Autism and the serotonin transporter: the long and short of it. *Mol. Psychiatry* 10, 1110–1116. doi: 10.1038/sj.mp.4001724

D'Hooge, R., Nagels, G., Franck, F., Bakker, C., Reyniers, E., Storm, K., et al. (1997). Mildly impaired water maze performance in male Fmr1 knockout mice. *Neuroscience* 76, 367–376. doi: 10.1016/s0306-4522(96)00224-2

Di Giovanni, G., Di Matteo, V., Pierucci, M., Benigno, A., and Esposito, E. (2006). Serotonin involvement in the basal ganglia pathophysiology: could the 5-HT2C receptor be a new target for therapeutic strategies? *Curr. Med. Chem.* 13, 3069–3081. doi: 10.2174/092986706778521805

Di Martino, A., Kelly, C., Grzadzinski, R., Zuo, X.-N., Mennes, M., Mairena, M. A., et al. (2011). Aberrant striatal functional connectivity in children with autism. *Biol. Psychiatry* 69, 847–856. doi: 10.1016/j.biopsych.2010.10.029

Dibbens, L. M., Tarpey, P. S., Hynes, K., Bayly, M. A., Scheffer, I. E., Smith, R., et al. (2008). X-linked protocadherin 19 mutations cause female-limited epilepsy and cognitive impairment. *Nat. Genet.* 40, 776–781. doi: 10.1038/ng.149

Dodero, L., Damiano, M., Galbusera, A., Bifone, A., Tsaftsaris, S. A., Scattoni, M. L., et al. (2013). Neuroimaging evidence of major morpho-anatomical and functional abnormalities in the BTBR T+ TF/J mouse model of autism. *PLoS One* 8:e76655. doi: 10.1371/journal.pone.0076655

Dolan, B. M., Duron, S. G., Campbell, D. A., Vollrath, B., Rao, B. S., Ko, H.-Y., et al. (2013). Rescue of fragile X syndrome phenotypes in Fmr1 KO mice by the small-molecule PAK inhibitor FRAX486. *Proc. Natl. Acad. Sci. U S A* 110, 5671–5676. doi: 10.1073/pnas.1219383110

Dölen, G., and Bear, M. F. (2008). Role for metabotropic glutamate receptor 5 (mGluR5) in the pathogenesis of fragile X syndrome. *J. Physiol.* 586, 1503–1508. doi: 10.1113/jphysiol.2008.150722

Dölen, G., Osterweil, E., Rao, B. S., Smith, G. B., Auerbach, B. D., Chattarji, S., et al. (2007). Correction of fragile X syndrome in mice. *Neuron* 56, 955–962. doi: 10.1016/j.neuron.2007.12.001

Doyle, C. A., and McDougle, C. J. (2012). Pharmacologic treatments for the behavioral symptoms associated with autism spectrum disorders across the lifespan. *Dialogues Clin. Neurosci.* 14, 263–279. doi: 10.31887/DCNS.2012.14.3/cdoyle

Drapeau, E., Dorr, N. P., Elder, G. A., and Buxbaum, J. D. (2014). Absence of strong strain effects in behavioral analyses of Shank3-deficient mice. *Dis. Model. Mech.* 7, 667–681. doi: 10.1242/dmm.013821

Draper, A., Stephenson, M. C., Jackson, G. M., Pépés, S., Morgan, P. S., Morris, P. G., et al. (2014). Increased GABA contributes to enhanced control over motor excitability in Tourette syndrome. *Curr. Biol.* 24, 2343–2347. doi: 10.1016/j.cub.2014.08.038

Duffney, L. J., Wei, J., Cheng, J., Liu, W., Smith, K. R., Kittler, J. T., et al. (2013). Shank3 deficiency induces NMDA receptor hypofunction *via* an actin-dependent mechanism. *J. Neurosci.* 33, 15767–15778. doi: 10.1523/JNEUROSCI.1175-13.2013

Dunn, J. T., Mroczek, J., Patel, H. R., and Ragozzino, M. E. (2020). Tandospirone, a partial 5-HT1$_A$ receptor agonist, administered systemically or into anterior cingulate attenuates repetitive behaviors in Shank3B mice. *Int. J. Neuropsychopharmacol.* 23, 533–542. doi: 10.1093/ijnp/pyaa047

Dunn, H. G., Stoessl, A. J., Ho, H. H., MacLeod, P. M., Poskitt, K. J., Doudet, D. J., et al. (2002). Rett syndrome: investigation of nine patients, including PET scan. *Can. J. Neurol. Sci.* 29, 345–357. doi: 10.1017/s0317167100002213

Eadie, B. D., Cushman, J., Kannangara, T. S., Fanselow, M. S., and Christie, B. R. (2012). NMDA receptor hypofunction in the dentate gyrus and impaired context discrimination in adult Fmr1 knockout mice. *Hippocampus* 22, 241–254. doi: 10.1002/hipo.20890

Egea, J., and Klein, R. (2007). Bidirectional Eph-ephrin signaling during axon guidance. *Trends Cell Biol.* 17, 230–238. doi: 10.1016/j.tcb.2007.03.004

Ehlers, M. D. (1999). Synapse structure: glutamate receptors connected by the shanks. *Curr. Biol.* 9, R848–R850. doi: 10.1016/s0960-9822(00)80043-3

Ehninger, D., Han, S., Shilyansky, C., Zhou, Y., Li, W., Kwiatkowski, D. J., et al. (2008). Reversal of learning deficits in a Tsc2+/− mouse model of tuberous sclerosis. *Nat. Med.* 14, 843–848. doi: 10.1038/nm1788

Ehninger, D., and Silva, A. J. (2011). Rapamycin for treating Tuberous sclerosis and Autism spectrum disorders. *Trends Mol. Med.* 17, 78–87. doi: 10.1016/j.molmed.2010.10.002

Eissa, N., Al-Houqani, M., Sadeq, A., Ojha, S. K., Sasse, A., and Sadek, B. (2018). Current enlightenment about etiology and pharmacological treatment of autism spectrum disorder. *Front. Neurosci.* 12:304. doi: 10.3389/fnins.2018.00304

El-Kordi, A., Winkler, D., Hammerschmidt, K., Kästner, A., Krueger, D., Ronnenberg, A., et al. (2013). Development of an autism severity score for mice using Nlgn4 null mutants as a construct-valid model of heritable monogenic autism. *Behav. Brain Res.* 251, 41–49. doi: 10.1016/j.bbr.2012.11.016

Ellegood, J., Anagnostou, E., Babineau, B., Crawley, J., Lin, L., Genestine, M., et al. (2015). Clustering autism: using neuroanatomical differences in 26 mouse models to gain insight into the heterogeneity. *Mol. Psychiatry* 20, 118–125. doi: 10.1038/mp.2014.98

Ellegood, J., Babineau, B. A., Henkelman, R. M., Lerch, J. P., and Crawley, J. N. (2013). Neuroanatomical analysis of the BTBR mouse model of autism using magnetic resonance imaging and diffusion tensor imaging. *NeuroImage* 70, 288–300. doi: 10.1016/j.neuroimage.2012.12.029

Ellegood, J., Henkelman, R. M., and Lerch, J. P. (2012). Neuroanatomical assessment of the integrin β3 mouse model related to autism and the serotonin system using high resolution MRI. *Front. Psychiatry* 3:37. doi: 10.3389/fpsyt.2012.00037

Ellegood, J., Pacey, L. K., Hampson, D. R., Lerch, J. P., and Henkelman, R. M. (2010). Anatomical phenotyping in a mouse model of fragile X syndrome with magnetic resonance imaging. *NeuroImage* 53, 1023–1029. doi: 10.1016/j.neuroimage.2010.03.038

Ernst, A., and Smelik, P. (1966). Site of action of dopamine and apomorphine on compulsive gnawing behaviour in rats. *Experientia* 22, 837–838. doi: 10.1007/BF01897450

Errijgers, V., Fransen, E., D'Hooge, R., De Deyn, P. P., and Kooy, R. F. (2008). Effect of genetic background on acoustic startle response in fragile X knockout mice. *Genet. Res.* 90, 341–345. doi: 10.1017/S0016672308009415

Espinosa, F., Xuan, Z., Liu, S., and Powell, C. M. (2015). Neuroligin 1 modulates striatal glutamatergic neurotransmission in a pathway and NMDAR subunit-specific manner. *Front. Synaptic Neurosci.* 7:11. doi: 10.3389/fnsyn.2015.00011

Estanislau, C., Díaz-Morán, S., Cañete, T., Blázquez, G., Tobeña, A., and Fernández-Teruel, A. (2013). Context-dependent differences in grooming behavior among the NIH heterogeneous stock and the Roman high- and low-avoidance rats. *Neurosci. Res.* 77, 187–201. doi: 10.1016/j.neures.2013.09.012

Estanislau, C., Veloso, A. W. N., Filgueiras, G. B., Maio, T. P., Dal-Cól, M. L. C., Cunha, D. C., et al. (2019). Rat self-grooming and its relationships with anxiety, dearousal and perseveration: evidence for a self-grooming trait. *Physiol. Behav.* 209:112585. doi: 10.1016/j.physbeh.2019.112585

Ethell, I. M., Irie, F., Kalo, M. S., Couchman, J. R., Pasquale, E. B., and Yamaguchi, Y. (2001). EphB/syndecan-2 signaling in dendritic spine morphogenesis. *Neuron* 31, 1001–1013. doi: 10.1016/s0896-6273(01)00440-8

Etherton, M., Földy, C., Sharma, M., Tabuchi, K., Liu, X., Shamloo, M., et al. (2011). Autism-linked neuroligin-3 R451C mutation differentially alters hippocampal and cortical synaptic function. *Proc. Natl. Acad. Sci. U S A* 108, 13764–13769. doi: 10.1073/pnas.1111093108

Etherton, M. R., Blaiss, C. A., Powell, C. M., and Südhof, T. C. (2009). Mouse neurexin-1α deletion causes correlated electrophysiological and behavioral

changes consistent with cognitive impairments. *Proc. Natl. Acad. Sci. U S A* 106, 17998–18003. doi: 10.1073/pnas.0910297106

Fatemi, S. H., Halt, A. R., Realmuto, G., Earle, J., Kist, D. A., Thuras, P., et al. (2002). Purkinje cell size is reduced in cerebellum of patients with autism. *Cell. Mol. Neurobiol.* 22, 171–175. doi: 10.1023/a:1019861721160

Feliciano, P., Zhou, X., Astrovskaya, I., Turner, T. N., Wang, T., Brueggeman, L., et al. (2019). Exome sequencing of 457 autism families recruited online provides evidence for autism risk genes. *NPJ Genomic Med.* 4:19. doi: 10.1038/s41525-019-0093-8

Felix-Ortiz, A. C., and Tye, K. M. (2014). Amygdala inputs to the ventral hippocampus bidirectionally modulate social behavior. *J. Neurosci.* 34, 586–595. doi: 10.1523/JNEUROSCI.4257-13.2014

Fentress, J. C. (1988). Expressive contexts, fine structure and central mediation of rodent grooming. *Ann. N Y Acad. Sci.* 525, 18–26. doi: 10.1111/j.1749-6632.1988.tb38592.x

Filice, F., Lauber, E., Vörckel, K. J., Wöhr, M., and Schwaller, B. (2018). 17-β estradiol increases parvalbumin levels in Pvalb heterozygous mice and attenuates behavioral phenotypes with relevance to autism core symptoms. *Mol. Autism* 9:15. doi: 10.1186/s13229-018-0199-3

Filippini, A., Bonini, D., Lacoux, C., Pacini, L., Zingariello, M., Sancillo, L., et al. (2017). Absence of the fragile X mental retardation protein results in defects of RNA editing of neuronal mRNAs in mouse. *RNA Biol.* 14, 1580–1591. doi: 10.1080/15476286.2017.1338232

Filosa, A., Paixão, S., Honsek, S. D., Carmona, M. A., Becker, L., Feddersen, B., et al. (2009). Neuron-glia communication *via* EphA4/ephrin-A3 modulates LTP through glial glutamate transport. *Nat. Neurosci.* 12, 1285–1292. doi: 10.1038/nn.2394

Florijn, W. J., Holtmaat, A. J., de Lang, H., Spierenburg, H., Gispen, W. H., and Versteeg, D. H. (1993). Peptide-induced grooming behavior and caudate nucleus dopamine release. *Brain Res.* 625, 169–172. doi: 10.1016/0006-8993(93)90151-c

Floyd, N. S., Price, J. L., Ferry, A. T., Keay, K. A., and Bandler, R. (2000). Orbitomedial prefrontal cortical projections to distinct longitudinal columns of the periaqueductal gray in the rat. *J. Comp. Neurol.* 422, 556–578. doi: 10.1002/1096-9861(20000710)422:4<556::aid-cne6>3.0.co;2-u

Fraser, M. M., Bayazitov, I. T., Zakharenko, S. S., and Baker, S. J. (2008). Phosphatase and tensin homolog, deleted on chromosome 10 deficiency in brain causes defects in synaptic structure, transmission and plasticity, and myelination abnormalities. *Neuroscience* 151, 476–488. doi: 10.1016/j.neuroscience.2007.10.048

Fraser, M. M., Zhu, X., Kwon, C. H., Uhlmann, E. J., Gutmann, D. H., and Baker, S. J. (2004). Pten loss causes hypertrophy and increased proliferation of astrocytes *in vivo*. *Cancer Res.* 64, 7773–7779. doi: 10.1158/0008-5472.CAN-04-2487

Frisch, C., Hüsch, K., Angenstein, F., Kudin, A., Kunz, W., Elger, C. E., et al. (2009). Dose-dependent memory effects and cerebral volume changes after *in utero* exposure to valproate in the rat. *Epilepsia* 50, 1432–1441. doi: 10.1111/j.1528-1167.2008.01943.x

Fung, L. K., Mahajan, R., Nozzolillo, A., Bernal, P., Krasner, A., Jo, B., et al. (2016). Pharmacologic treatment of severe irritability and problem behaviors in autism: a systematic review and meta-analysis. *Pediatrics* 137, S124–S135. doi: 10.1542/peds.2015-2851K

Gandhi, R. M., Kogan, C. S., and Messier, C. (2014). 2-Methyl-6-(phenylethynyl) pyridine (MPEP) reverses maze learning and PSD-95 deficits in fMRI knock-out mice. *Front. Cell. Neurosci.* 8:70. doi: 10.3389/fncel.2014.00070

Gao, Y., Vasilyev, D. V., Goncalves, M. B., Howell, F. V., Hobbs, C., Reisenberg, M., et al. (2010). Loss of retrograde endocannabinoid signaling and reduced adult neurogenesis in diacylglycerol lipase knock-out mice. *J. Neurosci.* 30, 2017–2024. doi: 10.1523/JNEUROSCI.5693-09.2010

Gao, R., Zaccard, C. R., Shapiro, L. P., Dionisio, L. E., Martin-de-Saavedra, M. D., Piguel, N. H., et al. (2019). The CNTNAP2-CASK complex modulates GluA1 subcellular distribution in interneurons. *Neurosci. Lett.* 701, 92–99. doi: 10.1016/j.neulet.2019.02.025

Gao, P., Zhang, J., Yokoyama, M., Racey, B., Dreyfus, C., Black, I., et al. (1996). Regulation of topographic projection in the brain: Elf-1 in the hippocamposeptal system. *Proc. Natl. Acad. Sci. U S A* 93, 11161–11166. doi: 10.1073/pnas.93.20.11161

Gargiulo, P. A., and Donoso, A. O. (1996). Distinct grooming patterns induced by intracerebroventricular injection of CRH, TRH and LHRH in male rats. *Braz. J. Med. Biol. Res.* 29, 375–379.

Gau, S. S.-F., Liao, H.-M., Hong, C.-C., Chien, W.-H., and Chen, C.-H. (2012). Identification of two inherited copy number variants in a male with autism supports two-hit and compound heterozygosity models of autism. *Am. J. Med. Genet. B Neuropsychiatr. Genet.* 159, 710–717. doi: 10.1002/ajmg.b.32074

Gdalyahu, A., Lazaro, M., Penagarikano, O., Golshani, P., Trachtenberg, J. T., and Gescwind, D. H. (2015). The autism related protein contactin-associated protein-like 2 (CNTNAP2) stabilizes new spines: an *in vivo* mouse study. *PLoS One* 10:e0125633. doi: 10.1371/journal.pone.0125633

Gencer, O., Emiroglu, F. N., Miral, S., Baykara, B., Baykara, A., and Dirik, E. (2008). Comparison of long-term efficacy and safety of risperidone and haloperidol in children and adolescents with autistic disorder. An open label maintenance study. *Eur. Child Adolesc. Psychiatry* 17, 217–225. doi: 10.1007/s00787-007-0656-6

Gerfen, C. R. (1995). Dopamine receptor function in the basal ganglia. *Clin. Neuropharmacol.* 18, S162–S177. doi: 10.1002/mds.870080303

Gerfen, C. R., Engber, T. M., Mahan, L. C., Susel, Z., Chase, T. N., Monsma, F. J., et al. (1990). D1 and D2 dopamine receptor-regulated gene expression of striatonigral and striatopallidal neurons. *Science* 250, 1429–1432. doi: 10.1126/science.2147780

Gerke, P., Benzing, T., Höhne, M., Kispert, A., Frotscher, M., Walz, G., et al. (2006). Neuronal expression and interaction with the synaptic protein CASK suggest a role for Neph1 and Neph2 in synaptogenesis. *J. Comp. Neurol.* 498, 466–475. doi: 10.1002/cne.21064

Geschwind, D. H. (2011). Genetics of autism spectrum disorders. *Trends Cogn. Sci.* 15, 409–416. doi: 10.1016/j.tics.2011.07.003

Geschwind, D. H., and State, M. W. (2015). Gene hunting in autism spectrum disorder: on the path to precision medicine. *Lancet Neurol.* 14, 1109–1120. doi: 10.1016/S1474-4422(15)00044-7

Ghidoni, B. B. Z. (2007). Rett syndrome. *Child Adolesc. Psychiatr. Clin. N. Am.* 16, 723–743. doi: 10.1016/j.chc.2007.03.004

Gholizadeh, S., Arsenault, J., Xuan, I. C. Y., Pacey, L. K., and Hampson, D. R. (2014). Reduced phenotypic severity following adeno-associated virus-mediated Fmr1 gene delivery in fragile X mice. *Neuropsychopharmacology* 39, 3100–3111. doi: 10.1038/npp.2014.167

Gispen, W. H., and Isaacson, R. L. (1981). ACTH-induced excessive grooming in the rat. *Pharmacol. Ther.* 12, 209–246. doi: 10.1016/0163-7258(81)90081-4

Gogolla, N., LeBlanc, J. J., Quast, K. B., Südhof, T. C., Fagiolini, M., and Hensch, T. K. (2009). Common circuit defect of excitatory-inhibitory balance in mouse models of autism. *J. Neurodev. Disord.* 1, 172–181. doi: 10.1007/s11689-009-9023-x

Golden, C. E., Buxbaum, J. D., and De Rubeis, S. (2018). Disrupted circuits in mouse models of autism spectrum disorder and intellectual disability. *Curr. Opin. Neurobiol.* 48, 106–112. doi: 10.1016/j.conb.2017.11.006

Gotham, K., Bishop, S. L., Hus, V., Huerta, M., Lund, S., Buja, A., et al. (2013). Exploring the relationship between anxiety and insistence on sameness in autism spectrum disorders. *Autism Res.* 6, 33–41. doi: 10.1002/aur.1263

Gould, G. G., Hensler, J. G., Burke, T. F., Benno, R. H., Onaivi, E. S., and Daws, L. C. (2011). Density and function of central serotonin (5-HT) transporters, 5-$HT1_A$ and 5-$HT2_A$ receptors and effects of their targeting on BTBR T+ tf/J mouse social behavior. *J. Neurochem.* 116, 291–303. doi: 10.1111/j.1471-4159.2010.07104.x

Gould, B. R., and Zingg, H. H. (2003). Mapping oxytocin receptor gene expression in the mouse brain and mammary gland using an oxytocin receptor-LacZ reporter mouse. *Neuroscience* 122, 155–167. doi: 10.1016/s0306-4522(03)00283-5

Grabrucker, A. M. (2013). Environmental factors in autism. *Front. Psychiatry* 3:118. doi: 10.3389/fpsyt.2012.00118

Grabrucker, A. M., Schmeisser, M. J., Schoen, M., and Boeckers, T. M. (2011). Postsynaptic ProSAP/Shank scaffolds in the cross-hair of synaptopathies. *Trends Cell Biol.* 21, 594–603. doi: 10.1016/j.tcb.2011.07.003

Grayton, H. M., Missler, M., Collier, D. A., and Fernandes, C. (2013). Altered social behaviours in neurexin 1α knockout mice resemble core symptoms in neurodevelopmental disorders. *PLoS One* 8:e67114. doi: 10.1371/journal.pone.0067114

Green, S. A., Ben-Sasson, A., Soto, T. W., and Carter, A. S. (2012). Anxiety and sensory over-responsivity in toddlers with autism spectrum disorders: bidirectional effects across time. *J. Autism Dev. Disord.* 42, 1112–1119. doi: 10.1007/s10803-011-1361-3

Greer, J. M., and Capecchi, M. R. (2002). Hoxb8 is required for normal grooming behavior in mice. *Neuron* 33, 23–34. doi: 10.1016/s0896-6273(01)00564-5

Gremel, C. M., Chancey, J. H., Atwood, B. K., Luo, G., Neve, R., Ramakrishnan, C., et al. (2016). Endocannabinoid modulation of orbitostriatal circuits gates habit formation. *Neuron* 90, 1312–1324. doi: 10.1016/j.neuron.2016.04.043

Gross, C., Banerjee, A., Tiwari, D., Longo, F., White, A. R., Allen, A., et al. (2019). Isoform-selective phosphoinositide 3-kinase inhibition ameliorates a broad range of fragile X syndrome-associated deficits in a mouse model. *Neuropsychopharmacology* 44, 324–333. doi: 10.1038/s41386-018-0150-5

Grove, J., Ripke, S., Als, T. D., Mattheisen, M., Walters, R. K., Won, H., et al. (2019). Identification of common genetic risk variants for autism spectrum disorder. *Nat. Genet.* 51, 431–444. doi: 10.1038/s41588-019-0344-8

Grunwald, I. C., Korte, M., Adelmann, G., Plueck, A., Kullander, K., Adams, R. H., et al. (2004). Hippocampal plasticity requires postsynaptic ephrinBs. *Nat. Neurosci.* 7, 33–40. doi: 10.1038/nn1164

Grunwald, I. C., Korte, M., Wolfer, D., Wilkinson, G. A., Unsicker, K., Lipp, H.-P., et al. (2001). Kinase-independent requirement of EphB2 receptors in hippocampal synaptic plasticity. *Neuron* 32, 1027–1040. doi: 10.1016/s0896-6273(01)00550-5

Guilmatre, A., Huguet, G., Delorme, R., and Bourgeron, T. (2014). The emerging role of SHANK genes in neuropsychiatric disorders. *Dev. Neurobiol.* 74, 113–122. doi: 10.1002/dneu.22128

Gulisano, M., Barone, R., Alaimo, S., Ferro, A., Pulvirenti, A., Cirnigliaro, L., et al. (2020). Disentangling restrictive and repetitive behaviors and social impairments in children and adolescents with gilles de la tourette syndrome and autism spectrum disorder. *Brain Sci.* 10:308. doi: 10.3390/brainsci10050308

Gundelfinger, E. D., Boeckers, T. M., Baron, M. K., and Bowie, J. U. (2006). A role for zinc in postsynaptic density asSAMbly and plasticity? *Trends Biochem. Sci.* 31, 366–373. doi: 10.1016/j.tibs.2006.05.007

Guo, H., Duyzend, M. H., Coe, B. P., Baker, C., Hoekzema, K., Gerdts, J., et al. (2019). Genome sequencing identifies multiple deleterious variants in autism patients with more severe phenotypes. *Genet. Med.* 21, 1611–1620. doi: 10.1038/s41436-018-0380-2

Gurney, M. E., Cogram, P., Deacon, R. M., Rex, C., and Tranfaglia, M. (2017). Multiple behavior phenotypes of the fragile-X syndrome mouse model respond to chronic inhibition of phosphodiesterase-4D (PDE4D). *Sci. Rep.* 7:14653. doi: 10.1038/s41598-017-15028-x

Haas, B. W., Barnea-Goraly, N., Lightbody, A. A., Patnaik, S. S., Hoeft, F., Hazlett, H., et al. (2009). Early white-matter abnormalities of the ventral frontostriatal pathway in fragile X syndrome. *Dev. Med. Child Neurol.* 51, 593–599. doi: 10.1111/j.1469-8749.2009.03295.x

Haber, S. N., and Calzavara, R. (2009). The cortico-basal ganglia integrative network: the role of the thalamus. *Brain Res. Bull.* 78, 69–74. doi: 10.1016/j.brainresbull.2008.09.013

Haberl, M. G., Zerbi, V., Veltien, A., Ginger, M., Heerschap, A., and Frick, A. (2015). Structural-functional connectivity deficits of neocortical circuits in the fMR1−/y mouse model of autism. *Sci. Adv.* 1:e1500775. doi: 10.1126/sciadv.1500775

Hadley, C., Hadley, B., Ephraim, S., Yang, M., and Lewis, M. H. (2006). Spontaneous stereotypy and environmental enrichment in deer mice (*Peromyscus maniculatus*): reversibility of experience. *Appl. Anim. Behav. Sci.* 97, 312–322. doi: 10.1016/j.applanim.2005.08.006

Hagerman, R. J., Berry-Kravis, E., Hazlett, H. C., Bailey, D. B. Jr., Moine, H., Kooy, R. F., et al. (2017). Fragile X syndrome. *Nat. Rev. Dis. Primers* 3:17065. doi: 10.1038/nrdp.2017.65

Hallahan, B. P., Craig, M. C., Toal, F., Daly, E. M., Moore, C. J., Ambikapathy, A., et al. (2011). *In vivo* brain anatomy of adult males with Fragile X syndrome: an MRI study. *NeuroImage* 54, 16–24. doi: 10.1016/j.neuroimage.2010.08.015

Han, S., Tai, C., Jones, C. J., Scheuer, T., and Catterall, W. A. (2014). Enhancement of inhibitory neurotransmission by $GABA_A$ receptors having α2,3-subunits ameliorates behavioral deficits in a mouse model of autism. *Neuron* 81, 1282–1289. doi: 10.1016/j.neuron.2014.01.016

Han, S., Tai, C., Westenbroek, R. E., Frank, H. Y., Cheah, C. S., Potter, G. B., et al. (2012). Autistic-like behaviour in $Scn1a^{+/-}$ mice and rescue by enhanced GABA-mediated neurotransmission. *Nature* 489, 385–390. doi: 10.1038/nature11356

Harony-Nicolas, H., Kay, M., du Hoffmann, J., Klein, M. E., Bozdagi-Gunal, O., Riad, M., et al. (2017). Oxytocin improves behavioral and electrophysiological deficits in a novel Shank3-deficient rat. *eLife* 6:e18904. doi: 10.7554/eLife.18904

Hashemi, E., Ariza, J., Rogers, H., Noctor, S. C., and Martínez-Cerdeño, V. (2017). The number of parvalbumin-expressing interneurons is decreased in the prefrontal cortex in autism. *Cereb. Cortex* 27, 1931–1943. doi: 10.1093/cercor/bhw021

Hayashi, E., Kuratani, K., Kinoshita, M., and Hara, H. (2010). Pharmacologically distinctive behaviors other than burying marbles during the marble burying test in mice. *Pharmacology* 86, 293–296. doi: 10.1159/000321190

Heimer, L., Van Hoesen, G. W., Trimble, M., and Zahm, D. S. (2007). *Anatomy of Neuropsychiatry: The New Anatomy of the Basal Forebrain and Its Implications for Neuropsychiatric Illness.* New York, NY: Academic Press.

Henderson, C., Wijetunge, L., Kinoshita, M. N., Shumway, M., Hammond, R. S., Postma, F. R., et al. (2012). Reversal of disease-related pathologies in the fragile X mouse model by selective activation of $GABA_B$ receptors with arbaclofen. *Sci. Transl. Med.* 4:152ra128. doi: 10.1126/scitranslmed.3004218

Henkemeyer, M., Itkis, O. S., Ngo, M., Hickmott, P. W., and Ethell, I. M. (2003). Multiple EphB receptor tyrosine kinases shape dendritic spines in the hippocampus. *J. Cell Biol.* 163, 1313–1326. doi: 10.1083/jcb.200306033

Herman, G. E., Butter, E., Enrile, B., Pastore, M., Prior, T. W., and Sommer, A. (2007). Increasing knowledge of PTEN germline mutations: two additional patients with autism and macrocephaly. *Am. J. Med. Genet. A* 143A, 589–593. doi: 10.1002/ajmg.a.31619

Héroult, M., Schaffner, F., and Augustin, H. G. (2006). Eph receptor and ephrin ligand-mediated interactions during angiogenesis and tumor progression. *Exp. Cell Res.* 312, 642–650. doi: 10.1055/s-0040-1719018

Hines, R. M., Wu, L., Hines, D. J., Steenland, H., Mansour, S., Dahlhaus, R., et al. (2008). Synaptic imbalance, stereotypies, and impaired social interactions in mice with altered neuroligin 2 expression. *J. Neurosci.* 28, 6055–6067. doi: 10.1523/JNEUROSCI.0032-08.2008

Hisaoka, T., Komori, T., Kitamura, T., and Morikawa, Y. (2018). Abnormal behaviours relevant to neurodevelopmental disorders in Kirrel3-knockout mice. *Sci. Rep.* 8:1408. doi: 10.1038/s41598-018-19844-7

Hollander, E., Anagnostou, E., Chaplin, W., Esposito, K., Haznedar, M. M., Licalzi, E., et al. (2005). Striatal volume on magnetic resonance imaging and repetitive behaviors in autism. *Biol. Psychiatry* 58, 226–232. doi: 10.1016/j.biopsych.2005.03.040

Homberg, J. R., van den Akker, M., Raasø, H. S., Wardeh, G., Binnekade, R., Schoffelmeer, A. N., et al. (2002). Enhanced motivation to self-administer cocaine is predicted by self-grooming behaviour and relates to dopamine release in the rat medial prefrontal cortex and amygdala. *Eur. J. Neurosci.* 15, 1542–1550. doi: 10.1046/j.1460-9568.2002.01976.x

Hong, W., Kim, D.-W., and Anderson, D. J. (2014). Antagonistic control of social versus repetitive self-grooming behaviors by separable amygdala neuronal subsets. *Cell* 158, 1348–1361. doi: 10.1016/j.cell.2014.07.049

Horev, G., Ellegood, J., Lerch, J. P., Son, Y.-E. E., Muthuswamy, L., Vogel, H., et al. (2011). Dosage-dependent phenotypes in models of 16p11. 2 lesions found in autism. *Proc. Natl. Acad. Sci. U S A* 108, 17076–17081. doi: 10.1073/pnas.1114042108

Hosie, S., Malone, D. T., Liu, S., Glass, M., Adlard, P. A., Hannan, A. J., et al. (2018). Altered amygdala excitation and CB1 receptor modulation of aggressive behavior in the neuroligin-3^{R451C} mouse model of autism. *Front. Cell. Neurosci.* 12:234. doi: 10.3389/fncel.2018.00234

Houwing, D. J., Heijkoop, R., Olivier, J. D. A., and Snoeren, E. M. S. (2019). Perinatal fluoxetine exposure changes social and stress-coping behavior in adult rats housed in a seminatural environment. *Neuropharmacology* 151, 84–97. doi: 10.1016/j.neuropharm.2019.03.037

Hu, X. Z., Lipsky, R. H., Zhu, G., Akhtar, L. A., Taubman, J., Greenberg, B. D., et al. (2006). Serotonin transporter promoter gain-of-function genotypes are linked to obsessive-compulsive disorder. *Am. J. Hum. Genet.* 78, 815–826. doi: 10.1086/503850

Huang, H.-S., Burns, A. J., Nonneman, R. J., Baker, L. K., Riddick, N. V., Nikolova, V. D., et al. (2013). Behavioral deficits in an Angelman syndrome model: effects of genetic background and age. *Behav. Brain Res.* 243, 79–90. doi: 10.1016/j.bbr.2012.12.052

Huang, F., Chen, X., Jiang, X., Niu, J., Cui, C., Chen, Z., et al. (2019). Betaine ameliorates prenatal valproic-acid-induced autism-like behavioral abnormalities in mice by promoting homocysteine metabolism. *Psychiatry Clin. Neurosci.* 73, 317–322. doi: 10.1111/pcn.12833

Hung, A. Y., Futai, K., Sala, C., Valtschanoff, J. G., Ryu, J., Woodworth, M. A., et al. (2008). Smaller dendritic spines, weaker synaptic transmission, but enhanced spatial learning in mice lacking Shank1. *J. Neurosci.* 28, 1697–1708. doi: 10.1523/JNEUROSCI.3032-07.2008

Huang, J., and Manning, B. D. (2008). The TSC1-TSC2 complex: a molecular switchboard controlling cell growth. *Biochem. J.* 412, 179–190. doi: 10.1042/BJ20080281

Hynes, K., Tarpey, P., Dibbens, L. M., Bayly, M. A., Berkovic, S. F., Smith, R., et al. (2010). Epilepsy and mental retardation limited to females with PCDH19 mutations can present *de novo* or in single generation families. *J. Med. Genet.* 47, 211–216. doi: 10.1136/jmg.2009.068817

Ifergan, I., Kebir, H., Terouz, S., Alvarez, J. I., Lécuyer, M. A., Gendron, S., et al. (2011). Role of Ninjurin-1 in the migration of myeloid cells to central nervous system inflammatory lesions. *Ann. Neurol.* 70, 751–763. doi: 10.1002/ana.22519

Inoki, K., Corradetti, M. N., and Guan, K.-L. (2005). Dysregulation of the TSC-mTOR pathway in human disease. *Nat. Genet.* 37, 19–24. doi: 10.1038/ng1494

Iossifov, I., Ronemus, M., Levy, D., Wang, Z., Hakker, I., Rosenbaum, J., et al. (2012). *De novo* gene disruptions in children on the autistic spectrum. *Neuron* 74, 285–299. doi: 10.1016/j.neuron.2012.04.009

Ishiguro, A., Inagaki, M., and Kaga, M. (2007). Stereotypic circling behavior in mice with vestibular dysfunction: asymmetrical effects of intrastriatal microinjection of a dopamine agonist. *Int. J. Neurosci.* 117, 1049–1064. doi: 10.1080/00207450600936874

Jamain, S., Quach, H., Betancur, C., Råstam, M., Colineaux, C., Gillberg, I. C., et al. (2003). Mutations of the X-linked genes encoding neuroligins NLGN3 and NLGN4 are associated with autism. *Nat. Genet.* 34, 27–29. doi: 10.1038/ng1136

Jang, Y. S., Kang, J. H., Woo, J. K., Kim, H. M., Hwang, J. I., Lee, S. J., et al. (2016). Ninjurin1 suppresses metastatic property of lung cancer cells through inhibition of interleukin 6 signaling pathway. *Int. J. Cancer* 139, 383–395. doi: 10.1002/ijc.30021

Jaramillo, T. C., Speed, H. E., Xuan, Z., Reimers, J. M., Liu, S., and Powell, C. M. (2016). Altered striatal synaptic function and abnormal behaviour in Shank3 exon4-9 deletion mouse model of autism. *Autism Res.* 9, 350–375. doi: 10.1002/aur.1529

Jardim, M. C., and Guimarães, F. S. (2001). GABAergic and glutamatergic modulation of exploratory behavior in the dorsomedial hypothalamus. *Pharmacol. Biochem. Behav.* 69, 579–584. doi: 10.1016/s0091-3057(01)00560-3

Jia, Y. F., Wininger, K., Peyton, L., Ho, A. M., and Choi, D. S. (2021). Astrocytic glutamate transporter 1 (GLT1) deficient mice exhibit repetitive behaviors. *Behav. Brain Res.* 396:112906. doi: 10.1016/j.bbr.2020.112906

Jiang, Y.-H., Pan, Y., Zhu, L., Landa, L., Yoo, J., Spencer, C., et al. (2010). Altered ultrasonic vocalization and impaired learning and memory in Angelman syndrome mouse model with a large maternal deletion from Ube3a to Gabrb3. *PLoS One* 5:e12278. doi: 10.1371/journal.pone.0012278

Jiang, Y.-H., Yuen, R. K., Jin, X., Wang, M., Chen, N., Wu, X., et al. (2013). Detection of clinically relevant genetic variants in autism spectrum disorder by whole-genome sequencing. *Am. J. Hum. Genet.* 93, 249–263. doi: 10.1016/j.ajhg.2013.06.012

Jiujias, M., Kelley, E., and Hall, L. (2017). Restricted, repetitive behaviors in autism spectrum disorder and obsessive-compulsive disorder: a comparative review. *Child Psychiatry Hum. Dev.* 48, 944–959. doi: 10.1007/s10578-017-0717-0

Joyner, C. P., Myrick, L. C., Crossland, J. P., and Dawson, W. D. (1998). Deer mice as laboratory animals. *ILAR J.* 39, 322–330. doi: 10.1093/ilar.39.4.322

Jung, C. K., and Herms, J. (2014). Structural dynamics of dendritic spines are influenced by an environmental enrichment: an *in vivo* imaging study. *Cereb. Cortex* 24, 377–384. doi: 10.1093/cercor/bhs317

Jung, K.-M., Sepers, M., Henstridge, C. M., Lassalle, O., Neuhofer, D., Martin, H., et al. (2012). Uncoupling of the endocannabinoid signalling complex in a mouse model of fragile X syndrome. *Nat. Commun.* 3:1080. doi: 10.1038/ncomms2045

Kalueff, A. V., and Nutt, D. J. (2007). Role of GABA in anxiety and depression. *Depress. Anxiety* 24, 495–517. doi: 10.1002/da.20262

Kalueff, A. V., and Tuohimaa, P. (2004a). Contrasting grooming phenotypes in C57Bl/6 and 129S1/SvImJ mice. *Brain Res.* 1028, 75–82. doi: 10.1016/j.brainres.2004.09.001

Kalueff, A. V., and Tuohimaa, P. (2004b). Grooming analysis algorithm for neurobehavioural stress research. *Brain Res. Protoc.* 13, 151–158. doi: 10.1016/j.brainresprot.2004.04.002

Kalueff, A. V., and Tuohimaa, P. (2005a). Contrasting grooming phenotypes in three mouse strains markedly different in anxiety and activity (129S1, BALB/c and NMRI). *Behav. Brain Res.* 160, 1–10. doi: 10.1016/j.bbr.2004.11.010

Kalueff, A. V., and Tuohimaa, P. (2005b). The grooming analysis algorithm discriminates between different levels of anxiety in rats: potential utility for neurobehavioural stress research. *J. Neurosci. Methods* 143, 169–177. doi: 10.1016/j.jneumeth.2004.10.001

Kalueff, A. V., and Tuohimaa, P. (2005c). Mouse grooming microstructure is a reliable anxiety marker bidirectionally sensitive to GABAergic drugs. *Eur. J. Pharmacol.* 508, 147–153. doi: 10.1016/j.ejphar.2004.11.054

Kalueff, A. V., Ren-Patterson, R. F., and Murphy, D. L. (2007). The developing use of heterozygous mutant mouse models in brain monoamine transporter research. *Trends Pharmacol. Sci.* 28, 122–127. doi: 10.1016/j.tips.2007.01.002

Kalueff, A. V., Ren-Patterson, R. F., LaPorte, J. L., and Murphy, D. L. (2008). Domain interplay concept in animal models of neuropsychiatric disorders: a new strategy for high-throughput neurophenotyping research. *Behav. Brain Res.* 188, 243–249. doi: 10.1016/j.bbr.2007.11.011

Kalueff, A. V., Stewart, A. M., Song, C., Berridge, K. C., Graybiel, A. M., and Fentress, J. C. (2016). Neurobiology of rodent self-grooming and its value for translational neuroscience. *Nat. Rev. Neurosci.* 17, 45–59. doi: 10.1038/nrn.2015.8

Kametani, H. (1988). Analysis of age-related changes in stress-induced grooming in the rat. Differential behavioral profile of adaptation to stress. *Ann. N. Y. Acad. Sci.* 525, 101–113. doi: 10.1111/j.1749-6632.1988.tb38599.x

Kano, M., Ohno-Shosaku, T., Hashimotodani, Y., Uchigashima, M., and Watanabe, M. (2009). Endocannabinoid-mediated control of synaptic transmission. *Physiol. Rev.* 89, 309–380. doi: 10.1152/physrev.00019.2008

Karimi, P., Kamali, E., Mousavi, S. M., and Karahmadi, M. (2017). Environmental factors influencing the risk of autism. *J. Res. Med. Sci.* 22:27. doi: 10.4103/1735-1995.200272

Karler, R., Bedingfield, J. B., Thai, D. K., and Calder, L. D. (1997). The role of the frontal cortex in the mouse in behavioral sensitization to amphetamine. *Brain Res.* 757, 228–235. doi: 10.1016/s0006-8993(97)00221-7

Karler, R., Calder, L. D., Thai, D. K., and Bedingfield, J. B. (1998). The role of dopamine in the mouse frontal cortex: a new hypothesis of behavioral sensitization to amphetamine and cocaine. *Pharmacol. Biochem. Behav.* 61, 435–443. doi: 10.1016/s0091-3057(98)00133-6

Karvat, G., and Kimchi, T. (2014). Acetylcholine elevation relieves cognitive rigidity and social deficiency in a mouse model of autism. *Neuropsychopharmacology* 39, 831–840. doi: 10.1038/npp.2013.274

Kas, M. J., Fernandes, C., Schalkwyk, L. C., and Collier, D. A. (2007). Genetics of behavioural domains across the neuropsychiatric spectrum; of mice and men. *Mol. Psychiatry* 12, 324–330. doi: 10.1038/sj.mp.4001979

Kassim, A. B. B. M., and Mohamed, N. H. B. (2019). The global prevalence and diagnosis of autism spectrum disorder (ASD) among young children. *Southeast Asia Psychol. J.* 7, 26–45.

Katz, R. J., and Roth, K. A. (1979). Stress induced grooming in the rat—an endorphin mediated syndrome. *Neurosci. Lett.* 13, 209–212. doi: 10.1016/0304-3940(79)90043-0

Kaufman, J., Yang, B.-Z., Douglas-Palumberi, H., Grasso, D., Lipschitz, D., Houshyar, S., et al. (2006). Brain-derived neurotrophic factor-5-HTTLPR gene interactions and environmental modifiers of depression in children. *Biol. Psychiatry* 59, 673–680. doi: 10.1016/j.biopsych.2005.10.026

Kazdoba, T. M., Leach, P. T., and Crawley, J. N. (2016). Behavioral phenotypes of genetic mouse models of autism. *Genes Brain Behav.* 15, 7–26. doi: 10.1111/gbb.12256

Kent, J. M., Kushner, S., Ning, X., Karcher, K., Ness, S., Aman, M., et al. (2013). Risperidone dosing in children and adolescents with autistic disorder: a double-blind, placebo-controlled study. *J. Autism Dev. Disord.* 43, 1773–1783. doi: 10.1007/s10803-012-1723-5

Khakh, B. S., and Sofroniew, M. V. (2015). Diversity of astrocyte functions and phenotypes in neural circuits. *Nat. Neurosci.* 18, 942–952. doi: 10.1038/nn.4043

Kim, S., Burette, A., Chung, H. S., Kwon, S.-K., Woo, J., Lee, H. W., et al. (2006). NGL family PSD-95-interacting adhesion molecules regulate excitatory synapse formation. *Nat. Neurosci.* 9, 1294–1301. doi: 10.1038/nn1763

Kim, T. W., Kang, Y. K., Park, Z. Y., Kim, Y.-H., Hong, S. W., Oh, S. J., et al. (2014). SH3RF2 functions as an oncogene by mediating PAK4 protein stability. *Carcinogenesis* 35, 624–634. doi: 10.1093/carcin/bgt338

Kim, Y. S., and Leventhal, B. L. (2015). Genetic epidemiology and insights into interactive genetic and environmental effects in autism spectrum disorders. *Biol. Psychiatry* 77, 66–74. doi: 10.1016/j.biopsych.2014.11.001

Kim, H., Lim, C.-S., and Kaang, B.-K. (2016). Neuronal mechanisms and circuits underlying repetitive behaviors in mouse models of autism spectrum disorder. *Behav. Brain Funct.* 12:3. doi: 10.1186/s12993-016-0087-y

Kim, E. C., Patel, J., Zhang, J., Soh, H., Rhodes, J. S., Tzingounis, A. V., et al. (2020). Heterozygous loss of epilepsy gene KCNQ2 alters social, repetitive and exploratory behaviors. *Genes Brain Behav.* 19:e12599. doi: 10.1111/gbb.12599

Kim, I. H., Rossi, M. A., Aryal, D. K., Racz, B., Kim, N., Uezu, A., et al. (2015). Spine pruning drives antipsychotic-sensitive locomotion *via* circuit control of striatal dopamine. *Nat. Neurosci.* 18, 883–891. doi: 10.1038/nn.4015

Kim, J.-W., Seung, H., Kim, K. C., Gonzales, E. L. T., Oh, H. A., Yang, S. M., et al. (2017). Agmatine rescues autistic behaviors in the valproic acid-induced animal model of autism. *Neuropharmacology* 113, 71–81. doi: 10.1016/j.neuropharm.2016.09.014

King, B. H., Hollander, E., Sikich, L., McCracken, J. T., Scahill, L., Bregman, J. D., et al. (2009). Lack of efficacy of citalopram in children with autism spectrum disorders and high levels of repetitive behavior: citalopram ineffective in children with autism. *Arch. Gen. Psychiatry* 66, 583–590. doi: 10.1001/archgenpsychiatry.2009.30

Kinsey, S. G., Bailey, M. T., Sheridan, J. F., Padgett, D. A., and Avitsur, R. (2007). Repeated social defeat causes increased anxiety-like behavior and alters splenocyte function in C57BL/6 and CD-1 mice. *Brain Behav. Immun.* 21, 458–466. doi: 10.1016/j.bbi.2006.11.001

Kiyatkin, E. A., and Rebec, G. V. (1999). Striatal neuronal activity and responsiveness to dopamine and glutamate after selective blockade of D1 and D2 dopamine receptors in freely moving rats. *J. Neurosci.* 19, 3594–3609. doi: 10.1523/JNEUROSCI.19-09-03594.1999

Klein, R. (2004). Eph/ephrin signaling in morphogenesis, neural development and plasticity. *Curr. Opin. Cell Biol.* 16, 580–589. doi: 10.1016/j.ceb.2004.07.002

Klein, R. (2009). Bidirectional modulation of synaptic functions by Eph/ephrin signaling. *Nat. Neurosci.* 12, 15–20. doi: 10.1038/nn.2231

Komorowska, J., and Pellis, S. M. (2004). Regulatory mechanisms underlying novelty-induced grooming in the laboratory rat. *Behav. Processes* 67, 287–293. doi: 10.1016/j.beproc.2004.05.001

Kouser, M., Speed, H. E., Dewey, C. M., Reimers, J. M., Widman, A. J., Gupta, N., et al. (2013). Loss of predominant Shank3 isoforms results in hippocampus-dependent impairments in behavior and synaptic transmission. *J. Neurosci.* 33, 18448–18468. doi: 10.1523/JNEUROSCI.3017-13.2013

Kreienkamp, H.-J. (2008). "Scaffolding proteins at the postsynaptic density: shank as the architectural framework," in *Protein-Protein Interactions as New Drug Targets*, eds E. Klussmann and J. Scott (Berlin: Springer), 365–380.

Krueger, D. D., Osterweil, E. K., Chen, S. P., Tye, L. D., and Bear, M. F. (2011). Cognitive dysfunction and prefrontal synaptic abnormalities in a mouse model of fragile X syndrome. *Proc. Natl. Acad. Sci. U S A* 108, 2587–2592. doi: 10.1073/pnas.1013855108

Kullander, K., and Klein, R. (2002). Mechanisms and functions of Eph and ephrin signalling. *Nat. Rev. Mol. Cell Biol.* 3, 475–486. doi: 10.1038/nrm856

Kumar, M., Duda, J. T., Hwang, W. T., Kenworthy, C., Ittyerah, R., Pickup, S., et al. (2014). High resolution magnetic resonance imaging for characterization of the neuroligin-3 knock-in mouse model associated with autism spectrum disorder. *PLoS One* 9:e109872. doi: 10.1371/journal.pone.0109872

Kwon, C.-H., Luikart, B. W., Powell, C. M., Zhou, J., Matheny, S. A., Zhang, W., et al. (2006). Pten regulates neuronal arborization and social interaction in mice. *Neuron* 50, 377–388. doi: 10.1016/j.neuron.2006.03.023

Lai, M.-C., Lombardo, M. V., and Baron-Cohen, S. (2014). Autism. *Lancet* 383, 896–910. doi: 10.1016/S0140-6736(13)61539-1

Langen, M., Leemans, A., Johnston, P., Ecker, C., Daly, E., Murphy, C. M., et al. (2012). Fronto-striatal circuitry and inhibitory control in autism: findings from diffusion tensor imaging tractography. *Cortex* 48, 183–193. doi: 10.1016/j.cortex.2011.05.018

LaSalle, J. M. (2013). Epigenomic strategies at the interface of genetic and environmental risk factors for autism. *J. Hum. Genet.* 58, 396–401. doi: 10.1038/jhg.2013.49

Lauber, E., Filice, F., and Schwaller, B. (2018). Dysregulation of parvalbumin expression in the *Cntnap2*$^{-/-}$ mouse model of autism spectrum disorder. *Front. Mol. Neurosci.* 11:262. doi: 10.3389/fnmol.2018.00262

Lauterborn, J. C., Rex, C. S., Kramár, E., Chen, L. Y., Pandyarajan, V., Lynch, G., et al. (2007). Brain-derived neurotrophic factor rescues synaptic plasticity in a mouse model of fragile X syndrome. *J. Neurosci.* 27, 10685–10694. doi: 10.1523/JNEUROSCI.2624-07.2007

Le, H., Ahn, B. J., Lee, H. S., Shin, A., Chae, S., Lee, S. Y., et al. (2017). Disruption of Ninjurin1 leads to repetitive and anxiety-like behaviors in mice. *Mol. Neurobiol.* 54, 7353–7368. doi: 10.1007/s12035-016-0207-6

Lee, B., Lee, K., Panda, S., Gonzales-Rojas, R., Chong, A., Bugay, V., et al. (2018). Nanoparticle delivery of CRISPR into the brain rescues a mouse model of fragile X syndrome from exaggerated repetitive behaviours. *Nat. Biomed. Eng.* 2, 497–507. doi: 10.1038/s41551-018-0252-8

Lee, H. J., Macbeth, A. H., Pagani, J. H., and Young, W. S. III. (2009). Oxytocin: the great facilitator of life. *Prog. Neurobiol.* 88, 127–151. doi: 10.1016/j.pneurobio.2009.04.001

Leonzino, M., Ponzoni, L., Braida, D., Gigliucci, V., Busnelli, M., Ceresini, I., et al. (2019). Impaired approach to novelty and striatal alterations in the oxytocin receptor deficient mouse model of autism. *Horm. Behav.* 114:104543. doi: 10.1016/j.yhbeh.2019.06.007

Lever, A. G., and Geurts, H. M. (2016). Psychiatric co-occurring symptoms and disorders in young, middle-aged, and older adults with autism spectrum disorder. *J. Autism Dev. Disord.* 46, 1916–1930. doi: 10.1007/s10803-016-2722-8

Levitt, P., and Campbell, D. B. (2009). The genetic and neurobiologic compass points toward common signaling dysfunctions in autism spectrum disorders. *J. Clin. Invest.* 119, 747–754. doi: 10.1172/JCI37934

Levy, D., Ronemus, M., Yamrom, B., Lee, Y.-H., Leotta, A., Kendall, J., et al. (2011). Rare *de novo* and transmitted copy-number variation in autistic spectrum disorders. *Neuron* 70, 886–897. doi: 10.1016/j.neuron.2011.05.015

Lewis, M. H., and Bodfish, J. W. (1998). Repetitive behavior disorders in autism. *Ment. Retardat. Dev.* 4, 80–89.

Lewis, M., and Kim, S.-J. (2009). The pathophysiology of restricted repetitive behavior. *J. Neurodev. Disord.* 1, 114–132. doi: 10.1007/s11689-009-9019-6

Lewis, M. H., Primiani, C. T., and Muehlmann, A. M. (2019). Targeting dopamine D2, adenosine A2A, and glutamate mGlu5 receptors to reduce repetitive behaviors in deer mice. *J. Pharmacol. Exp. Ther.* 369, 88–97. doi: 10.1124/jpet.118.256081

Lewis, M. H., Tanimura, Y., Lee, L. W., and Bodfish, J. W. (2007). Animal models of restricted repetitive behavior in autism. *Behav. Brain Res.* 176, 66–74. doi: 10.1016/j.bbr.2006.08.023

Li, Y.-C., Kellendonk, C., Simpson, E. H., Kandel, E. R., and Gao, W.-J. (2011). D2 receptor overexpression in the striatum leads to a deficit in inhibitory transmission and dopamine sensitivity in mouse prefrontal cortex. *Proc. Natl. Acad. Sci. U S A* 108, 12107–12112. doi: 10.1073/pnas.1109718108

Li, W., and Pozzo-Miller, L. (2020). Dysfunction of the corticostriatal pathway in autism spectrum disorders. *J. Neurosci. Res.* 98, 2130–2147. doi: 10.1002/jnr.24560

Lidstone, J., Uljarević, M., Sullivan, J., Rodgers, J., McConachie, H., Freeston, M., et al. (2014). Relations among restricted and repetitive behaviors, anxiety and sensory features in children with autism spectrum disorders. *Res. Autism Spectr. Disord.* 8, 82–92. doi: 10.1016/j.rasd.2013.10.001

Lim, J., Ryu, J., Kang, S., Noh, H. J., and Kim, C. H. (2019). Autism-like behaviors in male mice with a Pcdh19 deletion. *Mol. Brain* 12:95. doi: 10.1186/s13041-019-0519-3

Lin, J. C., Ho, W.-H., Gurney, A., and Rosenthal, A. (2003). The netrin-G1 ligand NGL-1 promotes the outgrowth of thalamocortical axons. *Nat. Neurosci.* 6, 1270–1276. doi: 10.1038/nn1148

Liu, J., and Moghaddam, B. (1995). Regulation of glutamate efflux by excitatory amino acid receptors: evidence for tonic inhibitory and phasic excitatory regulation. *J. Pharmacol. Exp. Ther.* 274, 1209–1215.

Lonetti, G., Angelucci, A., Morando, L., Boggio, E. M., Giustetto, M., and Pizzorusso, T. (2010). Early environmental enrichment moderates the behavioral and synaptic phenotype of MeCP2 null mice. *Biol. Psychiatry* 67, 657–665. doi: 10.1016/j.biopsych.2009.12.022

Lopez, B. R., Lincoln, A. J., Ozonoff, S., and Lai, Z. (2005). Examining the relationship between executive functions and restricted, repetitive symptoms of autistic disorder. *J. Autism Dev. Disord.* 35, 445–460. doi: 10.1007/s10803-005-5035-x

Lord, C., Brugha, T. S., Charman, T., Cusack, J., Dumas, G., Frazier, T., et al. (2020). Autism spectrum disorder. *Nat. Rev. Dis. Primers* 6:5. doi: 10.1038/s41572-019-0138-4

Lord, C., Cook, E. H., Leventhal, B. L., and Amaral, D. G. (2000). Autism spectrum disorders. *Neuron* 28, 355–363. doi: 10.1016/s0896-6273(00)00115-x

Lu, H., Ash, R. T., He, L., Kee, S. E., Wang, W., Yu, D., et al. (2016). Loss and gain of MeCP2 cause similar hippocampal circuit dysfunction that is rescued by deep brain stimulation in a Rett syndrome mouse model. *Neuron* 91, 739–747. doi: 10.1016/j.neuron.2016.07.018

Lugo, J. N., Smith, G. D., Arbuckle, E. P., White, J., Holley, A. J., Floruta, C. M., et al. (2014). Deletion of PTEN produces autism-like behavioral deficits and alterations in synaptic proteins. *Front. Mol. Neurosci.* 7:27. doi: 10.3389/fnmol.2014.00027

Maenner, M. J., Shaw, K. A., Baio, J., Washington, A., Patrick, M., DiRienzo, M., et al (2020). Prevalence of autism spectrum disorder among children aged 8 years—autism and developmental disabilities monitoring network, 11 sites, United States, 2016. *MMWR Surveill. Summ.* 69:1. doi: 10.15585/mmwr.ss6904a1

Mahmood, U., Ahn, S., Yang, E.-J., Choi, M., Kim, H., Regan, P., et al. (2018). Dendritic spine anomalies and PTEN alterations in a mouse model of VPA-induced autism spectrum disorder. *Pharmacol. Res.* 128, 110–121. doi: 10.1016/j.phrs.2017.08.006

Mahmoud, S., Gharagozloo, M., Simard, C., and Gris, D. (2019). Astrocytes maintain glutamate homeostasis in the CNS by controlling the balance between glutamate uptake and release. *Cells* 8:184. doi: 10.3390/cells8020184

Malone, R. P., and Waheed, A. (2009). The role of antipsychotics in the management of behavioural symptoms in children and adolescents with autism. *Drugs* 69, 535–548. doi: 10.2165/00003495-200969050-00003

Maneeton, N., Maneeton, B., Putthisri, S., Woottiluk, P., Narkpongphun, A., and Srisurapanont, M. (2018). Risperidone for children and adolescents with autism spectrum disorder: a systematic review. *Neuropsychiatr. Dis. Treat.* 14, 1811–1820. doi: 10.2147/NDT.S151802

Mardirossian, S., Rampon, C., Salvert, D., Fort, P., and Sarda, N. (2009). Impaired hippocampal plasticity and altered neurogenesis in adult Ube3a maternal deficient mouse model for Angelman syndrome. *Exp. neurol.* 220, 341–348. doi: 10.1016/j.expneurol.2009.08.035

Martin, E. A., Muralidhar, S., Wang, Z., Cervantes, D. C., Basu, R., Taylor, M. R., et al. (2015). The intellectual disability gene Kirrel3 regulates target-specific mossy fiber synapse development in the hippocampus. *eLife* 4:e09395. doi: 10.7554/eLife.09395

Martínez, A., and Soriano, E. (2005). Functions of ephrin/Eph interactions in the development of the nervous system: emphasis on the hippocampal system. *Brain Res. Rev.* 49, 211–226. doi: 10.1016/j.jenvman.2020.111781

Masi, A., DeMayo, M. M., Glozier, N., and Guastella, A. J. (2017). An overview of autism spectrum disorder, heterogeneity and treatment options. *Neurosci. Bull.* 33, 183–193. doi: 10.1007/s12264-017-0100-y

Matsukawa, H., Akiyoshi-Nishimura, S., Zhang, Q., Luján, R., Yamaguchi, K., Goto, H., et al. (2014). Netrin-G/NGL complexes encode functional synaptic diversification. *J. Neurosci.* 34, 15779–15792. doi: 10.1523/JNEUROSCI.1141-14.2014

Matsuki, M., Kabara, M., Saito, Y., Shimamura, K., Minoshima, A., Nishimura, M., et al. (2015). Ninjurin1 is a novel factor to regulate angiogenesis through the function of pericytes. *Circ. J.* 79, 1363–1371. doi: 10.1253/circj.CJ-14-1376

Matta, S. M., Moore, Z., Walker, F. R., Hill-Yardin, E. L., and Crack, P. J. (2020). An altered glial phenotype in the $NL3^{R451C}$ mouse model of autism. *Sci. Rep.* 10:14492. doi: 10.1038/s41598-020-71171-y

Mazurek, M. O., Vasa, R. A., Kalb, L. G., Kanne, S. M., Rosenberg, D., Keefer, A., et al. (2013). Anxiety, sensory over-responsivity and gastrointestinal problems in children with autism spectrum disorders. *J. Abnorm. Child Psychol.* 41, 165–176. doi: 10.1007/s10802-012-9668-x

Mazzocco, M. M., Pulsifer, M., Fiumara, A., Cocuzza, M., Nigro, F., Incorpora, G., et al. (1998). Brief report: autistic behaviors among children with fragile X or Rett syndrome: implications for the classification of pervasive developmental disorder. *J. Autism and Dev. Disord.* 28, 321–328. doi: 10.1023/a:1026012703449

McBride, P. A., Anderson, G. M., Hertzig, M. E., Sweeney, J. A., Kream, J., Cohen, D. J., et al. (1989). Serotonergic responsivity in male young adults with autistic disorder: results of a pilot study. *Arch. Gen. Psychiatry* 46, 213–221. doi: 10.1001/archpsyc.1989.01810030019003

McCracken, J. T., McGough, J., Shah, B., Cronin, P., Hong, D., Aman, M. G., et al. (2002). Risperidone in children with autism and serious behavioral problems. *N. Engl. J. Med.* 347, 314–321. doi: 10.1056/NEJMoa013171

McDougle, C., Naylor, S. T., Cohen, D. J., Aghajanian, G. K., Heninger, G. R., and Price, L. H. (1996). Effects of tryptophan depletion in drug-free adults with autistic disorder. *Arch. Gen. Psychiatry* 53, 993–1000. doi: 10.1001/archpsyc.1996.01830110029004

McDougle, C. J., Scahill, L., Aman, M. G., McCracken, J. T., Tierney, E., Davies, M., et al. (2005). Risperidone for the core symptom domains of autism: results from the study by the autism network of the research units on pediatric psychopharmacology. *Am. J. Psychiatry* 162, 1142–1148. doi: 10.1176/appi.ajp.162.6.1142

McDougle, C. J., Stigler, K. A., Erickson, C. A., and Posey, D. J. (2008). Atypical antipsychotics in children and adolescents with autistic and other pervasive developmental disorders. *J. Clin. Psychiatry* 69, 15–20.

McFarlane, H. G., Kusek, G., Yang, M., Phoenix, J., Bolivar, V., and Crawley, J. (2008). Autism-like behavioral phenotypes in BTBR T+tf/J mice. *Genes Brain Behav.* 7, 152–163. doi: 10.1111/j.1601-183X.2007.00330.x

McGrath, M. J., Campbell, K. M., Veldman, M. B., and Burton, F. H. (1999). Anxiety in a transgenic mouse model of cortical-limbic neuro-potentiated compulsive behavior. *Behav. Pharmacol.* 10, 435–443. doi: 10.1097/00008877-199909000-00001

McNaughton, C. H., Moon, J., Strawderman, M. S., Maclean, K. N., Evans, J., and Strupp, B. J. (2008). Evidence for social anxiety and impaired social cognition in a mouse model of fragile X syndrome. *Behav. Neurosci.* 122, 293–300. doi: 10.1037/0735-7044.122.2.293

McPheeters, M. L., Warren, Z., Sathe, N., Bruzek, J. L., Krishnaswami, S., Jerome, R. N., et al. (2011). A systematic review of medical treatments for children with autism spectrum disorders. *Pediatrics* 127, e1312–e1321. doi: 10.1542/peds.2011-0427

Mehta, M. V., Gandal, M. J., and Siegel, S. J. (2011). mGluR5-antagonist mediated reversal of elevated stereotyped, repetitive behaviors in the VPA model of autism. *PLoS One* 6:e26077. doi: 10.1371/journal.pone.0026077

Mei, Y., Monteiro, P., Zhou, Y., Kim, J.-A., Gao, X., Fu, Z., et al. (2016). Adult restoration of Shank3 expression rescues selective autistic-like phenotypes. *Nature* 530, 481–484. doi: 10.1038/nature16971

Meikle, L., Pollizzi, K., Egnor, A., Kramvis, I., Lane, H., Sahin, M., et al. (2008). Response of a neuronal model of tuberous sclerosis to mammalian target of rapamycin (mTOR) inhibitors: effects on mTORC1 and Akt signaling lead to improved survival and function. *J. Neurosci.* 28, 5422–5432. doi: 10.1523/JNEUROSCI.0955-08.2008

Meikle, L., Talos, D. M., Onda, H., Pollizzi, K., Rotenberg, A., Sahin, M., et al. (2007). A mouse model of tuberous sclerosis: neuronal loss of Tsc1 causes dysplastic and ectopic neurons, reduced myelination, seizure activity and limited survival. *J. Neurosci.* 27, 5546–5558. doi: 10.1523/JNEUROSCI.5540-06.2007

Mejias, R., Adamczyk, A., Anggono, V., Niranjan, T., Thomas, G. M., Sharma, K., et al. (2011). Gain-of-function glutamate receptor interacting protein 1 variants

alter GluA2 recycling and surface distribution in patients with autism. *Proc. Natl. Acad. Sci. U S A* 108, 4920–4925. doi: 10.1073/pnas.1102233108

Mejias, R., Chiu, S.-L., Han, M., Rose, R., Gil-Infante, A., Zhao, Y., et al. (2019). Purkinje cell-specific Grip1/2 knockout mice show increased repetitive self-grooming and enhanced mGluR5 signaling in cerebellum. *Neurobiol. Dis.* 132:104602. doi: 10.1016/j.nbd.2019.104602

Mercer, A. A., Palarz, K. J., Tabatadze, N., Woolley, C. S., and Raman, I. M. (2016). Sex differences in cerebellar synaptic transmission and sex-specific responses to autism-linked Gabrb3 mutations in mice. *eLife* 5:e07596. doi: 10.7554/eLife.07596

Meyza, K., and Blanchard, D. (2017). The BTBR mouse model of idiopathic autism-current view on mechanisms. *Neurosci. Biobehav. Rev.* 76, 99–110. doi: 10.1016/j.neubiorev.2016.12.037

Miral, S., Gencer, O., Inal-Emiroglu, F. N., Baykara, B., Baykara, A., and Dirik, E. (2008). Risperidone versus haloperidol in children and adolescents with AD: a randomized, controlled, double-blind trial. *Eur. Child Adolesc. Psychiatry* 17, 1–8. doi: 10.1007/s00787-007-0620-5

Modabbernia, A., Velthorst, E., and Reichenberg, A. (2017). Environmental risk factors for autism: an evidence-based review of systematic reviews and meta-analyses. *Mol. Autism* 8:13. doi: 10.1186/s13229-017-0121-4

Modi, B., Pimpinella, D., Pazienti, A., Zacchi, P., Cherubini, E., and Griguoli, M. (2019). Possible implication of the CA2 hippocampal circuit in social cognition deficits observed in the neuroligin 3 knock-out mouse, a non-syndromic animal model of autism. *Front. Psychiatry* 10:513. doi: 10.3389/fpsyt.2019.00513

Molofsky, A. V., Krenick, R., Ullian, E., Tsai, H.-H., Deneen, B., Richardson, W. D., et al. (2012). Astrocytes and disease: a neurodevelopmental perspective. *Genes Dev.* 26, 891–907. doi: 10.1101/gad.188326.112

Monteiro, P., and Feng, G. (2017). SHANK proteins: roles at the synapse and in autism spectrum disorder. *Nat. Rev. Neurosci.* 18, 147–157. doi: 10.1038/nrn.2016.183

Moon, J.-S., Beaudin, A., Verosky, S., Driscoll, L., Weiskopf, M., Levitsky, D., et al. (2006). Attentional dysfunction, impulsivity, and resistance to change in a mouse model of fragile X syndrome. *Behav. Neurosci.* 120, 1367–1369. doi: 10.1037/0735-7044.120.6.1367

Morency, M. A., Stewart, R. J., and Beninger, R. J. (1985). Effects of unilateral microinjections of sulpiride into the medial prefrontal cortex on circling behavior of rats. *Prog. Neuropsychopharmacol. Biol. Psychiatry* 9, 735–738. doi: 10.1016/0278-5846(85)90051-x

Moretti, P., Bouwknecht, J. A., Teague, R., Paylor, R., and Zoghbi, H. Y. (2005). Abnormalities of social interactions and home-cage behavior in a mouse model of Rett syndrome. *Hum. Mol. Genet.* 14, 205–220. doi: 10.1093/hmg/ddi016

Morikawa, Y., Komori, T., Hisaoka, T., Ueno, H., Kitamura, T., and Senba, E. (2007). Expression of mKirre in the developing sensory pathways: its close apposition to nephrin-expressing cells. *Neuroscience* 150, 880–886. doi: 10.1016/j.neuroscience.2007.10.013

Moss, J., and Howlin, P. (2009). Autism spectrum disorders in genetic syndromes: implications for diagnosis, intervention and understanding the wider autism spectrum disorder population. *J. Intellect. Disabil. Res.* 53, 852–873. doi: 10.1111/j.1365-2788.2009.01197.x

Moy, S. S., and Nadler, J. J. (2008). Advances in behavioral genetics: mouse models of autism. *Mol. Psychiatry* 13, 4–26. doi: 10.1038/sj.mp.4002082

Moy, S. S., Nadler, J. J., Magnuson, T. R., and Crawley, J. N. (2006). Mouse models of autism spectrum disorders: the challenge for behavioral genetics. *Am. J. Med. Genet. C Semin. Med. Genet.* 142, 40–51. doi: 10.1002/ajmg.c.30081

Moy, S. S., Nadler, J. J., Poe, M. D., Nonneman, R. J., Young, N. B., Koller, B. H., et al. (2008a). Development of a mouse test for repetitive, restricted behaviors: relevance to autism. *Behav. Brain Res.* 188, 178–194. doi: 10.1016/j.bbr.2007.10.029

Moy, S. S., Nadler, J. J., Young, N. B., Nonneman, R. J., Segall, S. K., Andrade, G. M., et al. (2008b). Social approach and repetitive behavior in eleven inbred mouse strains. *Behav. Brain Res.* 191, 118–129. doi: 10.1016/j.bbr.2008.03.015

Moy, S. S., Nadler, J. J., Young, N. B., Perez, A., Holloway, L. P., Barbaro, R. P., et al. (2007). Mouse behavioral tasks relevant to autism: phenotypes of 10 inbred strains. *Behav. Brain Res.* 176, 4–20. doi: 10.1016/j.bbr.2006.07.030

Muehlmann, A., Edington, G., Mihalik, A., Buchwald, Z., Koppuzha, D., Korah, M., et al. (2012). Further characterization of repetitive behavior in C58 mice: developmental trajectory and effects of environmental enrichment. *Behav. Brain Res.* 235, 143–149. doi: 10.1016/j.bbr.2012.07.041

Muhle, R., Trentacoste, S. V., and Rapin, I. (2004). The genetics of autism. *Pediatrics* 113, e472–e486. doi: 10.1542/peds.113.5.e472

Murai, K. K., Nguyen, L. N., Irie, F., Yamaguchi, Y., and Pasquale, E. B. (2003). Control of hippocampal dendritic spine morphology through ephrin-A3/EphA4 signaling. *Nat. Neurosci.* 6, 153–160. doi: 10.1038/nn994

Nagarajan, N., Jones, B. W., West, P. J., Marc, R. E., and Capecchi, M. R. (2018). Corticostriatal circuit defects in Hoxb8 mutant mice. *Mol. Psychiatry* 23, 1868–1877. doi: 10.1038/mp.2017.180

Nardone, S., and Elliott, E. (2016). The interaction between the immune system and epigenetics in the etiology of autism spectrum disorders. *Front. Neurosci.* 10:329. doi: 10.3389/fnins.2016.00329

Naviaux, J. C., Wang, L., Li, K., Bright, A. T., Alaynick, W. A., Williams, K. R., et al. (2015). Antipurinergic therapy corrects the autism-like features in the Fragile X (fMRI knockout) mouse model. *Mol. Autism* 6:1. doi: 10.1186/2040-2392-6-1

Neumann-Haefelin, E., Kramer-Zucker, A., Slanchev, K., Hartleben, B., Noutsou, F., Martin, K., et al. (2010). A model organism approach: defining the role of Neph proteins as regulators of neuron and kidney morphogenesis. *Hum. Mol. Genet.* 19, 2347–2359. doi: 10.1093/hmg/ddq108

Nimmo-Smith, V., Heuvelman, H., Dalman, C., Lundberg, M., Idring, S., Carpenter, P., et al. (2020). Anxiety disorders in adults with autism spectrum disorder: a population-based study. *J. Autism Dev. Disord.* 50, 308–318. doi: 10.1007/s10803-019-04234-3

Nin, M. S., Ferri, M. K., Couto-Pereira, N. S., Souza, M. F., Azeredo, L. A., Agnes, G., et al. (2012). The effect of intra-nucleus accumbens administration of allopregnanolone on δ and γ2 $GABA_A$ receptor subunit mRNA expression in the hippocampus and on depressive-like and grooming behaviors in rats. *Pharmacol. Biochem. Behav.* 103, 359–366. doi: 10.1016/j.pbb.2012.09.002

Nishida, K., Nakayama, K., Yoshimura, S., and Murakami, F. (2011). Role of Neph2 in pontine nuclei formation in the developing hindbrain. *Mol. Cell. Neurosci.* 46, 662–670. doi: 10.1016/j.mcn.2011.01.007

Niu, M., Han, Y., Dy, A. B. C., Du, J., Jin, H., Qin, J., et al. (2017). Autism symptoms in fragile X syndrome. *J. Child Neurol.* 32, 903–909. doi: 10.1177/0883073817712875

Njung'e, K., and Handley, S. L. (1991). Evaluation of marble-burying behavior as a model of anxiety. *Pharmacol. Biochem. Behav.* 38, 63–67. doi: 10.1016/0091-3057(91)90590-x

Nolan, S. O., and Lugo, J. N. (2018). Reversal learning paradigm reveals deficits in cognitive flexibility in the fMR1 knockout male mouse. *F1000Res.* 7:711. doi: 10.12688/f1000research.14969.1

Nosyreva, E. D., and Huber, K. M. (2006). Metabotropic receptor-dependent long-term depression persists in the absence of protein synthesis in the mouse model of fragile X syndrome. *J. Neurophysiol.* 95, 3291–3295. doi: 10.1152/jn.01316.2005

O'Leary, T. P., Gunn, R. K., and Brown, R. E. (2013). What are we measuring when we test strain differences in anxiety in mice? *Behav. Genet.* 43, 34–50. doi: 10.1007/s10519-012-9572-8

Obeso, J. A., and Lanciego, J. L. (2011). Past, present, and future of the pathophysiological model of the Basal Ganglia. *Front. Neuroanat.* 5:39. doi: 10.3389/fnana.2011.00039

Orefice, L. L., Zimmerman, A. L., Chirila, A. M., Sleboda, S. J., Head, J. P., and Ginty, D. D. (2016). Peripheral mechanosensory neuron dysfunction underlies tactile and behavioral deficits in mouse models of ASDs. *Cell* 166, 299–313. doi: 10.1016/j.cell.2016.05.033

Page, D. T., Kuti, O. J., Prestia, C., and Sur, M. (2009). Haploinsufficiency for Pten and serotonin transporter cooperatively influences brain size and social behavior. *Proc. Natl. Acad. Sci. U S A* 106, 1989–1994. doi: 10.1073/pnas.0804428106

Palmen, S. J., and van Engeland, H. (2004). Review on structural neuroimaging findings in autism. *J. Neural Transm.* 111, 903–929. doi: 10.1007/s00702-003-0068-9

Palmer, A., and Klein, R. (2003). Multiple roles of ephrins in morphogenesis, neuronal networking, and brain function. *Genes Dev.* 17, 1429–1450. doi: 10.1101/gad.1093703

Panayotis, N., Pratte, M., Borges-Correia, A., Ghata, A., Villard, L., and Roux, J.-C. (2011). Morphological and functional alterations in the substantia nigra pars compacta of the Mecp2-null mouse. *Neurobiol. Dis.* 41, 385–397. doi: 10.1016/j.nbd.2010.10.006

Parr-Brownlie, L. C., and Hyland, B. I. (2005). Bradykinesia induced by dopamine D2 receptor blockade is associated with reduced motor cortex activity in the rat. *J. Neurosci.* 25, 5700–5709. doi: 10.1523/JNEUROSCI.0523-05.2005

Paylor, R., Yuva-Paylor, L. A., Nelson, D. L., and Spencer, C. M. (2008). Reversal of sensorimotor gating abnormalities in fMR1 knockout mice carrying a human Fmr1 transgene. *Behav. Neurosci.* 122, 1371–1371. doi: 10.1037/a0013047

Peça, J., Feliciano, C., Ting, J. T., Wang, W., Wells, M. F., Venkatraman, T. N., et al. (2011). Shank3 mutant mice display autistic-like behaviours and striatal dysfunction. *Nature* 472, 437–442. doi: 10.1038/nature09965

Peier, A. M., McIlwain, K. L., Kenneson, A., Warren, S. T., Paylor, R., and Nelson, D. L. (2000). (Over)correction of fMR1 deficiency with YAC transgenics: behavioral and physical features. *Hum. Mol. Genet.* 9, 1145–1159. doi: 10.1093/hmg/9.8.1145

Peixoto, R. T., Wang, W., Croney, D. M., Kozorovitskiy, Y., and Sabatini, B. L. (2016). Early hyperactivity and precocious maturation of corticostriatal circuits in Shank3B$^{-/-}$ mice. *Nat. Neurosci.* 19, 716–724. doi: 10.1038/nn.4260

Peñagarikano, O., Abrahams, B. S., Herman, E. I., Winden, K. D., Gdalyahu, A., Dong, H., et al. (2011). Absence of CNTNAP2 leads to epilepsy, neuronal migration abnormalities, and core autism-related deficits. *Cell* 147, 235–246. doi: 10.1016/j.cell.2011.08.040

Perry, W., Minassian, A., Lopez, B., Maron, L., and Lincoln, A. (2007). Sensorimotor gating deficits in adults with autism. *Biol. Psychiatry* 61, 482–486. doi: 10.1016/j.biopsych.2005.09.025

Persico, A. M., and Bourgeron, T. (2006). Searching for ways out of the autism maze: genetic, epigenetic and environmental clues. *Trends Neurosci.* 29, 349–358. doi: 10.1016/j.tins.2006.05.010

Petrenko, A., Gulyaev, M., Tischenko, D., Petuchov, V., and Abbasova, K. (2013). Effects of prenatal treatment with valproic acid (VPA) on offspring of epileptic adult rats: MRI investigation. *J. Neurosci. Neuroengineering* 2, 1–7. doi: 10.1166/jnsne.2013.1085

Pham, D. H., Tan, C. C., Homan, C. C., Kolc, K. L., Corbett, M. A., McAninch, D., et al. (2017). Protocadherin 19 (PCDH19) interacts with paraspeckle protein NONO to co-regulate gene expression with estrogen receptor alpha (ERα). *Hum. Mol. Genet.* 26, 2042–2052. doi: 10.1093/hmg/ddx094

Pierce, K., and Courchesne, E. (2001). Evidence for a cerebellar role in reduced exploration and stereotyped behavior in autism. *Biol. Psychiatry* 49, 655–664. doi: 10.1016/s0006-3223(00)01008-8

Pietropaolo, S., Guilleminot, A., Martin, B., d'Amato, F. R., and Crusio, W. E. (2011). Genetic-background modulation of core and variable autistic-like symptoms in Fmr1 knock-out mice. *PLoS One* 6:e17073. doi: 10.1371/journal.pone.0017073

Pignatelli, M., Piccinin, S., Molinaro, G., Di Menna, L., Riozzi, B., Cannella, M., et al. (2014). Changes in mGlu5 receptor-dependent synaptic plasticity and coupling to homer proteins in the hippocampus of Ube3A hemizygous mice modeling angelman syndrome. *J. Neurosci.* 34, 4558–4566. doi: 10.1523/JNEUROSCI.1846-13.2014

Pobbe, R. L., Defensor, E. B., Pearson, B. L., Bolivar, V. J., Blanchard, D. C., and Blanchard, R. J. (2011). General and social anxiety in the BTBR T+ tf/J mouse strain. *Behav. Brain Res.* 216, 446–451. doi: 10.1016/j.bbr.2010.08.039

Pobbe, R. L., Pearson, B. L., Defensor, E. B., Bolivar, V. J., Young, W. S. III., Lee, H. J., et al. (2012). Oxytocin receptor knockout mice display deficits in the expression of autism-related behaviors. *Horm. Behav.* 61, 436–444. doi: 10.1016/j.yhbeh.2011.10.010

Portmann, T., Yang, M., Mao, R., Panagiotakos, G., Ellegood, J., Dolen, G., et al. (2014). Behavioral abnormalities and circuit defects in the basal ganglia of a mouse model of 16p11. 2 deletion syndrome. *Cell Rep.* 7, 1077–1092. doi: 10.1016/j.celrep.2014.03.036

Postorino, V., Kerns, C. M., Vivanti, G., Bradshaw, J., Siracusano, M., and Mazzone, L. (2017). Anxiety disorders and obsessive-compulsive disorder in individuals with autism spectrum disorder. *Curr. Psychiatry Rep.* 19:92. doi: 10.1007/s11920-017-0846-y

Powell, S. B., Newman, H. A., McDonald, T. A., Bugenhagen, P., and Lewis, M. H. (2000). Development of spontaneous stereotyped behavior in deer mice: effects of early and late exposure to a more complex environment. *Dev. Psychobiol.* 37, 100–108. doi: 10.1002/1098-2302(200009)37:2<100::AID-DEV5>3.3.CO;2-Y

Presti, M. F., Gibney, B. C., and Lewis, M. H. (2004). Effects of intrastriatal administration of selective dopaminergic ligands on spontaneous stereotypy in mice. *Physiol. Behav.* 80, 433–439. doi: 10.1016/j.physbeh.2003.09.008

Presti, M. F., Mikes, H. M., and Lewis, M. H. (2003). Selective blockade of spontaneous motor stereotypy *via* intrastriatal pharmacological manipulation. *Pharmacol. Biochem. Behav.* 74, 833–839. doi: 10.1016/s0091-3057(02)01081-x

Prince, J. E., Brignall, A. C., Cutforth, T., Shen, K., and Cloutier, J.-F. (2013). Kirrel3 is required for the coalescence of vomeronasal sensory neuron axons into glomeruli and for male-male aggression. *Development* 140, 2398–2408. doi: 10.1242/dev.087262

Qiu, S., Aldinger, K. A., and Levitt, P. (2012). Modeling of autism genetic variations in mice: focusing on synaptic and microcircuit dysfunctions. *Dev. Neurosci.* 34, 88–100. doi: 10.1159/000336644

Qualls-Creekmore, E., and Münzberg, H. (2018). Modulation of feeding and associated behaviors by lateral hypothalamic circuits. *Endocrinology* 159, 3631–3642. doi: 10.1210/en.2018-00449

Quintero-Rivera, F., Sharifi-Hannauer, P., and Martinez-Agosto, J. A. (2010). Autistic and psychiatric findings associated with the 3q29 microdeletion syndrome: case report and review. *Am. J. Med. Genet. A* 152, 2459–2467. doi: 10.1128/JCM.02955-20

Rademacher, S., and Eickholt, B. J. (2019). PTEN in autism and neurodevelopmental disorders. *Cold Spring Harb. Perspect. Med.* 9:a036780. doi: 10.1101/cshperspect.a036780

Radyushkin, K., Hammerschmidt, K., Boretius, S., Varoqueaux, F., El-Kordi, A., Ronnenberg, A., et al. (2009). Neuroligin-3-deficient mice: model of a monogenic heritable form of autism with an olfactory deficit. *Genes Brain Behav.* 8, 416–425. doi: 10.1111/j.1601-183X.2009.00487.x

Ramaswami, G., and Geschwind, D. H. (2018). Genetics of autism spectrum disorder *Handb. Clin. Neurol.* 147, 321–329. doi: 10.1016/B978-0-444-63233-3.00021-X

Reiner, A., and Anderson, K. D. (1990). The patterns of neurotransmitter and neuropeptide co-occurrence among striatal projection neurons: conclusions based on recent findings. *Brain Res. Rev.* 15, 251–265. doi: 10.1016/0165-0173(90)90003-7

Reiss, A. L., Faruque, F., Naidu, S., Abrams, M., Beaty, T., Bryan, R. N., et al. (1993). Neuroanatomy of Rett syndrome: a volumetric imaging study. *Ann. Neurol.* 34, 227–234. doi: 10.1002/ana.410340220

Reis-Silva, T. M., Sandini, T. M., Calefi, A. S., Orlando, B. C. G., Moreira, N., Lima, A. P. N., et al. (2019). Stress resilience evidenced by grooming behaviour and dopamine levels in male mice selected for high and low immobility using the tail suspension test. *Eur. J. Neurosci.* 50, 2942–2954. doi: 10.1111/ejn.14409

Reith, R. M., McKenna, J., Wu, H., Hashmi, S. S., Cho, S.-H., Dash, P. K., et al. (2013). Loss of Tsc2 in Purkinje cells is associated with autistic-like behavior in a mouse model of tuberous sclerosis complex. *Neurobiol. Dis.* 51, 93–103. doi: 10.1016/j.nbd.2012.10.014

Reynolds, S., Urruela, M., and Devine, D. P. (2013). Effects of environmental enrichment on repetitive behaviors in the BTBR T+tf/J mouse model of autism. *Autism Res.* 6, 337–343. doi: 10.1002/aur.1298

Richler, J., Bishop, S. L., Kleinke, J. R., and Lord, C. (2007). Restricted and repetitive behaviors in young children with autism spectrum disorders. *J. Autism Dev. Disord.* 37, 73–85. doi: 10.1007/s10803-006-0332-6

Rinaldi, T., Kulangara, K., Antoniello, K., and Markram, H. (2007). Elevated NMDA receptor levels and enhanced postsynaptic long-term potentiation induced by prenatal exposure to valproic acid. *Proc. Natl. Acad. Sci. U S A* 104, 13501–13506. doi: 10.1073/pnas.0704391104

Rodenas-Cuadrado, P., Ho, J., and Vernes, S. C. (2014). Shining a light on CNTNAP2: complex functions to complex disorders. *Eur. J. Hum. Genet.* 22, 171–178. doi: 10.1038/ejhg.2013.100

Roeling, T., Veening, J., Peters, J., Vermelis, M., and Nieuwenhuys, R. (1993). Efferent connections of the hypothalamic "grooming area" in the rat. *Neuroscience* 56, 199–225. doi: 10.1016/0306-4522(93)90574-y

Rojas, D. C., Peterson, E., Winterrowd, E., Reite, M. L., Rogers, S. J., and Tregellas, J. R. (2006). Regional gray matter volumetric changes in autism

associated with social and repetitive behavior symptoms. *BMC Psychiatry* 6:56. doi: 10.1186/1471-244X-6-56

Ronemus, M., Iossifov, I., Levy, D., and Wigler, M. (2014). The role of *de novo* mutations in the genetics of autism spectrum disorders. *Nat. Rev. Genet.* 15, 133–141. doi: 10.1038/nrg3585

Rothwell, P. E., Fuccillo, M. V., Maxeiner, S., Hayton, S. J., Gokce, O., Lim, B. K., et al. (2014). Autism-associated neuroligin-3 mutations commonly impair striatal circuits to boost repetitive behaviors. *Cell* 158, 198–212. doi: 10.1016/j.cell.2014.04.045

Roullet, F. I., and Crawley, J. N. (2011). Mouse models of autism: testing hypotheses about molecular mechanisms. *Curr. Top. Behav. Neurosci.* 7, 187–212. doi: 10.1007/7854_2010_113

Rubenstein, J. L. (2010). Three hypotheses for developmental defects that may underlie some forms of autism spectrum disorder. *Curr. Opin. Neurol.* 23, 118–123. doi: 10.1097/WCO.0b013e328336eb13

Russell, K. M., Frost, K. M., and Ingersoll, B. (2019). The relationship between subtypes of repetitive behaviors and anxiety in children with autism spectrum disorder. *Res. Autism Spectr. Disord.* 62, 48–54. doi: 10.1007/s10803-016-2884-4

Russell, A. J., Murphy, C. M., Wilson, E., Gillan, N., Brown, C., Robertson, D. M., et al. (2016). The mental health of individuals referred for assessment of autism spectrum disorder in adulthood: a clinic report. *Autism* 20, 623–627. doi: 10.1177/1362361315604271

Ryan, S. G., Chance, P. F., Zou, C.-H., Spinner, N. B., Golden, J. A., and Smietana, S. (1997). Epilepsy and mental retardation limited to females: an X-linked dominant disorder with male sparing. *Nat. Genet.* 17, 92–95. doi: 10.1038/ng0997-92

Ryan, B. C., Young, N. B., Crawley, J. N., Bodfish, J. W., and Moy, S. S. (2010). Social deficits, stereotypy and early emergence of repetitive behavior in the C58/J inbred mouse strain. *Behav. Brain Res.* 208, 178–188. doi: 10.1016/j.bbr.2009.11.031

Sagar, A., Bishop, J. R., Tessman, D. C., Guter, S., Martin, C. L., and Cook, E. H. (2013). Co-occurrence of autism, childhood psychosis and intellectual disability associated with a *de novo* 3q29 microdeletion. *Am. J. Med. Genet. A* 161, 845–849. doi: 10.1002/ajmg.a.35754

Sajdyk, T. J., and Shekhar, A. (2000). Sodium lactate elicits anxiety in rats after repeated GABA receptor blockade in the basolateral amygdala. *Eur. J. Pharmacol.* 394, 265–273. doi: 10.1016/s0014-2999(00)00128-x

Sala, C., Vicidomini, C., Bigi, I., Mossa, A., and Verpelli, C. (2015). Shank synaptic scaffold proteins: keys to understanding the pathogenesis of autism and other synaptic disorders. *J. Neurochem.* 135, 849–858. doi: 10.1111/jnc.13232

Sala, M., Braida, D., Lentini, D., Busnelli, M., Bulgheroni, E., Capurro, V., et al. (2011). Pharmacologic rescue of impaired cognitive flexibility, social deficits, increased aggression and seizure susceptibility in oxytocin receptor null mice: a neurobehavioral model of autism. *Biol. Psychiatry* 69, 875–882. doi: 10.1016/j.biopsych.2010.12.022

Samaco, R. C., Fryer, J. D., Ren, J., Fyffe, S., Chao, H.-T., Sun, Y., et al. (2008). A partial loss of function allele of methyl-CpG-binding protein 2 predicts a human neurodevelopmental syndrome. *Hum. Mol. Genet.* 17, 1718–1727. doi: 10.1093/hmg/ddn062

Sangu, N., Shimojima, K., Takahashi, Y., Ohashi, T., Tohyama, J., and Yamamoto, T. (2017). A 7q31.33q32.1 microdeletion including LRRC4 and *GRM8* is associated with severe intellectual disability and characteristics of autism. *Hum. Genome Var.* 4:17001. doi: 10.1038/hgv.2017.1

Sansal, I., and Sellers, W. R. (2004). The biology and clinical relevance of the PTEN tumor suppressor pathway. *J. Clin. Oncol.* 22, 2954–2963. doi: 10.1200/JCO.2004.02.141

Satterstrom, F. K., Kosmicki, J. A., Wang, J., Breen, M. S., De Rubeis, S., An, J.-Y., et al. (2020). Large-scale exome sequencing study implicates both developmental and functional changes in the neurobiology of autism. *Cell* 180, 568.e23–584.e23. doi: 10.1016/j.cell.2019.12.036

Scahill, L., and Challa, S. A. (2016). "Repetitive behavior in children with autism spectrum disorder: similarities and differences with obsessive-compulsive disorder," in *Psychiatric Symptoms and Comorbidities in Autism Spectrum Disorder*, eds L. Mazzone and B. Vitiello (Cham: Springer), 39–50.

Scahill, L., Koenig, K., Carroll, D. H., and Pachler, M. (2007). Risperidone approved for the treatment of serious behavioral problems in children with autism. *J. Child Adolesc. Psychiatr. Nurs.* 20, 188–190. doi: 10.1111/j.1744-6171.2007.00112.x

Scahill, L., McDougle, C. J., Aman, M. G., Johnson, C., Handen, B., Bearss, K., et al. (2012). Effects of risperidone and parent training on adaptive functioning in children with pervasive developmental disorders and serious behavioral problems. *J. Am. Acad. Child Adolesc. Psychiatry* 51, 136–146. doi: 10.1016/j.jaac.2011.11.010

Schaefer, G. B., and Mendelsohn, N. J. (2013). Clinical genetics evaluation in identifying the etiology of autism spectrum disorders: 2013 guideline revisions. *Genet. Med.* 15, 399–407. doi: 10.1038/gim.2013.32

Schmeisser, M. J. (2015). Translational neurobiology in Shank mutant mice—model systems for neuropsychiatric disorders. *Ann. Anat.* 200, 115–117. doi: 10.1016/j.aanat.2015.03.006

Schmeisser, M. J., Ey, E., Wegener, S., Bockmann, J., Stempel, A. V., Kuebler, A., et al. (2012). Autistic-like behaviours and hyperactivity in mice lacking ProSAP1/Shank2. *Nature* 486, 256–260. doi: 10.1038/nature11015

Schneider, T., and Przewocki, R. (2005). Behavioral alterations in rats prenatally exposed to valproic acid: animal model of autism. *Neuropsychopharmacology* 30, 80–89. doi: 10.1038/sj.npp.1300518

Schneider, T., Turczak, J., and Przewocki, R. (2006). Environmental enrichment reverses behavioral alterations in rats prenatally exposed to valproic acid: issues for a therapeutic approach in autism. *Neuropsychopharmacology* 31, 36–46. doi: 10.1038/sj.npp.1300767

Sealey, L., Hughes, B., Sriskanda, A., Guest, J., Gibson, A., Johnson-Williams, L., et al. (2016). Environmental factors in the development of autism spectrum disorders. *Environ. Int.* 88, 288–298. doi: 10.1016/j.envint.2015.12.021

Sears, L. L., Vest, C., Mohamed, S., Bailey, J., Ranson, B. J., and Piven, J. (1999). An MRI study of the basal ganglia in autism. *Prog. Neuropsychopharmacol. Biol. Psychiatry* 23, 613–624. doi: 10.1016/s0278-5846(99)00020-2

Sellin, L., Huber, T. B., Gerke, P., Quack, I., Pavenstädt, H., and Walz, G. (2003). NEPH1 defines a novel family of podocin interacting proteins. *FASEB J.* 17, 115–117. doi: 10.1096/fj.02-0242fje

Serizawa, S., Miyamichi, K., Takeuchi, H., Yamagishi, Y., Suzuki, M., and Sakano, H. (2006). A neuronal identity code for the odorant receptor-specific and activity-dependent axon sorting. *Cell* 127, 1057–1069. doi: 10.1016/j.cell.2006.10.031

Sforazzini, F., Bertero, A., Dodero, L., David, G., Galbusera, A., Scattoni, M. L., et al. (2016). Altered functional connectivity networks in acallosal and socially impaired BTBR mice. *Brain Struct. Funct.* 221, 941–954. doi: 10.1007/s00429-014-0948-9

Shafritz, K. M., Dichter, G. S., Baranek, G. T., and Belger, A. (2008). The neural circuitry mediating shifts in behavioral response and cognitive set in autism. *Biol. Psychiatry* 63, 974–980. doi: 10.1016/j.biopsych.2007.06.028

Shah, M. M., Migliore, M., Valencia, I., Cooper, E. C., and Brown, D. A. (2008). Functional significance of axonal Kv7 channels in hippocampal pyramidal neurons. *Proc. Natl. Acad. Sci. U S A* 105, 7869–7874. doi: 10.1073/pnas.0802805105

Shah, A. A., Sjovold, T., and Treit, D. (2004). Inactivation of the medial prefrontal cortex with the $GABA_A$ receptor agonist muscimol increases open-arm activity in the elevated plus-maze and attenuates shock-probe burying in rats. *Brain Res.* 1028, 112–115. doi: 10.1016/j.brainres.2004.08.061

Shahbazian, M. D., Young, J. I., Yuva-Paylor, L. A., Spencer, C. M., Antalffy, B. A., Noebels, J. L., et al. (2002). Mice with truncated MeCP2 recapitulate many Rett syndrome features and display hyperacetylation of histone H3. *Neuron* 35, 243–254. doi: 10.1016/s0896-6273(02)00768-7

Sharma, A., and Shaw, S. R. (2012). Efficacy of risperidone in managing maladaptive behaviors for children with autistic spectrum disorder: a meta-analysis. *J. Pediatr. Health Care* 26, 291–299. doi: 10.1016/j.pedhc.2011.02.008

Shavitt, R. G., Hounie, A. G., Rosário Campos, M. C., and Miguel, E. C. (2006). Tourette's syndrome. *Psychiatr. Clin. North Am.* 29, 471–486. doi: 10.1016/j.psc.2006.02.005

Shea, S., Turgay, A., Carroll, A., Schulz, M., Orlik, H., Smith, I., et al. (2004). Risperidone in the treatment of disruptive behavioral symptoms in children

with autistic and other pervasive developmental disorders. *Pediatrics* 114, e634–e641. doi: 10.1542/peds.2003-0264-F

Sheng, M., and Kim, E. (2000). The Shank family of scaffold proteins. *J. Cell Sci.* 113, 1851–1856.

Shi, R., Redman, P., Ghose, D., Hwang, H., Liu, Y., Ren, X., et al. (2017). Shank proteins differentially regulate synaptic transmission. *eNeuro* 4:ENEURO.0163-15.2017. doi: 10.1523/ENEURO.0163-15.2017

Shin, W., Kweon, H., Kang, R., Kim, D., Kim, K., Kang, M., et al. (2019). Scn2a haploinsufficiency in mice suppresses hippocampal neuronal excitability, excitatory synaptic drive and long-term potentiation and spatial learning and memory. *Front. Mol. Neurosci.* 12:145. doi: 10.3389/fnmol.2019.00145

Shonesy, B. C., Bluett, R. J., Ramikie, T. S., Báldi, R., Hermanson, D. J., Kingsley, P. J., et al. (2014). Genetic disruption of 2-arachidonoylglycerol synthesis reveals a key role for endocannabinoid signaling in anxiety modulation. *Cell Rep.* 9, 1644–1653. doi: 10.1016/j.celrep.2014.11.001

Shonesy, B. C., Parrish, W. P., Haddad, H. K., Stephenson, J. R., Báldi, R., Bluett, R. J., et al. (2018). Role of striatal direct pathway 2-arachidonoylglycerol signaling in sociability and repetitive behavior. *Biol. Psychiatry* 84, 304–315. doi: 10.1016/j.biopsych.2017.11.036

Shukla, T., de la Peña, J. B., Perish, J. M., Ploski, J. E., Stumpf, C. R., Webster, K. R., et al. (2020). A highly selective MNK inhibitor rescues deficits associated with fragile X syndrome in mice. *Neurotherapeutics* doi: 10.1007/s13311-020-00932-4 [Epub ahead of print].

Silverman, J. L., Pride, M., Hayes, J., Puhger, K., Butler-Struben, H., Baker, S., et al. (2015). $GABA_B$ receptor agonist R-baclofen reverses social deficits and reduces repetitive behavior in two mouse models of autism. *Neuropsychopharmacology* 40, 2228–2239. doi: 10.1038/npp.2015.66

Silverman, J. L., Smith, D. G., Rizzo, S. J. S., Karras, M. N., Turner, S. M., Tolu, S. S., et al. (2012). Negative allosteric modulation of the mGluR5 receptor reduces repetitive behaviors and rescues social deficits in mouse models of autism. *Sci. Transl. Med.* 4:131ra151. doi: 10.1126/scitranslmed.3003501

Silverman, J. L., Tolu, S. S., Barkan, C. L., and Crawley, J. N. (2010). Repetitive self-grooming behavior in the BTBR mouse model of autism is blocked by the mGluR5 antagonist MPEP. *Neuropsychopharmacology* 35, 976–989. doi: 10.1038/npp.2009.201

Silverman, J. L., Turner, S. M., Barkan, C. L., Tolu, S. S., Saxena, R., Hung, A. Y., et al. (2011). Sociability and motor functions in Shank1 mutant mice. *Brain Res.* 1380, 120–137. doi: 10.1016/j.brainres.2010.09.026

Sinclair, D., Featherstone, R., Naschek, M., Nam, J., Du, A., Wright, S., et al. (2017). GABA-B agonist baclofen normalizes auditory-evoked neural oscillations and behavioral deficits in the Fmr1 knockout mouse model of fragile X syndrome. *Eneuro* 4:ENEURO.0380-16.2017. doi: 10.1523/ENEURO.0380-16.2017

Singewald, N., Salchner, P., and Sharp, T. (2003). Induction of c-Fos expression in specific areas of the fear circuitry in rat forebrain by anxiogenic drugs. *Biol. Psychiatry* 53, 275–283. doi: 10.1016/s0006-3223(02)01574-3

Snow, W. M., Hartle, K., and Ivanco, T. L. (2008). Altered morphology of motor cortex neurons in the VPA rat model of autism. *Dev. Psychobiol.* 50, 633–639. doi: 10.1002/dev.20337

Sosnoski, D., Emanuel, B., Hawkins, A., van Tuinen, P., Ledbetter, D., Nussbaum, R., et al. (1988). Chromosomal localization of the genes for the vitronectin and fibronectin receptors alpha subunits and for platelet glycoproteins IIb and IIIa. *J. Clin. Invest.* 81, 1993–1998. doi: 10.1172/JCI113548

Soto, F., Watkins, K. L., Johnson, R. E., Schottler, F., and Kerschensteiner, D. (2013). NGL-2 regulates pathway-specific neurite growth and lamination, synapse formation and signal transmission in the retina. *J. Neurosci.* 33, 11949–11959. doi: 10.1523/JNEUROSCI.1521-13.2013

Soto, F., Zhao, L., and Kerschensteiner, D. (2018). Synapse maintenance and restoration in the retina by NGL2. *eLife* 7:e30388. doi: 10.7554/eLife.30388

Specchio, N., Marini, C., Terracciano, A., Mei, D., Trivisano, M., Sicca, F., et al. (2011). Spectrum of phenotypes in female patients with epilepsy due to protocadherin 19 mutations. *Epilepsia* 52, 1251–1257. doi: 10.1111/j.1528-1167.2011.03063.x

Spencer, C., Alekseyenko, O., Serysheva, E., Yuva-Paylor, L., and Paylor, R. (2005). Altered anxiety-related and social behaviors in the fMR1 knockout mouse model of fragile X syndrome. *Genes Brain Behav.* 4, 420–430. doi: 10.1111/j.1601-183X.2005.00123.x

Spencer, C. M., Graham, D. F., Yuva-Paylor, L. A., Nelson, D. L., and Paylor, R. (2008). Social behavior in fMR1 knockout mice carrying a human FMR1 transgene. *Behav. Neurosci.* 122, 710–715. doi: 10.1037/0735-7044.122.3.710

Spruijt, B. M., Cools, A. R., Ellenbroek, B. A., and Gispen, W. H. (1986). Dopaminergic modulation of ACTH-induced grooming. *Eur. J. Pharmacol.* 120, 249–256. doi: 10.1016/0014-2999(86)90465-6

Spruijt, B. M., van Hooff, J. A., and Gispen, W. H. (1992). Ethology and neurobiology of grooming behavior. *Physiol. Rev.* 72, 825–852. doi: 10.1152/physrev.1992.72.3.825

Squillace, M., Dodero, L., Federici, M., Migliarini, S., Errico, F., Napolitano, F., et al. (2014). Dysfunctional dopaminergic neurotransmission in asocial BTBR mice. *Transl. Psychiatry* 4:e427. doi: 10.1038/tp.2014.69

Stearns, N., Schaevitz, L., Bowling, H., Nag, N., Berger, U., and Berger-Sweeney, J. (2007). Behavioral and anatomical abnormalities in Mecp2 mutant mice: a model for Rett syndrome. *Neuroscience* 146, 907–921. doi: 10.1016/j.neuroscience.2007.02.009

Stratis, E. A., and Lecavalier, L. (2013). Restricted and repetitive behaviors and psychiatric symptoms in youth with autism spectrum disorders. *Res. Autism Spectr. Disord.* 7, 757–766. doi: 10.1016/j.rasd.2013.02.017

Stubbs, G., Henley, K., and Green, J. (2016). Autism: will vitamin D supplementation during pregnancy and early childhood reduce the recurrence rate of autism in newborn siblings? *Med. Hypotheses* 88, 74–78. doi: 10.1016/j.mehy.2016.01.015

Subramaniam, B., Naidu, S., and Reiss, A. L. (1997). Neuroanatomy in Rett syndrome: cerebral cortex and posterior fossa. *Neurology* 48, 399–407. doi: 10.1212/wnl.48.2.399

Südhof, T. C. (2008). Neuroligins and neurexins link synaptic function to cognitive disease. *Nature* 455, 903–911. doi: 10.1038/nature07456

Sultana, R., Ghandi, T., M. Davila, A., Lee, C. C., and Ogundele, O. M. (2018). Upregulated SK2 expression and impaired CaMKII phosphorylation are shared synaptic defects between 16p11. 2del and 129S: Δdisc1 mutant mice. *ASN Neuro* 11:1759091419847891. doi: 10.1177/1759091418817641

Sun, T., Song, Z., Tian, Y., Tian, W., Zhu, C., Ji, G., et al. (2019). Basolateral amygdala input to the medial prefrontal cortex controls obsessive-compulsive disorder-like checking behavior. *Proc. Natl. Acad. Sci. U S A* 116, 3799–3804. doi: 10.1073/pnas.1814292116

Sungur, A. Ö., Vörckel, K. J., Schwarting, R. K., and Wöhr, M. (2014). Repetitive behaviors in the Shank1 knockout mouse model for autism spectrum disorder: developmental aspects and effects of social context. *J. Neurosci. Methods* 234, 92–100. doi: 10.1016/j.jneumeth.2014.05.003

Sutcliffe, J. S., Delahanty, R. J., Prasad, H. C., McCauley, J. L., Han, Q., Jiang, L., et al. (2005). Allelic heterogeneity at the serotonin transporter locus (SLC6A4) confers susceptibility to autism and rigid-compulsive behaviors. *Am. J. Hum. Genet.* 77, 265–279. doi: 10.1086/432648

Suvrathan, A., Hoeffer, C. A., Wong, H., Klann, E., and Chattarji, S. (2010). Characterization and reversal of synaptic defects in the amygdala in a mouse model of fragile X syndrome. *Proc. Natl. Acad. Sci. U S A* 107, 11591–11596. doi: 10.1073/pnas.1002262107

Swanwick, C. C., Larsen, E. C., and Banerjee-Basu, S. (2011). "Genetic heterogeneity of autism spectrum disorders," in *Autism Spectrum Disorders: The Role of Genetics in Diagnosis and Treatment*, eds S. I. Deutsch and M. R. Urbano (Rikela: InTech), 65–82.

Szechtman, H., Ahmari, S. E., Beninger, R. J., Eilam, D., Harvey, B. H., Edemann-Callesen, H., et al. (2017). Obsessive-compulsive disorder: insights from animal models. *Neurosci. Biobehav. Rev.* 76, 254–279. doi: 10.1016/j.neubiorev.2016.04.019

Tabuchi, K., Blundell, J., Etherton, M. R., Hammer, R. E., Liu, X., Powell, C. M., et al. (2007). A neuroligin-3 mutation implicated in autism increases inhibitory synaptic transmission in mice. *Science* 318, 71–76. doi: 10.1126/science.1146221

Takahata, R., and Moghaddam, B. (2003). Activation of glutamate neurotransmission in the prefrontal cortex sustains the motoric and dopaminergic effects of phencyclidine. *Neuropsychopharmacology* 28, 1117–1124. doi: 10.1038/sj.npp.1300127

Takamiya, K., Mao, L., Huganir, R. L., and Linden, D. J. (2008). The glutamate receptor-interacting protein family of GluR2-binding proteins

is required for long-term synaptic depression expression in cerebellar Purkinje cells. *J. Neurosci.* 28, 5752–5755. doi: 10.1523/JNEUROSCI.0654-08.2008

Tanaka, M., DeLorey, T. M., Delgado-Escueta, A., and Olsen, R. W. (2012). "GABRB3, epilepsy and neurodevelopment," in *Jasper's Basic Mechanisms of the Epilepsies [Internet]*, 4th Edn. eds Jeffrey Noebels, Massimo Avoli, Michael Rogawski, Richard Olsen, and Antonio Delgado-Escueta (Bethesda, MD: National Center for Biotechnology Information US).

Tang, A.-H., and Alger, B. E. (2015). Homer protein-metabotropic glutamate receptor binding regulates endocannabinoid signaling and affects hyperexcitability in a mouse model of fragile X syndrome. *J. Neurosci.* 35, 3938–3945. doi: 10.1523/JNEUROSCI.4499-14.2015

Tanimura, Y., King, M. A., Williams, D. K., and Lewis, M. H. (2011). Development of repetitive behavior in a mouse model: roles of indirect and striosomal basal ganglia pathways. *Int. J. Dev. Neurosci.* 29, 461–467. doi: 10.1016/j.ijdevneu.2011.02.004

Tanimura, Y., Vaziri, S., and Lewis, M. H. (2010). Indirect basal ganglia pathway mediation of repetitive behavior: attenuation by adenosine receptor agonists. *Behav. Brain Res.* 210, 116–122. doi: 10.1016/j.bbr.2010.02.030

Tanimura, A., Yamazaki, M., Hashimotodani, Y., Uchigashima, M., Kawata, S., Abe, M., et al. (2010). The endocannabinoid 2-arachidonoylglycerol produced by diacylglycerol lipase α mediates retrograde suppression of synaptic transmission. *Neuron* 65, 320–327. doi: 10.1016/j.neuron.2010.01.021

Tanimura, Y., Yang, M. C., and Lewis, M. H. (2008). Procedural learning and cognitive flexibility in a mouse model of restricted, repetitive behaviour. *Behav. Brain Res.* 189, 250–256. doi: 10.1016/j.bbr.2008.01.001

Tavazoie, S. F., Alvarez, V. A., Ridenour, D. A., Kwiatkowski, D. J., and Sabatini, B. L. (2005). Regulation of neuronal morphology and function by the tumor suppressors Tsc1 and Tsc2. *Nat. Neurosci.* 8, 1727–1734. doi: 10.1038/nn1566

Taylor, G. T., Lerch, S., and Chourbaji, S. (2017). Marble burying as compulsive behaviors in male and female mice. *Acta Neurobiol. Exp.* 77, 254–260.

Thakkar, K. N., Polli, F. E., Joseph, R. M., Tuch, D. S., Hadjikhani, N., Barton, J. J., et al. (2008). Response monitoring, repetitive behaviour and anterior cingulate abnormalities in autism spectrum disorders (ASD). *Brain* 131, 2464–2478. doi: 10.1093/brain/awn099

Thomas, A., Burant, A., Bui, N., Graham, D., Yuva-Paylor, L. A., and Paylor, R. (2009). Marble burying reflects a repetitive and perseverative behavior more than novelty-induced anxiety. *Psychopharmacology* 204, 361–373. doi: 10.1007/s00213-009-1466-y

Thomas, A. M., Bui, N., Perkins, J. R., Yuva-Paylor, L. A., and Paylor, R. (2012). Group I metabotropic glutamate receptor antagonists alter select behaviors in a mouse model for fragile X syndrome. *Psychopharmacology* 219, 47–58. doi: 10.1007/s00213-011-2375-4

Tordjman, S., Somogyi, E., Coulon, N., Kermarrec, S., Cohen, D., Bronsard, G., et al. (2014). Gene× Environment interactions in autism spectrum disorders: role of epigenetic mechanisms. *Front. Psychiatry* 5:53. doi: 10.3389/fpsyt.2014.00053

Triplett, J. W., and Feldheim, D. A. (2012). Eph and ephrin signaling in the formation of topographic maps. *Semin. Cell Dev. Biol.* 23, 7–15. doi: 10.1016/j.semcdb.2011.10.026

Tsujino, N., Nakatani, Y., Seki, Y., Nakasato, A., Nakamura, M., Sugawara, M., et al. (2007). Abnormality of circadian rhythm accompanied by an increase in frontal cortex serotonin in animal model of autism. *Neurosci. Res.* 57, 289–295. doi: 10.1016/j.neures.2006.10.018

Turner, K. C., Frost, L., Linsenbardt, D., McIlroy, J. R., and Müller, R.-A. (2006). Atypically diffuse functional connectivity between caudate nuclei and cerebral cortex in autism. *Behav. Brain Funct.* 2:34. doi: 10.1186/1744-9081-2-34

Turner, G., Webb, T., Wake, S., and Robinson, H. (1996). Prevalence of fragile X syndrome. *Am. J. Med. Genet.* 64, 196–197. doi: 10.1002/(SICI)1096-8628(19960712)64:1<196::AID-AJMG35>3.0.CO;2-G

Ullrich, M., Weber, M., Post, A., Popp, S., Grein, J., Zechner, M., et al. (2018). OCD-like behavior is caused by dysfunction of thalamo-amygdala circuits and upregulated TrkB/ERK-MAPK signaling as a result of SPRED2 deficiency. *Mol. Psychiatry* 23, 444–458. doi: 10.1038/mp.2016.232

Um, S. M., Ha, S., Lee, H., Kim, J., Kim, K., Shin, W., et al. (2018). NGL-2 deletion leads to autistic-like behaviors responsive to NMDAR modulation. *Cell Rep.* 23, 3839–3851. doi: 10.1016/j.celrep.2018.05.087

Vaccarino, F. J., and Franklin, K. (1982). Dopamine mediates ipsi-and contraversive circling elicited from the substantia nigra. *Pharmacol. Biochem. Behav.* 17, 431–434. doi: 10.1016/0091-3057(82)90300-8

van Steensel, F. J., Bögels, S. M., and Perrin, S. (2011). Anxiety disorders in children and adolescents with autistic spectrum disorders: a meta-analysis. *Clin. Child Fam. Psychol. Rev.* 14, 302–317. doi: 10.1007/s10567-011-0097-0

Varea, O., Martin-de-Saavedra, M. D., Kopeikina, K. J., Schürmann, B., Fleming, H. J., Fawcett-Patel, J. M., et al. (2015). Synaptic abnormalities and cytoplasmic glutamate receptor aggregates in contactin associated protein-like 2/Caspr2 knockout neurons. *Proc. Natl. Acad. Sci. U S A* 112, 6176–6181. doi: 10.1073/pnas.1423205112

Varga, E. A., Pastore, M., Prior, T., Herman, G. E., and McBride, K. L. (2009). The prevalence of PTEN mutations in a clinical pediatric cohort with autism spectrum disorders, developmental delay and macrocephaly. *Genet. Med.* 11, 111–117. doi: 10.1097/GIM.0b013e31818fd762

Vasa, R. A., and Mazurek, M. O. (2015). An update on anxiety in youth with autism spectrum disorders. *Curr. Opin. Psychiatry* 28, 83–90. doi: 10.1097/YCO.0000000000000133

Veenema, A. H., Meijer, O. C., de Kloet, E. R., Koolhaas, J. M., and Bohus, B. G. (2003). Differences in basal and stress-induced HPA regulation of wild house mice selected for high and low aggression. *Horm. Behav.* 43, 197–204. doi: 10.1016/s0018-506x(02)00013-2

Veenstra-VanderWeele, J., Muller, C. L., Iwamoto, H., Sauer, J. E., Owens, W. A., Shah, C. R., et al. (2012). Autism gene variant causes hyperserotonemia, serotonin receptor hypersensitivity, social impairment and repetitive behavior. *Proc. Natl. Acad. Sci. U S A* 109, 5469–5474. doi: 10.1073/pnas.1112345109

Velíšek, L., Velíšková, J., Ravizza, T., Giorgi, F. S., and Moshé, S. L. (2005). Circling behavior and [^{14}C] 2-deoxyglucose mapping in rats: possible implications for autistic repetitive behaviors. *Neurobiol. Dis.* 18, 346–355. doi: 10.1016/j.nbd.2004.10.012

Verhoeven, J. S., De Cock, P., Lagae, L., and Sunaert, S. (2010). Neuroimaging of autism. *Neuroradiology* 52, 3–14. doi: 10.1007/s00234-009-0583-y

Wahlsten, D., Metten, P., and Crabbe, J. C. (2003). Survey of 21 inbred mouse strains in two laboratories reveals that BTBR T/+ tf/tf has severely reduced hippocampal commissure and absent corpus callosum. *Brain Res.* 971, 47–54. doi: 10.1016/s0006-8993(03)02354-0

Walsh, T., McClellan, J. M., McCarthy, S. E., Addington, A. M., Pierce, S. B., Cooper, G. M., et al. (2008). Rare structural variants disrupt multiple genes in neurodevelopmental pathways in schizophrenia. *Science* 320, 539–543. doi: 10.1126/science.1155174

Wang, L., Almeida, L. E., Spornick, N. A., Kenyon, N., Kamimura, S., Khaibullina, A., et al. (2015). Modulation of social deficits and repetitive behaviors in a mouse model of autism: the role of the nicotinic cholinergic system. *Psychopharmacology* 232, 4303–4316. doi: 10.1007/s00213-015-4058-z

Wang, X., Bey, A. L., Katz, B. M., Badea, A., Kim, N., David, L. K., et al. (2016). Altered mGluR5-Homer scaffolds and corticostriatal connectivity in a Shank3 complete knockout model of autism. *Nat. Commun.* 7:11459. doi: 10.1038/ncomms11459

Wang, Y., Billon, C., Walker, J. K., and Burris, T. P. (2016). Therapeutic effect of a synthetic RORα/γ agonist in an animal model of autism. *ACS Chem. Neurosci.* 7, 143–148.

Wang, W., Li, C., Chen, Q., van der Goes, M.-S., Hawrot, J., Yao, A. Y., et al. (2017). Striatopallidal dysfunction underlies repetitive behavior in Shank3-deficient model of autism. *J. Clin. Invest.* 127, 1978–1990. doi: 10.1172/JCI87997

Wang, X., McCoy, P. A., Rodriguiz, R. M., Pan, Y., Je, H. S., Roberts, A. C., et al. (2011). Synaptic dysfunction and abnormal behaviors in mice lacking major isoforms of Shank3. *Hum. Mol. Genet.* 20, 3093–3108. doi: 10.1093/hmg/ddr212

Wang, S., Tan, N., Zhu, X., Yao, M., Wang, Y., Zhang, X., et al. (2018). Sh3rf2 haploinsufficiency leads to unilateral neuronal development deficits and autistic-like behaviors in mice. *Cell Rep.* 25, 2963.e6–2971.e6. doi: 10.1016/j.celrep.2018.11.044

Wang, Y., Zeng, C., Li, J., Zhou, Z., Ju, X., Xia, S., et al. (2018). PAK2 haploinsufficiency results in synaptic cytoskeleton impairment and autism-related behavior. *Cell Rep.* 24, 2029–2041. doi: 10.1016/j.celrep.2018.07.061

Way, S. W., McKenna, J. III., Mietzsch, U., Reith, R. M., Wu, H. C.-J., and Gambello, M. J. (2009). Loss of Tsc2 in radial glia models the brain pathology

of tuberous sclerosis complex in the mouse. *Hum. Mol. Genet.* 18, 1252–1265. doi: 10.1093/hmg/ddp025

Weeber, E. J., Jiang, Y.-H., Elgersma, Y., Varga, A. W., Carrasquillo, Y., Brown, S. E., et al. (2003). Derangements of hippocampal calcium/calmodulin-dependent protein kinase II in a mouse model for Angelman mental retardation syndrome. *J. Neurosci.* 23, 2634–2644. doi: 10.1523/JNEUROSCI.23-07-02634.2003

Welch, J. M., Lu, J., Rodriguiz, R. M., Trotta, N. C., Peca, J., Ding, J.-D., et al. (2007). Cortico-striatal synaptic defects and OCD-like behaviours in Sapap3-mutant mice. *Nature* 448, 894–900. doi: 10.1038/nature06104

Whitehouse, C. M., and Lewis, M. H. (2015). Repetitive behavior in neurodevelopmental disorders: clinical and translational findings. *Behav. Anal.* 38, 163–178. doi: 10.1007/s40614-015-0029-2

Whitehouse, C. M., Curry-Pochy, L. S., Shafer, R., Rudy, J., and Lewis, M. H. (2017). Reversal learning in C58 mice: modeling higher order repetitive behavior. *Behav. Brain Res.* 332, 372–378. doi: 10.1016/j.bbr.2017.06.014

Whitney, E. R., Kemper, T. L., Bauman, M. L., Rosene, D. L., and Blatt, G. J. (2008). Cerebellar Purkinje cells are reduced in a subpopulation of autistic brains: a stereological experiment using calbindin-D28k. *Cerebellum* 7, 406–416. doi: 10.1007/s12311-008-0043-y

Wilhelm, M., Kukekov, N. V., Schmit, T. L., Biagas, K. V., Sproul, A. A., Gire, S., et al. (2012). Sh3rf2/POSHER protein promotes cell survival by ring-mediated proteasomal degradation of the c-Jun N-terminal kinase scaffold POSH (Plenty of SH3s) protein. *J. Biol. Chem.* 287, 2247–2256. doi: 10.1074/jbc.M111.269431

Wilkes, B., and Lewis, M. (2018). The neural circuitry of restricted repetitive behavior: magnetic resonance imaging in neurodevelopmental disorders and animal models. *Neurosci. Biobehav. Rev.* 92, 152–171. doi: 10.1016/j.neubiorev.2018.05.022

Willatt, L., Cox, J., Barber, J., Cabanas, E. D., Collins, A., Donnai, D., et al. (2005). 3q29 microdeletion syndrome: clinical and molecular characterization of a new syndrome. *Am. J. Hum. Genet.* 77, 154–160. doi: 10.1086/431653

Wöhr, M., Orduz, D., Gregory, P., Moreno, H., Khan, U., Vörckel, K. J., et al. (2015). Lack of parvalbumin in mice leads to behavioral deficits relevant to all human autism core symptoms and related neural morphofunctional abnormalities. *Transl. Psychiatry* 5:e525. doi: 10.1038/tp.2015.19

Wöhr, M., Roullet, F. I., and Crawley, J. N. (2011). Reduced scent marking and ultrasonic vocalizations in the BTBR T+ tf/J mouse model of autism. *Genes Brain Behav.* 10, 35–43. doi: 10.1111/j.1601-183X.2010.00582.x

Wöhr, M., Silverman, J. L., Scattoni, M. L., Turner, S. M., Harris, M. J., Saxena, R., et al. (2013). Developmental delays and reduced pup ultrasonic vocalizations but normal sociability in mice lacking the postsynaptic cell adhesion protein neuroligin2. *Behav. Brain Res.* 251, 50–64. doi: 10.1016/j.bbr.2012.07.024

Wolmarans, D. W., Brand, L., Stein, D. J., and Harvey, B. H. (2013). Reappraisal of spontaneous stereotypy in the deer mouse as an animal model of obsessive-compulsive disorder (OCD): response to escitalopram treatment and basal serotonin transporter (SERT) density. *Behav. Brain Res.* 256, 545–553. doi: 10.1016/j.bbr.2013.08.049

Won, H., Lee, H.-R., Gee, H. Y., Mah, W., Kim, J.-I., Lee, J., et al. (2012). Autistic-like social behaviour in Shank2-mutant mice improved by restoring NMDA receptor function. *Nature* 486, 261–265. doi: 10.1038/nature11208

Wong, M., Ess, K. C., Uhlmann, E. J., Jansen, L. A., Li, W., Crino, P. B., et al. (2003). Impaired glial glutamate transport in a mouse tuberous sclerosis epilepsy model. *Ann. Neurol.* 54, 251–256. doi: 10.1002/ana.10648

Wong, D. F., Ricaurte, G., Gründer, G., Rothman, R., Naidu, S., Singer, H., et al. (1998). Dopamine transporter changes in neuropsychiatric disorders. *Adv. Pharmacol.* 42, 219–223. doi: 10.1016/s1054-3589(08)60732-2

Woo, J., Kwon, S.-K., Choi, S., Kim, S., Lee, J.-R., Dunah, A. W., et al. (2009). Trans-synaptic adhesion between NGL-3 and LAR regulates the formation of excitatory synapses. *Nat. Neurosci.* 12, 428–437. doi: 10.1038/nn.2279

Wu, K., Hanna, G. L., Rosenberg, D. R., and Arnold, P. D. (2012). The role of glutamate signaling in the pathogenesis and treatment of obsessive-compulsive disorder. *Pharmacol. Biochem. Behav.* 100, 726–735. doi: 10.1016/j.pbb.2011.10.007

Wurzman, R., Forcelli, P. A., Griffey, C. J., and Kromer, L. F. (2015). Repetitive grooming and sensorimotor abnormalities in an Ephrin-A knockout model for autism spectrum disorders. *Behav. Brain Res.* 278, 115–128. doi: 10.1016/j.bbr.2014.09.012

Xu, H.-Y., Liu, Y.-J., Xu, M.-Y., Zhang, Y.-H., Zhang, J.-X., and Wu, Y.-J. (2012). Inactivation of the bed nucleus of the stria terminalis suppresses the innate fear responses of rats induced by the odor of cat urine. *Neuroscience* 221, 21–27. doi: 10.1016/j.neuroscience.2012.06.056

Xu, J., Marshall, J. J., Fernandes, H. B., Nomura, T., Copits, B. A., Procissi, D., et al. (2017). Complete disruption of the kainate receptor gene family results in corticostriatal dysfunction in mice. *Cell Rep.* 18, 1848–1857. doi: 10.1016/j.celrep.2017.01.073

Xu, T., and Pandey, S. C. (2000). Cellular localization of serotonin$_{2A}$ ($5HT_{2A}$) receptors in the rat brain. *Brain Res. Bull.* 51, 499–505. doi: 10.1016/s0361-9230(99)00278-6

Yamaguchi, Y., and Pasquale, E. B. (2004). Eph receptors in the adult brain. *Curr. Opin. Neurobiol.* 14, 288–296. doi: 10.1016/j.conb.2004.04.003

Yan, Q., Rammal, M., Tranfaglia, M., and Bauchwitz, R. (2005). Suppression of two major Fragile X syndrome mouse model phenotypes by the mGluR5 antagonist MPEP. *Neuropharmacology* 49, 1053–1066. doi: 10.1016/j.neuropharm.2005.06.004

Yang, M., Bozdagi, O., Scattoni, M. L., Wöhr, M., Roullet, F. I., Katz, A. M., et al. (2012). Reduced excitatory neurotransmission and mild autism-relevant phenotypes in adolescent Shank3 null mutant mice. *J. Neurosci.* 32, 6525–6541. doi: 10.1523/JNEUROSCI.6107-11.2012

Yau, S., Bettio, L., Vetrici, M., Truesdell, A., Chiu, C., Chiu, J., et al. (2018). Chronic minocycline treatment improves hippocampal neuronal structure, NMDA receptor function and memory processing in fMRI knockout mice. *Neurobiol. Dis.* 113, 11–22. doi: 10.1016/j.nbd.2018.01.014

Yilmazer-Hanke, D. M., Roskoden, T., Zilles, K., and Schwegler, H. (2003). Anxiety-related behavior and densities of glutamate, $GABA_A$, acetylcholine and serotonin receptors in the amygdala of seven inbred mouse strains. *Behav. Brain Res.* 145, 145–159. doi: 10.1016/s0166-4328(03)00107-4

Yu, Y., Chaulagain, A., Pedersen, S. A., Lydersen, S., Leventhal, B. L., Szatmari, P., et al. (2020). Pharmacotherapy of restricted/repetitive behavior in autism spectrum disorder:a systematic review and meta-analysis. *BMC Psychiatry* 20:121. doi: 10.1186/s12888-020-2477-9

Yu, X., Taylor, A. M., Nagai, J., Golshani, P., Evans, C. J., Coppola, G., et al. (2018). Reducing astrocyte calcium signaling *in vivo* alters striatal microcircuits and causes repetitive behavior. *Neuron* 99, 1170.e9–1187.e9. doi: 10.1016/j.neuron.2018.08.015

Yu, X., Wang, G., Gilmore, A., Yee, A. X., Li, X., Xu, T., et al. (2013). Accelerated experience-dependent pruning of cortical synapses in ephrin-A2 knockout mice. *Neuron* 80, 64–71. doi: 10.1016/j.neuron.2013.07.014

Yue, C., and Yaari, Y. (2006). Axo-somatic and apical dendritic Kv7/M channels differentially regulate the intrinsic excitability of adult rat CA1 pyramidal cells. *J. Neurophysiol.* 95, 3480–3495. doi: 10.1152/jn.01333.2005

Yuen, R. K., Merico, D., Bookman, M., Howe, J. L., Thiruvahindrapuram, B., Patel, R. V., et al. (2017). Whole genome sequencing resource identifies 18 new candidate genes for autism spectrum disorder. *Nat. Neurosci.* 20, 602–611. doi: 10.1038/nn.4524

Zablotsky, B., Black, L. I., Maenner, M. J., Schieve, L. A., Danielson, M. L., Bitsko, R. H., et al. (2019). Prevalence and trends of developmental disabilities among children in the United States: 2009–2017. *Pediatrics* 144:e20190811. doi: 10.1542/peds.2019-0811

Zamberletti, E., Gabaglio, M., Piscitelli, F., Brodie, J. S., Woolley-Roberts, M., Barbiero, I., et al. (2019). Cannabidivarin completely rescues cognitive deficits and delays neurological and motor defects in male *Mecp2* mutant mice. *J. Psychopharmacol.* 33, 894–907. doi: 10.1177/0269881119844184

Zandt, F., Prior, M., and Kyrios, M. (2007). Repetitive behaviour in children with high functioning autism and obsessive compulsive disorder. *J. Autism Dev. Disord.* 37, 251–259. doi: 10.1007/s10803-006-0158-2

Zeng, L.-H., Ouyang, Y., Gazit, V., Cirrito, J. R., Jansen, L. A., Ess, K. C., et al. (2007). Abnormal glutamate homeostasis and impaired synaptic plasticity and learning in a mouse model of tuberous sclerosis complex. *Neurobiol. Dis.* 28, 184–196. doi: 10.1016/j.nbd.2007.07.015

Zeng, L. H., Xu, L., Gutmann, D. H., and Wong, M. (2008). Rapamycin prevents epilepsy in a mouse model of tuberous sclerosis complex. *Ann. Neurol.* 63, 444–453. doi: 10.1002/ana.21331

Zerbi, V., Ielacqua, G. D., Markicevic, M., Haberl, M. G., Ellisman, M. H., A-Bhaskaran, A., et al. (2018). Dysfunctional autism risk genes cause circuit-specific connectivity deficits with distinct developmental trajectories. *Cereb. Cortex* 28, 2495–2506. doi: 10.1093/cercor/bhy046

Zhang, L., and Alger, B. E. (2010). Enhanced endocannabinoid signaling elevates neuronal excitability in fragile X syndrome. *J. Neurosci.* 30, 5724–5729. doi: 10.1523/JNEUROSCI.0795-10.2010

Zhang, W.-N., Bast, T., and Feldon, J. (2002). Effects of hippocampal N-methyl-[D]-aspartate infusion on locomotor activity and prepulse inhibition: Differences between the dorsal and ventral hippocampus. *Behav. Neurosci.* 116, 72–84. doi: 10.1037/0735-7044.116.1.72

Zhang, C., Kalueff, A. V., and Song, C. (2019). Minocycline ameliorates anxiety-related self-grooming behaviors and alters hippocampal neuroinflammation, GABA and serum cholesterol levels in female Sprague–Dawley rats subjected to chronic unpredictable mild stress. *Behav. Brain Res.* 363, 109–117. doi: 10.1016/j.bbr.2019.01.045

Zhang, Y. V., Ormerod, K. G., and Littleton, J. T. (2017). Astrocyte Ca^{2+} influx negatively regulates neuronal activity. *eNeuro* 4:ENEURO.0340-16.2017. doi: 10.1523/ENEURO.0340-16.2017

Zhou, M. S., Nasir, M., Farhat, L. C., Kook, M., Artukoglu, B. B., and Bloch, M. H. (2020). Meta-analysis: pharmacologic treatment of restricted and repetitive behaviors in autism spectrum disorders. *J. Am. Acad. Child Adolesc. Psychiatry* doi: 10.1016/j.jaac.2020.03.007 [Epub ahead of print].

Zhou, Y., Kaiser, T., Monteiro, P., Zhang, X., Van der Goes, M. S., Wang, D., et al. (2016). Mice with Shank3 mutations associated with ASD and schizophrenia display both shared and distinct defects. *Neuron* 89, 147–162. doi: 10.1016/j.neuron.2015.11.023

Zhou, L.-T., Ye, S.-H., Yang, H.-X., Zhou, Y.-T., Zhao, Q.-H., Sun, W.-W., et al. (2017). A novel role of fragile X mental retardation protein in pre-mRNA alternative splicing through RNA-binding protein 14. *Neuroscience* 349, 64–75. doi: 10.1016/j.neuroscience.2017.02.044

Zieba, J., Sinclair, D., Sebree, T., Bonn-Miller, M., Gutterman, D., Siegel, S., et al. (2019). Cannabidiol (CBD) reduces anxiety-related behavior in mice *via* an FMRP-independent mechanism. *Pharmacol. Biochem. Behav.* 181, 93–100. doi: 10.1016/j.pbb.2019.05.002

Conflict of Interest: The authors declare that the research was conducted in the absence of any commercial or financial relationships that could be construed as a potential conflict of interest.

frontiers in Genetics

BRIEF RESEARCH REPORT
published: 12 July 2021
doi: 10.3389/fgene.2021.683959

Camk2a-Cre and *Tshz3* Expression in Mouse Striatal Cholinergic Interneurons: Implications for Autism Spectrum Disorder

*Xavier Caubit†, Elise Arbeille†, Dorian Chabbert, Florence Desprez, Imane Messak, Ahmed Fatmi, Bianca Habermann, Paolo Gubellini and Laurent Fasano**

Aix-Marseille University, CNRS, IBDM, UMR 7288, Marseille, France

Camk2a-Cre mice have been widely used to study the postnatal function of several genes in forebrain projection neurons, including cortical projection neurons (CPNs) and striatal medium-sized spiny neurons (MSNs). We linked heterozygous deletion of *TSHZ3/Tshz3* gene to autism spectrum disorder (ASD) and used *Camk2a-Cre* mice to investigate the postnatal function of *Tshz3*, which is expressed by CPNs but not MSNs. Recently, single-cell transcriptomics of the adult mouse striatum revealed the expression of *Camk2a* in interneurons and showed *Tshz3* expression in striatal cholinergic interneurons (SCINs), which are attracting increasing interest in the field of ASD. These data and the phenotypic similarity between the mice with *Tshz3* haploinsufficiency and *Camk2a-Cre*-dependent conditional deletion of *Tshz3* (*Camk2a-cKO*) prompted us to better characterize the expression of *Tshz3* and the activity of *Camk2a-Cre* transgene in the striatum. Here, we show that the great majority of *Tshz3*-expressing cells are SCINs and that all SCINs express *Tshz3*. Using lineage tracing, we demonstrate that the *Camk2a-Cre* transgene is expressed in the SCIN lineage where it can efficiently elicit the deletion of the *Tshz3*-floxed allele. Moreover, transcriptomic and bioinformatic analysis in *Camk2a-cKO* mice showed dysregulated striatal expression of a number of genes, including genes whose human orthologues are associated with ASD and synaptic signaling. These findings identifying the expression of the *Camk2a-Cre* transgene in SCINs lineage lead to a reappraisal of the interpretation of experiments using *Camk2a-Cre*-dependent gene manipulations. They are also useful to decipher the cellular and molecular substrates of the ASD-related behavioral abnormalities observed in *Tshz3* mouse models.

Keywords: ***Camk2a-Cre***, ***TSHZ3***, **striatal cholinergic interneurons, autism spectrum disorder,** ***Mus musculus***

OPEN ACCESS

Edited by:
Yu-Chih Lin,
Hussman Institute for Autism, United States

Reviewed by:
Max Tischfield, Rutgers, The State University of New Jersey, United States
Nathalie Dehorter, Australian National University, Australia

***Correspondence:**
Laurent Fasano
laurent.fasano@univ-amu.fr

†These authors share first authorship

Specialty section:
This article was submitted to Neurogenomics, a section of the journal Frontiers in Genetics

Received: *22 March 2021*
Accepted: *21 June 2021*
Published: *12 July 2021*

Citation:
Caubit X, Arbeille E, Chabbert D, Desprez F, Messak I, Fatmi A, Habermann B, Gubellini P and Fasano L (2021) Camk2a-Cre and Tshz3 Expression in Mouse Striatal Cholinergic Interneurons: Implications for Autism Spectrum Disorder. Front. Genet. 12:683959. doi: 10.3389/fgene.2021.683959

INTRODUCTION

The corticostriatal (CStr) circuitry is critically involved in functions ranging from motor control and habit formation to cognition. Defective development and dysfunction of CStr circuits have been linked to several brain disorders, including Huntington's disease, Parkinson's disease, and autism spectrum disorder (ASD) (Shepherd, 2013; Li and Pozzo-Miller, 2020). The striatum receives

its main excitatory input from two types of cortical projection neurons (CPNs): intratelencephalic (IT) neurons and pyramidal-tract (PT) neurons. IT and PT neurons that project to the striatum reside mostly in the deep cortical layer (L) 5 (Reiner et al., 2010; Shepherd, 2013). Their primary striatal targets are the medium-sized spiny projection neurons (MSNs) (Sohur et al., 2012), which represent 90–95% of the neurons in the striatum (Gerfen and Surmeier, 2011). The remaining 5–10% of striatal neurons are aspiny interneurons, initially categorized into three main subpopulations, among which one population of striatal cholinergic interneurons (SCINs) (Kawaguchi, 1997). There is growing evidence for a higher diversity of striatal interneurons, based on studies on their developmental origin, gene expression profile, and electrophysiological properties and connectivity. These data define at least 6–7 classes of GABAergic interneurons (Munoz-Manchado et al., 2018; Tepper et al., 2018) and reveal that also SCINs are a heterogeneous population (Ahmed et al., 2019). Though few in number, striatal interneurons, and SCINs in particular, play a key functional role by modulating striatal activity through distinct connections with MSNs and/or other interneurons (Tepper et al., 2018; Abudukeyoumu et al., 2019).

We previously reported in mouse that heterozygous deletion of *Tshz3*, the gene encoding the transcription factor TSHZ3 (teashirt zinc-finger homeobox family member 3, also known as ZFP537), drives ASD-relevant behavioral abnormalities (Caubit et al., 2016), paralleled by altered transmission and plasticity at CStr synapses. Having shown that *Tshz3* is expressed within the CStr circuit in both L5 CPNs and a few striatal cells that are not MSNs (Caubit et al., 2016), we performed conditional *Tshz3* deletion using the *Camk2a-Cre* transgene, which is known to be active in CPNs from postnatal day 2–3 onward (Casanova et al., 2001; Li et al., 2017). We found that it results in a behavioral phenotype similar to *Tshz3* heterozygous mice, also associated with altered CStr function (Chabbert et al., 2019). These findings pointed to the CStr pathway as a main player in the ASD syndrome linked to *TSHZ3* deficiency. Recently, single-cell RNA sequencing (scRNA-seq) profiling showed that the striatal cells with the highest expression of *Tshz3* are SCINs: the levels of *Tshz3* transcripts in these cells are comparable to those found in CPNs, whereas they are very low in parvalbumin/tyrosine hydroxylase interneurons and almost null in the other striatal cell populations (Munoz-Manchado et al., 2018; Saunders et al., 2018). scRNA-seq data also revealed that the *Camk2a*, considered as being expressed in MSNs (von Schimmelmann et al., 2016; Andrade et al., 2017), is also expressed in subpopulations of striatal interneurons (Saunders et al., 2018). Given the phenotypic similarity between the heterozygous and conditional *Tshz3* mouse models, and the literature linking dysfunction of striatal circuits (Li and Pozzo-Miller, 2020) and altered cholinergic function to ASD (Karvat and Kimchi, 2014; Rapanelli et al., 2017), here we characterized in SCINs the expression of *Tshz3* and the activity of the *CamK2a-Cre* transgene using genetic lineage tracing (Heffner et al., 2012). Based on our results showing that the majority of SCINs express *Tshz3* and the *Camk2a*-Cre transgene, we characterized the molecular changes in the striatum resulting from *Tshz3* deletion using the *Camk2a*-Cre mice.

RESULTS

The *Tshz3* Gene and the *Camk2a-Cre* Transgene Are Expressed in SCINs

In the adult striatum, there are few TSHZ3-positive cells that are not MSNs (Caubit et al., 2016) and recent transcriptomic analysis of mouse striatum suggested *Tshz3* expression in SCINs (Munoz-Manchado et al., 2018; Saunders et al., 2018). To test this hypothesis, we performed double choline acetyltransferase (CHAT) and TSHZ3 immunohistochemistry in wild-type mice, confirming the expression of TSHZ3 in SCINs (**Figure 1A**). We also confirmed that, as reported in other tissues (Caubit et al., 2008), the expression of the $Tshz3^{lacZ}$ allele in the striatum, revealed by beta-galactosidase (ß-Gal) staining, recapitulates the expression pattern of endogenous TSHZ3: accordingly, the density of TSHZ3-postive neurons in control mice is on the same range of the density of ß-Gal-positive neurons in $Tshz3^{+/lacZ}$ mice (**Figures 1B–D**). Moreover, these densities are in agreement with those reported in the literature (Matamales et al., 2016). Finally, double CHAT and ß-Gal staining in the striatum (**Figures 1D,E**) revealed that, in average, 90.4% of TSHZ3-expressing cells are SCINs and, conversely, 98.9% of SCINs co-express TSHZ3.

To further characterize the expression of the *Camk2a-Cre* transgene in the striatum, we performed a lineage tracing experiment by crossing *Camk2a-Cre* mice (Casanova et al., 2001) with *Rosa26-STOP-lacZ* mice (Mao et al., 1999). In these *Camk2a-Cre;Rosa26-STOP-lacZ* mice, the Cre activity resulted in the deletion of the STOP signal enabling *lacZ* expression in Cre-expressing cells and all their progeny. Accordingly, numerous ß-Gal-immunoreactive cells could be detected in the cerebral cortex and the striatum, consistent with *Camk2a* expression in CPNs and MSNs (**Figure 2A**). In addition, CHAT immunostaining showed that the majority (∼80%) of SCINs are also ß-Gal-positive (**Figures 2A,B**). Therefore, in the CStr circuit, *Tshz3* and *CamK2a* are co-expressed in CPNs and SCINs.

The *Camk2a-Cre* Efficiently Deletes the *Tshz3*-Floxed Allele in SCINs

We then examined whether *Camk2a-Cre* expression by SCINs can drive the deletion of *Tshz3*. To address this issue, *Camk2a-Cre* mice were crossed with $Tshz3^{flox/flox}$ mice to obtain *Tshz3* conditional knock-out (*Camk2a-cKO*) mice. In this model we found that both the number of TSHZ3-positive cells (**Figures 3A,B**) and the levels of *Tshz3* mRNA (**Figure 3C**) in the striatum are dramatically reduced, while the density of CHAT-positive neurons is unchanged compared to control (**Figures 3D,E**). The remaining TSHZ3-positive cells do not exhibit a specific spatial distribution (data not shown).

Genes Differentially Expressed in the Striatum of *Camk2a-cKO* Mice Are Associated With ASD

Analysis of the RNA-seq data from the striatum of *Camk2a-cKO* mice (**Supplementary Table 1A**) revealed 210 differentially

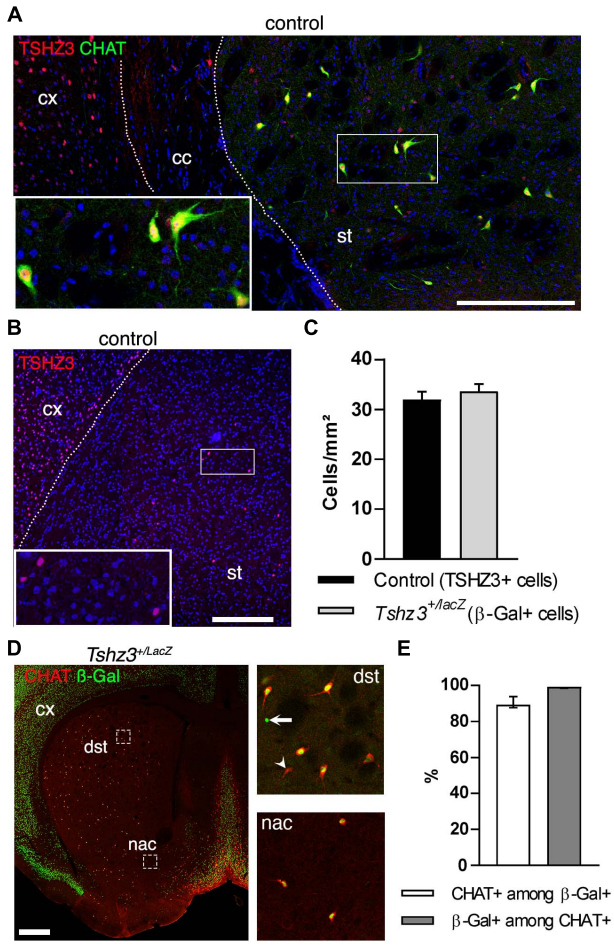

FIGURE 1 | TSHZ3 is expressed in SCINs. **(A)** Immunostaining in a control mouse showing the expression of TSHZ3 and CHAT that identifies SCINs. Scale bar, 200 μm. **(B)** Immunostaining showing the expression of TSHZ3 in a control mouse. Scale bar, 250 μm. **(C)** Density of TSHZ3-positive (1791 cells in 56.0 mm^2 from eight control mice) and ß-Gal-positive (954 cells in 28.1 mm^2 from four *Tshz3*$^{+/LacZ}$ mice) striatal cells ($P = 0.5225$, Student's *t*-test; data are expressed as mean + SEM). **(D)** Immunostaining showing the expression of ß-Gal (TSHZ3) and CHAT. Scale bar, 500 μm. Framed regions are shown on the right; arrow shows a ß-Gal-positive/CHAT-negative cell; arrowhead shows a CHAT-positive/ß-Gal-negative cell. **(E)** Percentage of CHAT-positive cells among ß-Gal-positive (TSHZ3+) cells, and vice-versa (12 sections from four *Tshz3*$^{+/LacZ}$ mice; data are expressed as median with interquartile range). cc, corpus callosum; cx, cerebral cortex; st, striatum. Nuclei in **A,B** are counterstained with DAPI (blue).

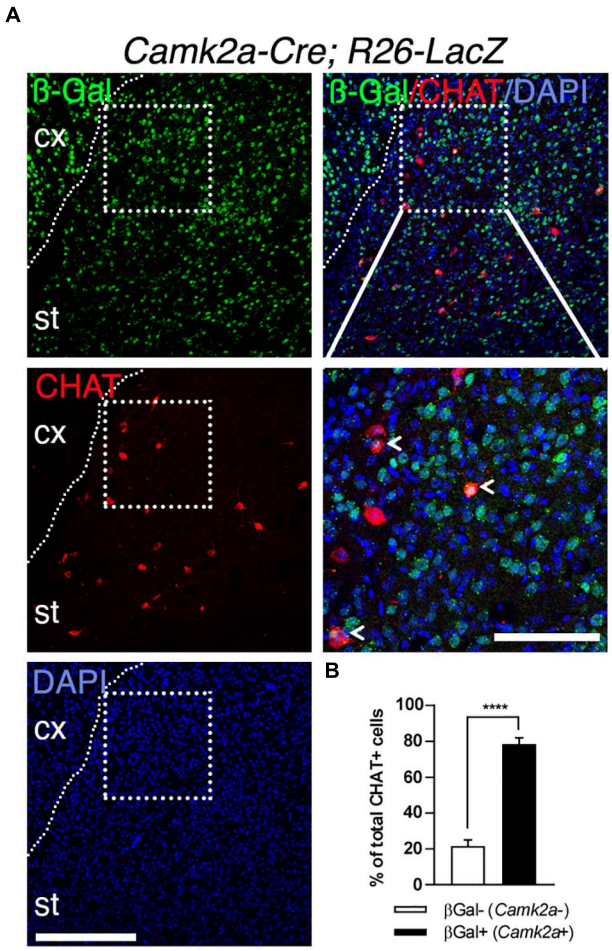

FIGURE 2 | Expression of *Camk2a-Cre* in SCINs. **(A)** Coronal brain section from a *Camk2a-Cre;Rosa26-stop-LacZ* mouse stained for ß-Gal (TSHZ3) and CHAT. Scale bar, 200 μm. The boxed region is magnified to show ß-Gal/CHAT double positive SCINs (arrowheads). Scale bar, 100 μm. **(B)** Distribution of ß-Gal-negative and ß-Gal-positive cells among CHAT-positive cells (20 sections from three mice per genotype; ****$P < 0.0001$, Student's *t*-test; data are expressed as means + SEM). cx, cerebral cortex; st, striatum. Nuclei were counterstained with DAPI (blue).

expressed genes (DEGs) with increased expression and 515 DEGs with decreased expression (false discovery rate cut-off = 0.075, $\log_2$ fold change > |0.25|) (**Supplementary Table 1B**). *Tshz3* itself is the most strongly downregulated gene. Comparison of the DEGs with scRNA-seq analysis of striatal interneurons (Munoz-Manchado et al., 2018) identified thirteen DEGs (*Bad, Dnpep, Fstl1, Galnt18, Hdac5, Id3, Mrpl54, Ncaph2, Ntrk1, Osbpl6, Sez6l, Tnrc18*, and *Tshz3*) expressed in SCINs. To further characterize the DEGs, we performed functional and enrichment analyses using EnrichR (Kuleshov et al., 2016) and g:Profiler (Raudvere et al., 2019). These analyses confirmed enrichment for genes expressed in the striatum (**Supplementary Tables 1C–E**) and revealed KEGG pathways mainly involved in mitochondrial function and neurological disorders (**Figure 4A** and **Supplementary Tables 1F–H**). We quantified the representation of 36 mitochondrial processes within the DEGs, using the MitoXplorer pipeline (Yim et al., 2020). This analysis revealed that DEGs are distributed in 31 mitochondrial processes, especially within oxidative phosphorylation, translation as well as replication and transcription (**Supplementary Figure 1**). The KEGG pathway enrichment analysis also identified the association of DEGs in three pathways (glutamatergic synapse, Wnt signaling, and mTOR signaling) associated with ASD (BRITE H02111) (**Supplementary Tables 1F,G**). We also performed enrichment

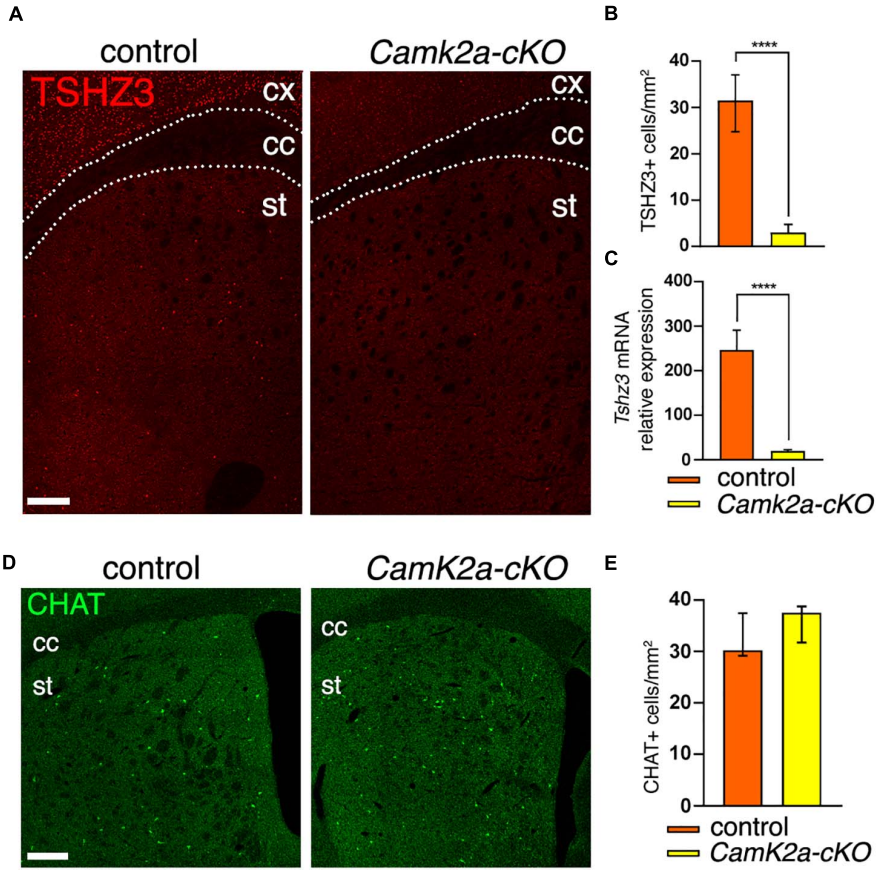

FIGURE 3 | Loss of *Tshz3* in SCINs in *Camk2a-cKO* mice. **(A)** Coronal brain sections from control and *Camk2a-cKO* mice stained for TSHZ3. Scale bar, 500 μm. **(B)** Densities of TSHZ3-positive cells in the striatum of control and *Camk2a-cKO* mice (898 cells in 28.1 mm^2 and 95 cells in 26.3 mm^2 for control and *Camk2a-cKO*, respectively, from three mice per genotype; ****$P < 0.0001$, Mann–Whitney test). **(C)** *Tshz3* mRNA levels analyzed by RNA-seq in control and *Camk2a-cKO* striata (****$P_{adj} < 1.00E\text{-}14$, $Log_2FC = -2.26$; data expressed as mean + SEM). **(D)** Coronal brain sections from control and *Camk2a-cKO* mice stained for CHAT. Scale bar, 300 μm **(E)** Densities of CHAT-positive SCINs in control and *Camk2a-cKO* mice (758 cells in 23.6 mm^2 and 629 cells in 17.1 mm^2 for control and *Camk2a-cKO*, respectively, from three mice per genotype; $P = 0.1014$, Mann–Whitney test). Cell counts in **B,E** were performed on the whole striatal surface. Data in **B,E** are expressed as median with interquartile range. cc, corpus callosum; cx, cerebral cortex; st, striatum.

analysis on phenotypes predefined by MGI (Mouse Genome Informatics mammalian phenotypes) and found that DEGs are significantly enriched with phenotypes of impaired coordination and hyperactivity (adjusted *P*-value < 0.05) (**Supplementary Table 1I**). Comparing the 718 human orthologs (**Supplementary Table 1J**) of the 725 DEGs with the SFARI autism gene list (Abrahams et al., 2013) identified 54 genes (**Supplementary Table 1K**). Almost half of these genes (25/54 = 46%) belong to the high confidence ASD candidates (SFARI categories 1 and 2). Amongst the ASD candidate gene set, the most significant KEGG pathways and biological processes are related to synaptic signaling (**Figure 4B** and **Supplementary Table 2**). We then proceeded to identify the DEGs present in both the striatum (725 DEGs; this study) and the cerebral cortex (1025 DEGs) (Chabbert et al., 2019) of *Camk2a-cKO* mice. This analysis identified 235 genes regulated in these two brain regions (**Supplementary Table 3A**), showing that most of the genes regulated by *Tshz3* are unique to the striatum or the cerebral cortex, suggesting cell-context specificity. Indeed, 196 genes regulated in both these brain structures are differentially responsive (activated in one brain part and repressed in the other, or vice versa), showing that even genes regulated by TSHZ3 both in the striatum and the cerebral cortex can be controlled by distinct mechanisms (**Supplementary Table 3B**). Comparing the 233 human orthologs (**Supplementary Table 3C**) of the 235 DEGs with SFARI identifies 15 genes including *TSHZ3* (**Supplementary Table 3D**). Last, functional and enrichment analysis using EnrichR reveals pathways involved in mitochondrial function and neurological disorders (**Supplementary Tables 3E–H**).

DISCUSSION

As main findings, this study show that (i) all SCINs express TSHZ3 and the main striatal population expressing TSHZ3 are SCINs; (ii) the *Camk2a-Cre* transgene is expressed in the SCIN lineage; (iii) conditional deletion of *Tshz3* using the *Camk2a-Cre* mediates efficient *Tshz3* deletion in SCINs and drives changes in

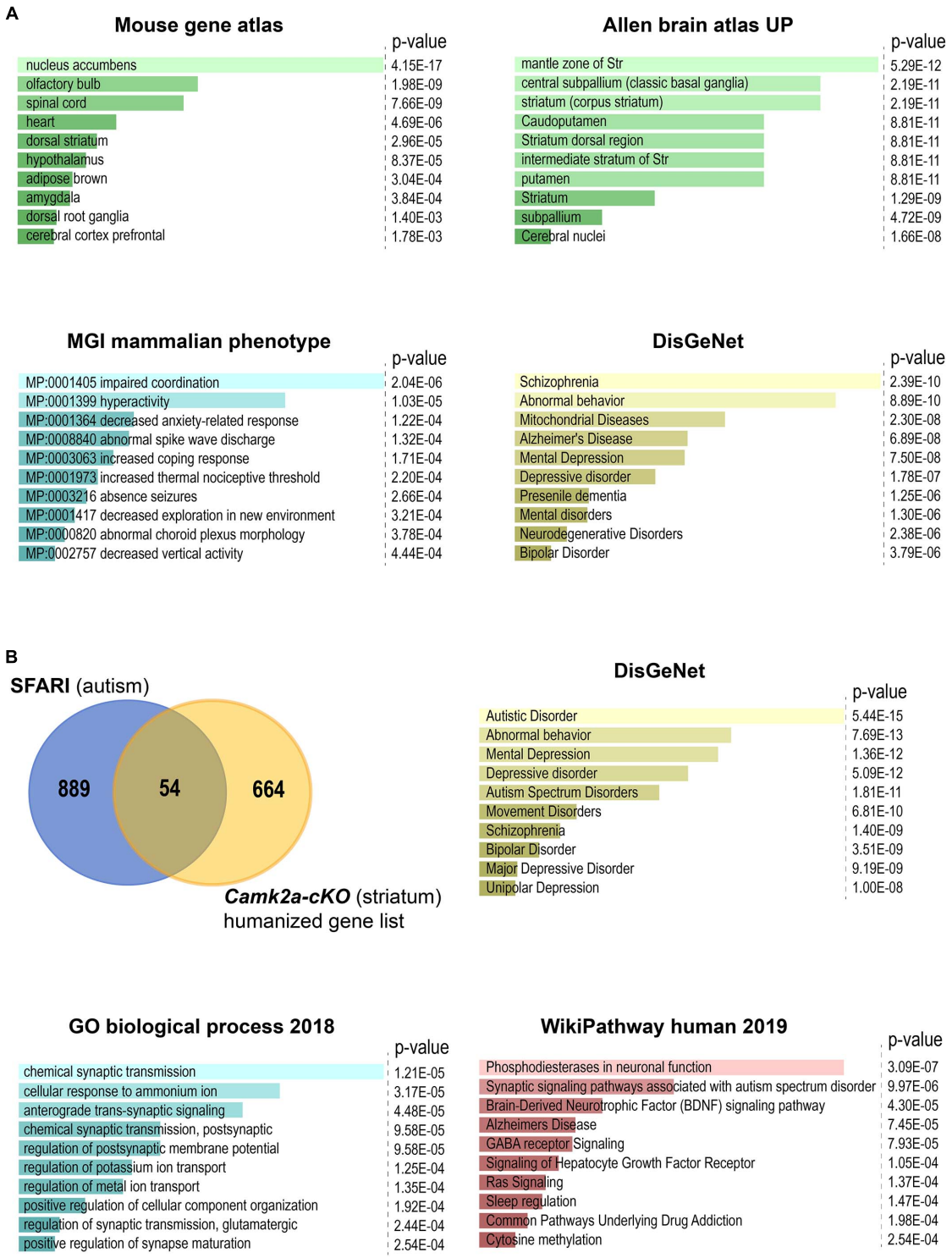

FIGURE 4 | Enrichment analysis using EnrichR of DEGs between *Camk2a-cKO* and control. The bar plots show the top 10 terms selected according to their *P*-value. All enrichment results are also shown in **Supplementary Tables 2**, **3**. **(A)** Analysis of all the DEGs. Highest-scoring is found for: nucleus accumbens, which is part of the ventral striatum, in the mouse gene atlas; terms related to striatum in the Allen brain atlas UP category; impaired coordination, which is commonly associated with ASD, in the MGI mammalian phenotype database; neurological disorders in the crowd-based DisGeNet. **(B)** Analysis of the 54 genes overlapping between the SFARI gene list and human orthologs of our list of DEGs. Highest scoring is found: in DisGeNet for autistic disorder (to note the strong overlap between these terms and those issued from the DisGeNet analysis of the overall set of DEGs); in Gene Ontology Biological Process for terms related to synaptic transmission and membrane potential; in human WikiPathways, for terms related to synaptic signaling pathways, including pathways associated with ASD.

the expression of 725 genes in the striatum, among which 196 are also differentially expressed in the cerebral cortex, suggesting profound alteration of striatal function. These results call to more caution in the interpretation of experiments using *Camk2a-Cre*-dependent gene manipulations and point to SCINs as potential players in the ASD-relevant behavioral abnormalities triggered by *Tshz3* loss in both the heterozygous deletion model (Caubit et al., 2016) and the conditional model using the *Camk2a-Cre* transgene (Chabbert et al., 2019).

Unreported recombinase activity using Cre driver lines can be due to ectopic expression of the *Cre* transgene but also to unappreciated expression of the driver gene itself (Heffner et al., 2012). The *Camk2a* gene has been reported to be expressed postnatally (Bayer et al., 1999) in specific brain regions, including the cerebral cortex and the striatum (Casanova et al., 2001). While the *Camk2a-Cre* transgene has been extensively used to study the postnatal function of genes highly expressed in projection neurons of these regions, as CPNs (Li et al., 2017) and MSNs (von Schimmelmann et al., 2016; Andrade et al., 2017), its expression and/or activity has not been specifically examined in striatal interneurons. To date, expression profiles available in gene expression atlas [i.e., Allen Brain Atlas (Lein et al., 2007)] do not provide information on the striatal cells expressing *CamK2a* and it is only recently that scRNA-seq reported the expression of *CamK2a* not only in MSNs but also in striatal interneurons (Saunders et al., 2018). In this context, genetic lineage tracing represents an efficient way to determine which cellular types express or have once expressed the *CamK2a-Cre* transgene whatever its developmental/postnatal expression profile. As MSNs represent 90% of all striatal neurons, expression of the reporter gene in a specific interneuron class, such as SCINs that constitute less than 2% of the total striatal population, cannot be addressed unless a specific marker for the latter is used. Here, we reveal the expression of the *Camk2a-Cre* transgene in the SCIN lineage by co-immunostaining for the reporter ß-Gal and for CHAT in the striatum of *Camk2a-Cre;Rosa26-STOP-lacZ* mice. The ß-Gal reporter is not detected in the whole SCIN population but in ∼80% of them. This could be due to methodological limitations, such as inefficient excision of the STOP cassette, and/or reflect the diversity of these interneurons recently emphasized by studies of their developmental origin and birthdate (Allaway and Machold, 2017), molecular and electrophysiological profile, and connectivity (Ahmed et al., 2019). In addition, our results call for a better characterization of the expression pattern of the *CamK2a-Cre* transgene, critical for the interpretation of the results generated using this Cre line. In particular, they raise the question of the contribution of SCINs to the phenotypes observed in mouse models of *Tshz3*-deficiency. For instance, we show that the *Tshz3* gene associated with autism (Caubit et al., 2016; Chabbert et al., 2019), known to be expressed in CPNs, is also expressed in SCINs. Moreover, expression of *Cre* allows efficient recombination of the *Tshz3*-floxed allele in SCINs without affecting their viability, as previously shown for CPNs. Therefore, *Tshz3* deletion in both CPNs and SCINs might contribute to altered functioning of the CStr circuitry in the heterozygous *Tshz3* as well as in the conditional *Camk2a-cKO* mouse models. It is worth noting that, although in low number, SCINs are tonically active neurons that represent the main source of striatal cholinergic tone, and act as key regulators of striatal function in health and diseases. Despite evidence for the role of the cholinergic system in the etiology of ASD (Karvat and Kimchi, 2014), the specific involvement of SCINs remains poorly investigated. The findings of this study raise the question of the respective contribution of SCINs and CPNs to the *TSHZ3*-related ASD phenotype.

In addition, we found 725 DEGs in the striatum of *Camk2a-cKO* mice. These gene expression changes might occur in part in SCINs, in particular for the DEGs reported as specific for these interneurons (Munoz-Manchado et al., 2018) as well as in the few *Tshz3*-positive/CHAT-negative striatal cells, in CPN axons (Kim and Jung, 2020) and, in a non-cell autonomous way, in other striatal components. Indeed, we previously reported that *Tshz3* deletion results in altered transmission and plasticity at corticostriatal synapses (Chabbert et al., 2019), which could in turn affect gene expression in their striatal targets (mainly MSNs). *Tshz3* loss in SCINs might also alter their morphofunctional properties and thereby indirectly impact gene expression in their striatal targets. Regarding the pathways dysregulated in the striatum of *Camk2a-cKO* mice, enrichment analysis highlights synaptic activity and mitochondrial function pathways, whose alterations are suggested to contribute to ASD development (Citrigno et al., 2020; Rojas-Charry et al., 2021). In the same line, testing for enrichment of MGI mammalian phenotypes associated with the DEGs identified impaired coordination and hyperactivity, two behaviors that frequently accompany ASD. Similarly, enrichment for Elsevier pathway collection identified DEGs involved in epilepsy, which is found at higher rates in children with ASD than the general population. In conclusion, here we show that conditional *Tshz3* deletion using the *Camk2a-Cre* transgene targets not only CPNs (Casanova et al., 2001; Li et al., 2017) but, unexpectedly, also SCINs, triggering dramatic changes in striatal gene expression. These data call for possible reconsideration of previous findings obtained using *Camk2a-Cre*-dependent gene deletion, and for careful characterization of transgenic Cre mouse lines.

MATERIALS AND METHODS

Mouse Strains and Genotyping

The $Tshz3^{lacZ}$, $Tshz3^{flox/flox}$, *Camk2a-Cre* [*CaMK2a-iCre* BAC (CKC)] and *Rosa26-STOP-lacZ* mouse lines have been described previously (Mao et al., 1999; Casanova et al., 2001; Caubit et al., 2008; Chabbert et al., 2019). Male heterozygous *Camk2a-Cre* mice were crossed with female $Tshz3^{flox/flox}$ to obtain *Tshz3* conditional knock-out (cKO) mice (*Camk2a-cKO*) (Casanova et al., 2001). Littermate $Camk2a\text{-}Cre^{-/-}$ mice were used as control. Animals carrying the $Tshz3^{flox}$ allele and $Tshz3^{\Delta}$ allele were genotyped as described previously (Chabbert et al., 2019).

Immunohistochemistry and Histology

All stains were performed on coronal 40 μm cryostat brain sections of postnatal day (P) 28–34 mice, cut at the level of the rostral striatum, from bregma 0 to +1.18 mm, AP (Paxinos

and Franklin, 2001). For TSHZ3 immunostaining, brains were immediately removed after euthanasia and frozen in dry ice until use; before incubation with the antibodies, sections were fixed in 4% paraformaldehyde (PFA) for 15 min, then washed twice for 5 min in PBS. For TSHZ3 and CHAT double immunodetection, mice were anesthetized (ketamine + xylazine, 100 + 10 mg/kg, respectively, i.p.) and transcardially perfused with PBS. Brains were immediately dissected out, post-fixed by immersion 2 h in 4% paraformaldehyde in PBS, placed in 30% sucrose in PBS overnight and frozen in dry ice until sectioning. For the other stains, mice under anesthesia were transcardially perfused with 4% PFA in PBS. Brains were removed and post-fixed in 4% PFA for at least 2 h before cryostat sectioning. For all stains, brain sections were washed with PBS and blocked in PBST (0.3% Triton X-100 in 1xPBS) with 5% BSA for 1 h at room temperature. Sections were then incubated in primary antibody diluted in blocking solution (PBST, 1% BSA) overnight at 4°C with the following primary antibodies: goat anti-CHAT (1:100, Millipore, AB144P), rabbit anti-ß-Galactosidase (1:1,000, Cappel, 599762) and guinea-pig anti-TSHZ3 (1:2,000; ref. Caubit et al., 2008). Sections were then washed with PBS three times and incubated overnight at 4°C in secondary antibodies diluted 1:1,000 in blocking solution: donkey anti-guinea pig Cy3 and donkey anti-goat Cy3 (Jackson ImmunoResearch Laboratories); donkey anti-goat Alexa Fluor 488, Donkey anti-Goat AlexaFluor 568 and donkey anti-rabbit Alexa Fluor 488 (Life Technologies). Sections were stained using a 300 μM DAPI intermediate solution (1:1,000, Molecular Probes, Cat# B34650). Sections were then washed with PBS three times, mounted on Superfrost Plus slides (Fischer Scientific) and coverslipped for imaging on a laser scanning confocal microscope (Zeiss LSM780 with Quasar detection module). Spectral detection bandwidths (nm) were set at 411-473 for DAPI, 498-568 for GFP and 568-638 for Cy3; pinhole was set to 1 Airy unit. Unbiased counting of CHAT-, TSHZ3-, and ß-Gal-positive neurons were done on the whole surface the dorsal striatum (excluding the nucleus accumbens) of confocal images using ImageJ software (see figure legends for details). Images were assembled using Photoshop 21.2.3. Statistical analysis was performed using GraphPad Prism 7.05. Data were analyzed by unpaired Student's *t*-test or by Mann–Whitney test when they passed or not, respectively, the D'Agostino–Pearson normality test. A P-value < 0.001 was considered significant.

RNA Sequencing Analysis

Three independent replicates, each containing the dorsal striata from 3 to 4 *Camk2a-cKO* mice and littermate controls (P34), were prepared for analysis. RNA and cDNA preparation, as well as cDNA sequencing, were performed as previously reported (Chabbert et al., 2019). We used STAR (Dobin et al., 2013) with standard parameters to align RNA-seq reads to the latest release of the mouse genome (mm10) downloaded from UCSC (as of March 2020). Read counting was performed using featureCounts (Liao et al., 2014). One replicate of control and one of *Camk2a-cKO* were discarded before further analysis due to inconsistent clustering during principal component analysis. Differential expression analysis was done using DESeq2 (Love et al., 2014). DESeq2 results, as well as the list of DEGs used for enrichment analysis and KEGG pathway mapping (representing genes with a FDR ≤ 0.075 and a fold change of 1.25 (log2FC: $|0.25|$), are shown in **Supplementary Table 1B**. Enrichment analysis was done using EnrichR (Chen et al., 2013; Kuleshov et al., 2016).

Quantitative RT-qPCR

Total RNA from control and *Tshz3* mutant (P28) cerebral cortex was prepared using Rneasy Plus Universal Mini Kit gDNA eliminator (Qiagen™) and first strand cDNA was synthesized using iScript Reverse Transcription Supermix kit (Bio-RAD™). Real-time quantitative PCR (RT-qPCR) was performed on a CFX96 qPCR detection system (Bio-RAD™) using SYBR® GreenER™ qPCR SuperMixes (Life Technologies™). RT-qPCR conditions: 40 cycles of 95°C for 15 s and 60°C for 60 s. Analyses were performed in triplicate. Transcript levels were first normalized to the housekeeping gene *Gapdh*. Primer sequences used for RT-qPCR: *Gapdh* Forward: 5′-GTCTCCTGCGACTTCAACAGCA-3′; *Gapdh* Reverse: 5′-ACCACCCTGTTGCTGTAGCCGT-3′. *Tshz3* Forward: 5′-CACTCCTTCCAGCATCTCTGAG-3′; *Tshz3* Reverse: 5′-TAGCAGGTGCTGAGGATTCCAG-3′. Statistical analysis was performed by unpaired Student's *t*-tests by using the qbasePLUS software version 2 (Biogazelle). A P-value < 0.05 was considered significant.

URLs

http://dropviz.org
https://www.genome.jp/kegg/brite.html
http://mitoxplorer.ibdm.univ-mrs.fr.

DATA AVAILABILITY STATEMENT

The data that support the findings of this study are available from the corresponding author upon reasonable request. Raw data (FastQ files) from the sequencing experiment (triplicates from wild-type and *Tshz3*-mutant striatum) and raw abundance measurements for genes (read counts) for each sample are available from Gene Expression Omnibus (GEO) under accession GSE157658, which should be quoted in any manuscript discussing the data.

ETHICS STATEMENT

The animal study was reviewed and approved by "Comité National de Réflexion Ethique sur l'Expérimentation Animale n°14" (ID numbers 57-07112012, 2019020811238253-V2 #19022, and 2020031615241974-V5 #25232) and were in agreement with the recommendations of the European Communities Council Directive (2010/63/EU).

AUTHOR CONTRIBUTIONS

EA, XC, DC, and FD performed the histological experiments and quantitative analyses. EA, XC, and FD performed the CHAT cell lineage experiments. AF and XC prepared the samples for RNA-seq. BH and IM performed the RNA-seq analysis, pathway analysis, and enrichment analysis. EA and XC generated and maintained the transgenic mouse lines. XC, LF, BH, and PG conceived the project, supervised the work and wrote the manuscript. All authors contributed to the article and approved the submitted version.

FUNDING

Microscopy was performed at the imaging platform of the IBDM and we acknowledge France-BioImaging/PiCsL infrastructure (ANR-10-INSB-04-01); the IBDM is affiliated with NeuroMarseille, the Aix-Marseille University neuroscience network supported by the Excellence Initiative of Aix-Marseille University A*MIDEX "Investissements d'Avenir" program (AMX-19-IET-004), with MarMara (AMX-19-IET-007) and with NeuroSchool, the Aix-Marseille University graduate school in neuroscience supported by the A*MIDEX and the "Investissements d'Avenir" program (nEURo*AMU, ANR-17-EURE-0029 grant). This work was supported by the French Research National Agency (ANR) "TSHZ3inASD" project grant n° ANR-17-CE16-0030-01 (to LF and BH), the *Fédération pour la Recherche sur le Cerveau* (FRC) (to LF), the *Centre National de la Recherche Scientifique* (CNRS), and Aix-Marseille University. DC was supported by a Ph.D. grant from the MESRI (*Ministère de l'Enseignement Supérieur, de la Recherche et de l'Innovation*). EA was supported by a post-doctoral fellowship from the ANR-17-CE16-0030-01 grant.

ACKNOWLEDGMENTS

We thank G. Schütz (DKFZ, Germany) for providing the *CaMK2a-iCre* mice and the IBDM mouse facility. We also acknowledge the Languedoc-Roussillon facility Montpellier GenomiX (MGX) and thank Dany Severac and Emeric Dubois for RNA sequencing.

SUPPLEMENTARY MATERIAL

The Supplementary Material for this article can be found online at: https://www.frontiersin.org/articles/10.3389/fgene.2021.683959/full#supplementary-material

Supplementary Figure 1 | Interactome view of 36 mitochondrial processes within the DEGs. Striatal DEGs are distributed in 31 mitochondrial processes, especially within oxidative phosphorylation, translation as well as replication and transcription. Individual bubbles represent genes of a process; blue and red, indicate up- or down-regulated genes within a process, respectively. Bubble size indicates log2 fold change values. This scheme was built using the "Interactome View" tool available on mitoXplorer web-plateform http://mitoxplorer.ibdm.univ-mrs.fr/index.php.

REFERENCES

Abrahams, B. S., Arking, D. E., Campbell, D. B., Mefford, H. C., Morrow, E. M., Weiss, L. A., et al. (2013). Sfari gene 2.0: a community-driven knowledgebase for the autism spectrum disorders (asds). *Mol. Autism* 4:36. doi: 10.1186/2040-2392-4-36

Abudukeyoumu, N., Hernandez-Flores, T., Garcia-Munoz, M., and Arbuthnott, G. W. (2019). Cholinergic modulation of striatal microcircuits. *Eur. J. Neurosci.* 49, 604–622. doi: 10.1111/ejn.13949

Ahmed, N. Y., Knowles, R., and Dehorter, N. (2019). New insights into cholinergic neuron diversity. *Front. Mol. Neurosci.* 12:204. doi: 10.3389/fnmol.2019.00204

Allaway, K. C., and Machold, R. (2017). Developmental specification of forebrain cholinergic neurons. *Dev. Biol.* 421, 1–7. doi: 10.1016/j.ydbio.2016.11.007

Andrade, E. C., Musante, V., Horiuchi, A., Matsuzaki, H., Brody, A. H., Wu, T., et al. (2017). Arpp-16 is a striatal-enriched inhibitor of protein phosphatase 2a regulated by microtubule-associated serine/threonine kinase 3 (mast 3 kinase). *J. Neurosci.* 37, 2709–2722. doi: 10.1523/JNEUROSCI.4559-15.2017

Bayer, K. U., Lohler, J., Schulman, H., and Harbers, K. (1999). Developmental expression of the cam kinase ii isoforms: ubiquitous gamma- and delta-cam kinase ii are the early isoforms and most abundant in the developing nervous system. *Brain Res. Mol. Brain Res.* 70, 147–154. doi: 10.1016/s0169-328x(99)00131-x

Casanova, E., Fehsenfeld, S., Mantamadiotis, T., Lemberger, T., Greiner, E., Stewart, A. F., et al. (2001). A camkiialpha icre bac allows brain-specific gene inactivation. *Genesis* 31, 37–42.

Caubit, X., Gubellini, P., Andrieux, J., Roubertoux, P. L., Metwaly, M., Jacq, B., et al. (2016). Tshz3 deletion causes an autism syndrome and defects in cortical projection neurons. *Nat. Genet.* 48, 1359–1369. doi: 10.1038/ng.3681

Caubit, X., Lye, C. M., Martin, E., Core, N., Long, D. A., Vola, C., et al. (2008). Teashirt 3 is necessary for ureteral smooth muscle differentiation downstream of shh and bmp4. *Development* 135, 3301–3310.

Chabbert, D., Caubit, X., Roubertoux, P. L., Carlier, M., Habermann, B., Jacq, B., et al. (2019). Postnatal tshz3 deletion drives altered corticostriatal function and autism spectrum disorder-like behavior. *Biol. Psychiatry* 86, 274–285. doi: 10.1016/j.biopsych.2019.03.974

Chen, E. Y., Tan, C. M., Kou, Y., Duan, Q., Wang, Z., Meirelles, G. V., et al. (2013). Enrichr: interactive and collaborative html5 gene list enrichment analysis tool. *BMC Bioinform.* 14:128. doi: 10.1186/1471-2105-14-128

Citrigno, L., Muglia, M., Qualtieri, A., Spadafora, P., Cavalcanti, F., Pioggia, G., et al. (2020). The mitochondrial dysfunction hypothesis in autism spectrum disorders: current status and future perspectives. *Int. J. Mol. Sci.* 21:5785. doi: 10.3390/ijms21165785

Dobin, A., Davis, C. A., Schlesinger, F., Drenkow, J., Zaleski, C., Jha, S., et al. (2013). Star: ultrafast universal rna-seq aligner. *Bioinformatics* 29, 15–21. doi: 10.1093/bioinformatics/bts635

Gerfen, C. R., and Surmeier, D. J. (2011). Modulation of striatal projection systems by dopamine. *Annu. Rev. Neurosci.* 34, 441–466. doi: 10.1146/annurev-neuro-061010-113641

Heffner, C. S., Herbert Pratt, C., Babiuk, R. P., Sharma, Y., Rockwood, S. F., Donahue, L. R., et al. (2012). Supporting conditional mouse mutagenesis with a comprehensive cre characterization resource. *Nat. Commun.* 3:1218. doi: 10.1038/ncomms2186

Karvat, G., and Kimchi, T. (2014). Acetylcholine elevation relieves cognitive rigidity and social deficiency in a mouse model of autism. *Neuropsychopharmacology* 39, 831–840. doi: 10.1038/npp.2013.274

Kawaguchi, Y. (1997). Neostriatal cell subtypes and their functional roles. *Neurosci. Res.* 27, 1–8. doi: 10.1016/s0168-0102(96)01134-0

Kim, E., and Jung, H. (2020). Local mrna translation in long-term maintenance of axon health and function. *Curr. Opin. Neurobiol.* 63, 15–22. doi: 10.1016/j.conb.2020.01.006

Kuleshov, M. V., Jones, M. R., Rouillard, A. D., Fernandez, N. F., Duan, Q., Wang, Z., et al. (2016). Enrichr: a comprehensive gene set enrichment analysis web server 2016 update. *Nucleic Acids Res.* 44, W90–W97. doi: 10.1093/nar/gkw377

Lein, E. S., Hawrylycz, M. J., Ao, N., Ayres, M., Bensinger, A., Bernard, A., et al. (2007). Genome-wide atlas of gene expression in the adult mouse brain. *Nature* 445, 168–176. doi: 10.1038/nature05453

Li, W., and Pozzo-Miller, L. (2020). Dysfunction of the corticostriatal pathway in autism spectrum disorders. *J. Neurosci. Res.* 98, 2130–2147. doi: 10.1002/jnr.24560

Li, Y., You, Q. L., Zhang, S. R., Huang, W. Y., Zou, W. J., Jie, W., et al. (2017). Satb2 ablation impairs hippocampus-based long-term spatial memory and short-term working memory and immediate early genes (iegs)-mediated hippocampal synaptic plasticity. *Mol. Neurobiol.* doi: 10.1007/s12035-017-0531-5 [Epub ahead of print].

Liao, Y., Smyth, G. K., and Shi, W. (2014). Featurecounts: an efficient general purpose program for assigning sequence reads to genomic features. *Bioinformatics* 30, 923–930. doi: 10.1093/bioinformatics/btt656

Love, M. I., Huber, W., and Anders, S. (2014). Moderated estimation of fold change and dispersion for rna-seq data with deseq2. *Genome Biol.* 15:550. doi: 10.1186/s13059-014-0550-8

Mao, X., Fujiwara, Y., and Orkin, S. H. (1999). Improved reporter strain for monitoring cre recombinase-mediated DNA excisions in mice. *Proc. Natl. Acad. Sci. U. S. A.* 96, 5037–5042. doi: 10.1073/pnas.96.9.5037

Matamales, M., Gotz, J., and Bertran-Gonzalez, J. (2016). Quantitative imaging of cholinergic interneurons reveals a distinctive spatial organization and a functional gradient across the mouse striatum. *PLoS One* 11:e0157682. doi: 10.1371/journal.pone.0157682

Munoz-Manchado, A. B., Bengtsson Gonzales, C., Zeisel, A., Munguba, H., Bekkouche, B., Skene, N. G., et al. (2018). Diversity of interneurons in the dorsal striatum revealed by single-cell rna sequencing and patchseq. *Cell Rep.* 24, 2179–2190.e7. doi: 10.1016/j.celrep.2018.07.053

Paxinos, G., and Franklin, K. B. J. (2001). *The Mouse Brain in Stereotaxic Coordinates*, 2nd Edn. Cambridge, MA: Academic Press.

Rapanelli, M., Frick, L. R., Xu, M., Groman, S. M., Jindachomthong, K., Tamamaki, N., et al. (2017). Targeted interneuron depletion in the dorsal striatum produces autism-like behavioral abnormalities in male but not female mice. *Biol. Psychiatry* 82, 194–203. doi: 10.1016/j.biopsych.2017.01.020

Raudvere, U., Kolberg, L., Kuzmin, I., Arak, T., Adler, P., Peterson, H., et al. (2019). G:Profiler: a web server for functional enrichment analysis and conversions of gene lists (2019 update). *Nucleic Acids Res.* 47, W191–W198. doi: 10.1093/nar/gkz369

Reiner, A., Hart, N. M., Lei, W., and Deng, Y. (2010). Corticostriatal projection neurons – dichotomous types and dichotomous functions. *Front. Neuroanat.* 4:142. doi: 10.3389/fnana.2010.00142

Rojas-Charry, L., Nardi, L., Methner, A., and Schmeisser, M. J. (2021). Abnormalities of synaptic mitochondria in autism spectrum disorder and related neurodevelopmental disorders. *J. Mol. Med. (Berl.)* 99, 161–178. doi: 10.1007/s00109-020-02018-2

Saunders, A., Macosko, E. Z., Wysoker, A., Goldman, M., Krienen, F. M., de Rivera, H., et al. (2018). Molecular diversity and specializations among the cells of the adult mouse brain. *Cell* 174, 1015–1030e1016. doi: 10.1016/j.cell.2018.07.028

Shepherd, G. M. (2013). Corticostriatal connectivity and its role in disease. *Nat. Rev. Neurosci.* 14, 278–291. doi: 10.1038/nrn3469

Sohur, U. S., Padmanabhan, H. K., Kotchetkov, I. S., Menezes, J. R., and Macklis, J. D. (2012). Anatomic and molecular development of corticostriatal projection neurons in mice. *Cereb. Cortex* 24, 293–303. doi: 10.1093/cercor/bhs342

Tepper, J. M., Koos, T., Ibanez-Sandoval, O., Tecuapetla, F., Faust, T. W., and Assous, M. (2018). Heterogeneity and diversity of striatal gabaergic interneurons: update 2018. *Front. Neuroanat.* 12:91. doi: 10.3389/fnana.2018.00091

von Schimmelmann, M., Feinberg, P. A., Sullivan, J. M., Ku, S. M., Badimon, A., Duff, M. K., et al. (2016). Polycomb repressive complex 2 (prc2) silences genes responsible for neurodegeneration. *Nat. Neurosci.* 19, 1321–1330. doi: 10.1038/nn.4360

Yim, A., Koti, P., Bonnard, A., Marchiano, F., Durrbaum, M., Garcia-Perez, C., et al. (2020). Mitoxplorer, a visual data mining platform to systematically analyze and visualize mitochondrial expression dynamics and mutations. *Nucleic Acids Res.* 48, 605–632. doi: 10.1093/nar/gkz1128

Conflict of Interest: The authors declare that the research was conducted in the absence of any commercial or financial relationships that could be construed as a potential conflict of interest.

frontiers in Cellular Neuroscience

ORIGINAL RESEARCH
published: 30 July 2021
doi: 10.3389/fncel.2021.692232

An Autism-Associated *de novo* Mutation in GluN2B Destabilizes Growing Dendrites by Promoting Retraction and Pruning

*Jacob A. Bahry[1,2], Karlie N. Fedder-Semmes[3], Michael P. Sceniak[1] and Shasta L. Sabo[1,2,4]**

[1] Department of Biology, Central Michigan University, Mount Pleasant, MI, United States, [2] Graduate Program in Biochemistry, Cell and Molecular Biology, Central Michigan University, Mount Pleasant, MI, United States, [3] Department of Pharmacology, Case Western Reserve University, Cleveland, OH, United States, [4] Neuroscience Program, Central Michigan University, Mount Pleasant, MI, United States

Mutations in *GRIN2B*, which encodes the GluN2B subunit of NMDA receptors, lead to autism spectrum disorders (ASD), but the pathophysiological mechanisms remain unclear. Recently, we showed that a GluN2B variant that is associated with severe ASD (GluN2B^{724t}) impairs dendrite morphogenesis. To determine which aspects of dendrite growth are affected by GluN2B^{724t}, we investigated the dynamics of dendrite growth and branching in rat neocortical neurons using time-lapse imaging. GluN2B^{724t} expression shifted branch motility toward retraction and away from extension. GluN2B^{724t} and wild-type neurons formed new branches at similar rates, but mutant neurons exhibited increased pruning of dendritic branches. The observed changes in dynamics resulted in nearly complete elimination of the net expansion of arbor size and complexity that is normally observed during this developmental period. These data demonstrate that ASD-associated mutant GluN2B interferes with dendrite morphogenesis by reducing rates of outgrowth while promoting retraction and subsequent pruning. Because mutant dendrites remain motile and capable of growth, it is possible that reducing pruning or promoting dendrite stabilization could overcome dendrite arbor defects associated with *GRIN2B* mutations.

Keywords: autism, neurodevelopment, GluN2B (NMDA receptor subunit NR2B), dendrite development, *GRIN2B* gene, NMDA receptor, live imaging

OPEN ACCESS

Edited by:
Yu-Chih Lin,
Hussman Institute for Autism, United States

Reviewed by:
Deepak Prakash Srivastava, King's College London, United Kingdom
Stanislava Pankratova, University of Copenhagen, Denmark

***Correspondence:**
Shasta L. Sabo
sabo1s@cmich.edu

Specialty section:
This article was submitted to Cellular Neuropathology, a section of the journal Frontiers in Cellular Neuroscience

Received: *07 April 2021*
Accepted: *06 July 2021*
Published: *30 July 2021*

Citation:
Bahry JA, Fedder-Semmes KN, Sceniak MP and Sabo SL (2021) An Autism-Associated de novo Mutation in GluN2B Destabilizes Growing Dendrites by Promoting Retraction and Pruning. Front. Cell. Neurosci. 15:692232. doi: 10.3389/fncel.2021.692232

INTRODUCTION

Autism spectrum disorder (ASD) is a neurodevelopmental disorder (NDD) characterized by restricted, repetitive behavior, and social deficits. A small number of genes have been identified as having a high probability of bearing mutations that cause sporadic ASD (Abrahams et al., 2013). One of these high-confidence genes is *GRIN2B*. *GRIN2B* encodes the GluN2B subunit of NMDA receptors, ionotropic glutamate receptors that are essential for plasticity and brain development (Sanz-Clemente et al., 2013). Recently, *GRIN2B* has been identified as 1 of the 10 genes most likely to be key nodes that may control the larger network of autism risk genes (Fan et al., 2020).

Homozygous *GRIN2B* knockout mice die perinatally, indicating that GluN2B is required for neural development (Kutsuwada et al., 1996).

Many *GRIN2B* mutations have been identified among individuals with ASD and other NDDs (Myers et al., 2011; O'Roak et al., 2011, 2012, 2014; Tarabeux et al., 2011; Talkowski et al., 2012; Yoo et al., 2012; De Rubeis et al., 2014; Iossifov et al., 2014; Kenny et al., 2014; Pan et al., 2015; Sanders et al., 2015; Takasaki et al., 2016; Platzer et al., 2017). However, it is not yet understood how *GRIN2B* mutations lead to pathogenesis of NDDs. Studies in non-neuronal cells have begun evaluating how *GRIN2B* mutations affect NMDAR function by examining channel properties and subcellular trafficking (Swanger et al., 2016; Liu et al., 2017; Bell et al., 2018; Fedele et al., 2018; Vyklicky et al., 2018; Li et al., 2019; Sceniak et al., 2019), but only a few *GRIN2B* mutations have been studied in neurons (Liu et al., 2017; Sceniak et al., 2019).

The first ASD-associated *GRIN2B* mutation to be discovered was a *de novo* splice site mutation (O'Roak et al., 2011) that is predicted to truncate GluN2B within the second extracellular loop (S2), which forms part of the agonist binding domain (ABD). In addition to this variant (GluN2B^{724t}), four more *GRIN2B* mutations have been identified among individuals with ASD or intellectual disability that also lead to truncation within S2 (Endele et al., 2010; Kenny et al., 2014; Stessman et al., 2017). Furthermore, 32 protein-altering mutations occur in the ABD, 20 of which are within S2 (Swanger et al., 2016; Platzer et al., 2017; Stessman et al., 2017).

We recently demonstrated that GluN2B^{724t} expression causes a striking impairment in dendrite morphogenesis, leading to reduced dendrite length and complexity (Sceniak et al., 2019). This reduction in dendritic arborization was associated with a lack of mutant subunit surface trafficking and distribution into dendrites. Further, dendritic spine number was likely decreased by the presence of GluN2B^{724t} since spine density was unaltered (Sceniak et al., 2019). Dendrite morphology directly affects the extent of synaptic connectivity, the number of potential synaptic partners a neuron interacts with, and dendritic filtering of postsynaptic responses (Ledda and Paratcha, 2017; Martínez-Cerdeño, 2017). Therefore, restricting dendrite length and branching is expected to change what information is received by a neuron, as well as how that information is processed by a neuron, consistent with the hypothesis that abnormal dendrite morphogenesis leads to symptoms of ASD and ID.

Dendritic arbors are established through repeated cycles of formation of new branches followed by their elongation (Lohmann and Wong, 2005; Yoong et al., 2019). Ultimately, nascent branches are either stabilized or retracted and eliminated. Distinct molecular mechanisms underlie different aspects of dendrite growth (Vaillant et al., 2002; Baumert et al., 2020; Wilson et al., 2020). For example, glutamate-mediated signaling through mGluR5 receptors leads to Ckd5-mediated phosphorylation of delta-catenin. Interestingly, unphosphorylated delta-catenin promotes extension, whereas phosphorylated delta-catenin favors branching over extension (Baumert et al., 2020). As a result, altering glutamate signaling can shift growth from extension to branching. Therefore, it is important to define which features of dendrite growth are impaired in ASD. Here, we sought to address this issue by studying the dynamics of dendrite elongation, branching, stabilization, and pruning. Through live imaging of developing cortical neurons, we found that GluN2B^{724t} impeded dendrite development by reducing elongation and promoting dendritic pruning. These data suggest that ASD mutations contribute to ASD pathophysiology by shifting the dynamics of dendrite growth away from extension and toward branch elimination, thereby reducing dendritic arbor size and complexity and disrupting normal circuit development and function. Based on the observations presented here, it will be important to explore whether promoting dendrite outgrowth and branch stabilization can reverse the dendrite maldevelopment caused by mutant GluN2B.

RESULTS

To investigate how ASD-associated mutations restrict dendritic arbor size and complexity, we used live, time-lapse confocal microscopy to examine the dynamics of dendrite growth. We focused on a mutation that is predicted to truncate GluN2B in the S2 lobe of the ABD at amino acid 724 (GluN2B^{724t}; O'Roak et al., 2011; **Figure 1A**). Rat neurons were transfected with either GluN2B^{WT} or GluN2B^{724t} tagged with GFP, along with tdTomato to fill dendrites. Imaging was performed at 5–9 days *in vitro* (DIV), a period of highly active dendrite growth and branching. Consistent with our previous observations in more mature neurons (Sceniak et al., 2019), 5–9 DIV neurons expressing GluN2B^{724t} appeared to have fewer, as well as shorter, dendrites than GluN2B^{WT} neurons (**Figure 1B**). Time-lapse images were collected over 4 h (**Figure 1B**; **Supplementary Videos 1, 2**), and terminal dendrites were tracked for the following fates: extension, retraction, pruning, and branching (**Figure 2**). Terminal dendrites were analyzed because they are the segments that are actively growing.

Here, we chose to express GluN2B^{WT} and GluN2B^{724t} on a wild-type background to reflect the heterozygous nature of patients with ASD. We previously showed that the effect of GluN2B on dendrite development was not due to overexpression of GluN2B (Sceniak et al., 2019). Furthermore, exogenous expression of *GRIN2B* does not alter the expression levels of other NMDAR subunits (Kutsuwada et al., 1996; Morikawa et al., 1998; Tang et al., 1999; Philpot et al., 2007; von Engelhardt et al., 2008), so the results reported here are likely not due to upregulation of other NMDAR subunits. It is also worth noting that the effects observed here are cell-autonomous since a small percentage (typically less than 2%) of cells express GFP-GluN2B constructs.

ASD-Associated Mutant GluN2B Reduces Dendrite Elongation but Not Motility

Because we observed shorter dendrites in GluN2B^{724t} neurons when compared to GluN2B^{WT} neurons, we asked whether reduced dendrite length stems from either reduced elongation or increased retraction. To do so, we measured changes in dendrite

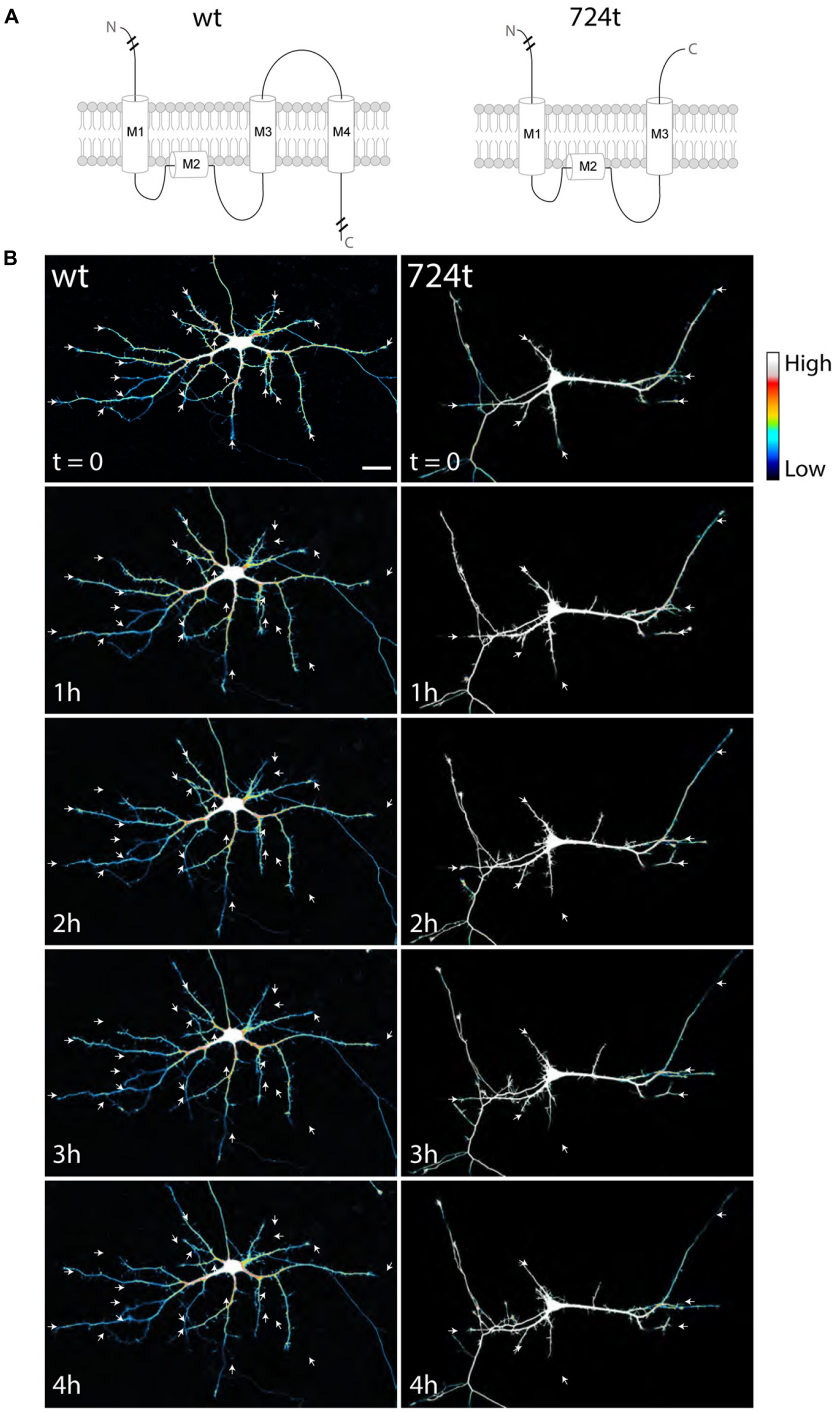

FIGURE 1 | Developing neurons expressing ASD-mutant GluN2B have smaller dendrites. **(A)** Schematic of GluN2B^{WT} (*left*) and GluN2B^{724t} (*right*). M1, M2, M3, and M4 represent membrane domains. To focus on the mutation site, full amino and carboxy termini are not depicted when indicated by line breaks. **(B)** Representative images of neurons (5–9 DIV) transfected with mutant (*right)* or wildtype (*left*) GFP-tagged GluN2B (not shown) and tdTomato (color coded with an intensity scale, as indicated by the color key). Arrows point to terminal ends of dendrites. Imaging times are displayed in hours, relative to the start of imaging. Scale bar, 25 μm.

length over time. For these analyses, terminal dendrites must have been greater than 7 μm over the time period analyzed. Dendrites that branched during the imaging period were not included in this analysis.

First, to determine whether mutant dendrites grow at a different net rate than wildtype dendrites, we traced terminal dendrites in the first and last frames of the movies. GluN2B^{724t} dendrites averaged a significantly smaller net gain in length than

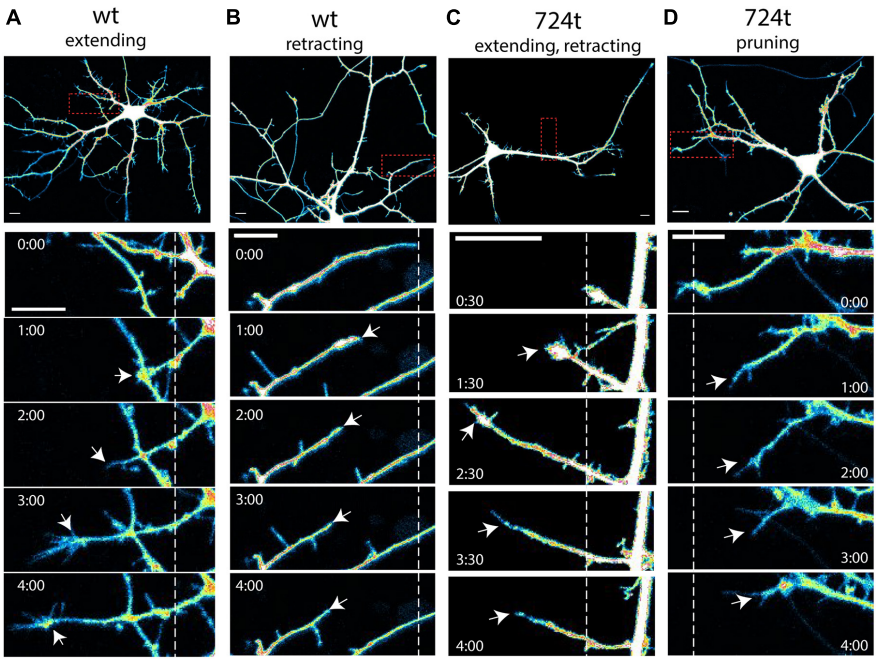

FIGURE 2 | Examples of terminal dendrite dynamics. Both wild-type and mutant neurons were observed extending, retracting, branching, and pruning. **(A–D)** Representative images of dendrite behavior. *Top panels*, low magnification view of individual neurons, visualized by imaging of tdTomato cytoplasmic fills. Areas within the *red boxes* are magnified in the time-lapse panels below each neuron. *Dashed lines* indicate the positions of each dendrite tip at the beginning of imaging. *White arrows* indicate the position of the dendrite tip in each frame. Growth cones were considered the tips of dendrites, rather than individual filopodia. Imaging times are displayed relative to the start of imaging (*0:00*) and span 4 h. Intensities are colored as in **Figure 1**. *Scale bars*, 10 μm. **(A)** wildtype dendrite extending and remaining terminal (*white arrows*). **(B)** Wildtype dendrite retracting and remaining terminal (*white arrows*). **(C)** GluN2B^{724t} dendrite emerging, growing, and then retracting (*white arrows*). **(D)** GluN2B^{724t} dendrite retracting and pruning (*white arrows*).

GluN2B^{WT} dendrites (**Figure 3A**; GluN2B^{WT}: 6.87 ± 1.48 μm, n = 113 dendrites from 14 cells and GluN2B^{724t}: 1.14 ± 1.75 μm, n = 93 dendrites from 14 cells; p = 0.018). In addition, more mutant dendrites netted a loss of length (**Figure 3B**). To further delineate the mechanisms of reduced net growth of mutant neurons, we analyzed the instantaneous growth rate of terminal dendrites. By examining the instantaneous growth rate, we could remove contaminating effects of periods when dendrites were neither extending nor retracting since only frames with detectable movement were analyzed. Consistent with what we observed over 4 h, GluN2B^{724t} dendrites elongated more slowly (**Figure 3C**; GluN2B^{WT}: 0.73 ± 0.23 μm/min, n = 565 movements from 113 dendrites and GluN2B^{724t}: -0.22 ± 0.21 μm/min, n = 465 movements from 93 dendrites; p = 0.0008). However, the absolute values of the instantaneous rate of change for wildtype and mutant neurons were similar (**Figure 3D**; GluN2B^{WT}: 3.47 ± 0.18 μm/min, n = 565 movements from 113 dendrites and GluN2B^{724t}: 3.23 ± 0.14 μm/min, n = 465 movements from 93 dendrites; p = 0.7147), indicating that GluN2B^{724t} dendrites were not less motile than GluN2B^{WT} dendrites.

Mutant dendrites could have reduced growth either: (i) because elongation is decreased or (ii) because retraction is increased. To distinguish between these possibilities, we separately analyzed extension and retraction. First, we evaluated rates of extension and retraction. The average rate of extension did not differ for wildtype and mutant dendrites (**Figure 3E**; GluN2B^{WT}: 5.56 ± 0.38 μm/min, n = 194 movements from 113 dendrites and GluN2B^{724t}: 5.26 ± 0.28 μm/min, n = 115 movements from 93 dendrites; p = 0.5255). The rates of retraction for both GluN2B^{WT} and GluN2B^{724t} were also similar (**Figure 3F**; GluN2B^{WT}: -4.80 ± 0.35 μm/min, n = 140 movements from 113 dendrites and GluN2B^{724t}: -4.88 ± 0.25 μm/min, n = 144 movements from 93 dendrites; p = 0.3121). Given that net growth was substantially reduced in mutant neurons (**Figures 3A,C**) while rates of extension and retraction were similar (**Figures 3E,F**), these data suggest that growing dendrites must spend less time extending and/or more time retracting in neurons expressing GluN2B^{724t}. We found that both of these changes occur (**Figure 3G**; GluN2B^{WT}: 1.72 ± 0.11 frames extending, 1.24 ± 0.09 frames retracting, and 2.04 ± 0.12 frames not changing length; GluN2B^{724t}: 1.24 ± 0.11 frames extending, 1.548 ± 0.11 frames retracting, 2.22 ± 0.12 frames not changing; p = 0.0017, 0.0283, and 0.2138, respectively). Therefore, expression of GluN2B^{724t} shifts dendrite dynamics away from extension and toward retraction, leading to shorter dendrite arbors.

GluN2B^{724t} Expression Promotes Pruning of Dendrite Branches

Neurons expressing GluN2B^{724t} also have fewer branches (Sceniak et al., 2019). To determine whether we could capture

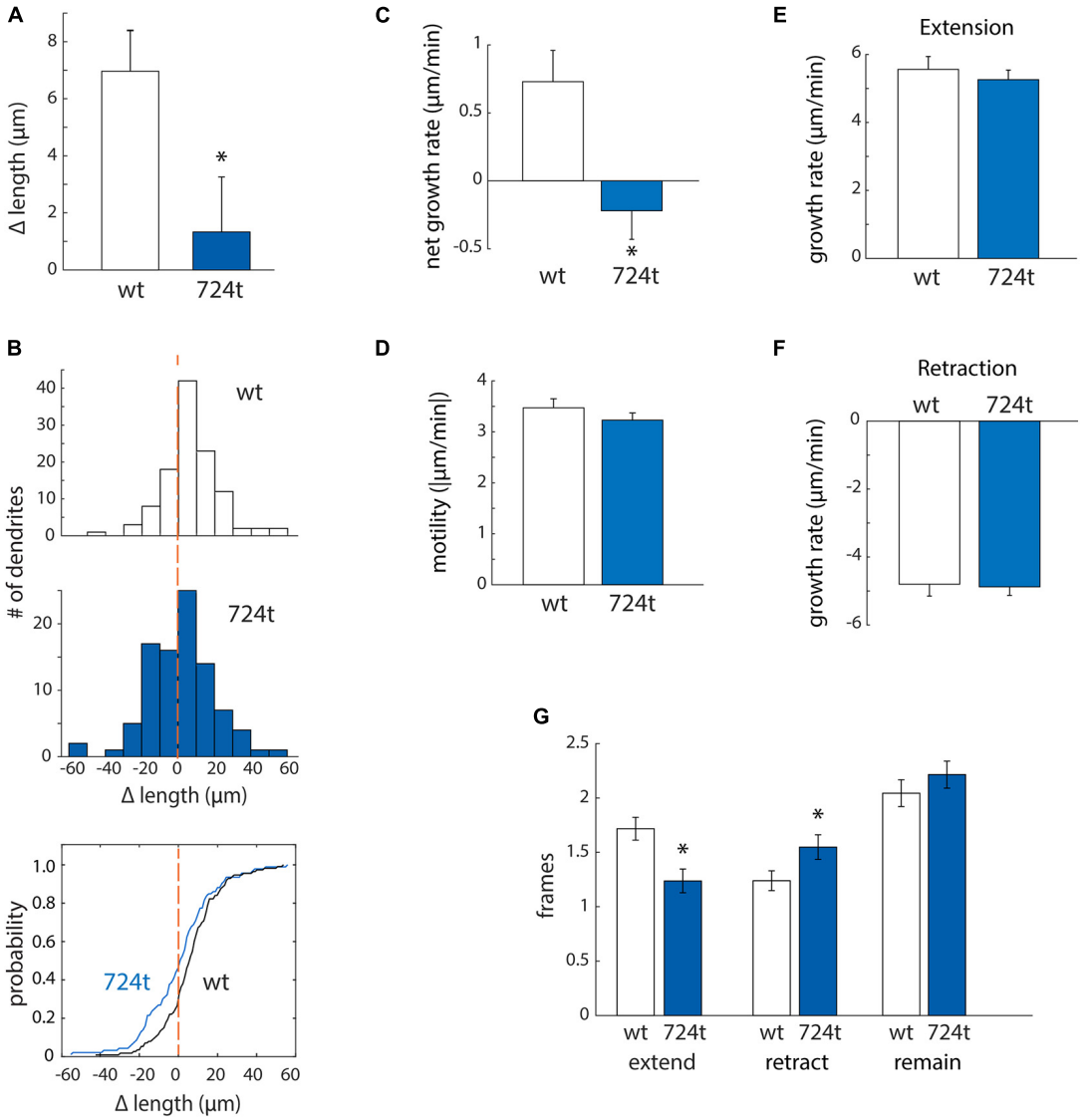

FIGURE 3 | ASD-associated mutant GluN2B leads to a bias toward retraction of growing dendrites, while wild-type dendrites tend to elongate. **(A,B)** ASD-associated mutation in GluN2B disrupts dendrite growth kinetics. Quantification of the average change in length of terminal dendrites for neurons expressing GluN2B^{WT} (*white*) or GluN2B^{724t} (*blue*) from eight independent experiments. **(A)** Over 4 h, neurons expressing GluN2B^{724t} had reduced net growth. Data represent means ± S.E. (*p = 0.018, n = 14 GluN2B^{WT} neurons, and 14 GluN2B^{724t} neurons). **(B)** ASD-associated mutation in GluN2B biases net growth of dendrites toward retraction and away from extension. *Top and middle panels,* histograms represent the number of dendrites that lengthen or shorten, separated into bins of 10 μm, with negative values representing a terminal dendrite becoming shorter over 4 h of live imaging. *Bottom panel,* cumulative probability distribution of changes in dendrite length. GluN2B^{WT} (n = 113 dendrites), and GluN2B^{724t} (n = 93 dendrites). *Dashed orange lines,* zero change in length. **(C,D)** ASD-mutant GluN2B reduces the net rate of dendrite outgrowth but not overall motility of terminal dendrites. Lengths of terminal dendrites were measured every 12 min for 1 h. Data represent means ± S.E. (n = 113 GluN2B^{WT} dendrites, and 93 GluN2B^{724t} dendrites). **(C)** ASD-associated mutant dendrites elongated at a reduced rate, compared to neurons expressing GluN2B^{WT} (*p = 0.0008). **(D)** Overall motility of terminal dendrites was similar for neurons transfected with either wildtype or mutant GluN2B (p = 0.7147). Motility represents all movements, regardless of direction, and was quantified by averaging the absolute values of instantaneous growth rates. Rates of extension [**(E)**, p = 0.5255] and retraction [**(F)**, p = 0.3121] were similar in ASD and WT neurons. Time spent extending [**(G)**, left, p = 0.0017] and retracting [**(G)**, middle, p = 0.0283] were significantly different, however. Time spent not actively extending or retracting was similar for ASD and WT neurons [**(G)**, right, p = 0.2138]. Each frame represents 12 min.

that change in branching in our imaging time period, we analyzed the net change in the number of terminal dendrites. Within this analysis, positive values corresponded to dendrites gained from branching, and negative values represented pruned dendrites. Mutant neurons tended to lose dendrite branches, whereas wild-type neurons did not (**Figure 4A**; GluN2B^{WT}: 0.00 ± 0.08, n = 14 cells and GluN2B^{724t}: -0.30 ± 0.10, n = 14 cells; p = 0.0302). Although there was a net loss of branches in the mutant, these dendrites were still dynamic since the mean of the absolute values of all branch gains and losses was not significantly different

in mutant and wild type neurons (**Figure 4B**; GluN2B^{WT}: 0.32 ± 0.07, n = 14 cells and GluN2B^{724t}: 0.48 ± 0.09, n = 14 cells; p = 0.2553).

Apical and basal dendrites of pyramidal cells are differentially affected by mutation or loss of two autism-associated genes, Epac2 and TAO2 (de Anda et al., 2012; Srivastava et al., 2012). This raises the question of whether apical and basal dendrites are similarly affected by GluN2B^{724t}. To test this, we quantified the net change in number of terminal dendrite branches for only the principal/apical dendrites. In wild-type and mutant neurons, a similar percentage of the total population of terminal dendrites belonged to the principal dendrite arbor (GluN2B^{WT}: 67.74 ± 0.09%, n = 13 cells and GluN2B^{724t}: 60.69 ± 0.08%, n = 13 cells; p = 0.5378). Interestingly, the stability of apical branches did not differ when comparing wild-type and mutant neurons: in 4 h of imaging, the same proportion of wild-type and mutant GluN2B neurons lost apical branches (2 out of 13 neurons for both GluN2B^{WT} and GluN2B^{724t}) GluN2B^{WT}. In addition, apical dendrites gained 1.15 ± 0.42 branches (n = 13 cells), and GluN2B^{724t} apical dendrites gained 0.46 ± 0.39 branches (n = 13 cells; p = 0.2787), even though the mutant neurons tended to lose dendrite branches in the same movies (**Figure 4A**).

The observed reduction in dendrite branching could stem from either reduced formation of new branches or increased elimination of existing branches. To distinguish between these two possibilities, we analyzed branching and pruning of individual dendrites. Dendrites that existed at the start of recording could have one of three possible fates: branch, prune, or remain terminal (i.e., neither branch nor prune). Within our 4 h imaging period, a higher percentage of GluN2B^{724t} dendrites pruned (**Figure 4C**; wt: 4.6%, n = 131 and 724t: 25.9%, n = 139 dendrites). Conversely, a lower percentage of mutant dendrites remained terminal (**Figure 4C**; GluN2B^{WT}: 86.3%, n = 131 and GluN2B^{724t}: 66.9%, n = 139). Interestingly, rates of formation of new branches were similar in wild-type and mutant neurons (**Figure 4C**; GluN2B^{WT}: 9.2%, n = 131 and GluN2B^{724t}: 7.2%, n = 139). These data suggest that dendrites of neurons transfected with GluN2B^{724t} were less stable and had an increased bias toward pruning.

The observed bias toward pruning could be from more cells having dendrites that prune, or from more dendrites pruning per cell. We found that a higher percentage of mutant neurons had dendrites that pruned (**Figure 4D**; GluN2B^{WT}: 50%, n = 14 cells and GluN2B^{724t}: 86%, n = 14 cells). Of the neurons that had pruned dendrites, there was no difference in the number of transient dendrites per cell [**Figure 4E**, 5.29 ± 0.71 (wt) and 4.17 ± 0.94 (724t); n = 7 GluN2B^{WT} and 12 GluN2B^{724t} neurons; p = 0.114]. This shows two things: (1) more neurons expressing GluN2B^{724t} had pruned dendrites, and (2) of the cells that had pruned dendrites, neurons expressing mutant and wildtype GluN2B had a similar number of dendrites that pruned.

For the dendrites that pruned, we next asked whether the pruning process occurred more rapidly in GluN2B^{724t} expressing neurons by analyzing the rate of elimination of pruned branches. All imaging frames were included in the calculations, including frames with advances or no movement. The rate of elimination was increased for GluN2B^{724t}-expressing neurons compared to GluN2B^{WT}-expressing neurons [**Figure 4F**; -0.055 ± 0.018 μm/min (GluN2B^{WT}), -0.174 ± 0.035 μm/min (GluN2B^{724t}); p = 0.008; n = 37 GluN2B^{WT} dendrites from seven neurons and 50 GluN2B^{724t} dendrites from 12 neurons]. Together, our data indicate that ASD mutant GluN2B destabilizes growing dendrites, leading to increased rates of branch pruning, which ultimately leads to reduced arbor complexity.

DISCUSSION

Despite abundant evidence that GluN2B influences dendrite growth and arborization (Ewald et al., 2008; Espinosa et al., 2009; Sepulveda et al., 2010; Bustos et al., 2014; Keith et al., 2019), the specific role of GluN2B in the dynamics of dendrite outgrowth and branching remains poorly understood. In the Xenopus tectal system, GluN2B over-expression did not alter branch additions or retractions but increased the appearance of transient dendrites, defined as existing no longer than 2 h (Ewald et al., 2008). Here, we found that rodent cortical neurons expressing GluN2B^{724t} had more retraction events, fewer stable dendrites, and more transient branches than wild-type neurons. In our experiments, transient dendrites corresponded to dendrites that existed at the start of imaging but did not persist for the entire 4 h imaging period. Although transient dendrites are defined somewhat differently in these two studies, both point to a role for GluN2B in regulation of dendrite turn-over and stability. Overall, these data suggest that ASD-associated *GRIN2B* mutations may disrupt normal GluN2B-dependent stabilization of nascent dendrites. GluN2B^{724t} may restrict dendrite outgrowth and branching by either inhibiting downstream signals that stabilize growing dendrites or by activating signaling pathways that promote retraction and pruning.

In cortical pyramidal neurons, apical and basal dendrites are distinct subcellular compartments. Here, we found that ASD mutant GluN2B lead to a net loss of terminal dendrites. However, in the same movies, apical/principal dendrite branches were unaffected by GluN2B^{724t}, indicating that apical and basal dendritic arbors are differentially affected by GluN2B^{724t}. Our observations are consistent with previous studies demonstrating that basal dendrite arbors are specifically reduced by expression of ASD-associated mutations in Epac2 (Srivastava et al., 2012) and loss of the ASD-associated TAO2 (de Anda et al., 2012). Interestingly, it was recently shown that GluN2B antagonists preferentially reduced basal dendrite branch number without significantly changing apical dendrite branching in cortical pyramidal neurons in organotypic slices (Gonda et al., 2020).

The synaptotrophic hypothesis posits that dendritic arbors are stabilized and shaped by concomitant synapse formation (Vaughn, 1989; Wong and Ghosh, 2002; Cline and Haas, 2008; Valnegri et al., 2015). This hypothesis is supported by observations that, in *Xenopus* tectal neurons, strong synapses are associated with stabilized dendrites, while weak synapses are not (Wu et al., 1999). Supporting a role for NMDARs in mediating synaptotrophic dendrite growth in mammalian cortex, NMDAR activation stabilizes stellate cell dendrites that form synapses with appropriate presynaptic partners (Mizuno et al., 2014). In

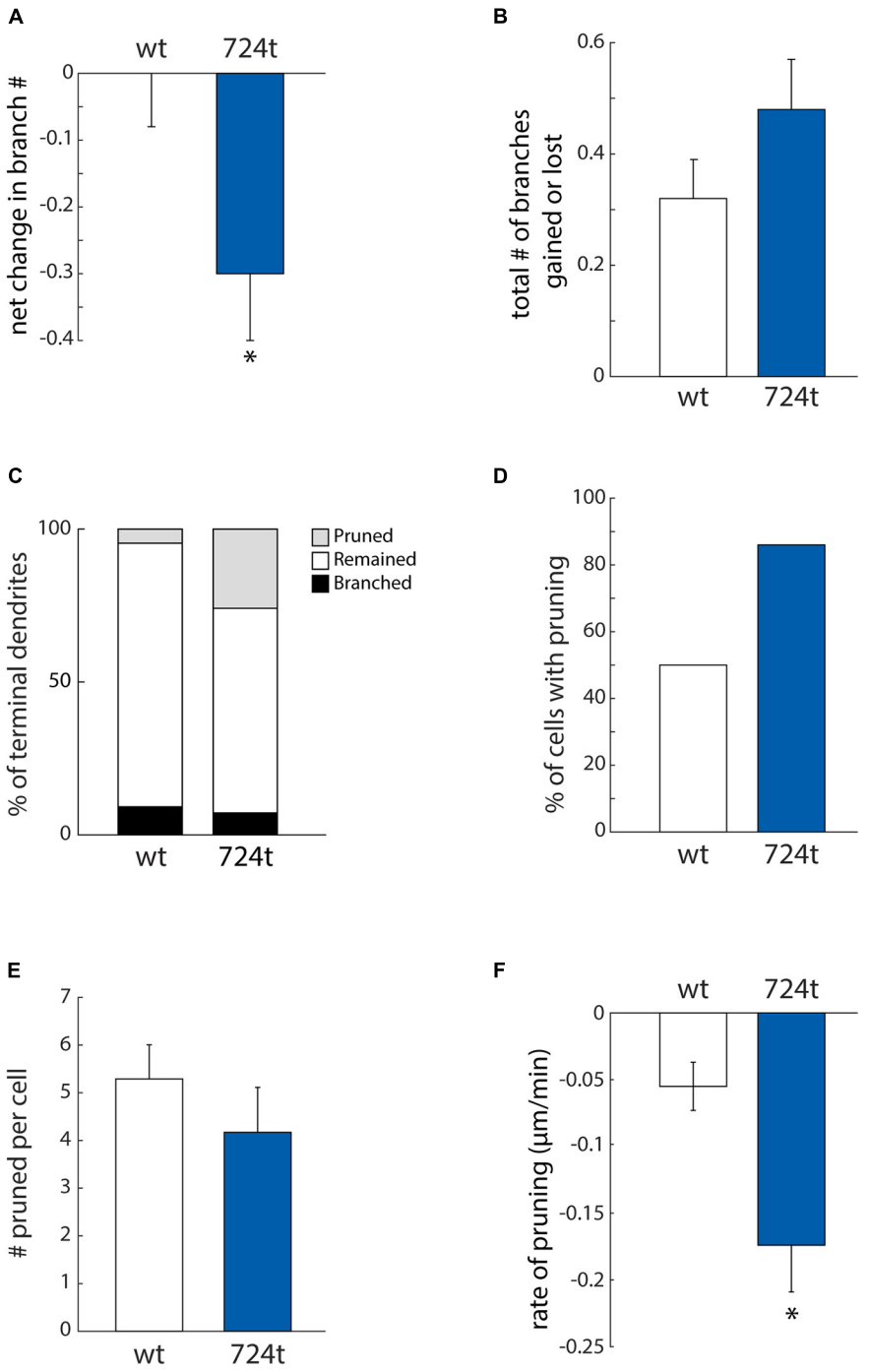

FIGURE 4 | ASD-associated mutation in GluN2B increases dendrite pruning but does not affect formation of new branches. **(A)** ASD mutant neurons (*blue bars*) display a net loss of terminal dendrite branches, while wild-type neurons (*white bars*) have a stable number of terminal dendrites. Positive values represent gain of dendrite branches, while negative values represent loss of dendrite branches. Data represent the mean ± S.E. (*p = 0.0302, n = 14 GluN2B^{WT}, and 14 GluN2B^{724t} neurons). **(B)** To calculate the total change in the number of terminal dendrites per cell per hour, both gains and losses of dendrites are represented as positive values. The ASD-associated mutation did not have a significant impact on the total change in the number of terminal dendrites (p = 0.2553). **(C)** Outcomes for terminal dendrites. A higher percentage of ASD-mutant dendrites were pruned, while a higher percentage of wild-type dendrites remained stable as terminal dendrites. The percentages of dendrites that branched were similar for mutant and wild-type dendrites. **(A–C)** For each cell, data were collected every hour for 4 h. **(D)** An increased percentage of ASD-associated mutant neurons had at least one pruned terminal dendrite over a 4-h time period, as compared to wild-type neurons. **(E)** Neurons that had at least one pruned dendrite had a similar number of pruned dendrites. Data represent the mean ± S.E. (p = 0.114, n = 7 GluN2B^{WT}, and 12 Glun2B^{724t} neurons). **(F)** Pruned dendrites retracted at a significantly faster rate for neurons expressing GluN2B^{724t} compared to neurons expressing GluN2B^{WT} (p = 0.008, n = 37 GluN2B^{WT}, and 50 GluN2B^{724t} dendrites).

this study, local activation of synaptic NMDARs was proposed to stabilize dendrite branches and promote their elongation, while global NMDAR signaling reduced dendrite extension and decreased the motility of terminal dendrite branches throughout the dendritic arbor.

It seems likely that the impaired dendrite elongation and branching that we observed in ASD mutant neurons is coupled to reduced synaptogenesis. Here, we observed that terminal dendrites are less stable and more likely to be eliminated in neurons transfected with GluN2B^{724t} than with GluN2B^{WT}. We previously showed that dendrites of mutant neurons form fewer spine synapses (Sceniak et al., 2019), but we do not yet know whether the number of non-spine synapses formed with dendrite shafts is similarly reduced. On one hand, if synaptotrophic mechanisms couple dendrite growth and synaptogenesis, then reduced stability of terminal dendrites and increased pruning could be downstream of reduced synaptogenesis. In addition, mutant NMDARs could reduce synapse strength, contributing to a deficit in dendrite stabilization. On the other hand, abnormal dendrite growth dynamics might drive the loss in synapse number in GluN2B^{724t} neurons: smaller, simplified dendrites may encounter fewer appropriate synaptic partners as they grow, driving a reduction in synapse formation.

The etiology of autism remains unclear; although, it is believed that autism is related to defects in neuronal connectivity in higher-order association areas (Geschwind and Levitt, 2007). Magnetic resonance imaging has provided evidence of both large-scale and small-scale changes in connectivity (Maximo et al., 2014), supporting this theory. Most research examining the cellular basis of connectivity abnormalities in ASD has focused on spine number and morphology or synaptic function (Kelleher and Bear, 2008; Bourgeron, 2009; Phillips and Pozzo-Miller, 2015; Varghese et al., 2017). However, it remains unclear how mutations in ASD-associated proteins cause changes in connectivity. One hypothesis is that morphological abnormalities in dendritic arbors lead to altered connectivity (Kulkarni and Firestein, 2012; Copf, 2016). Consistent with this hypothesis, our results suggest that in forms of ASD characterized by lower synapse number, ASD mutations may contribute to reduced connectivity by impairing dendrite outgrowth and stabilization.

Understanding how ASD mutations alter dendrite growth and stabilization is essential: if the bias in dendrite growth dynamics can be shifted toward outgrowth and stabilization, perhaps dendrite architecture can be restored. Because diagnosis of ASD often occurs after dendrite development is complete, it will be interesting to determine whether dendrite defects can be reversed later in development, after diagnosis of ASD.

MATERIALS AND METHODS

All studies were conducted with an approved protocol from the Case Western Reserve University Institutional Animal Care and Use Committee or the Central Michigan University Institutional Animal Care and Use Committee, in compliance with the National Institutes of Health guidelines for care and use of experimental animals.

Neuronal Cell Culture and Transfection

Neurons and astrocytes were derived from cortices of wild-type Sprague Dawley rats at 0–1 days postnatal. Neurons were grown on a confluent monolayer of astrocytes at 5% CO_2. Astrocytes were plated on 18 mm coverslips made of German glass (Carolina Scientific) that were acid cleaned then coated with a mixture of collagen and poly-D-lysine and grown in MEM without phenol red (Gibco), supplemented with N2 (Gibco), 10% fetal calf serum (Gibco or HyClone), 20% glucose, glutamax (Gibco), and Primocin (Invivogen). When astrocytes formed a confluent monolayer, neurons were plated on top of the astrocytes. Co-cultures were maintained in neuronal medium: Neurobasal-A (Gibco) with B27 (Gibco) and without antibiotics or phenol red, as previously described (Bury and Sabo, 2011, 2014; Sceniak et al., 2012). Half of the medium was replaced with fresh, equilibrated neuronal medium every 3–5 days.

Neurons were co-transfected with pEGFP-GluN2B constructs (2.6 μg DNA/coverslip) along with tdTomato (0.4 μg DNA/coverslip) at 2 DIV using the calcium phosphate method (Berry et al., 2012; Sceniak et al., 2019). pEGFP-GluN2B constructs were previously described (Sceniak et al., 2019). EGFP is inserted in the amino-terminal extracellular domain after the signal peptide. tdTomato-N1 was Addgene plasmid 54642.

Live Imaging of Neurons

Neurons were imaged live at 5–9 DIV. A coverslip was transferred to a sterile, closed imaging chamber (Warner Instruments) and bathed in warmed (37°C) Hibernate-A low-fluorescence medium (Gibco), supplemented with glutamax (Gibco). The chamber was mounted on the microscope stage and enclosed in a custom-made warming box (32–35°C). GFP was used to identify cells that expressed GluN2B constructs. Large neurons with pyramidal somas, based on tdTomato fills, were chosen for imaging. Only healthy cells were imaged, as determined by the appearance of the soma under DIC and a smooth axon without fragmentation or blebbing. Transfection efficiency was sufficiently low that individual filled neurons could be imaged without interference from nearby neurons. Imaging was with a Nikon C1 Plus confocal system, Eclipse Ti-E microscope, 20X (NA 0.75) Plan Apo objective, and 590/50 nm bandpass filter to visualize tdTomato fills. A perfect focus system was used to maintain focus. Eighty images were collected at 3-min intervals over 4 h. Scanning frame times were kept minimal at 14.7 s per image. Gains were set to clearly visualize thin dendrites while minimizing saturation in thicker dendrites and were kept constant during imaging. Images were taken with pixel sizes ranging from 205.1 to 250.3 nm.

Dendrite Analysis

Fiji (ImageJ 2.0.0-rc-65/1.51w) was used to track dendrite growth and branching, based on the tdTomato fills. Individual terminal dendrite branches were traced throughout the movies for further quantification, as described in detail below for each measure presented. Analysis was limited to neurons that remained healthy throughout the 4 h imaging period. Dendrites were identified

based on their morphology (shorter than the axon, tapered). MATLAB was used to plot the data. Since the data were not normally distributed (not shown), statistical comparisons were made using Wilcoxon rank sum tests in MATLAB.

To quantify the change in length of terminal dendrites, dendrites longer than 7 μm were traced at the start (t = 0 h) and end (t = 4 h) of imaging. To calculate a net change in length, the difference between starting and ending lengths was determined, then these values were averaged for each neuron. Statistical analysis was performed using the average of each neuron. Histograms represent data for individual dendrites.

To determine instantaneous growth rates, terminal dendrites greater than 7 μm long were traced every 12 min for 1 h. This analysis interval was sufficient to capture all quantifiable movements. The instantaneous net growth rate corresponds to the average rate of change in length for all movements. The instantaneous motility corresponds to the mean of the absolute values of instantaneous growth rates. The rate of retraction was calculated by averaging growth rates for all movements resulting in loss of at least 2 μm of dendrite in 12 min. Similarly, the rate of extension is the mean of movements that added at least 2 μm of dendrite length in 12 min.

Pruning dendrites were defined as dendrites that existed at the start of imaging but retracted until no longer visible. Branching dendrites were defined as dendrites that existed at the start of imaging but became branched into 2 or more dendrites during imaging. Dendrites that remained terminal were dendrites that may have gained or lost length but never disappeared or branched. For analysis of the net change in the number of terminal dendrites, the total number of terminal dendrites per neuron was recorded each hour for 4 h. For apical dendrite analysis, the first and last frames of movies were compared for addition or loss of terminal dendrites.

To determine retraction rates for pruned dendrites, we recorded the length of each dendrite every 12 min until the dendrite was completely gone. Changes in length were divided by 12, and every pruned branch was treated as independent for statistical analysis. Transient dendrites were not considered fully pruned until they completely disappeared. This ensured that we did not include dendrites that might eventually regrow in the analysis of pruning.

DATA AVAILABILITY STATEMENT

The raw data supporting the conclusions of this article will be made available by the authors, without undue reservation.

ETHICS STATEMENT

The animal study was reviewed and approved by Case Western Reserve University Institutional Animal Care and Use Committee and Central Michigan University Institutional Animal Care and Use Committee.

AUTHOR CONTRIBUTIONS

KF-S collected data and edited the manuscript. MS analyzed data and edited the manuscript. JB and SS analyzed data and wrote the manuscript. All authors contributed to the article and approved the submitted version.

FUNDING

This work was supported by a Research Starter grant from the Simons Foundation Autism Research Initiative and funds from Central Michigan University.

SUPPLEMENTARY MATERIAL

The Supplementary Material for this article can be found online at: https://www.frontiersin.org/articles/10.3389/fncel.2021.692232/full#supplementary-material

Supplementary Video 1 | Representative movie example of a GluN2B^{WT} GFP-GluN2B neuron. Neuron was six DIV. Movie spans 4-h of imaging. Images were collected every 3 min. Frame time was 14.718 s. This neuron is also shown in **Figure 1B**. Scale bar, 25 μm.

Supplementary Video 2 | Representative movie example of a GluN2B^{724t} GFP-GluN2B neuron. Neuron was seven DIV. Movie spans 4-h of imaging. Images were collected every 3 min. Frame time was 14.718 s. This neuron is also shown in **Figure 1B**. Scale bar, 25 μm.

REFERENCES

Abrahams, B. S., Arking, D. E., Campbell, D. B., Mefford, H. C., Morrow, E. M., Weiss, L. A., et al. (2013). SFARI Gene 2.0: a community-driven knowledgebase for the autism spectrum disorders (ASDs). *Mol. Autism* 4:36. doi: 10.1186/2040-2392-4-36

Baumert, R., Ji, H., Paulucci-Holthauzen, A., Wolfe, A., Sagum, C., Hodgson, L., et al. (2020). Novel phospho-switch function of delta-catenin in dendrite development. *J. Cell Biol.* 219:e201909166.

Bell, S., Maussion, G., Jefri, M., Peng, H., Theroux, J. F., Silveira, H., et al. (2018). Disruption of GRIN2B impairs differentiation in human neurons. *Stem Cell Reports* 11, 183–196. doi: 10.1016/j.stemcr.2018.05.018

Berry, C. T., Sceniak, M. P., Zhou, L., and Sabo, S. L. (2012). Developmental up-regulation of vesicular glutamate transporter-1 promotes neocortical presynaptic terminal development. *PLoS One* 7:e50911. doi: 10.1371/journal.pone.0050911

Bourgeron, T. (2009). A synaptic trek to autism. *Curr. Opin. Neurobiol.* 19, 231–234. doi: 10.1016/j.conb.2009.06.003

Bury, L. A., and Sabo, S. L. (2011). Coordinated trafficking of synaptic vesicle and active zone proteins prior to synapse formation. *Neural Dev.* 6:24. doi: 10.1186/1749-8104-6-24

Bury, L. A., and Sabo, S. L. (2014). Dynamic mechanisms of neuroligin-dependent presynaptic terminal assembly in living cortical neurons. *Neural Dev.* 9:13. doi: 10.1186/1749-8104-9-13

Bustos, F. J., Varela-Nallar, L., Campos, M., Henriquez, B., Phillips, M., Opazo, C., et al. (2014). PSD95 suppresses dendritic arbor development in mature hippocampal neurons by occluding the clustering of NR2B-NMDA receptors. *PLoS One* 9:e94037. doi: 10.1371/journal.pone.0094037

Cline, H., and Haas, K. (2008). The regulation of dendritic arbor development and plasticity by glutamatergic synaptic input: a review of the synaptotrophic hypothesis. *J. Physiol.* 586, 1509–1517. doi: 10.1113/jphysiol.2007.150029

Copf, T. (2016). Impairments in dendrite morphogenesis as etiology for neurodevelopmental disorders and implications for therapeutic treatments. *Neurosci. Biobehav. Rev.* 68, 946–978. doi: 10.1016/j.neubiorev.2016.04.008

de Anda, F. C., Rosario, A. L., Durak, O., Tran, T., Gräff, J., Meletis, K., et al. (2012). Autism spectrum disorder susceptibility gene TAOK2 affects basal dendrite formation in the neocortex. *Nat. Neurosci.* 15, 1022–1031. doi: 10.1038/nn.3141

De Rubeis, S., He, X., Goldberg, A. P., Poultney, C. S., Samocha, K., Ercument Cicek, A., et al. (2014). Synaptic, transcriptional and chromatin genes disrupted in autism. *Nature* 515, 209–215.

Endele, S., Rosenberger, G., Geider, K., Popp, B., Tamer, C., Stefanova, I., et al. (2010). Mutations in GRIN2A and GRIN2B encoding regulatory subunits of NMDA receptors cause variable neurodevelopmental phenotypes. *Nat. Genet.* 42, 1021–1026. doi: 10.1038/ng.677

Espinosa, J. S., Wheeler, D. G., Tsien, R. W., and Luo, L. (2009). Uncoupling dendrite growth and patterning: single-cell knockout analysis of NMDA receptor 2B. *Neuron* 62, 205–217. doi: 10.1016/j.neuron.2009.03.006

Ewald, R. C., Van Keuren-Jensen, K. R., Aizenman, C. D., and Cline, H. T. (2008). Roles of NR2A and NR2B in the development of dendritic arbor morphology in vivo. *J. Neurosci.* 28, 850–861. doi: 10.1523/jneurosci.5078-07.2008

Fan, C., Gao, Y., Liang, G., Huang, L., Wang, J., Yang, X., et al. (2020). Transcriptomics of Gabra4 knockout mice reveals common NMDAR pathways underlying autism, memory, and epilepsy. *Mol. Autism* 11:13.

Fedele, L., Newcombe, J., Topf, M., Gibb, A., Harvey, R. J., and Smart, T. G. (2018). Disease-associated missense mutations in GluN2B subunit alter NMDA receptor ligand binding and ion channel properties. *Nat. Commun.* 9:957.

Geschwind, D. H., and Levitt, P. (2007). Autism spectrum disorders: developmental disconnection syndromes. *Curr. Opin. Neurobiol.* 17, 103–11. doi: 10.1016/j.conb.2007.01.009

Gonda, S., Giesen, J., Sieberath, A., West, F., Buchholz, R., Klatt, O., et al. (2020). GluN2B but not GluN2A for basal dendritic growth of cortical pyramidal neurons. *Front. Neuroanat.* 14:571351. doi: 10.3389/fnana.2020.571351

Iossifov, I., O'Roak, B. J., Sanders, S. J., Ronemus, M., Krumm, N., Levy, D., et al. (2014). The contribution of de novo coding mutations to autism spectrum disorder. *Nature* 515, 216–221.

Keith, R. E., Azcarate, J. M., Keith, M. J., Hung, C. W., Badakhsh, M. F., and Dumas, T. C. (2019). Direct intracellular signaling by the carboxy terminus of NMDA receptor GluN2 subunits regulates dendritic morphology in hippocampal CA1 pyramidal neurons. *Neuroscience* 396, 138–153. doi: 10.1016/j.neuroscience.2018.11.021

Kelleher, R. J., and Bear, M. F. (2008). The autistic neuron: troubled translation? *Cell* 135, 401–406. doi: 10.1016/j.cell.2008.10.017

Kenny, E. M., Cormican, P., Furlong, S., Heron, E., Kenny, G., Fahey, C., et al. (2014). Excess of rare novel loss-of-function variants in synaptic genes in schizophrenia and autism spectrum disorders. *Mol. Psychiatry* 19, 872–879. doi: 10.1038/mp.2013.127

Kulkarni, V. A., and Firestein, B. L. (2012). The dendritic tree and brain disorders. *Mol. Cell. Neurosci.* 50, 10–20. doi: 10.1016/j.mcn.2012.03.005

Kutsuwada, T., Sakimura, K., Manabe, T., Takayama, C., Katakura, N., Kushiya, E., et al. (1996). Impairment of suckling response, trigeminal neuronal pattern formation, and hippocampal LTD in NMDA receptor epsilon 2 subunit mutant mice. *Neuron* 16, 333–344. doi: 10.1016/s0896-6273(00)80051-3

Ledda, F., and Paratcha, G. (2017). Mechanisms regulating dendritic arbor patterning. *Cell. Mol. Life Sci.* 74, 4511–4537. doi: 10.1007/s00018-017-2588-8

Li, J., Zhang, J., Tang, W., Mizu, R. K., Kusumoto, H., XiangWei, W., et al. (2019). De novo GRIN variants in NMDA receptor M2 channel pore-forming loop are associated with neurological diseases. *Hum. Mutat.* 40, 2393–2413. doi: 10.1002/humu.23895

Liu, S., Zhou, L., Yuan, H., Vieira, M., Sanz-Clemente, A., Badger, J. D. 2nd, et al. (2017). A rare variant identified within the GluN2B C-terminus in a patient with autism affects NMDA receptor surface expression and spine density. *J. Neurosci.* 37, 4093–4102. doi: 10.1523/jneurosci.0827-16.2017

Lohmann, C., and Wong, R. O. (2005). Regulation of dendritic growth and plasticity by local and global calcium dynamics. *Cell Calcium* 37, 403–409. doi: 10.1016/j.ceca.2005.01.008

Martínez-Cerdeño, V. (2017). Dendrite and spine modifications in autism and related neurodevelopmental disorders in patients and animal models. *Dev. Neurobiol.* 77, 393–404. doi: 10.1002/dneu.22417

Maximo, J. O., Cadena, E. J., and Kana, R. K. (2014). The implications of brain connectivity in the neuropsychology of autism. *Neuropsychol. Rev.* 24, 16–31. doi: 10.1007/s11065-014-9250-0

Mizuno, H., Luo, W., Tarusawa, E., Saito, Y. M., Sato, T., Yoshimura, Y., et al. (2014). NMDAR-regulated dynamics of layer 4 neuronal dendrites during thalamocortical reorganization in neonates. *Neuron* 82, 365–379. doi: 10.1016/j.neuron.2014.02.026

Morikawa, E., Mori, H., Kiyama, Y., Mishina, M., Asano, T., and Kirino, T. (1998). Attenuation of focal ischemic brain injury in mice deficient in the epsilon1 (NR2A) subunit of NMDA receptor. *J. Neurosci.* 18, 9727–9732. doi: 10.1523/jneurosci.18-23-09727.1998

Myers, R. A., Casals, F., Gauthier, J., Hamdan, F. F., Keebler, J., Boyko, A. R., et al. (2011). A population genetic approach to mapping neurological disorder genes using deep resequencing. *PLoS Genet.* 7:e1001318. doi: 10.1371/journal.pgen.1001318

O'Roak, B. J., Deriziotis, P., Lee, C., Vives, L., Schwartz, J. J., Girirajan, S., et al. (2011). Exome sequencing in sporadic autism spectrum disorders identifies severe de novo mutations. *Nat. Genet.* 43, 585–589. doi: 10.1038/ng.835

O'Roak, B. J., Stessman, H. A., Boyle, E. A., Witherspoon, K. T., Martin, B., Lee, C., et al. (2014). Recurrent de novo mutations implicate novel genes underlying simplex autism risk. *Nat. Commun.* 5:5595.

O'Roak, B. J., Vives, L., Fu, W., Egertson, J. D., Stanaway, I. B., Phelps, I. G., et al. (2012). Multiplex targeted sequencing identifies recurrently mutated genes in autism spectrum disorders. *Science* 338, 1619–1622. doi: 10.1126/science.1227764

Pan, Y., Chen, J., Guo, H., Ou, J., Peng, Y., Liu, Q., et al. (2015). Association of genetic variants of GRIN2B with autism. *Sci. Rep.* 5:8296.

Phillips, M., and Pozzo-Miller, L. (2015). Dendritic spine dysgenesis in autism related disorders. *Neurosci. Lett.* 601, 30–40. doi: 10.1016/j.neulet.2015.01.011

Philpot, B. D., Cho, K. K., and Bear, M. F. (2007). Obligatory role of NR2A for metaplasticity in visual cortex. *Neuron* 53, 495–502. doi: 10.1016/j.neuron.2007.01.027

Platzer, K., Yuan, H., Schutz, H., Winschel, A., Chen, W., Hu, C., et al. (2017). GRIN2B encephalopathy: novel findings on phenotype, variant clustering, functional consequences and treatment aspects. *J. Med. Genet.* 54, 460–470.

Sanders, S. J., He, X., Willsey, A. J., Ercan-Sencicek, A. G., Samocha, K. E., Cicek, A. E., et al. (2015). Insights into autism spectrum disorder genomic architecture and biology from 71 risk loci. *Neuron* 87, 1215–1233.

Sanz-Clemente, A., Nicoll, R. A., and Roche, K. W. (2013). Diversity in NMDA receptor composition: many regulators, many consequences. *Neuroscientist* 19, 62–75. doi: 10.1177/1073858411435129

Sceniak, M. P., Berry, C. T., and Sabo, S. L. (2012). Facilitation of neocortical presynaptic terminal development by NMDA receptor activation. *Neural Dev.* 7:8. doi: 10.1186/1749-8104-7-8

Sceniak, M. P., Fedder, K. N., Wang, Q., Droubi, S., Babcock, K., Patwardhan, S., et al. (2019). An autism-associated mutation in GluN2B prevents NMDA receptor trafficking and interferes with dendrite growth. *J. Cell Sci.* 132:jcs232892.

Sepulveda, F. J., Bustos, F. J., Inostroza, E., Zúñiga, F. A., Neve, R. L., Montecino, M., et al. (2010). Differential roles of NMDA receptor subtypes NR2A and NR2B in dendritic branch development and requirement of RasGRF1. *J. Neurophysiol.* 103, 1758–1770. doi: 10.1152/jn.00823.2009

Srivastava, D. P., Woolfrey, K. M., Jones, K. A., Anderson, C. T., Smith, K. R., Russell, T. A., et al. (2012). An autism-associated variant of Epac2 reveals a role for Ras/Epac2 signaling in controlling basal dendrite maintenance in mice. *PLoS Biol.* 10:e1001350. doi: 10.1371/journal.pbio.1001350

Stessman, H. A. F., Xiong, B., Coe, B. P., Wang, T., Hoekzema, K., Fenckova, M., et al. (2017). Targeted sequencing identifies 91 neurodevelopmental-disorder risk genes with autism and developmental-disability biases. *Nat. Genet.* 49, 515–526. doi: 10.1038/ng.3792

Swanger, S. A., Chen, W., Wells, G., Burger, P. B., Tankovic, A., Bhattacharya, S., et al. (2016). Mechanistic insight into NMDA receptor dysregulation by rare variants in the GluN2A and GluN2B agonist binding domains. *Am. J. Hum. Genet.* 99, 1261–1280. doi: 10.1016/j.ajhg.2016.10.002

Takasaki, Y., Koide, T., Wang, C., Kimura, H., Xing, J., Kushima, I., et al. (2016). Mutation screening of GRIN2B in schizophrenia and autism spectrum disorder in a Japanese population. *Sci. Rep.* 6:33311.

Talkowski, M. E., Rosenfeld, J. A., Blumenthal, I., Pillalamarri, V., Chiang, C., Heilbut, A., et al. (2012). Sequencing chromosomal abnormalities reveals neurodevelopmental loci that confer risk across diagnostic boundaries. *Cell* 149, 525–537. doi: 10.1016/j.cell.2012.03.028

Tang, Y. P., Shimizu, E., Dube, G. R., Rampon, C., Kerchner, G. A., Zhuo, M., et al. (1999). Genetic enhancement of learning and memory in mice. *Nature* 401, 63–69. doi: 10.1038/43432

Tarabeux, J., Kebir, O., Gauthier, J., Hamdan, F. F., Xiong, L., Piton, A., et al. (2011). Rare mutations in N-methyl-D-aspartate glutamate receptors in autism spectrum disorders and schizophrenia. *Trans. Psychiatry* 1:e55. doi: 10.1038/tp.2011.52

Vaillant, A. R., Zanassi, P., Walsh, G. S., Aumont, A., Alonso, A., and Miller, F. D. (2002). Signaling mechanisms underlying reversible, activity-dependent dendrite formation. *Neuron* 34, 985–998. doi: 10.1016/s0896-6273(02)00717-1

Valnegri, P., Puram, S. V., and Bonni, A. (2015). Regulation of dendrite morphogenesis by extrinsic cues. *Trends Neurosci.* 38, 439–447. doi: 10.1016/j.tins.2015.05.003

Varghese, M., Keshav, N., Jacot-Descombes, S., Warda, T., Wicinski, B., Dickstein, D. L., et al. (2017). Autism spectrum disorder: neuropathology and animal models. *Acta Neuropathol.* 134, 537–566.

Vaughn, J. E. (1989). Fine structure of synaptogenesis in the vertebrate central nervous system. *Synapse* 3, 255–285. doi: 10.1002/syn.890030312

von Engelhardt, J., Doganci, B., Jensen, V., Hvalby, Ø, Göngrich, C., Taylor, A., et al. (2008). Contribution of hippocampal and extra-hippocampal NR2B-containing NMDA receptors to performance on spatial learning tasks. *Neuron* 60, 846–860. doi: 10.1016/j.neuron.2008.09.039

Vyklicky, V., Krausova, B., Cerny, J., Ladislav, M., Smejkalova, T., Kysilov, B., et al. (2018). Surface expression, function, and pharmacology of disease-associated mutations in the membrane domain of the human GluN2B subunit. *Front. Mol. Neurosci.* 11:110. doi: 10.3389/fnmol.2018.00110NODOI

Wilson, E., Rudisill, T., Kirk, B., Johnson, C., Kemper, P., and Newell-Litwa, K. (2020). Cytoskeletal regulation of synaptogenesis in a model of human fetal brain development. *J. Neurosci. Res.* 98:2148–2165. doi: 10.1002/jnr.24692

Wong, R. O., and Ghosh, A. (2002). Activity-dependent regulation of dendritic growth and patterning. *Nat. Rev. Neurosci.* 3, 803–812. doi: 10.1038/nrn941

Wu, G. Y., Zou, D. J., Rajan, I., and Cline H. (1999). Dendritic dynamics *in vivo* change during neuronal maturation. *J. Neurosci.* 19, 4472–4483. doi: 10.1523/JNEUROSCI.19-11-04472.1999

Yoo, H. J., Cho, I. H., Park, M., Yang, S. Y., and Kim, S. A. (2012). Family based association of GRIN2A and GRIN2B with Korean autism spectrum disorders. *Neurosci. Lett.* 512, 89–93. doi: 10.1016/j.neulet.2012.01.061

Yoong, L. F., Pai, Y. J., and Moore, A. W. (2019). Stages and transitions in dendrite arbor differentiation. *Neurosci. Res.* 138, 70–78. doi: 10.1016/j.neures.2018.09.015

Conflict of Interest: The authors declare that the research was conducted in the absence of any commercial or financial relationships that could be construed as a potential conflict of interest.

Publisher's Note: All claims expressed in this article are solely those of the authors and do not necessarily represent those of their affiliated organizations, or those of the publisher, the editors and the reviewers. Any product that may be evaluated in this article, or claim that may be made by its manufacturer, is not guaranteed or endorsed by the publisher.

Advantages of publishing in Frontiers

OPEN ACCESS
Articles are free to read for greatest visibility and readership

FAST PUBLICATION
Around 90 days from submission to decision

HIGH QUALITY PEER-REVIEW
Rigorous, collaborative, and constructive peer-review

TRANSPARENT PEER-REVIEW
Editors and reviewers acknowledged by name on published articles

Frontiers
Avenue du Tribunal-Fédéral 34
1005 Lausanne | Switzerland

Visit us: www.frontiersin.org
Contact us: frontiersin.org/about/contact

REPRODUCIBILITY OF RESEARCH
Support open data and methods to enhance research reproducibility

DIGITAL PUBLISHING
Articles designed for optimal readership across devices

FOLLOW US
@frontiersin

IMPACT METRICS
Advanced article metrics track visibility across digital media

EXTENSIVE PROMOTION
Marketing and promotion of impactful research

LOOP RESEARCH NETWORK
Our network increases your article's readership